

NUREG/IA-0135
CAMP006

International Agreement Report

Post-Test Analysis of PIPER-ONE PO-IC-2 Experiment by RELAP5/MOD3 Codes

Prepared by
R. Bovalini, F. D'Auria, G. M. Galassi, M. Mazzini

University of Pisa
Via Diotisalvi, 2
1-56126 Pisa
Italy

RECEIVED
DEC 05 1996
OSTI

Office of Nuclear Regulatory Research
U.S. Nuclear Regulatory Commission
Washington, DC 20555-0001

November 1996

DISTRIBUTION OF THIS DOCUMENT IS UNLIMITED

Prepared as part of
The Agreement on Research Participation and Technical Exchange
under the International Thermal-Hydraulic Code Assessment
and Maintenance Program (CAMP)

Published by
U.S. Nuclear Regulatory Commission

MASTER

AVAILABILITY NOTICE

Availability of Reference Materials Cited in NRC Publications

Most documents cited in NRC publications will be available from one of the following sources:

1. The NRC Public Document Room, 2120 L Street, NW., Lower Level, Washington, DC 20555-0001
2. The Superintendent of Documents, U.S. Government Printing Office, P. O. Box 37082, Washington, DC 20402-9328
3. The National Technical Information Service, Springfield, VA 22161-0002

Although the listing that follows represents the majority of documents cited in NRC publications, it is not intended to be exhaustive.

Referenced documents available for inspection and copying for a fee from the NRC Public Document Room include NRC correspondence and internal NRC memoranda; NRC bulletins, circulars, information notices, inspection and investigation notices; licensee event reports; vendor reports and correspondence; Commission papers; and applicant and licensee documents and correspondence.

The following documents in the NUREG series are available for purchase from the Government Printing Office: formal NRC staff and contractor reports, NRC-sponsored conference proceedings, international agreement reports, grantee reports, and NRC booklets and brochures. Also available are regulatory guides, NRC regulations in the *Code of Federal Regulations*, and *Nuclear Regulatory Commission Issuances*.

Documents available from the National Technical Information Service include NUREG-series reports and technical reports prepared by other Federal agencies and reports prepared by the Atomic Energy Commission, forerunner agency to the Nuclear Regulatory Commission.

Documents available from public and special technical libraries include all open literature items, such as books, journal articles, and transactions. *Federal Register* notices, Federal and State legislation, and congressional reports can usually be obtained from these libraries.

Documents such as theses, dissertations, foreign reports and translations, and non-NRC conference proceedings are available for purchase from the organization sponsoring the publication cited.

Single copies of NRC draft reports are available free, to the extent of supply, upon written request to the Office of Administration, Distribution and Mail Services Section, U.S. Nuclear Regulatory Commission, Washington, DC 20555-0001.

Copies of industry codes and standards used in a substantive manner in the NRC regulatory process are maintained at the NRC Library, Two White Flint North, 11545 Rockville Pike, Rockville, MD 20852-2738, for use by the public. Codes and standards are usually copyrighted and may be purchased from the originating organization or, if they are American National Standards, from the American National Standards Institute, 1430 Broadway, New York, NY 10018-3308.

DISCLAIMER NOTICE

This report was prepared under an international cooperative agreement for the exchange of technical information. Neither the United States Government nor any agency thereof, nor any of their employees, makes any warranty, expressed or implied, or assumes any legal liability or responsibility for any third party's use, or the results of such use, of any information, apparatus, product, or process disclosed in this report, or represents that its use by such third party would not infringe privately owned rights.



NUREG/IA-0135
CAMP006

International Agreement Report

Post-Test Analysis of PIPER-ONE PO-IC-2 Experiment by RELAP5/MOD3 Codes

Prepared by
R. Bovalini, F. D'Auria, G. M. Galassi, M. Mazzini

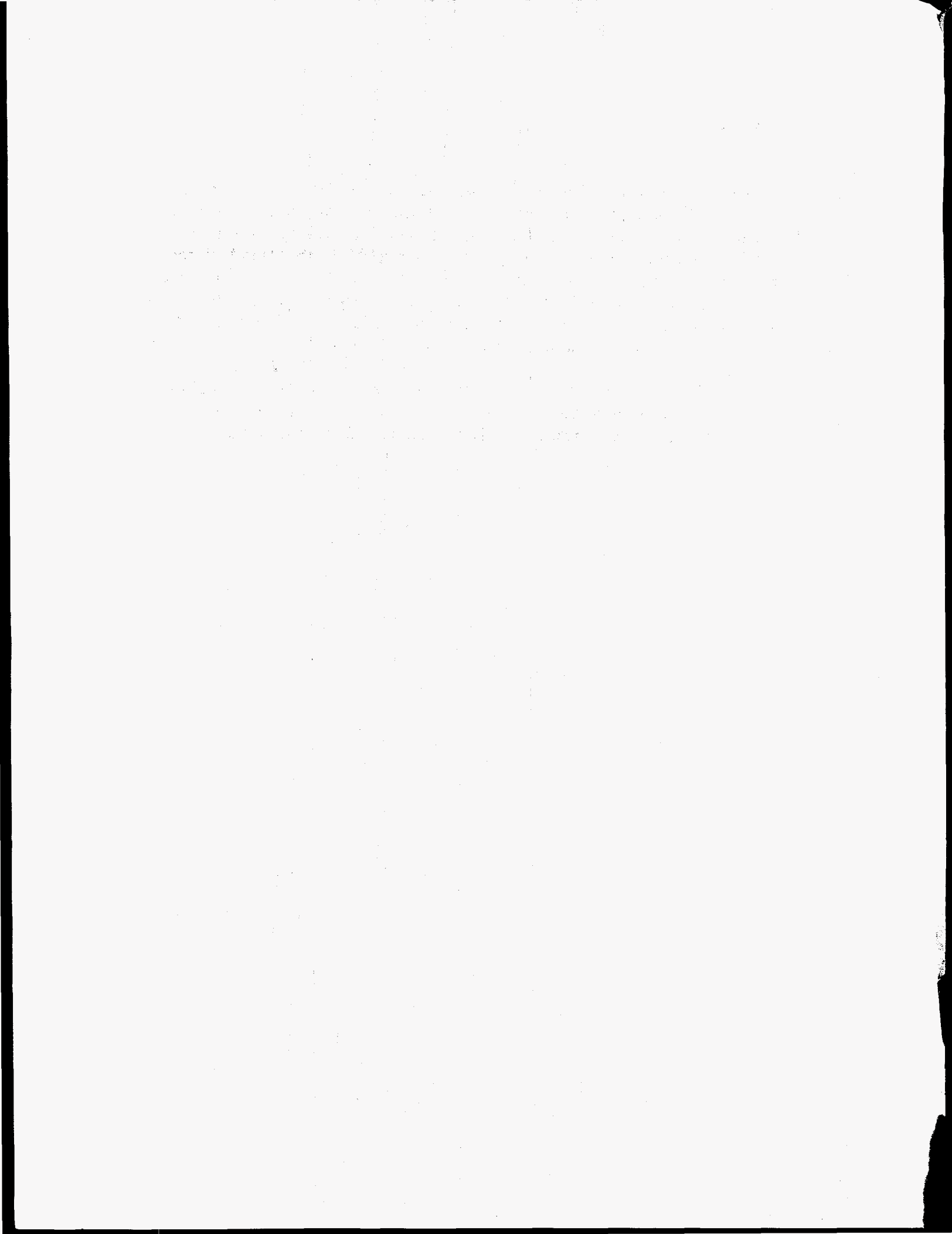
University of Pisa
Via Diotisalvi, 2
1-56126 Pisa
Italy

Office of Nuclear Regulatory Research
U.S. Nuclear Regulatory Commission
Washington, DC 20555-0001

November 1996

Prepared as part of
The Agreement on Research Participation and Technical Exchange
under the International Thermal-Hydraulic Code Assessment
and Maintenance Program (CAMP)

Published by
U.S. Nuclear Regulatory Commission



DISCLAIMER

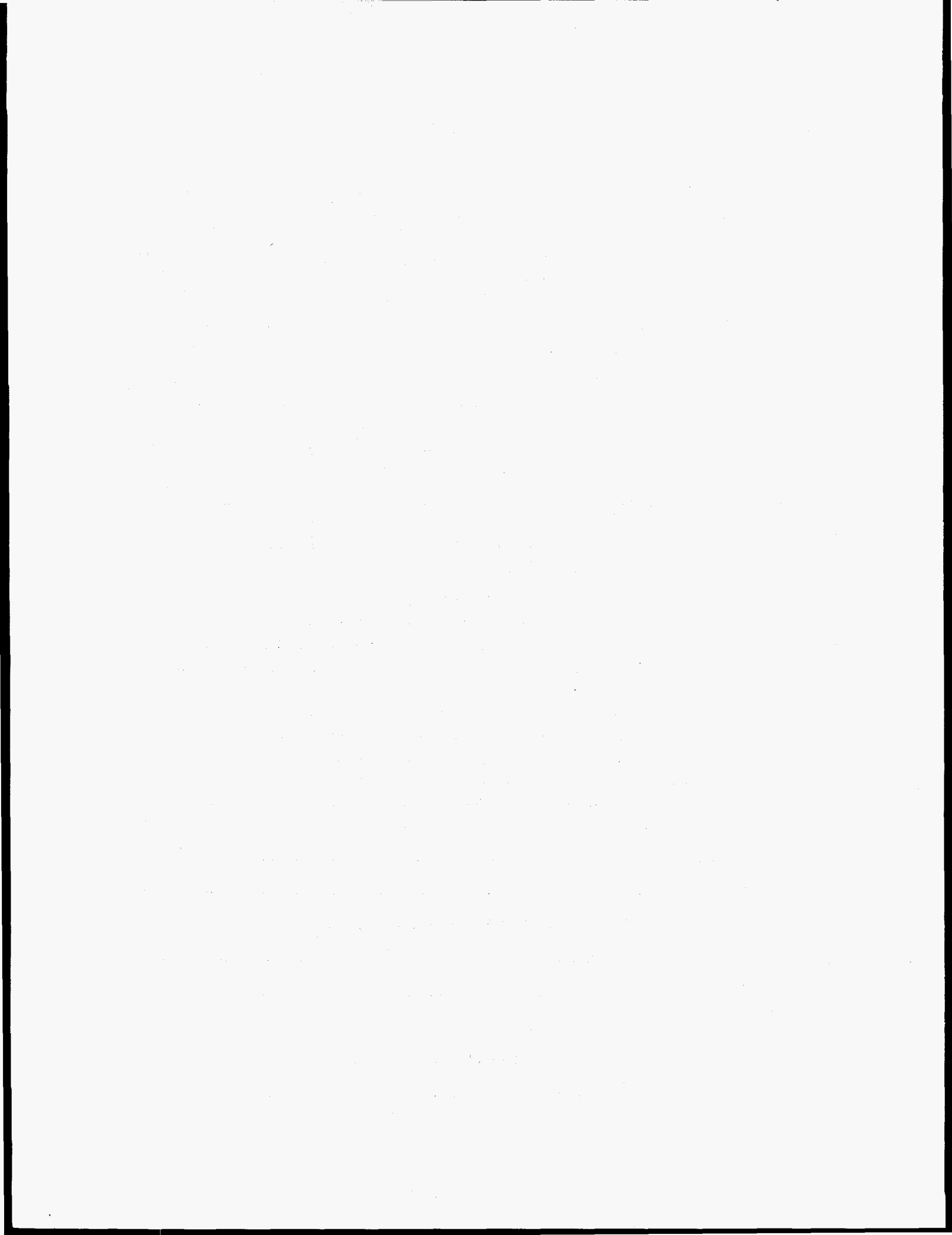
**Portions of this document may be illegible
in electronic image products. Images are
produced from the best available original
document.**

DISCLAIMER

This report was prepared as an account of work sponsored by an agency of the United States Government. Neither the United States Government nor any agency thereof, nor any of their employees, makes any warranty, express or implied, or assumes any legal liability or responsibility for the accuracy, completeness, or usefulness of any information, apparatus, product, or process disclosed, or represents that its use would not infringe privately owned rights. Reference herein to any specific commercial product, process, or service by trade name, trademark, manufacturer, or otherwise does not necessarily constitute or imply its endorsement, recommendation, or favoring by the United States Government or any agency thereof. The views and opinions of authors expressed herein do not necessarily state or reflect those of the United States Government or any agency thereof.

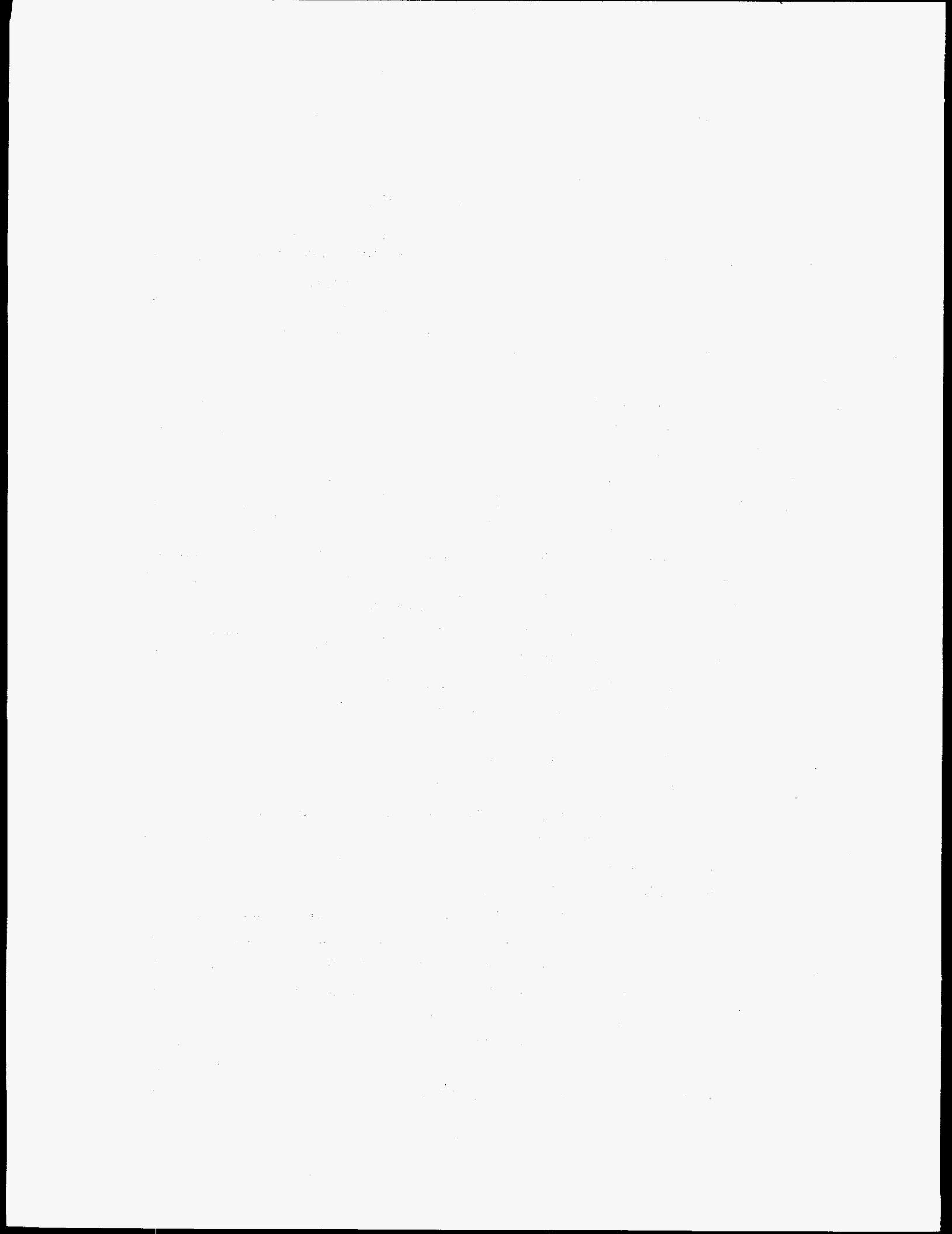
ABSTRACT

RELAP5/MOD3.1 was applied to the PO-IC-2 experiment performed in PIPER-ONE facility, which has been modified to reproduce typical isolation condenser thermal-hydraulic conditions. RELAP5 is a well known code widely used at the University of Pisa during the past seven years. RELAP5/MOD3.1 was the latest version of the code made available by the Idaho National Engineering Laboratory at the time of the reported study. PIPER-ONE is an experimental facility simulating a General Electric BWR-6 with volume and height scaling ratios of 1/2200 and 1./1, respectively. In the frame of the present activity a once-through heat exchanger immersed in a pool of ambient temperature water, installed approximately 10 m above the core, was utilized to reproduce qualitatively the phenomenologies expected for the Isolation Condenser in the simplified BWR (SBWR). The PO-IC-2 experiment is the flood up of the PO-SD-8 and has been designed to solve some of the problems encountered in the analysis of the PO-SD-8 experiment. A very wide analysis is presented hereafter including the use of different code versions.



CONTENTS

ABSTRACT	iii
LIST OF FIGURES	vii
LIST OF TABLES	ix
ACKNOWLEDGMENTS	xi
1. INTRODUCTION	1
2. DESCRIPTION OF THE EXPERIMENT	3
2.1 PIPER-ONE Facility	3
2.2 TEST PO-IC-2	11
2.2.1 Planning of the test	11
2.2.2 Test execution	11
2.2.3 Test results	11
3. ADOPTED CODES AND NODALIZATION	27
3.1 The used codes	27
3.2 Strategy of calculations and specific objectives	27
3.3 Adopted nodalization	27
4. ANALYSIS OF POST-TEST CALCULATION RESULTS	39
4.1 Steady state calculations (Phase 1 of the post-test analysis)	39
4.2 Reference calculation results (Phase 2 of the post-test analysis)	44
4.2.1 Primary circuit behavior	45
4.2.2 IC behavior	46
4.2.3 Heat transfer coefficient across the IC tubes	48
4.3 Sensitivity Calculations (Phase 3, of the Post-test analysis)	50
4.3.1 Significant results	51
4.3.2 Results in Apps. 2 and 4	68
4.3.3. Isolation of downcomer (App.3)	68
4.4 Scaling analysis	69
5. CONCLUSIONS	71
REFERENCES	73
APPENDIX 1: Results of reference calculation (Post-Test IC31).....	A1
APPENDIX 2: IC36 results	A2
APPENDIX 3: IC37 results	A3
APPENDIX 4: ICA6 results	A4
APPENDIX 5: Listing of RELAP5/Mod3.1 input	A5
APPENDIX 6: Overview of the scaling analysis	A6



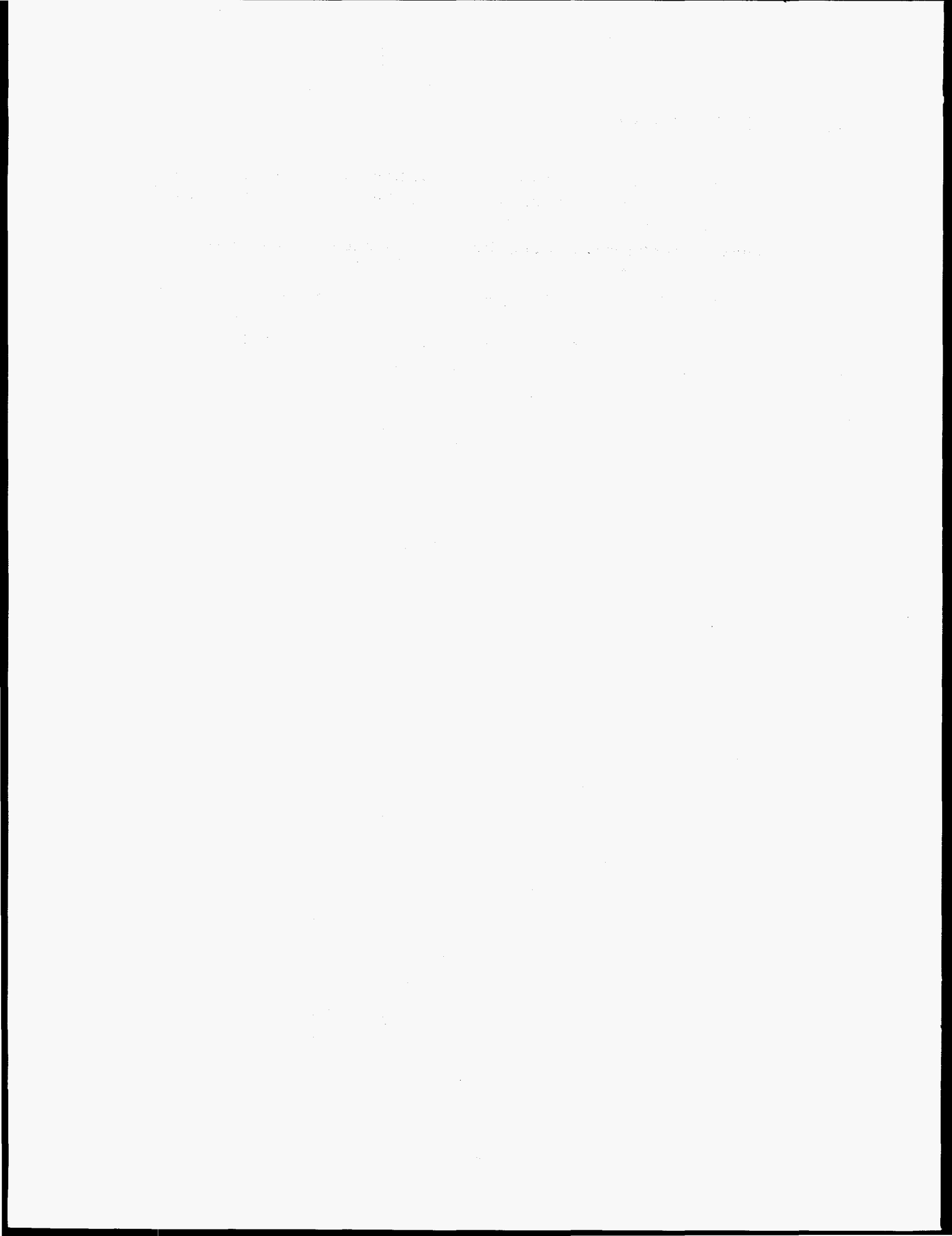
LIST OF FIGURES

Figure 1:	Sketch of PIPER-ONE facility	4
Figure 2:	Comparison between main regions in PIPER-ONE and in BWR-6	5
Figure 3:	Details of the heating rod of PIPER-ONE	5
Figure 4:	Connection between isolation condenser loop and PIPER-ONE loop	6
Figure 5:	Sketch of isolation condenser pool with temperature measurement locations (part A)	8
Figure 6:	Sketch of isolation condenser pool with temperature measurement locations (part B)	9
Figure 7:	Core power and lower plenum pressure	16
Figure 8:	Core power and fluid temperature in lower plenum	16
Figure 9:	Core power and downcomer level	17
Figure 10:	Core power and core level	17
Figure 11:	Pressure drop and flowrate across IC	18
Figure 12:	Tube "A" axial temperature distribution (external TC)	18
Figure 13:	Tube "A" internal and external TC (upper elevation)	19
Figure 14:	Tube "A" fluid temperature and external TC (middle elevation)	19
Figure 15:	Tubes "A," "B" and "C" fluid temperature (middle elevation)	20
Figure 16:	Tubes "A," "B" and "C" external TC (middle elevation)	20
Figure 17:	IC fluid temperatures (inlet center and outlet)	21
Figure 18:	Pool internal axial fluid temperatures	21
Figure 19:	Pool internal temperatures in different azimuthal positions	22
Figure 20:	Pool internal and external (upper elevation)	22
Figure 21:	Pool internal and external (middle elevation)	23
Figure 22:	Pool internal and external (lower elevation)	23
Figure 23:	Pool internal and external different positions	24
Figure 24:	Temperature at IC inlet comparison with saturation temperature	24
Figure 25:	Rod power and thermal power across IC	25
Figure 26:	Temperature jump across the wall	25
Figure 27:	Fluid temperature disuniformity across tubes	26
Figure 28:	Surface temperature disuniformities	26
Figure 29:	Nodalization of PIPER-ONE loop	37
Figure 30:	Measured and calculated trends of lower plenum pressure	42
Figure 31:	Measured and calculated trends of lower plenum temperature	42
Figure 32:	Measured and calculated trends of core level	43
Figure 33:	Measured and calculated trends of downcomer level	43
Figure 34:	Lower plenum pressure	52
Figure 35:	IC tubes wall surface temperature (external side level 3)	53

Figure 36: IC tubes fluid temperature (middle level 3)	53
Figure 37: IC outlet fluid temperature	54
Figure 38: Heat transfer coefficient at the inside of IC tubes wall (level 3)	54
Figure 39: Heat transfer coefficient at the outside of IC tubes wall (level 3)	55
Figure 40: Lower plenum pressure	55
Figure 41: IC tubes wall surface temperatures (external side level 3)	57
Figure 42: IC tubes fluid temperature (middle elevation)	57
Figure 43: IC outlet fluid temperature	58
Figure 44: Heat transfer coefficient at the inside of IC tubes wall (level 3)	58
Figure 45: Heat transfer coefficient at the outside of IC tubes wall (level 3)	59
Figure 46: Lower plenum pressure	59
Figure 47: IC tubes wall surface temperature (external side level 3)	60
Figure 48: IC tubes fluid temperature (middle elevation)	60
Figure 49: IC outlet fluid temperature	61
Figure 50: Heat transfer coefficient at the inside of IC tubes wall (level 3)	61
Figure 51: Heat transfer coefficient at the outside of IC tubes wall (level 3)	62
Figure 52: Lower plenum pressure	62
Figure 53: IC tubes wall surface temperature (external side level 3)	63
Figure 54: IC tubes fluid temperature (middle elevation)	63
Figure 55: IC outlet fluid temperature	64
Figure 56: Heat transfer coefficient at the inside of IC tubes wall (level 3)	64
Figure 57: Heat transfer coefficient at the outside of IC tubes wall (level 3)	65
Figure 58: Lower plenum pressure	65
Figure 59: IC tubes wall surface temperature (external side level 3)	66
Figure 60: IC tubes fluid temperature (middle elevation)	66
Figure 61: IC outlet fluid temperature	67
Figure 62: Heat transfer coefficient at the inside of IC tubes wall (level 3)	67
Figure 63: Heat transfer coefficient at the outside of IC tubes wall (level 3)	68

LIST OF TABLES

Table I:	Comparison between isolation condenser related data in PIPER-ONE and in SBWR	10
Table II:	PIPER-ONE test PO-IC-2: initial conditions	12
Table III:	PIPER-ONE test PO-IC-2: boundary conditions	12
Table IV:	PIPER-ONE test PO-IC-2: power history	12
Table V:	Details of nodes geometry in the RELAP5 nodalization	29
Table VI:	Details of relevant junction related parameters of RELAP5 nodalization	36
Table VII:	Comparison between measured and calculated initial conditions	41
Table VIII:	Comparison between measured and calculated boundary conditions	41
Table IXa:	Evaluation of the heat transfer coefficient (Ph.w.2)	49
Table IXb:	Evaluation of the heat transfer coefficient (Ph.w.4)	49
Table X:	List of calculations and varied parameters	50
Table XI:	Documented calculations	51



ACKNOWLEDGMENTS

The authors acknowledge the contribution of the technical staff of the Scalbatraio Laboratory for performing the experiments and in particular F. Mariotti, F. Pistelli, R. Centonze and F. Rosellini.

The University of Munchen student C. Rierter also contributed to the preparation of the facility for the experiment.

The authors gratefully acknowledge also D. Del Corso, for typing and editing this document.

Thanks are finally due to Dr. P. Marsili of ANPA for collaborating in defining the objectives of the activity and for revising the manuscript.

1. INTRODUCTION

Innovative reactors, (essentially AP-600 and SBWR) are characterized by simplification in the design and by the presence of passive systems. Experimental and theoretical research are needed to qualify the new components introduced in the design and to characterize the new thermalhydraulic scenarios expected during accidents. Available system codes have to be validated in order to be used for evaluating the thermalhydraulic performances of the new systems, especially in case of long lasting transients evolving at low pressure /1/.

In the frame of the activities carried out at University of Pisa related to the analysis of thermalhydraulic situations of interest to the mentioned reactors (e.g. refs. /2/, and /3/), three series of experiments have been carried out utilizing the PIPER-ONE facility. They were aimed at the experimental investigation of the behaviour of systems simulating the main features of the Gravity Driven Cooling System (GDCS, first series of experiments, refs. /4/) and of the reactor pressure vessel Isolation Condenser (IC, second and third series of experiments, refs. /5/ to /7/ and ref. /8/, respectively). At the same time Relap5/mod2 /9/, and mod3 /10/ codes have been extensively applied as best estimate tools to predict the transient scenarios of both SBWR and AP-600 reactors; (see also refs. /11/ and /12/).

PIPER-ONE is a General Electric BWR experimental simulator specifically designed in the early '80 to reproduce small break LOCAs transient scenarios (e.g. refs. /13/ - /15/). The volume scaling ratio is 1/2200, the height scaling ratio is 1/1 and the available core power is roughly 25% of the scaled full nominal power. The mentioned experiments were essentially devoted to a qualitative investigation of the thermalhydraulic conditions typical of the new components foreseen in the above reactors (essentially SBWR) and at setting up a data base suitable for code assessment. The distortions that characterize PIPER-ONE hardware in comparison with a scaled loop simulating SBWR, completely prevent a possible application of the measured data to reactor conditions: the core and downcomer heights, as well the distance between the Bottom of Active Fuel (BAF) and the Isolation Condenser top are important parameters not considered in the model.

The aforementioned applications to innovative reactors scenarios emphasized the codes inadequacies in producing reliable results when system pressure attains values below 0.5 MPa. Numerical deficiencies, limited ranges of validity of the utilized correlations and lack of user experience (i.e. difficulty to develop a suitable code use strategy) are retained mostly responsible of this situation.

The purposes of the activity described in the present document, that is the direct follow up of the post-test evaluation of the previous IC experiment PO-SD-8, ref. /7/, are essentially three:

- a) to give an outline of test results obtained during the high pressure part of the test PO-IC-2 also related to the study of the Isolation Condenser performance;
- b) to evaluate the capabilities of the latest version of Relap5/mod3 code (i.e. version 3.1) in reproducing the experimental scenario giving emphasis to the attempt of fixing the code limitations and the criteria for the optimal use of the code.
- c) to demonstrate possible improvement in the latest code version with respect to the previous one especially in relation to condensation.

In order to achieve these objectives the original Relap5/mod2 nodalization of the PIPER-ONE apparatus /16/, also modified to perform pre-test and post-test calculations of the test PO-SD-8 (e.g. refs. /7/ and /17/), was completely revised. In particular, the number of nodes was roughly doubled also considering the available computer code capabilities. This nodalization was qualified by the calculation of the test PO-SD-8 and was used extensively for stability analysis in PIPER-ONE loop, ref. /18/.

Many sensitivity calculations were performed in the present context to identify some unknown boundary conditions (e.g. spatial distribution of heat losses to the environment) and to optimize the user choices like the countercurrent flow limiting option in the annular region of steam separator to predict liquid deentrainment from the mixture flowing out from the core.

2. DESCRIPTION OF THE EXPERIMENT

2.1 PIPER-ONE Facility

The PIPER-ONE apparatus is an integral test facility designed for reproducing the behaviour of BWRs in thermalhydraulic transient, dominated by gravity forces.

The ENEL BWR plant installed at Caorso (I) was formerly taken as the reference prototype in the design of the apparatus. The reactor is a General Electric BWR-4 plant, equipped with a Mark II containment, but it has some features of the latest GE design (e.g., 8x8 fuel rod assembly). The situation of nuclear energy in Italy, at the beginning of the experimental phase, led to a revision of the original experimental programme. The BWR-6 plant, equipped with 624 fuel bundles was assumed at reference for the first test carried-out on the PIPER-ONE facility, chosen by OECD-CSNI as ISP 21 /19/; then, the latter was used as a reference plant for all the LOCA tests, which had already been performed.

The simplified sketch of the apparatus is shown in Fig. 1; it includes the main loop, the ECCS simulators (LPCI/CS, HPCI/CS) and the systems simulating ADS, SRV and steam line, as well as the blow-down line.

Nine zones can be identified in the main loop: lower plenum, core, core bypass (outside the core), guide tube region; upper plenum, region of separators and dryers, steam dome, upper downcomer, lower downcomer and jet pump region. The correspondence between the circuit and the vessel of the actual plant is shown in Fig. 2.

The volume scaling factor is about 1/2200, while the core cell geometry and the piezometric heads acting on the lower core support plate are the same in the model and in the reference plant.

The heated bundle consists of 16 (4x4) indirectly heated electrical rods, whose height, pitch and diameter are the same as in the reference plant (Fig. 3). The maximum available power is 320 kW, corresponding to about 25% of scaled full of the reference BWR.

The one-dimensionality as well as the overall simplicity of the apparatus are highlighted in Fig. 1; this is the direct outcome of the main objective of the research. In fact, the primary circuit was designed in such a way to have as far as possible:

- one dimensional cylindrical volumes (nodes in codes calculations);
- connections between adjacent nodes clearly defined (geometric discontinuities, Venturi nozzles, orifices);
- lack of items (such as pumps and control systems) which can originate confusing situations in code calculations.

The instrumentation system has features consistent with the fundamental philosophy of the facility design:

- direct measurements of integral or mean quantities (overall heat and mass entering or exiting from the primary circuit, collapsed levels in the various zones, mean temperatures in the volumes and interfacing structures, mean density in a section, etc.);
- measurement of the various quantities (such as fluid and structure temperatures) in the middle of the volumes and at the junctions connecting the various zones.

Roughly 250 transducers are part of the instrumentation system: rod surface temperatures, absolute pressures, differential pressures, flowrates, density and temperatures of the fluid and of the structures are measured in different zones of the loop.

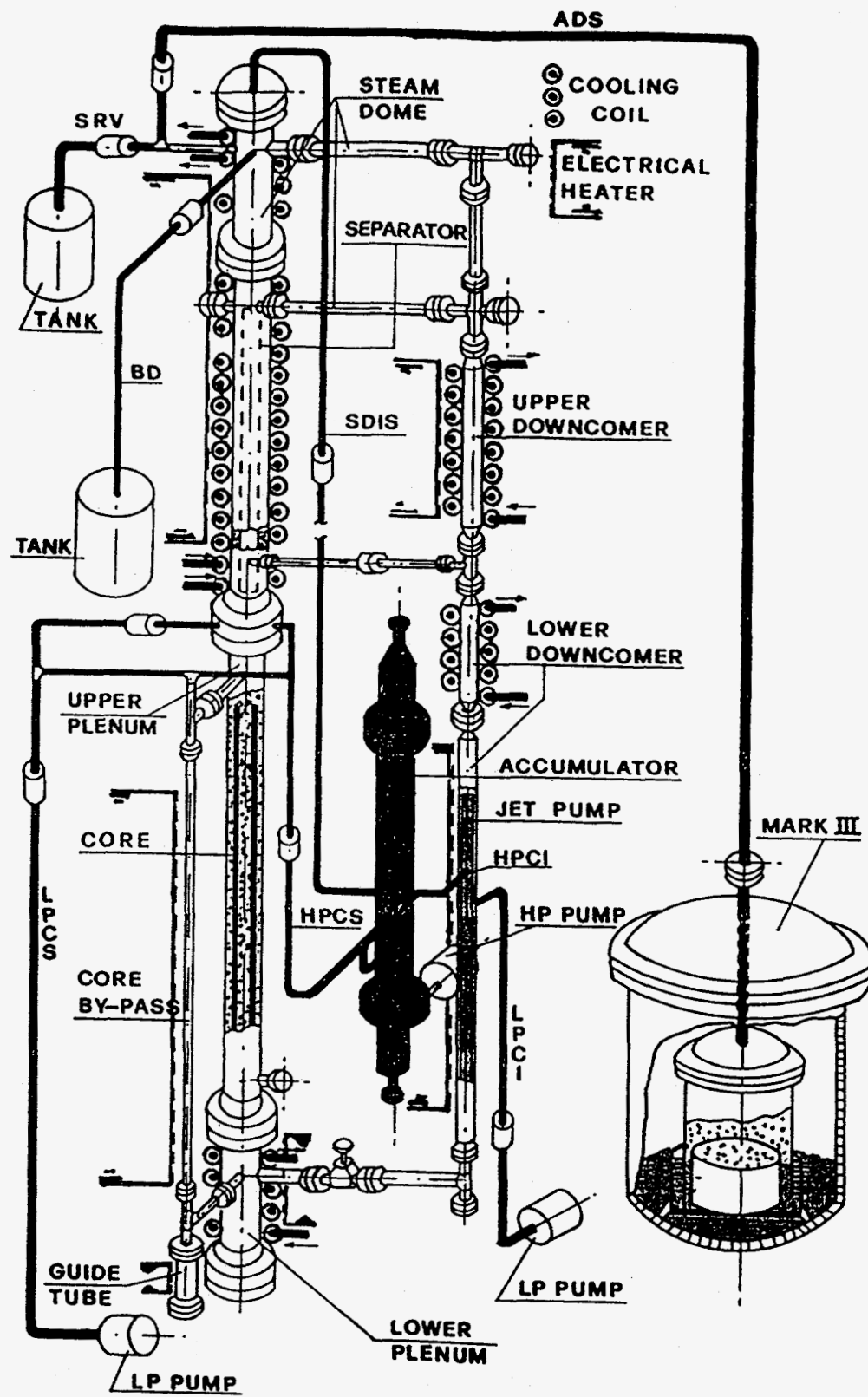


Fig. 1 - Sketch of PIPER-ONE facility

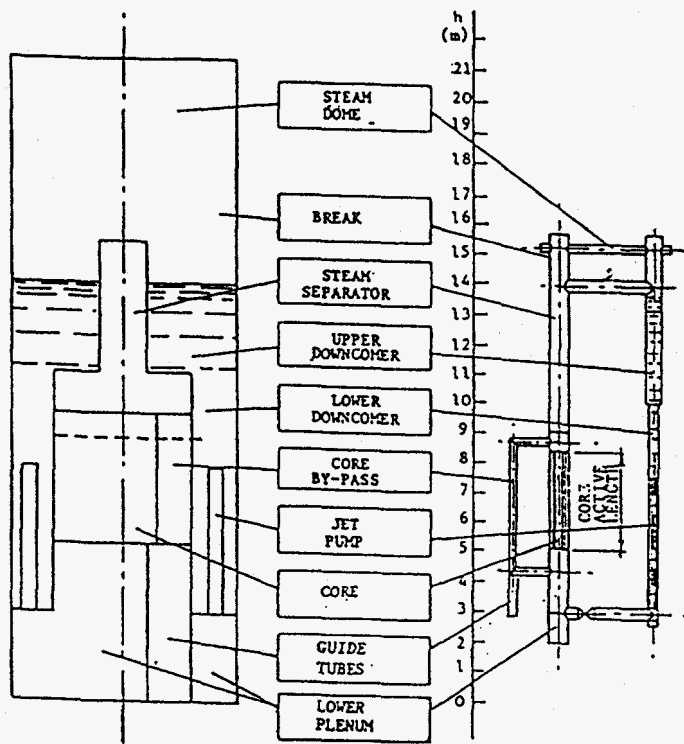


Fig. 2 - Comparison between main regions in PIPER-ONE and in BWR-6

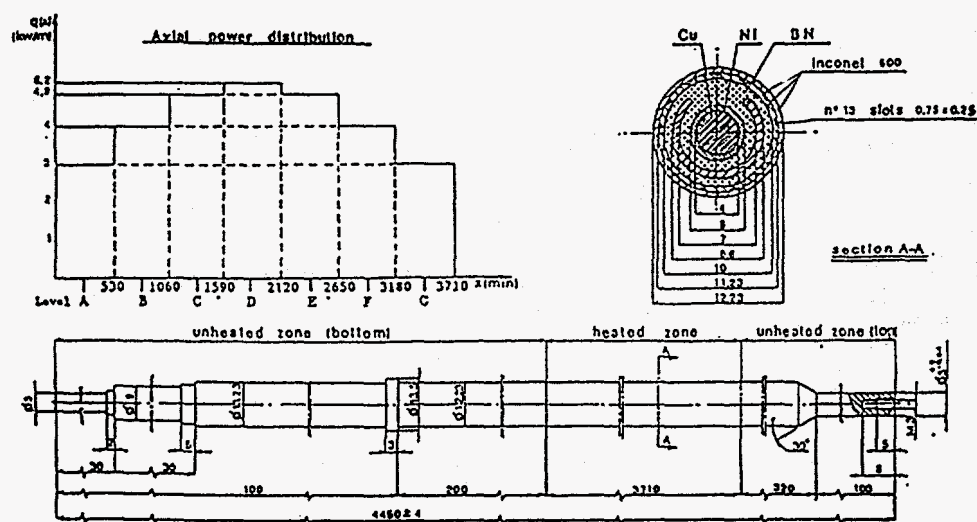


Fig. 3 - Details of the heating rod of PIPER-ONE

The data acquisition system can record 128 signals, with a frequency of up to 10 Hz for each signal. Particular care was taken to evaluate and maintain an adequate accuracy in measurements. The methodology developed (and adopted) includes:

- periodic calibration of all the transducers, in such a way to avoid or at least to reduce the systematic errors;
- control of the instrumentation system and of the related data acquisition system, before, during the preparation and at the end of each test. These checks reduce random errors and verify the correct operation of the measurement and data acquisition systems.

As already mentioned, the facility hardware was modified by inserting the loop, which can operate at the same pressure of the main circuit (Fig. 4).

The main component of Isolation Condenser loop is a heat exchanger consisting of a couple of flanges that support 12 pipes, 22 mm outer diameter and 0.4 m long; it is immersed in a tank of 1 m³ volume, containing stagnant water, located at 4th floor of the PIPER-ONE service structure. The heat exchanger is connected at the top and at the bottom respectively with the steam dome and the lower plenum of the main loop. In order to enhance natural convection inside the pool, a sort of shroud has been installed that divides the pool into two parts; a hot one and a cold one, the former encompassing the IC as can be seen in Fig. 5.

The Isolation Condenser loop is instrumented with a turbine flow-meter (Fig. 4) and a differential pressure transducer on the hot side (PD-IC-2 in Fig. 5) and a series of almost 30 thermocouples in various position of the IC and of the pool as can be derived from Figs. 5 and 6.

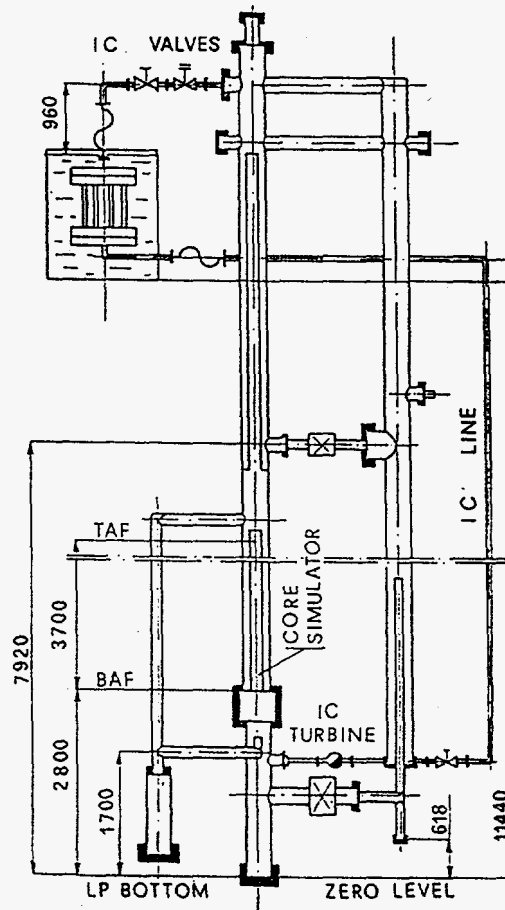


Fig. 4 - Connection between isolation condenser loop and PIPER-ONE loop

In particular, 5 thermocouples measure the primary side fluid temperature at the inlet (TF-IC-0), and outlet of the tubes bundle (TF-IC-4) and inside three different tubes (TF-IC-1 to 3); 7 thermocouples are installed on the outer surface of the tubes (TS-IC-1 to TS-IC-9, excluding the position 2 and 4); 2 thermocouples are installed on the inner surface of the tubes (TS-IC-2 and TS-IC-4); 14 thermocouples (TF-SC-1 to TF-SC-14) give a measure of the fluid temperature distribution in the pool. The distribution of thermocouple should give an idea of possible multidimensional phenomena in the pool and inside the IC. In addition, the instrumentation already available for measuring pressure, level and temperature in the different zones of PIPER-ONE apparatus is used.

Hardware restrictions preclude the possibility to have a system correctly scaled with respect to those provided for the new generation nuclear reactors, particularly the GE SBWR. This is evident from Table I, where relevant hardware data characterizing the Isolation Condenser loop installed in PIPER-ONE facility are compared with SBWR related data. In particular, Table I demonstrates that the heat transfer area of Isolation Condenser in PIPER-ONE is roughly five times larger than the ideal value. The distance between bottom of the active fuel and the Isolation Condenser and the height of the core itself are two of the most important parameters differentiating PIPER-ONE from SBWR. These essentially prevent any possibility of extrapolating PIPER-ONE experimental data to SBWR.

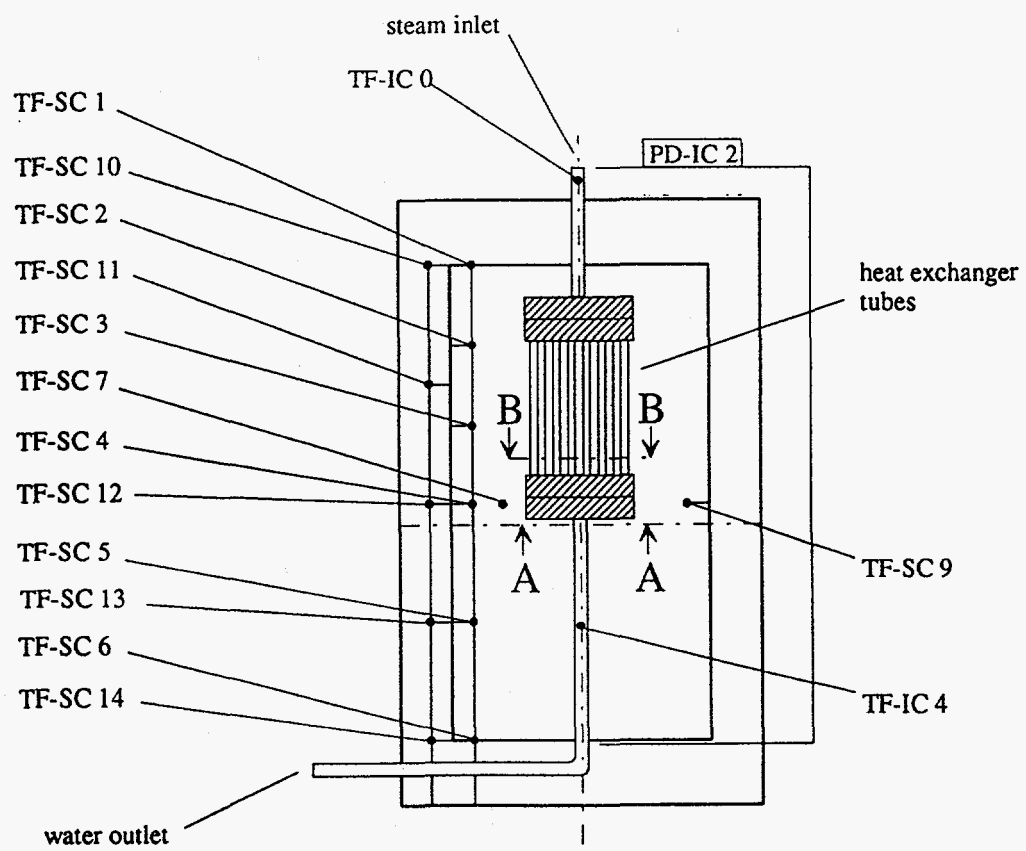
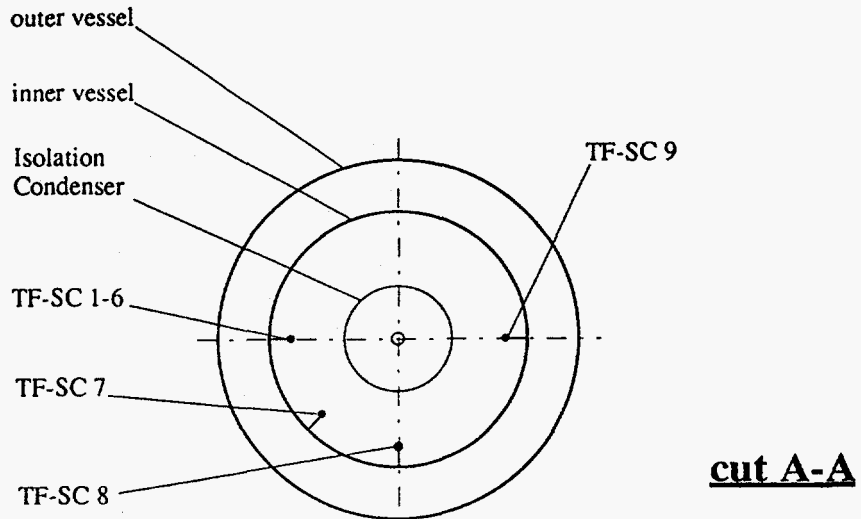
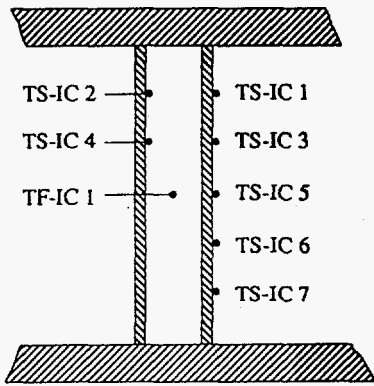
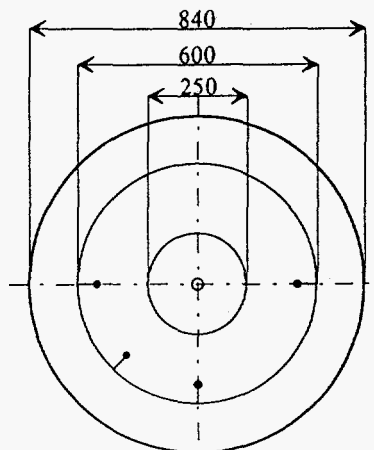
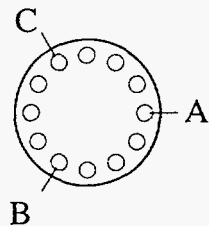


Fig. 5 - Sketch of isolation condenser pool with temperature measurement locations (part A)

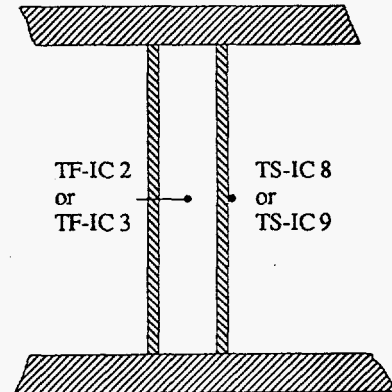
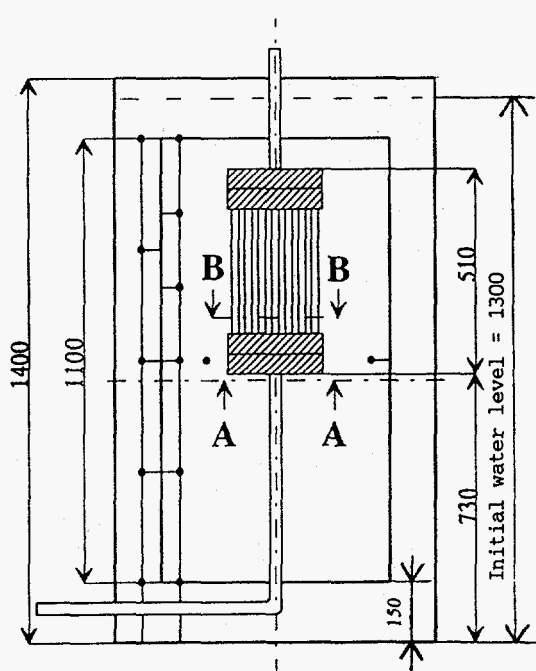
cut A-A



tube A



cut B-B



tubes B.C

Fig. 6 - Sketch of isolation condenser pool with temperature measurement locations (part B)

	QUANTITY	UNIT	PIPER-ONE	SBWR (°)	RATIO (+) PIPER-ONE/SBWR	IDEAL (+) VALUE OF THE RATIO PIPER-ONE/SBWR
1	Primary system volume	m ³	0.199	595.	1/2990	1/2990
2	Core height	m	3.710	2.743	1.35/1	1/1
3	Maximum nominal core power	MW	0.320	2000.	1/6200	1/2990
4	Value of 3% core power	MW	0.041 (-)	60.	1/1463	1/2990
5	Ratio (3% core power) /primary system volume	MW/m ³	0.206	0.1	2.06/1	1/1
6	Isolation condenser heat transfer area (++)	m ²	0.301	184	1/610	1/2990
7	Isolation condenser heat transfer area over primary system volume	m ⁻¹	1.512	0.31	4.9/1	1/1
8	Isolation condenser volume	m ³	0.0015	2.334	1/1556	1/2990
9	Isolation condenser volume over primary system volume	-	0.0075	0.0038	1.97/1	1/1
10	Isolation condenser heat transfer area over 3% core power	m ² /kW	7.341	3.066	2.39/1	1/1
11	Height of isolation condenser top related to bottom of active fuel	m	8.64	24.75	1/2.86	1/1
12	Diameter of a single tube	m	0.020	0.0508	1/2.54	1/1
13	Thickness of a single tube	m	0.0023	0.0023	1/1	1/1

(+) non-dimensional

(++) only tube bundles

(°) IC data have been taken from reference /21/

(-) related to BWR6

Tab. I - Comparison between isolation condenser related data in PIPER-ONE and in SBWR.

2.2 TEST PO-IC-2

2.2.1 Planning of the test

As already mentioned, test PO-IC-2 was the follow-up of the PIPER-ONE experiment PO-SD-8. Essentially, some discrepancies were found in the comparison measured-calculated trends in relation to variables representative of the IC behaviour; the lack of adequate local instrumentation in the IC prevented a complete characterization of the code-calculation adequacy. Furthermore, strong thermal stratification, as expected, took place in the cooling pool. The last two items led to the planning of the PO-IC-2 test as reported in ref. /8/.

Owing to the above, the instrumentation system was largely improved, now including the transducers discussed in the previous section A "shroud" was inserted into the pool to facilitate natural convection motion.

The original design of the PO-IC-2 experiment foresaw the same boundary and initial conditions as PO-SD-8 test; similar features were also foreseen for general test conduction (e.g. different core power levels, timings, etc.). Considering the presence of new devices installed in the PIPER-ONE facility (essentially active feedwater and steam line systems, ref. /18/), the initial part of the test should be addressed to characterizing PO behaviour in natural circulation. Unfortunately, the electrical power supply system suffered of heavy problems during the first attempt to carry out the experiment. Owing to this the maximum power was limited to less than 100 kW (i.e. 1/4 of the nominal value for the facility, roughly).

So, only two power steps were included in the final test design, at about 40 and 80 kW respectively, while primary circuit pressure was as specified, i.e. around 5 MPa (the same as in the experiment PO-SD-8). Relevant boundary and initial conditions are discussed in the following section.

2.2.2 Test execution

The execution of the PO-IC-2 test was essentially the same as test PO-SD-8; the "dynamic steady state", utilizing the active feedwater and steam line systems, was not performed and the usual "static steady state" was achieved.

The primary circuit was pressurized at the specified value by single phase and two-phase natural circulation with heat sources consisting of the core simulator and the structures heating system; before the test beginning, the liquid was drained to obtain the required levels in the downcomer and core regions.

The "static steady state" was achieved at zero core power and with structures electrical heating power switched on to compensate the heat losses (around 20 kW). The isolation condenser line was closed and almost full of ambient temperature liquid (60 mm above the top of IC heat exchanger).

At the beginning of the test, core heating power was switched on and almost simultaneously (see below) the IC line was open. Two core power levels, as already mentioned, were considered.

2.2.3 Test results

The initial and boundary conditions for the PIPER-ONE experiment PO- IC-2 are given in Tabs. II to IV. The two parts of the test ("low" and "medium" power, respectively) were carried out subsequently and in this way are also considered in the code calculation; so, initial conditions are only related to the "low" power phase.

32 measurement points were recorded during the test; most of these, are related to the IC loop and the remaining ones to the primary circuit. The measurement error band is that typical of all PO tests, because the established procedure of instrumentation check has been followed for carrying at the test. As an example the temperature signals have an error band (2σ) of $\pm 2K$ /19/.

PARAMETER	SIGN	UNIT	VALUE
LP pressure	PA-LP-1	MPa	5.1
LP fluid temperature	TF-LP-1	°C	262.5
Core level	LP-CC-1	m	11.9
Downcomer level	LP-LD-1	m	10.7
IC line fluid temperature	TF-IC-1	°C	17.5
IC pool fluid temperature	TF-SC-1	°C	17.5

Tab. II - PIPER-ONE test PO-IC-2: initial conditions

PARAMETER OR EVENT	TIME (s)
Test initiation	0.0
Power versus time	as in Tab. IV
IC top valve opens	4.0
IC bottom valve opens	32.0
IC top valve closes	508.0
IC top valve opens again	602.0
IC top and bottom valve close	1106.0
End of test	1184.0

Tab. III - PIPER-ONE test PO-IC-2: boundary conditions

TIME (°) (s)	POWER (kW)
0.0	0.0
5.0	41.60
438.0	41.60
440.7	0.0
586.1	0.0
588.0	70.47
590.0	73.30
1086.0	73.30
1088.0	0.0
1184.0	0.0

(°) from test start

Tab. IV - PIPER-ONE test PO-IC-2: power history

Primary circuit behaviour

Primary circuit pressure, lower plenum temperature, downcomer and core region levels are shown in Figs. 7 to 10, together with core power.

The IC was expected to remove almost 80 kW, ref. /7/; so the primary system pressure decrease until about 500 s (Fig. 7) is a foreseeable result considering that at the transient initiation (Tab. III) the IC line was opened and about 40 kW were supplied to the core simulator. In the second part of the transient, starting at about 600 s, the core power was very close to the IC removed power and primary circuit pressure was quite constant; a slight decrease of the pressure testifies that IC removed power is (slightly) larger than the power supplied to core simulator (73. kW).

The thermocouple producing the signal in Fig. 8, is installed in the zone of the lower plenum where the IC line is connected with the primary circuit: this explains the oscillations observable during the IC operation periods. In particular, oscillations amplitudes as large as 80 K have been measured as a consequence of cold liquid (coming from IC) mixing with hot liquid in the primary circuit.

Average cooling of the primary loop in the first phase of the experiment can also be deduced from observing core and downcomer regions levels in Figs. 9 and 10. In the second part of the experiment these levels remain quite constant. Unquantified dynamic effects are included in the level signal during the periods of IC operation; these are due to the natural circulation flowrate (0.5 - 0.7 kg/s) between core and downcomer.

IC system behaviour

The Isolation Condenser system behaviour has been characterized by the time trends reported in figures from 11 to 28.

The mass flowrate and the pressure drops across the IC are shown in Fig. 11. The mass flowrate signal, output of the turbine transducer, is not correct up to about 200 s. The pressure drop signal gives an idea of the filling and emptying of the IC tubes: starting from a situation with liquid level at the top of the component, a drop of the level up to about 2/3 of the tubes height can be observed in both the phases of the experiment. During the period of isolation of the line the internal side refills owing to abrupt steam condensation (this causes a shock wave that, among the other things, is the origin of problems in code calculations).

The axial tubes external surface temperatures (Fig. 12), show a large difference along the pipe high (around 50 K).

Other temperature differences can be observed in Figs. 13-17. A temperature jump of about 60 K roughly (the tubes thickness is 3 mm) is measured across the thickness in the upper part of the tubes (Fig. 13, see also Fig. 26); a larger temperature jump exists between the fluid and the external surface temperature (Fig. 14). Two-dimensional effects are indicated by Fig. 15, that shows the fluid temperature at the center of the two tubes: differences of the order of 20 K occur at the same elevation in two different tubes; moreover, the phenomenon repeats with the same characteristics in the two phases of the experiment. Radial disuniformities seem less important in the external surface (Fig. 16, see also Fig. 28); nevertheless, some additional analysis is needed to characterize the occurrence of multidimensional effects. Finally, fluid temperature variations between the inlet and the outlet of the IC can be drawn from Fig. 17; this shows that all the steam is condensed in the first half of IC, and the liquid outflowing from IC is highly subcooled (about 120 C).

Fluid temperatures inside the pool are shown in figures from 18 to 23. Essentially three aspects should be noted:

- a) strong temperature stratification exists: the fluid temperature differences between top and bottom is of the order of 70 K (Fig. 18);

- b) fluid temperatures are almost the same in the internal and the external sides of the shroud (Figs. from 20 to 23): this means that the shroud is not effective in enhancing natural circulation between the heated and the unheated part of the pool also due to the good heat conduction across the wall;
- c) maximum fluid temperature in the pool is always below the saturation temperature; i.e. no bulk boiling condition was achieved during the test.

Elaborations of the discussed signals are given in Figs. 24 to 28.

It can be noted that saturated steam (or two-phase mixture) is present at the IC inlet (Fig. 24).

The IC removed power is larger than the core supplied power in the first phase of the experiment and roughly the same in the second period; this is confirmed by the primary pressure that decreases in the first period and remains almost constant in the second one. The IC removed power is obtained from

$$\text{GIC} \bullet (\text{HGI} - \text{HFO})$$

where GIC is the IC flowrate, HGI is the steam saturation enthalpy at IC inlet (so it is assumed that only steam arrives from the primary circuit) and HFO is the liquid enthalpy at the IC outlet. Obviously the inadequacy of GIC in the first 200 s (see above) also reflects in the calculated IC power.

Temperature jumps are reported in Figs. 26 to 28.

Significant outcomes

Two main aspects can be emphasized from the analysis of the experimental data.

The former is connected with the constant value of the IC removed power, whatever is the electrical power supplied to the core simulator. This situation was already found in the previous experiment (test PO-SD-8, ref. /7/) albeit with a different primary circuit geometrical configuration and with different values (larger values) for core power. The phenomenon is a consequence of the about constant value of the IC flowrate. This occurs because the IC loop can be considered as one of the two parallel natural circulation flow paths for the two-phase mixture in the core region, the other one being the main loop with the downcomer. Actually, the overall flowrate across the core is the sum of flowrates crossing downcomer and IC. The driving heads are the pressure differentials between downcomer and core regions and between IC and core regions, respectively. Owing to geometry, the pressure drops across IC are higher than across the downcomer (ideally, with the same flowrate). As a consequence of this, increases of core power reflect as increases of mass flow across the downcomer.

The same conclusion can be reached considering that the pressure drop between the points connecting the IC to the primary loop are held nearly constant by the gravity head constituted by the liquid level in the downcomer that, at its time does not substantially change in the two periods of the experiment. As a final note, the overall gravity head in the IC line cannot change too much owing to the elevation of the IC component itself (the only zone where fluid density variations may occur assuming in any case complete condensation) that is less than 1/10 of the total axial length. Second order contributions to differences between the high and the low power periods as far as the overall IC removed power is concerned, come from:

- the progressive heating of the pool that in the high power period, may be compensated by the increase in the heat transfer coefficient on the outer part of the IC tubes;
- pressure variations in the primary circuit.

The latter aspect concerns the local behaviour of the heat transfer coefficient in the IC region. First of all it should be noted that the liquid level in the IC is almost the same during the two periods of the experiment (Fig. 11). Secondly, as already mentioned, temperature increases in the pool (of almost 70 K in the upper part, Fig. 18) have no or limited consequence upon the external surface tubes temperature (Fig. 12). Also the temperature jump between primary fluid and tubes external surface, remains almost constant as it results from Fig. 14. As a conclusion, notwithstanding variations of fluid conditions in the pool, the heat transfer phenomenon remains almost unchanged, when core power is varied.

An experimental verification of the link between IC and DC flowrates has been achieved recently, during the execution of another tests PO-IC-3, similar to PO-IC-2 but at low pressure (~ 0.5 MPa).

In the test PO-IC-3, after a period of quasi-steady conditions, a valve was open simulating a small break in lower DC. This lead to the stop in natural circulation between core and DC, due to the DC level lowering.

In this time period the IC flowrate increased.

It should be noted that both the above conclusions have been confirmed by code calculation results (see below) and seem directly applicable to nuclear power plant conditions: infact the described phenomena are not affected by the scale distortions of the PIPER-ONE apparatus.

Experimental errors

An extensive analysis for determining errors characterizing the experimental data was carried out in the occasion of the use of PIPER-ONE for the OECD/CSNI ISP 21, refs. /25/ to /27/. Details about methods for deriving measurement errors, can be found in ref. /28/.

The error concerned (i.e., error bands corresponding to two standard deviations) for the most relevant quantities, are as follows, ref. /28/:

- absolute pressure: ± 0.05 MPa;
- fluid temperature in primary loop: ± 2 K;
- core level: ± 0.1 m;
- downcomer level: ± 0.1 m;
- fluid temperature in the tank: ± 0.5 K;
- IC flowrate: ± 0.01 kg/s;
- core power: ± 1 KW (valid for the present test only);
- timing error (mainly for valves opening/closure): ± 2 s.

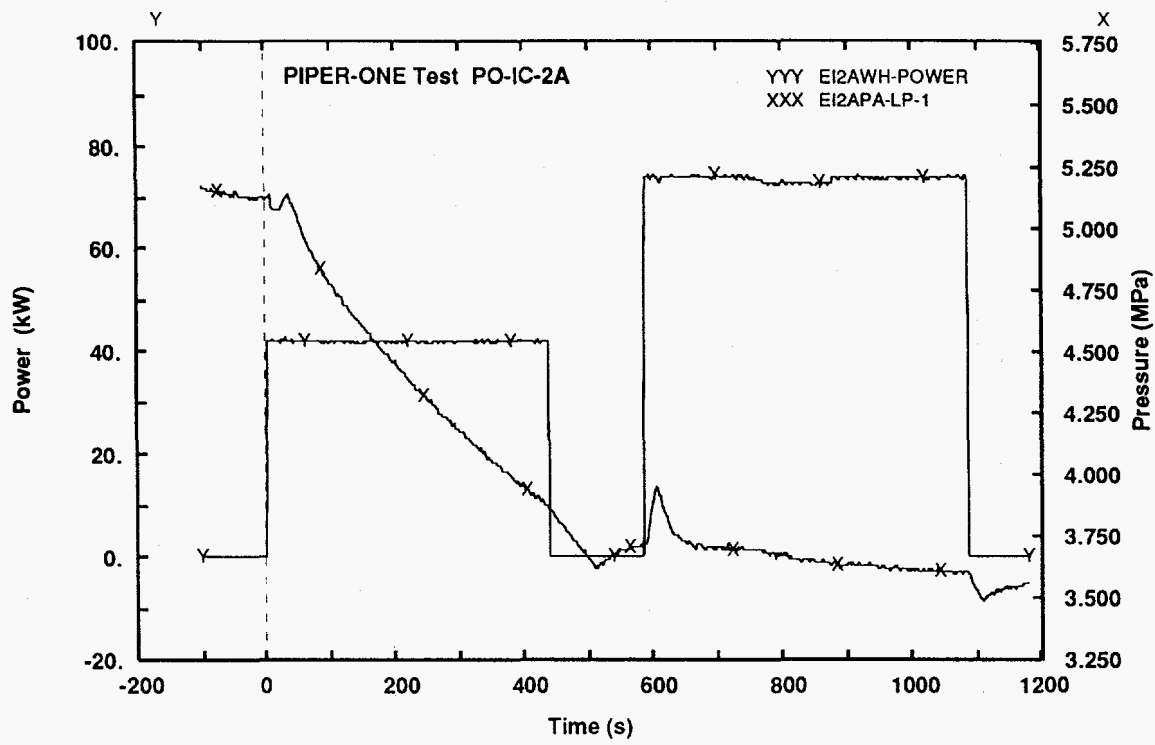


Fig. 7 - Core power and lower plenum pressure

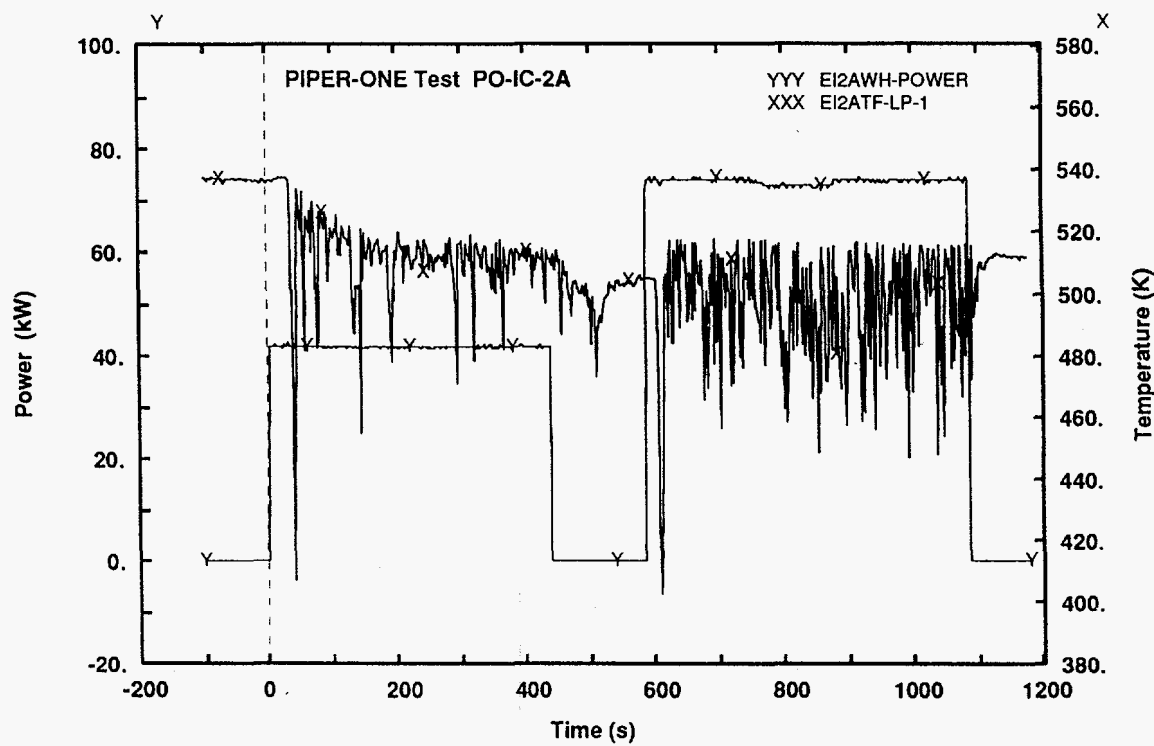


Fig. 8 - Core power and fluid temperature in lower plenum

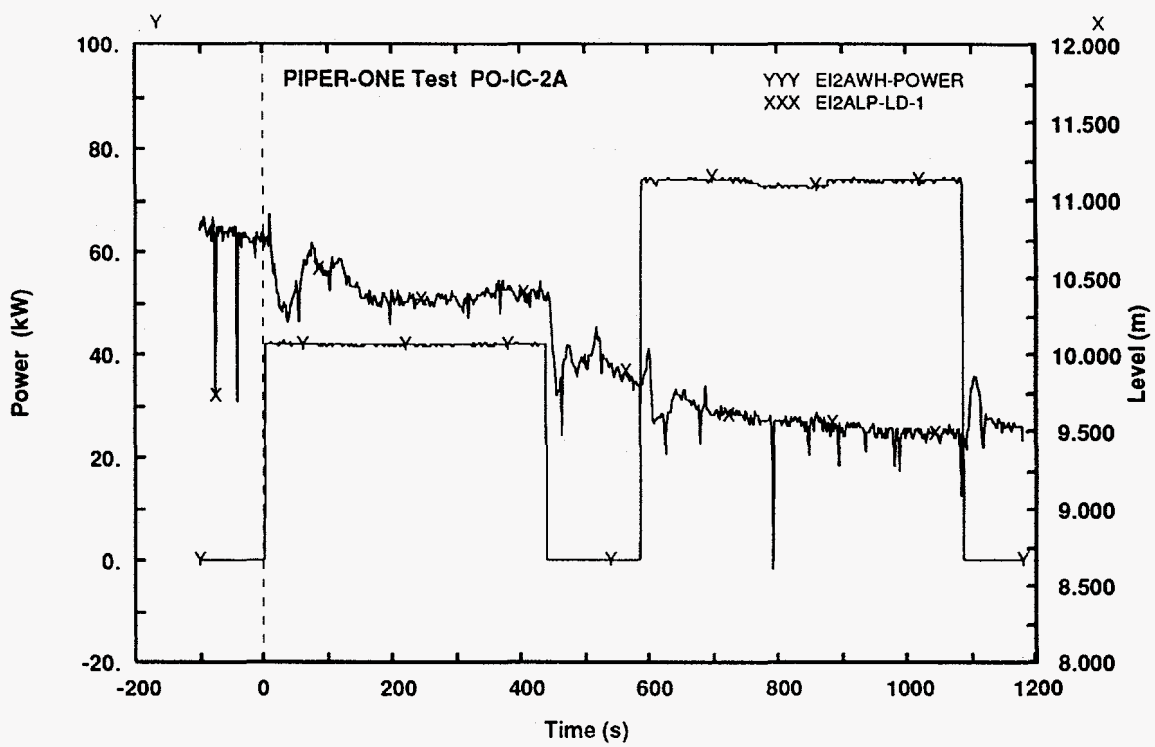


Fig. 9 - Core power and downcomer level

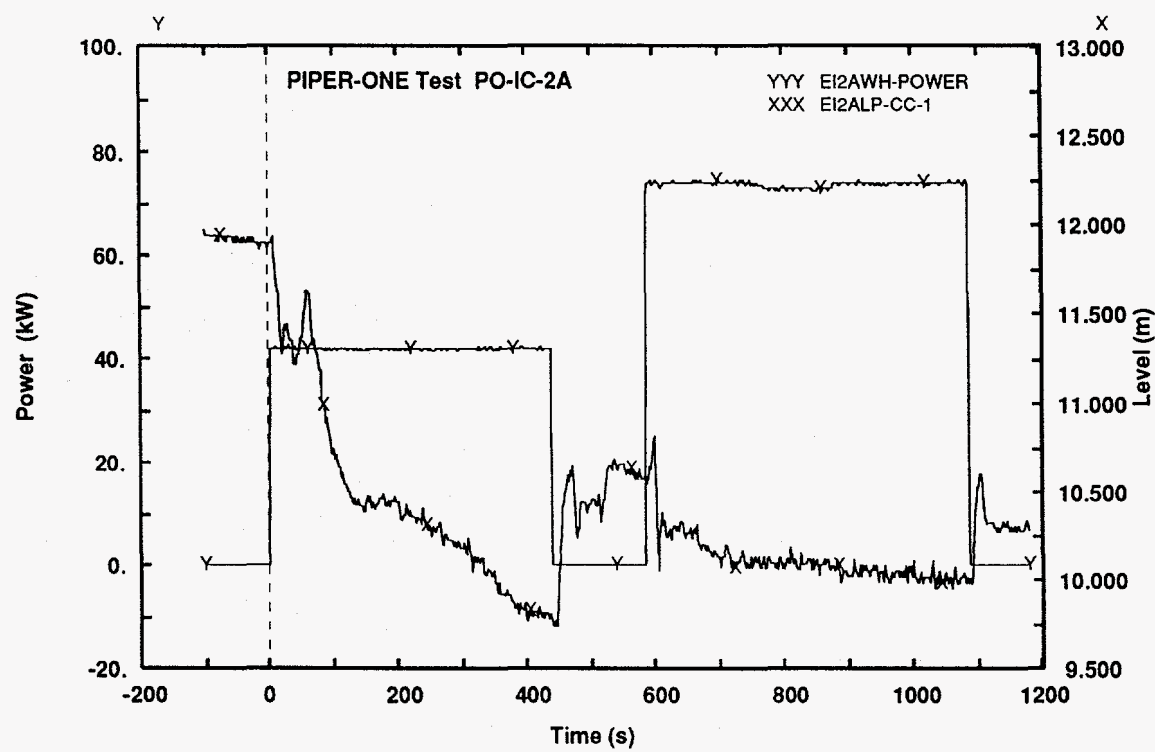


Fig. 10 - Core power and core level

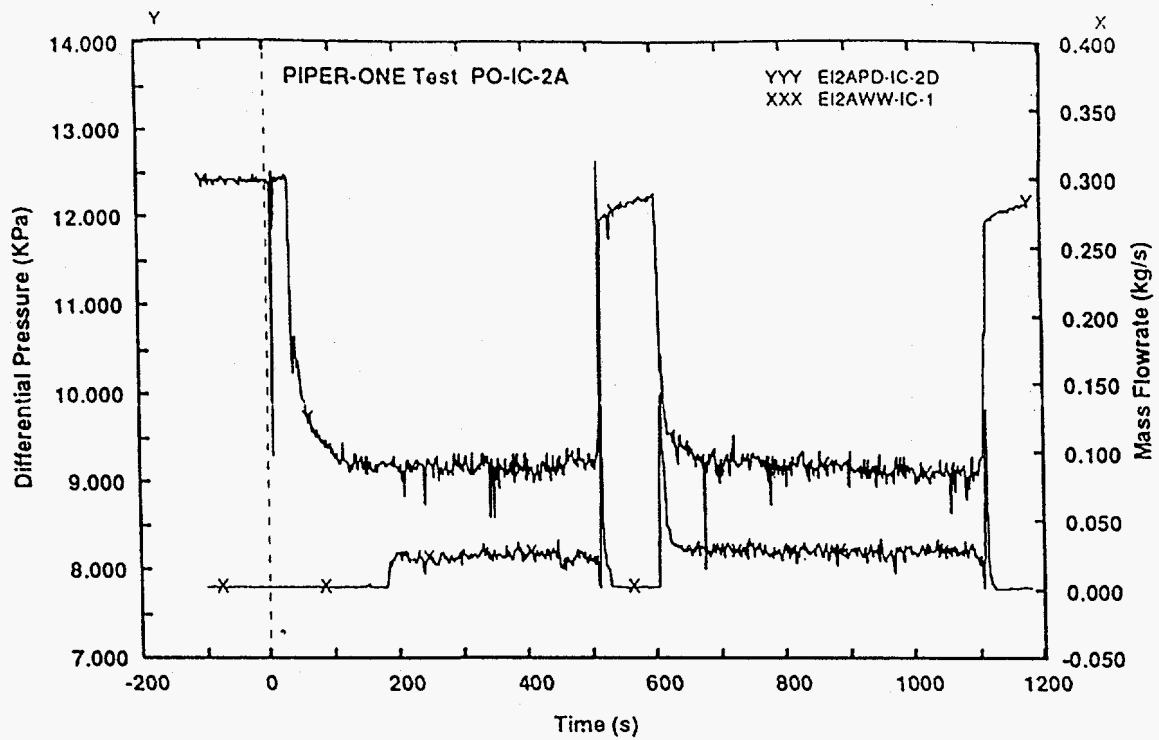


Fig. 11 - Pressure drop and flowrate across IC

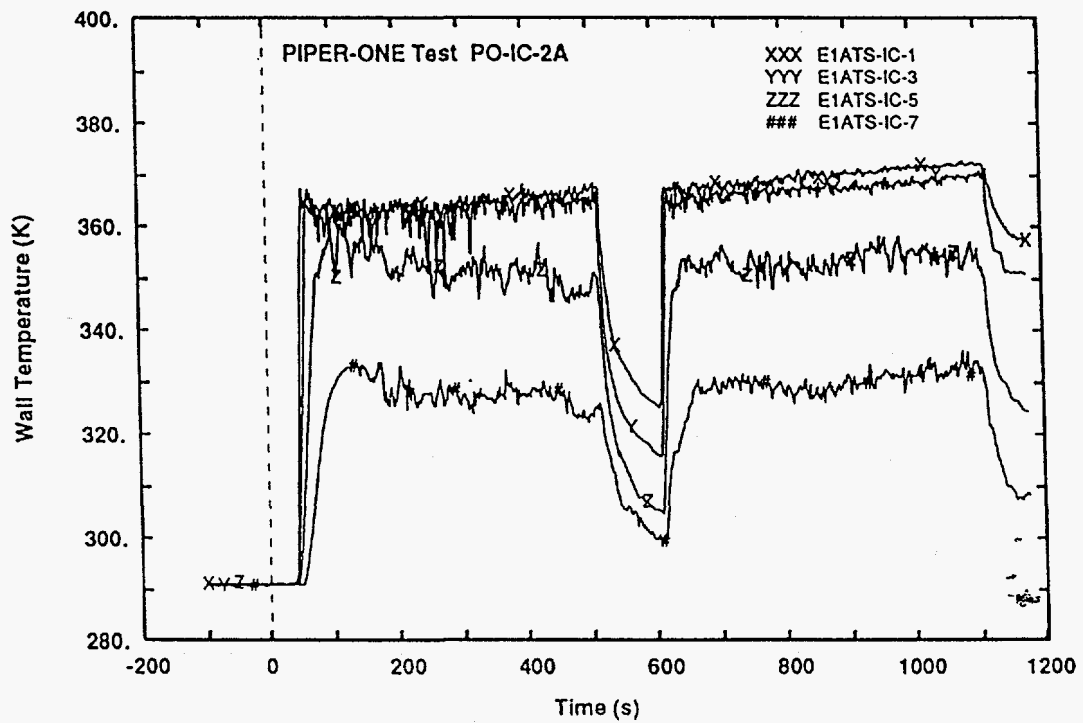


Fig. 12 - Tube "A" axial temperature distribution (external TC)

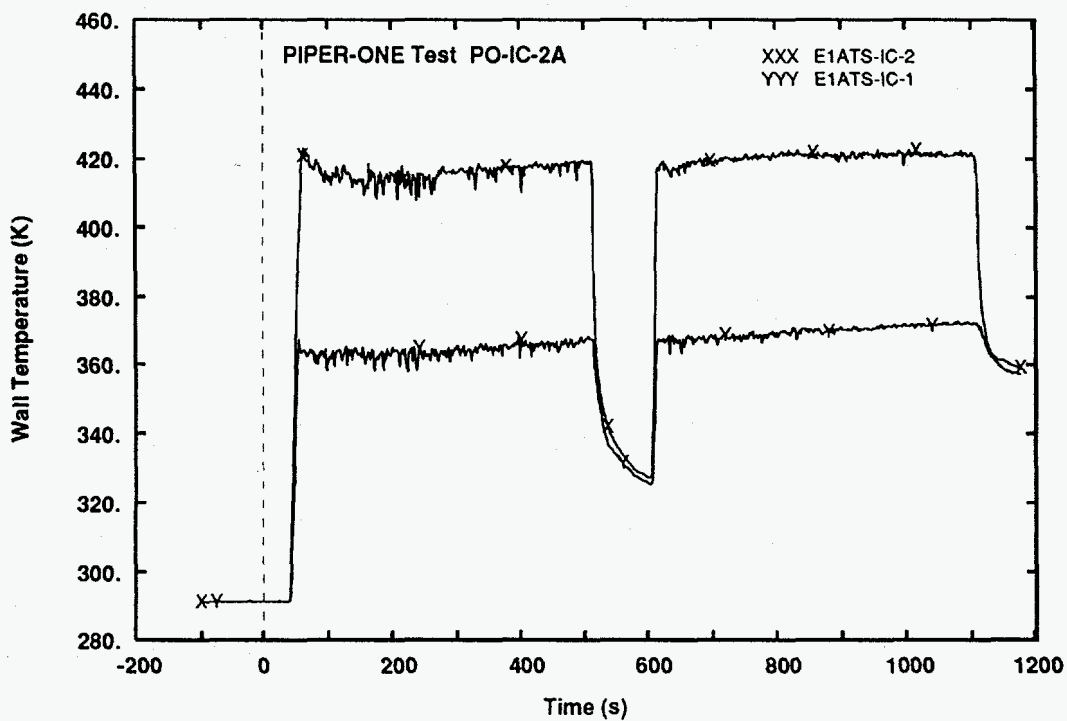


Fig. 13 - Tube "A" internal and external TC (upper elevation)

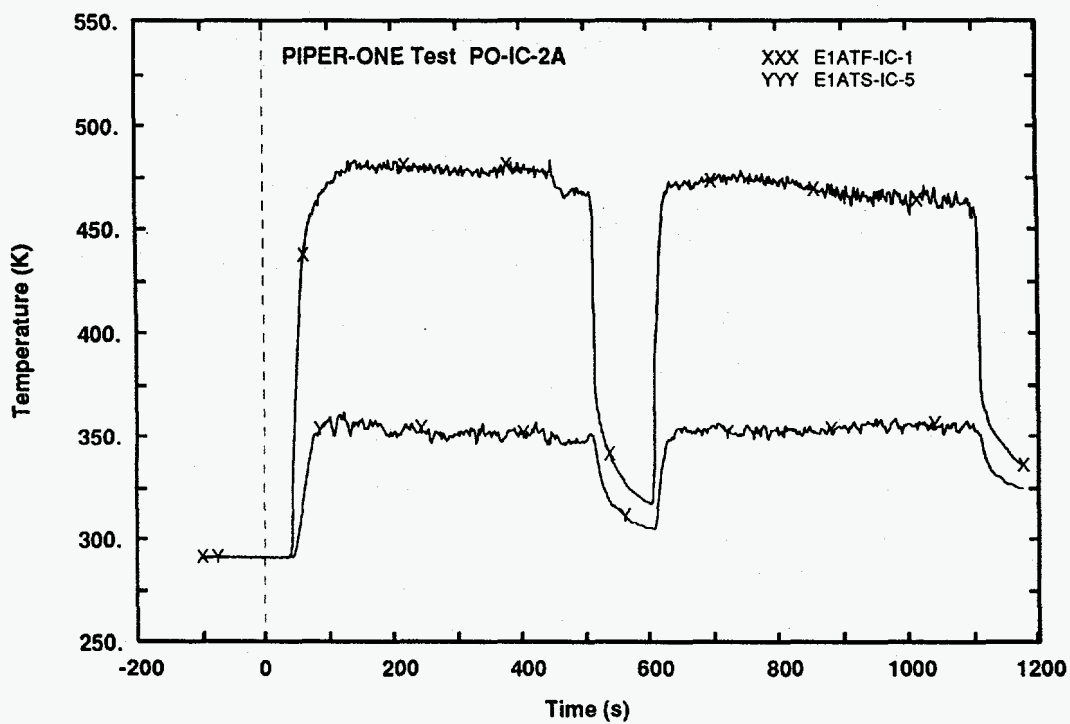


Fig. 14 - Tube "A" fluid temperature and external TC (middle elevation)

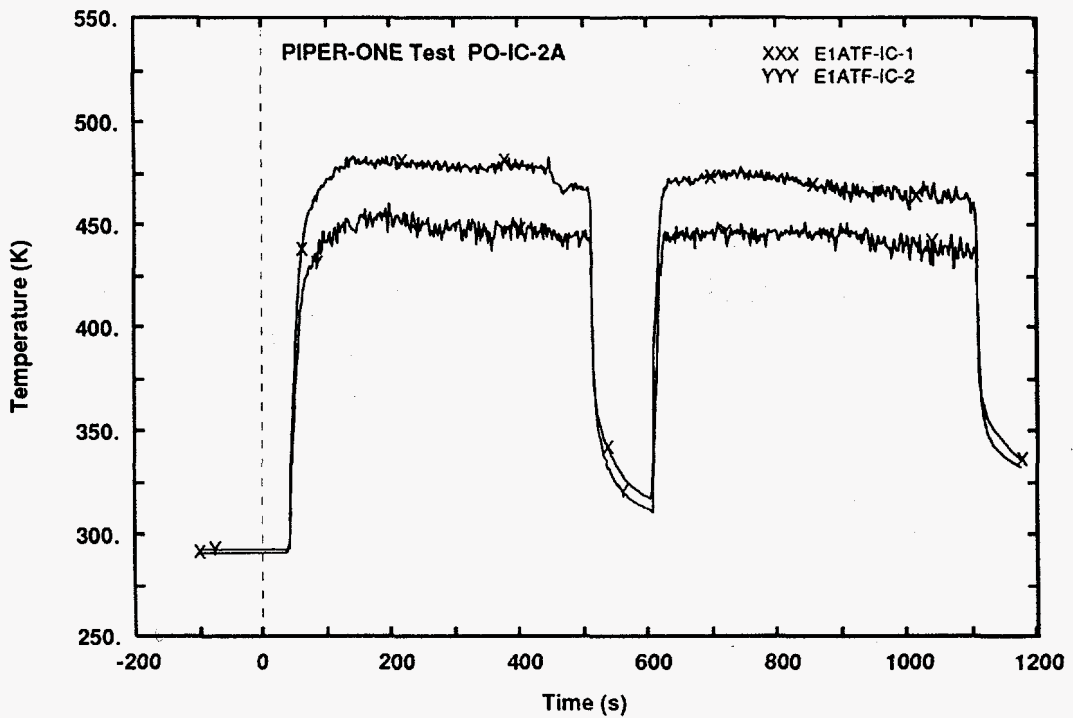


Fig. 15 - Tubes "A" and "B" fluid temperature (middle elevation)

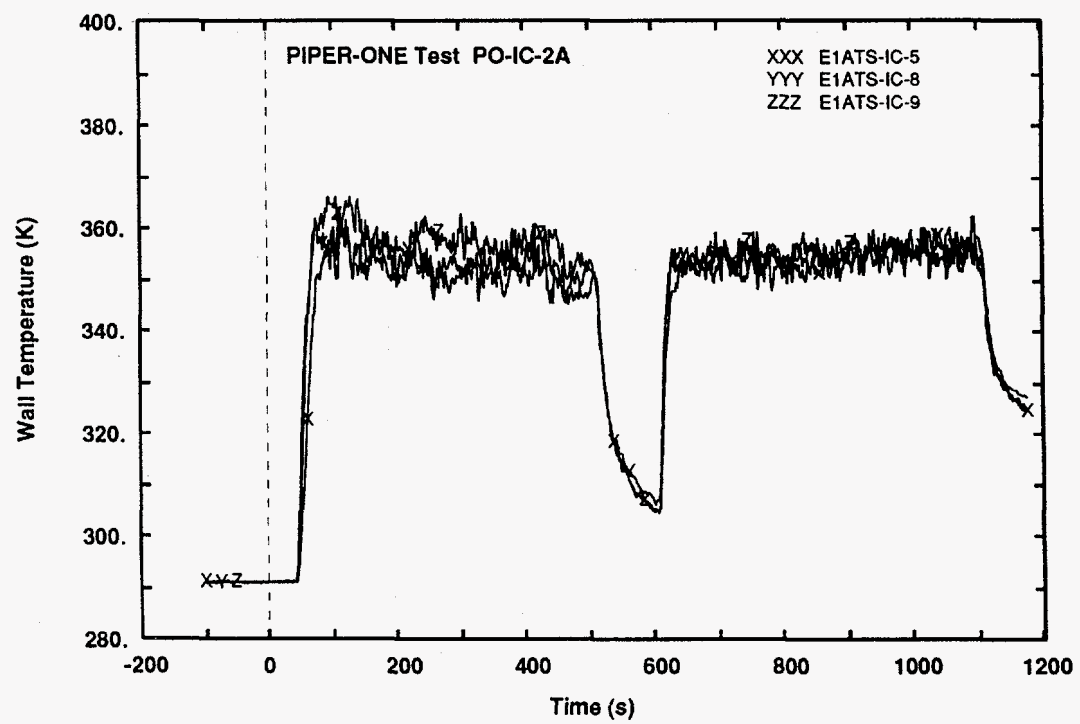


Fig. 16 - Tubes "A" "B" and "C" external TC (middle elevation)

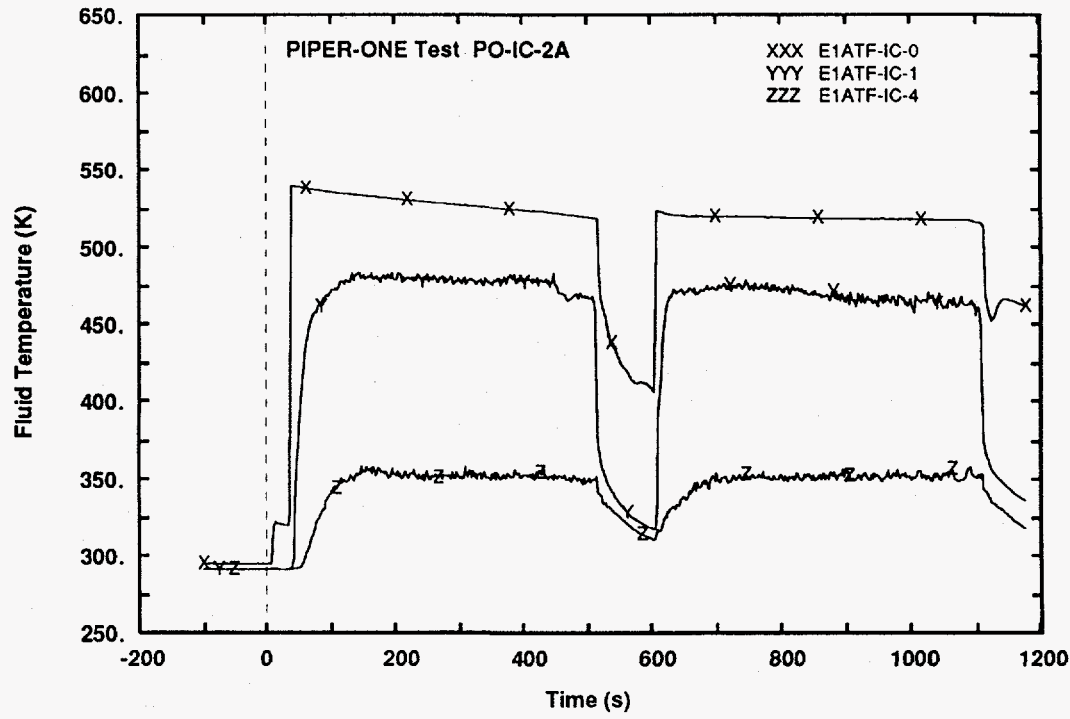


Fig. 17 - IC fluid temperatures (inlet, center and outlet)

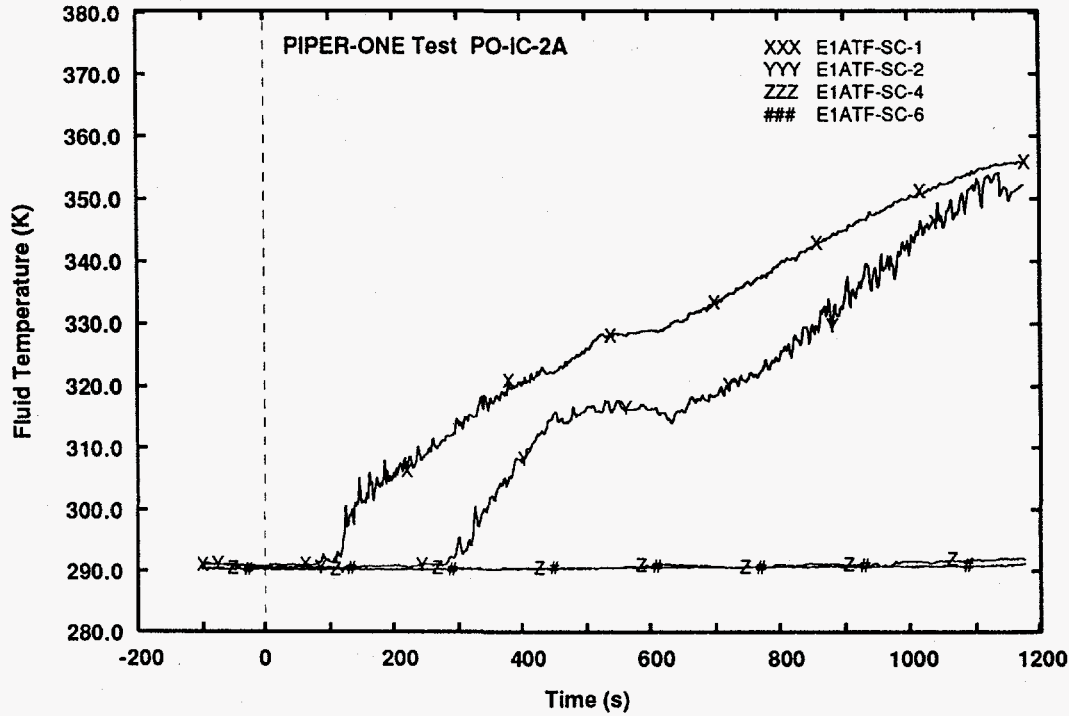


Fig. 18 -Pool internal axial fluid temperatures

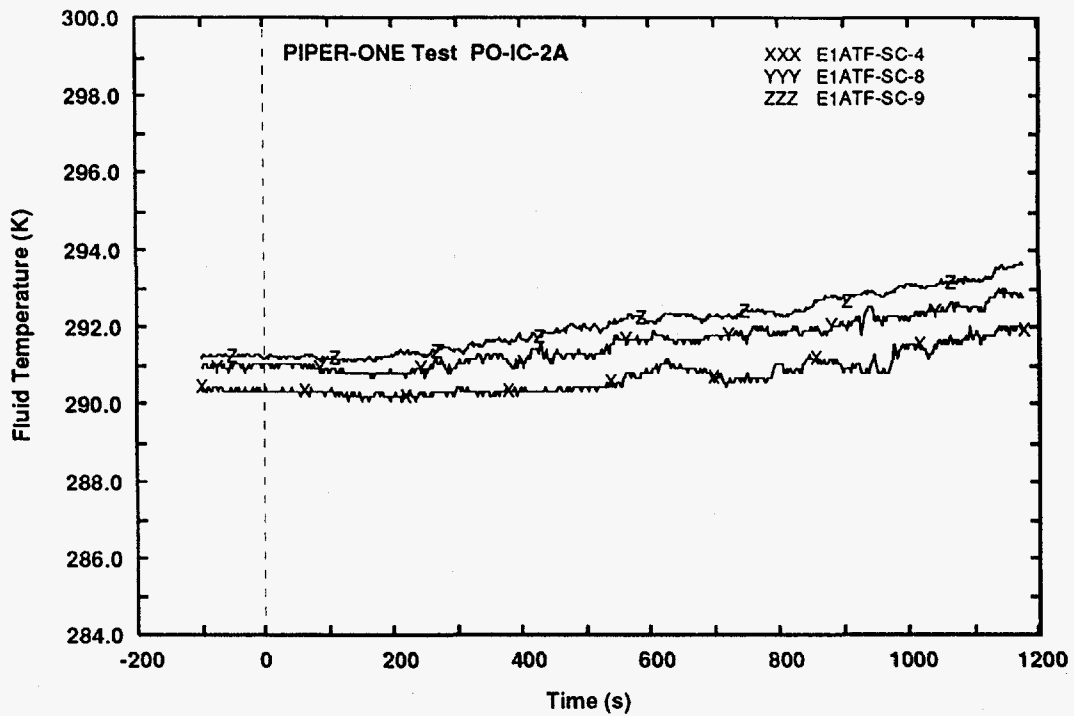


Fig. 19 - Pool internal temperatures in different azimuthal positions

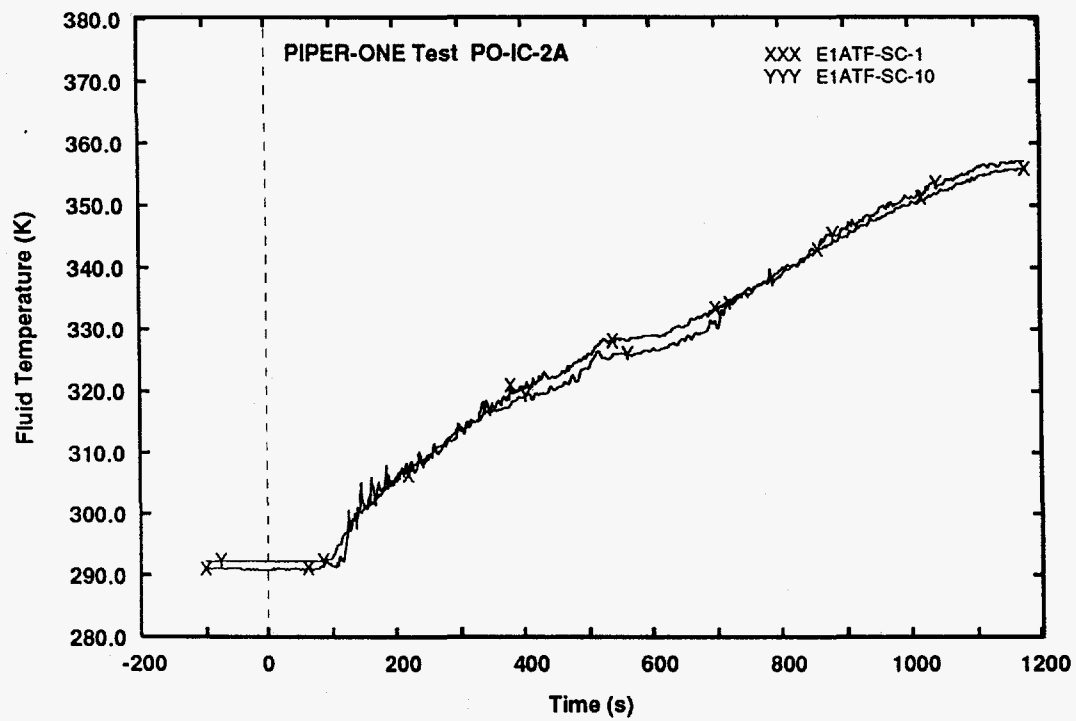


Fig. 20 - Pool temperatures, internal and external to shroud (upper elevation)

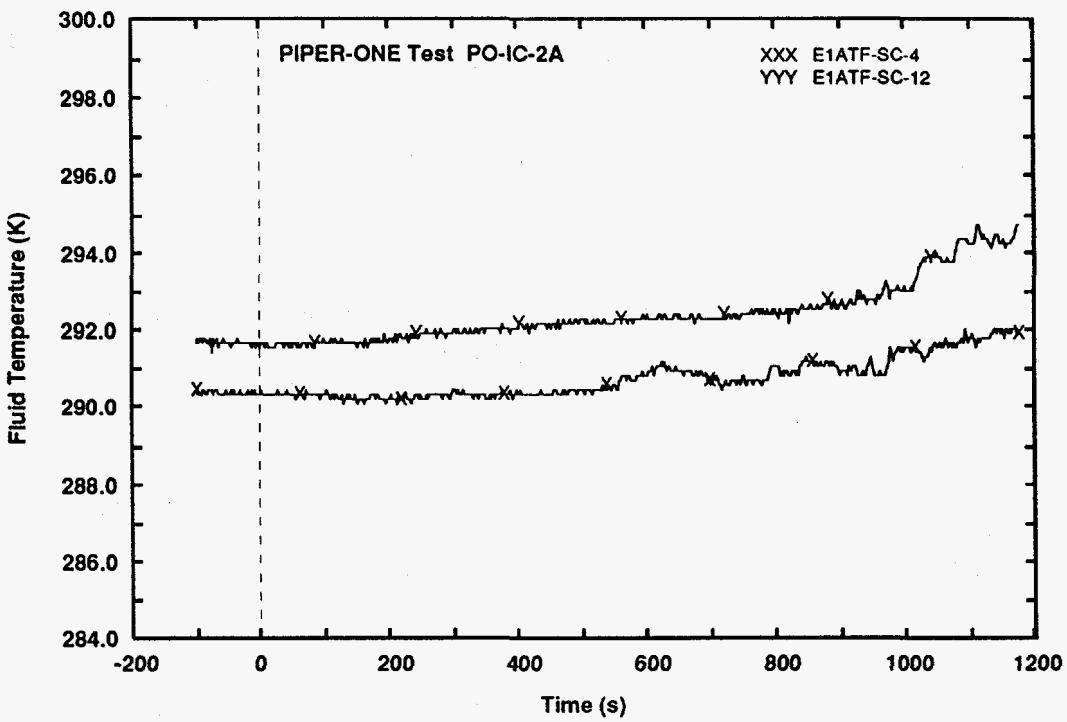


Fig. 21 - Pool temperatures, internal and external to shroud (middle elevation)

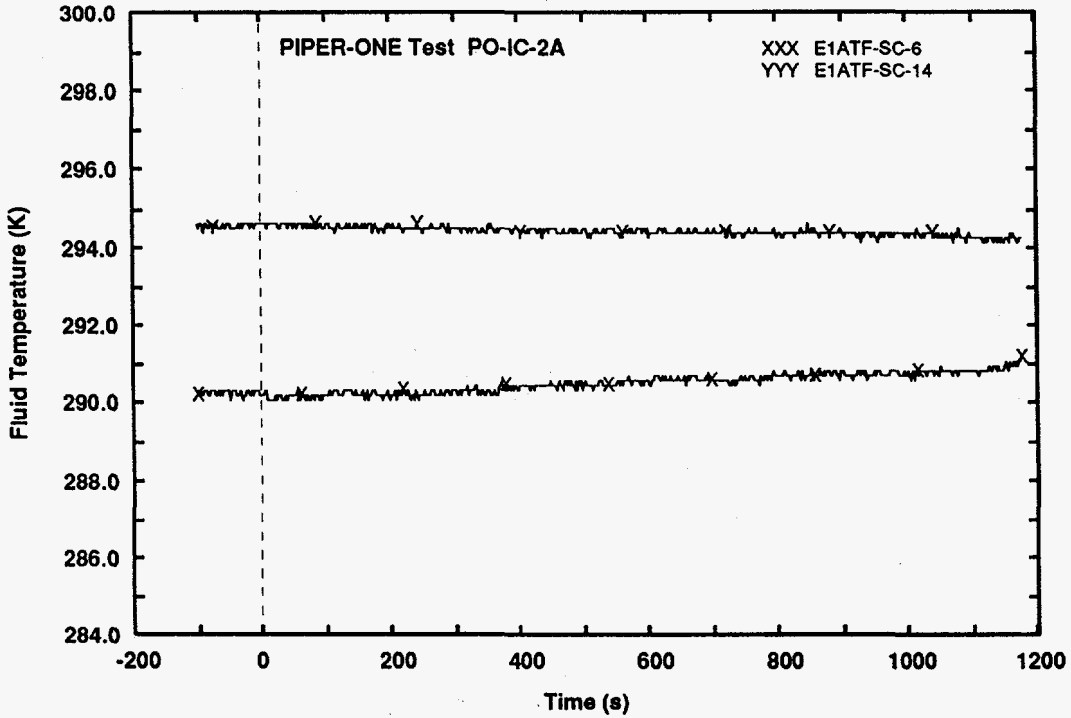


Fig. 22 - Pool temperatures, internal and external to shroud (lower elevation)

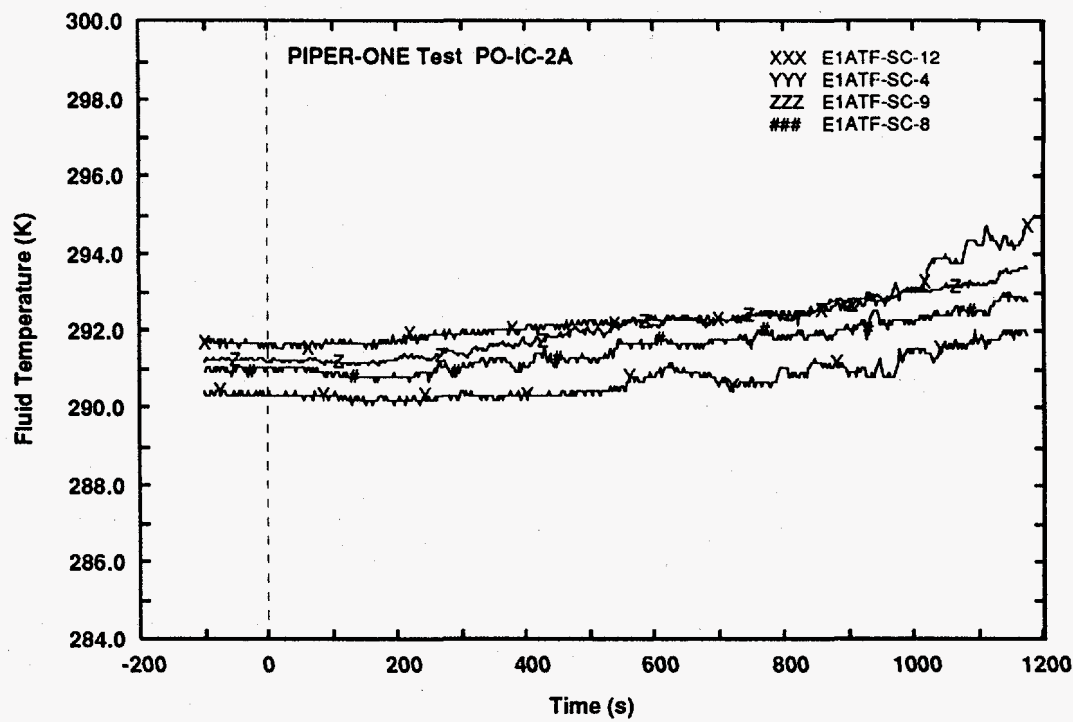


Fig. 23 - Pool temperatures (differential positions)

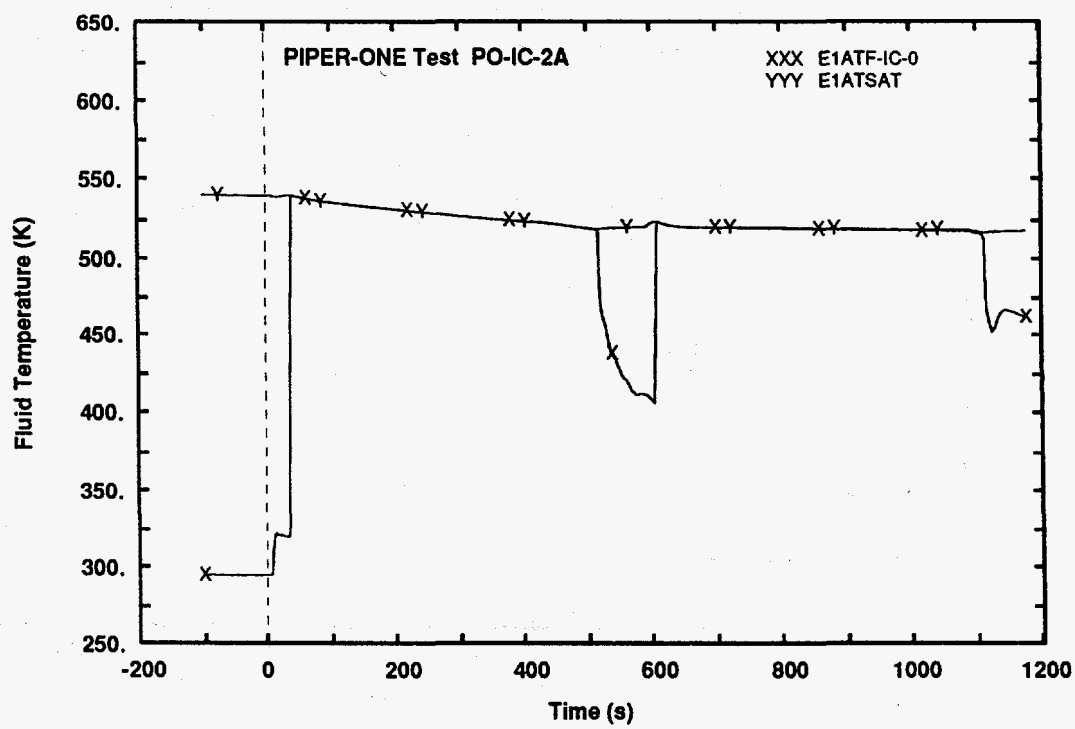


Fig. 24 - Temperature at IC inlet comparison with saturation temperature

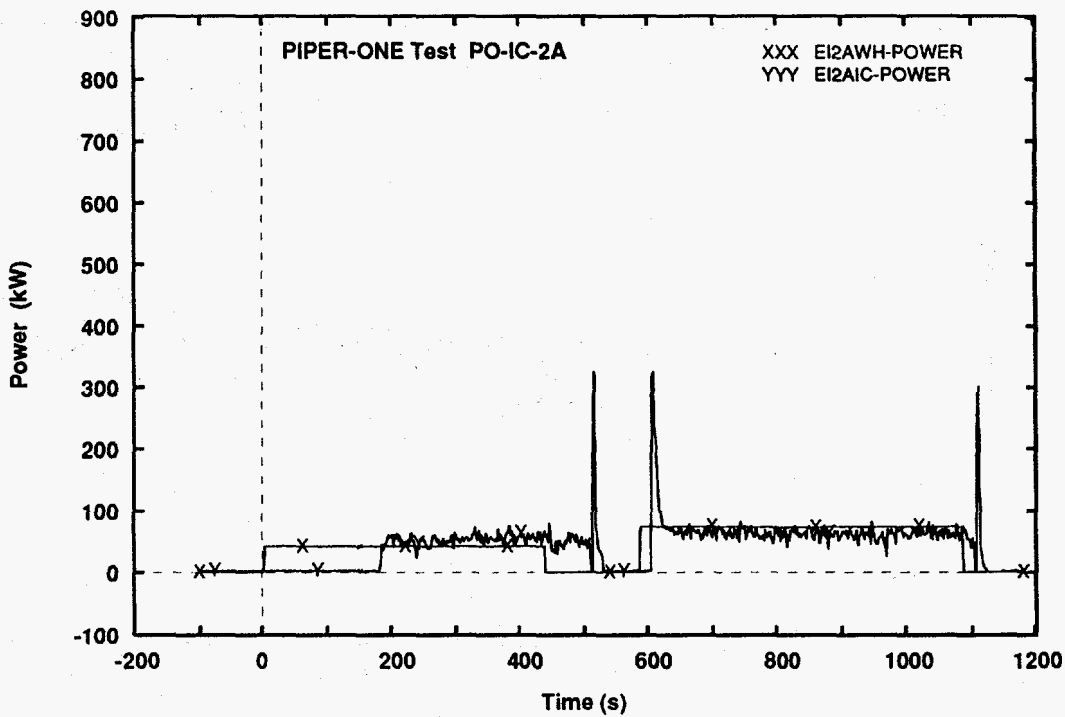


Fig. 25 - Rod power and thermal power across IC

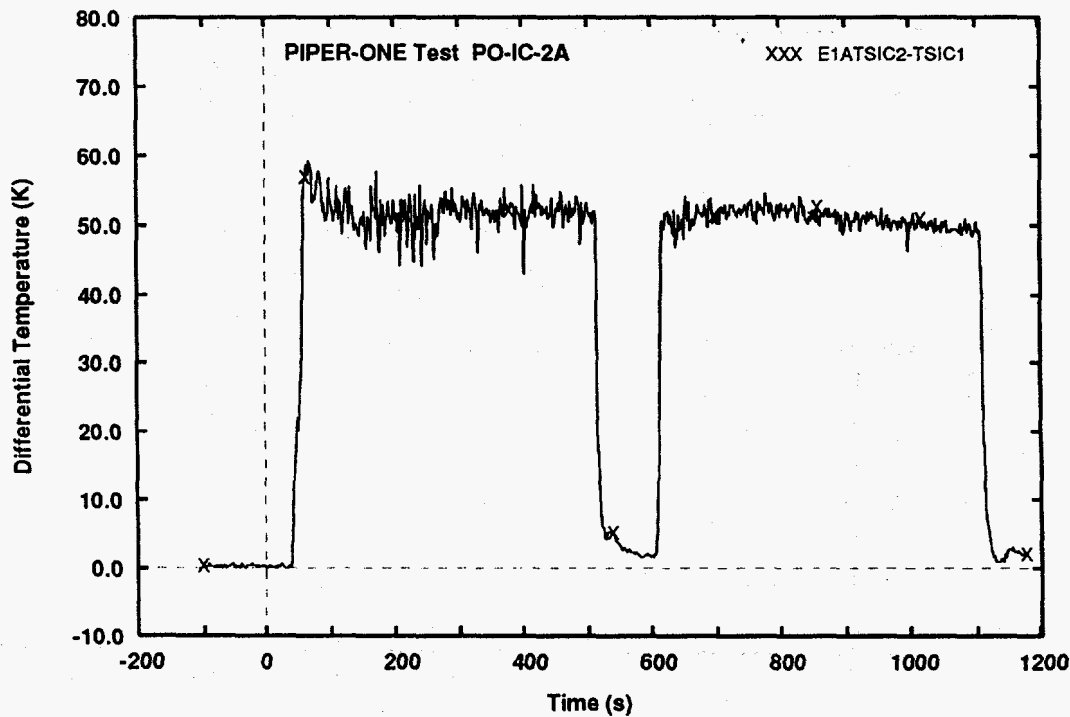


Fig. 26 - Temperature jump across the wall

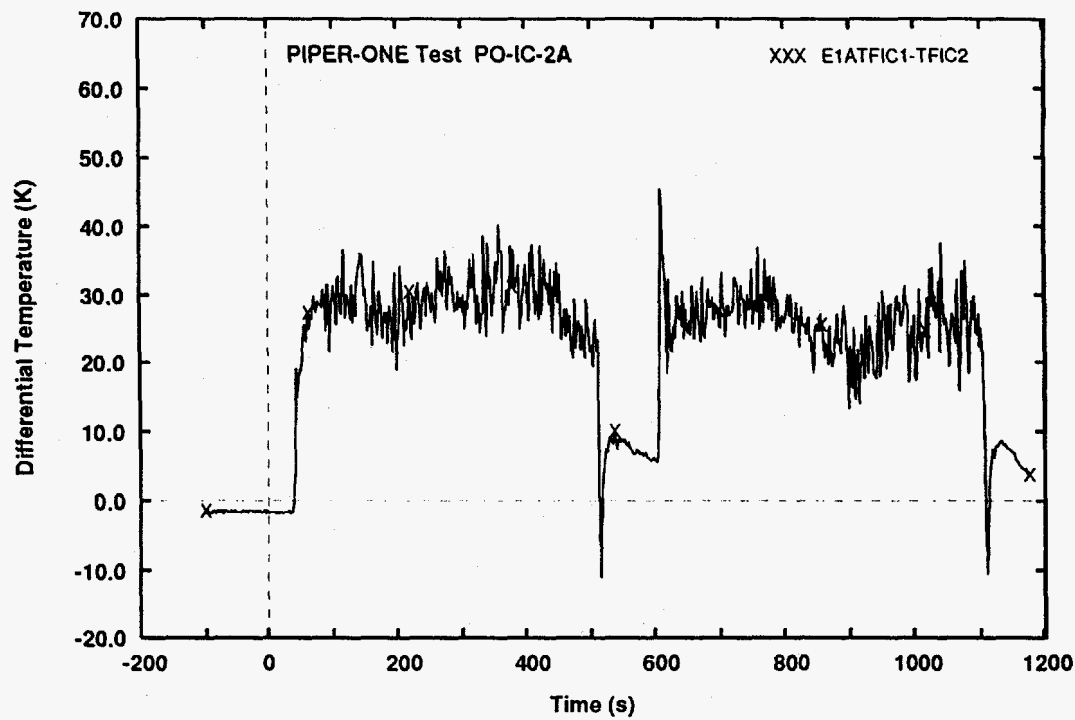


Fig. 27 - Fluid temperature disuniformity across tubes

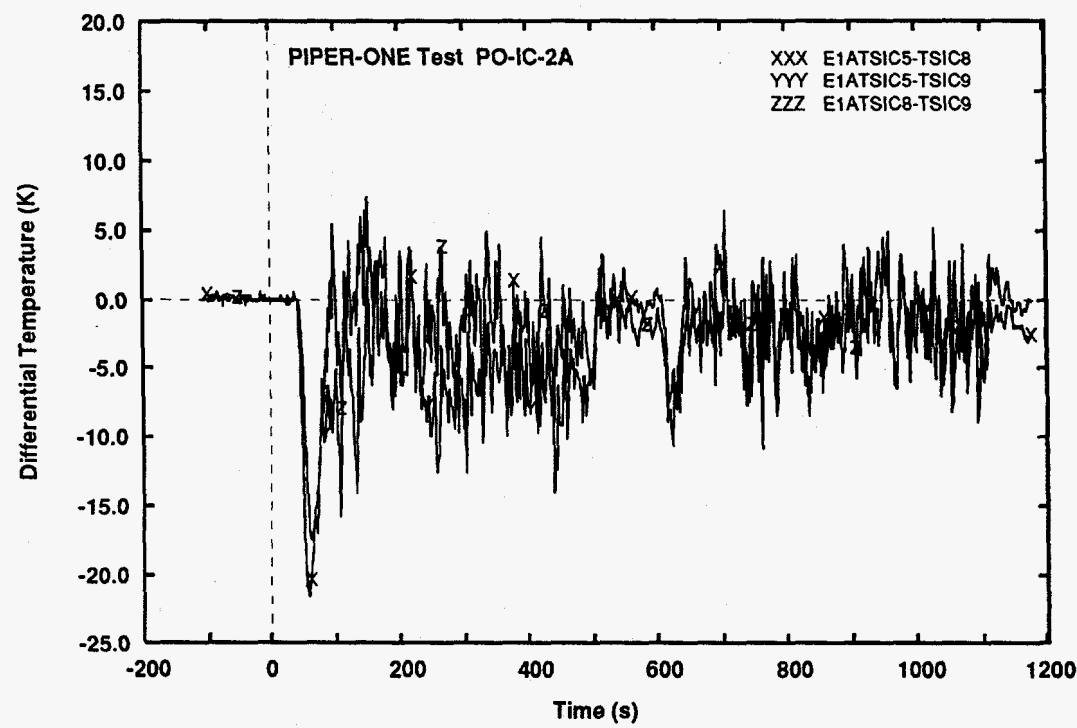


Fig. 28 - Surface temperature disuniformities

3. ADOPTED CODES AND NODALIZATION

3.1 The used codes

The standard version of the Relap5/mod3.1 has been adopted as reference code in the present study; none of the possible user selectable options has been activated when performing the reference calculation; necessary adjustments of initial and boundary conditions (see below), within the experimental uncertainty bands, have been done with this code version ("reference" code version) aiming at getting the "base calculation". The adopted standard version of Relap5/mod3.1 runs on an IBM RISC 6000.

Once the "base calculation" results have been obtained, previous code versions Relap5/mod2.5, Relap5/mod3 7J and Relap5/mod3 v80, running on Cray mainframe, IBM PC 486 and IBM RISC 6000 respectively, have been utilized, too.

3.2 Strategy of calculations and specific objectives

The overall strategy of the performed analysis aimed at assessing the capabilities of the reference code version and at identifying possible improvements with respect to previous code versions; sensitivity calculations considering variations in the nodalization have been performed in this framework.

An additional objective of the analysis was to confirm the explanation given for the reasons of constant IC flow when core power is varied.

3.3 Adopted nodalization

Considering the above objectives, the acquired experience in the use of the latest Relap5 code versions, the code user guidelines, ref. /19/, and the criteria proposed in ref. /20/ for nodalization development and qualification, a new PIPER-ONE input deck has been developed.

The sketch of the new nodalization is shown in Fig. 29. Actually this has been developed in the frame of the BIP (Boiling Instability Program) proposal, e.g. ref. /18/, and already used in that frame for the planning of experiments.

The main difference with respect to the original nodalization (e.g. ref. /16/) lies in the number of nodes that in this case is roughly three times larger. Moreover, the hardware modifications in the primary circuit of the facility have also been considered. In particular, the feedwater line has been added and the connection zone between downcomer and lower plenum and the region around the top of the separator have been slightly modified to better reproduce natural circulation in the reference reactor.

The IC system nodalization is essentially the same as adopted for the post-test analysis of the PO-SD-8 experiment (refs. /5/ and /6/); only the pool nodalization has been changed to account for the presence of a shroud enveloping the IC component.

Relevant input values related to the hydraulic volumes and to the connecting junctions of the nodalization, are summarized in Tabs. V and VI. The following items can be added to clarify Fig. 29 and the last tables:

- the nodes 100 to 140 (in total 14 nodes) represent the lower plenum which is connected with the jet-pump/downcomer region through the junction 325-03, with the core bypass through the junction 130-02 and with the IC system through the junction valve 550; -the hydraulic volumes 325, 330, 335 and 345 (11 nodes) are also part of the lower plenum and constitute the connection region downcomer - lower plenum;
- the nodes 200, from 1 to 16 represent the core: among these, the nodes 200-01 to 200-14

constitute the active region;

- the nodes 145 to 180 (in total 40 nodes) represent the core bypass that is connected to lower plenum and to the core exit region (through the junction 205-02);
- the upper plenum region is simulated by nodes from 205-01, to 220-02 (4 nodes) and include connections to core, core bypass and to the volume surrounding the fuel box simulator (see below);
- the volume surrounding the fuel box simulator has been included to preserve the square cross section for the fuel box, at the same time avoiding unrealistic thickness to maintain the pressure; it is connected with the main loop through the junction 360-01;
- the separator region consists of nodes from 220-03 to 220-20 (18 nodes) and is constituted by a "PIPE" component;
- the steam dome is constituted by vertical and horizontal parts, i.e. nodes from 235 to 265 (21 nodes) and includes connections with the separator through the junction 235-01, with the 'separator annulus' (see below) through the junction 235-02, with the downcomer through the junction 270-01, with the IC system through the junction 245-03 and with "external systems" like the steam line, the pressure control, the SRV and the ADS through the TMDPJUN 433 and valves from 443 to 473;
- the 'separator annulus' is a region outside the separator region and has been introduced to avoid the return of possible wall condensed liquid directly to the core region, volumes 225 and 230 (9 nodes); it is connected with the downcomer through an horizontal line including nodes 290 and 295;
- the downcomer is constituted by a cylindrical part consisting of hydraulic volumes from 270 to 310 (22 nodes) and by an annular part, hydraulic volume 320 (15 nodes) surrounding the jet pump simulator; the downcomer is connected with the steam dome/separator region through the junction 270-01, with the feedwater system through the TMDPJUN 453, with the separator annulus through the junction 300-03 and with the jet-pump through the junction 310-03;
- the jet-pump simulator is constituted by the cylindrical hydraulic component 315 (15 nodes) directly connected with the downcomer and the lower plenum region;
- structures heating systems and cooling systems are part of the nodalization and reflect the characteristics of the components in the facility (ref. /13/);
- emergency systems have also been included according to the design of PIPER-ONE, e.g. nodes 410, 420, etc.;
- the IC system consists of:
 - a) connecting pipes, i.e. hydraulic volumes 500 and 540 (37 nodes) connecting the IC to the primary circuit;
 - b) the heat exchange zone constituted by parallel tubes (i.e. hydraulic volume 515), inlet and outlet plena, (i.e. hydraulic volumes 510 and 520) and single outlet tube i.e. hydraulic volumes 525 (21 nodes);
 - c) the pool where the following zones can be recognized:
 - c1) the heat transfer region internal to the shroud i.e. hydraulic volumes 552, 560 and 561 (14 nodes);
 - c2) the outer annulus, i.e. hydraulic volumes 652, 660 and 661 (14 nodes);
 - c3) plenum regions, i.e. hydraulic volumes 551 and 562 (2 nodes);
 - c4) external pipes, i.e. hydraulic volumes 563 and 564 (44 nodes);
- structures are connected with each hydraulic volume: pipe walls have been separated from flanges;
- the active structures of the rod simulators have been subdivided into 10 radial meshes.

NODE	VOLUME (m ³ x 10 ³)	HEIGHT/LENGTH (m)	ZONE
100-01	3.212	0.3	Lower plenum
110-01	2.677	0.25	
110-02	2.677	0.25	
110-03	1.545	0.1443	
110-04	1.545	0.1443	
110-05	1.193	0.1114	
111-01	1.730	0.1615	
112-01	1.713	0.16	
115-01	1.869	0.1745	
120-01	1.944	0.2	
120-02	1.944	0.2	
130-01	1.488	0.176	
135-01	1.692	0.2	
140-01	1.692	0.2	
325-01	1.393	0.327	
330-01	0.85	0.185	
335-01	1.079	0.257	
335-02	1.079	0.257	
335-03	1.943	0.257	
335-04	1.943	0.257	
345-01	1.21	0.16	
345-02	0.247	0.18	
345-03	0.247	0.18	
345-04	0.343	0.25	
345-05	0.343	0.25	
TOTAL	34.961		
200-01	0.78	0.265	Core
200-02	0.78	0.265	
200-03	0.78	0.265	
200-04	0.78	0.265	
200-05	0.78	0.265	
200-06	0.78	0.265	
200-07	0.78	0.265	
200-08	0.78	0.265	
200-09	0.78	0.265	
200-10	0.78	0.265	

Tab. V - Details of nodes geometry in the RELAP5 nodalization

NODE	VOLUME (m ³ x 10 ³)	HEIGHT/LENGTH (m)	ZONE
200-11	0.78	0.265	
200-12	0.78	0.265	
200-13	0.78	0.265	
200-14	0.78	0.265	
200-15	0.814	0.229	
200-16	0.711	0.2	
TOTAL	12.445		
145-01	0.057	0.2	Bypass
145-02	0.057	0.2	
145-03	0.054	0.1892	
145-04	0.054	0.1892	
145-05	0.054	0.1892	
145-06	0.054	0.1892	
145-07	0.054	0.1892	
150-01	0.976	0.2468	
150-02	0.976	0.2468	
150-03	0.976	0.2468	
150-04	0.976	0.2468	
150-05	0.976	0.2468	
155-01	0.186	0.223	
160-01	0.178	0.2133	
160-02	0.178	0.2133	
160-03	0.178	0.2133	
160-04	0.178	0.2133	
160-05	0.178	0.2133	
160-06	0.178	0.2133	
160-07	0.178	0.2133	
160-08	0.178	0.2133	
160-09	0.178	0.2133	
160-10	0.178	0.2133	
165-01	0.168	0.2015	
170-01	0.196	0.235	
170-02	0.196	0.235	
170-03	0.196	0.235	
170-04	0.196	0.235	
170-05	0.196	0.235	
170-06	0.196	0.235	
170-07	0.196	0.235	
170-08	0.196	0.235	
170-09	0.196	0.235	

Tab. V - Details of nodes geometry in the RELAP5 nodalization (cont'ed)

NODE	VOLUME (m ³ x10 ³)	HEIGHT/LENGTH (m)	ZONE
170-10	0.196	0.235	
175-01	0.173	0.2075	
180-01	0.211	0.1776	
180-02	0.211	0.1776	
180-03	0.211	0.1776	
180-04	0.211	0.1776	
TOTAL	10.400		
205-01	1.262	0.22	Upper plenum
210-01	2.262	0.22	
220-01	2.200	0.214	
220-02	2.200	0.214	
TOTAL	8.924		
220-03	0.5651	0.2345	
220-04	0.5651	0.2345	
220-05	0.5651	0.2345	
220-06	0.5651	0.2345	
220-07	0.5651	0.2345	
220-08	0.5651	0.2345	
220-09	0.5651	0.2345	
220-10	0.5651	0.2345	
220-11	0.5651	0.2345	
220-12	0.5651	0.2345	
220-13	0.5651	0.2345	
220-14	0.5651	0.2345	
220-15	0.5651	0.2345	
220-15	0.5651	0.2345	
220-16	0.5651	0.2345	
220-17	0.5651	0.2345	
220-18	0.5651	0.2345	
220-19	0.5651	0.2345	
220-20	0.5651	0.2345	
225-01	2.447	0.34	
230-01	3.684	0.512	
230-02	3.375	0.469	
230-03	3.375	0.469	
230-04	3.375	0.469	
230-05	3.375	0.469	
230-06	3.375	0.469	
230-07	3.375	0.469	

Tab. V - Details of nodes geometry in the RELAP5 nodalization (cont'ed)

NODE	VOLUME (m ³ x10 ³)	HEIGHT/LENGTH (m)	ZONE
230-08	3.375	0.469	
235-01	2.554	0.246	
240-01	2.595	0.25	
240-02	2.595	0.25	
240-03	2.595	0.25	
240-04	2.595	0.25	
245-01	3.789	0.365	
250-01	1.555	0.289	
250-02	1.555	0.289	
250-03	1.555	0.289	
250-04	1.555	0.289	
250-05	1.555	0.289	
255-01	1.647	0.289	
255-02	1.647	0.289	
255-03	1.647	0.289	
255-04	1.647	0.289	
255-05	1.647	0.289	
260-01	1.662	0.25	
260-02	1.662	0.25	
260-03	1.662	0.25	
260-04	1.662	0.25	
265-01	1.635	0.246	
280-01	0.418	0.3295	
280-02	0.418	0.3295	
TOTAL	81.7548		
270-01	1.367	0.247	Downcomer and jet pump
275-01	2.009	0.362	
275-02	2.009	0.362	
275-03	2.009	0.362	
275-04	2.009	0.362	
280-01	1.660	0.3	
285-01	1.660	0.3	
285-02	1.660	0.3	
285-03	1.660	0.3	
285-04	1.660	0.3	
285-05	1.660	0.3	
285-06	1.660	0.3	

Tab. V - Details of nodes geometry in the RELAP5 nodalization (cont'ed)

NODE	VOLUME (m ³ x 10 ³)	HEIGHT/LENGTH (m)	ZONE
295-01	1.078	0.39	
295-02	1.078	0.39	
300-01	0.988	0.283	
305-01	1.012	0.29	
305-02	1.012	0.29	
305-03	1.012	0.29	
305-04	1.012	0.29	
305-05	1.012	0.29	
305-06	1.012	0.29	
305-07	1.012	0.29	
305-08	1.012	0.29	
310-01	1.385	0.325	
315-01	0.355	0.273	
315-02	0.355	0.273	
315-03	0.355	0.273	
315-04	0.355	0.273	
315-05	0.355	0.273	
315-06	0.355	0.273	
315-07	0.355	0.273	
315-08	0.355	0.273	
315-09	0.355	0.273	
315-10	0.355	0.273	
315-11	0.355	0.273	
315-12	0.355	0.273	
315-13	0.355	0.273	
315-14	0.355	0.273	
315-15	0.355	0.273	
320-01	0.737	0.273	
320-02	0.737	0.273	
320-03	0.737	0.273	
320-04	0.737	0.273	
320-05	0.737	0.273	
320-06	0.737	0.273	
320-07	0.737	0.273	
320-08	0.737	0.273	
320-09	0.737	0.273	
320-10	0.737	0.273	
320-11	0.737	0.273	
320-12	0.737	0.273	
320-13	0.737	0.273	
320-14	0.737	0.273	
320-15	0.737	0.273	
TOTAL	49.849		

Tab. V - Details of nodes geometry in the RELAP5 nodalization (cont'd)

NODE	VOLUME (m ³ x10 ³)	HEIGHT/LENGTH (m)	ZONE
360-01	1.926	0.429	Filler
370-01	2.379	0.53	
370-02	2.379	0.53	
370-03	2.379	0.53	
370-04	2.379	0.53	
370-05	2.379	0.53	
370-06	2.379	0.53	
370-07	2.379	0.53	
			IC
500-01	0.141	0.38	
500-02	0.141	0.38	
500-03	0.141	0.38	
500-04	0.141	0.38	
500-05	0.141	0.38	
500-06	0.115	0.312	
500-07	0.115	0.312	
500-08	0.115	0.312	
500-09	0.115	0.312	
500-10	0.078	0.212	
510-01	0.12	0.2	
515-01	0.1927	0.0632	
515-02	0.1927	0.0632	
515-03	0.1927	0.0632	
515-04	0.1927	0.0632	
515-05	0.1927	0.0632	
540-01	0.089	0.35	
540-02	0.089	0.35	
540-03	0.120	0.472	
540-04	0.120	0.472	
540-05	0.120	0.472	
540-06	0.120	0.472	
540-07	0.120	0.472	
540-08	0.120	0.472	
540-09	0.120	0.472	
540-10	0.120	0.472	
540-11	0.120	0.472	
540-12	0.120	0.472	
540-13	0.120	0.472	
540-14	0.120	0.472	
540-15	0.120	0.472	
540-16	0.120	0.472	
540-17	0.120	0.472	
540-18	0.120	0.472	
540-19	0.120	0.472	
540-20	0.120	0.472	

Tab. V - Details of nodes geometry in the RELAP5 nodalization (cont'd)

NODE	VOLUME (m ³ x10 ³)	HEIGHT/LENGTH (m)	ZONE
540-21	0.120	0.472	
540-22	0.120	0.472	
540-23	0.102	0.4	
540-24	0.076	0.3	
540-25	0.089	0.35	
540-26	0.089	0.35	
540-27	0.089	0.35	
TOTAL	5.2295		
551-01	55.755	0.07875	IC Tank
552-01	7.875	0.07875	
560-01	7.875	0.07875	
560-02	7.875	0.07875	
560-03	7.875	0.07875	
560-04	7.875	0.07875	
560-06	7.875	0.07875	
560-07	10.0	0.1	
560-08	5.1	0.1	
560-09	5.5	0.0632	
560-10	5.5	0.0632	
560-11	5.5	0.0632	
560-12	5.5	0.0632	
561-01	5.5	0.0632	
562-01	65.9	0.1	
652-01	47.88	0.07875	
660-01	47.88	0.07875	
660-02	47.88	0.07875	
660-03	47.88	0.07875	
660-04	47.88	0.07875	
660-05	47.88	0.07875	
660-05	47.88	0.07875	
660-06	47.88	0.07875	
660-07	60.8	0.1	
660-08	60.8	0.1	
660-09	38.43	0.0632	
660-10	38.43	0.0632	
660-11	38.43	0.0632	
660-12	38.43	0.0632	
TOTAL	868.29		

Tab. V - Details of nodes geometry in the RELAP5 nodalization (cont'ed)

SIGNIFICANT JUNCTION	FLOW AREA $m^2 \times 10^4$	K_D	K_R	POSITION
primary loop:				
130-02	2.86	0.	0.	bypass inlet
140-02	5.938	0.19	0.9	core inlet
205-01	16.49	14.5	10.6	core outlet
205-02	8.3	0.1	0.1	bypass outlet
220-02	24.1	0.	0.	separator inlet
235-01	24.1	0.	0.	separator outlet
235-02	3.94	100.	100.	separator annulus
235-03	42.6	0.1	0.1	steam dome lower connection
245-02	53.82	0.1	0.1	steam dome upper connection
310-02	27.	0.	0.	lower downcomer annulus
310-03	13.	1.	1.	jet pump inlet
340-00	8.5	1.	1.	lower plenum valve
IC loop				
505-00	3.	10.	10.	top valve
510-01	3.7	0.1	0.1	inlet pipe
510-02	3.	0.1	0.1	tube inlet
520-01	3.	0.1	0.1	tube outlet
520-02	1.7	0.1	0.1	outlet pipe
550-00	0.06	300.	-	bottom valve

Tab. VI - Details of relevant junction related parameters of RELAP5 nodalization

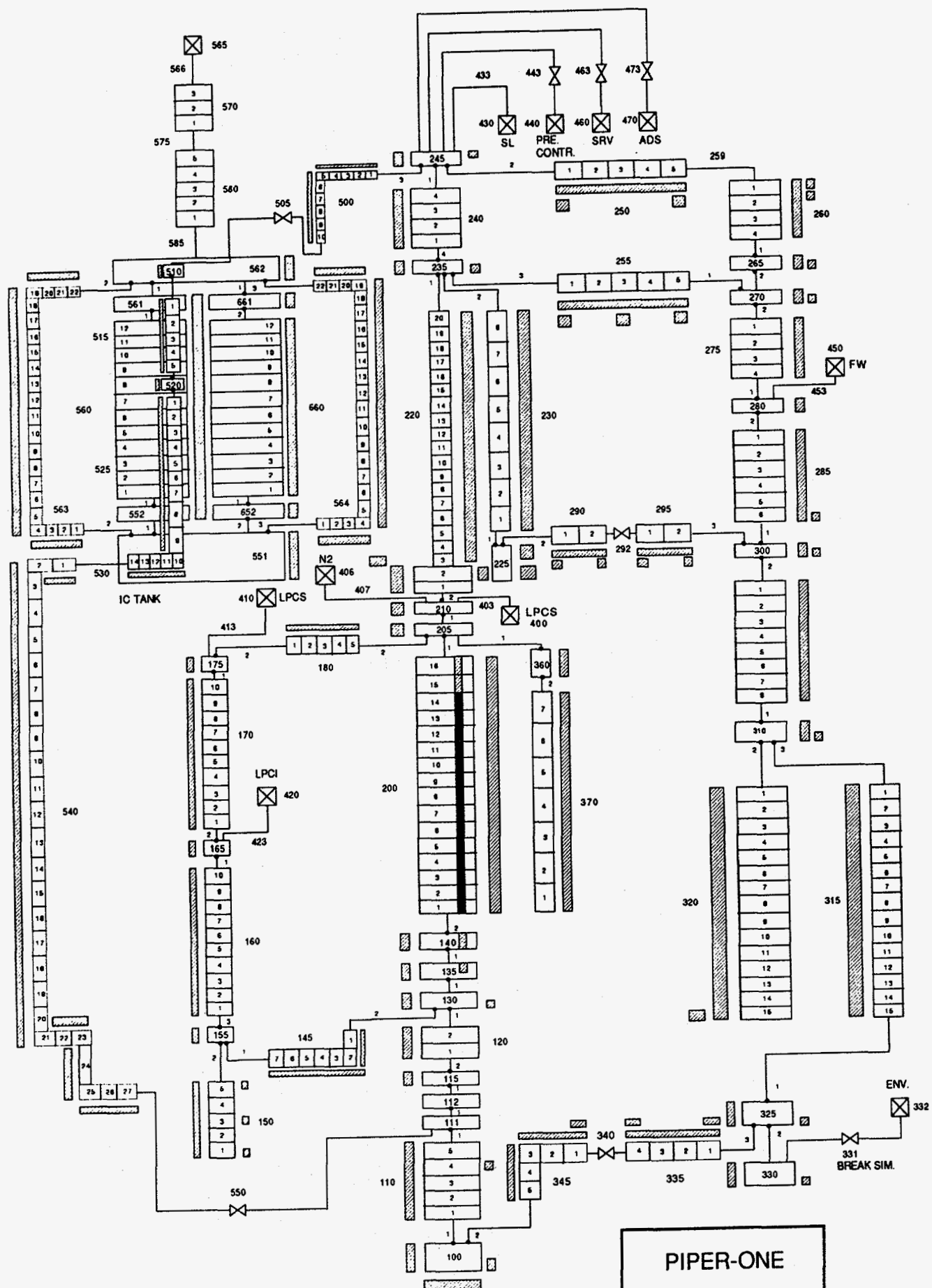


Fig. 29 - Nodalization of PIPER-ONE loop

4. ANALYSIS OF POST-TEST CALCULATION RESULTS

The pre-test results, that have been the basis for the design of the PO-IC-2 experiment, are not comparable with the actual data because of the differences between specified and actual values of the initial and boundary conditions. In particular, as already mentioned, the electrical power supply to the fuel rod simulator was limited to less than 100 kW.

For these reasons, the post-test analysis has comprised three phases:

1. achievement of good comparison between calculated and predicted trends of available primary circuit data;
2. definition of a reference calculation on the basis of the above activity;
3. execution of a series of sensitivity calculations aiming at reaching the stated objectives.

In the frame of the analysis at item 1., boundary and initial condition values related to the primary loop have been changed within the presumed experimental error bands, up to getting a satisfactory comparison between predicted and measured time trends in the primary circuit itself.

Once this process ended (this required a somewhat large effort because of the relative low power of the experiment⁺), the reference calculation results were also compared with the experimental values in the IC system (phase 2.).

The phase 3. of the analysis consisted of five different steps aiming at the evaluation of:

- 3a) influence of code version;
- 3b) influence of selected initial/boundary condition values;
- 3c) user effects;
- 3d) nodalization effects;
- 3e) sensitivity of code results when a geometric/hydraulic relevant parameter is changed in the input deck;

An additional calculation (identified as IC37 in the following) was performed to confirm the conclusions related to the reasons why IC flowrate remains constant when varying core supplied power; this is included in the above group 3e).

Finally, the results of a scaling analysis are shown; these demonstrate the suitability of the data base in relation to scenarios expected in SBWR plants (sect. 4.4).

4.1 Steady state calculations (Phase 1 of the post-test analysis)

As already mentioned, the main objective of the calculations was to match the primary circuit pressure trend.

The initial condition at the assumed "time zero" in the experiment was achieved at zero core power and zero flows inside feedwater and steam lines and at core inlet; structures heating systems were active to compensate heat losses to environment.

The very first series of calculations was carried out changing:

- * the fluid temperature values around the loop (+/- 3K around the saturation value);

⁺ This means that minor variations in the boundary and initial condition values (e.g. changes of heat losses of +/- 1 kw, of initial downcomer level of +/- 0.2 m, of the timing of opening/closure of IC valves of 2 s, consideration of primary circuit leaks as low as 0.0001 kg/s) have a sensible effect on primary pressure values as it happens in all tests performed at low power in any experimental facility, temperatures imbalances in the fluid and in the structures with main reference to the thick flanges.

- * the heat losses to environment (in the range 0 - 5 kW) and the related spatial distribution, excluding the heat losses through the chamber of rods electrical connectors (see below);
- * downcomer and core regions level (in the range +/- 1 m around the available experimental value).

Subsequently, a leak was introduced in the lower downcomer (leak flow varied in the range 0. - 0.05 kg/s starting from 600 s into the transient). Moreover, the time trend of the heat losses across the rod connectors zone has also been varied during the transient accounting for changes in the flows of the cooling nitrogen in this zone.

Finally IC valves characteristics, e.g. opening/closure time and actuation time (varied in the ranges +/- 1 s and +/- 2 s, respectively) have been changed.

The final situation considered for initial and boundary conditions can be seen in Tabs. VII and VIII including the comparison between calculated and measured (if available) values.

It should be noted that almost 30 code runs were necessary to achieve the reported final results.

The comparison between measured and calculated trends of primary pressure, lower plenum temperature and levels in the core region and in the downcomer, is given in Figs. 30 to 33. The calculated trends have been obtained from the code run IC31 (see below). A detailed analysis of the comparison can be found in sect. 4.2.

Here it is sufficient to emphasize three minor discrepancies in the pressure trend:

- at the transient beginning owing to the initial fluid temperature stratification not correctly considered in the code;
- during the phase of electrical power interruption mostly due to inadequate consideration of heat input to the fluid from the structures heating system;
- in the second phase of the test that is a consequence of the above.

The error in all the three cases is less than 0.1 MPa.

The measured lower plenum temperature is only bounded in the calculation (Fig. 31): this is due to the position of the thermocouple that is close to the connection between the main loop and the IC; in the Relap calculation an average volume related value is reported.

Larger differences appear from the level measurements (Figs. 32 and 33); in this case the reliability of the experimental signal is quite low. In the frame of the performed sensitivity calculations, it has been checked that large variations of these quantities (i.e. greater than the actual differences between measured and calculated trends) do not cause variations in the overall transient scenario with main reference to primary pressure and flowrate across the IC.

PARAMETER	UNIT	EXP	CALC (°)
LP pressure	MPa	5.1	5.1
LP temperature	°C	262.	258.5
Core level	m	11.9	11.8
DC level	m	10.7	10.5
IC line fluid temperature	°C	17.5	18.
IC pool fluid temperature	°C	17.5	18.
IC mass flowrate	kg/s	0.	0.
Core power	kW	0.	0.
Primary system heat losses: (*)			
- core region	kW	-	1.97
- steam dome	kW	-	8.5
- separator annulus	kW	-	-0.43
- upper downcomer	kW	-	-0.39
- lower downcomer	kW	-	3.4
- LP/core inlet	kW	-	2.5

(°) Reference case (IC31)

(*) Sign "-" refers to power added to the fluid, sign "+" to power lost

Tab. VII - Comparison between measured and calculated initial conditions

PARAMETER OR EVENT	TIME	
	EXP (s)	CALC (s)
Test initiation	0.	0.
Power versus time	as in Table IV	
IC top valve opens	4.	4.
IC bottom valve opens	32.	32.
IC top valve closes	508.	508.
IC bottom valve closes	-	508.
IC top valve opens	602.	605.
IC bottom valve opens	602.	606.
IC top and bottom valve close	1106.	1106.

Tab. VIII - Comparison between measured and calculated boundary conditions

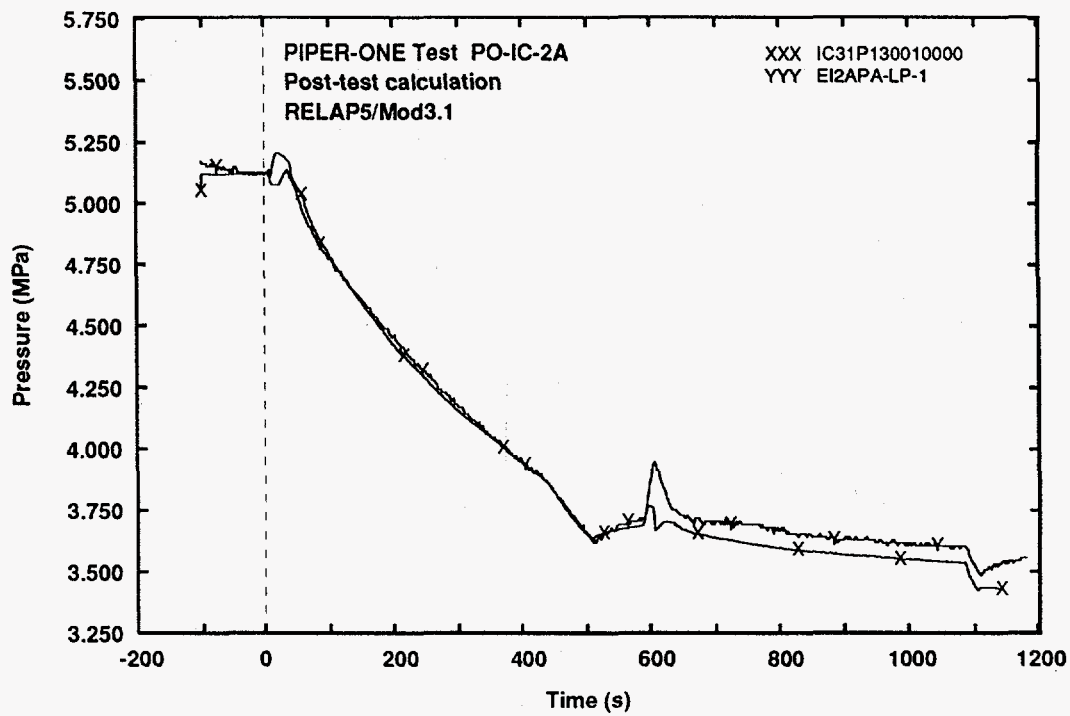


Fig. 30 - Measured and calculated trends of lower plenum pressure

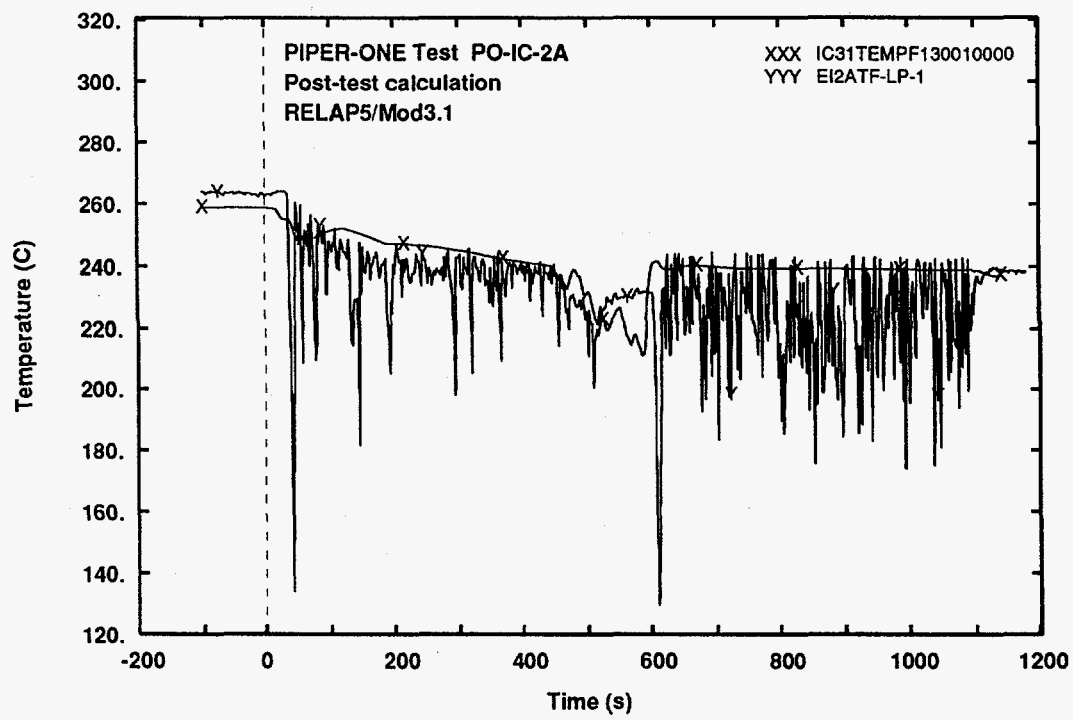


Fig. 31 - Measured and calculated trends of lower plenum temperature

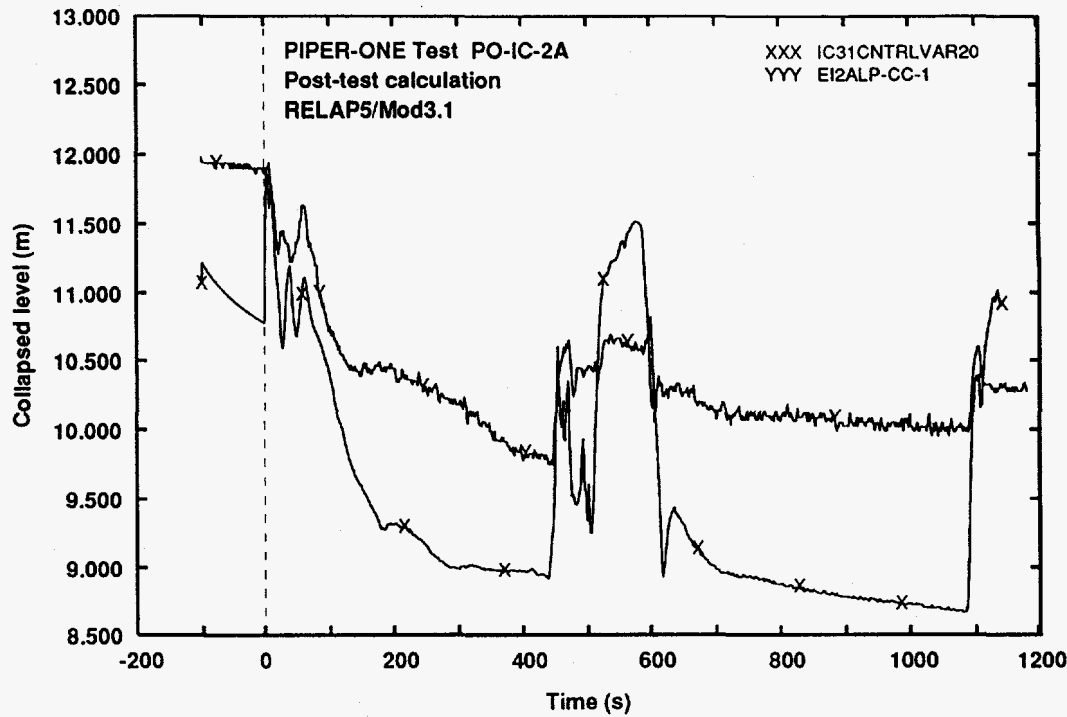


Fig. 32 - Measured and calculated trends of core level

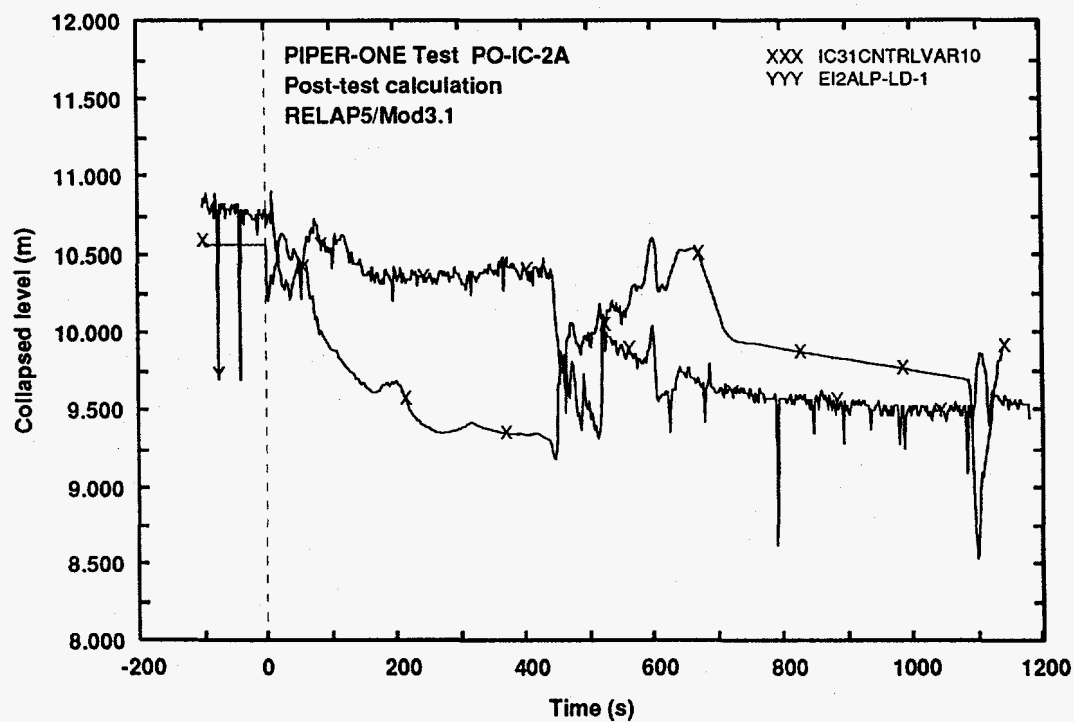


Fig. 33 - Measured and calculated trends of downcomer level

4.2 Reference calculation results (Phase 2 of the post test analysis)

Each of the performed calculations (see below) has been evaluated on the basis of 39 time trends of selected thermalhydraulic quantities. These can be subdivided into three main groups:

- A) variables related to the primary circuit that have been selected considering the availability of experimental data (the numbers into parentheses below refer to the identification of figures in the Appendices):
 - lower plenum pressure, (Fig. 1);
 - lower plenum fluid temperature, (Fig. 2);
 - rod surface temperature at level 9, (Fig. 3);
 - core region level, (Fig. 4);
 - downcomer levels, (Fig. 5);
 - core power, (Fig. 6);
- B) variables related to the IC system that have been selected considering the availability of experimental data:
 - mass flow rate, (Fig. 7);
 - differential pressure across the IC, (Fig. 8);
 - fluid temperatures along the IC system - primary side, (Figs. 9 - 12 and Fig. 27);
 - wall temperatures in the IC system, (Figs. 13 - 18);
 - fluid temperatures in the pool, (Figs. 19 - 26);
 - exchanged power across the IC (Fig. 28);
 - temperature difference between selected points (Figs. 29 - 31);
- C) calculated variables related to the IC system that are relevant for understanding the concerned phenomena and for evaluating the code behaviour:
 - heat transfer coefficients in the IC, (Figs. 32 - 34);
 - void fractions inside the IC tubes, (Fig. 35);
 - liquid and steam velocities inside the IC tubes, (Figs. 36 and 37);
 - internal and external heat transfer modes in the IC tubes (Figs. 38 and 39);
 - differences between steam and liquid temperature of primary fluid (Fig. 40).

The reference calculation results, that is case IC31, are reported in App. 1 (Figs. 1 - 40) and are discussed in the next section.

Computer related statistics

The calculations performed by RELAP5/Mod 3.1 have been run on the IBM RISC 6000, as results from sect. 3.1. The following relevant code run statistics applies (specifically related to the IC31 calculation):

- CPU time is of the order of 20000 s (Fig. 41 in App. 1);
- time step ranges between 0.05 and 0.1 s (Fig. 42 in App. 1), with the exception of the period of IC isolation.

The relation between code selected time step and imposed maximum time step can be seen in Fig. 43 of App. 1.

4.2.1 Primary circuit behaviour

In order to better address the comparison between measured and calculated trends, five phenomenological windows (Ph.W) can be distinguished looking at the primary circuit pressure (Fig. 1):

- * Ph.W 1 from transient beginning to 50 s: the prediction does not agree with the experiment owing to minor errors in initial conditions: the presence of a cold patch of liquid in the primary circuit (roughly 20 cm with less than 10 K of subcooling) or the initial temperature of the IC inlet pipe can be considered for improving the agreement between measured and calculated trends; however this does not affect the subsequent transient;
- * Ph.W 2 from 50 s to 440 s: this constitutes the low power part of the test. An excellent qualitative and quantitative agreement between measured and calculated trends can be observed: this demonstrates that the IC removed power is very well predicted;
- * Ph. W 3 from 440 s to 650 s: this includes the power shut-off period (i.e. from 440 s to 588 s) and the period necessary to achieve a "quasi steady-state" in the high power part of the test (i.e. from 588 s to 650 s). The disagreement in this Ph.W is mostly due to wrong estimation of the behaviour of the structure heating system, to the inaccurate modelling of the conduction heat transfer in the thick flanges (much larger number of meshes is required) and to the phenomena that occur inside the IC after its isolation. In particular, it is interesting to note that a sudden void collapse occurs in the IC primary system after its isolation; this brings the pressure from about 4 MPa to saturation values corresponding to the liquid temperature in the pool (i.e. of the order of 0.01 MPa). Two main consequences in terms of code calculation are:
 - a) the time step required to predict the condensation shock is very low (of the order of 1.e-6 s) and the code appeared not qualified in this connection;
 - b) the test conditions (essentially the insurge of liquid into the IC line) resulting from the shock occurrence affect the code prediction in the period 588 s to 650 s and are the main reason for the discrepancy in this period;
- * Ph.W 4 from 650 s to 1088 s: this constitutes the high power part of the test. An excellent qualitative agreement between measured and calculated trends can be noted; the difference between the two curves is a result of the previous Ph.W and is less than 0.1 MPa. Again the overall trend shows that the IC exchanged power is very well predicted;
- * Ph. W 5 from 1088 s to the end: power shutoff occurs in this period. The good agreement between measured and calculated trends confirms that the energy balance is well considered in the calculation.

It should be noted that the Ph.W 2 and 4 are of main interest in our study.

A few additional remarks related to the comparison between measured and predicted trends of the remaining primary circuit related quantities (Figs. 2 - 6 of App. 1) are as follows:

- the negative peaks in the measured lower plenum temperature (Fig. 2), as already mentioned, are due to the cold water coming from the IC; a volume averaged value is calculated by the code; the discrepancies during the Ph. W 3 are due to cold liquid stratification caused by the cooling of the rod connectors chamber;
- discrepancies in the rod surface temperatures are essentially due to the position of the thermocouple that does not coincide with the surface of the rod (Fig. 3);
- inaccuracies in the experimental signal and minor leaks from the primary circuit are to be considered when examining the discrepancies in levels (Figs. 4 and 5 of App. 1), as well as the fact that core and DC levels are influenced by the fluid velocity. However this does not hold for the lower DC level measurement (signal LP-LD-1); a code inadequacy

- seems evident in this respect;
- the calculated quantity is the heat transferred from the rods to the fluid while the experimental quantity is the electrical power supply to the rods: this explains the errors (not present during the "quasi steady-state") in the core power curves (Fig. 6 of App. 1).

4.2.2 IC behaviour

Primary System

The mass flowrate across the IC is quite well predicted by the code (Fig. 7 of App. 1); the zero flow resulting from the turbine signal in the first 200 s is originated by a malfunction of this device, as already mentioned. Peaks in the experiment during the Ph. W 1, 3 and 5 are not predicted. It can be concluded that the calculated result is within the experimental error bands in the Ph. W 2 and 4 that are of main interest in the present study.

Some more work is necessary to qualify the measured pressure drop signal (Fig. 8); nevertheless the prediction can be retained within the experimental error bands in the Ph. W 2 and 4.

The fluid temperatures at the IC inlet are represented in Figs. 9 and 27 of App. 1. The agreement between measured and calculated trends is quite good during all the considered Ph. W. Moreover, Fig. 27 shows that saturation temperature is measured and calculated during the Ph. W 2 and 4 at the IC entrance. The presence of subcooled liquid at the IC inlet during the Ph. W 1 and 3 can be deduced from the trends in Fig. 9, although information about absolute pressure in the IC line is not available.

Fluid temperature is very well predicted by the code at the center of the IC: the calculated trend (liquid temperature) lies between the two measured signals in Fig. 10 of App. 1. Subcooling in the lowest three nodes of the IC can be deduced from the analysis of Fig. 11 of App. 1: all the steam is condensed in the first two nodes in both the Ph. W 2 and 4.

The comparison of fluid temperatures at the outlet of the IC, Fig. 12 of App. 1, confirms that the overall heat transfer to the pool is satisfactorily predicted by the calculation: this appears to be true also considering separately the tubes region (where both condensation and heat transfer to the pool from subcooled liquid take place) and the single tube region (where only heat transfer to the pool from subcooled liquid takes place).

The data in Fig. 13 of App. 1 show an overestimation of the surface temperature by the code: this is true for all the surface temperatures, i.e. both in the inner and in the outer surface of the tubes, during the Ph. W 2 and 4, as it also results from Figs. 15, 16, 17, and 18 of App. 1. Considering that the overall power exchanged is quite well predicted, one can deduce a code error in predicting the heat transfer coefficient either in the inner surface or in the outer surface, either in both the surfaces (an average error of the external surface temperature of 20 K results in underestimating the heat transfer coefficient of about 20% in the conditions of Ph. W 2 at the top of the IC, see also sect. 4.2.3). This conclusion is also supported by the observation that measured and calculated surface temperatures are very close during the Ph. W 1, 3 and 5, i.e. when flowrate and exchanged power are nearly zero.

An abrupt external surface temperature change can be observed at about 900 s (Ph. W 4) in the calculation (Fig. 17 of App. 1): this is a consequence of a change in heat transfer coefficient from mode 2 (forced convection) to mode 3 (nucleate boiling) as it results from Fig. 39 of App. 1; mode 3 is also the heat transfer coefficient mode during the entire Ph. W 2 (Fig. 39).

Discrepancies between measured and calculated trends during the Ph. W 3 appear from Fig. 18 of App. 1; in this connection it should be noted that in order to perform the calculation in this Ph. W, it has been necessary to add two TMDPVOL and related TMDPJUN connected with the IC nodes: the reason for adding these components was to smooth the abrupt pressure collapse due to sudden condensation; the effect of the added

nodes can be seen, as far as Ph. W 3 is concerned, in the Fig. 18 of App. 1.

Pool

The good agreement between measured and calculated trends of pool temperature at different axial elevations (essentially, Figs. 19, 20, 23 and 24 of App. 1) constitutes an independent proof of the agreement in the overall exchanged power. Three additional aspects should be noted from the analysis of figures from 19 to 26 of App. 1:

- changes in the slope of the predicted trends during the Ph. W 3 (e.g. Fig. 19) are due to the necessity of the TMDPVOL discussed in the previous paragraphs;
- discrepancies in some measured and predicted trends (e.g. Fig. 20 or Fig. 26) are either of minor importance (only 3 K in Fig. 26, within the experimental error band), either due to different positions considered in the calculation and in the experiment (Fig. 20);
- external and internal side pool temperature are nearly the same demonstrating that conduction across the shroud prevents the possibility of establishing sufficient temperature difference to give rise to natural circulation inside the pool.

In definitive, from observing:

- a) fluid temperature at IC inlet, outlet and inside IC,
- b) surface temperatures in the tubes and,
- c) fluid temperature in the pool,

it can be deduced that variables a) and c) are well predicted (also flowrate and overall exchanged power are well predicted); but, variables b) are overestimated. The conclusion is that the heat transfer coefficients across the tubes (either on the internal or external surface) are calculated with some error (see sect. 4.2.3). Figures from 29 to 31 of App. 1 support this conclusion.

Furthermore, the temperature increase in the pool results from Fig. 31: the smooth increase of fluid temperature in the pool leads to a smooth decrease of the temperature difference between tubes inner wall surface temperature and pool temperature itself. Removed power remain constant: this means an average increase of the overall heat transfer coefficient during the experiment.

Calculated quantities

As already mentioned, calculated quantities that have not a corresponding measured trend are reported in Figs. 32 - 40 of App. 1.

As far as heat transfer coefficients are concerned during the Ph.W 2 and 4, the following observations can be made (Figs. 33 to 35 and 38, 39 of App. 1; inner and outer coefficients can be recognized by the last two digits in the variables labels at the right uppermost corner in the figures, "00" and "01", respectively):

- in the upper zone of the tubes Heat Transfer Coefficients at the inner wall (HTCI) are always smaller than Heat Transfer Coefficients at the outer wall (HTCO); in particular average values of HTCI and HTCO are 15000 and 18000 W/m²K, respectively;
- both HTCO and HTCI become noticeably lower along the axis reaching values as low as 1200 W/m²/K for HTCO in the bottom of the IC tubes;
- at the bottom of IC tubes HTCO is much smaller than HTCI, thus controlling the overall heat transfer process;
- the effect of the sharp transition from mode 2 to mode 3 of the HTCO can also be observed in Fig. 33 at about 900 s into the transient (see also Fig. 39 and the previous discussion);
- no sharp transitions during PH.W 2 and 4 can be observed in HTCI (Fig. 38).

The void fraction trends along the axis confirm that condensation is predicted only in the top two nodes simulating the IC tubes (Fig. 35): only liquid is present in the bottom three nodes during the whole experiment.

As reasonable, higher liquid velocities are calculated in the upper two nodes (liquid is entrained by steam, Fig. 36) than in the bottom three nodes.

An apparently unphysical steam velocity trend is calculated in the central node (upward oriented steam velocity in a node where void fraction is zero), Fig. 37: this does not happen in the two lowest nodes.

The degree of subcooling calculated for each of the 5 nodes representing the IC tubes, can be drawn from Fig. 40 of App. 1. It can be noted that, in the second IC node from the top (where both steam and liquid are simultaneously present and predicted void fraction around 0.9, Fig. 35), roughly 20 K subcooling are calculated during both Ph.W 2 and 4.

4.2.3 Heat transfer coefficient across the IC tubes

In order to better understand the comparison between calculated and experimental data in the reference calculation, relevant data were put in the frame of the Tabs. IXa and IXb, considering the Ph.W 2 and 4, respectively.

Each row deals with one of the five axial zones in which the IC tubes have been subdivided.

The first four columns deal with measured and calculated values of temperature differences between primary fluid and inner surface (T_{fi} and T_{wi}) and between outer surface and pool fluid (T_{wo} and T_{fo}). If surface temperature is not available from the experiment at a given level, the assumption is made, for that level, that calculated fluid temperature is the same in the experiment. This is justified by the comparisons between measured and calculated fluid temperatures (Figs. 9, 10, 12, 19, 20, 23, 24 of App. 1).

The second group of four columns deals with calculated values of exchanged power across each axial level at the inner (subscript "i") and at the outer surface of the IC tubes (subscript "o"). The four values of power (symbol "PO"), from left to right in the tables, have been calculated starting from inner "HTC", outer "HTC", inner "Q" value and outer "HTRNR" values, respectively (HTC, Q and HTRNR are Relap5 output quantities).

The following remarks can be done from the analysis of the tables, with reference to both the selected phenomenological windows:

- * exchanged power is much higher in the uppermost two nodes than in the remaining three bottom nodes;
- * power calculated from the HTC is not consistent with actual value at the inner surface in the uppermost three nodes;
- * only one temperature difference has been obtained for the inner surface: this seems not enough to draw conclusions;
- * experimental temperature differences at the outer surface are substantially lower than calculated values (factor 1.5 - 2): calculated heat transfer coefficient can be retained underestimated for the same amount. The presumable error coming from "fin" effect introduced by the externally welded thermocouples has not been considered in this conclusion.

In the above analysis, the assumption has been made that the phenomenon is quasi-stationary: this is supported by the time trends of the main quantities. Furthermore, the good agreement between measured and calculated levels (pressure drop inside the tubes) confirms this assumption.

Ph.w.2 (300. s)								
IC ZONE	T _{fi} - T _{wi}		T _{wo} - T _{fo}		P _{Oi}	P _{Oo}	P _{OQ,i}	P _{OH,o}
	EXP	CALC	EXP	CALC	CALC	CALC	CALC	CALC
1	106. (2)	39	50. (1)	76	21.8	73.	22.	23.3
2	-	70.5	68. (1)	84.5	11.2	59.	6÷23	14÷17
3	-	61.	50. (2)	85.	6.	30.	6.	6.
4	-	53.	-	62.	4.5	4.5	4.5	4.5
5	-	43.5	32. (2)	50.	3.2	3.1	3.2	3.1

T_{fi/o} = inside/outside fluid temperature

T_{wi/o} = inside /outside wall surface temperature

P_{Oi} = inside exchanged power evaluated from HTC

P_{Oo} = outside exchanged power evaluated from HTC

P_{OQ,i} = inside exchanged power calculated by code (variable "Q")

P_{OH,o} = outside exchanged power evaluated from heat flux (variable "HTRNR")

(1) = actual value

(2) = experimental fluid temperature equal to calculated one

Tab. IXa - Evaluation of the heat transfer coefficient (Ph.w.2)

Ph.w.4 (900. s)								
IC ZONE	T _{fi} - T _{wi}		T _{wo} - T _{fo}		P _{Oi}	P _{Oo}	P _{OQ,i}	P _{OH,o}
	EXP	CALC	EXP	CALC	CALC	CALC	CALC	CALC
1	94. (2)	33.5	25. (1)	44	22.8	4.6.	22.7	22.7
2	-	45.5	35. (1)	65	17.5	54.	5.2÷22	19÷15
3	-	61.	43. (2)	65.	5.7	22.9	5.5.	5.5
4	-	50.	-	53.	4.1	4.1	4.3	4.2
5	-	40.7	31. (2)	44.	3.	3.	3.1	3.1

T_{fi/o} = inside/outside fluid temperature

T_{wi/o} = inside /outside wall surface temperature

P_{Oi} = inside exchanged power evaluated from HTC

P_{Oo} = outside exchanged power evaluated from HTC

P_{OQ,i} = inside exchanged power by code (variable "Q")

P_{OH,o} = outside exchanged power evaluated from heat flux (variable "HTRNR")

(1) = actual value

(2) = experimental fluid temperature equal to calculated one

Tab. IXb - Evaluation of the heat transfer coefficient (Ph.w.4)

4.3 Sensitivity Calculations (Phase 3. of the Post-test analysis)

A large number of sensitivity calculations has been carried out as results from Tab. X, where the varied parameters have been reported together with some qualitatively significant effects on the results.

The calculation ICA6 was carried out with rough boundary conditions, already producing a "good" overall agreement with experimental data (App. 4). After that, some "tuning", changing the parameter values within the experimental error bands, was done: almost 30 calculations were performed, among which the IC19-IC31 specifically mentioned in Tab. X.

The result of the tuning was the reference calculation IC31 (App. 1).

Calculations from IC28 to IC36 in Tab. X aimed at finding parameters having large influence on the results: e.g. it was found that conduction heat transfer mesh size has almost no effect on the results (calculation IC32), while IC tubes node length introduces heavy oscillations in the relevant output quantities (calculation IC34).

Finally, calculation IC37 (App. 3) was carried out as a counterpart of calculation IC31 to demonstrate the influence of the presence of a large parallel circuit (i.e. vessel downcomer) upon the IC global performance.

CODE RUN	CHARACTERISTICS/VARIED PARAMETERS	MAIN RESULTS
ICA6 ⁽¹⁾	Rough boundary conditions	Overall system behaviour qualitatively predicted
IC19÷IC27	Sensitivity analyses - varied parameters: - heat losses (value and distribution) - core and downcomer initial levels; - core and downcomer initial liquid temperature distribution; - leaks in primary system; - IC valves operation.	Effects on primary system response ; minor changes on IC behaviour
IC31 ⁽²⁾	Reference case	
IC28÷IC30	Liquid surge in the IC line during the power switch-off and IC isolation phase. Varied parameter: - IC boundary condition modelling	Effect on primary system pressure soon after the power switch-on and IC restart
IC32	Heat exchanger modelling. Varied parameter: - IC tube structure mesh size	No effect
IC33/IC36 ⁽³⁾	- Heated diameter of IC tube wall external side	Large effect on IC outlet liquid temperature
IC34	- IC tube node number	Small effects on IC fluid temperature distribution and primary system behaviour Strong oscillations in the wall surface temperature of IC tubes
IC35	- IC tube material thermal conductivity	Small effects
IC37 ⁽⁴⁾	Recirculation rate in primary system. Varied parameter: - LP valve closure during transient	Step increase in IC mass flow rate

(1) Results in Appendix 4

(3) Results in Appendix 2

(2) Results in Appendix 1

(4) Results in Appendix 3

Tab. X - List of calculations and varied parameters

4.3.1 Significant results

Five main groups of calculations have been distinguished following the discussion under sect. 4. These are classified in Tab. XI where the varied parameter ranges are reported, if applicable. In the last part of Tab. XI, the differences between measured and calculated values of surface temperature in the lowest node of the IC tubes, are reported too. This is done at 100, 300 and 1000 s into the transient, the first two values belonging to Ph.W 2 and the last one to Ph.W. 4. It can be noted that in almost all the cases, calculated outer surface temperature values are larger than measured values (the consideration about possible thermocouples "fin" effect should be made here, too). Assuming that heat transfer power and fluid temperature are the same in the experiment and in the calculation, it can be concluded that calculated HTC values are lower than in the experiment, as it also results from sect. 4.2.3.

GROUP	CASE	VARIED PARAMETER	EFFECT ON PREDICTED IC PERFORMANCE		
			(TS-IC-7) - (HTTEMP150S0510)		
			100.s	300.s	1000.s
3a) INFLUENCE OF CODE VERSION	IC31*	USED CODE VERSION RELAP5/Mod3.1	-16.9	-17.1	-12.
	IC7J	RELAP5/Mod3V7J	-14.6	-0.1	-
	ICV8	RELAP5/Mod3V80	-14.8	-0.4	-
	ICM2	RELAP5/Mod2.5	-14.7	-14.8	-17.1
3b) INFLUENCE OF INITIAL AND BOUNDARY CONDITIONS	IC31*	INITIAL AND BOUNDARY CONDITIONS	-16.9	-17.1	-12.
	ICA6*		-12.9	-13.3	-4.6
3c) USER EFFECT	IC31*	IN/OUT FLOW TO IC CONTROL VOLUMES	-16.9	-17.1	-12.
	IC28		-16.7	-16.7	-11.8
	IC29		-16.9	-16.9	-11.4
	IC30 ^(*)		-16.9	-17.2	-
3d) NODALIZATION EFFECTS	IC31*	MESH NUMBER OF IC PIPE WALL: 10	-16.9	-17.1	-12.
		20	-17.1	-17.5	-12.4
	IC31	NODE NUMBER OF IC PIPE AND CORRESPONDING INTERNAL POOL ZONE: 5	-16.9	-17.1	-12.
		10	-10.6	-14.6	-8.4
	IC31	IC PIPE MATERIAL THERMAL CONDUCTIVITY STANDARD STEEL	-16.9	-17.2	-12.
		STANDARD STEEL *2	-17.3	-17.5	-12.3
	IC31*	HEATED DIAMETER IN THE EXTERNAL SIDE OF IC PIPE WALL: 0.005 m	-16.9	-17.1	-12.
		0.1 m	-43.7	-44.	-37.3
		0.001 m	-3.0	-3.4	0.3
3e) CHANGES OF RELEVANT PARAMETERS	IC37	LP-VALVE CLOSURE AT 300.s IN THE TRANSIENT	-16.6	-17.2	-31.9

(*) without control volumes in the IC

* Results in Appendix (see Tab. X)

Tab. XI - Documented calculations

In all cases, six quantities have been selected to characterize the influence of the varied parameter:

- lower plenum pressure;
- IC tubes surface temperature (external side level 3);
- IC tubes internal fluid temperature (level 3);
- IC outlet fluid temperature;
- IC HTC inside tubes (level 3);
- IC HTC outside tubes (level 3).

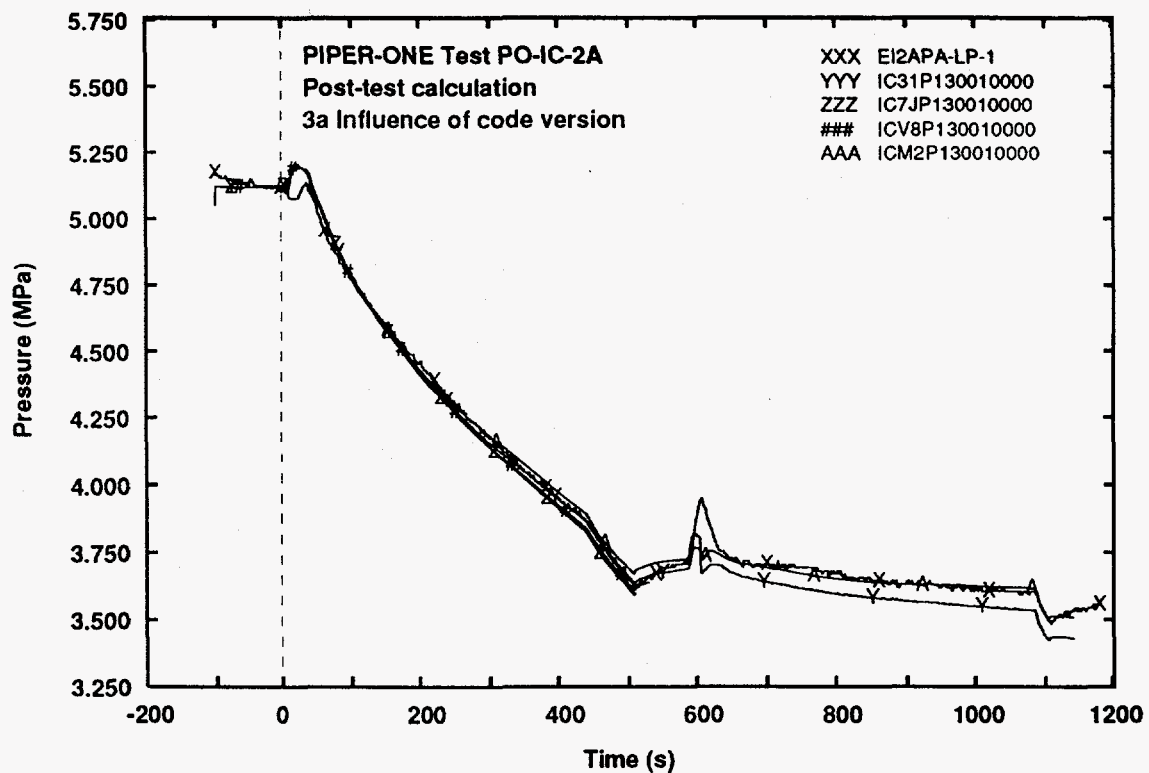


Fig. 34 - Lower plenum pressure

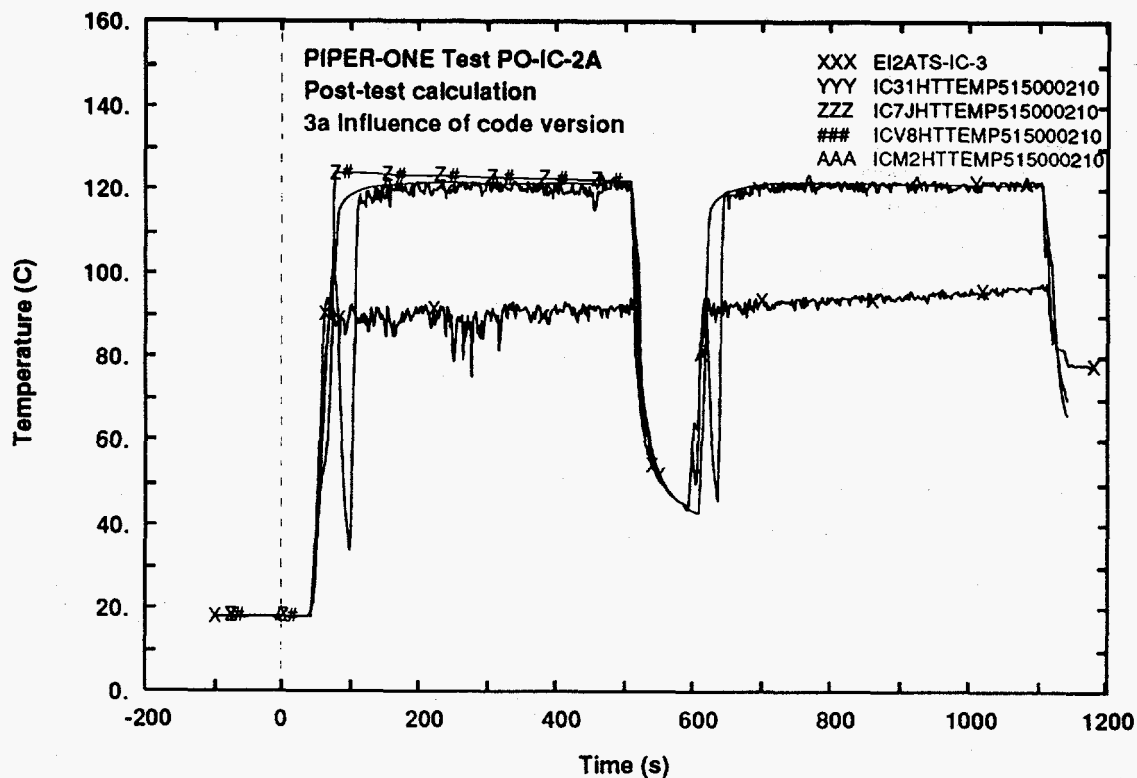


Fig. 35 - IC tubes wall surface temperature (external side level 3)

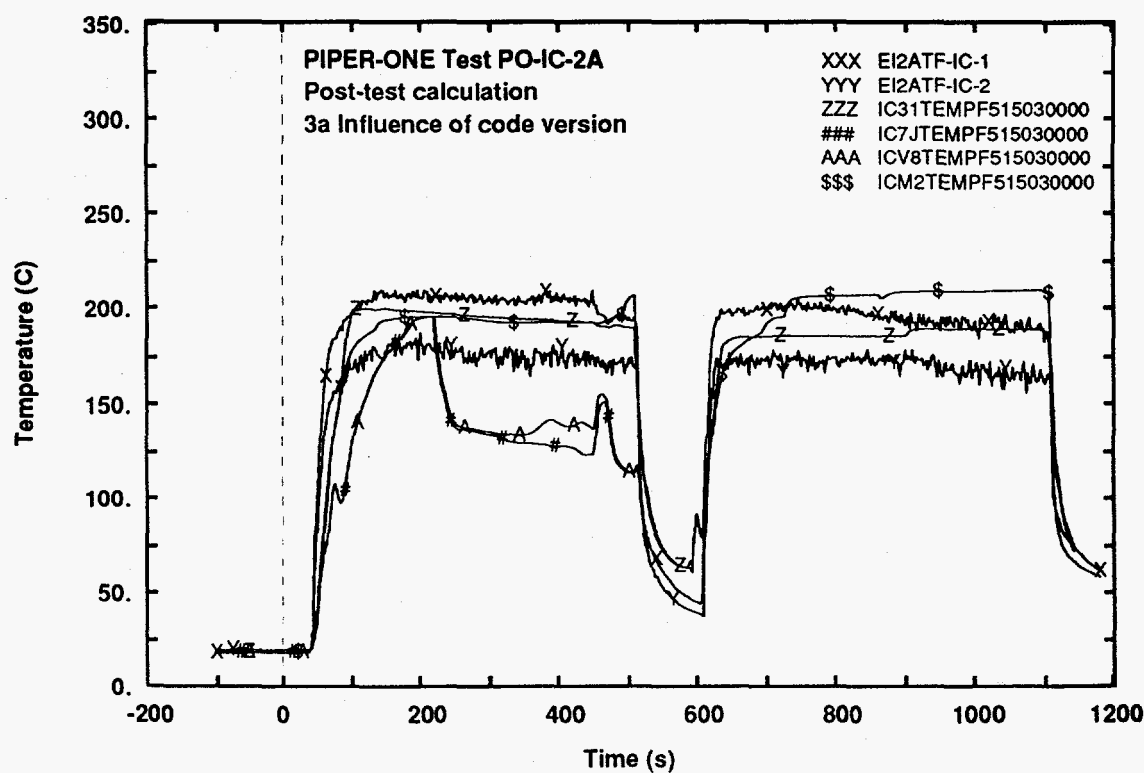


Fig. 36 - IC tubes fluid temperature (middle elevation)

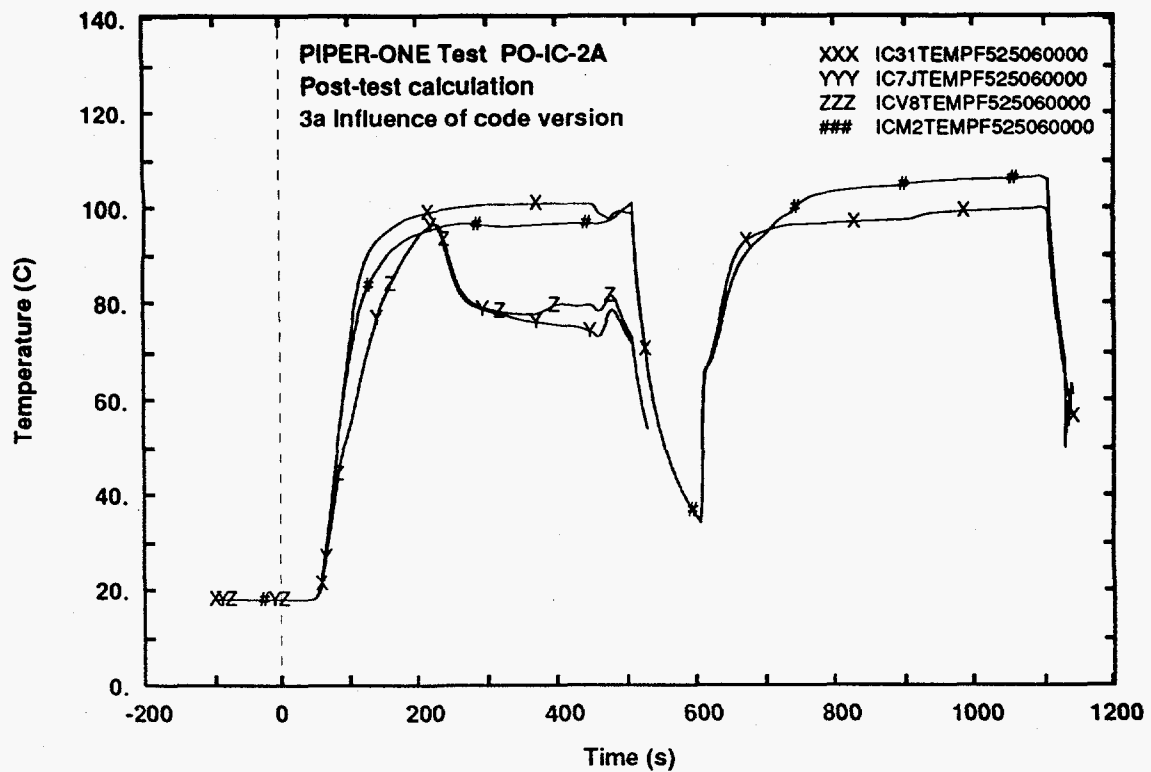


Fig. 37 - IC outlet fluid temperature

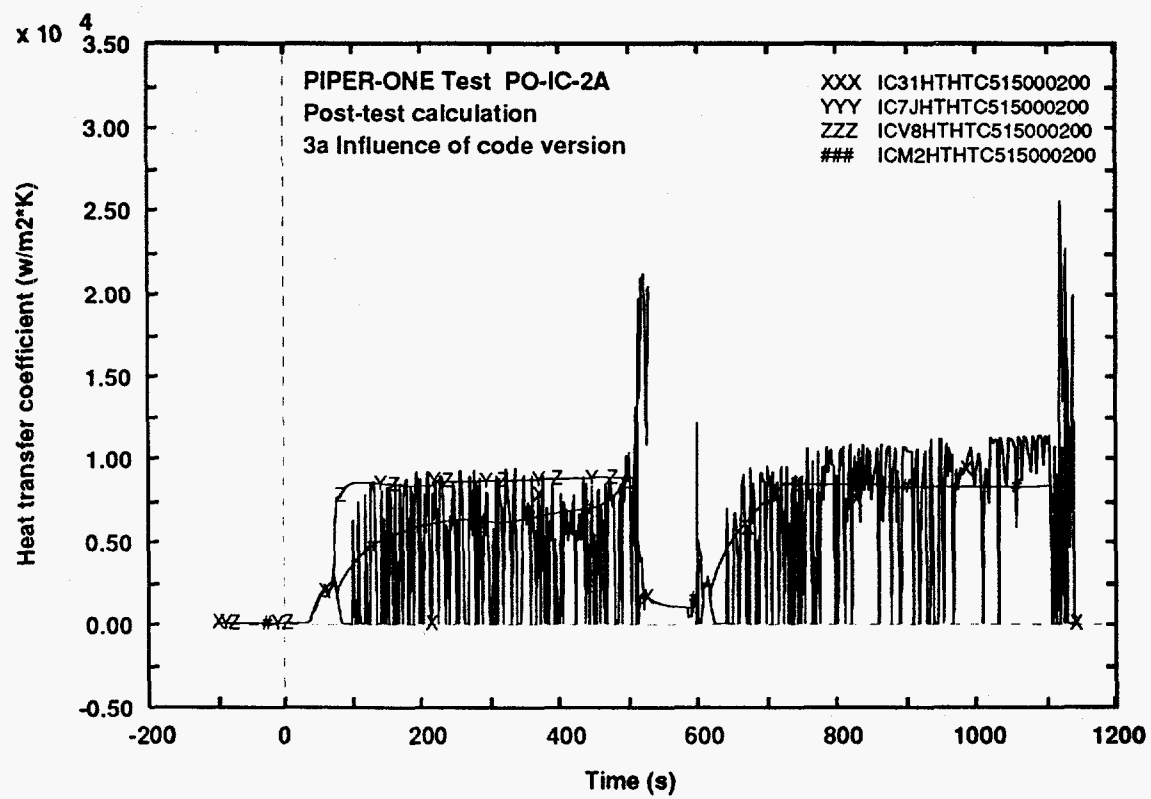


Fig. 38 - Heat transfer coefficient at the inside of IC tubes wall (level 3)

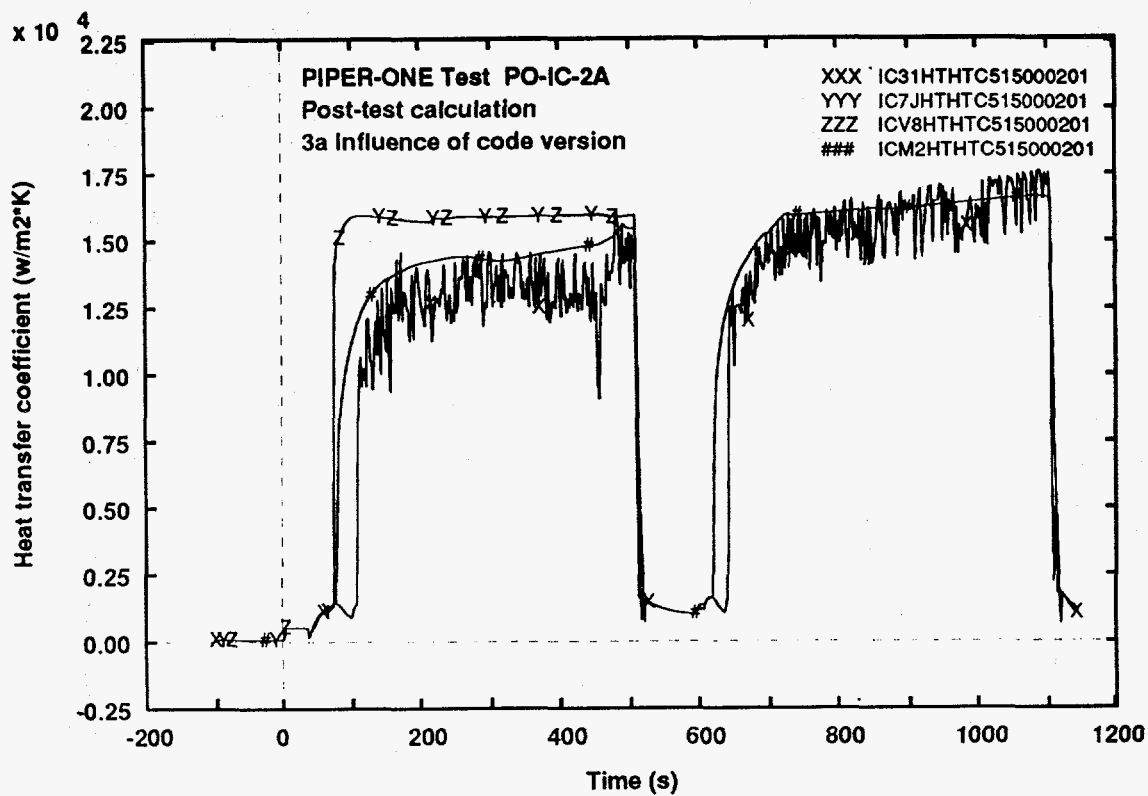


Fig. 39 - Heat transfer coefficient at the outside of IC tubes wall (level 3)

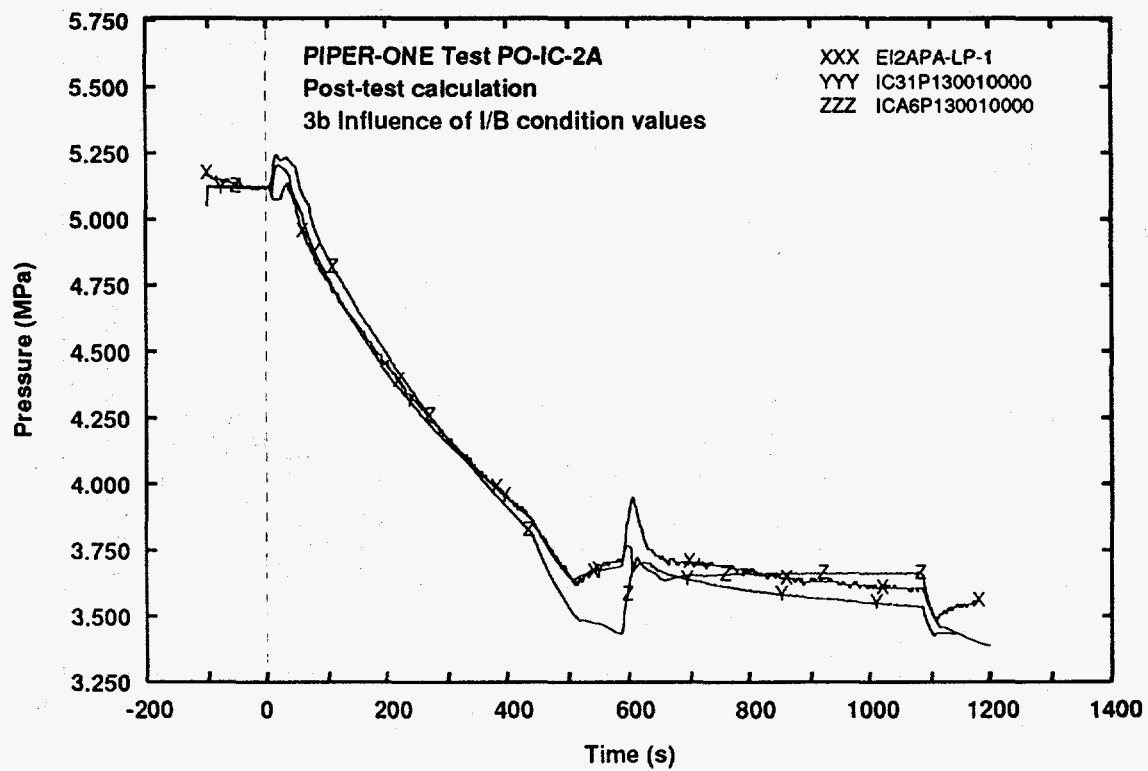


Fig. 40 - Lower plenum pressure

Influence of code version

The nodalization used for calculation IC31 has been modified (if necessary) and run with different code versions as specified in Tab. XI. The six selected quantities are compared in Figs. 34 to 39. Primary pressure is not very much affected by code version (Fig. 34). Overestimation of external temperature appears from all code versions (Fig. 35).

The unphysical behaviour for fluid temperature already noted in the analysis of the experiment PO-SD-8 by the 7J code version (ref. /6/), can also be noted in Figs. 36 and 37 also with reference to the v80 version.

Internal heat transfer coefficient is oscillating only in Relap5/mod3.1 (Figs. 38 and 39); HTC values are lower in the case of v 3.1. Calculations with 7J and v80 versions stopped at almost 500 s into the transient.

Influence of initial and boundary conditions

A large number of boundary conditions has been varied between ICA6 and IC31 calculations (ICA6 can be retained a blind post-test), as already mentioned. Differences in the results can be appreciated looking at figures from 40 to 45.

The influence of the considered changes cannot be retained relevant as far as the IC behaviour is concerned. HTC are lower in ICA6 than in IC31 calculations (Fig. 45).

User effects

Almost arbitrary conditions were imposed to run the calculations during PH.W 3, attempting to prevent calculation failure due to shock condensation.

Mostly, changes in the duration and phenomenology of Ph.W 3 can be noted in the results (Figs. 46 to 51); the influence on the subsequent Ph.W 4 seems negligible.

Nodalization effects

The studied nodalization effects include the increase in the number of conduction heat transfer meshes and the increase in the number of hydraulic nodes, (calculations IC32 and IC34 in Tab. XI, respectively). The change of steel conductivity (calculation IC35 in Tab. XI) has also been included in this group, although it could have been in the calculation group 3e) of Tab. XI. The results are shown in Figs. 52 - 57 with reference to the chosen six quantities: IC31 results are also reported.

The effects of these variations at a global level, i.e. considering primary circuit pressure (Fig. 52) or fluid temperature at the IC outlet (Fig. 55) are negligible. However, local effects can be very important as shown by the inner wall surface temperature in Fig. 53 and by the heat transfer coefficient in Fig. 57.

In particular the comparison of IC34 and IC31 related trends in Fig. 57 leads to the conclusion that (condensation) heat transfer coefficient should be in someway connected with node dimensions: a given HTC correlation can produce satisfactory results with nodes of given dimensions, but unacceptable results if node dimensions are changed.

Changes of relevant parameters

For simplicity, only the effect of hydraulic diameter change in the secondary side of the IC is discussed under this item. Calculations IC33 and IC36 are characterized by hydraulic diameters 20 times and 5 times, respectively, larger and lower than the value of the same quantity in calculation IC31. Relevant results are shown in Figs. 58 - 63.

This quantity has a strong effect both regarding primary pressure (Fig. 58) and IC related quantities, like fluid temperature at the outlet (Fig. 61) and heat transfer coefficient (Fig. 63).

The judgement about the preferable value for hydraulic diameter is difficult from the presented data.

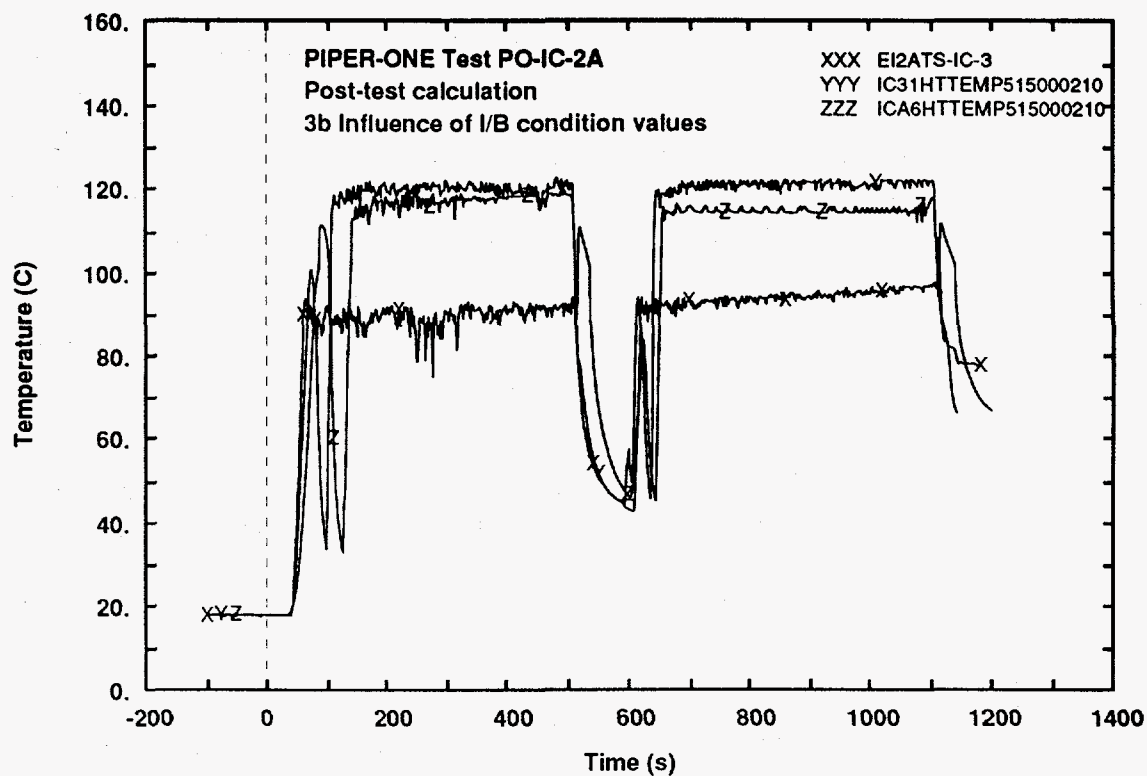


Fig. 41 - IC tubes wall surface temperature (external side level 3)

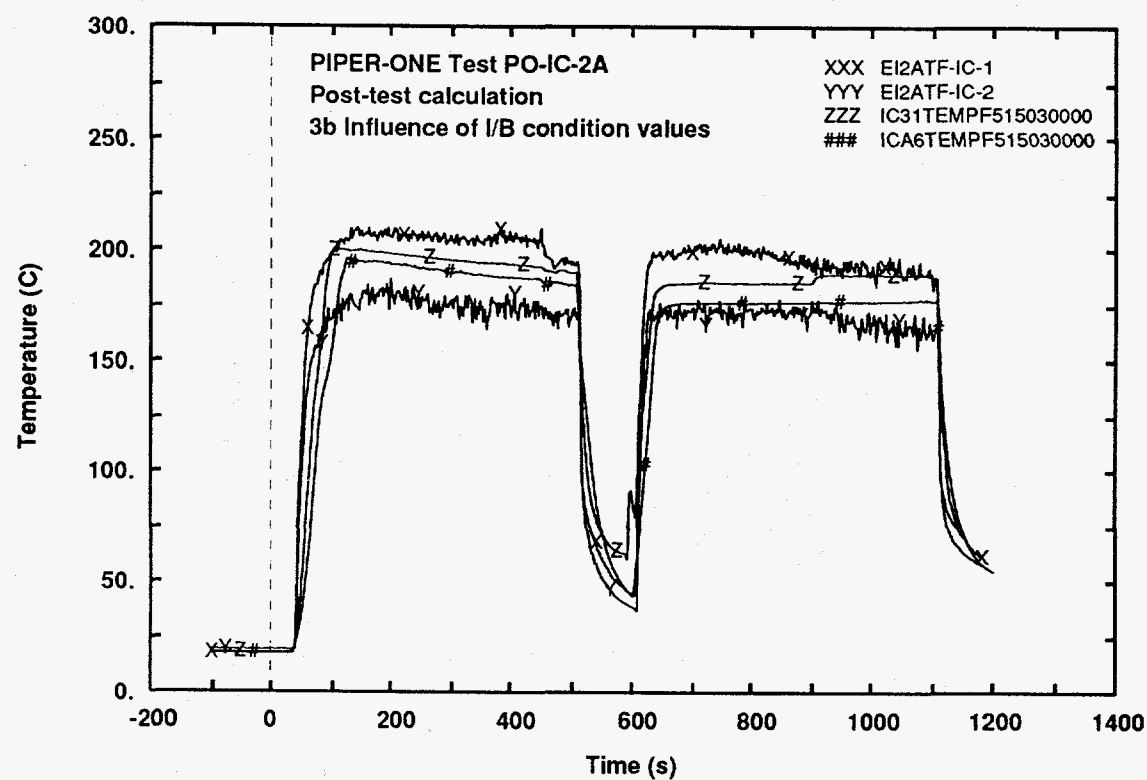


Fig. 42 - IC tubes fluid temperature (middle elevation)

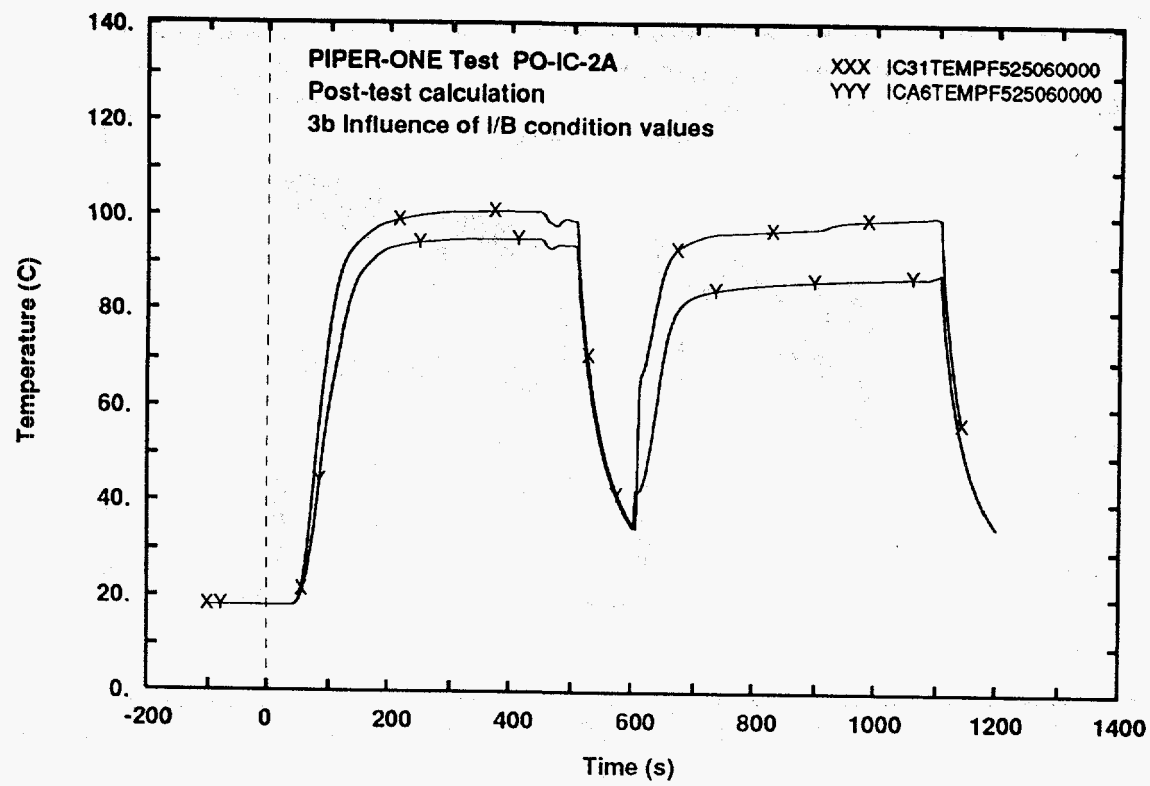


Fig. 43 - IC outlet fluid temperature

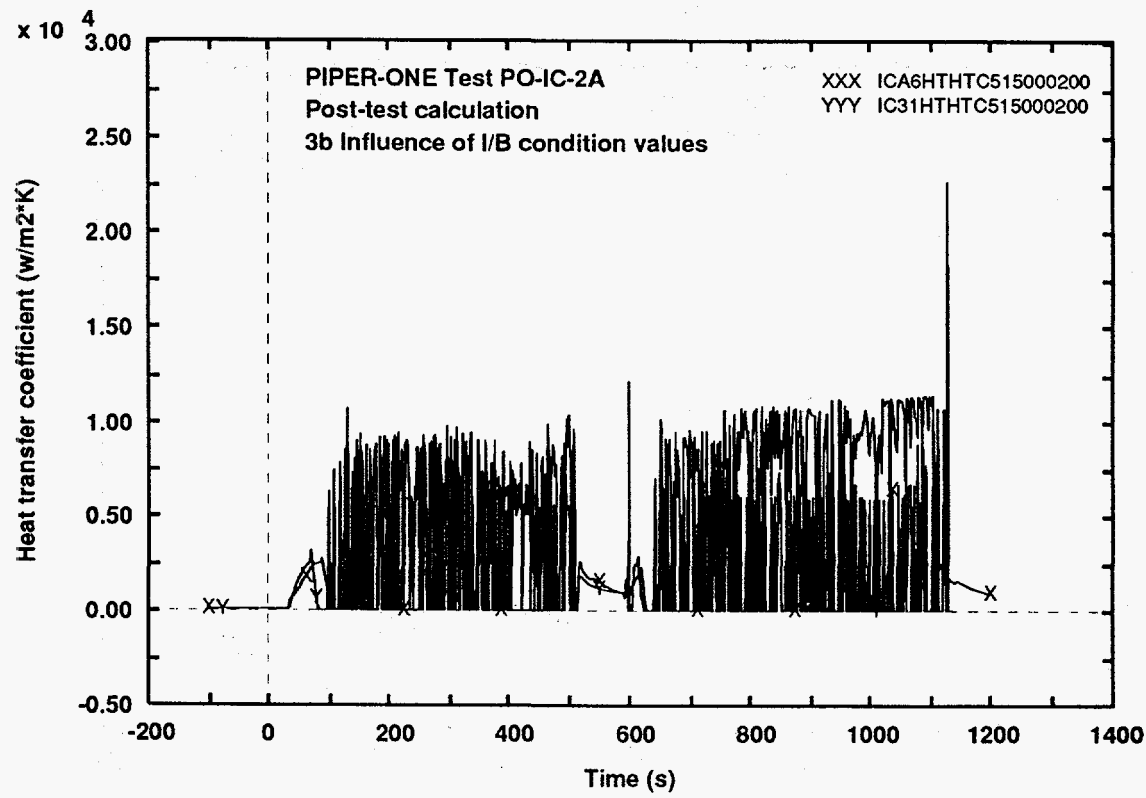


Fig. 44 - Heat transfer coefficient at the inside of IC tubes wall (level 3)

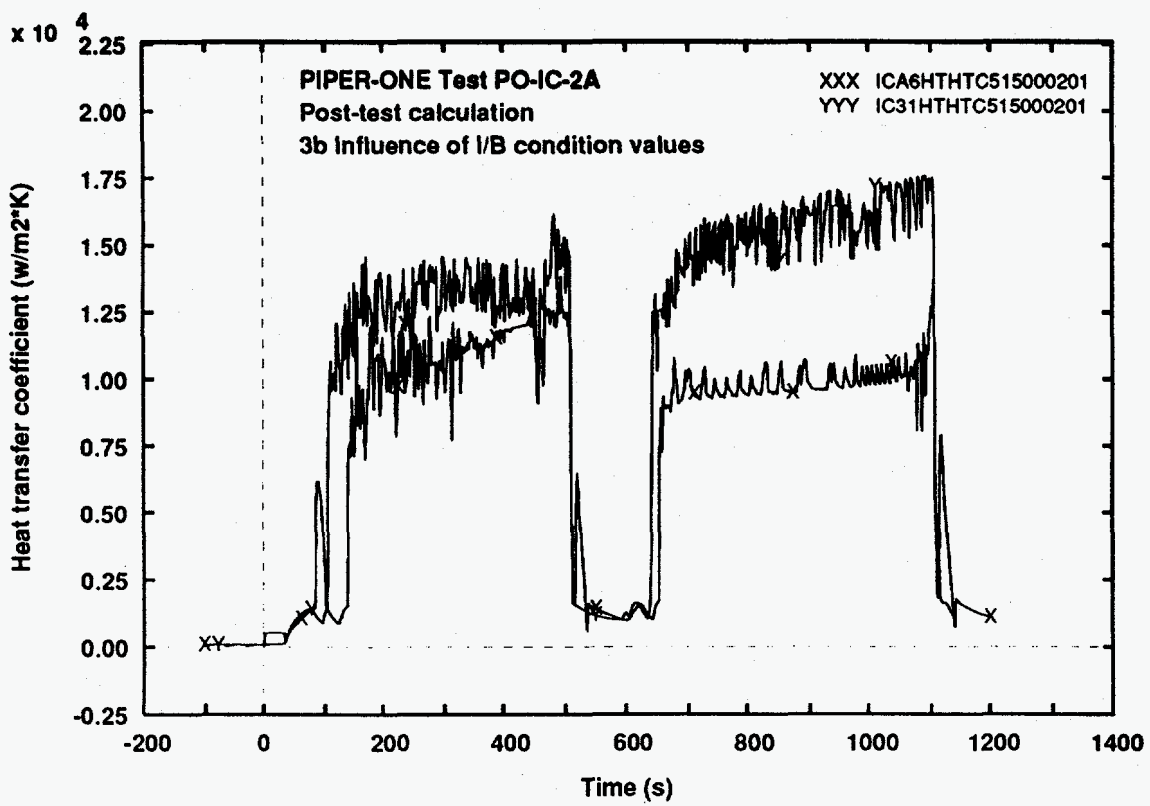


Fig. 45 - Heat transfer coefficient at the outside of IC tubes wall (level 3)

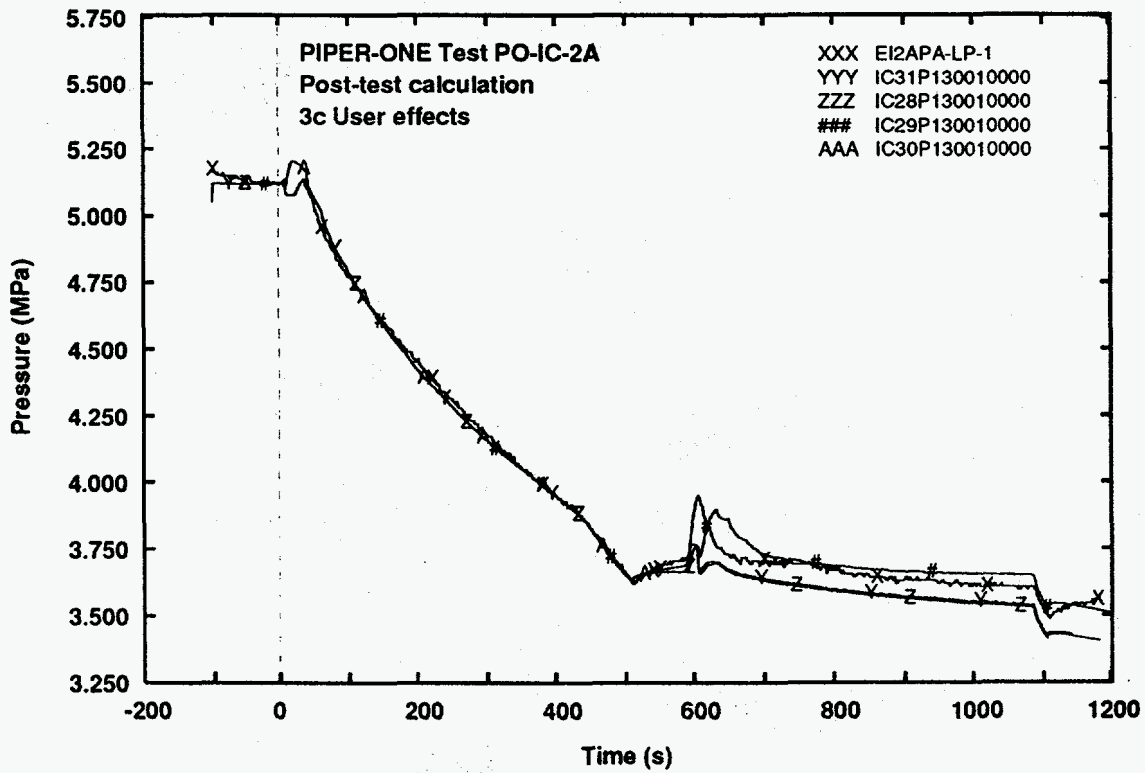


Fig. 46 - Lower plenum pressure

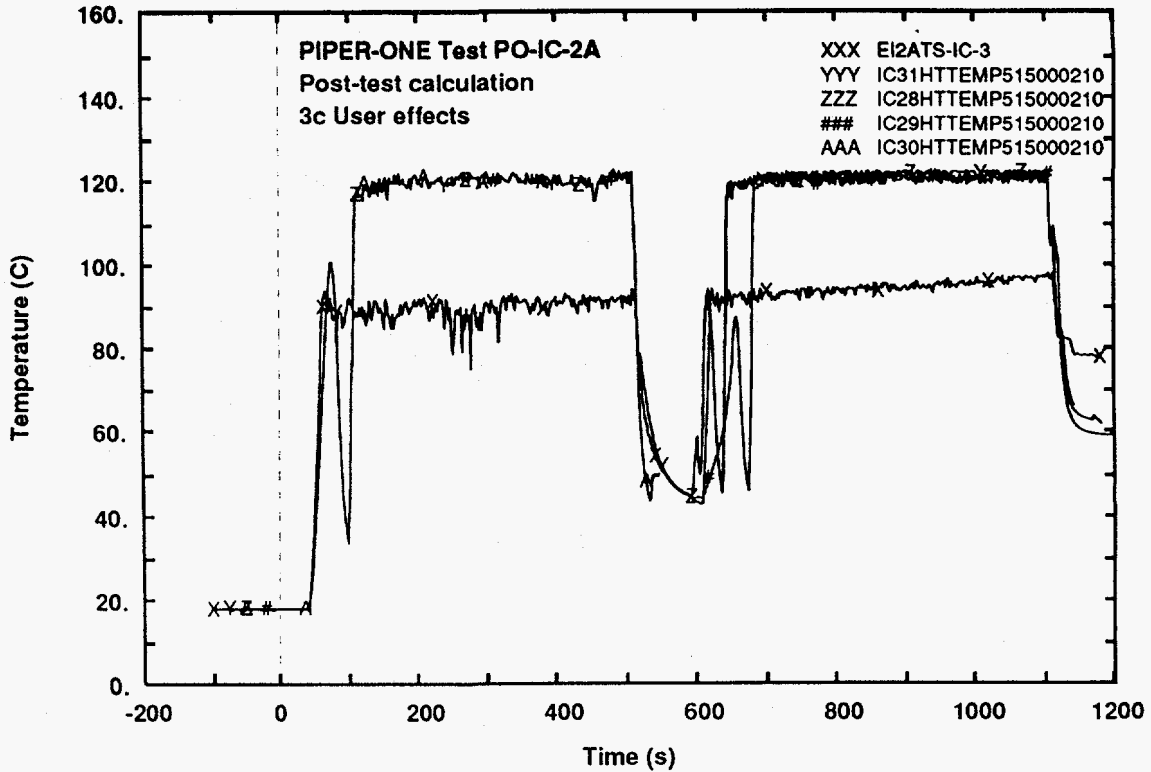


Fig. 47 - IC tubes wall surface temperature (external side level 3)

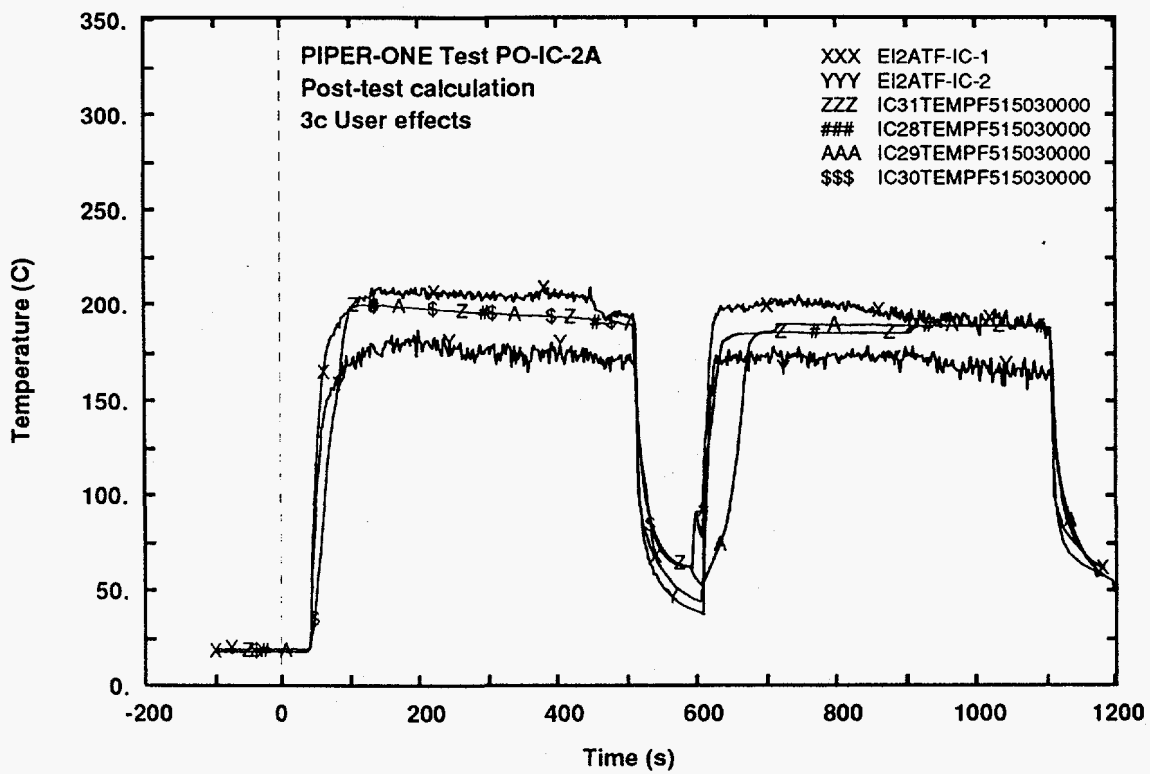


Fig. 48 - IC tubes fluid temperature (middle elevation)

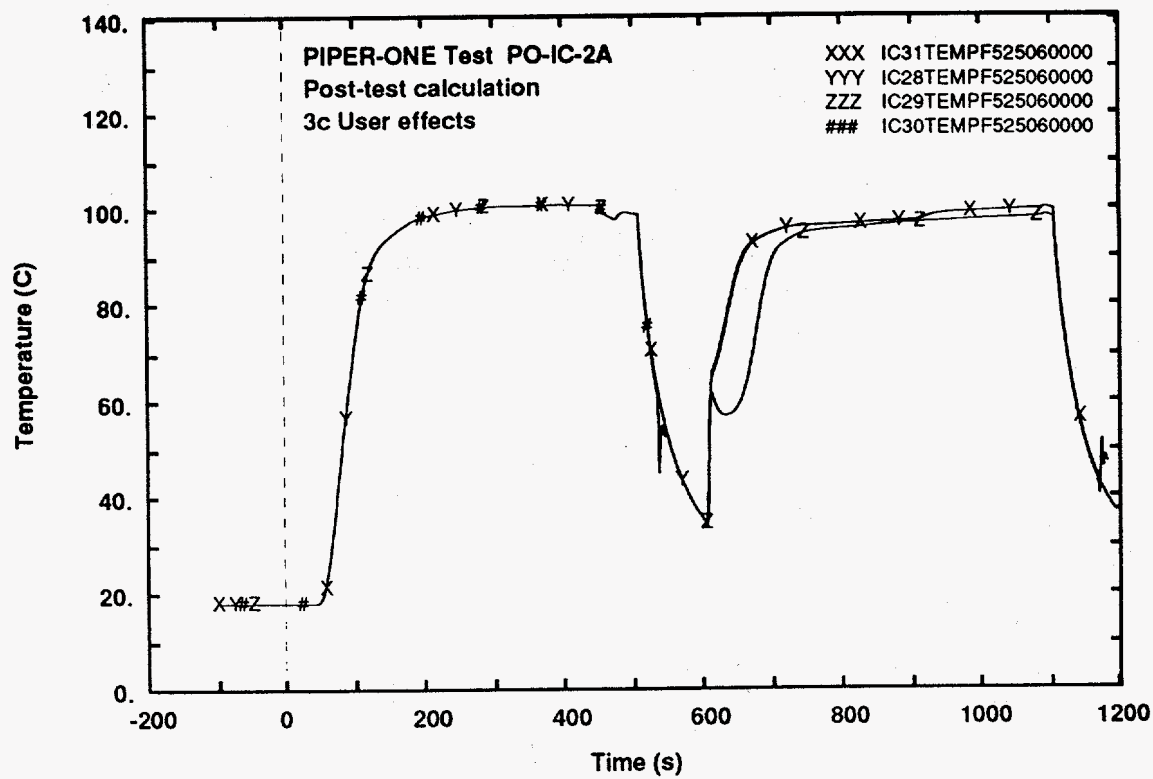


Fig. 49 - IC outlet fluid temperature

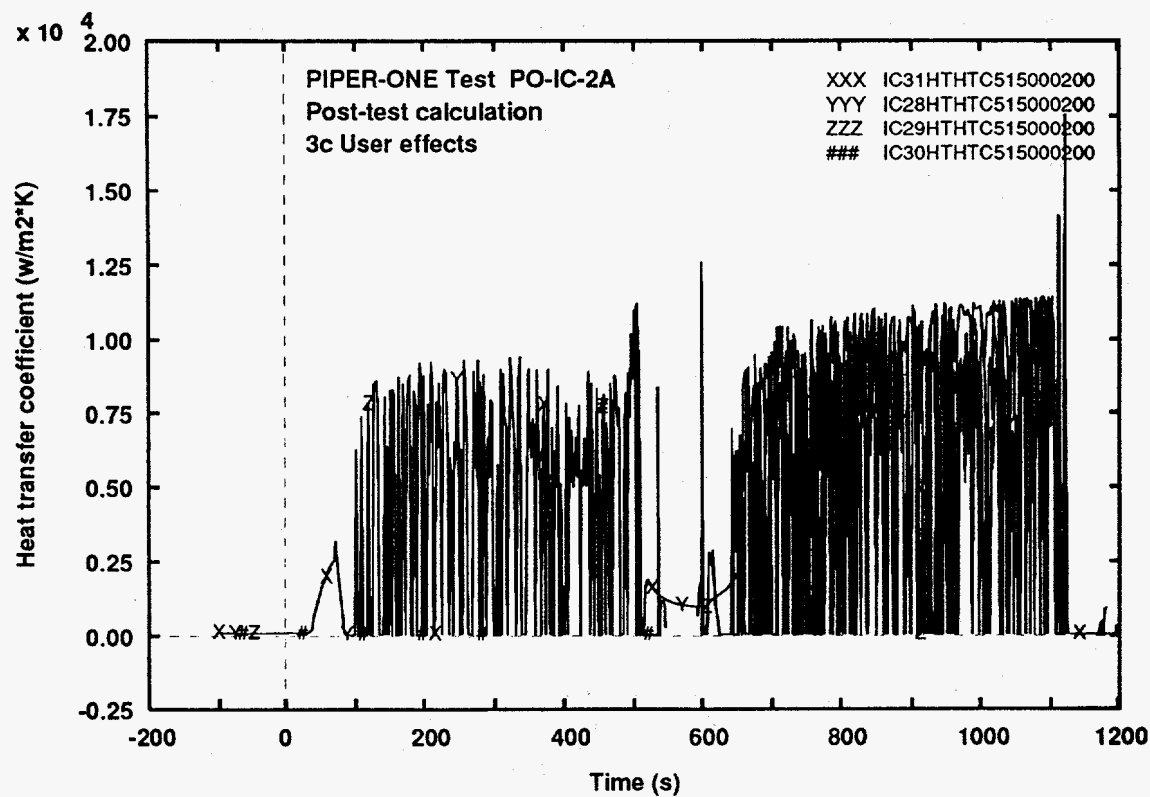


Fig. 50 - Heat transfer coefficient at the inside of IC tubes wall (level 3)

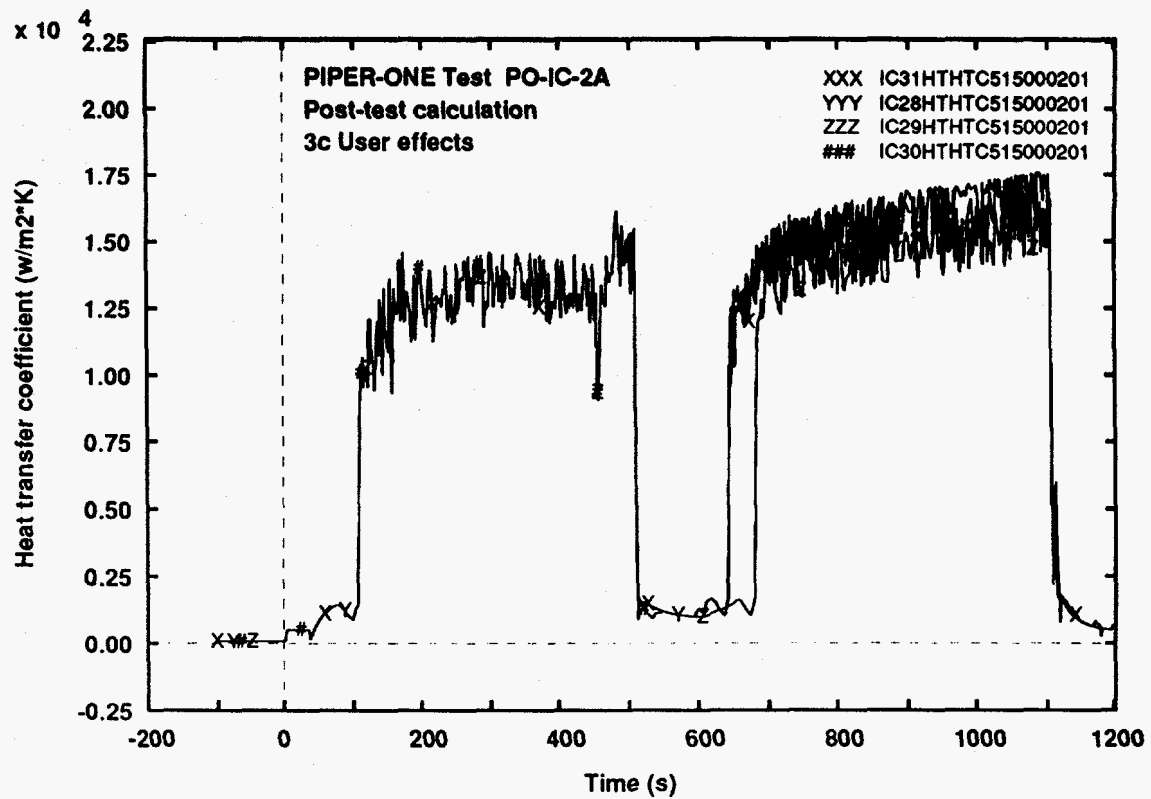


Fig. 51 - Heat transfer coefficient outside of IC tubes wall (level 3)

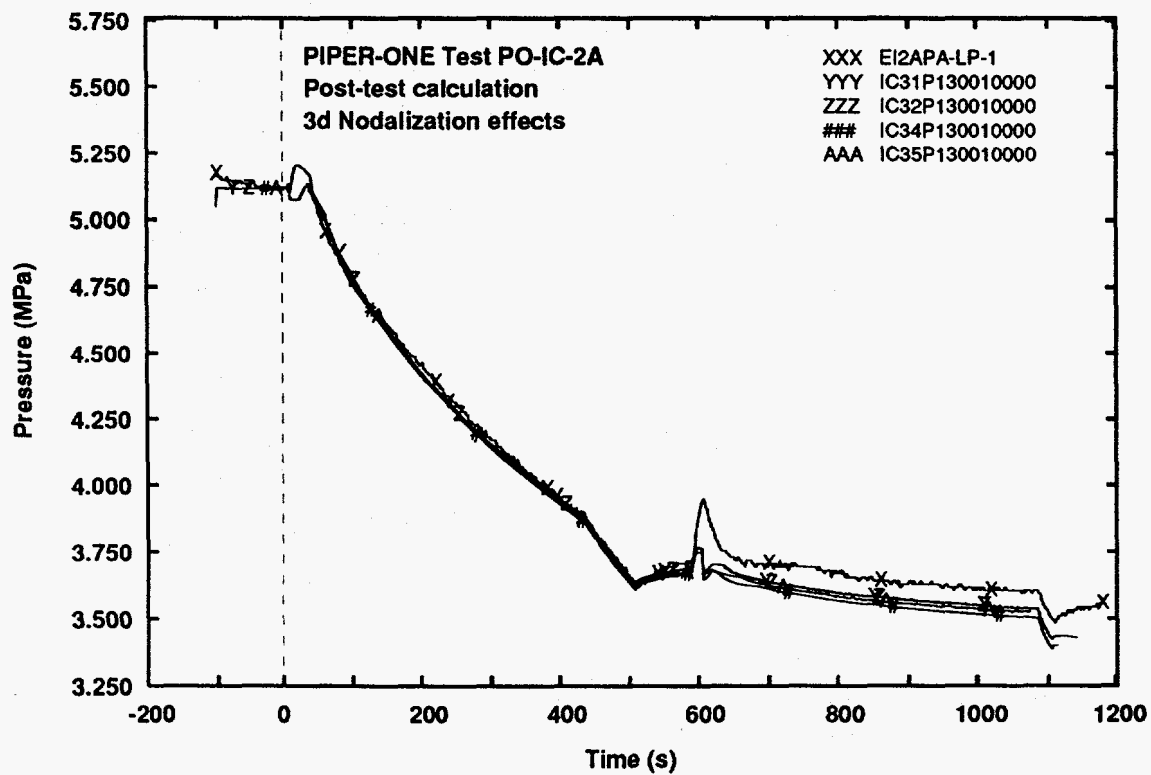


Fig. 52 - Lower plenum pressure

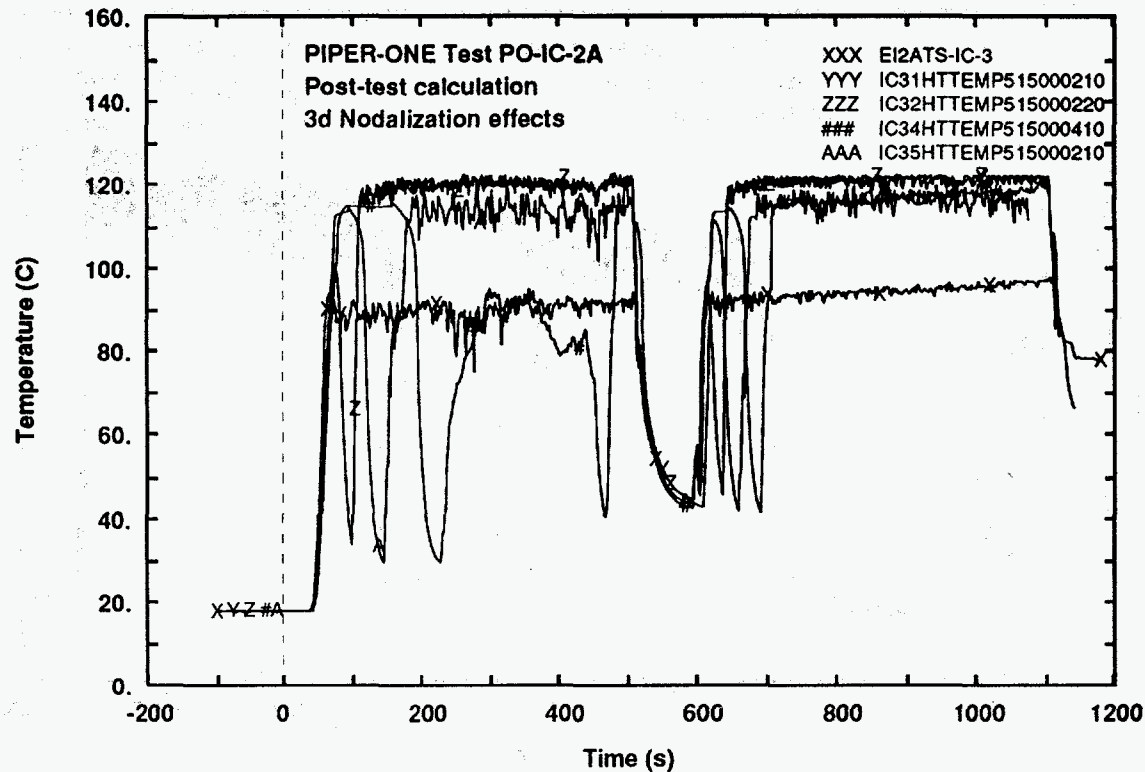


Fig. 53 - IC tubes wall surface temperature (external side level 3)

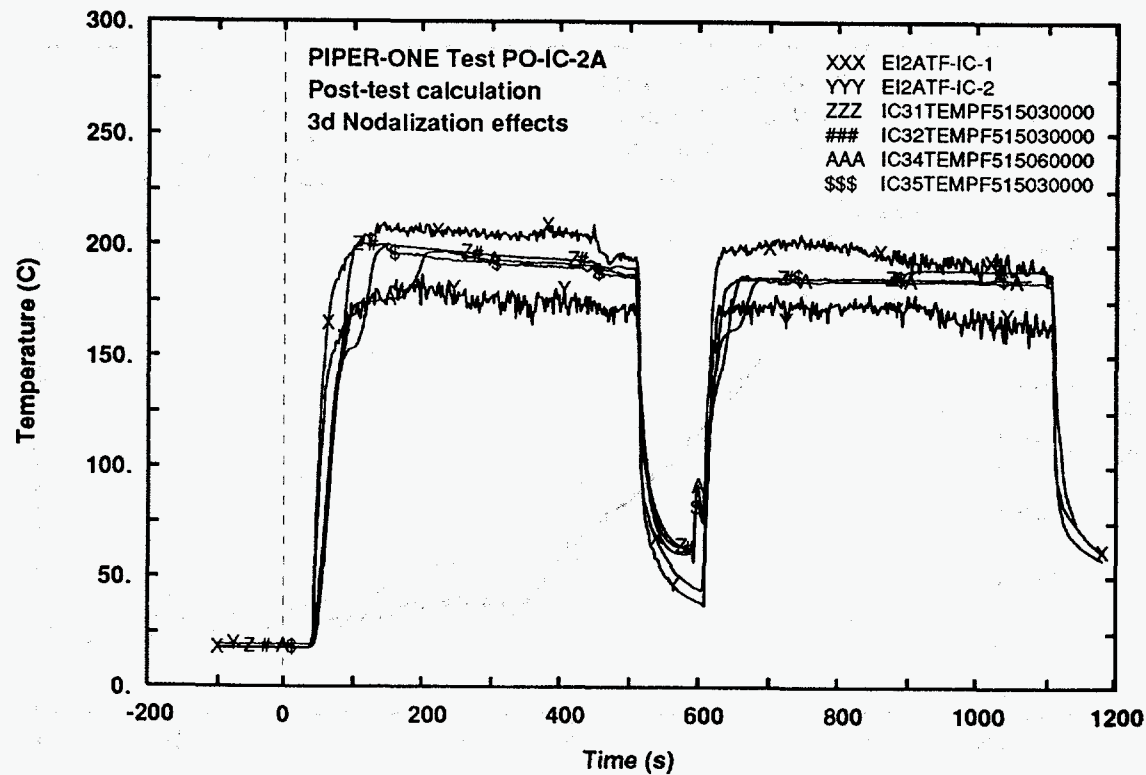


Fig. 54 - IC tubes fluid temperature (middle elevation)

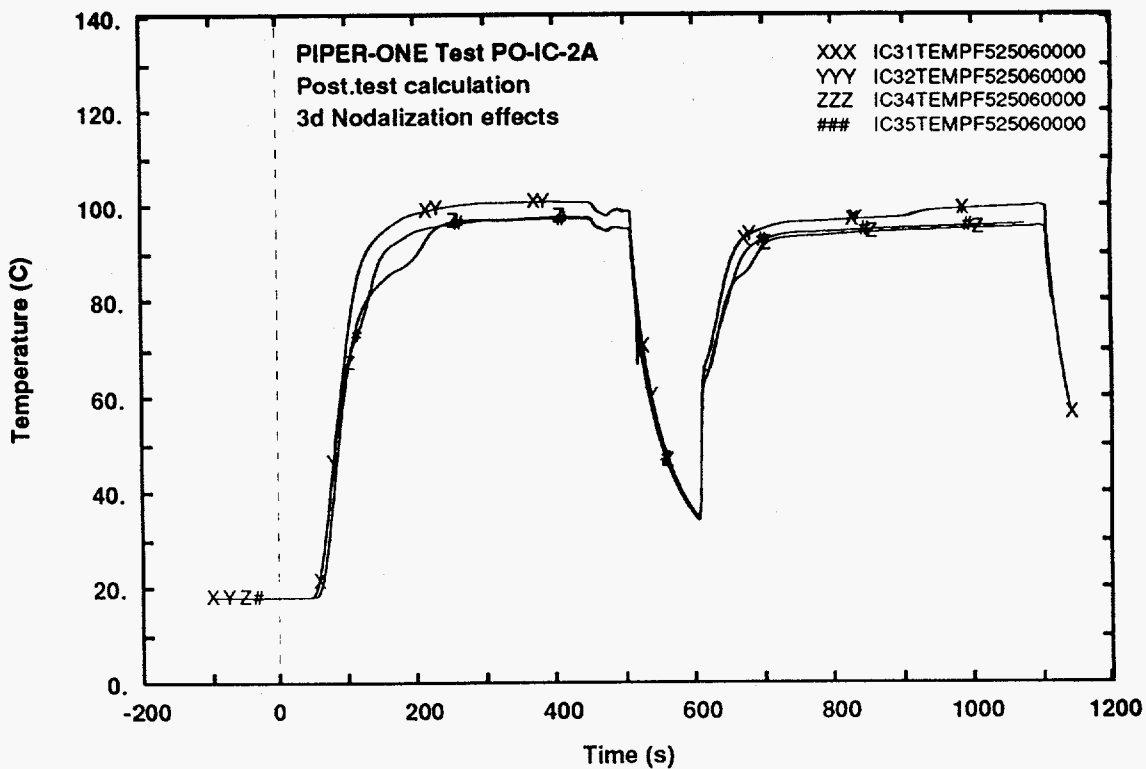


Fig. 55 - IC outlet fluid temperature

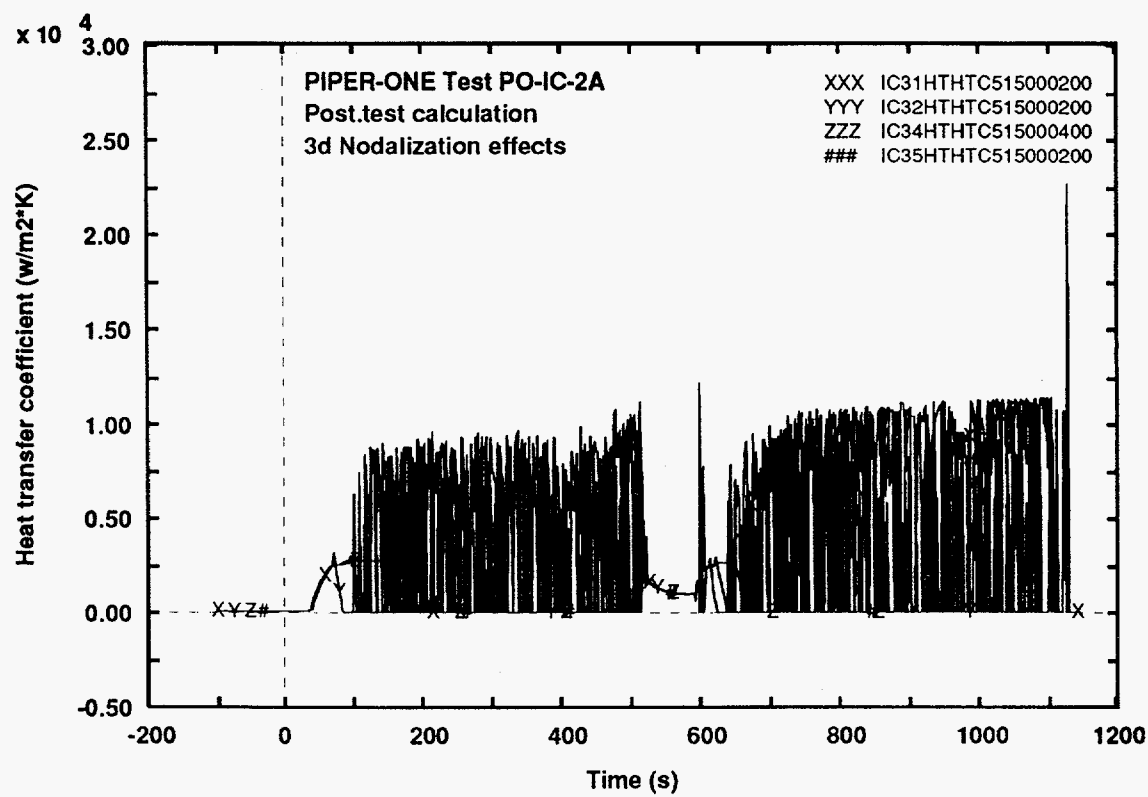


Fig. 56 - Heat transfer coefficient at the inside of IC tubes wall (level 3)

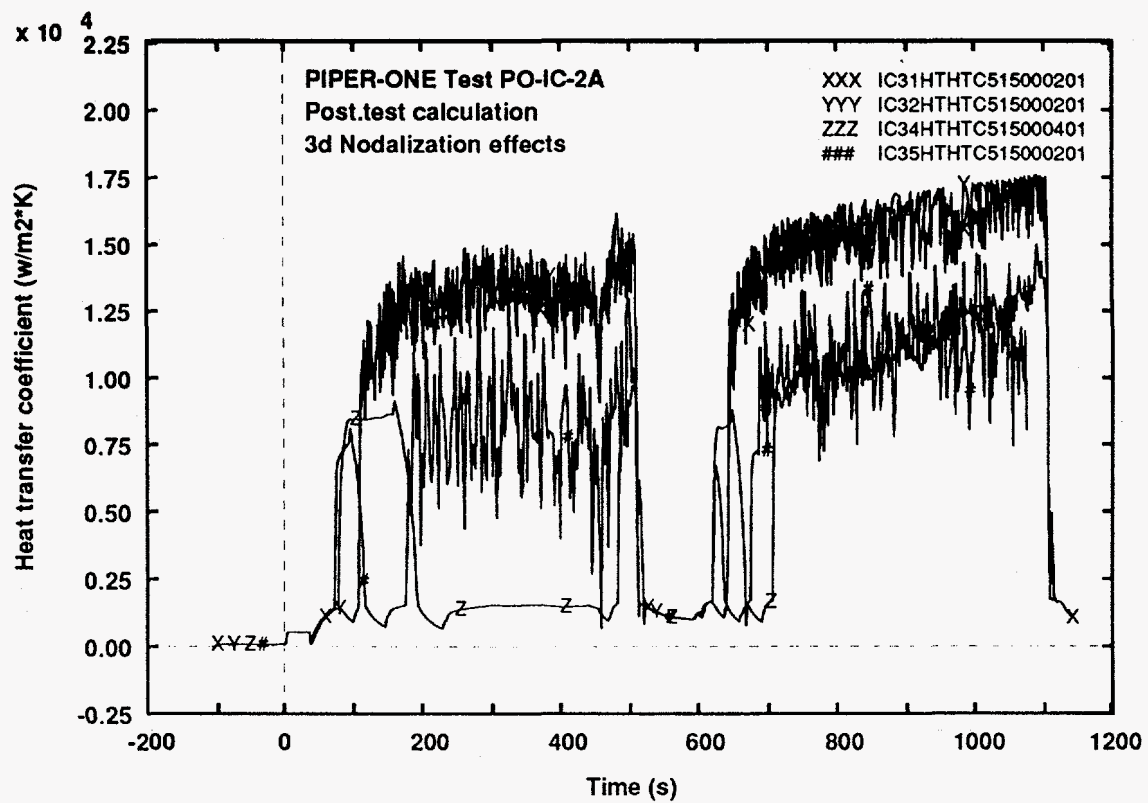


Fig. 57 - Heat transfer coefficient at the outside of IC tubes wall (level 3)

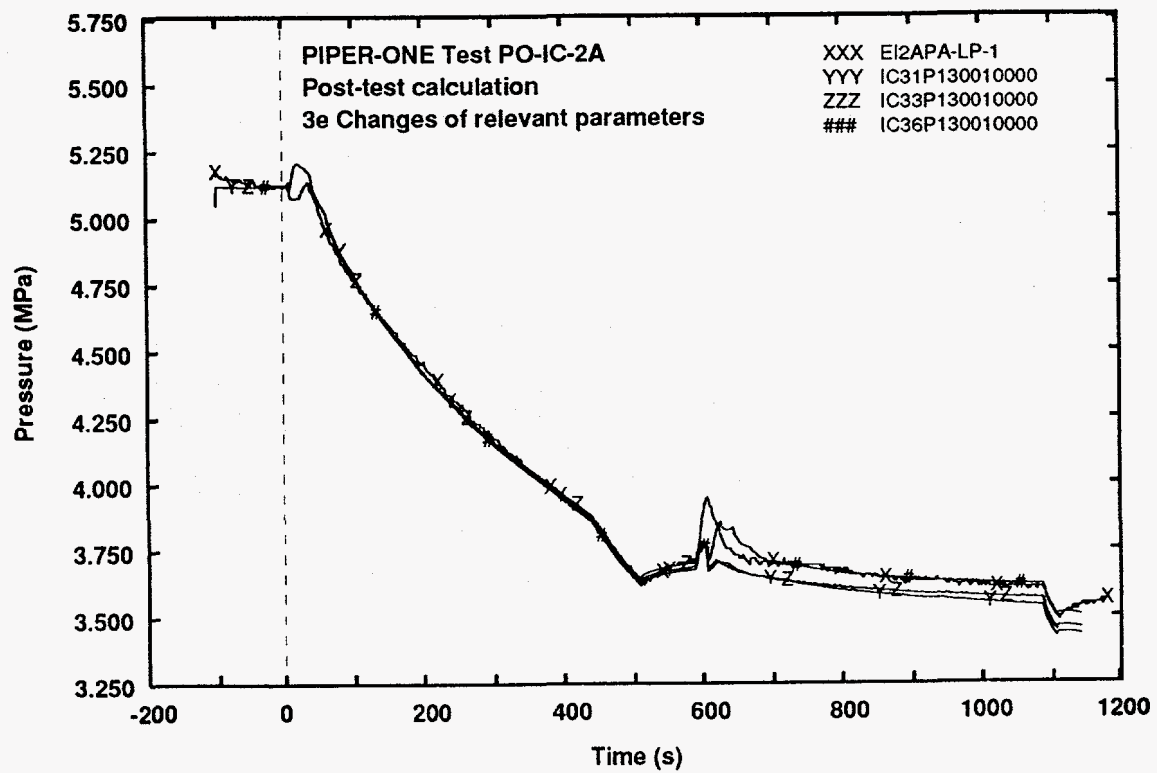


Fig. 58 - Lower plenum pressure

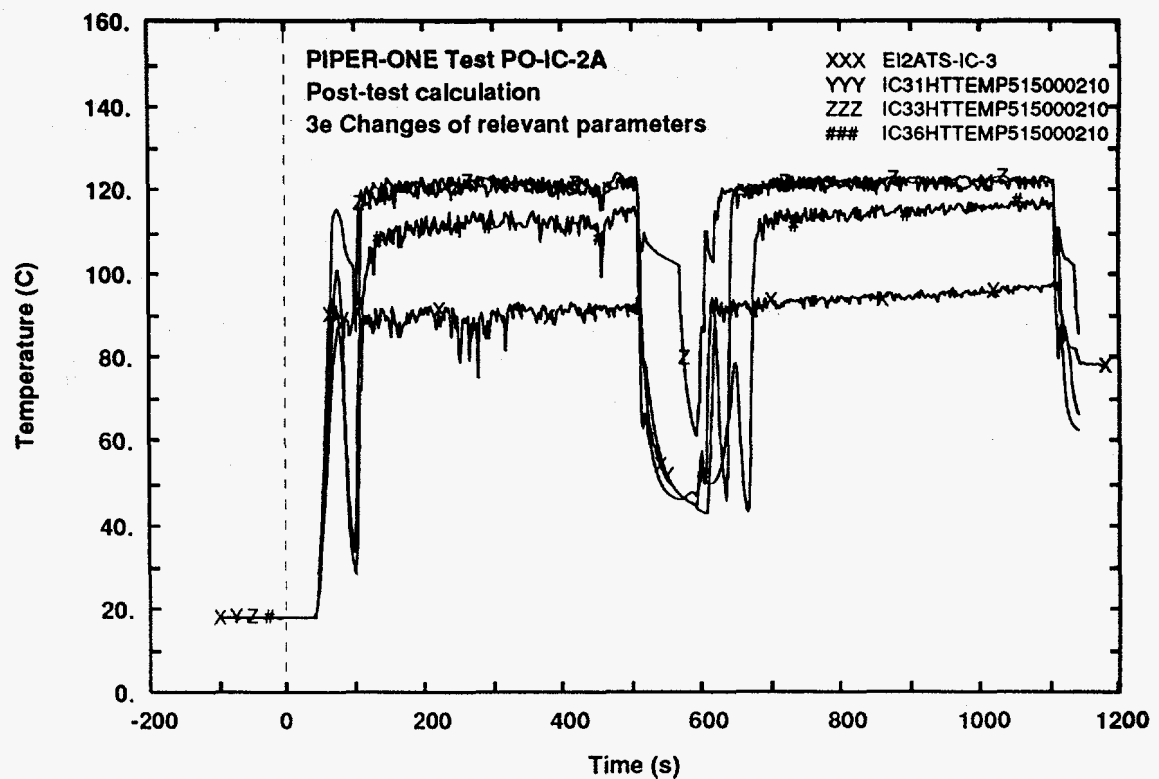


Fig. 59 - IC tubes wall surface temperature (external side level 3)

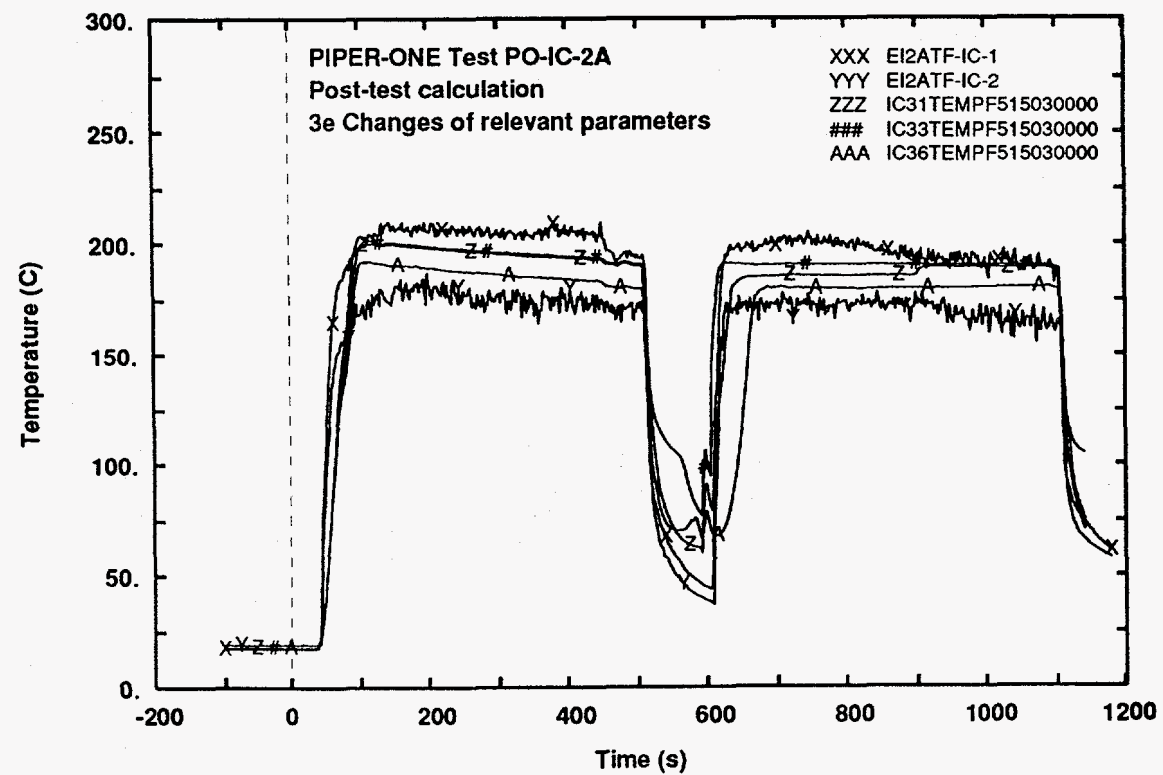


Fig. 60 - IC tubes fluid temperature (middle elevation)

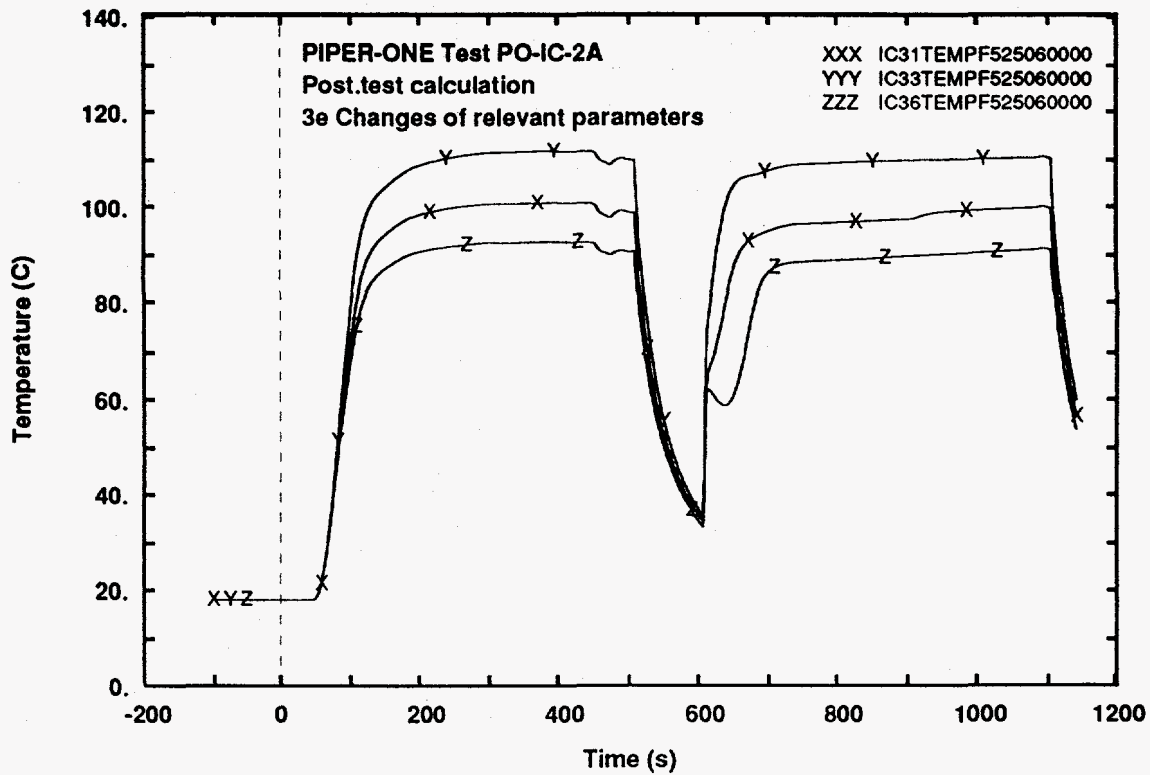


Fig. 61 - IC outlet fluid temperature

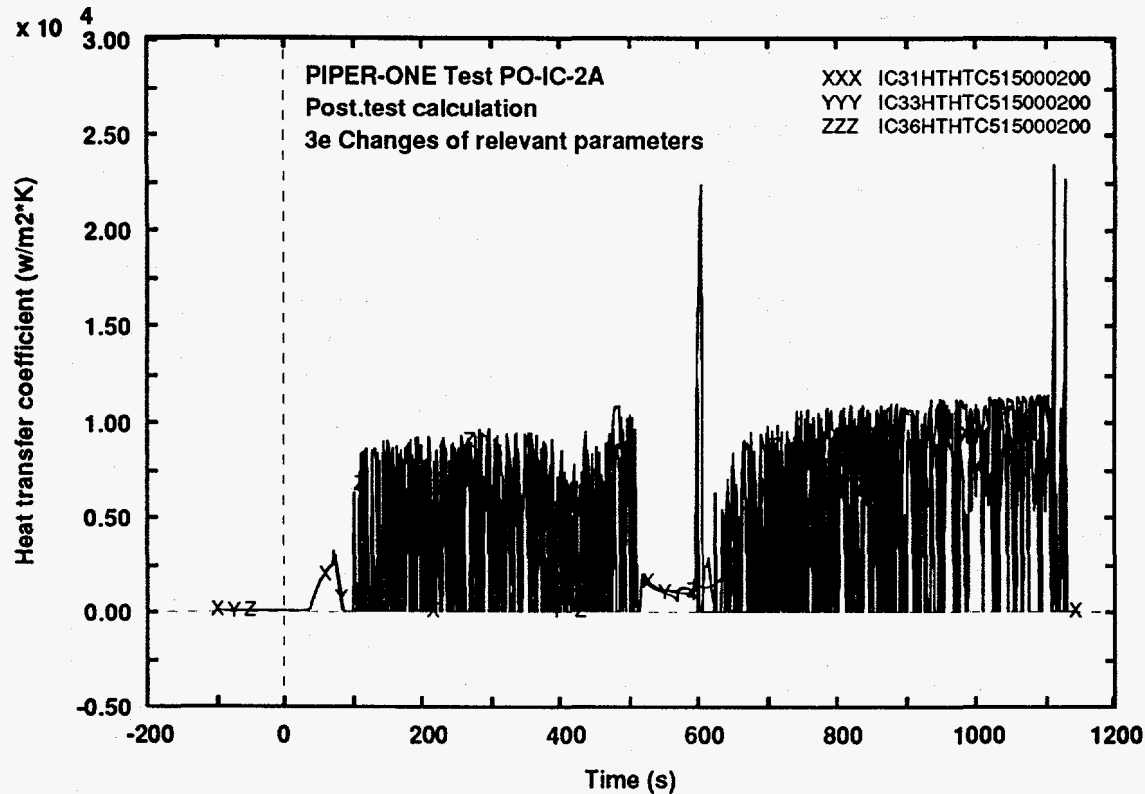


Fig. 62 - Heat transfer coefficient at the inside of IC tubes wall (level 3)

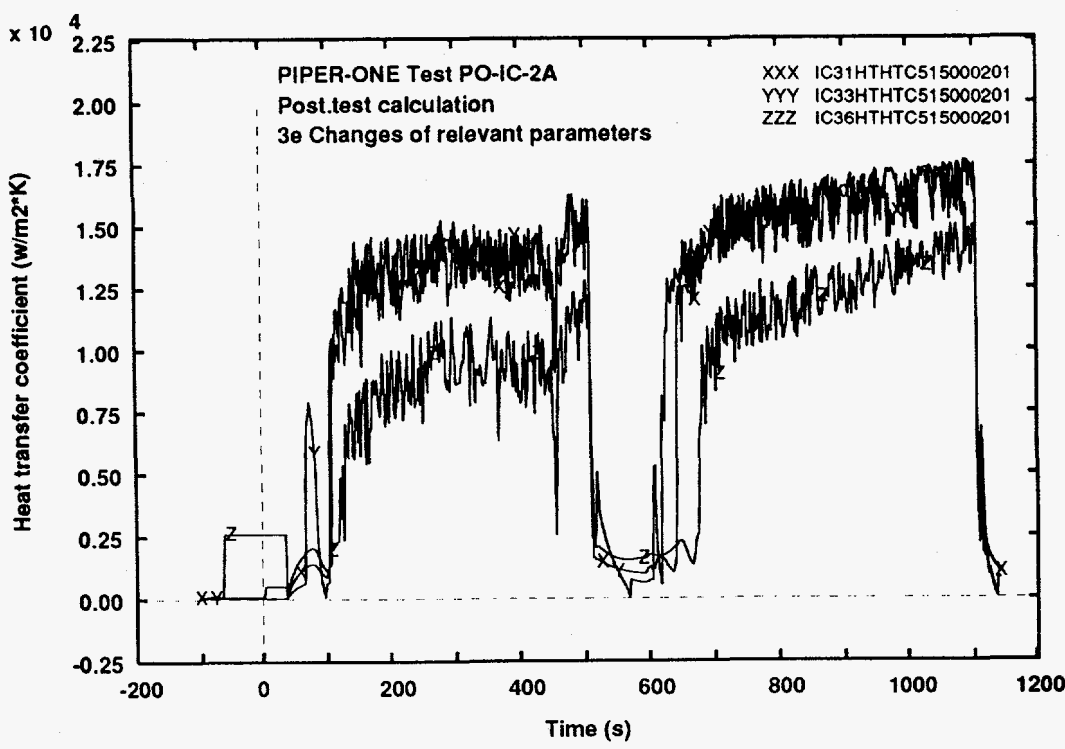


Fig. 63 - Heat transfer coefficient at the outside of IC tubes wall (level 3)

4.3.2 Results in Apps. 2 and 4

The results of calculation IC36 are shown in App. 2. It can be noted that the (arbitrary) variation (i.e. reduction) in the hydraulic diameter value of the pool nodes largely improves the comparison between measured and predicted wall temperatures (e.g. Figs. 17 and 18 in App. 2) with respect to the reference calculation IC31 (see also data in the last columns of Tab. XI). The primary side related quantities are either unaffected (e.g. downcomer level, Fig. 2 of App. 2), either better predicted (e.g. pressure, Fig. 1 in App. 2).

The results related to the calculation ICA6 are reported in App. 4, just because ICA6 can be considered as a blind post test. Some comments have already been given above.

4.3.3 Isolation of downcomer (App. 3)

The isolation of downcomer was assumed to demonstrate that IC flowrate and exchanged power increase with core supplied power, if the IC constitutes the only path for the steam coming from the core.

The IC37 calculation has the same input as the IC31 calculation, the only difference being the closure of the isolation valve between core and downcomer region at 300 s into the transient. The following effects can be noted:

- IC flowrate in Ph.W 2 increases after the isolation (Fig. 7 of App. 3);
- IC flowrate in Ph.W 4 is larger than in Ph.W 2 (Fig. 7 of App. 3);
- as a consequence of the above, IC exchanged power is also larger (Fig. 28 of App. 3) in Ph.W 4 with respect to Ph.W 2; this conclusion can also be inferred from the primary circuit pressure (Fig. 1 of App. 3) that decreases during Ph.W 4;
- condensing steam is present in the third volume from the top (Fig. 35 of App. 3): this is the local cause for the increase of the IC exchanged power as also results from observing HTC in Fig. 33 of App. 3;
- the pressure peak in Ph.W 3 is better predicted in calculation IC37 than in calculation IC31. This confirms the conclusion that pressure increase in the test is caused by steam production without circulation from the downcomer: the consequent stratification effect is underestimated by the code in the reference calculation.

4.4 Scaling analysis

The problem to be raised in the frame of a scaling study, can be synthesized by the following questions:

- ♦ is the experimental data base representative of situations expected in the reference plant (SBWR in this case)?
- ♦ are the code capabilities and limits (detected in this study) applicable to plant predictions?

The first question is addressed in the present framework (details in App. 6, ref. /22/). The second question needs the availability of counterpart tests; some aspects are discussed in ref. /23/.

A few details, taken from App. 6, are reported below.

The following parameters are considered in the analysis of scaling efforts:

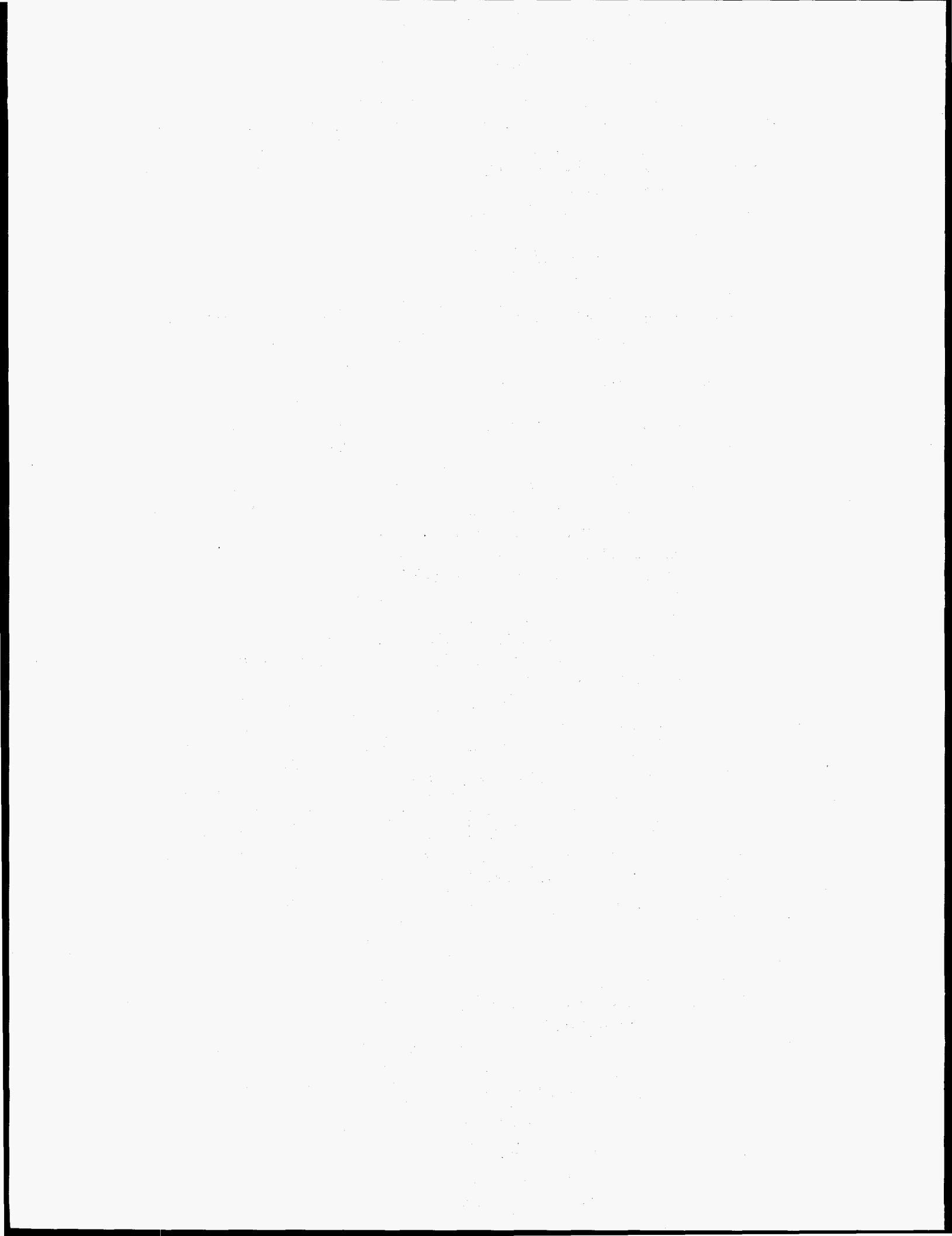
- 1) Elevation of IC relative to TAF;
- 2) Length of IC tubes;
- 3) Diameter of IC tubes;
- 4) Total heat exchange area of IC;
- 5) Inlet flow area of IC.

Each of the selected parameters is varied in the range from the actual value up to the right scaled value and for each variation a new nodalization is set up and a calculation is run. A final calculation is performed including all the variations at the same time.

The results can be summarized as follows:

- a) no new phenomena occurred in any of the calculations;
- b) the most important parameter in this analysis, i.e. the largest scaling distortions in PIPER-ONE apparatus, is constituted by the elevation of the IC (parameter nr. 1), above).

The qualitative scenario in the final calculation (i.e. the one including all the variations) does not differ from the experimental scenario.



5. CONCLUSIONS

The present document reports the analysis performed with Relap5 in relation to the PIPER-ONE experiment PO-IC-2. The test is the follow-up of the similar experiment PO-SD-8 and aims at characterizing phenomena connected with the operation of Isolation Condenser in a geometric configuration typical for SBWR. The test studied was conducted at high pressure (around 5 MPa) to study code performances in this situation.

Conclusion can be drawn in relation to:

- A) overall system performance;
- B) thermalhydraulic phenomena inside the IC;
- C) code capabilities;
- D) effect of various changes in the calculation conditions.

It has been confirmed that a constant removed power characterizes the IC performance (item A)) whatever are the primary loop thermalhydraulic conditions. From the analysis of experimental data supported by specific code calculations, the reason why IC exchanged power remains constant, when core power conditions are varied, has been made clear. This is a consequence of IC flowrate that is determined by the pressure difference created in the downcomer of the main loop; this remains almost constant during the performed experiment. Constant IC flowrate means constant condensation length in the IC tubes and constant transferred power to the pool (see also below).

The shroud put in the pool was not effective in provoking natural circulation because of the high conductivity across its wall, that led to fluid temperature stratification with the same characteristics in the inner and outer zones of the pool.

Heat transfer coefficients are several (3-7) times larger in the condensing zones of the IC tubes than in the single phase liquid region (item B)); the fluid pool temperature increase (up to 70 K) has a negligible role in this connection (high pressure steam). Liquid level in the IC remains almost constant when varying core power.

A new detailed nodalization of PIPER-ONE apparatus was adopted for this study. The standard version of Relap5/mod3.1 is able to catch the overall phenomenology during the four main periods of the experiment (item C)).

Discrepancies have been identified mainly concerning the IC tubes surface temperatures, that are overestimated by the code, particularly on the outer surface: this means underestimation by the code of the outer heat transfer coefficient, provided that the overall exchanged power is well predicted. However the possible "fin" effect originated by thermocouples has not been considered in this conclusion. An unphysically high heat transfer coefficient is produced in the output by the code although apparently not used (Tab. IX). During the phenomenological window nr 3 (i.e. during the period of power shut-off) the code was not able to simulate the condensation shock occurring in the IC line.

An extensive series of sensitivity calculations has been carried out (item D)). These demonstrated:

- * some improvements in the code results when passing from the earliest to the latest Relap5/mod3 code versions; however oscillations in condensation heat transfer value are much larger in the reference code version. Furthermore the transition logics from heat transfer mode 2 to 3 (and viceversa) could be improved;
- * changes in the equivalent diameter of the pool side of the IC has an important effect on the calculation of the local quantities like heat transfer coefficient and temperatures;
- * changes in nodalization can also have a noticeable effect as far as the calculation of the above mentioned quantities is concerned. The last item stressed the need to define some relationship between the (condensation) heat transfer coefficient and the average node

dimensions: this seems necessary to get reproducible results especially when condensation heat transfer is involved.

The performed scaling analysis (see also App. 6) demonstrated that the scaling distortions identified in the PIPER-ONE hardware, do not affect, qualitatively, the phenomena occurring during the selected experiments.

Analyses, related to the same test have been carried out by CATHARE code, e.g. ref. /24/.

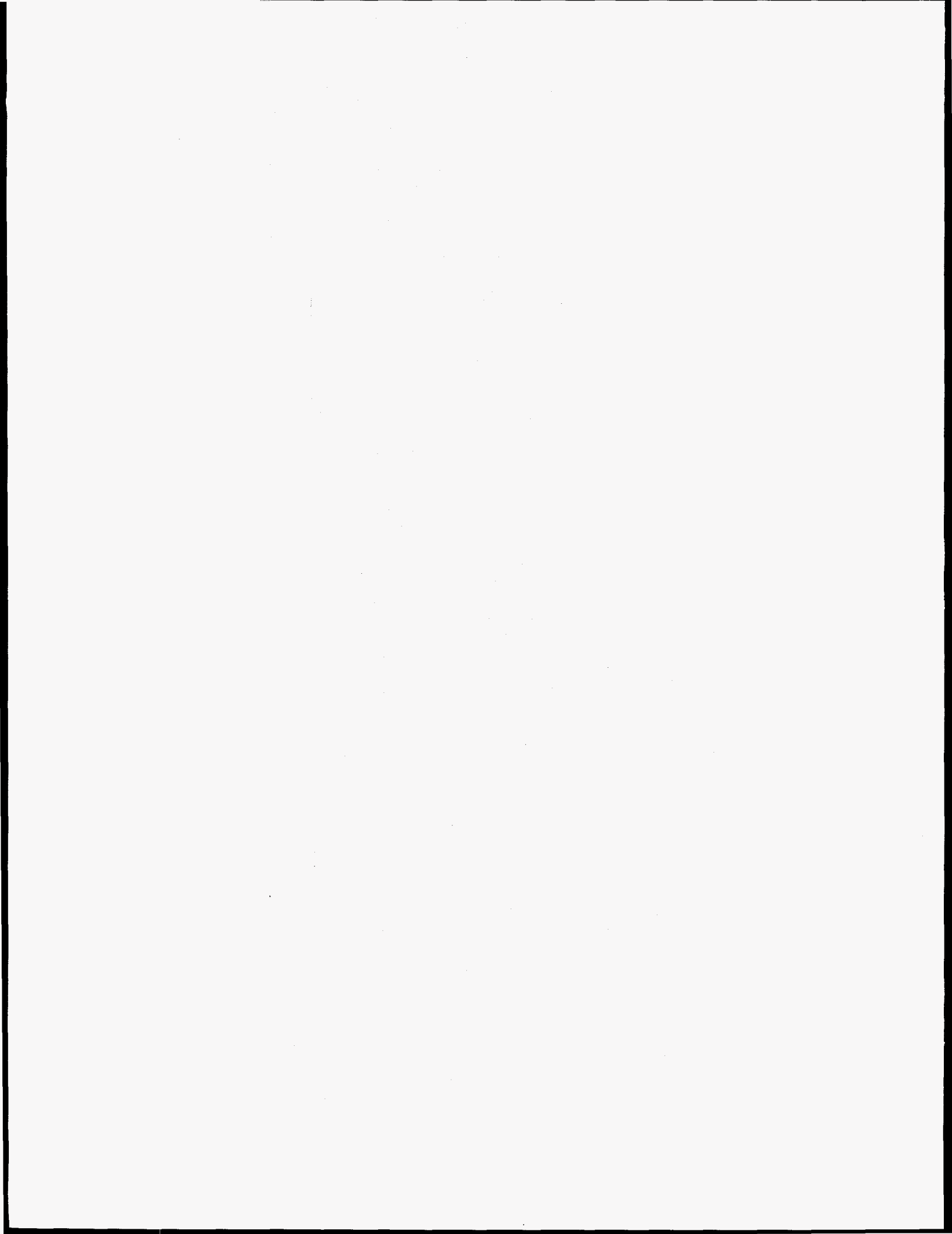
Further activity in this area includes the analysis of a companion experiment during which nitrogen gas was injected into the primary circuit and actually caused large degradation of the IC removed power.

REFERENCES

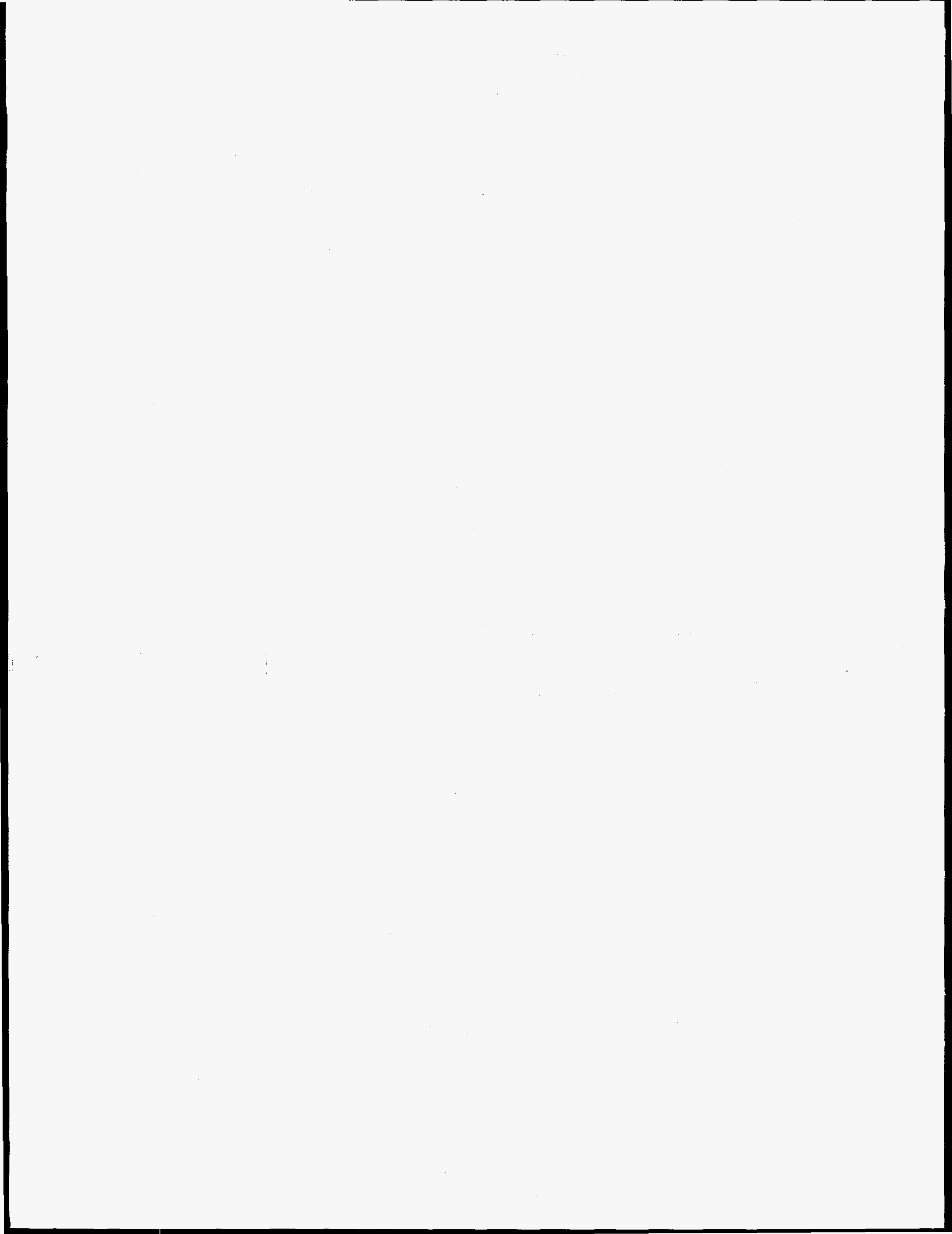
- /1/ D'Auria F., Modro M., Oriolo F., Tasaka K.: "Relevant Thermalhydraulic Aspects of New Generation LWR's"
CSNI Spec. Meet. On Transient Two-Phase Flow - System Thermalhydraulics, Aix-En-Provence (F), April 6-8, 1992.
- /2/ D'Auria F., Galassi G.M., Oriolo F.: "Thermalhydraulic Phenomena and Code Requirements for Future Reactors Safety Analysis"
Int. Conf. on Design and Safety of Nuclear Power Plants (ANP) - Tokyo (J), October 25-29, 1992.
- /3/ Andreuccetti P., Barbucci P., Donatini F., D'Auria F., Galassi G.M., Oriolo F.: "Capabilities of the RELAP5 in Simulating SBWR and AP-600 Thermalhydraulic Behaviour"
IAEA Technical Committee Meet. (TCM) on Progress in Development and Design Aspects of Advanced Water Cooled Reactors, Rome (I), September 9-12, 1991.
- /4/ Bovalini R., D'Auria F., Mazzini M.: "Experiments of Core Coolability by a Gravity Driven System Performed in Piper-One Apparatus"
ANS Winter Meeting, San Francisco (CA), November 10-15, 1991.
- /5/ Bovalini R., D'Auria F., Mazzini M., Vigni P.: "Isolation Condenser Performances in PIPER-ONE Apparatus"
1992 European Two-Phase Flow Group Meet., Stockholm (S), June 1-3, 1992.
- /6/ D'Auria F., Vigni P., Marsili P.: "Application of Relap5/Mod3 to the Evaluation of Isolation Condenser Performance"
Int. Conf. on Nuclear Engineering (ICONE-2) - San Francisco (US), March 21- 24, 1993
- /7/ Bovalini R., D'Auria F., Galassi G.M., Mazzini M.: "Piper-One Research: the Experiment PO-SD-8 Related to the Evaluation of Isolation Condenser Performance. Post-Test Analysis Carried out by Relap5/Mod3-7J code"
University of Pisa Report, DCMN - NT 200 (92), Pisa (I), November 1992.
- /8/ D'Auria F., Galassi G.M., Mazzini M., Pintore S.: "Ricerca Piper-One: specifiche dettagliate della prova PO-IC-2"
University of Pisa Report, DCMN - NT 234(94), Pisa (I), Giugno 1994.
- /9/ Ransom V.H., Wagner R.J., Trapp J.A., Jonhsen G.W., Miller C.S., Kiser D.M., Riemke R.A.: "Relap5/mod2 Code Manual - Vol. 1: Code Structure, Systems and Solution Methods"
NUREG/CR-4312 EGG 2396 - EGG Idaho Inc., March 1987.
- /10/ Carlson K.E., Riemke R.A., Rouhani S.Z., Shumway R.W., Weaver W.L.: "Relap5/Mod3 Code Manual - Volume II. User Guide and Input Requirements"
NUREG/CR-5535, June 1990.

- /11/ D'Auria F., Oriolo F., Bella L., Cavicchia V.: "AP-600 Thermalhydraulic Phenomenology: A Relap5/mod2 Model Simulation"
 Int. Conf. on New Trends in Nuclear System Thermohydraulics - Pisa (I), May 30 - June 2 1994
 Int. Top. Meeting on Advanced Reactor Safety - Pittsburgh (PA) April 17-21, 1994
- /12/ Barbucci P., Bella L., D'Auria F., Oriolo F.: "SBWR Thermalhydraulic Performance: a RELAP5/MOD2 Model Simulation"
 6th Int. Top. Meet. on Nuclear Reactor Thermalhydraulics, Grenoble (F), Oct. 5-8 1993
- /13/ Bovalini R., D'Auria F., Di Marco P., Galassi G.M., Giannecchini S., Mazzini M., Mariotti F., Piccinini L., Vigni P.: "PIPER-ONE: a Facility for the Simulation of SBLOCA in BWRs"
 Spec. Meet. on Small Break LOCA Analyses in LWRs, Pisa (I), June 23-27 1985
- /14/ Bovalini R., D'Auria F., Mazzini M., Pintore S., Vigni P.: "PIPER-ONE Research: Overview of the Experiments Carried out"
 9th Conf. of Italian Society of Heat Transport, Pisa (I), June 13-14 1991
- /15/ Bovalini R., D'Auria F., Mazzini M., Pintore S., Vigni P.: "PIPER-ONE Research: Lesson Learned"
 9th Conf. of Italian Society of Heat Transport, Pisa (I), June 13-14 1991
- /16/ D'Auria F., Fruttuoso G.: "OECD CSNI ISP 21, PIPER-ONE Test PO-SB-7: Post-Test Analysis Performed at Pisa University by RELAP5/MOD2 Code"
 University of Pisa Report, DCMN - RL 386 (89), Pisa (I), March 1989
 OECD CSNI 2nd Workshop on ISP 21, Calci (I), Apr. 13-14 1989
- /17/ D'Auria F., Galassi G.M., Mazzini M.: "PIPER-ONE Research: Specifications of PO-SD-8 Experiment" (in Italian)
 University of Pisa Report, DCMN - NT 190 (92), Pisa (I), Jan. 1992
- /18/ Ambrosini W., D'Auria F., Galassi G.M., Mazzini M., Virdis M.: "Preliminary Planning of BIP Tests to be Performed in PIPER-ONE Apparatus"
 University of Pisa Report, DCMN - NT 207 (93), Pisa (I), May 1993.
- /19/ D'Auria F., Mazzini M., Oriolo F., Paci S.: "Comparison Report of the OECD/CSNI International Standard Problem 21 (PIPER-ONE Experiment PO-SB-7)"
 CSNI Report Nr. 162, Paris (F), Nov. 1989
- /20/ Bajs T., Bonuccelli M., D'Auria F., Debrecin N., Galassi G.M.: "On Transient Qualification of LOBI/MOD2, SPES, LSTF, BETHSY and KRSKO Plant Nodalizations for RELAP5/MOD2 Code"
 University of Pisa Report, DCMN - NT 185(91), Pisa (I), Dec. 1991
- /21/ Brandani M., Rizzo F.L., Gesi E, James A.J.: "SBWR-IC &PCC Systems: an Approach to Passive Safety"
 IAEA Technical Committee Meet. (TCM) on Progress in Development and Design Aspects of Advanced Water Cooled Reactors, Rome (I), September 9-12, 1991

- /22/ D'Auria F., Faluomi V.: "Qualitative Analysis of Scaling Effects in Isolation Condenser Behaviour with RELAP5/MOD3.1 Thermalhydraulic Code"
ICONE-4 Conference, New Orleans (US), March 10-14, 1996
- /23/ D'Auria F., Faluomi V., Vigni P.: "Evaluation of Hardware Data in Thermalhydraulic Facilities Relevant to SBWR Technology"
2nd European Thermal Sciences and 14th UIT Nat. Heat Transfer Conf., Roma (I), May 29-31, 1996
- /24/ D'Auria F., Mazzini M., Kalli H., Sorjonen J.: "Application of CATHARE Code to the Isolation Condenser Experiment in PIPER-ONE Loop"
ICONE-4 Conference, New Orleans (US), March 10-14, 1996
- /25/ Billa C., D'Auria F., Di Marco P., Mazzini M., Vigni P.: "PIPER-ONE Research: Facility Description for OECD-CSNI International Standard Problem N. 21 (ISP 21)"
University of Pisa Report, DCMN - RL 246(86), Pisa (I), Sept. 1986
OECD CSNI 1st Workshop on ISP 21, Marina di Grosseto (I), Sept. 22-23 1986
- /26/ Cioni L., D'Auria F., Di Marco P., Galassi G.M., Mazzini M.: "PIPER-ONE Research: Boundary and Initial Conditions for OECD-CSNI International Standard Problem 21 (ISP 21)"
University of Pisa Report, DCMN - RL 247(86), Pisa (I), Sept. 1986
OECD CSNI 1st Workshop on ISP 21, Marina di Grosseto (I), Sept. 22-23 1986
- /27/ Billa C., Bovalini R., D'Auria F., Mazzini M., Oriolo F., Piccinini L. "PIPER-ONE Research: Available Instrumentation and Specifications for OECD- CSNI International Standard Problem 21 (ISP 21)"
University of Pisa Report, DCMN - RL 255(86), Pisa (I), Sept. 1986
OECD CSNI 1st Workshop on ISP 21, Marina di Grosseto (I), Sept. 22-23 1986
- /28/ Breghi M.P.: "Uncertainty Evaluation of the Measurements taken in PIPER-ONE Apparatus"
University of Pisa Report DCMN RL 382 (89), Pisa (I), 1989



APPENDIX 1:
RESULTS OF REFERENCE CALCULATION
(Post-Test IC 31)



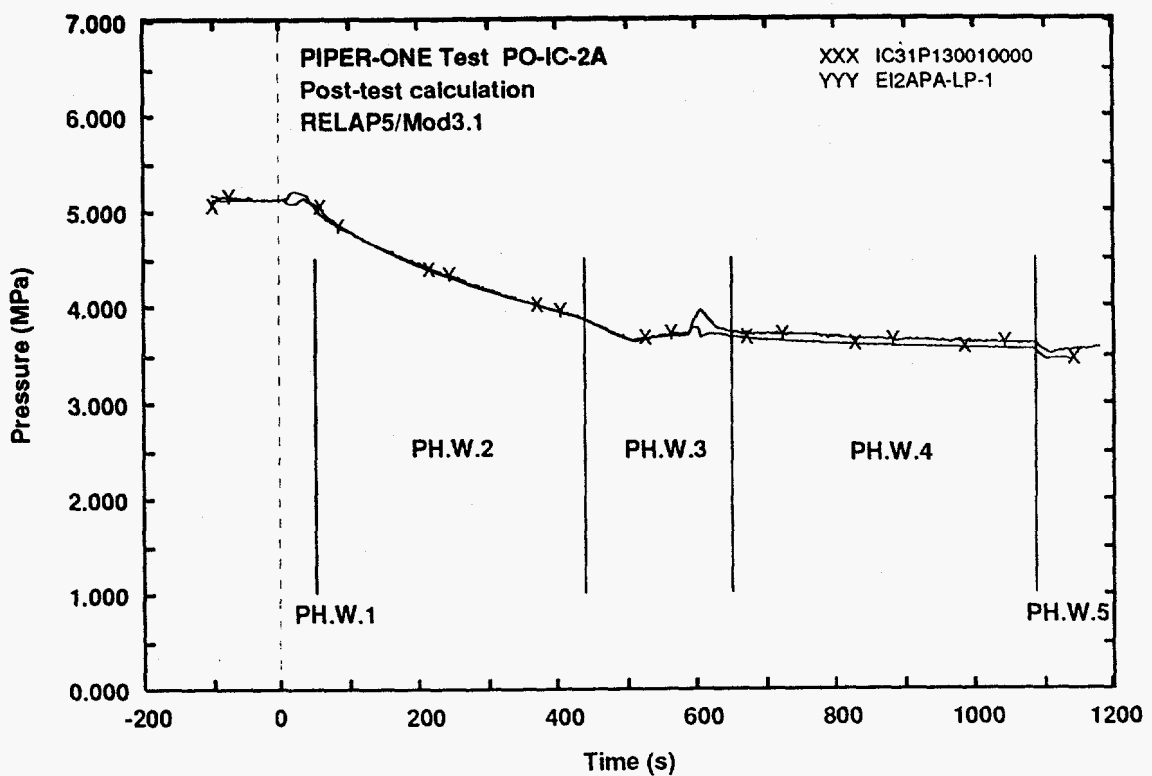


Fig. 1 - Measured and calculated trends of lower plenum pressure

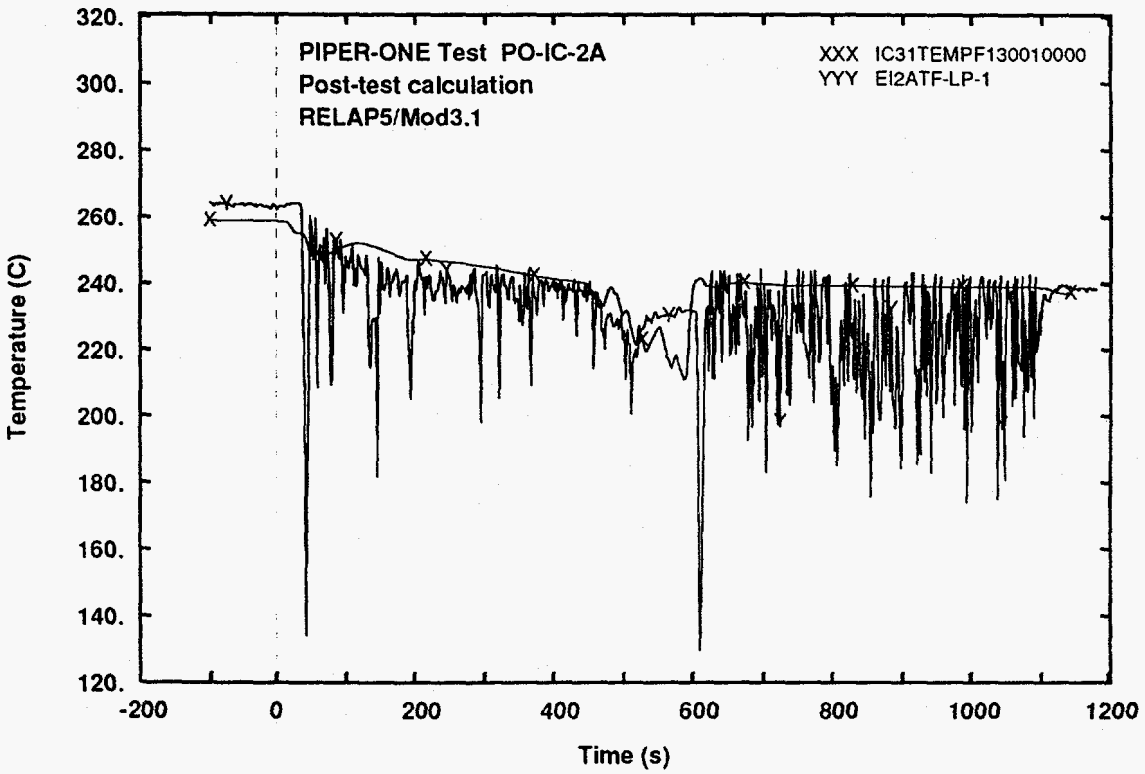


Fig. 2 - Measured and calculated trends of lower plenum temperature

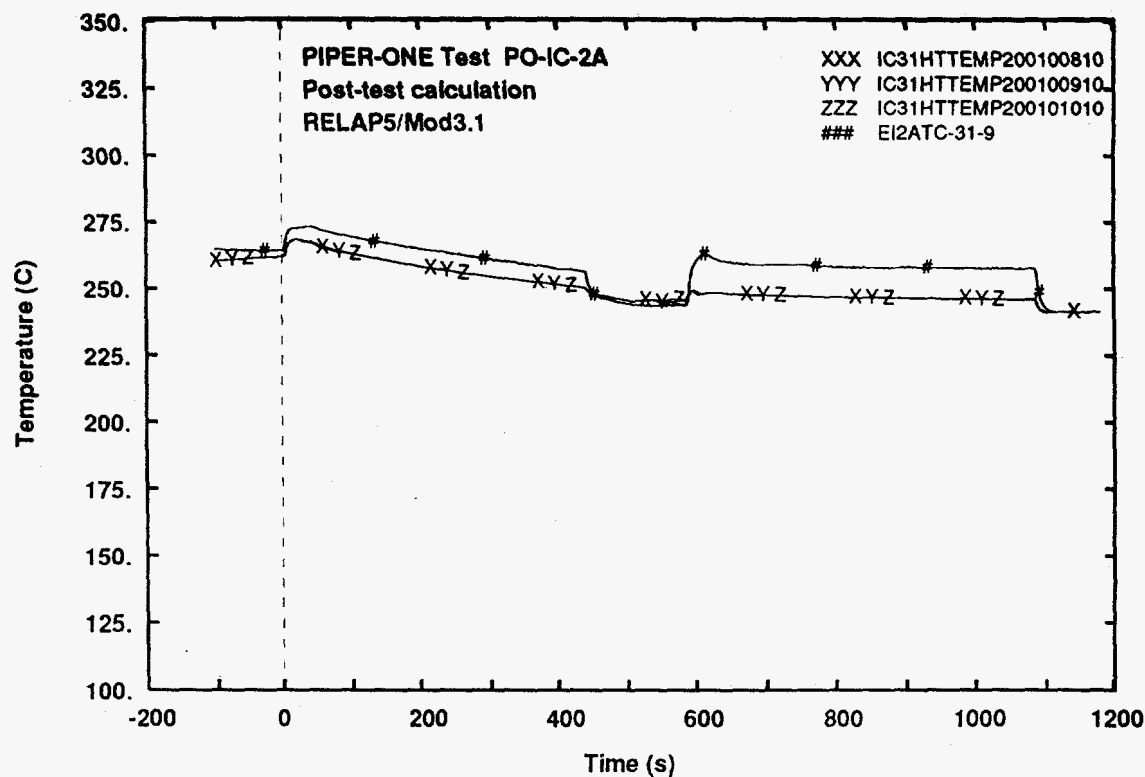


Fig. 3 - Measured and calculated trends of rod surface temperature (level 9)

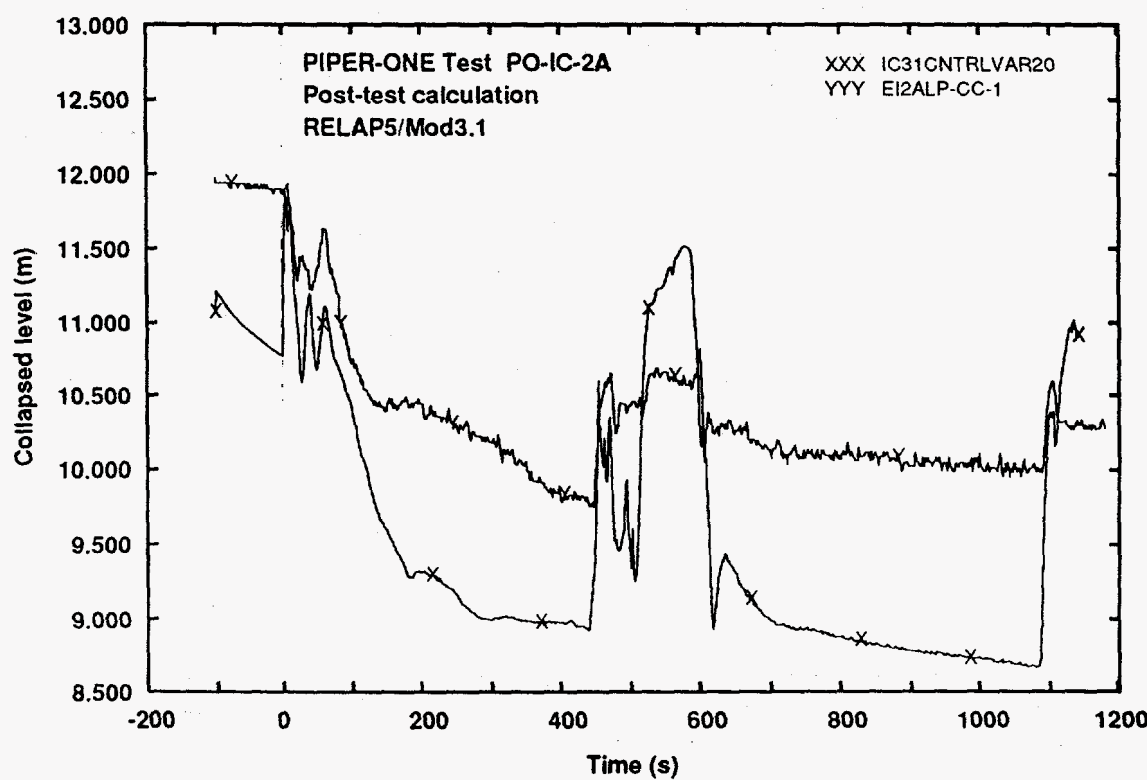


Fig. 4 - Measured and calculated trends of core level

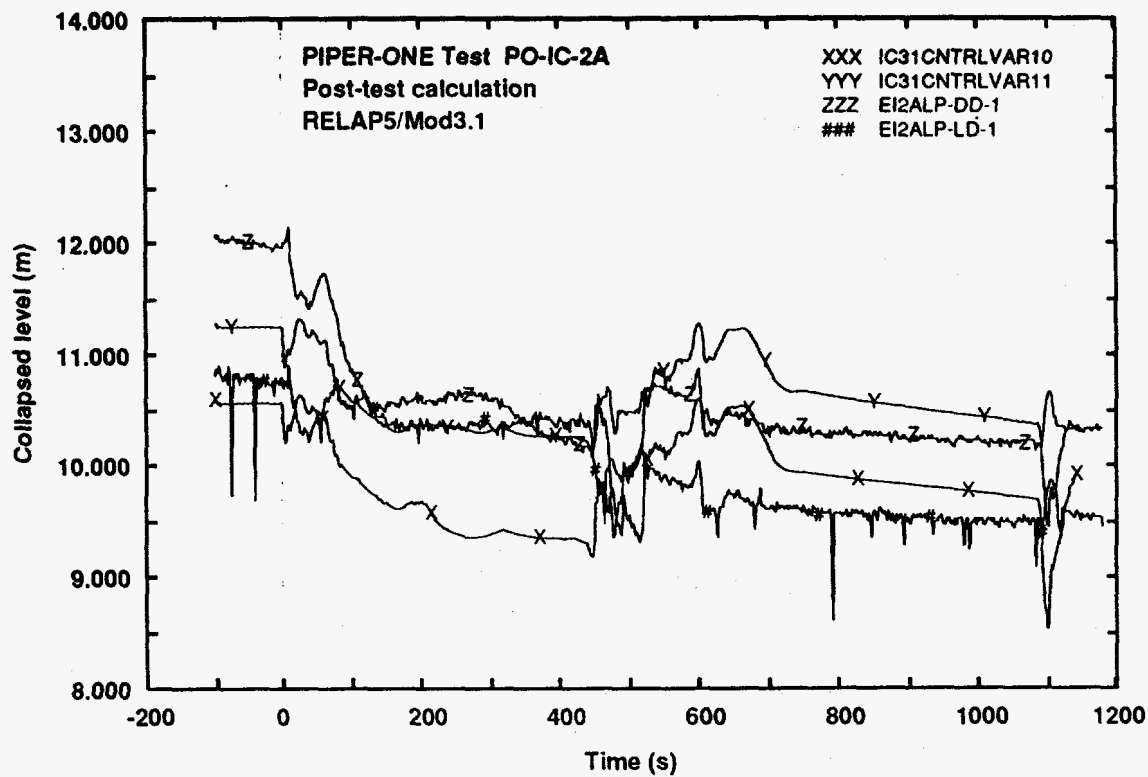


Fig. 5 - Measured and calculated trends of downcomer level

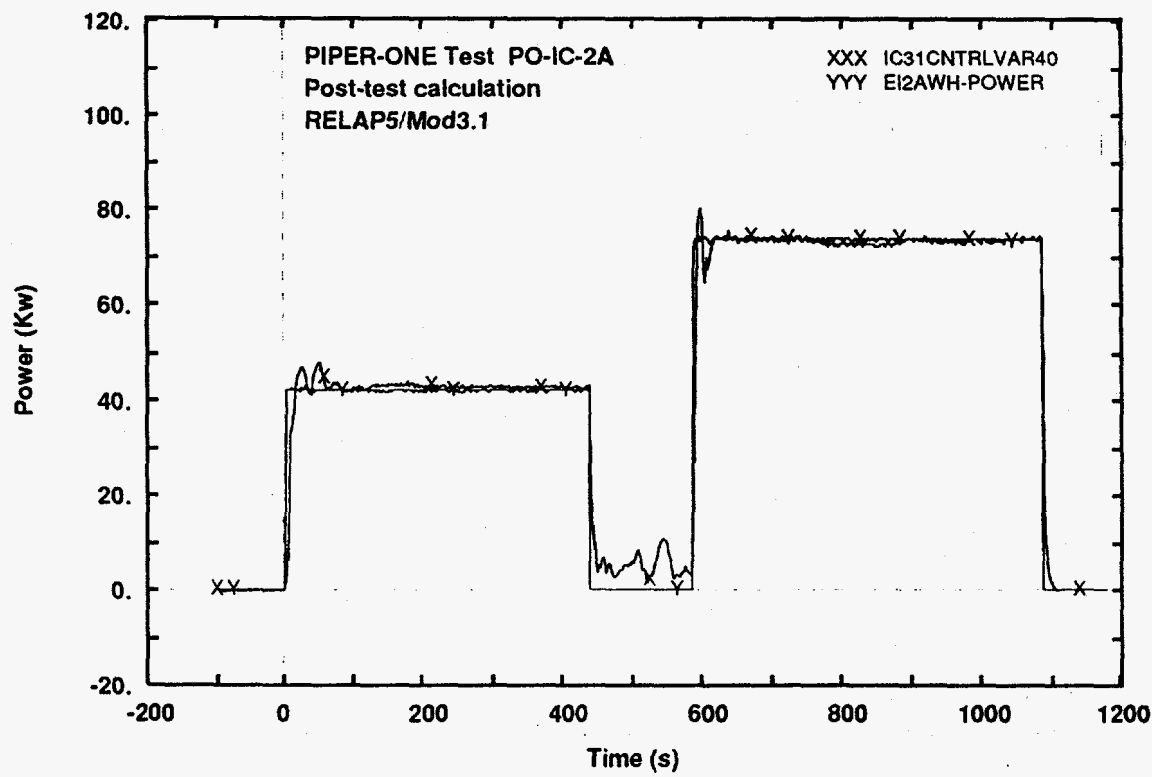


Fig. 6 - Measured and calculated trends of core power

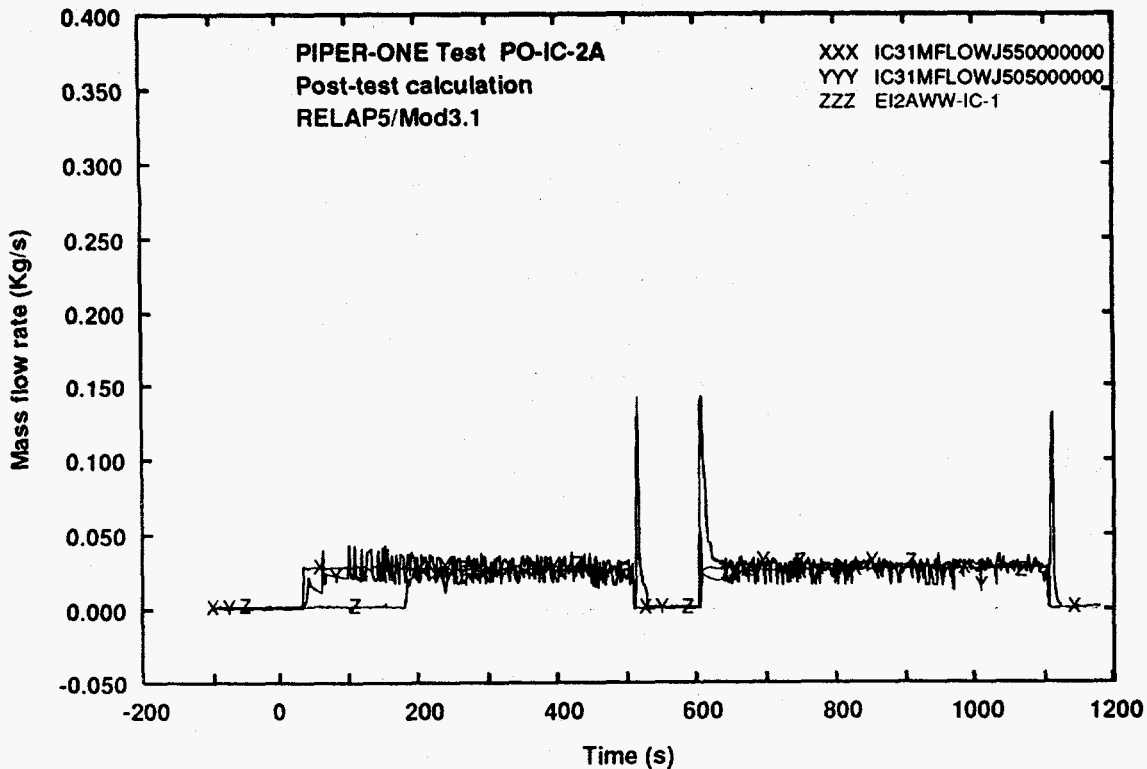


Fig. 7 - Measured and calculated trends of IC mass flow rate

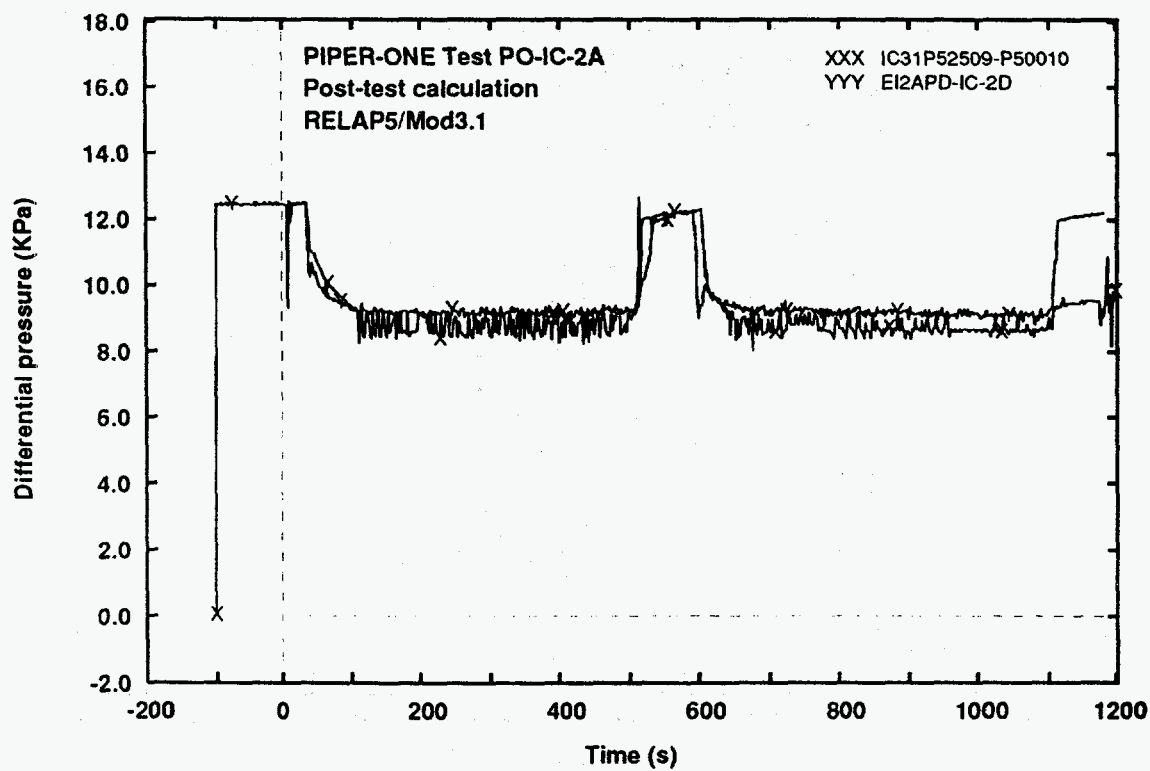


Fig. 8 - Measured and calculated trends of IC differential pressure

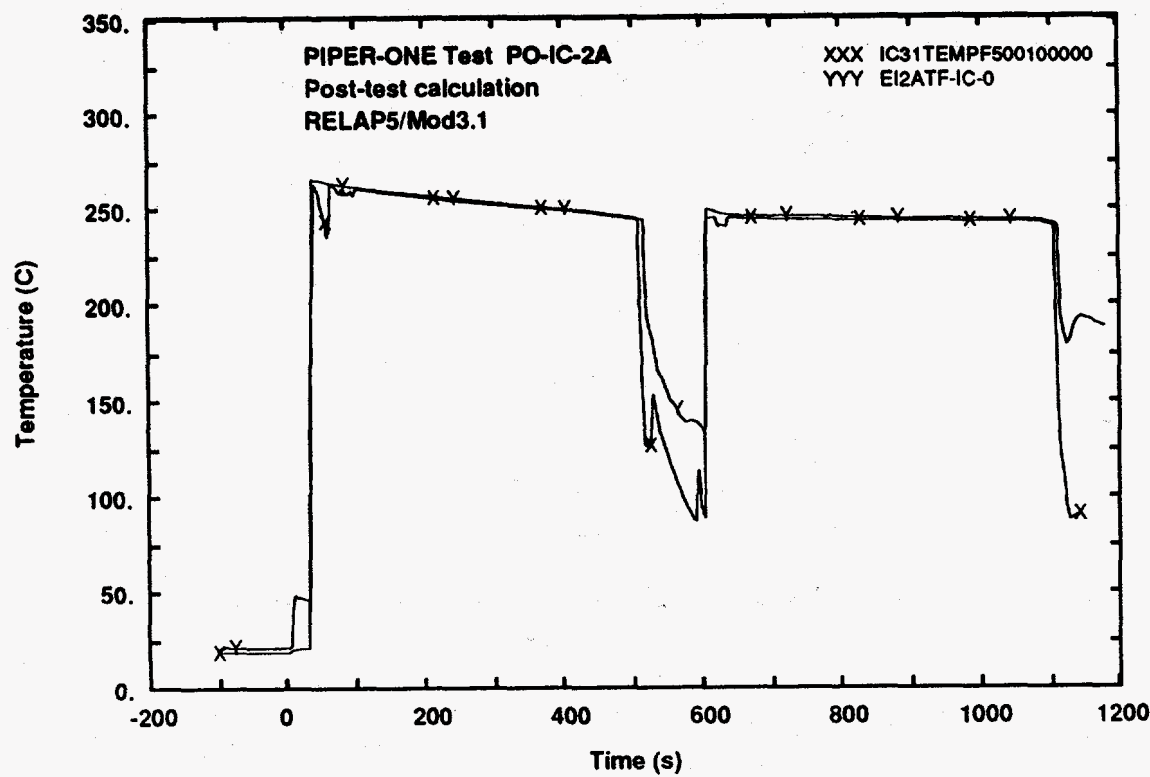


Fig. 9 - Measured and calculated trends of IC inlet fluid temperature

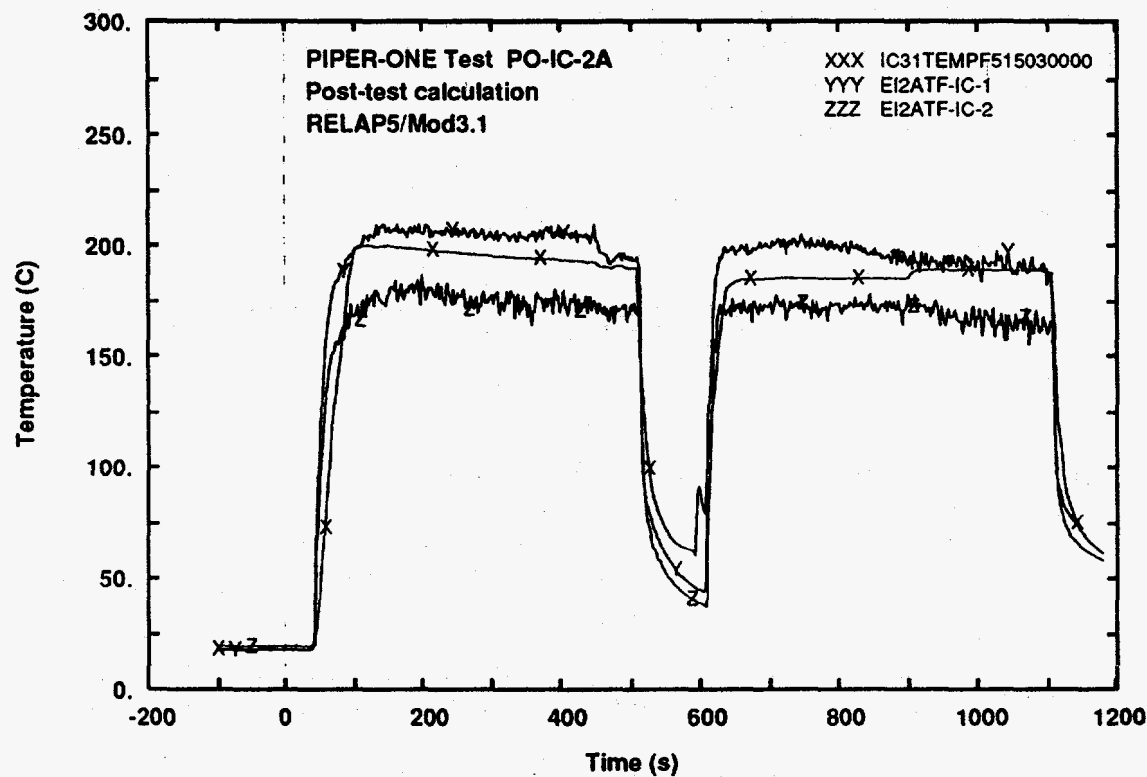


Fig. 10 - Measured and calculated trends of IC tubes fluid temperature
(middle elevation)

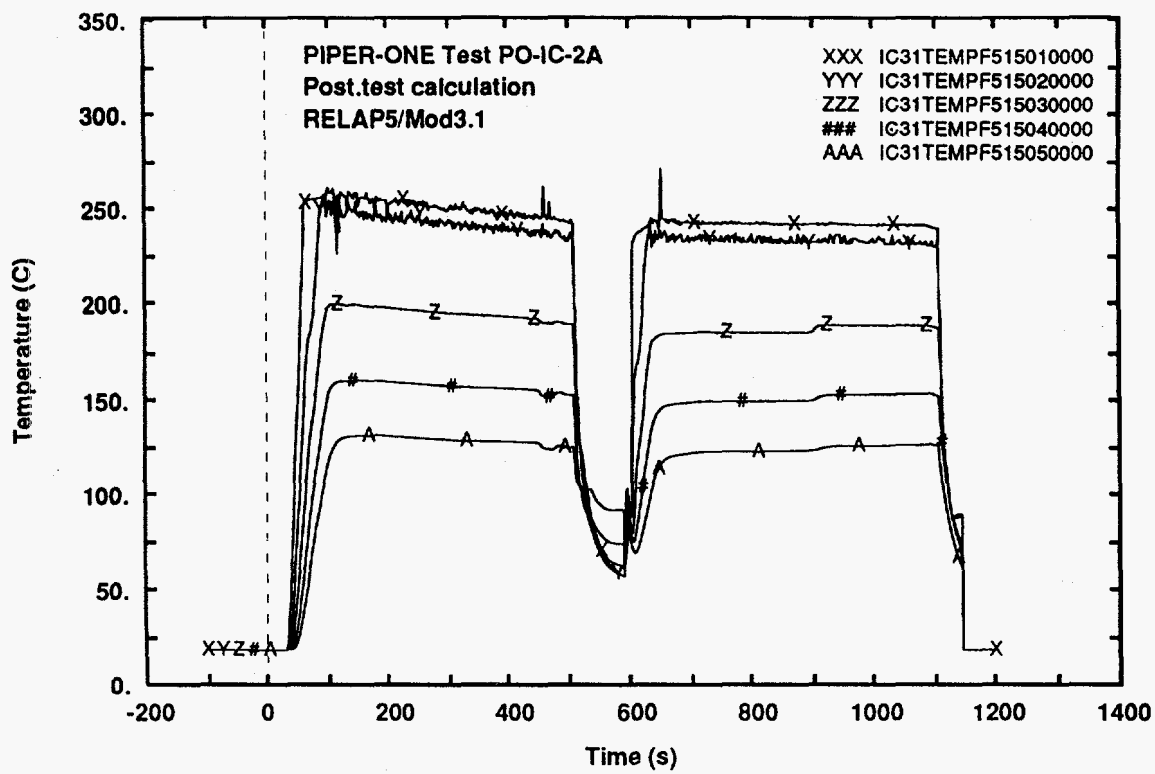


Fig. 11 - Calculated trends of IC fluid temperature along the axis

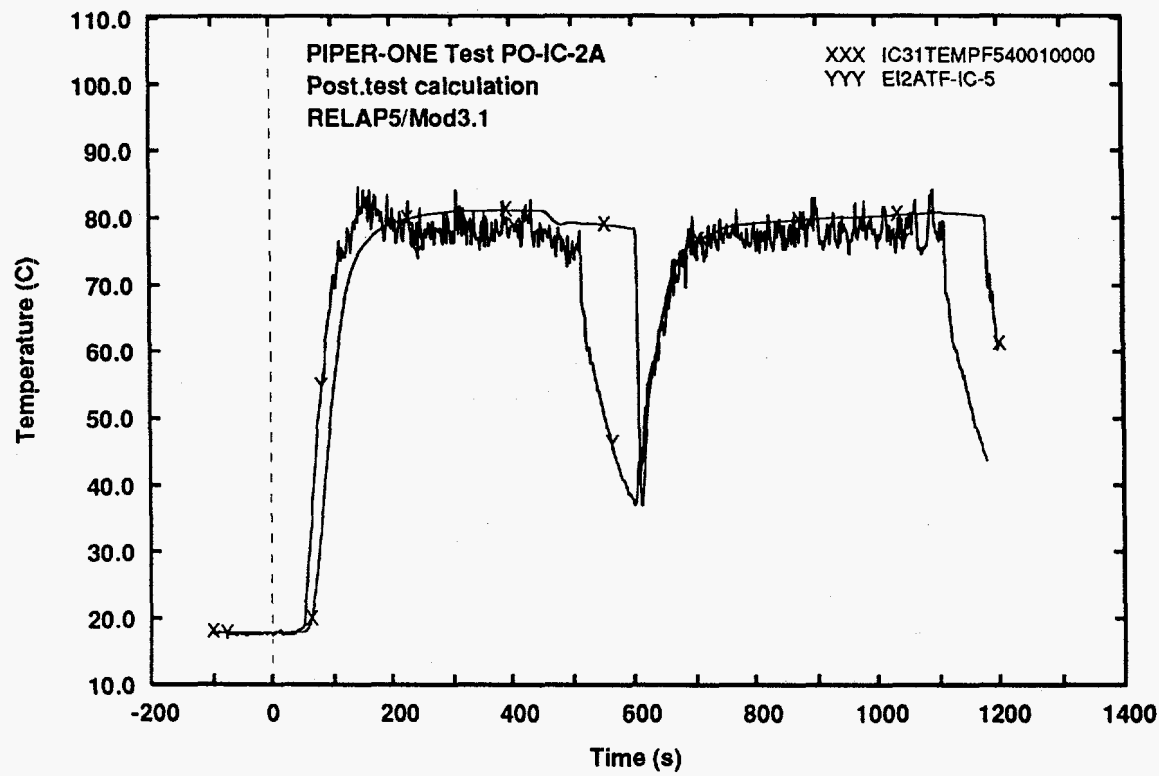


Fig. 12 - Measured and calculated trends of IC outlet fluid temperature

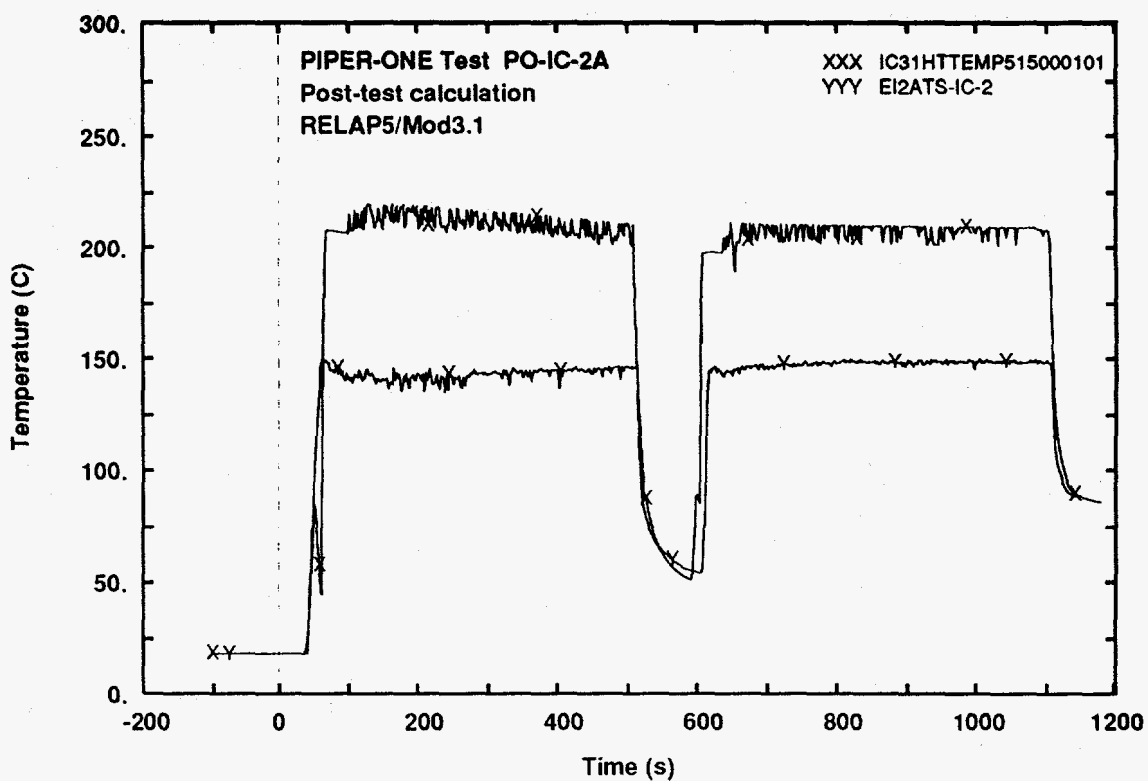


Fig. 13 - Measured and calculated trends of IC tubes wall surface temperature (internal side top elevation)

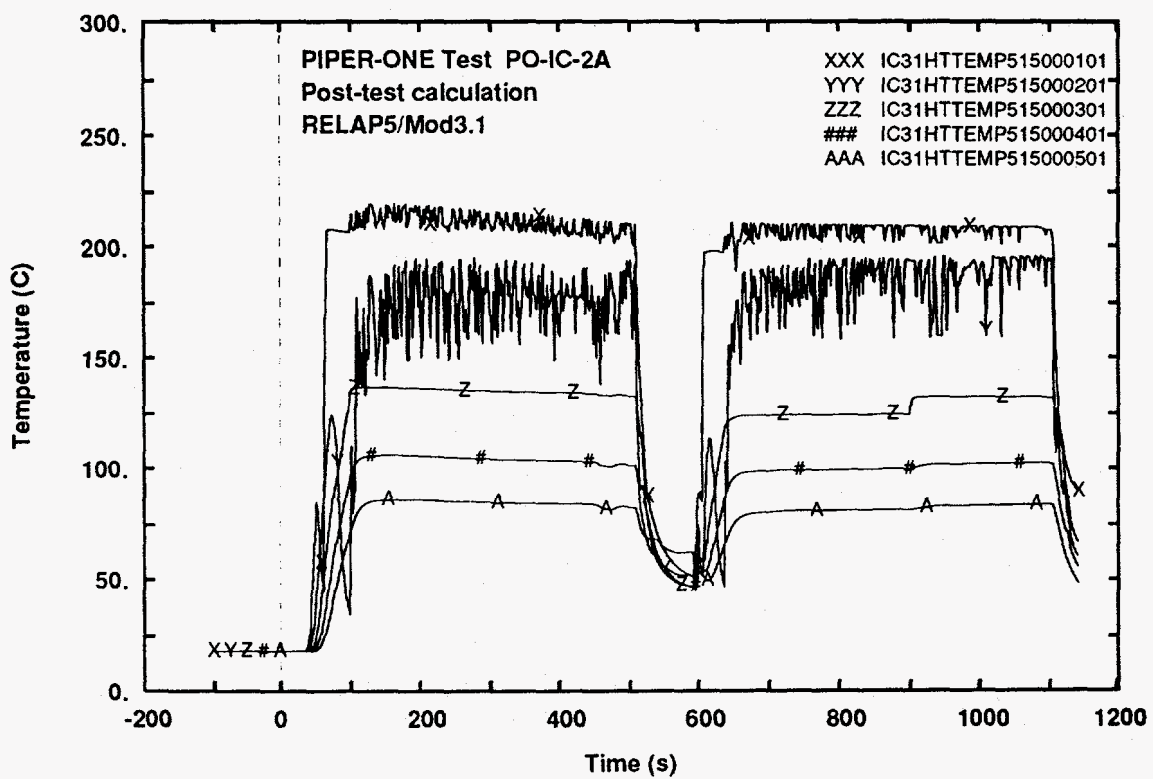


Fig. 14 - Calculated trends of IC tubes wall surface temperature along the axis (internal side)

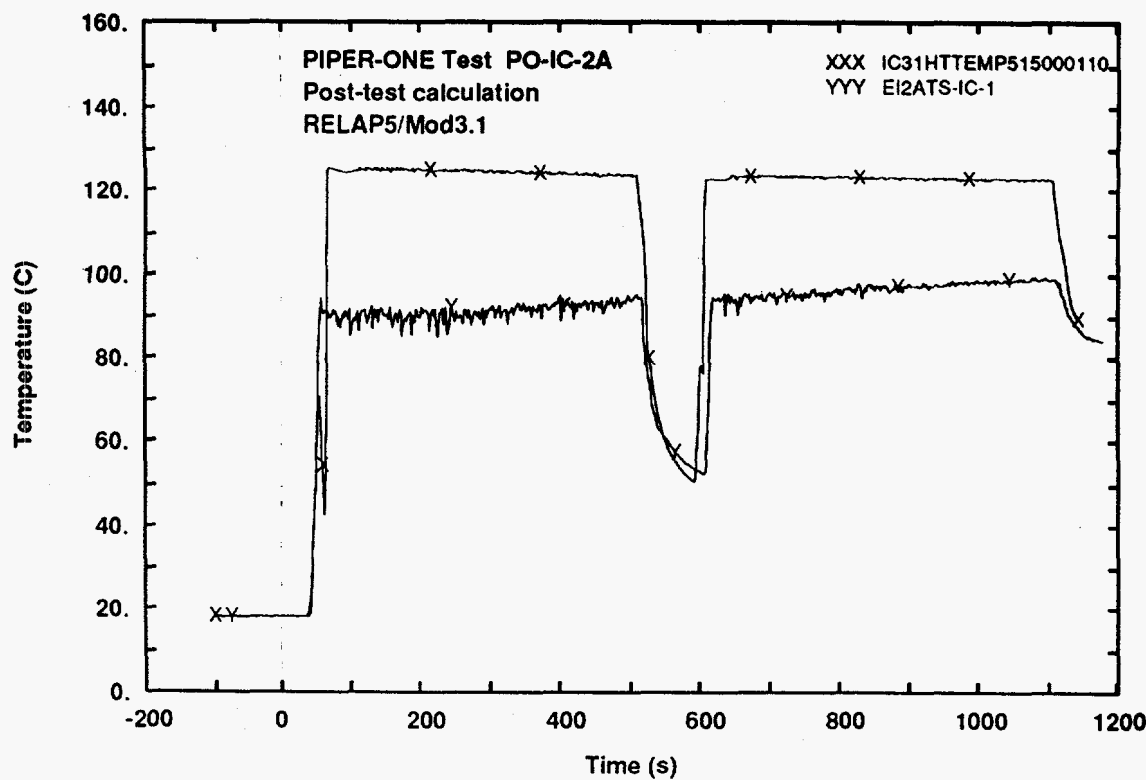


Fig. 15 - Measured and calculated trends of IC tubes wall surface temperature
(external side top elevation)

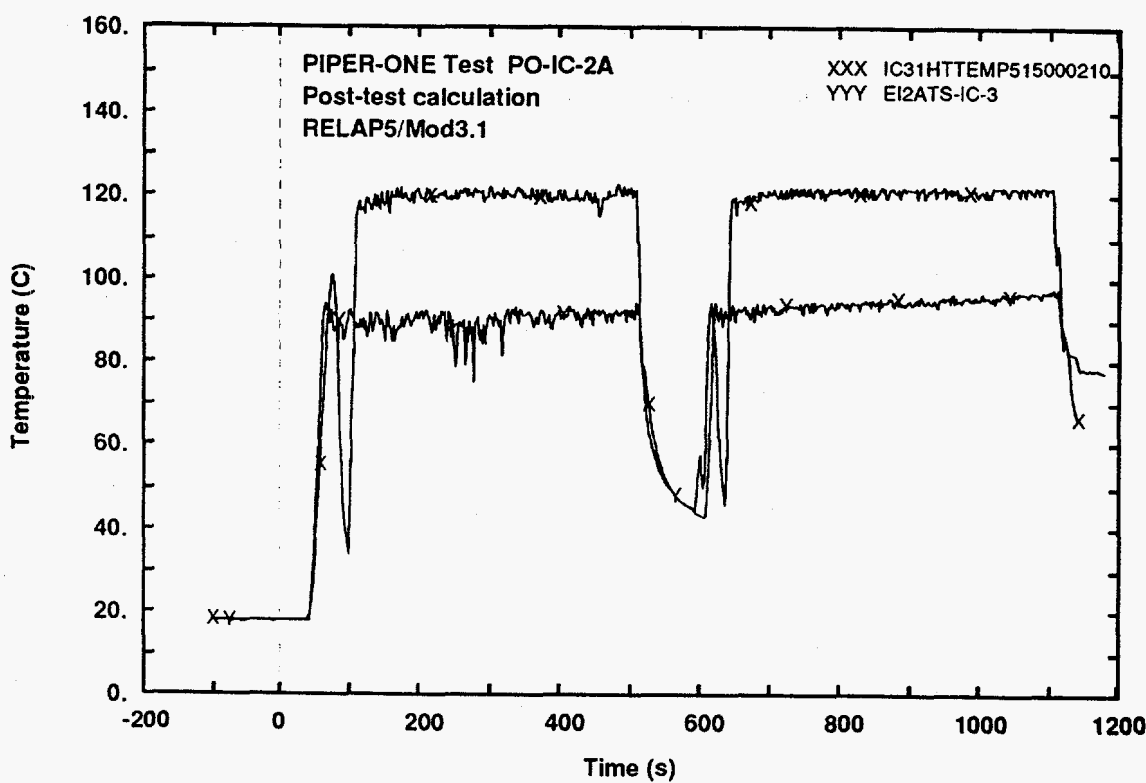


Fig. 16 - Measured and calculated trends of IC tubes wall surface temperature
(external side level 3)

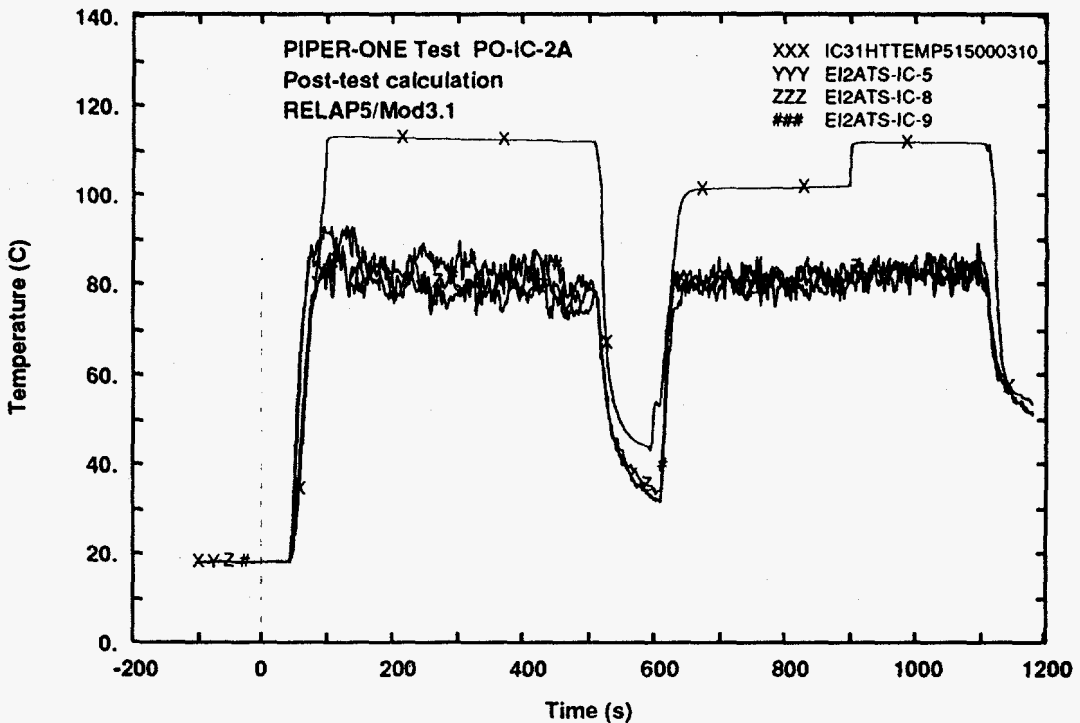


Fig. 17 - Measured and calculated trends of IC tubes wall surface temperature
(external side middle elevation)

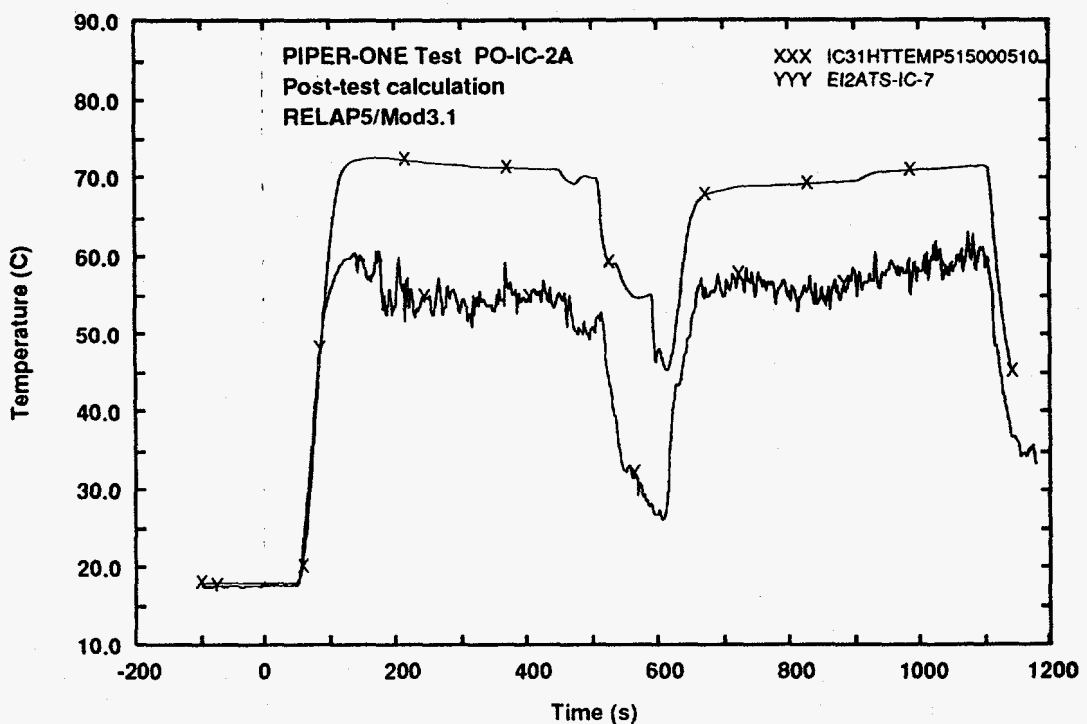


Fig. 18 - Measured and calculated trends of IC tubes wall surface temperature
(external side bottom elevation)

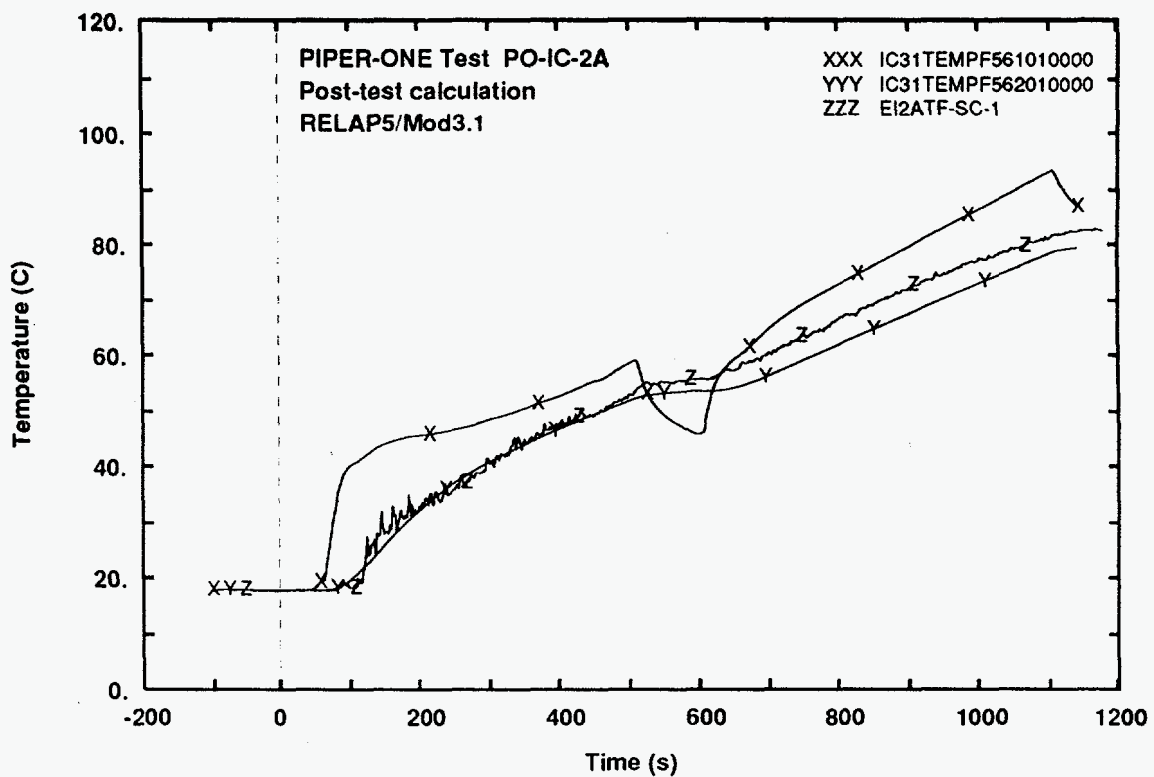


Fig. 19 - Measured and calculated trends of IC internal pool fluid temperature (top level)

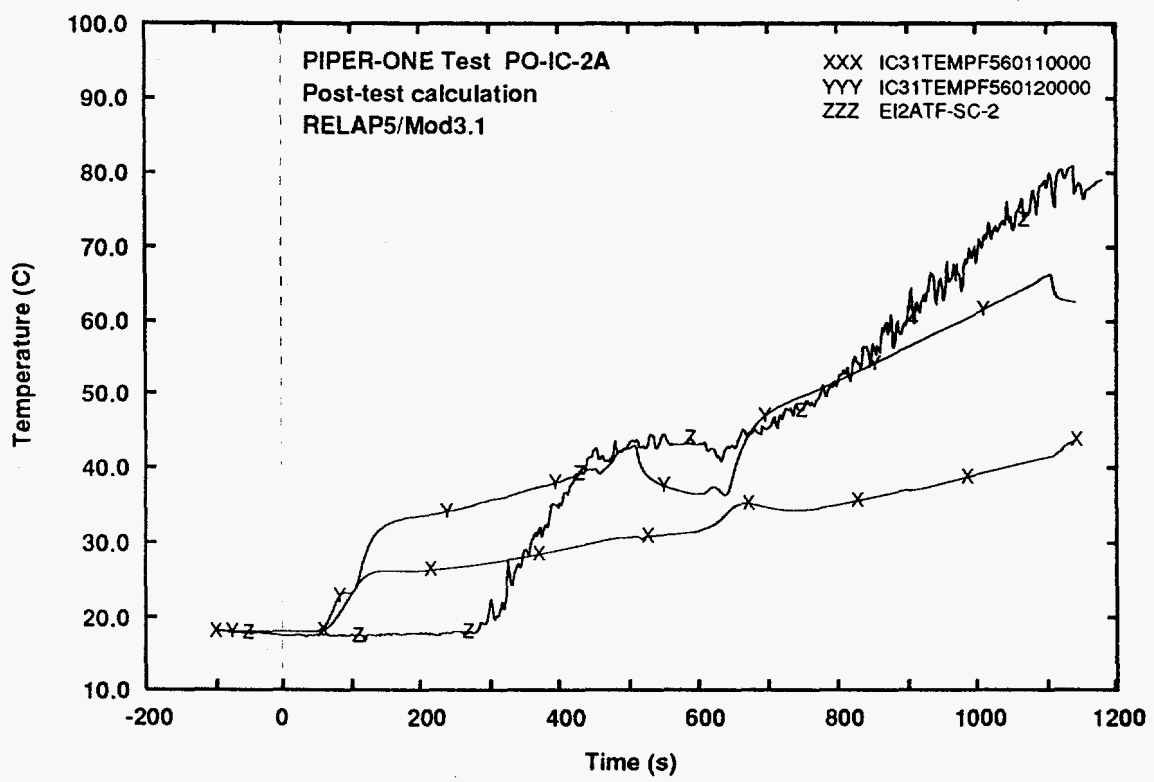


Fig. 20 - Measured and calculated trends of IC internal pool fluid temperature (level 2)

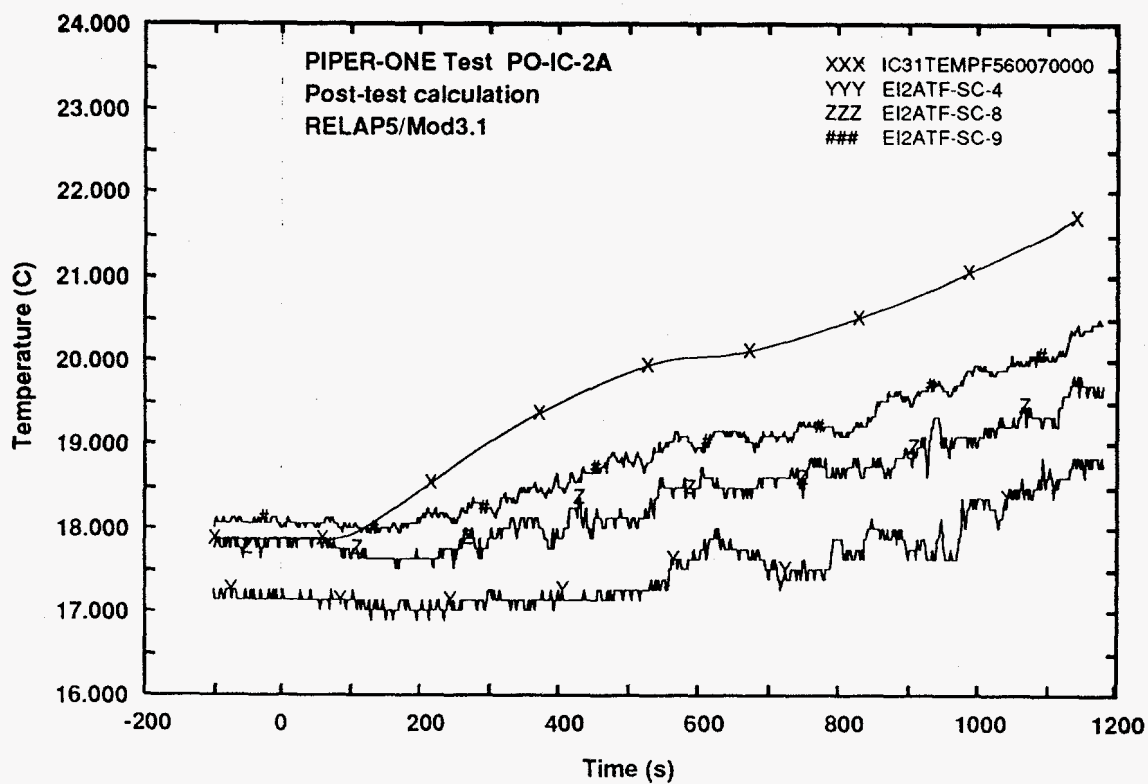


Fig. 21 - Measured and calculated trends of IC internal pool fluid temperature (middle level)

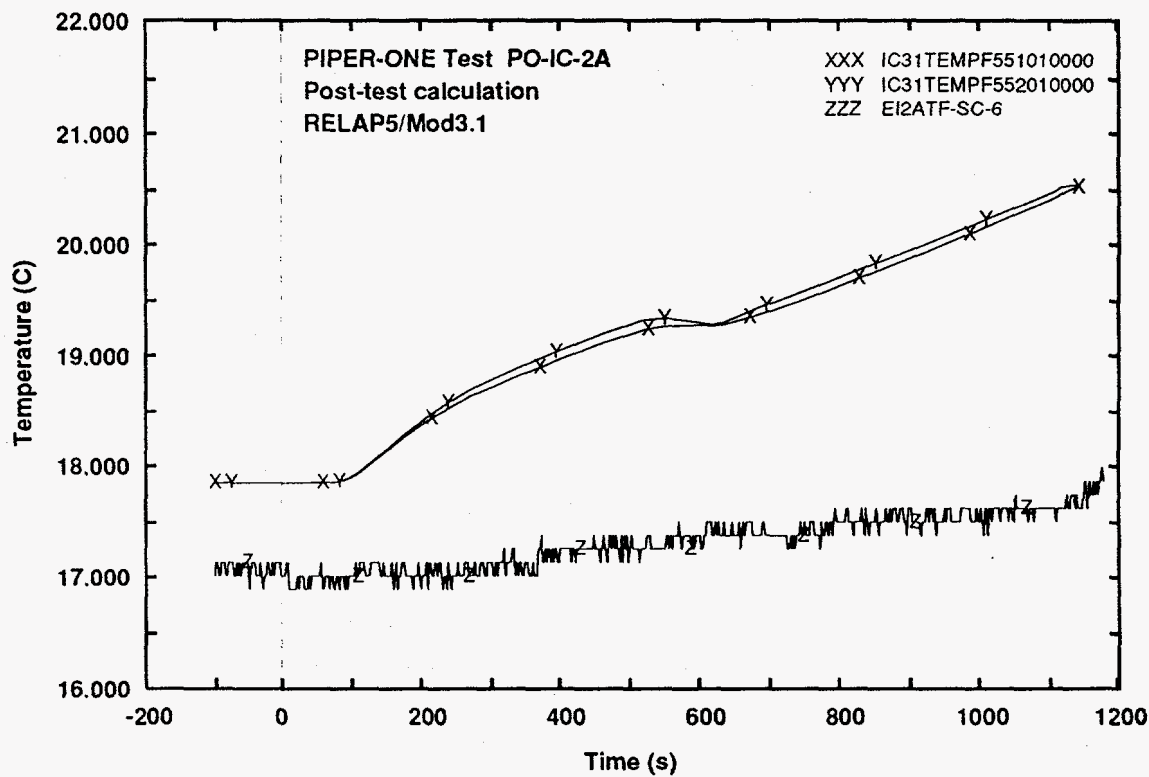


Fig. 22 - Measured and calculated trends of IC internal pool fluid temperature (bottom level)

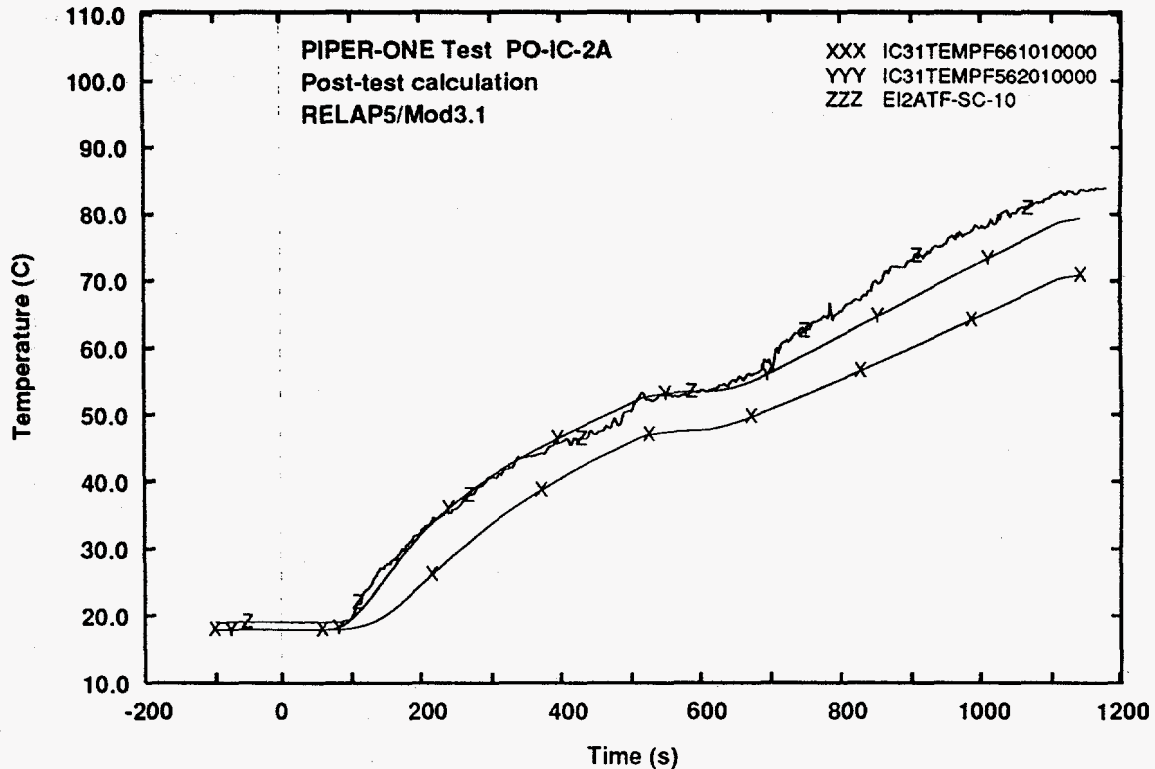


Fig. 23 - Measured and calculated trends of IC external pool fluid temperature (top level)

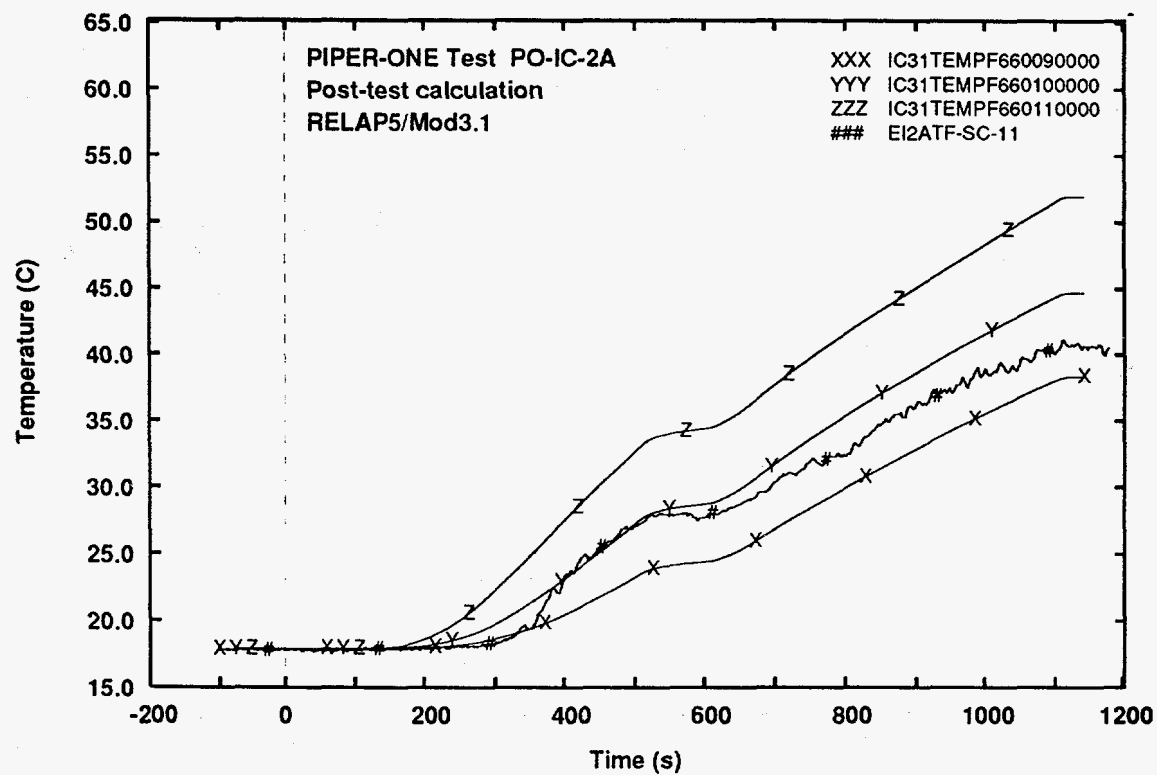


Fig. 24 - Measured and calculated trends of IC external pool fluid temperature (level 11)

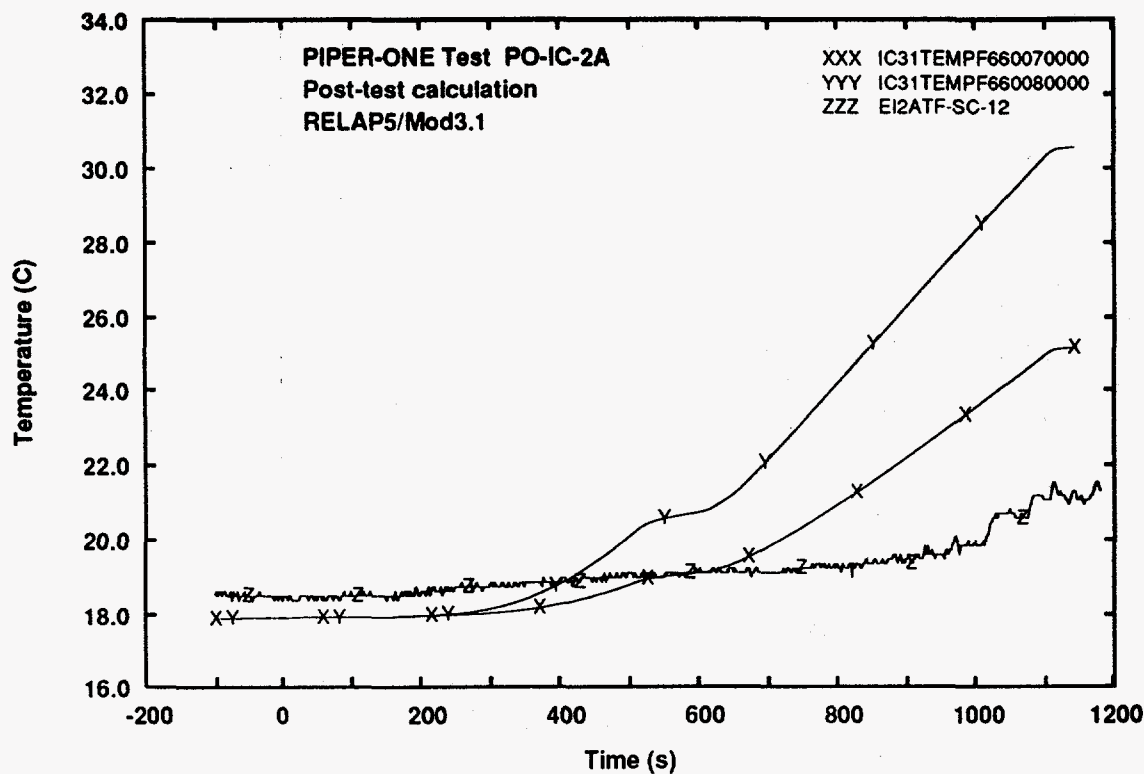


Fig. 25 - Measured and calculated trends of IC external pool fluid temperature (middle level)

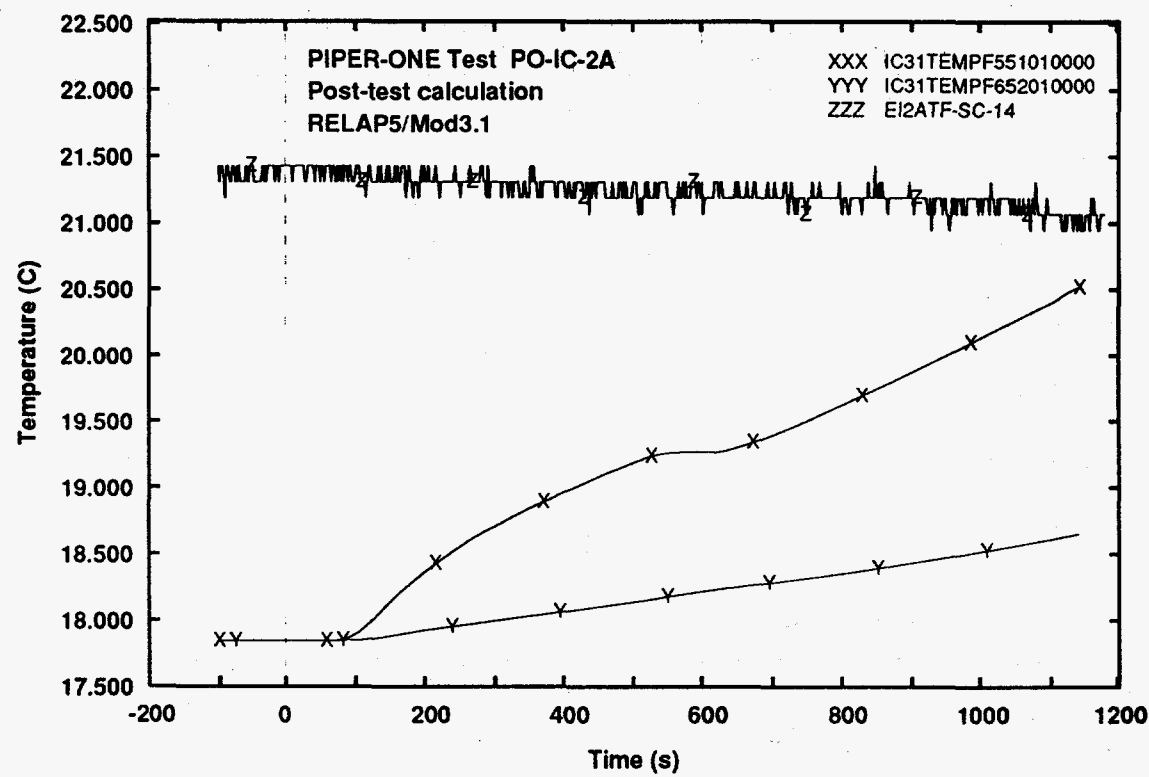


Fig. 26 - Measured and calculated trends of IC external pool fluid temperature (bottom level)

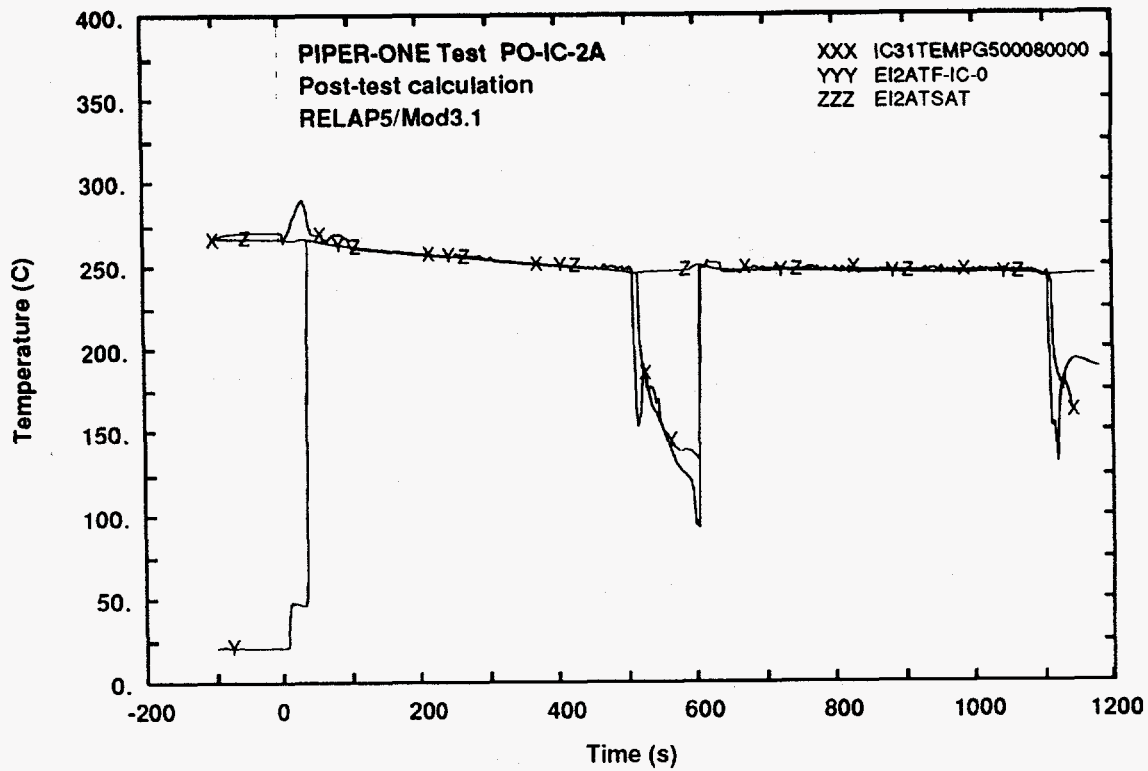


Fig. 27 - Measured and calculated trends of steam temperature at IC inlet
compared with experimental saturated temperature

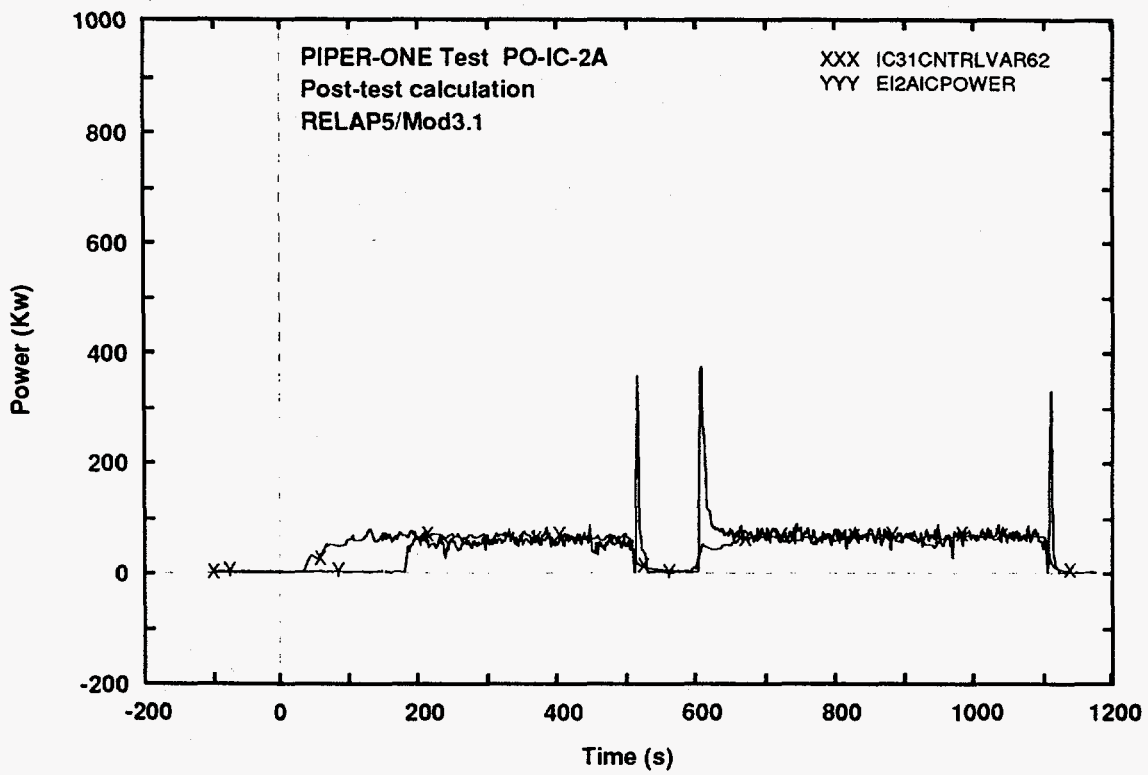


Fig. 28 - Measured and calculated trends of IC exchanged power

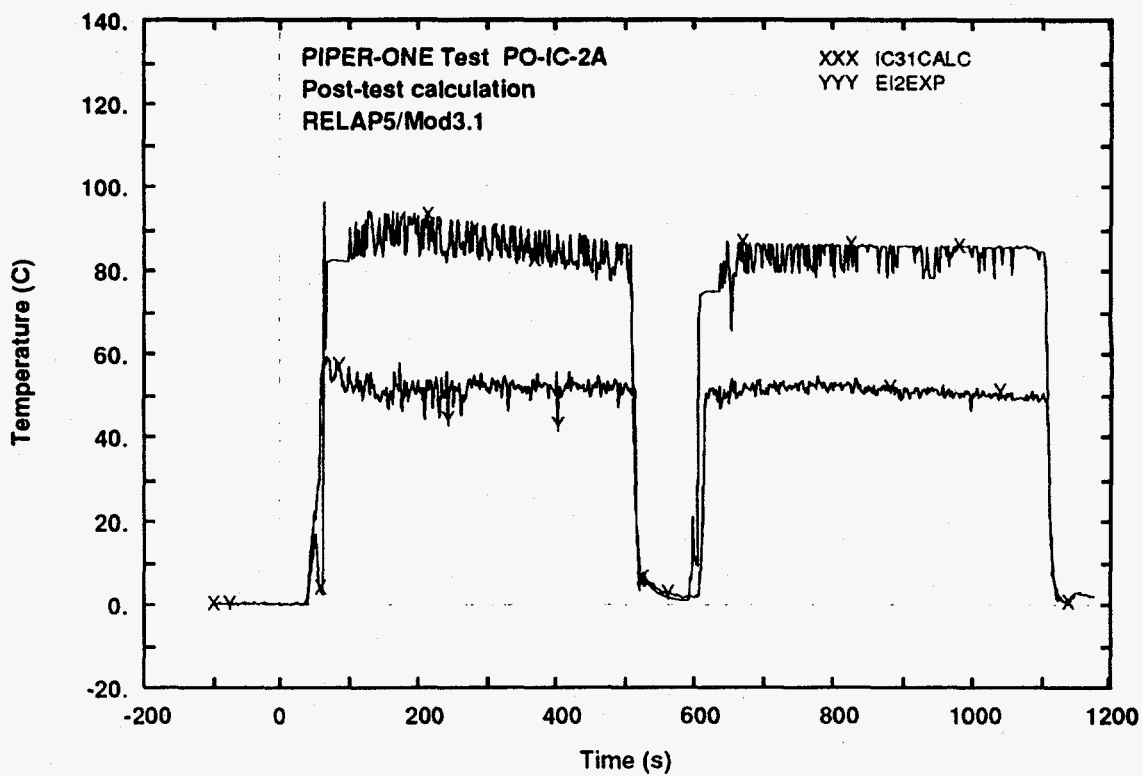


Fig. 29 - Measured and calculated trends of temperature difference between internal and external side of IC tubes wall (top elevation)

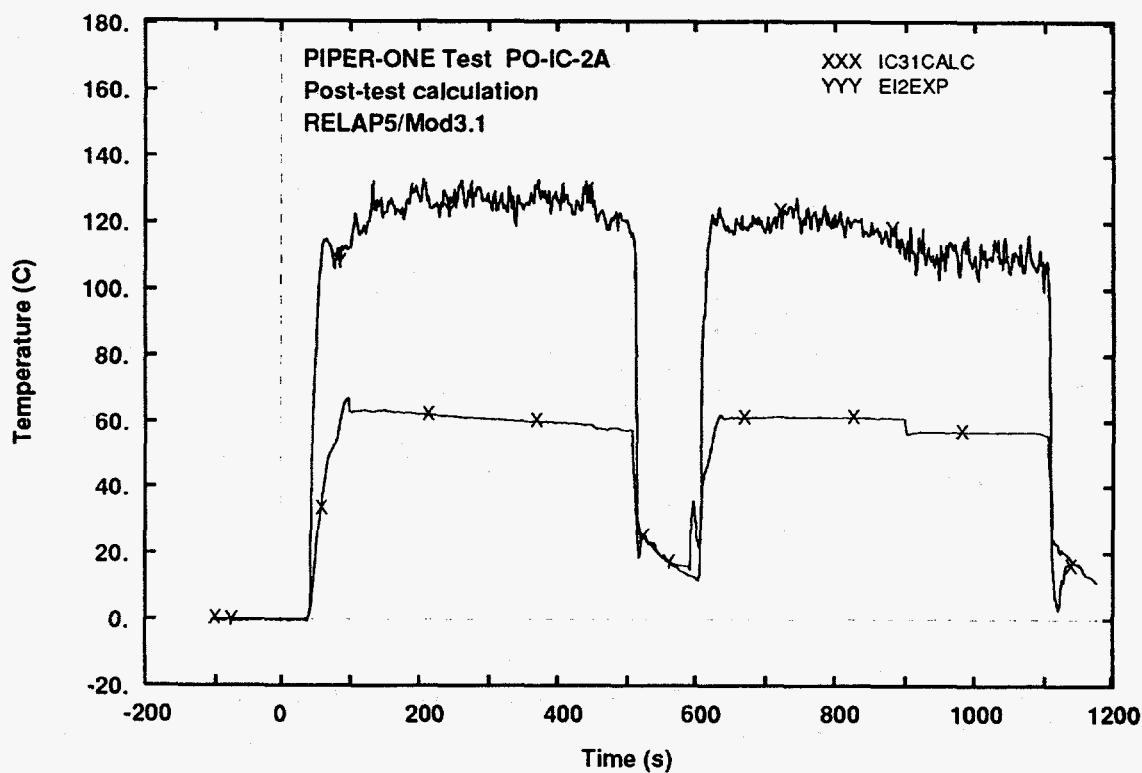


Fig. 30 - Measured and calculated trends of temperature difference between IC fluid and external side of IC tubes wall (middle elevation)

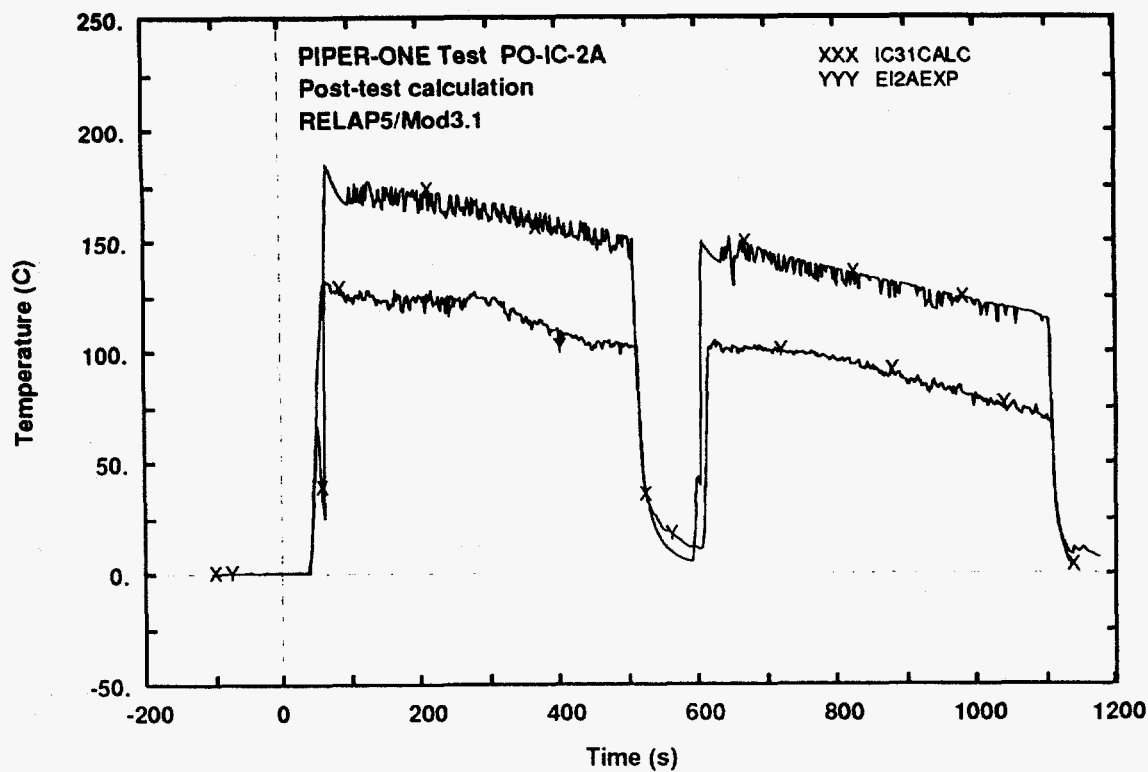


Fig. 31 - Measured and calculated trends of temperature difference between internal side of IC tubes wall and IC pool fluid temperature (top elevation)

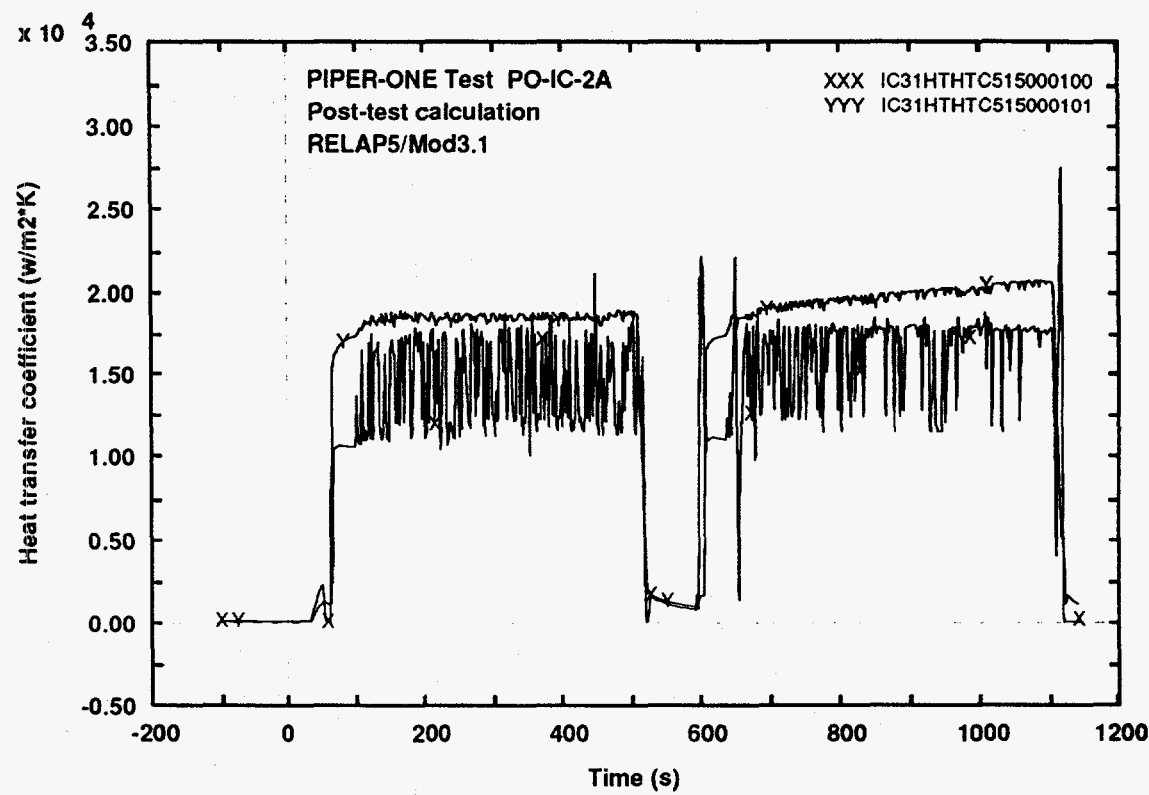


Fig. 32 - Calculated trends of the heat transfer coefficient at the inside and the outside of IC tubes wall (top elevation)

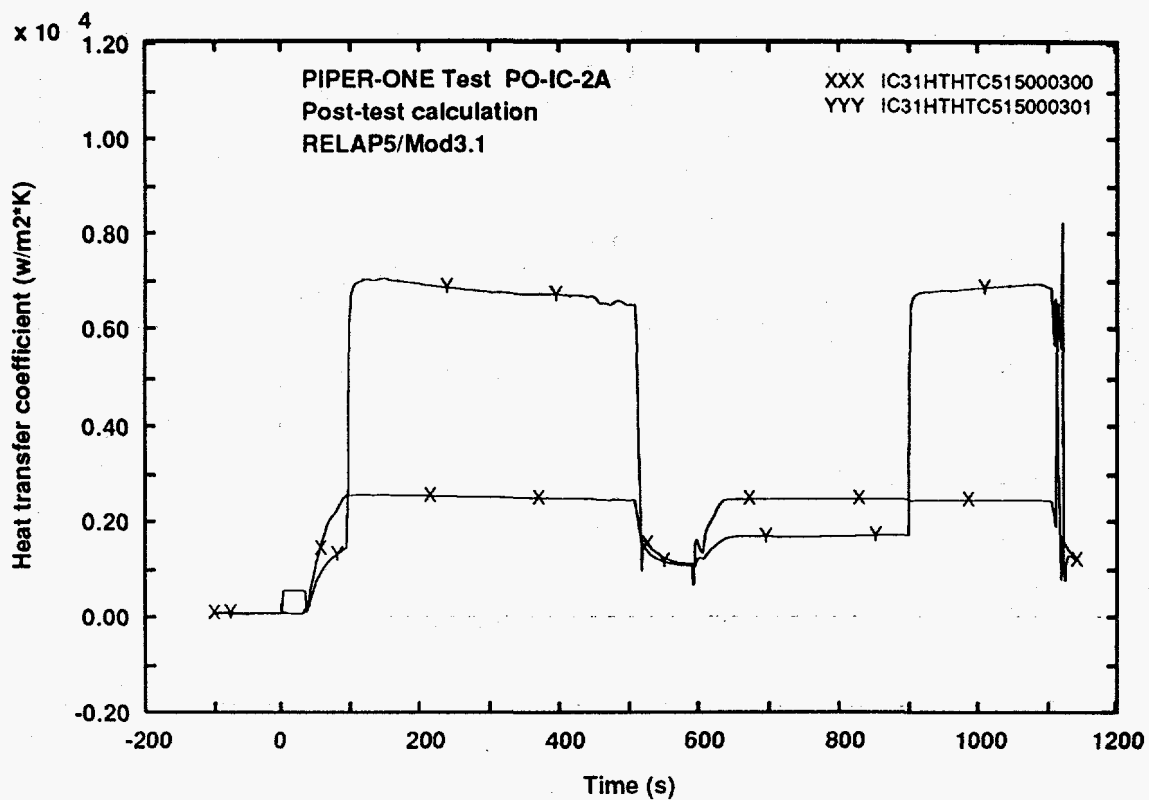


Fig. 33 - Calculated trends of the heat transfer coefficient at the inside and the outside of IC tubes wall (middle elevation)

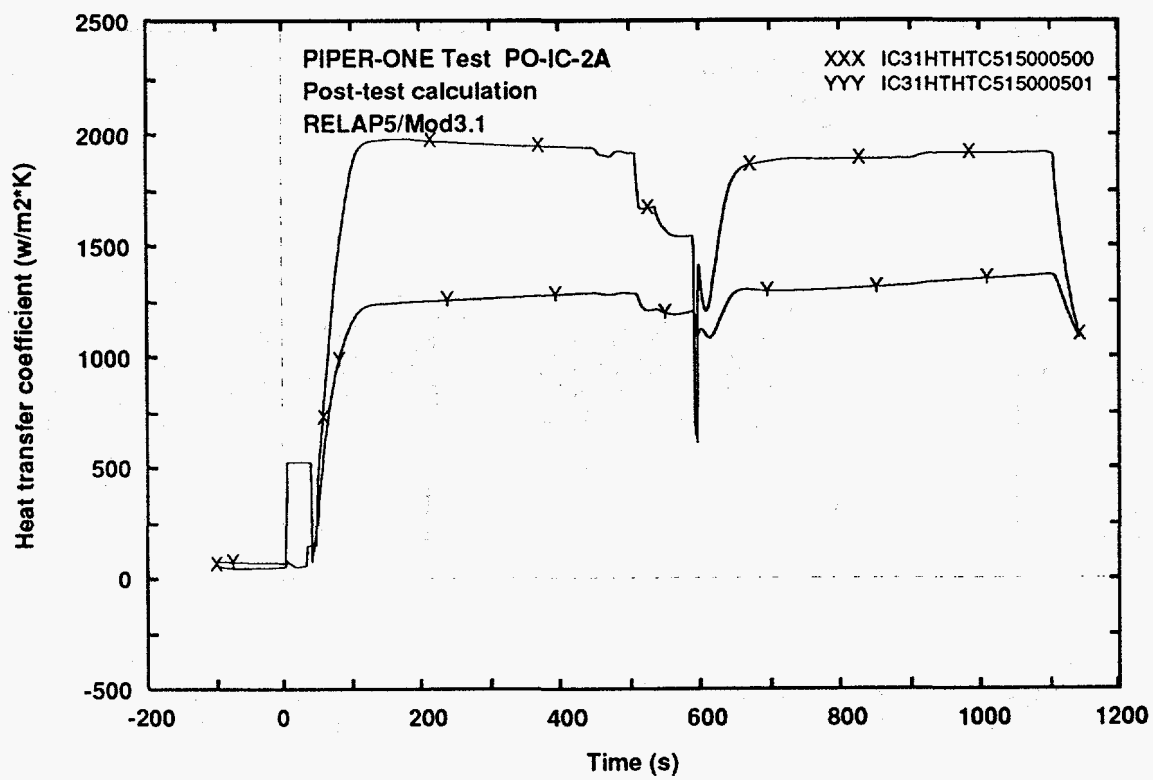


Fig. 34 - Calculated trends of the heat transfer coefficient at the inside and the outside of IC tubes wall (bottom elevation)

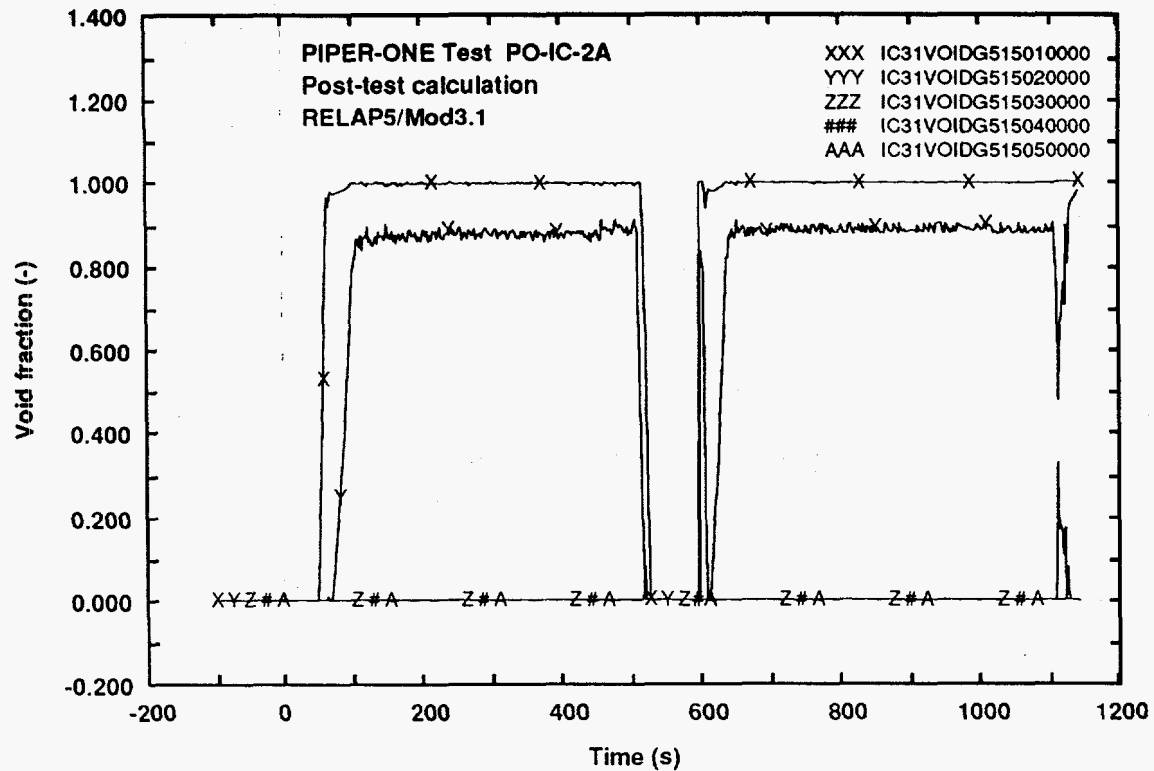


Fig. 35 - Calculated trends of IC tubes void fraction along the axis

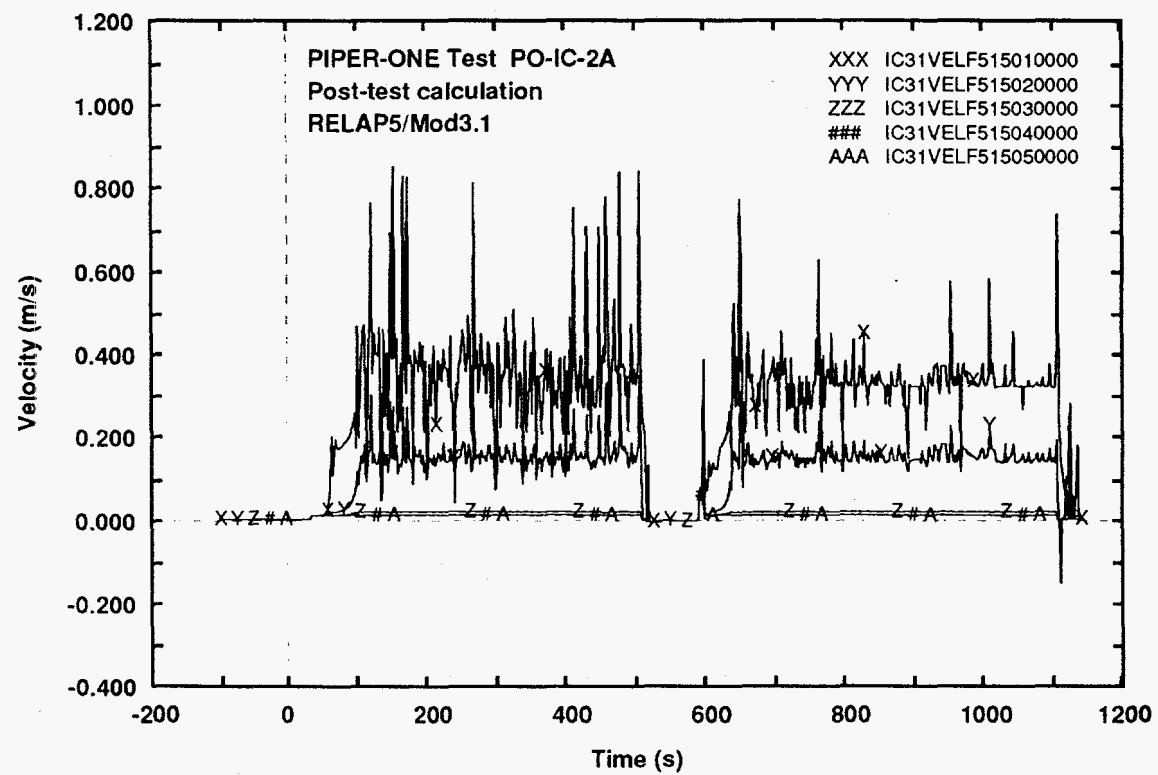


Fig. 36 - Calculated trends of IC tubes liquid velocity along the axis

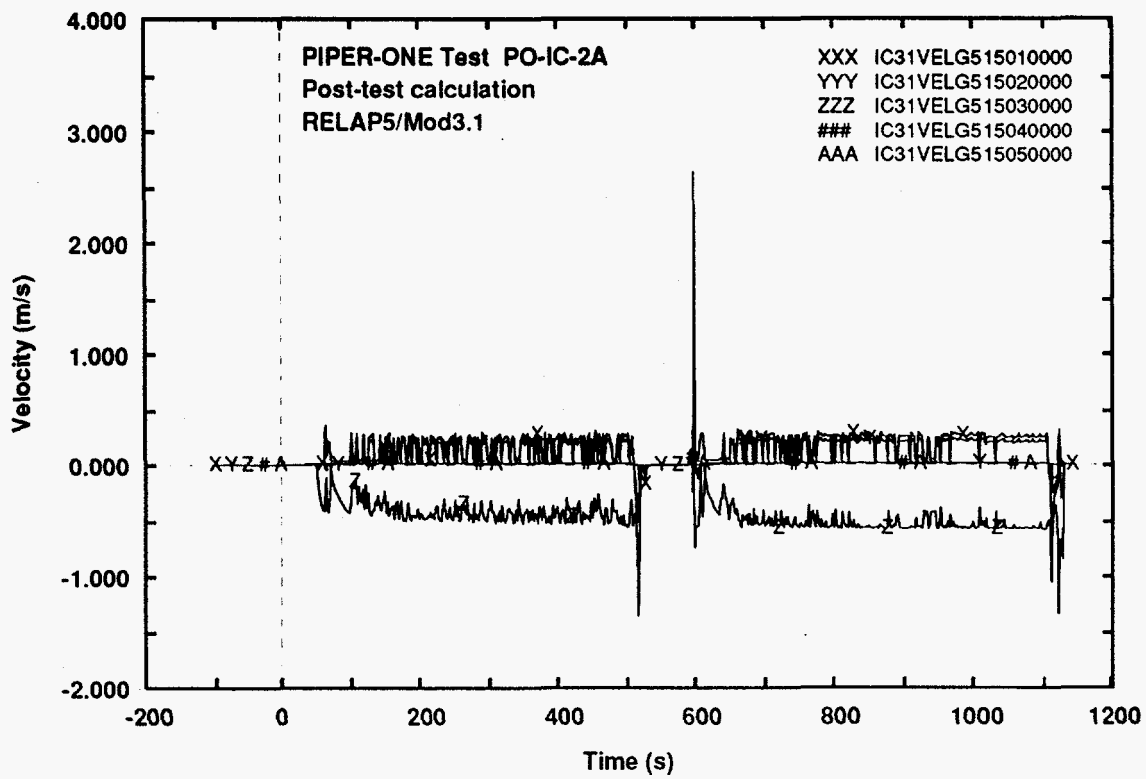


Fig. 37 - Calculated trends of IC tubes steam velocity along the axis

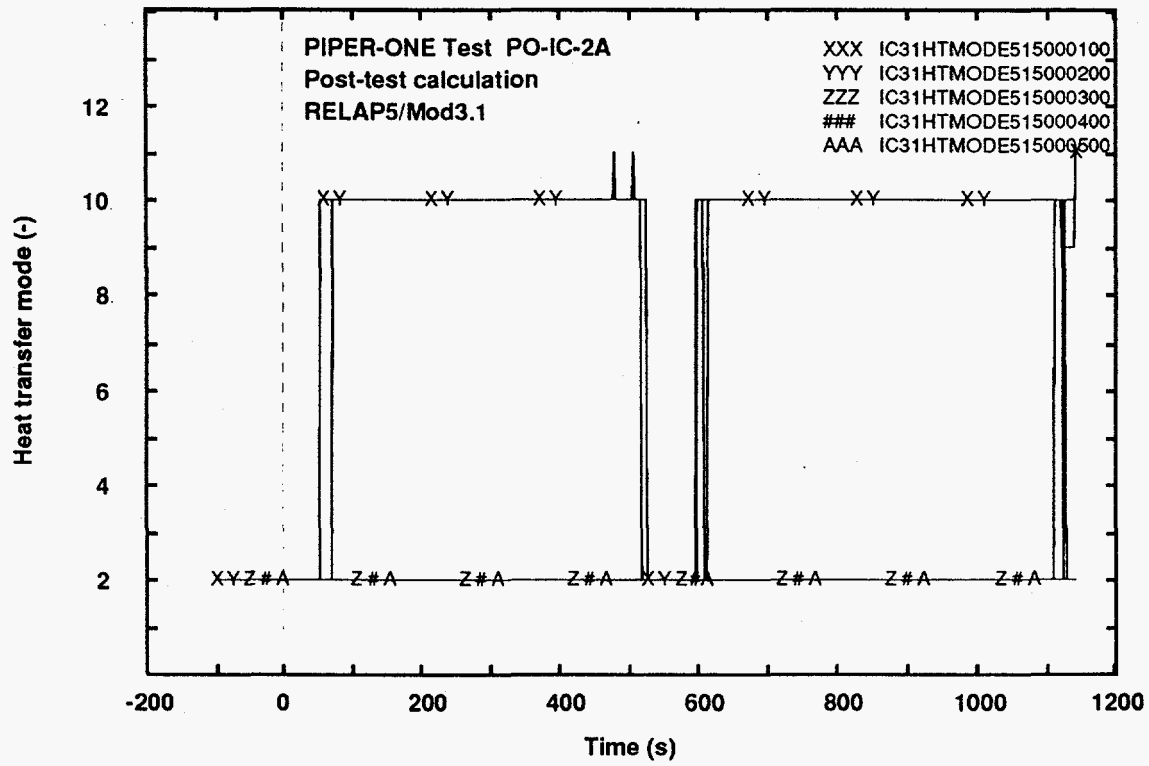


Fig. 38 - Calculated trends of IC tubes heat transfer mode (internal side)

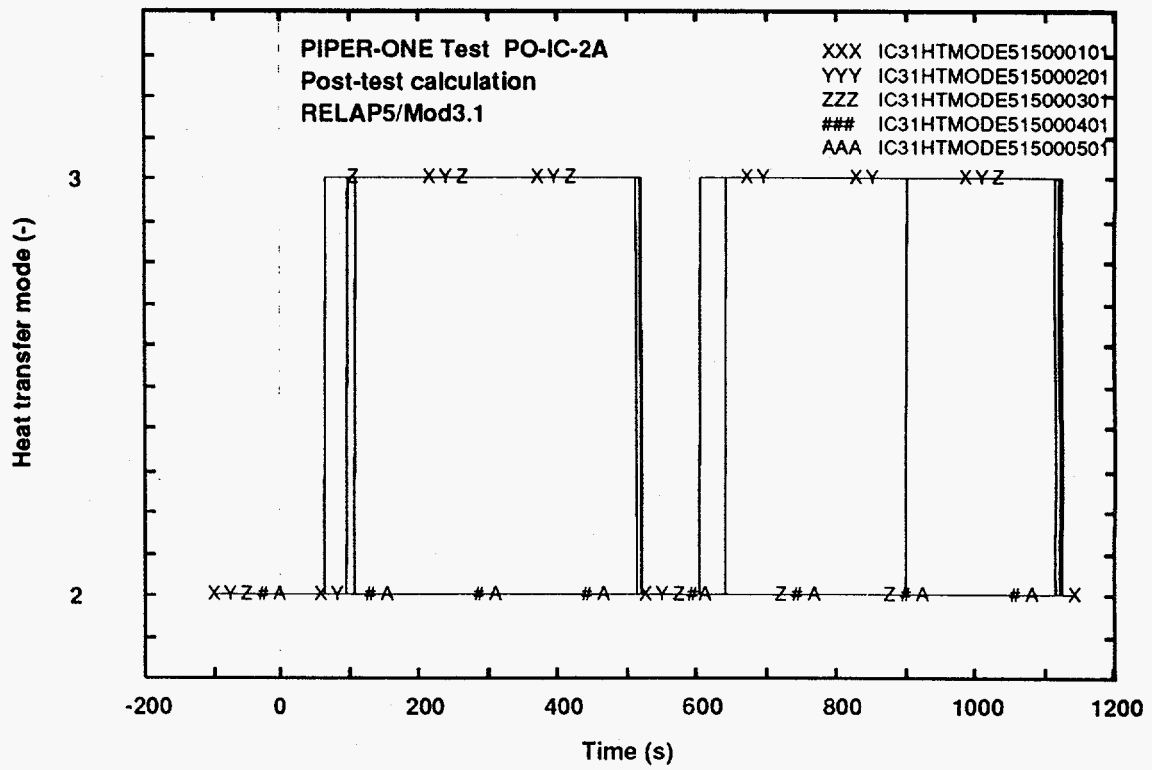


Fig. 39 - Calculated trends of IC tubes heat transfer mode (external side)

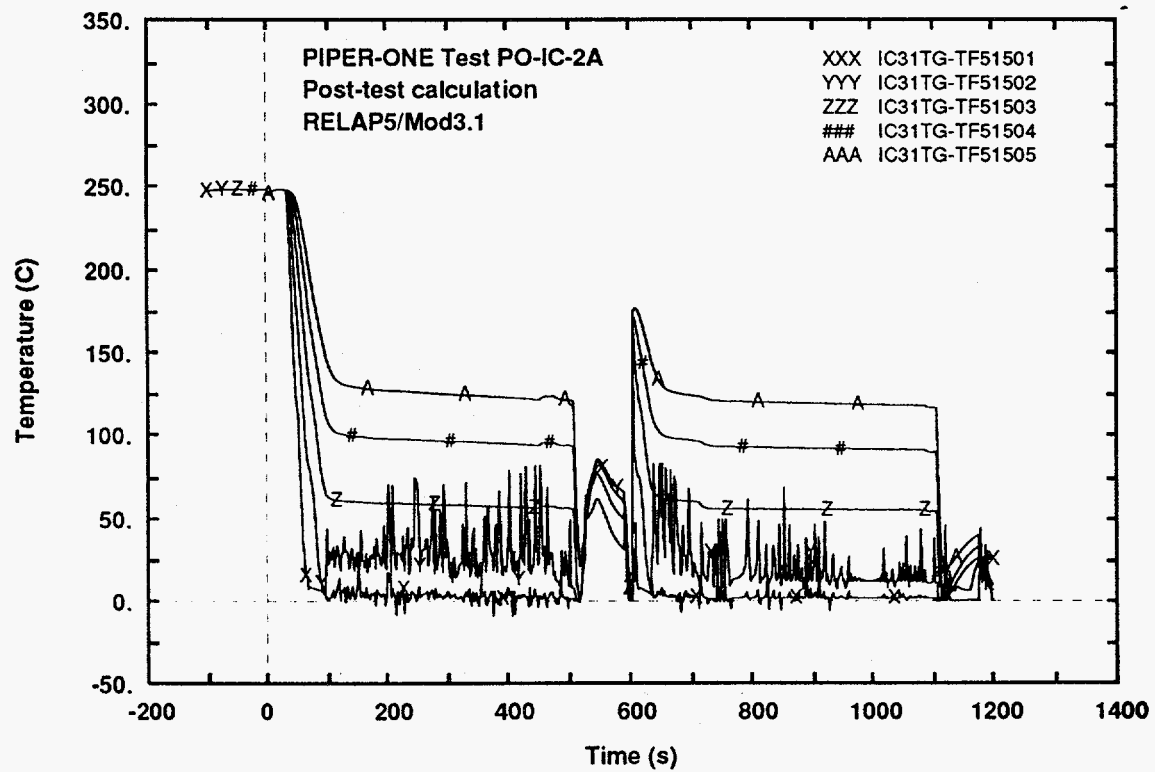


Fig. 40 - Calculated trends of subcooling degree inside IC tubes

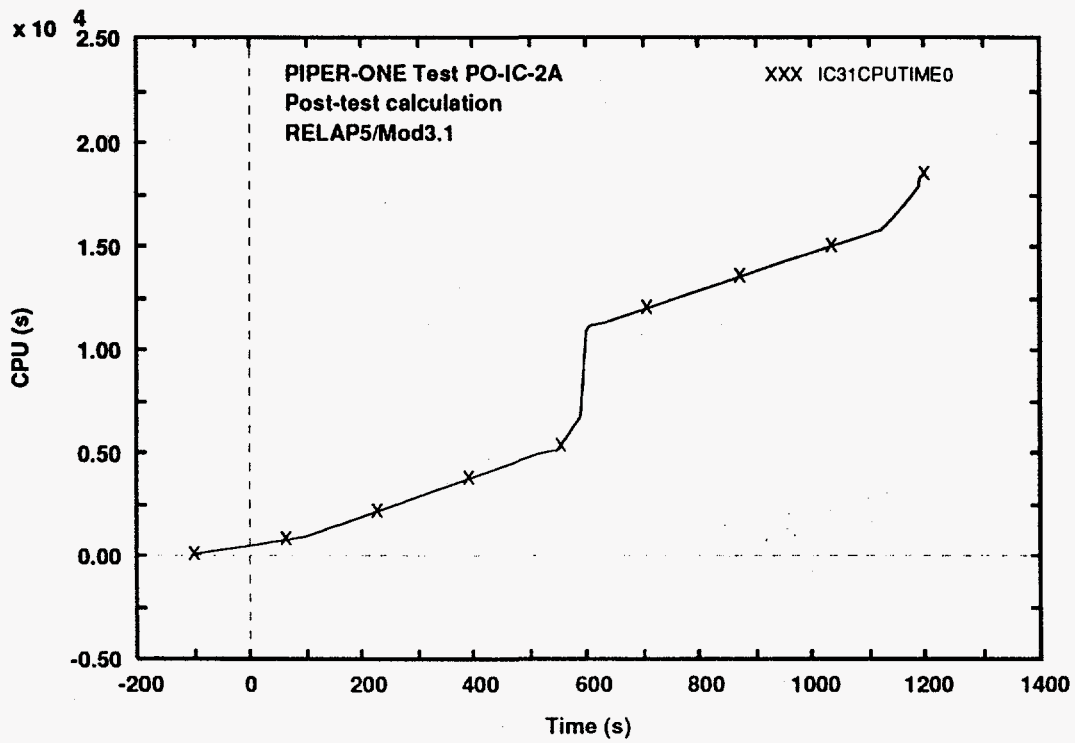


Fig. 41 - CPU versus transient time

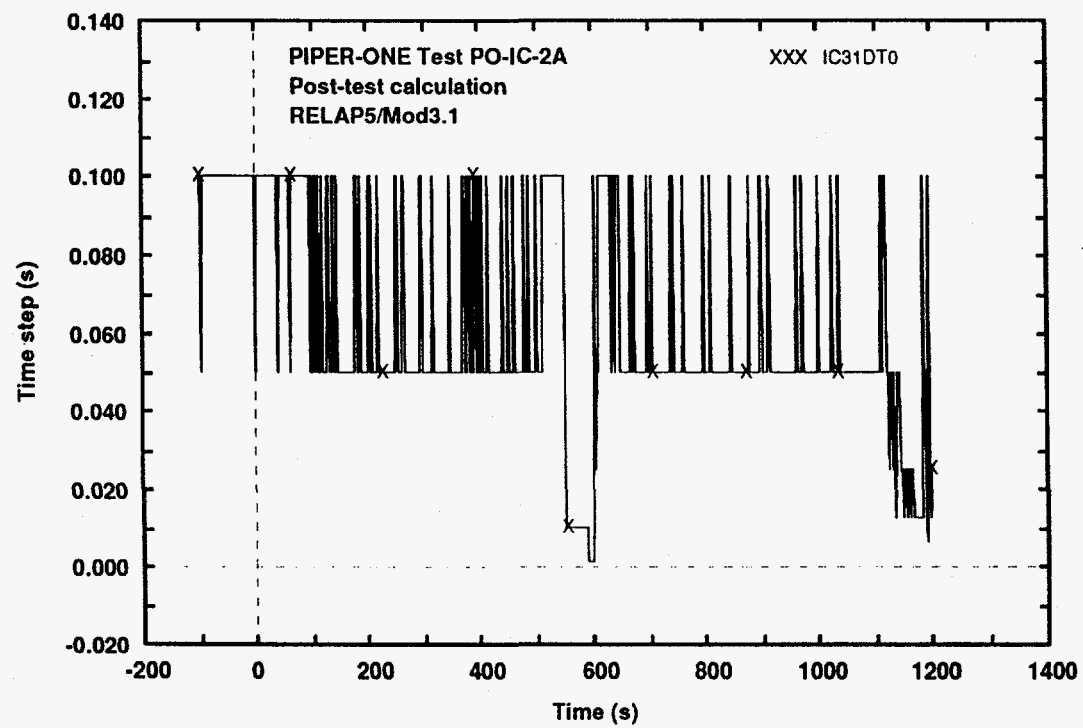


Fig. 42 - Time step versus transient time

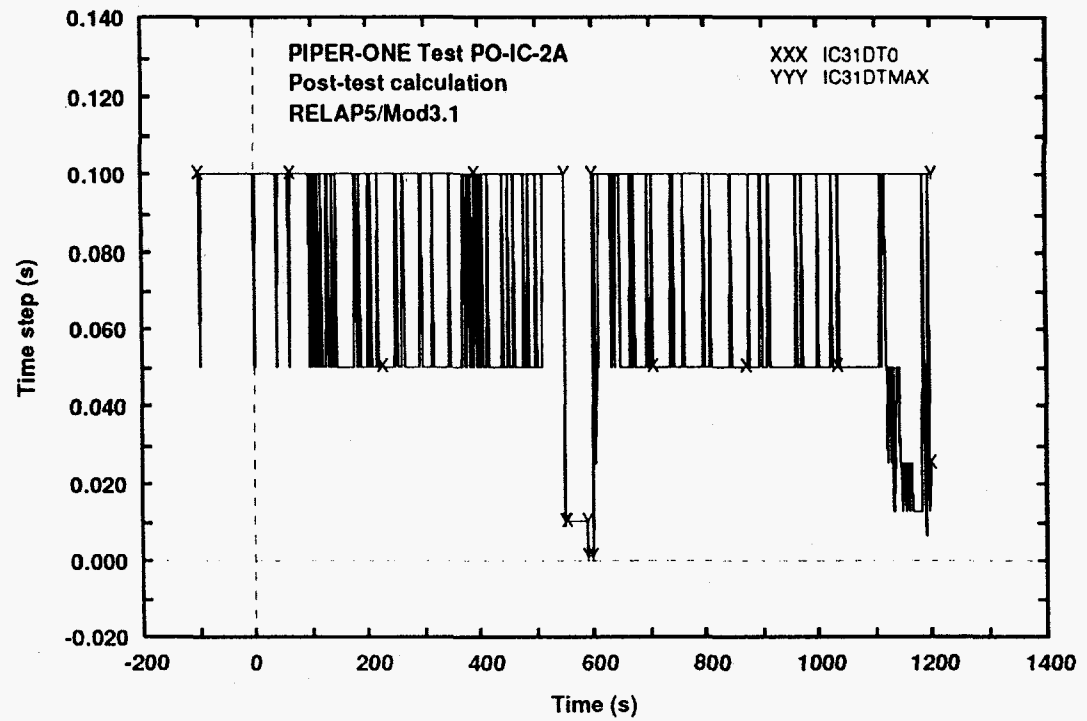


Fig. 43 - Time step and specified maximum time step versus transient time

APPENDIX 2:
IC 36 Results

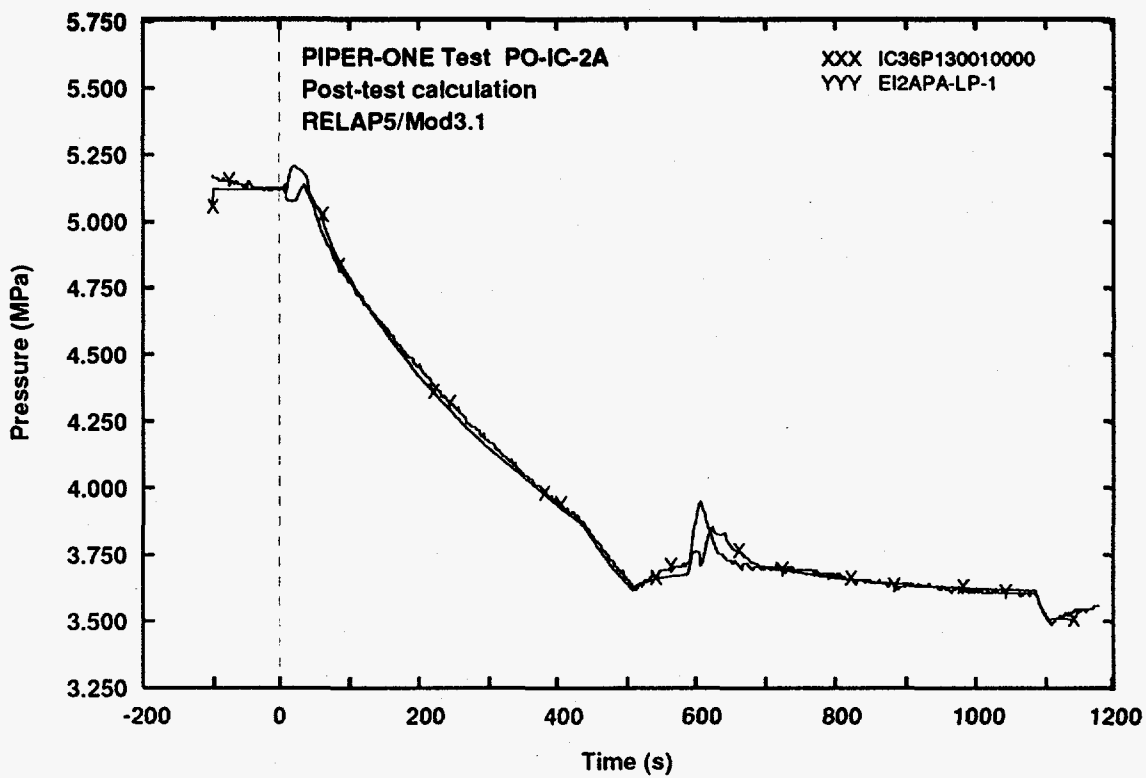


Fig. 1 - Measured and predicted trends of lower plenum pressure

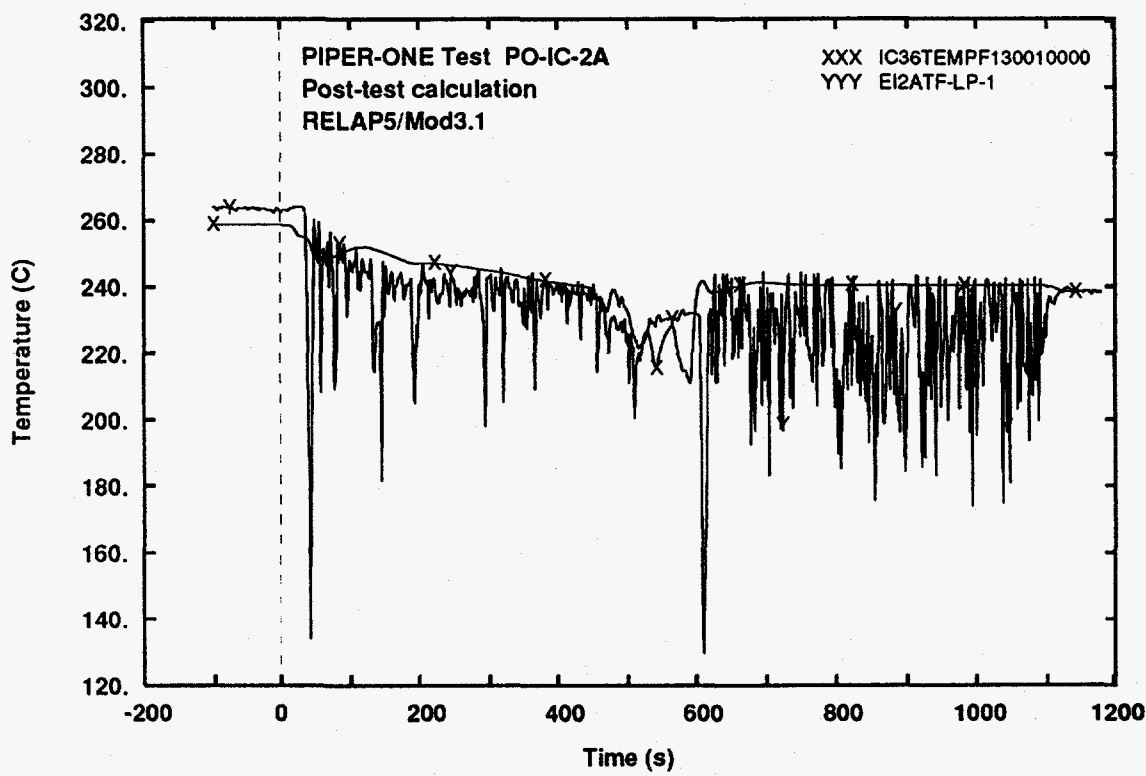


Fig. 2 - Measured and calculated trends of lower plenum temperature

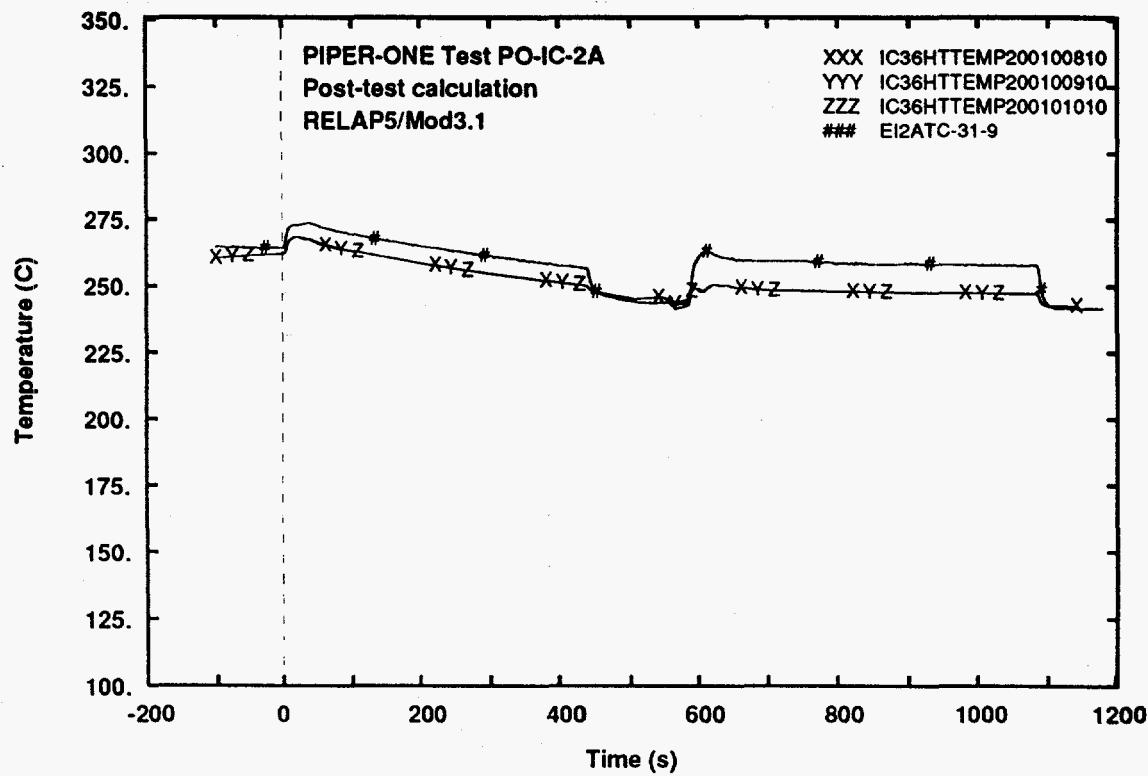


Fig. 3 - Measured and calculated trends of rod surface temperature (level 9)

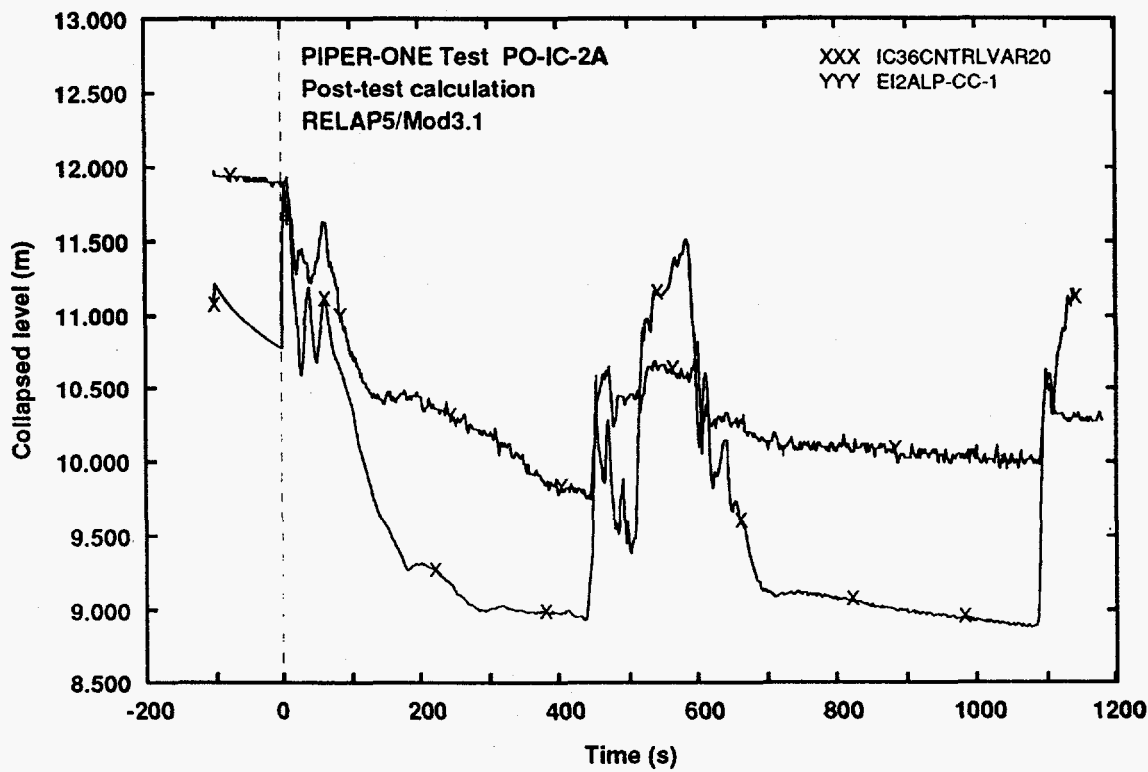


Fig. 4 - Measured and calculated trends of core level

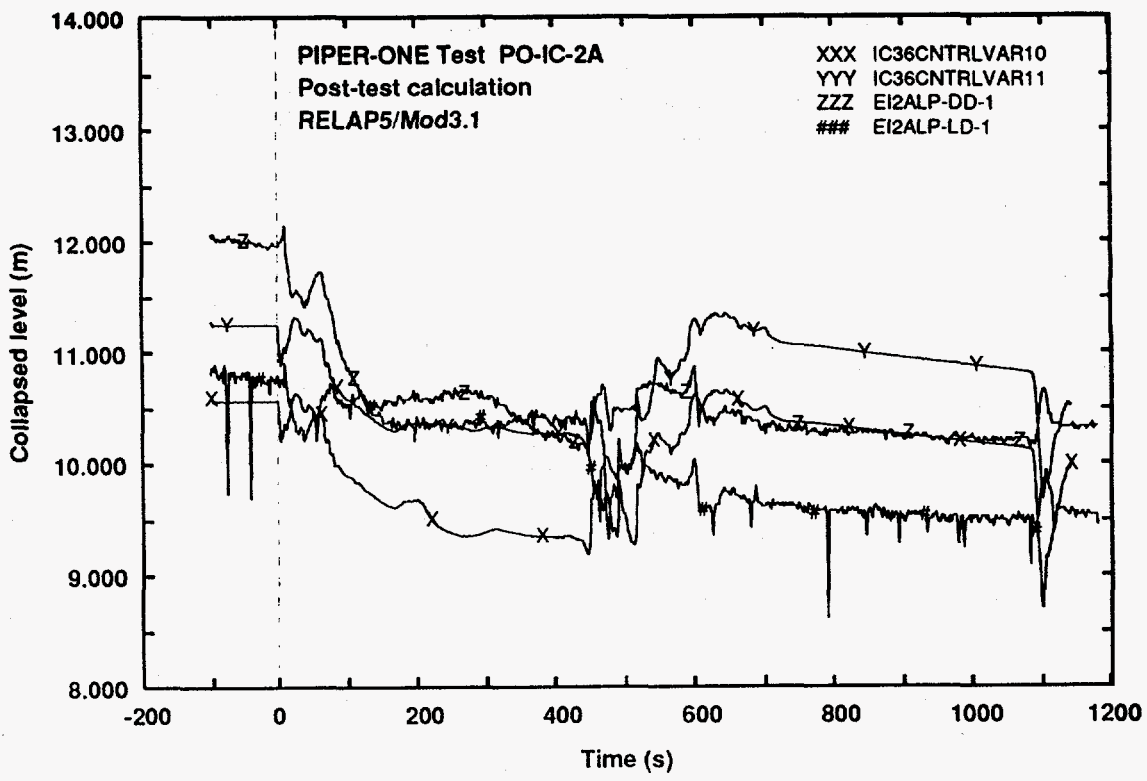


Fig. 5 - Measured and calculated trends of downcomer level

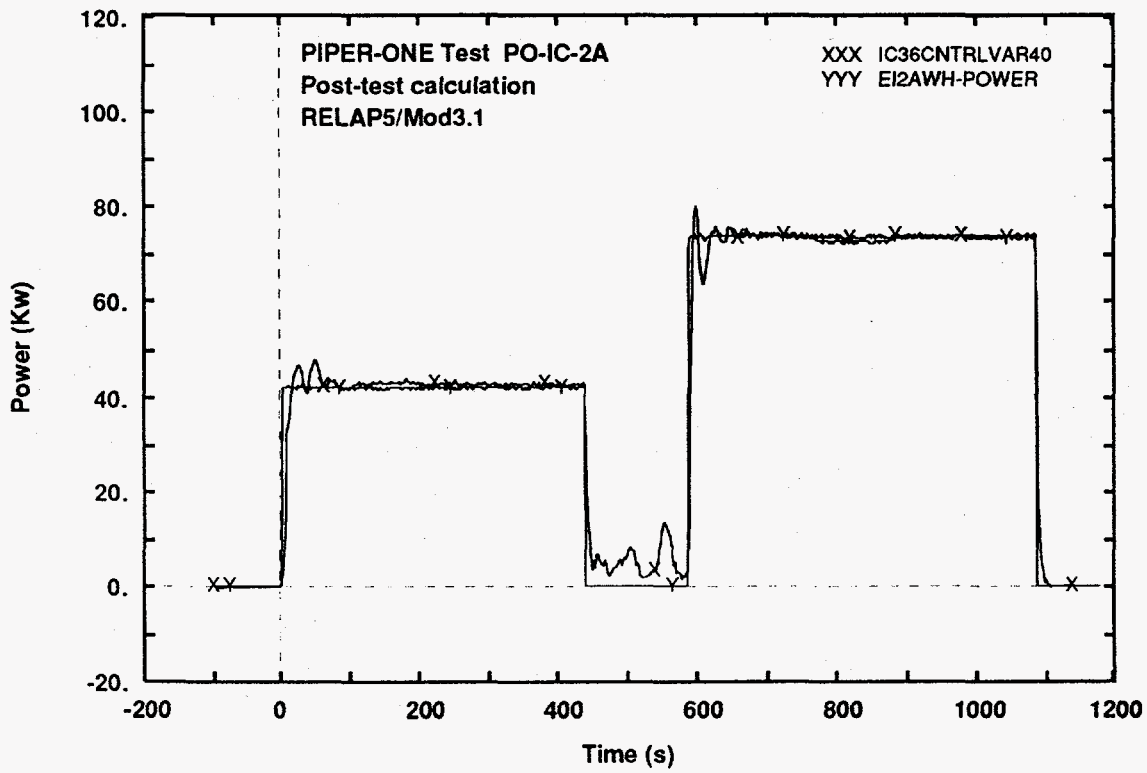


Fig. 6 - Measured and calculated trends of core power

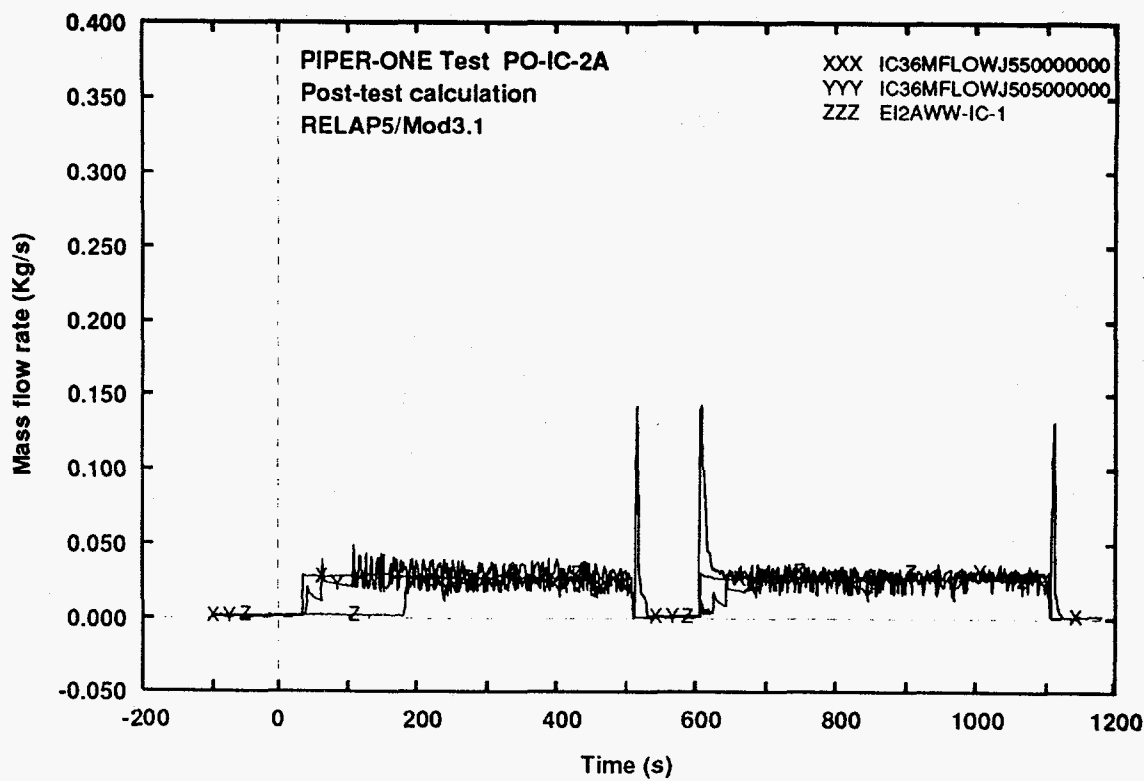


Fig. 7 - Measured and calculated trends of IC mass flow rate

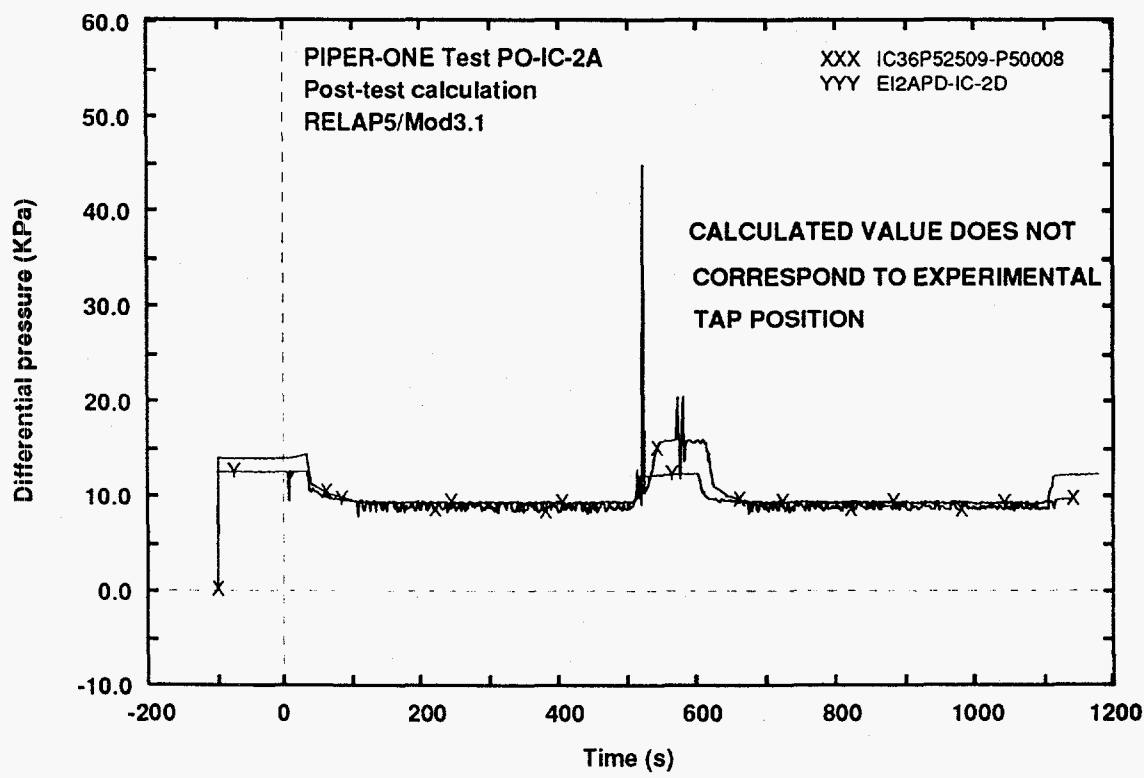


Fig. 8 - Measured and calculated trends of IC differential pressure

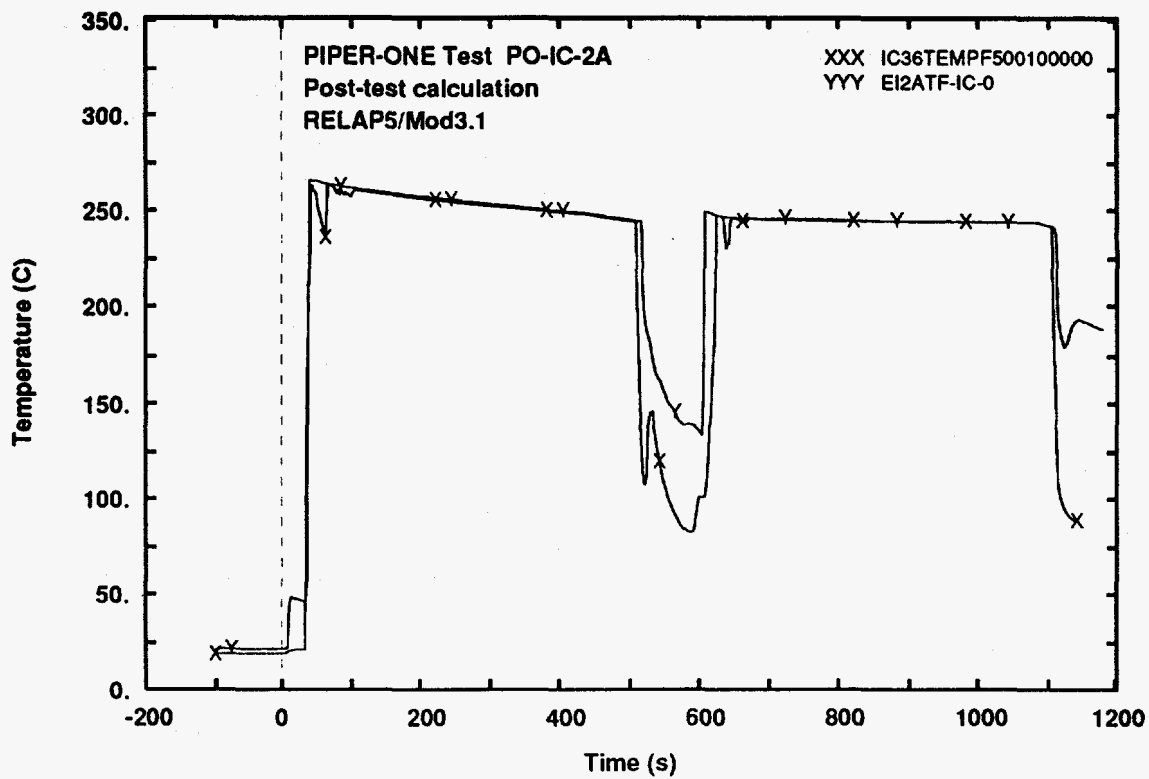
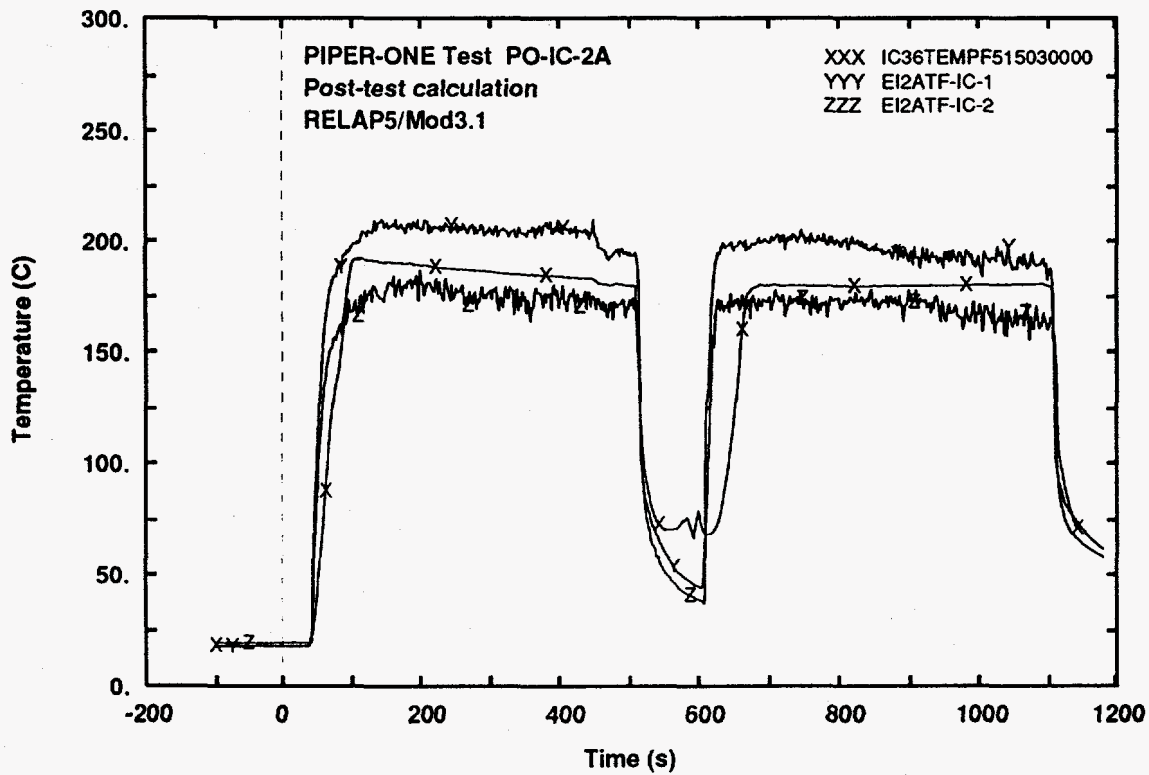


Fig. 9 - Measured and calculated trends of IC inlet fluid temperature



**Fig. 10 - Measured and calculated trends of IC tubes fluid temperature
(middle elevation)**

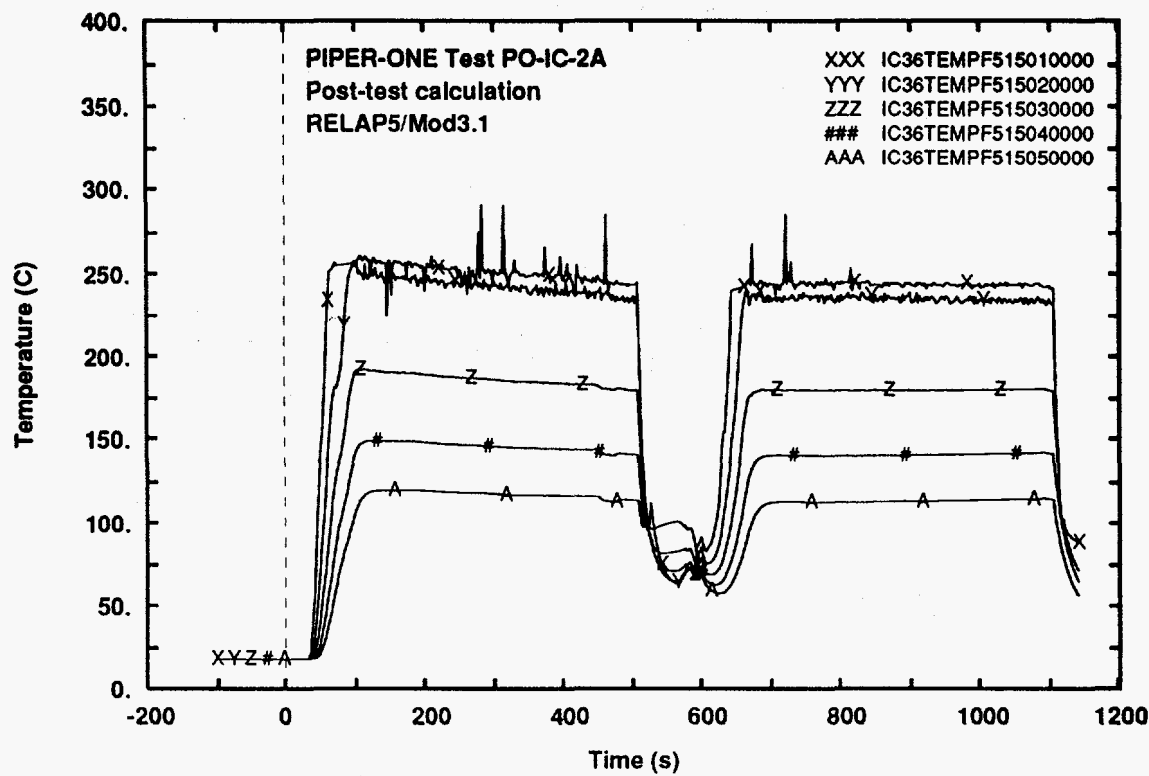


Fig. 11 - Calculated trends of IC tubes fluid temperature along the axis

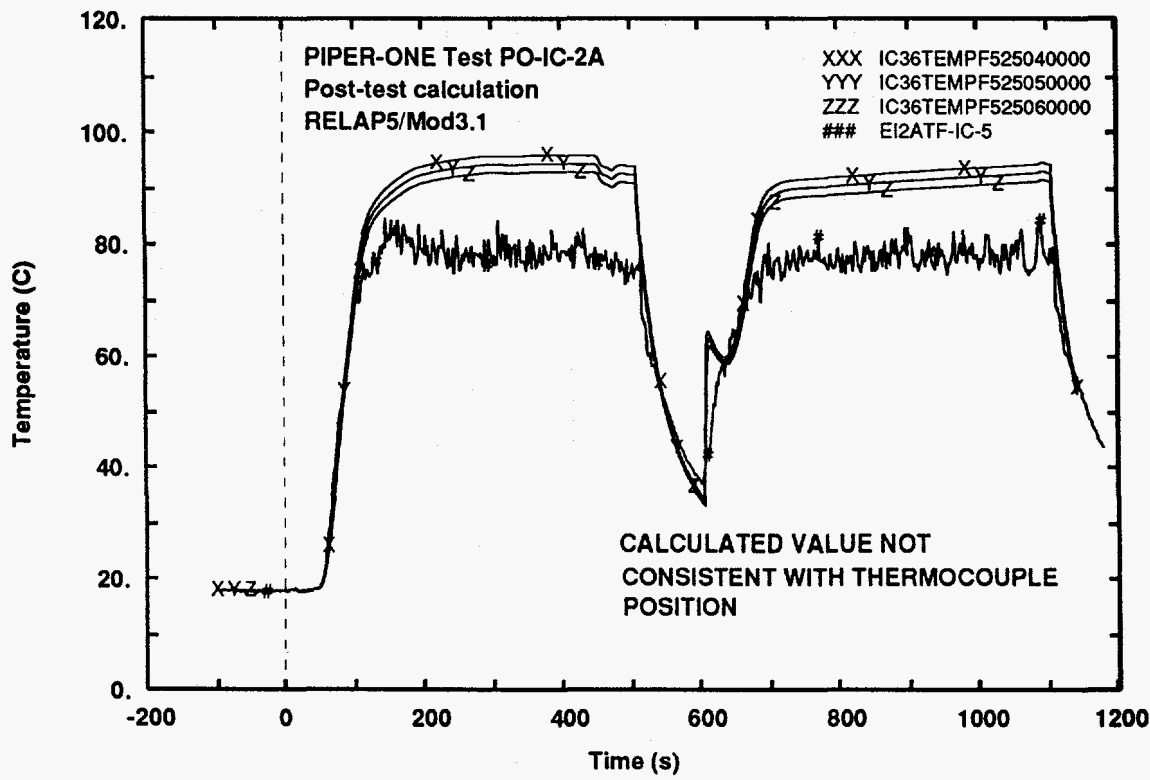


Fig. 12 - Measured and calculated trends of IC outlet fluid temperature

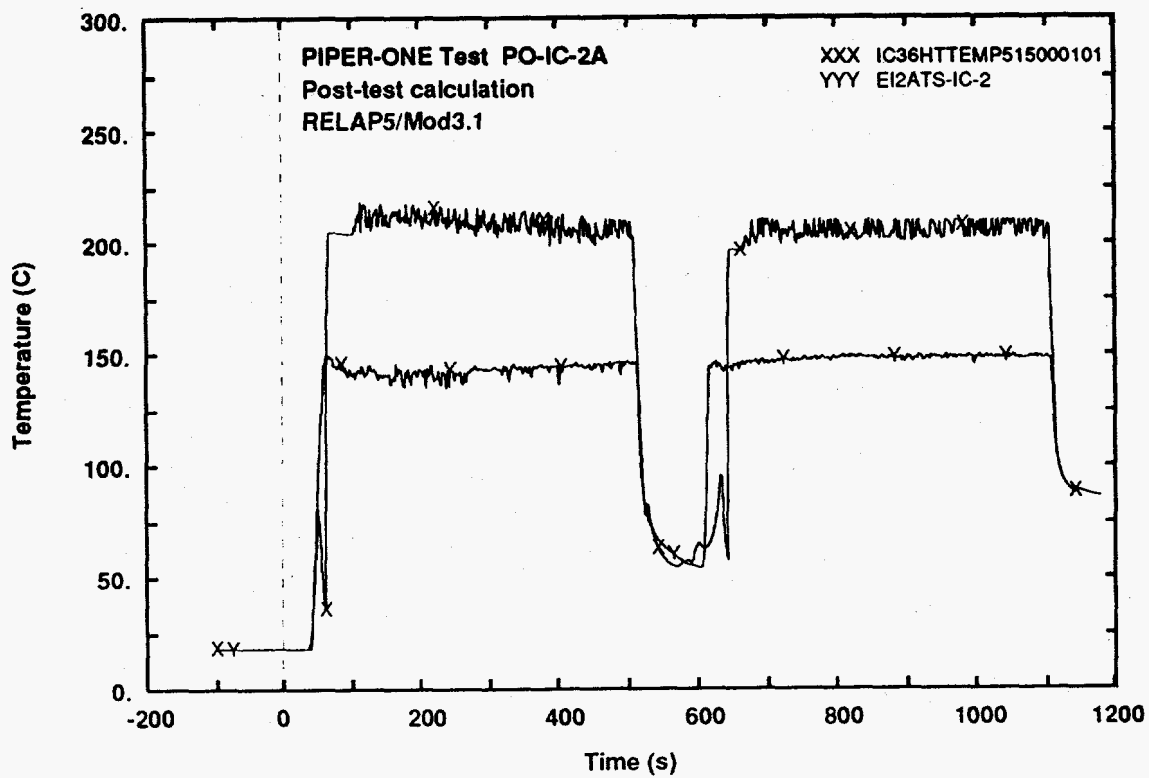


Fig. 13 - Measured and calculated trends of IC tubes wall surface temperature
(internal side top elevation)

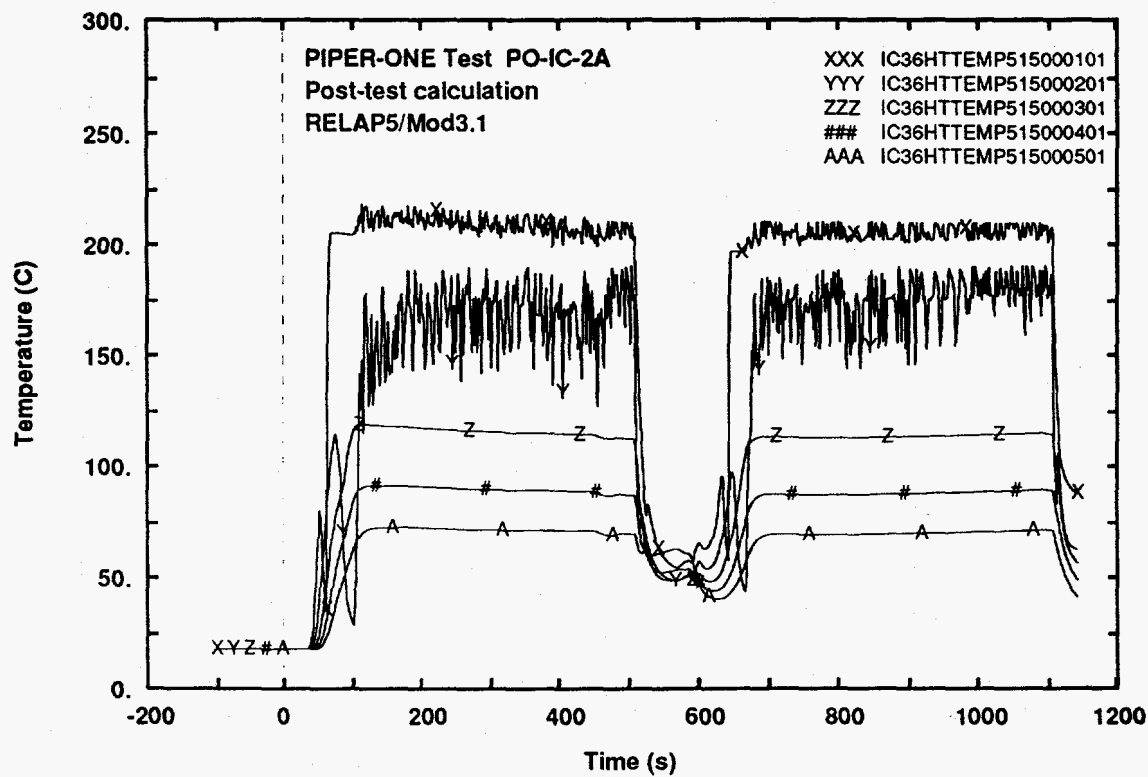


Fig. 14 - Calculated trends of IC tubes wall surface temperature along the axis
(internal side)

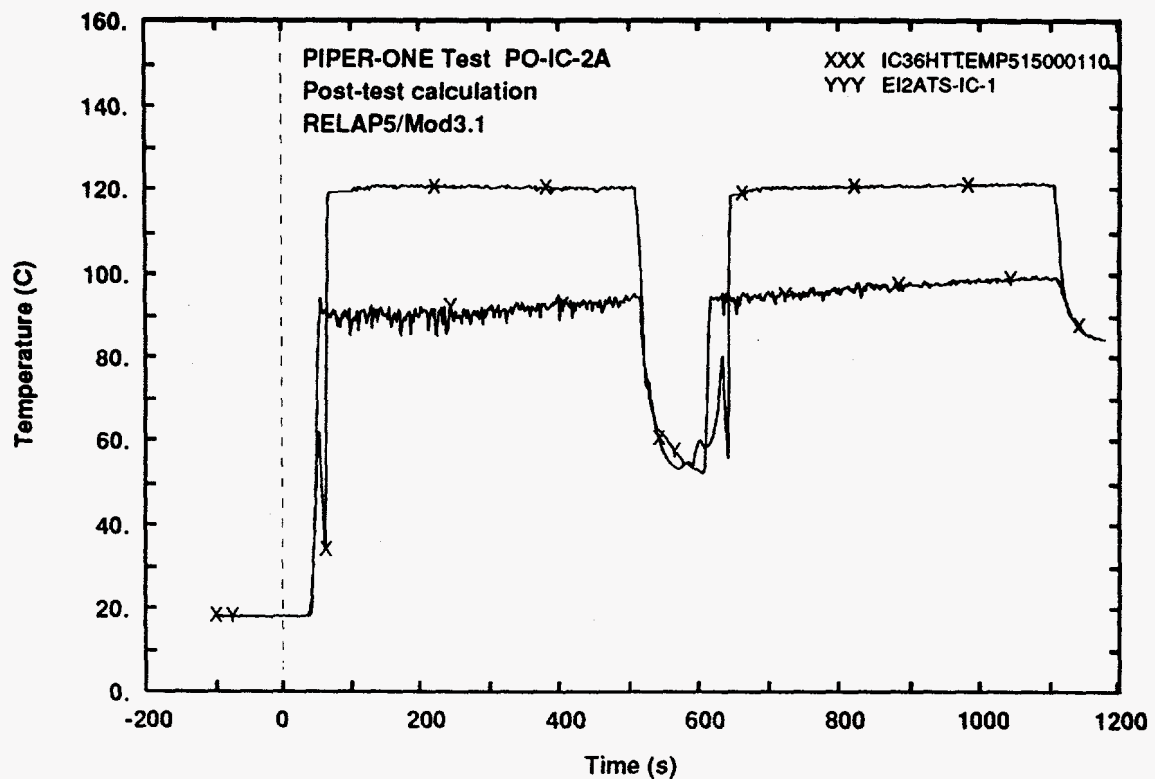


Fig. 15 - Measured and calculated trends of IC tubes wall surface temperature (external side top elevation)

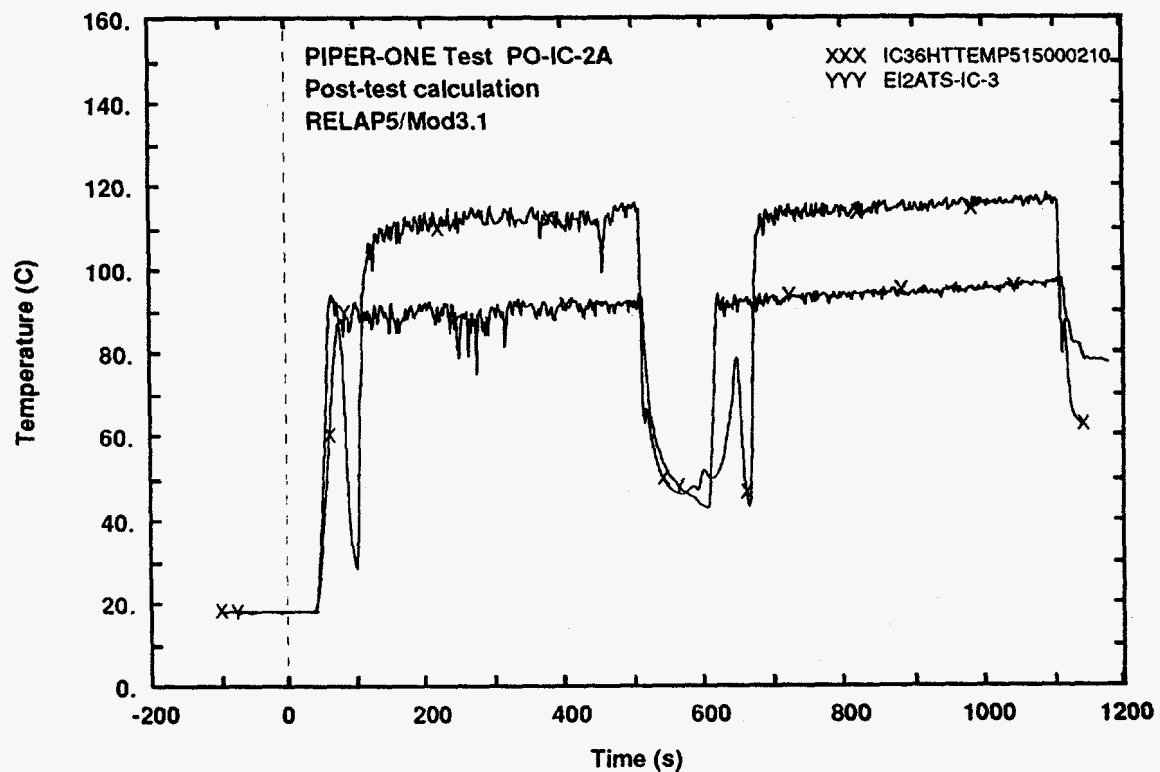


Fig. 16 - Measured and calculated trends of IC tubes wall surface temperature (external side level 3)

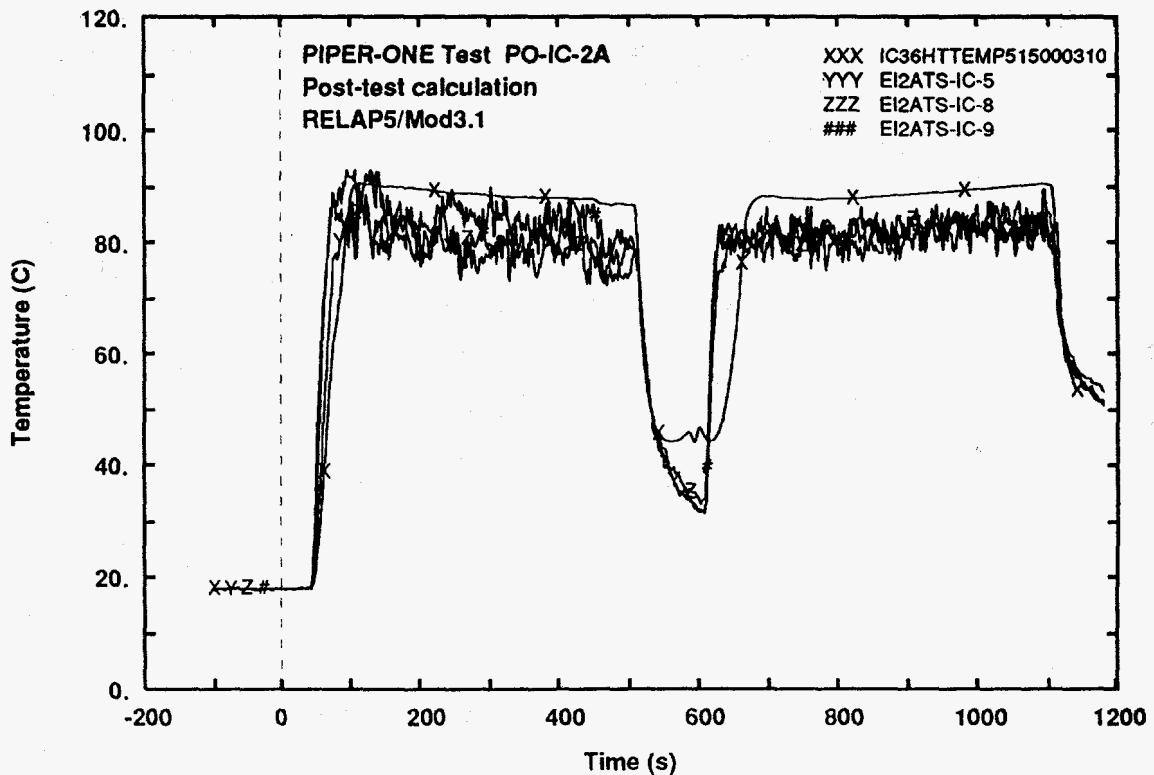


Fig. 17 - Measured and calculated trends of IC tubes wall surface temperature
(external side middle elevation)

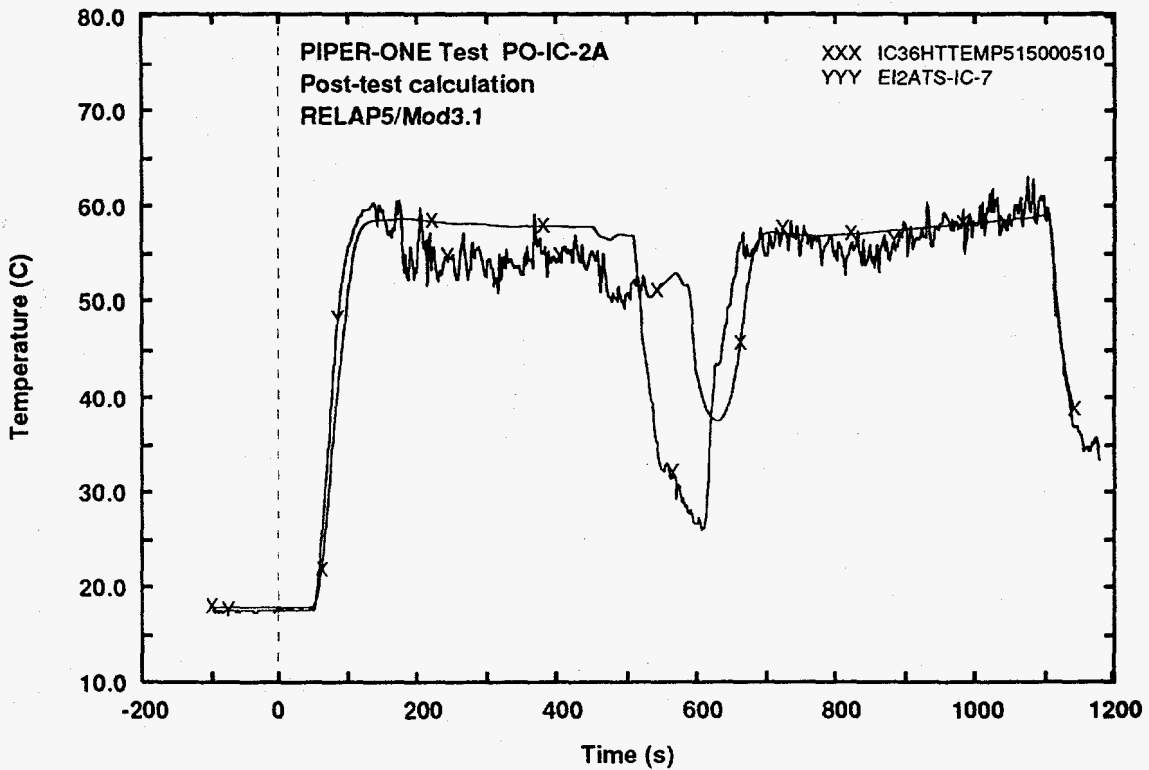


Fig. 18 - Measured and calculated trends of IC tubes wall surface temperature
(external side bottom elevation)

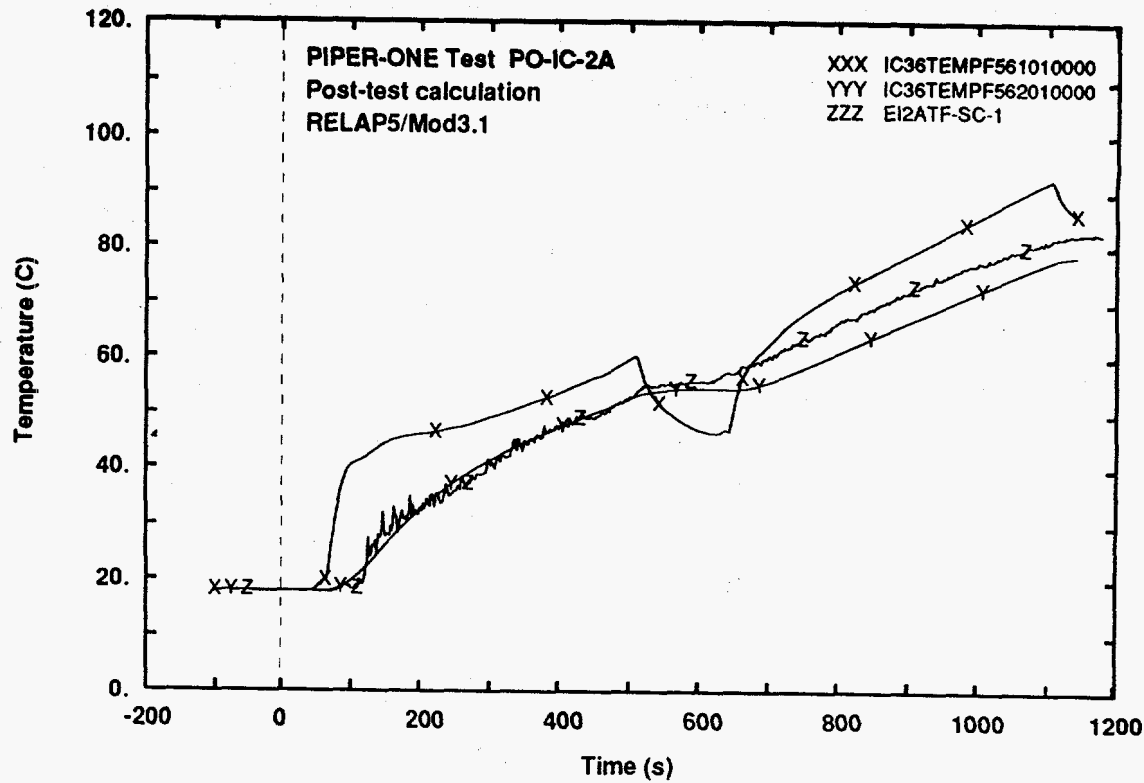


Fig. 19 - Measured and calculated trends of IC internal pool fluid temperature (top level)

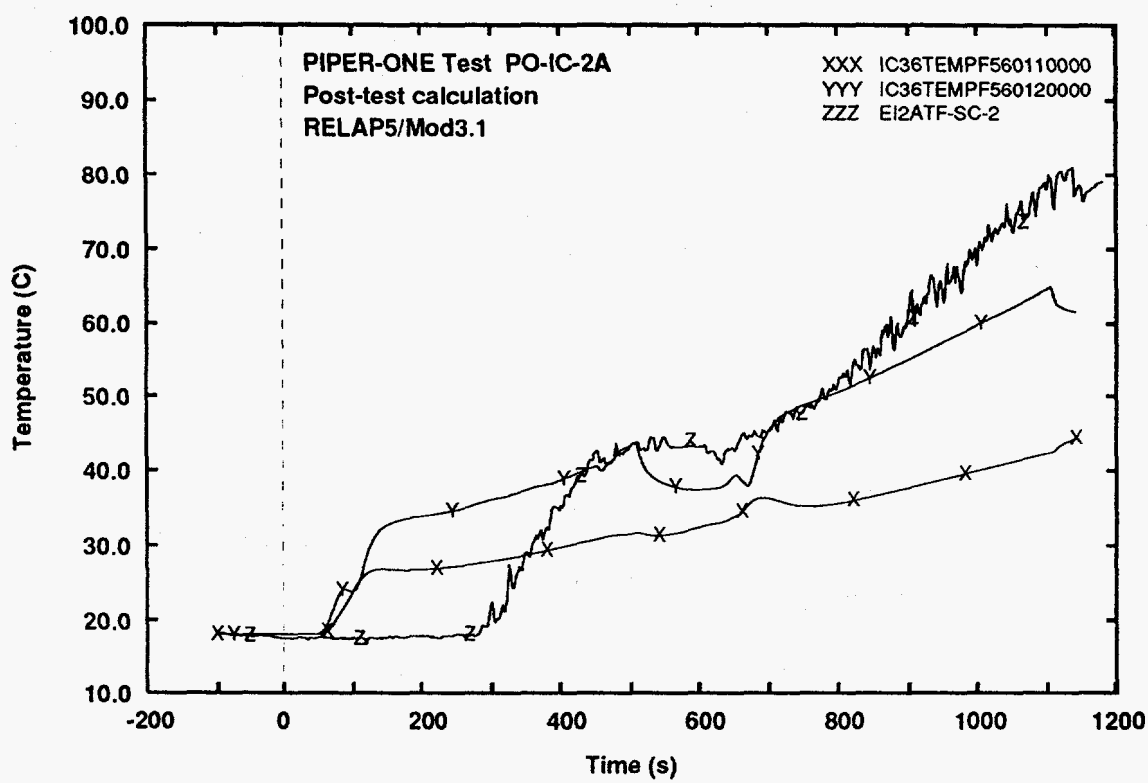


Fig. 20 - Measured and calculated trends of IC internal pool fluid temperature (level 2)

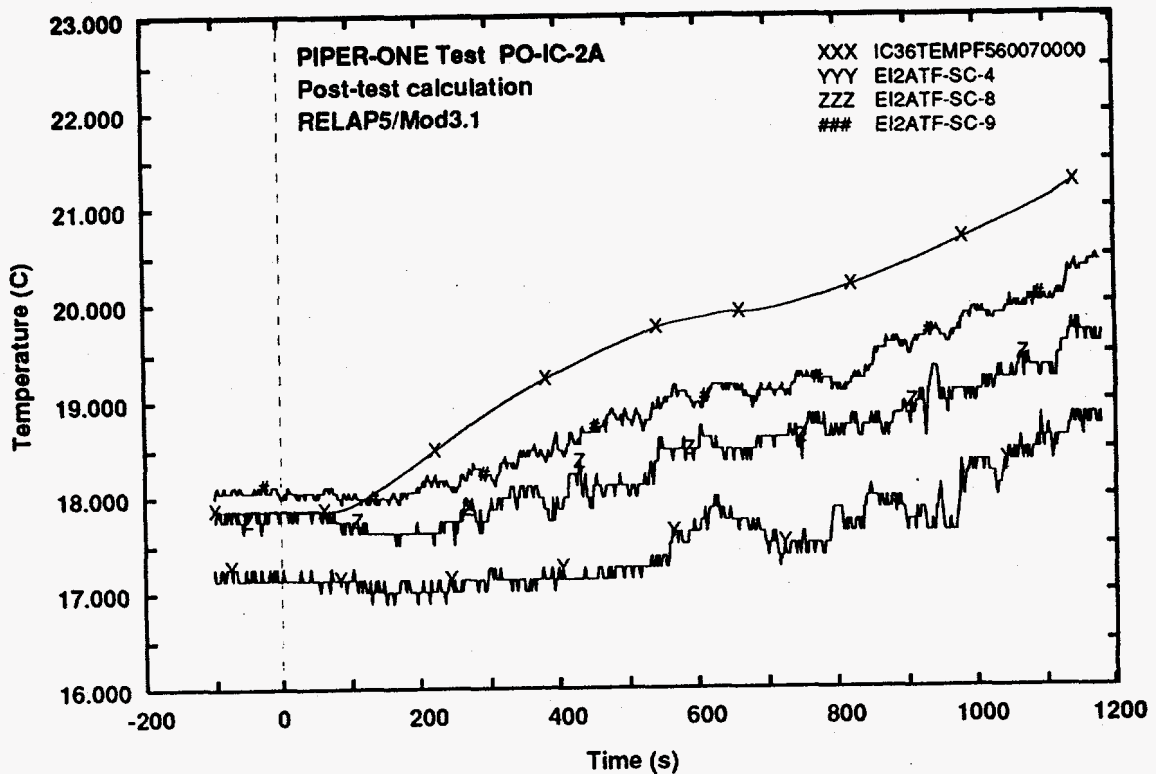


Fig. 21 - Measured and calculated trends of IC internal pool fluid temperature (middle level)

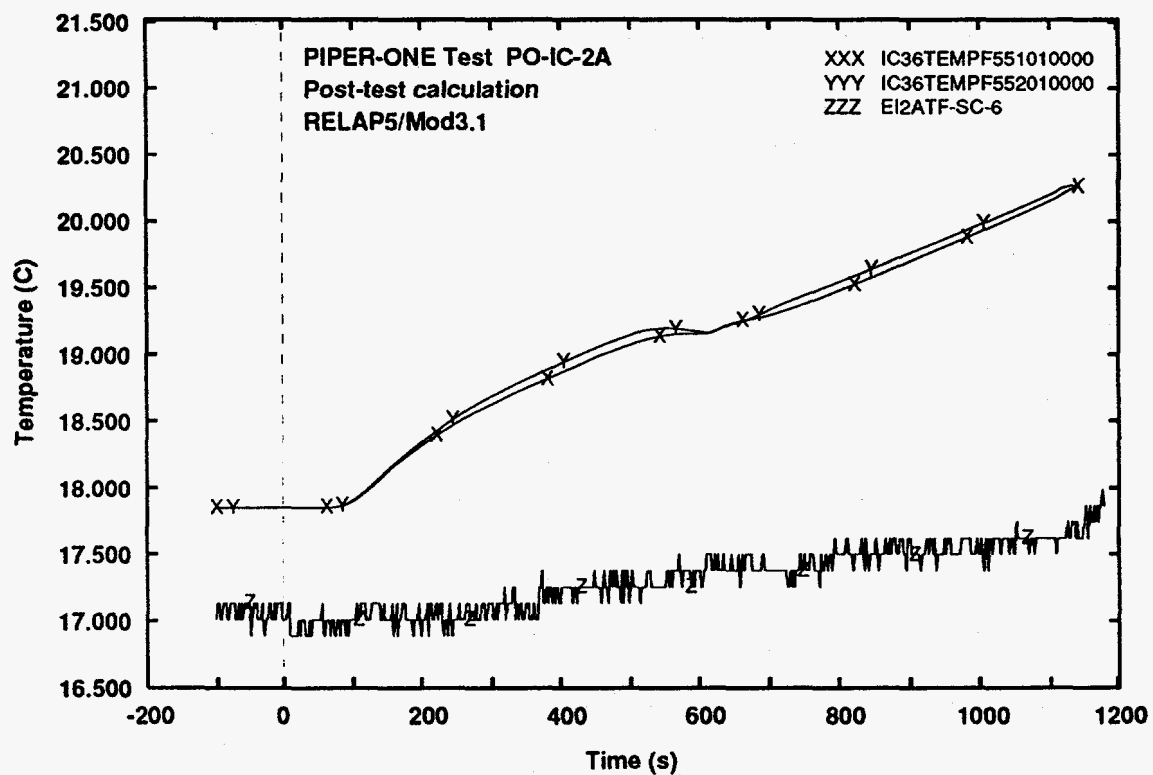


Fig. 22 - Measured and calculated trends of IC internal pool fluid temperature (bottom level)

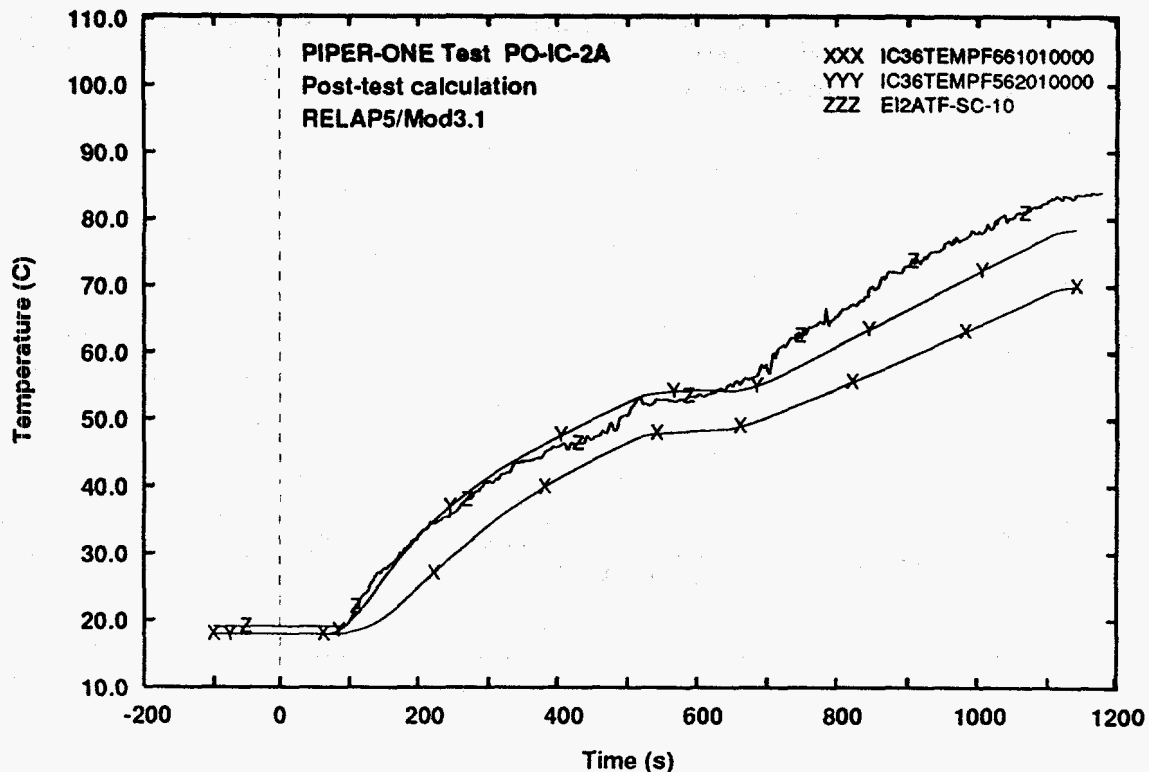


Fig. 23 - Measured and calculated trends of IC external pool fluid temperature (top level)

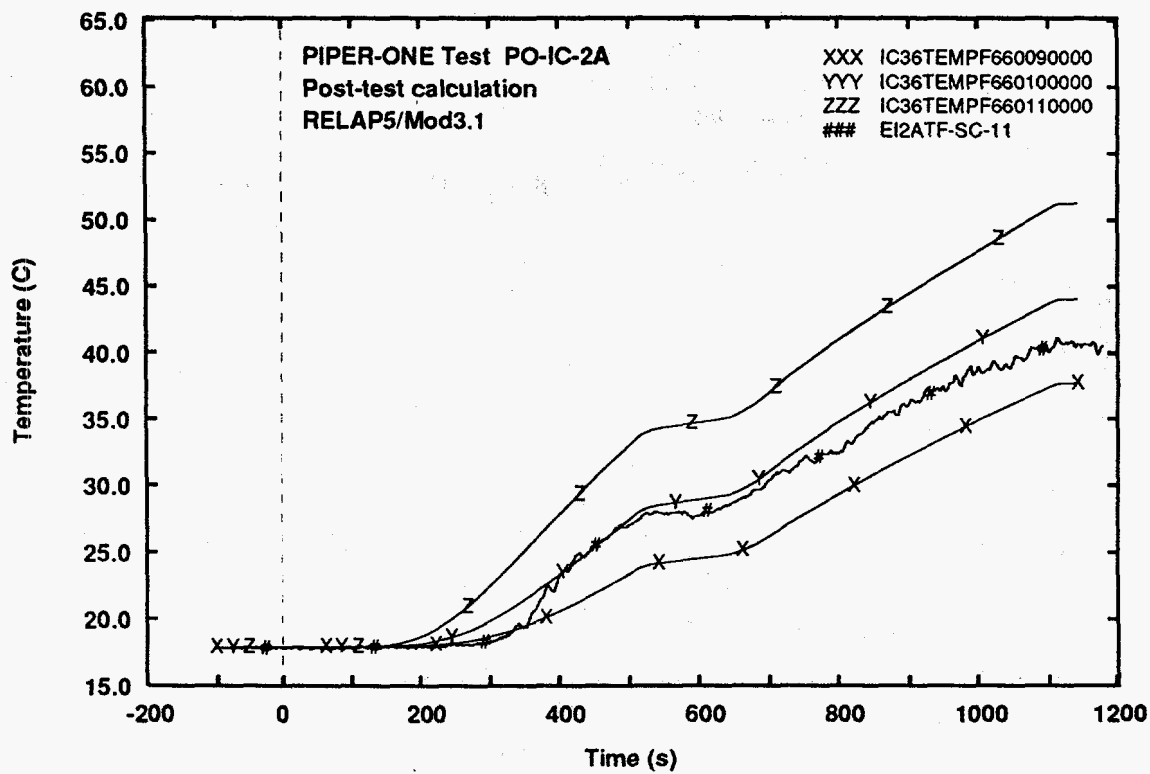


Fig. 24 - Measured and calculated trends of IC external pool fluid temperature (level 11)

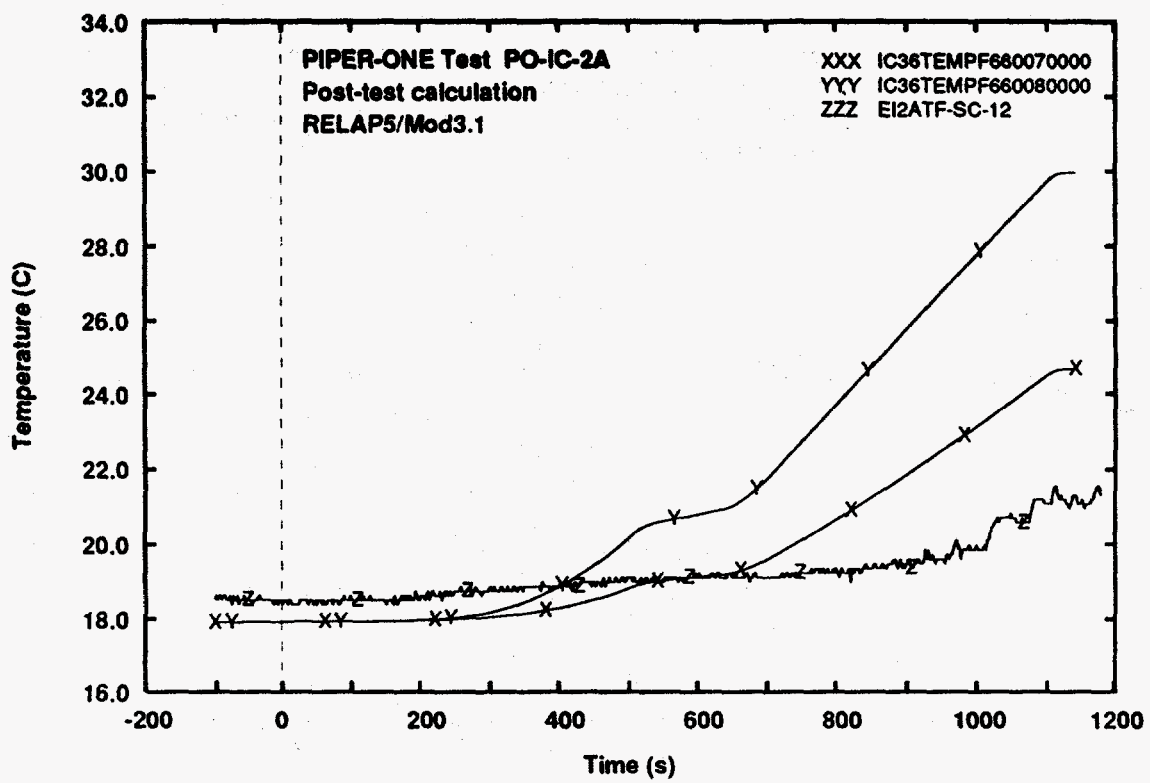


Fig. 25 - Measured and calculated trends of IC external pool fluid temperature (middle level)

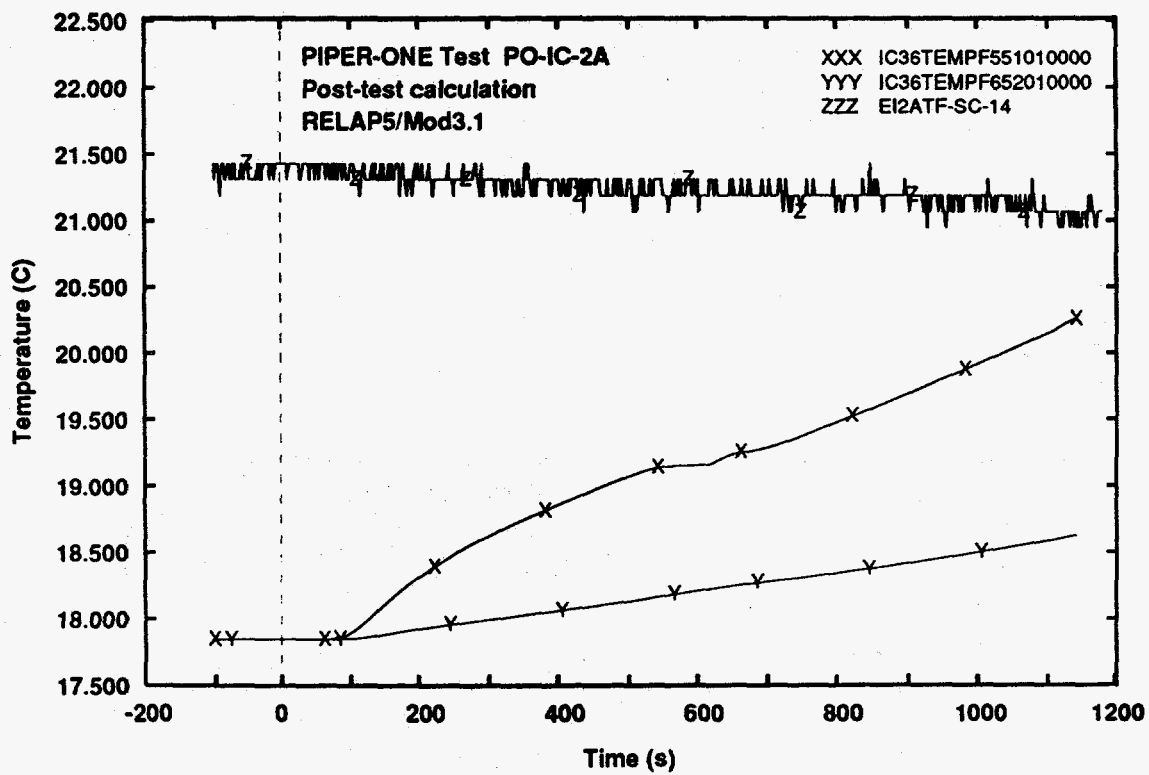


Fig. 26 - Measured and calculated trends of IC external pool fluid temperature (bottom level)

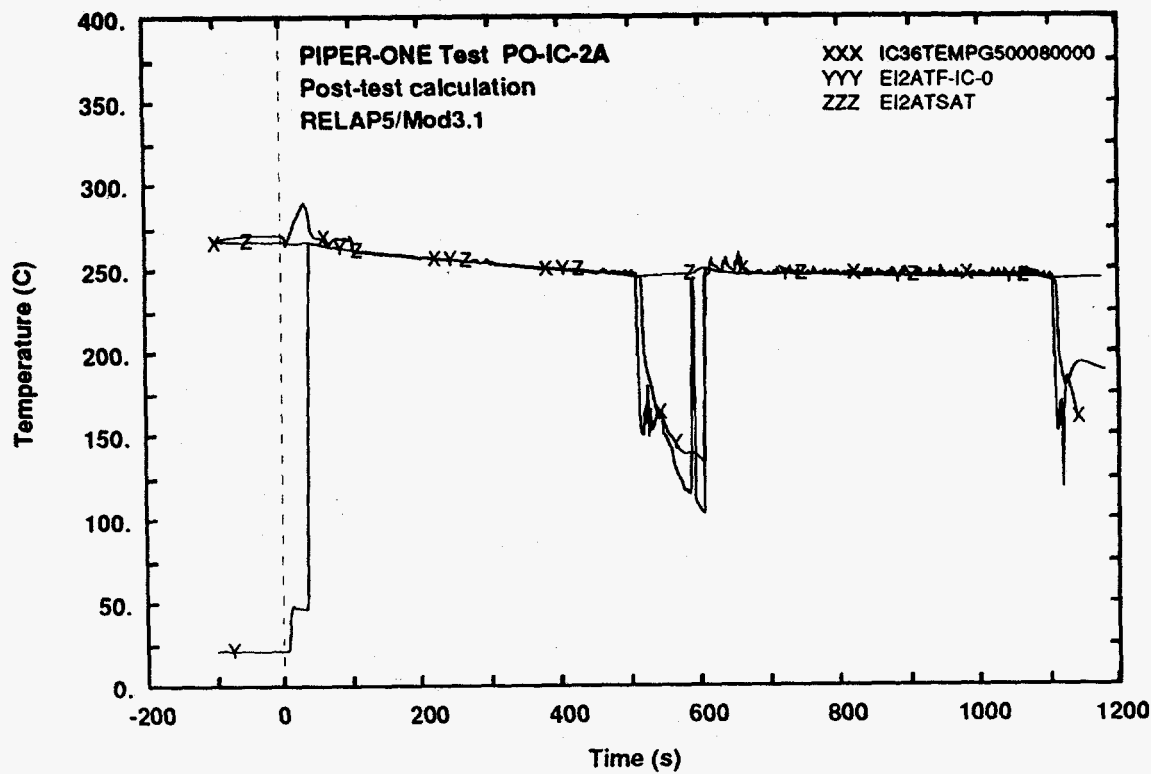


Fig. 27 - Measured and calculated trends of steam temperature at IC inlet compared with experimental saturated temperature

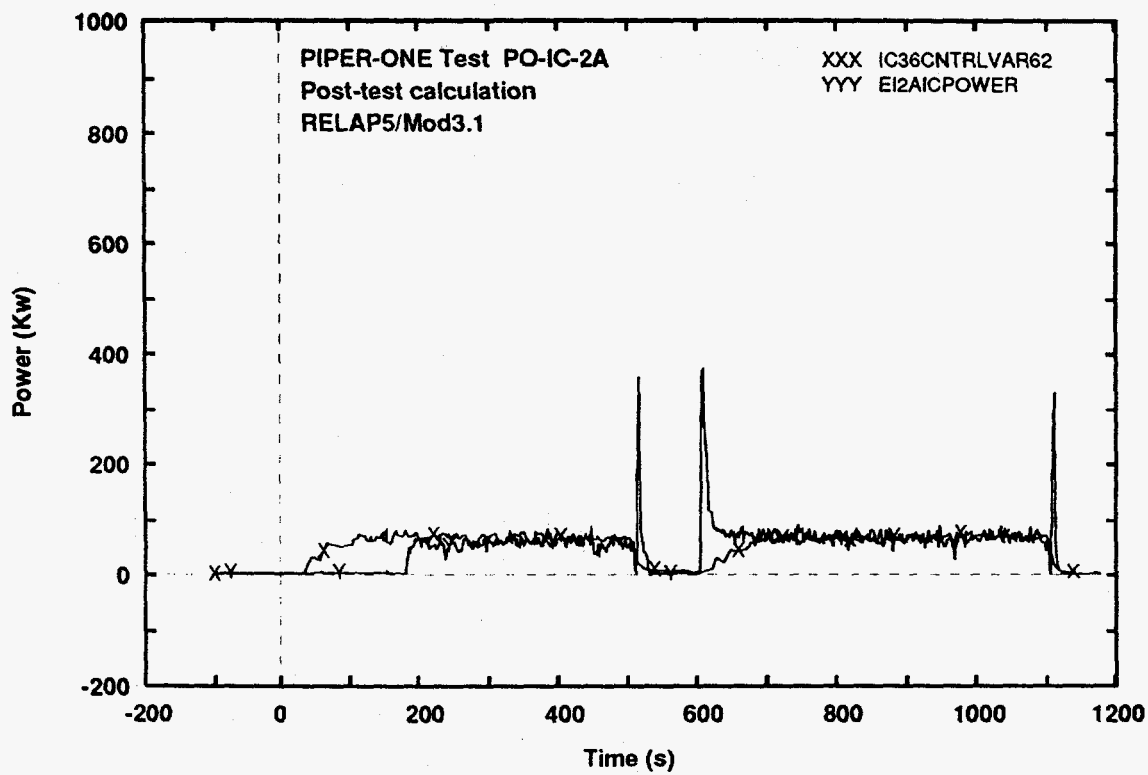


Fig. 28 - Measured and calculated trends of IC exchanged power

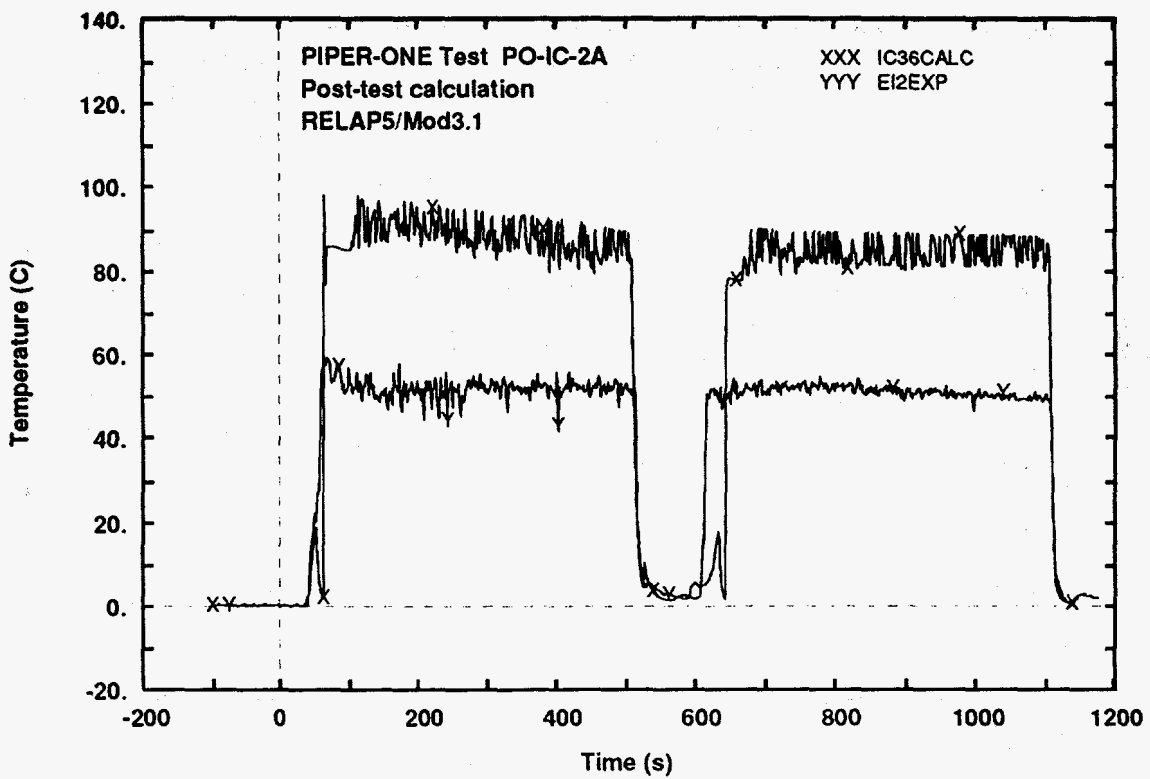


Fig. 29 - Measured and calculated trends of temperature difference between internal and external side of IC tubes wall (top elevation)

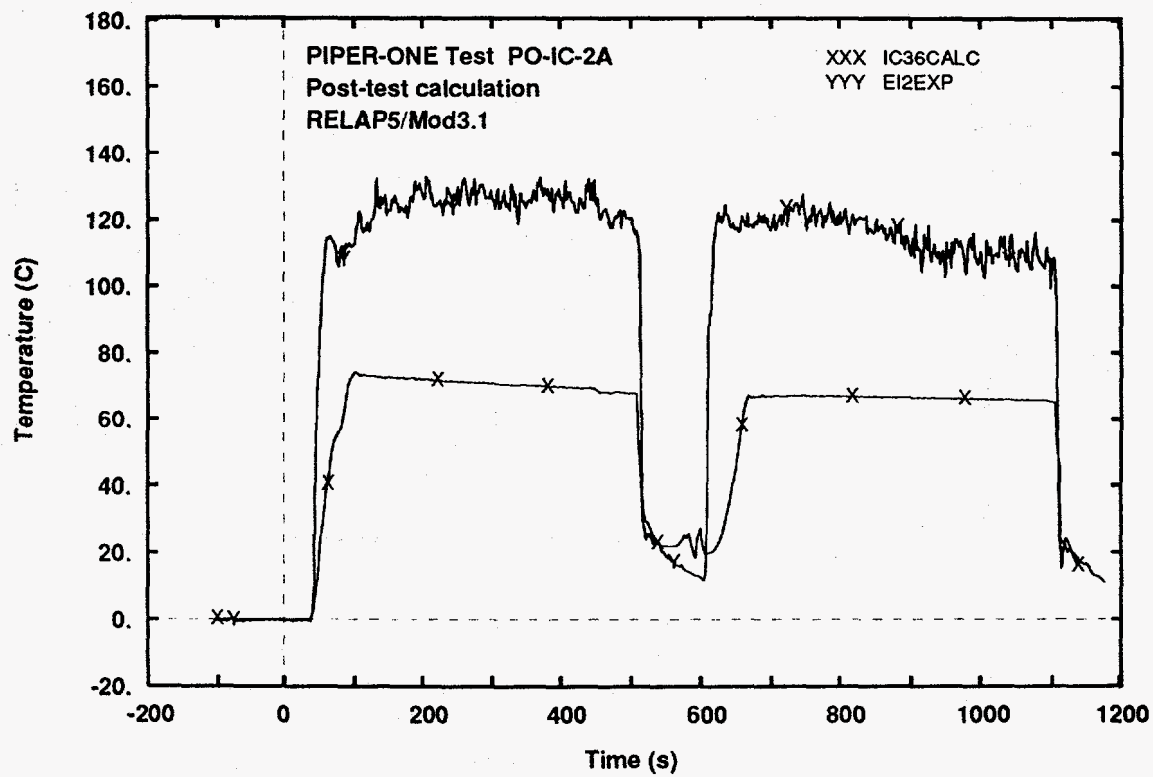


Fig. 30 - Measured and calculated trends of temperature difference between IC fluid and external side of IC tubes wall (middle elevation)

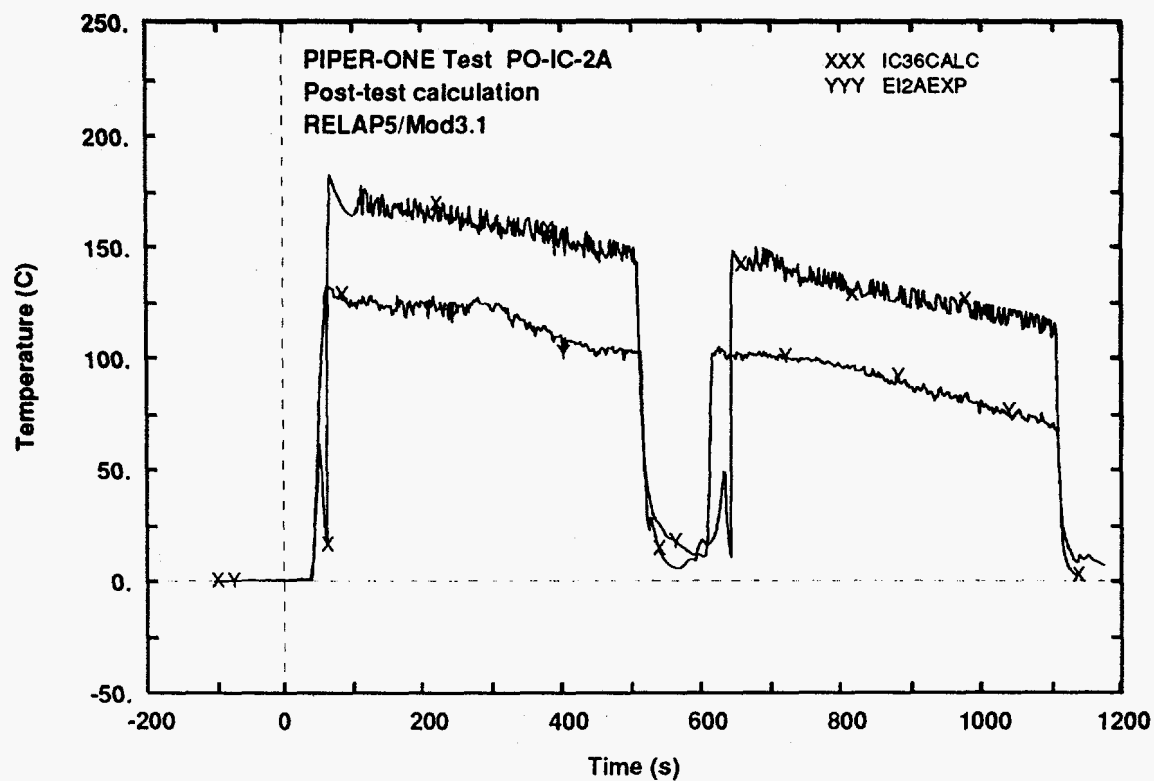


Fig. 31 - Measured and calculated trends of temperature difference between internal side of IC tubes wall and IC pool fluid temperature (top elevation)

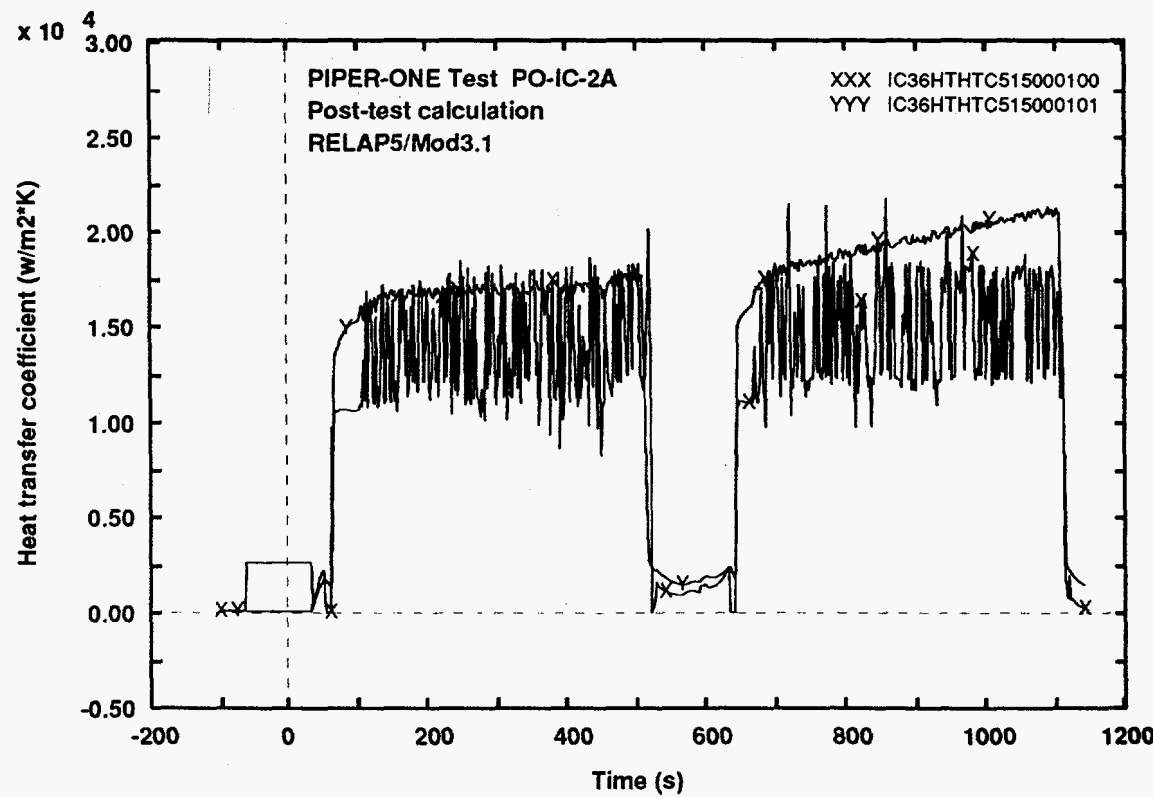


Fig. 32 - Calculated trends of the heat transfer coefficient at the inside and the outside of IC tubes wall (top elevation)

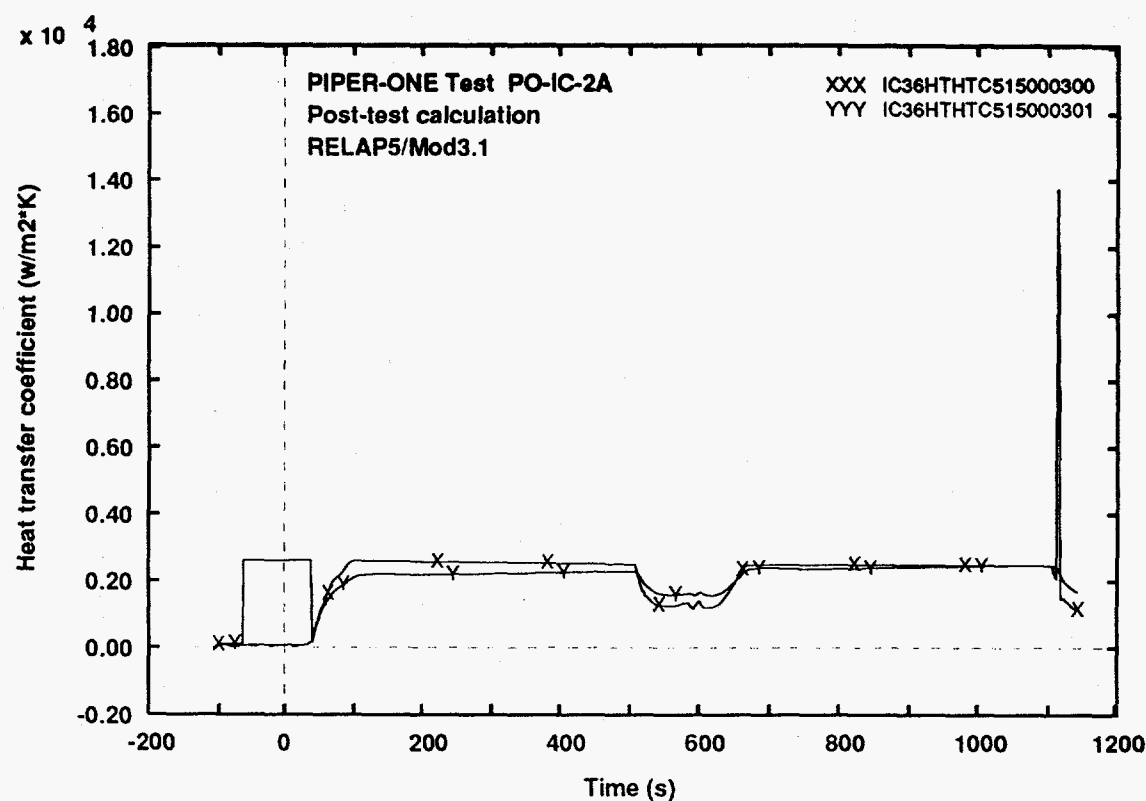


Fig. 33 - Calculated trends of the heat transfer coefficient at the inside and the outside of IC tubes wall (middle elevation)

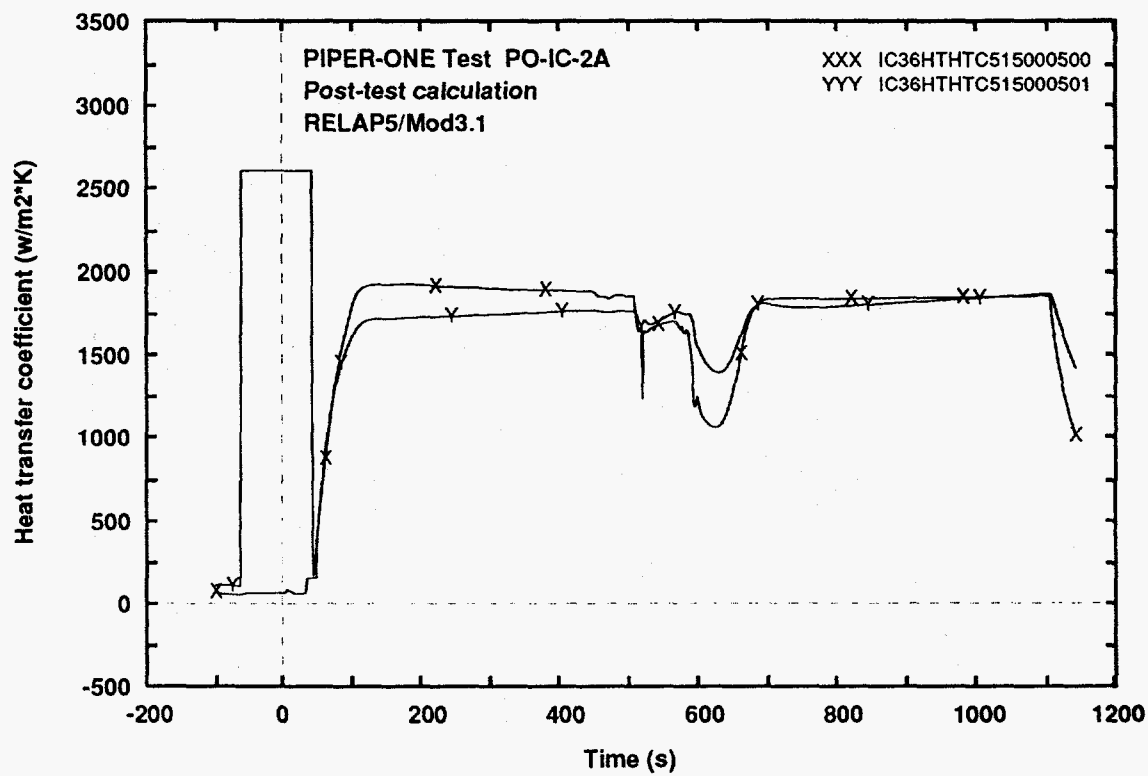


Fig. 34 - Calculated trends of the heat transfer coefficient at the inside and the outside of IC tubes wall (bottom elevation)

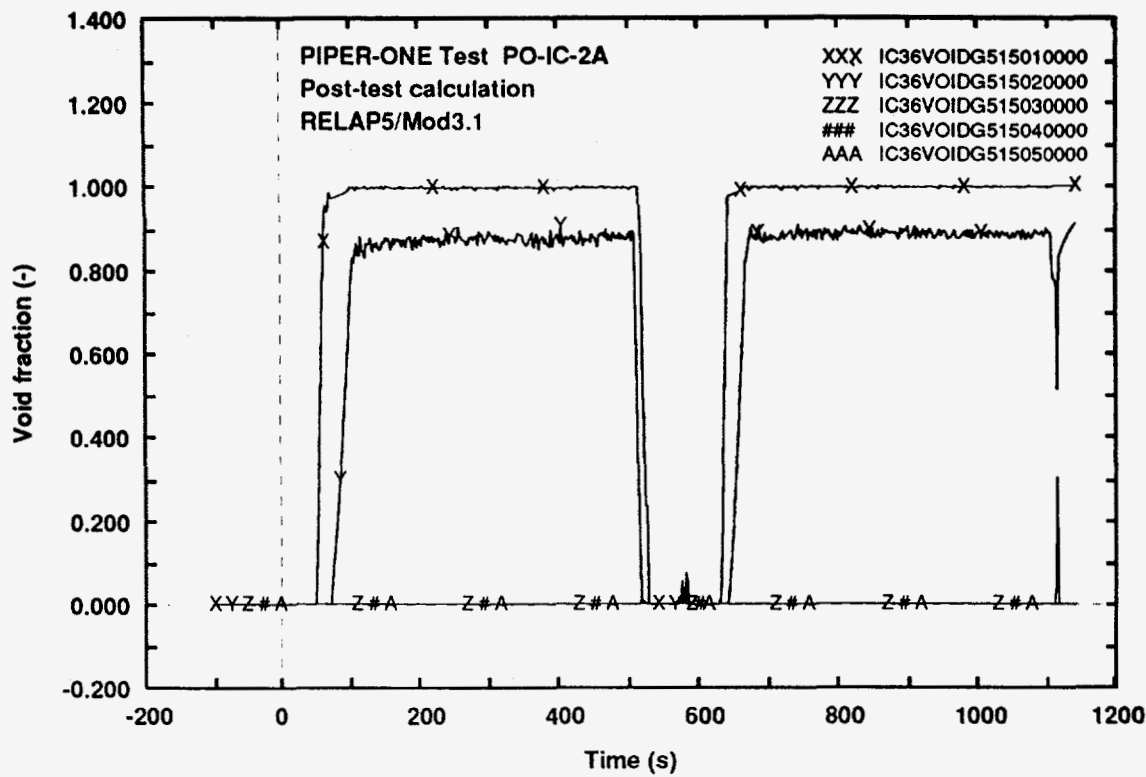


Fig. 35 - Calculated trends of IC tubes void fraction along the axis

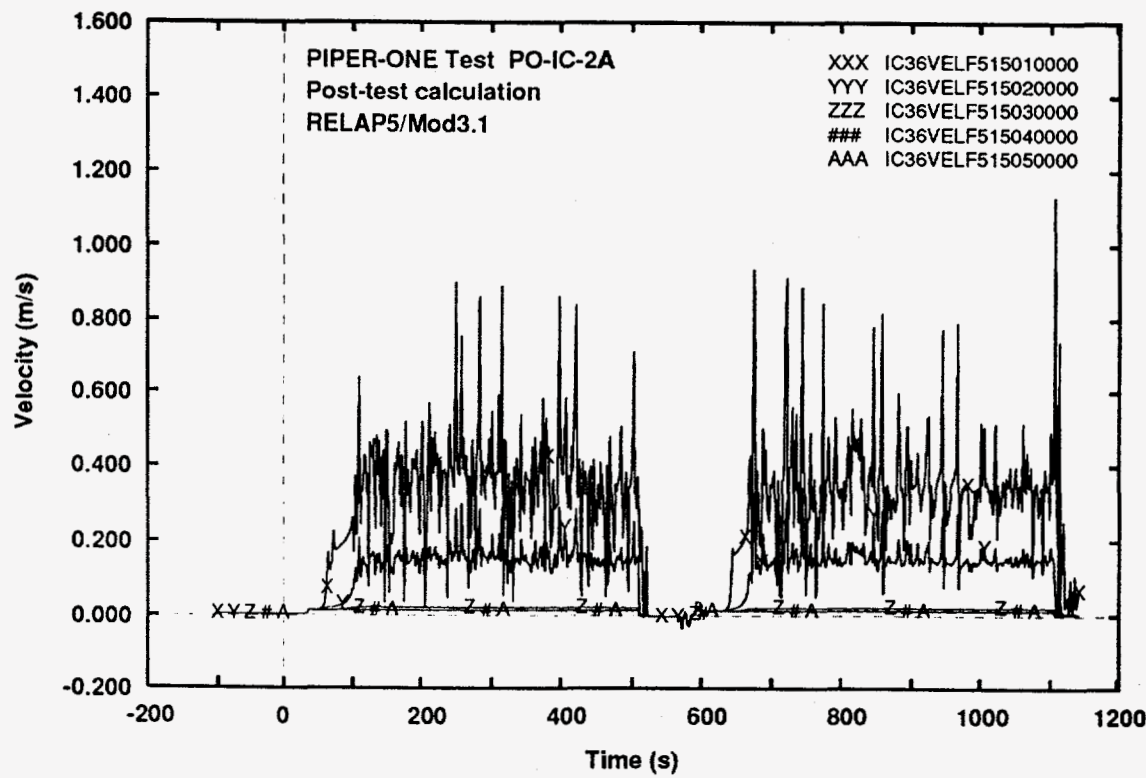


Fig. 36 - Calculated trends of IC tubes liquid velocity along the axis

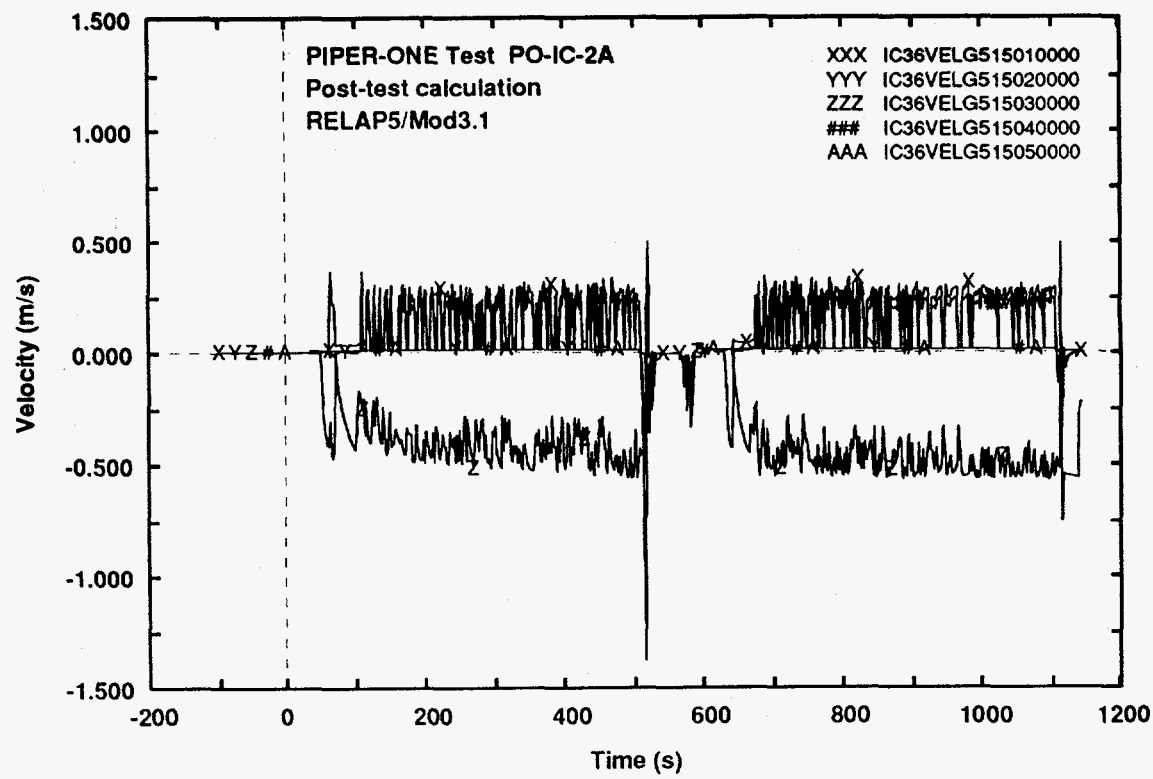


Fig. 37 - Calculated trends of IC tubes steam velocity along the axis

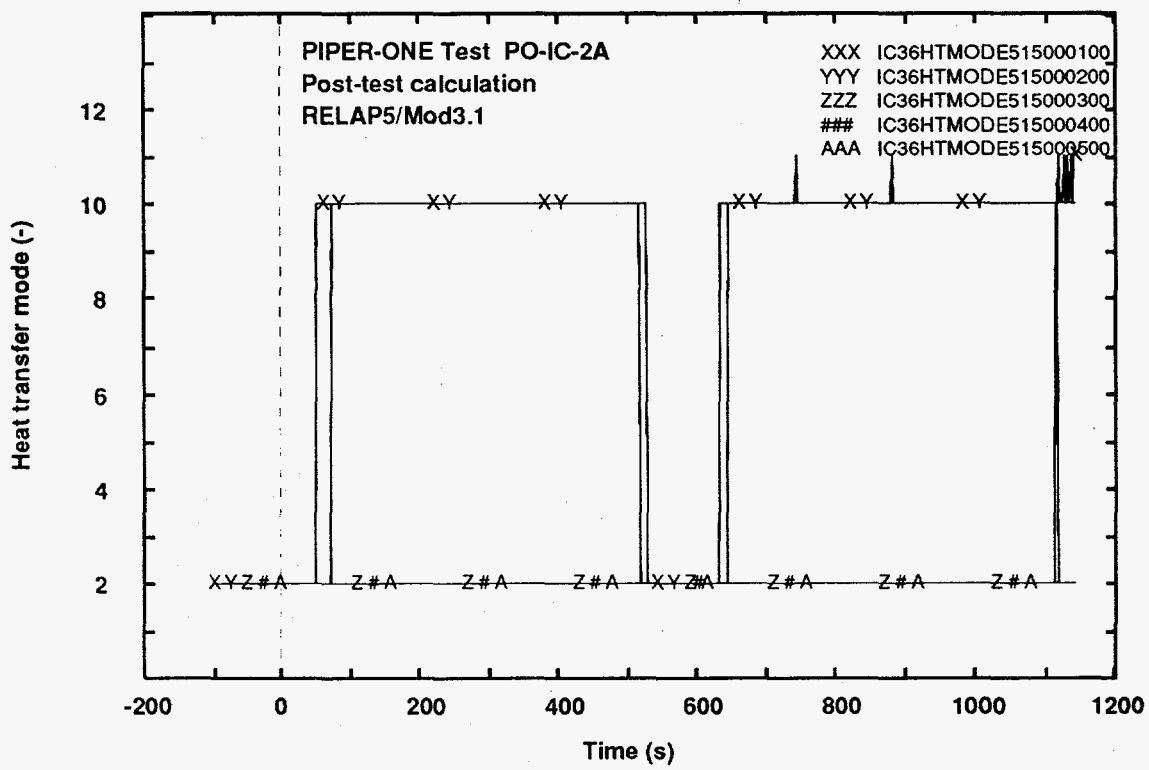


Fig. 38 - Calculated trends of IC tubes heat transfer mode (internal side)

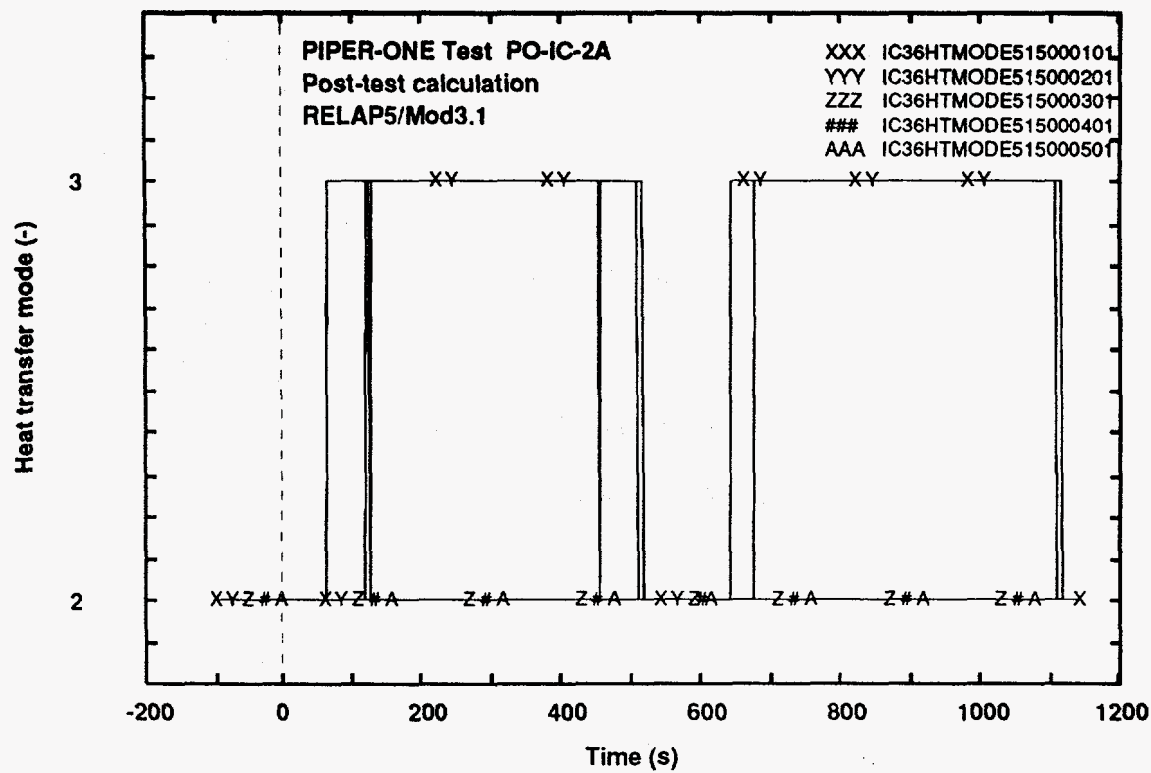
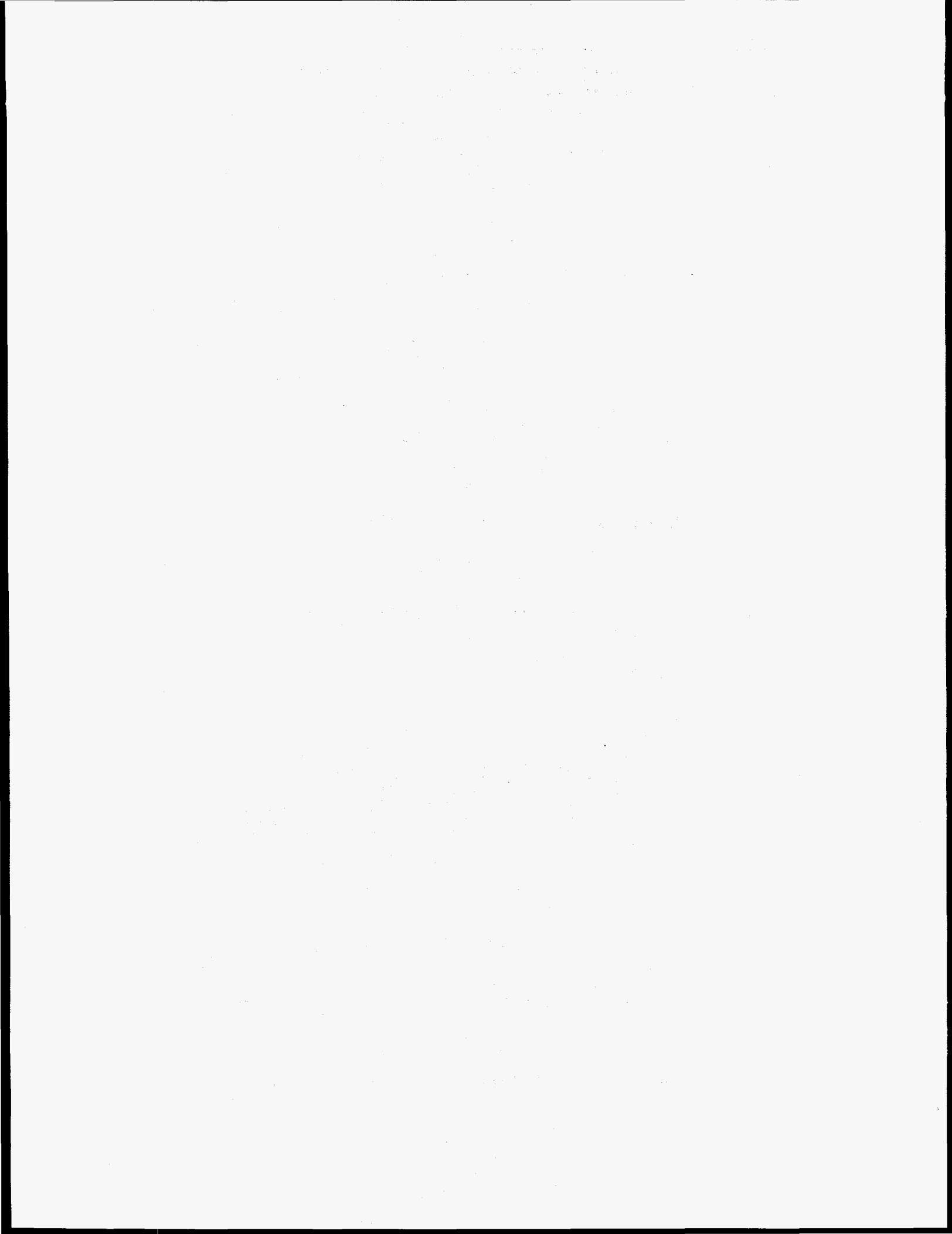


Fig. 39 - Calculated trends of IC tubes heat transfer mode (external side)

APPENDIX 3:
IC 37 Results



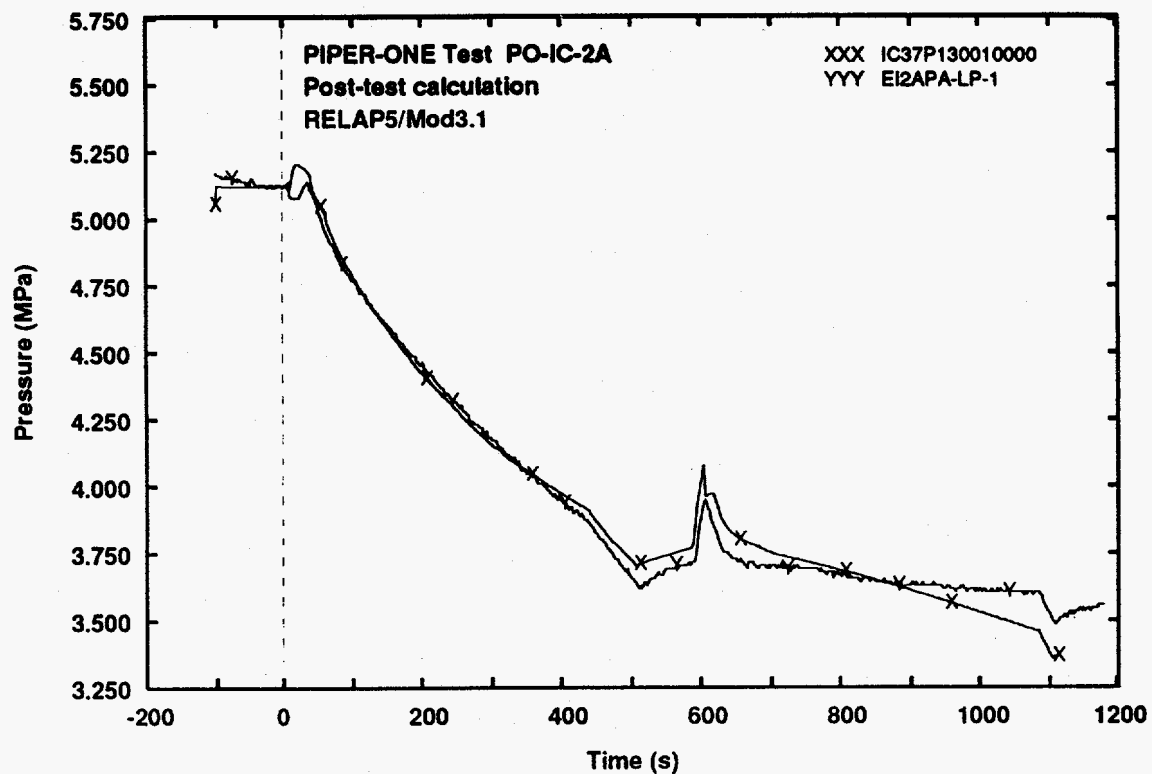


Fig. 1 - Measured and predicted trends of lower plenum pressure

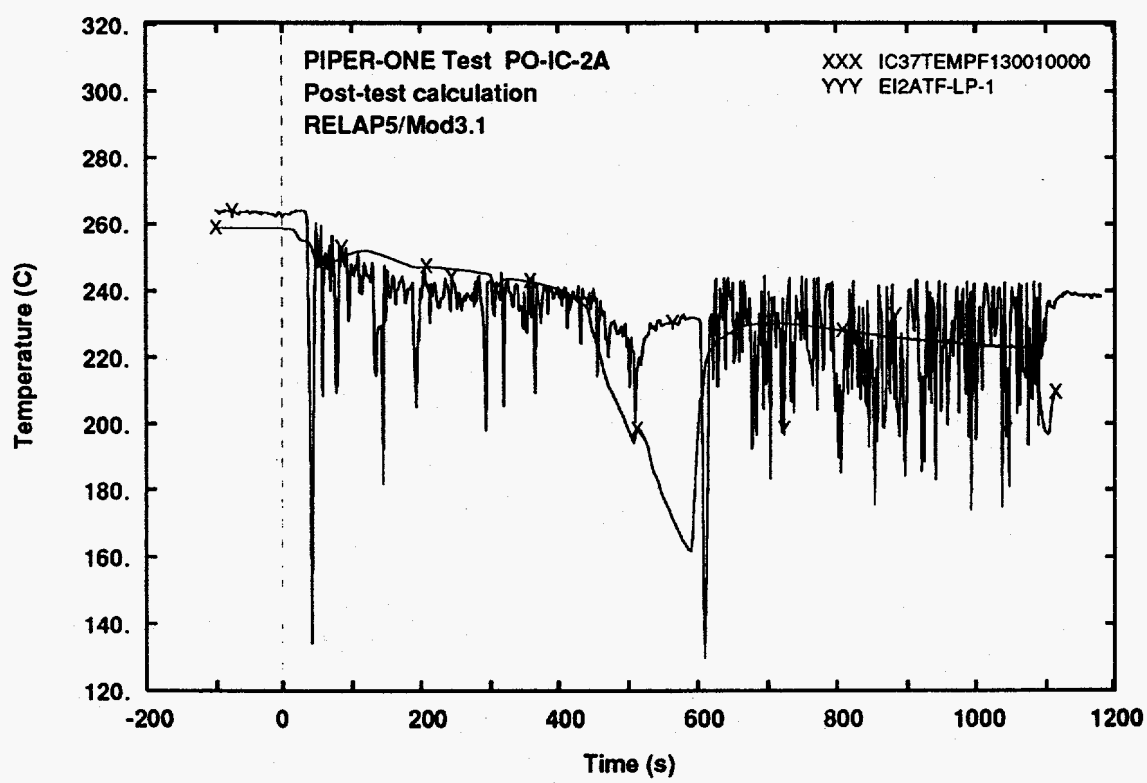


Fig. 2 - Measured and calculated trends of lower plenum temperature

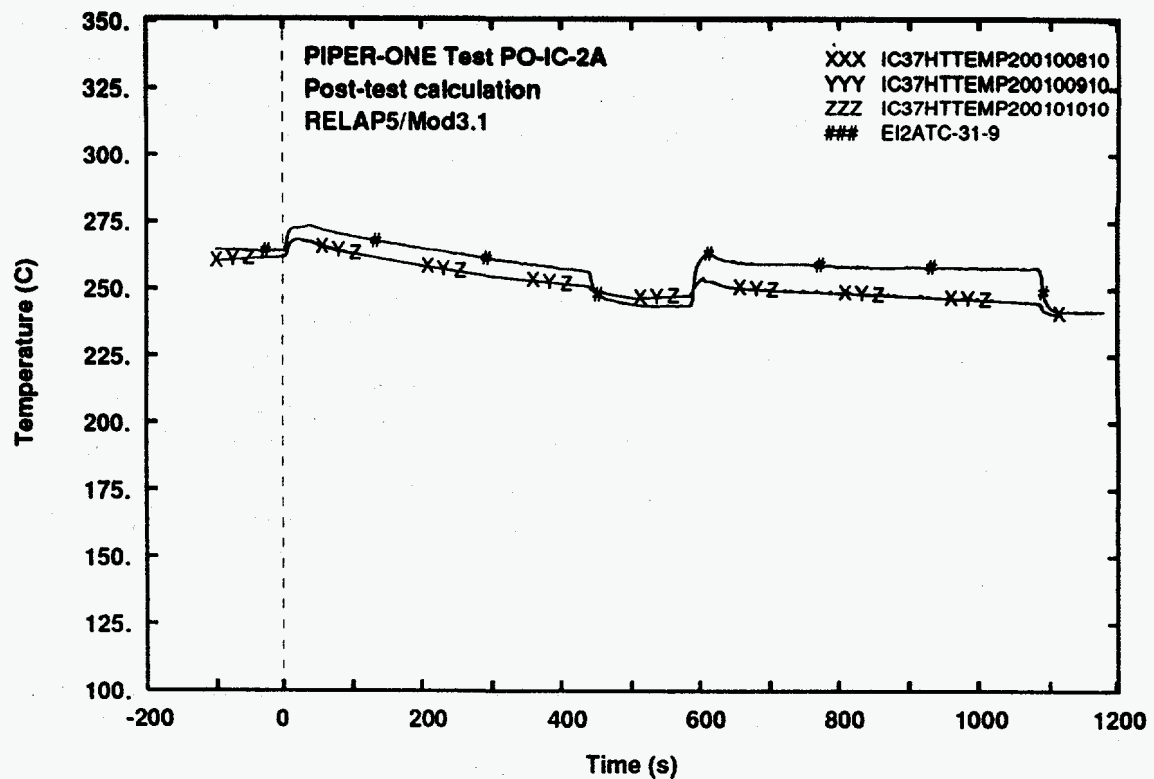


Fig. 3 - Measured and calculated trends of rod surface temperature (level 9)

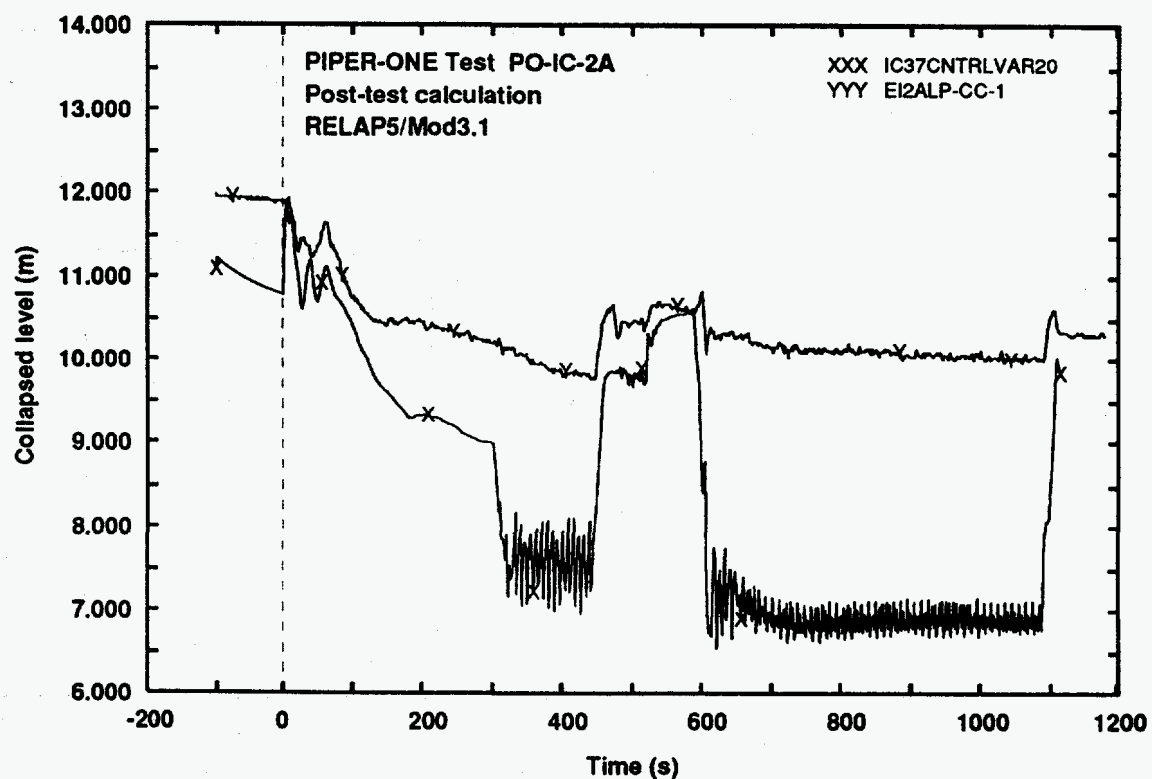


Fig. 4 - Measured and calculated trends of core level

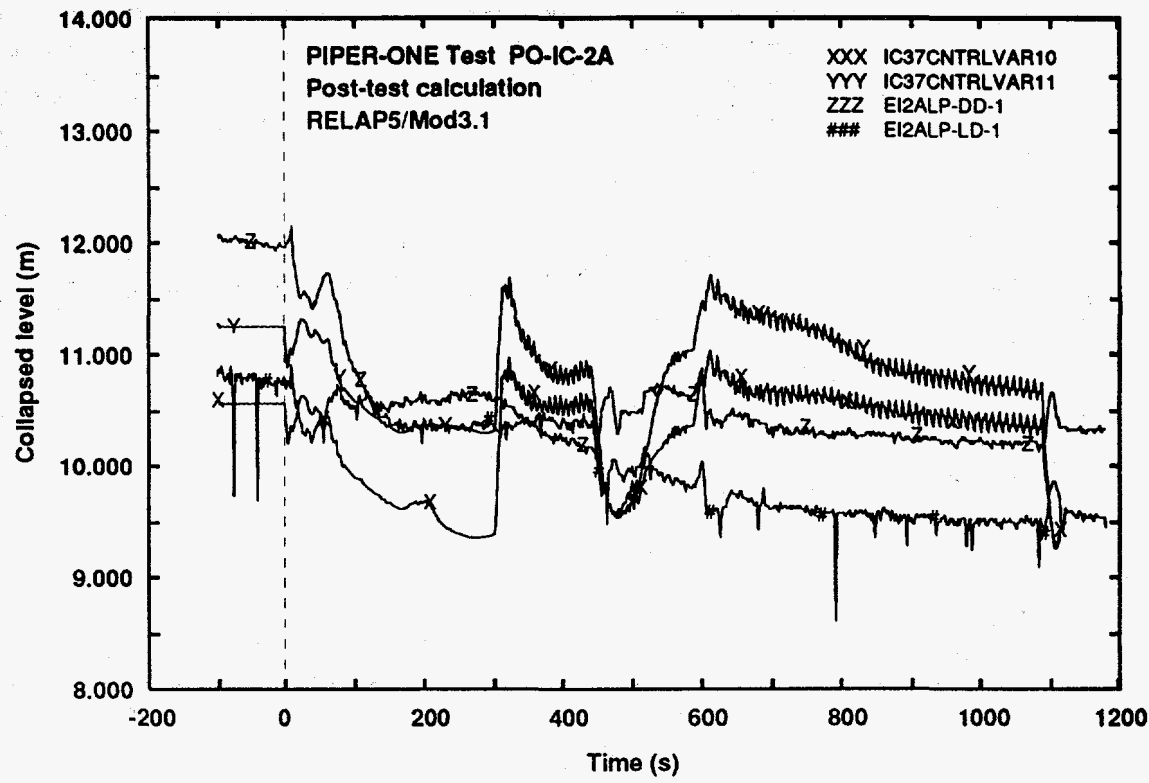


Fig. 5 - Measured and calculated trends of downcomer level

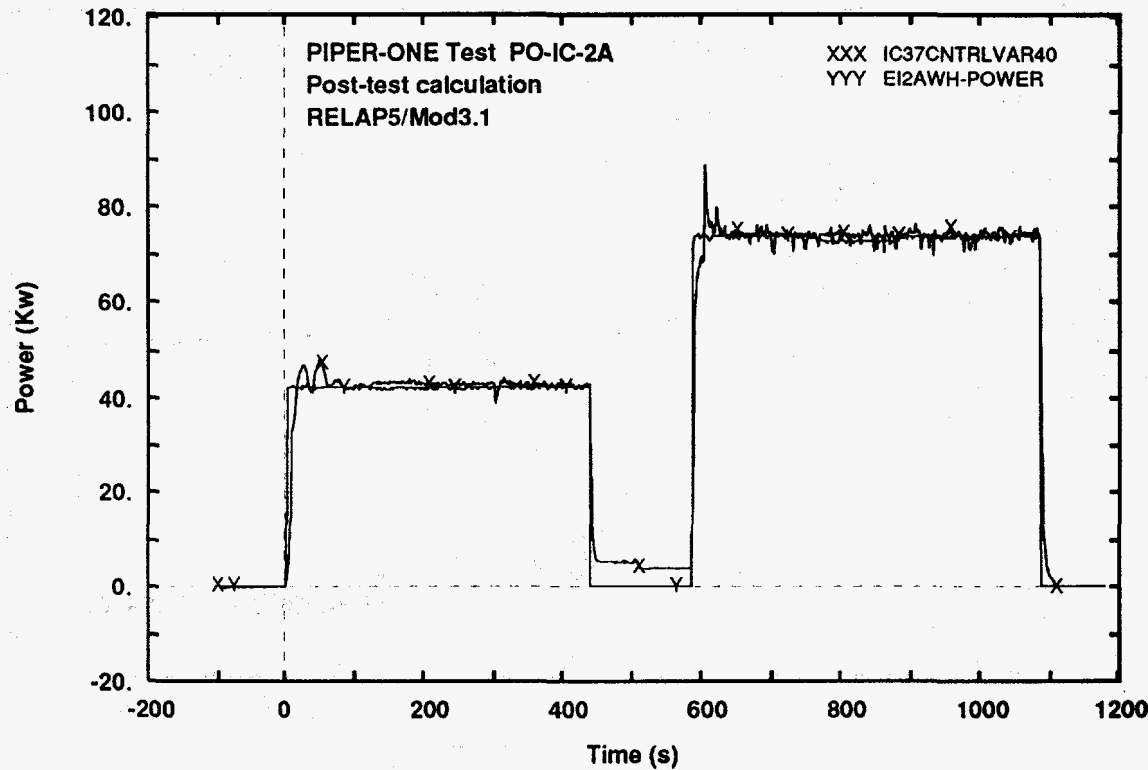


Fig. 6 - Measured and calculated trends of core power

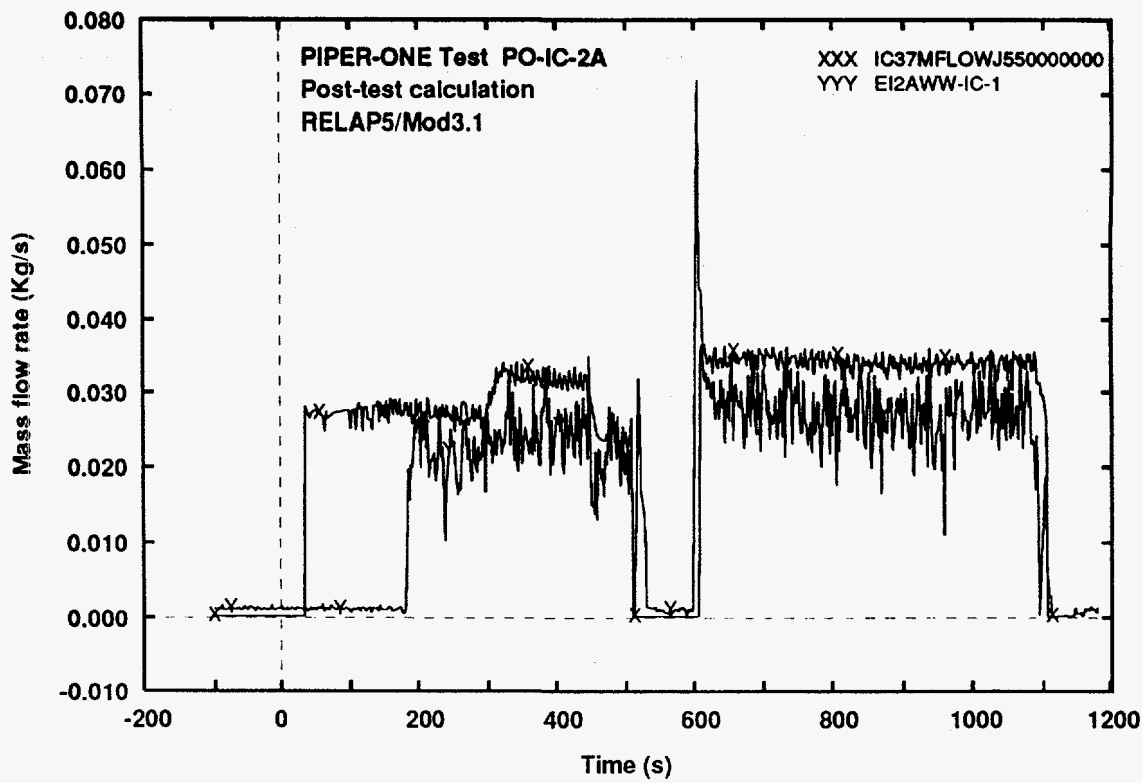


Fig. 7 - Measured and calculated trends of IC mass flow rate

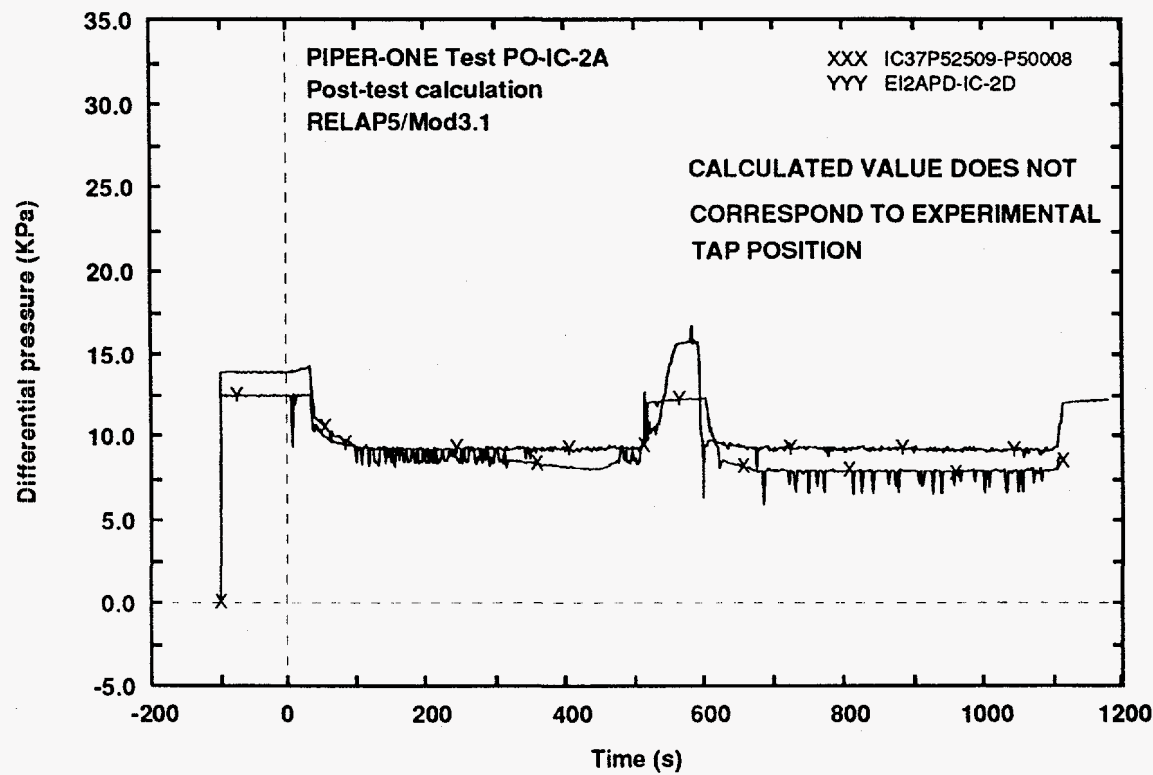


Fig. 8 - Measured and calculated trends of IC differential pressure

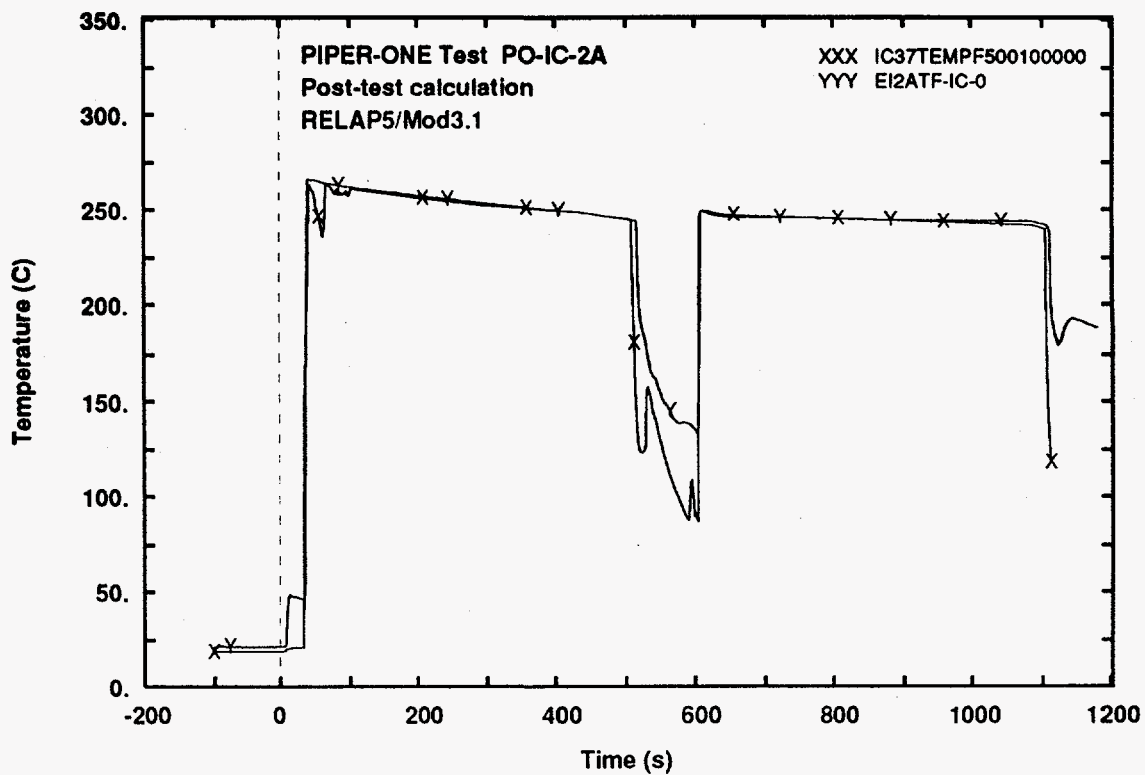


Fig. 9 - Measured and calculated trends of IC inlet fluid temperature

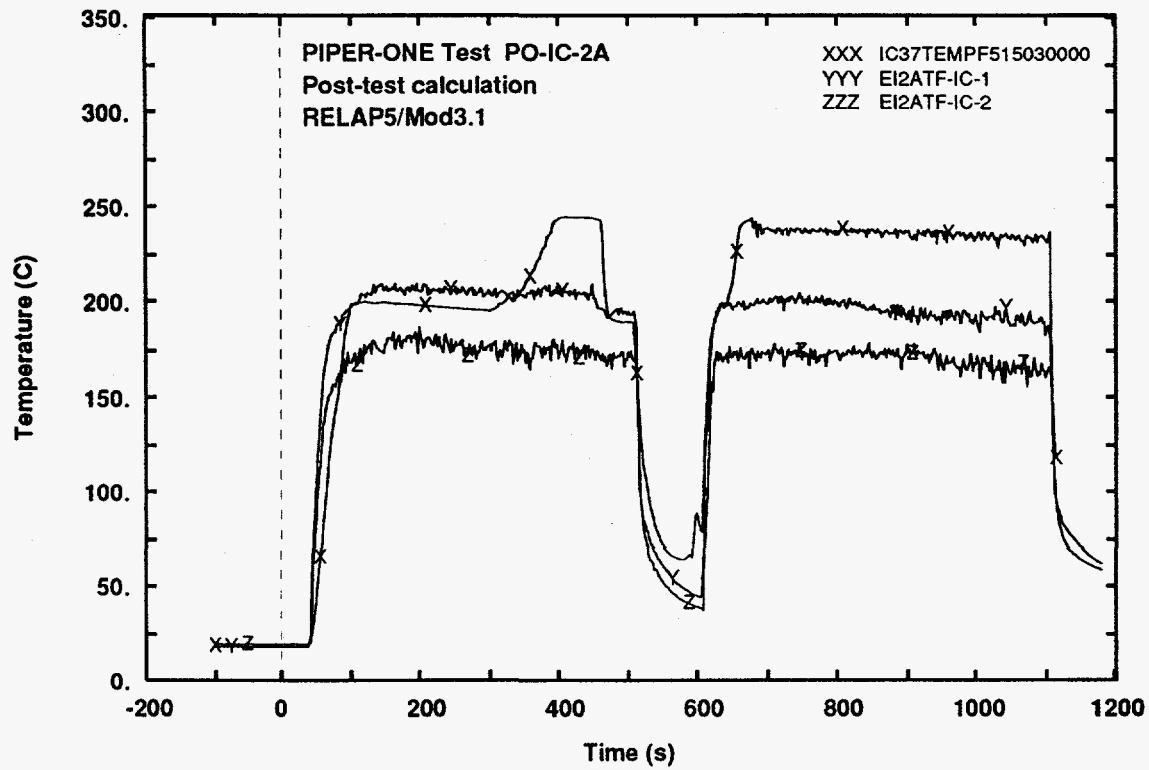


Fig. 10 - Measured and calculated trends of IC tubes fluid temperature
(middle elevation)

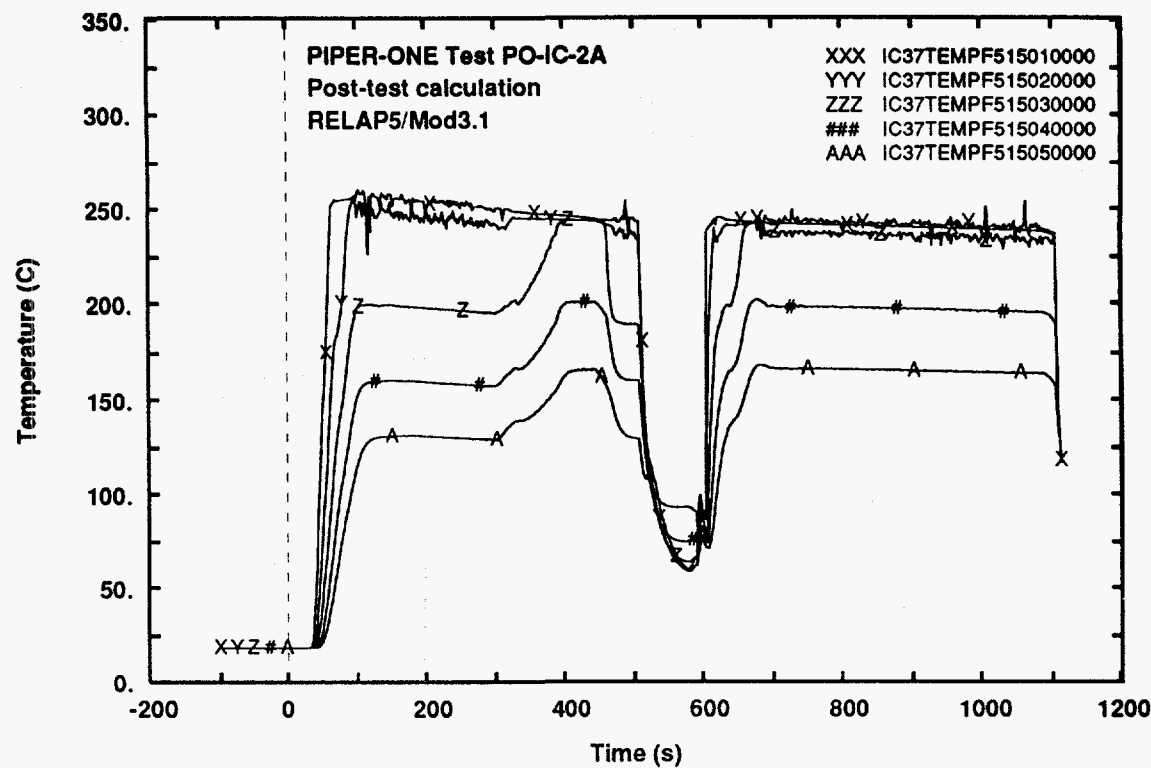


Fig. 11 - Calculated trends of IC tubes fluid temperature along the axis

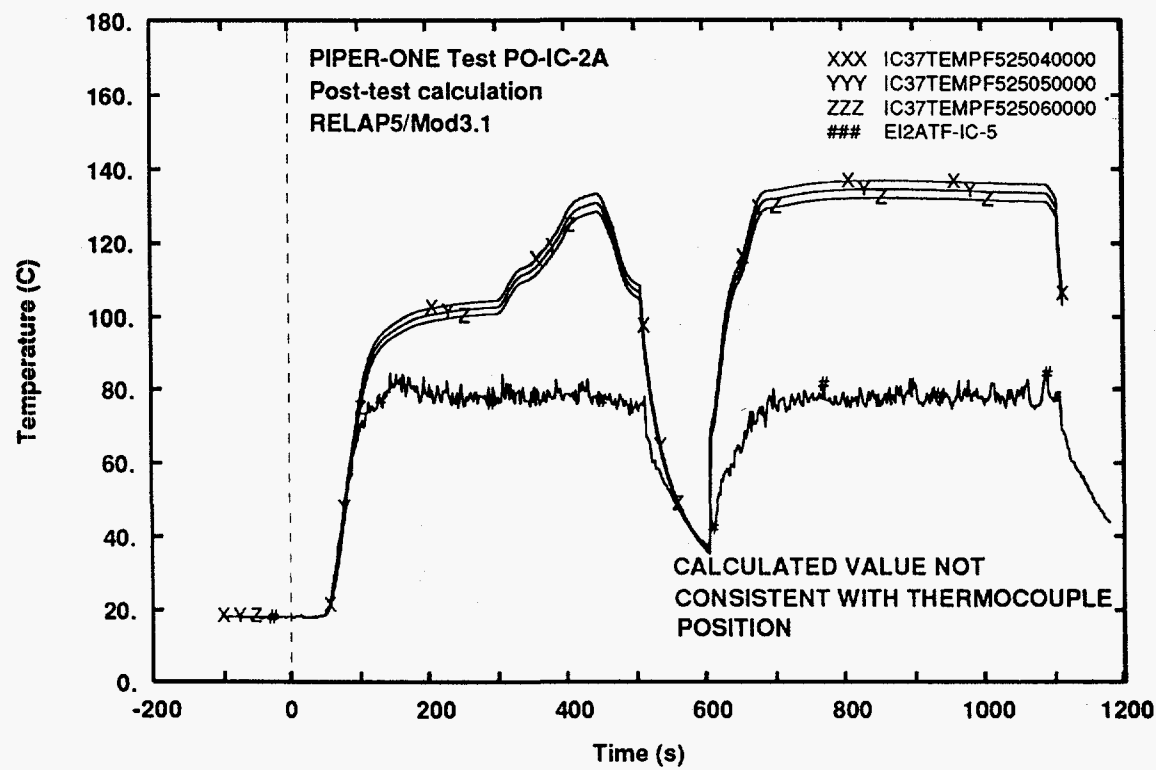
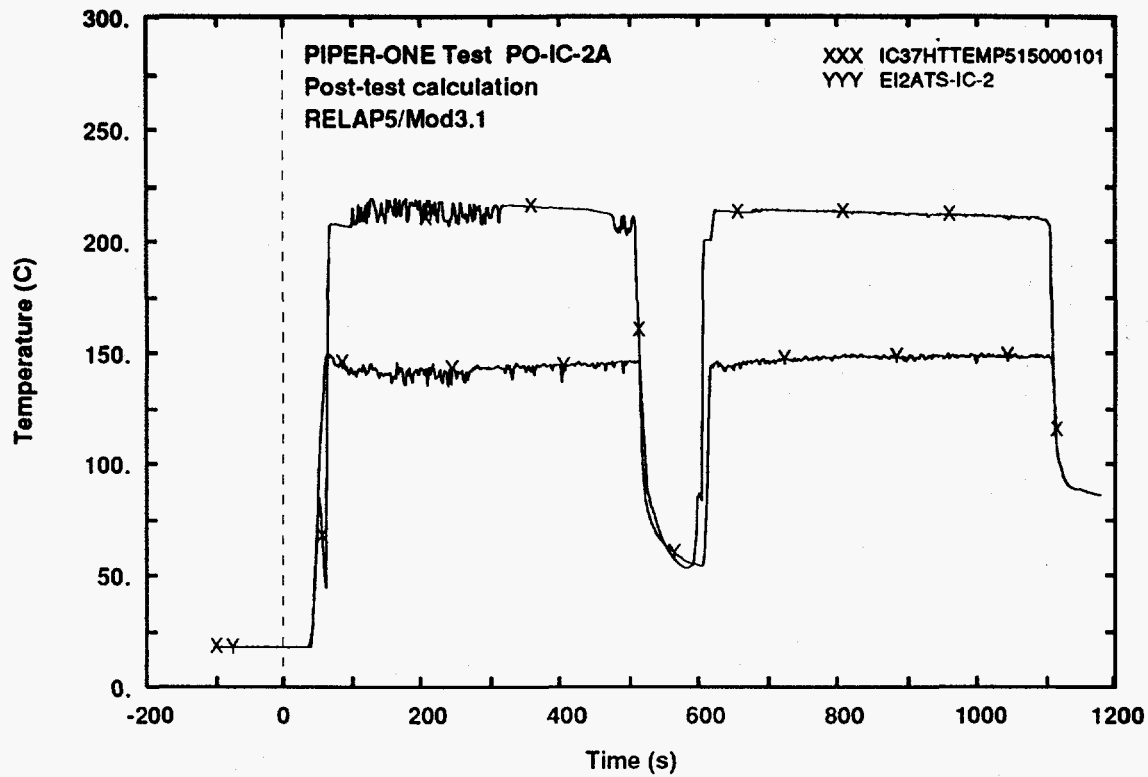
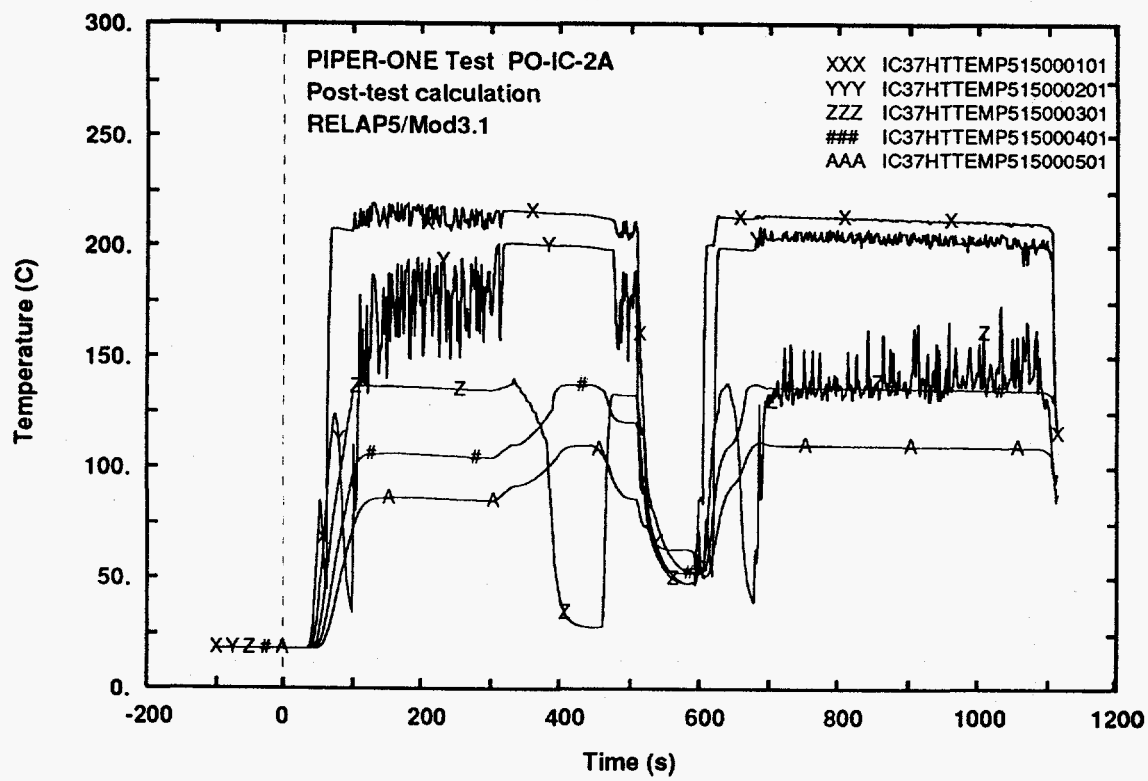


Fig. 12 - Measured and calculated trends of IC outlet fluid temperature



**Fig. 13 - Measured and calculated trends of IC tubes wall surface temperature
(internal side top elevation)**



**Fig. 14 - Calculated trends of IC tubes wall surface temperature along the axis
(internal side)**

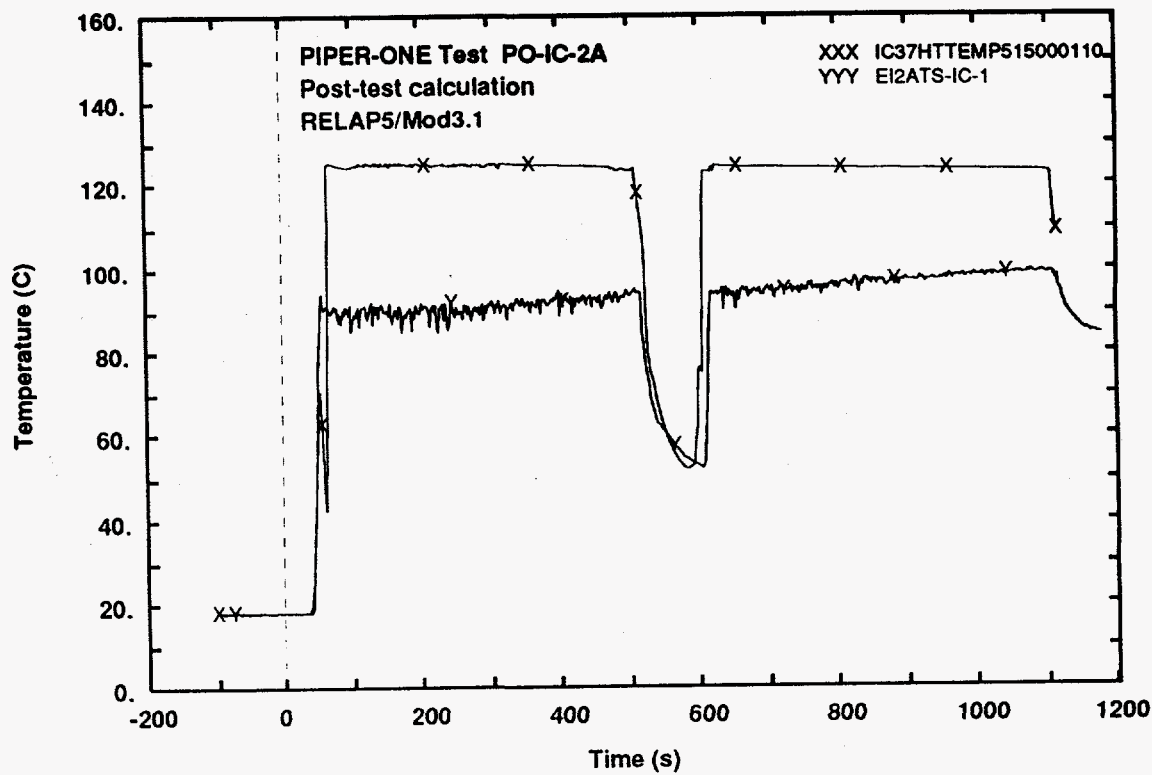


Fig. 15 - Measured and calculated trends of IC tubes wall surface temperature (external side top elevation)

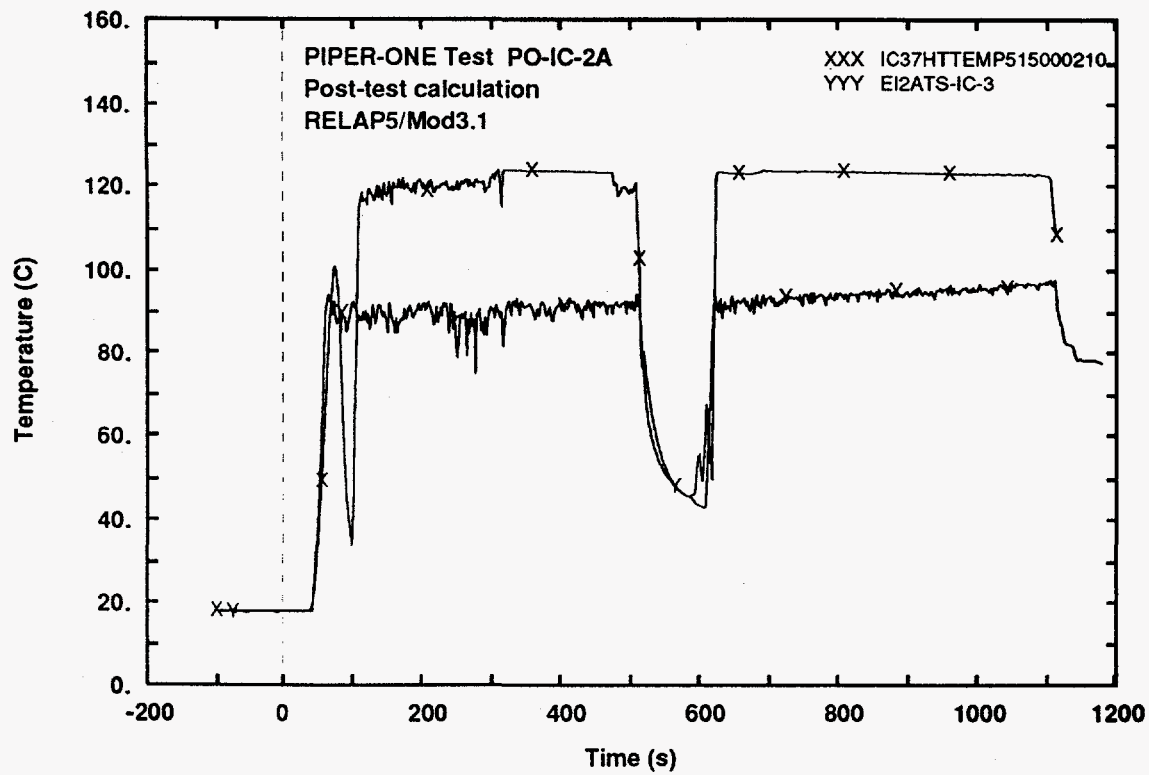


Fig. 16 - Measured and calculated trends of IC tubes wall surface temperature (external side level 3)

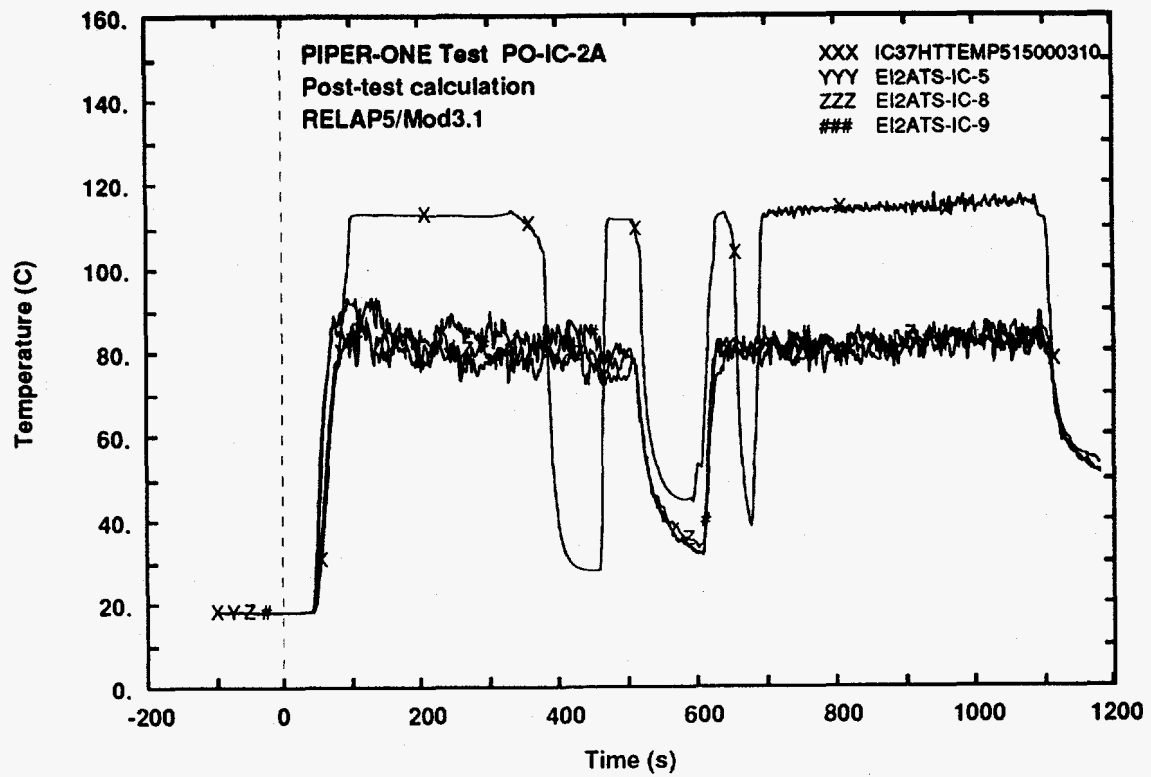


Fig. 17 - Measured and calculated trends of IC tubes wall surface temperature (external side middle elevation)

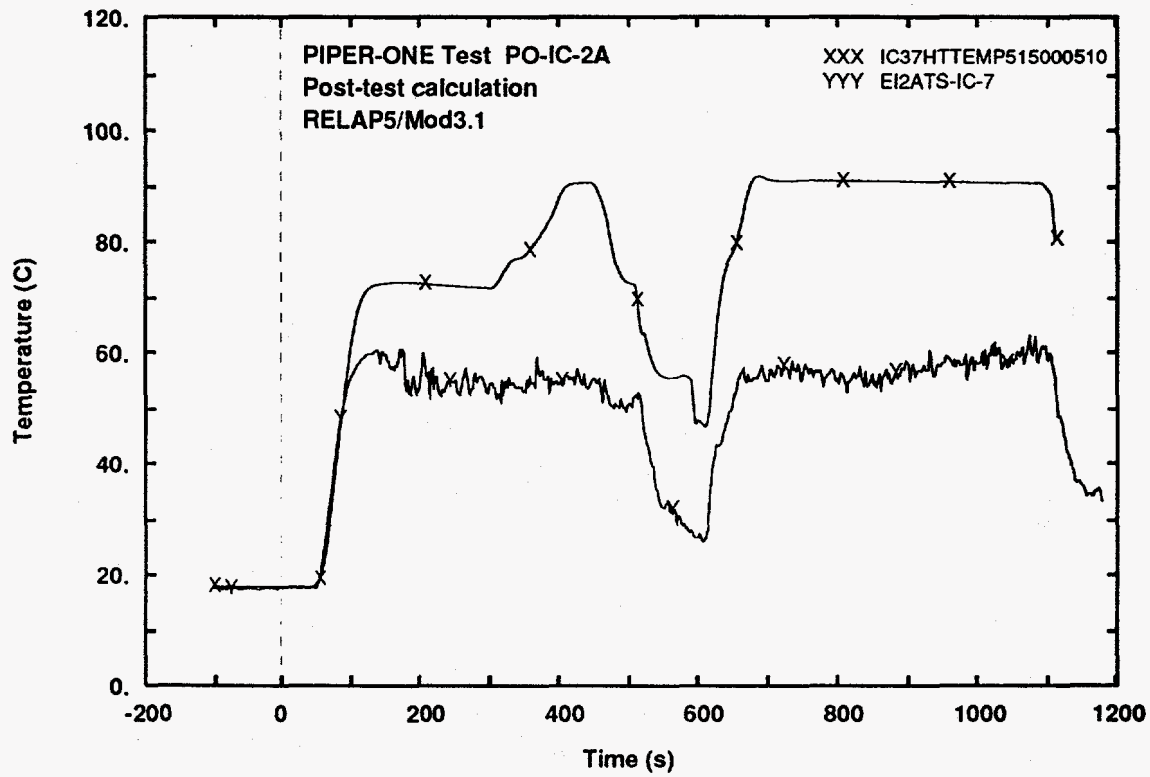


Fig. 18 - Measured and calculated trends of IC tubes wall surface temperature (external side bottom elevation)

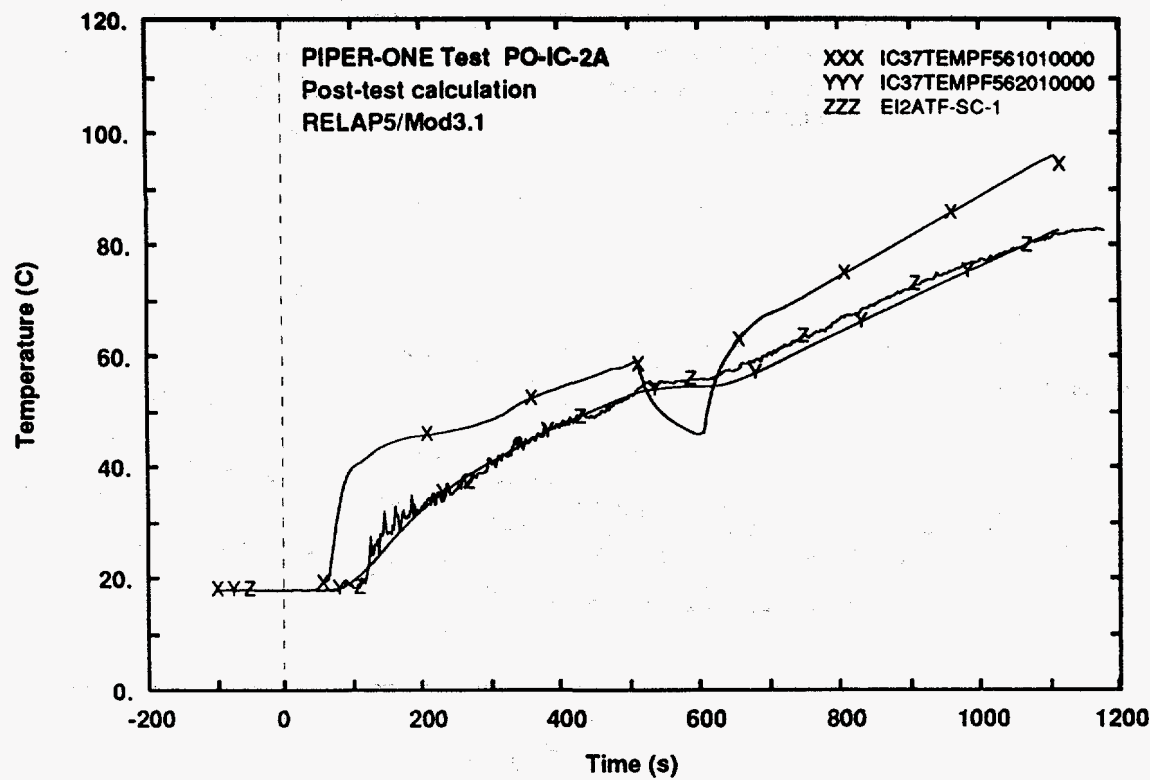


Fig. 19 - Measured and calculated trends of IC internal pool fluid temperature (top level)

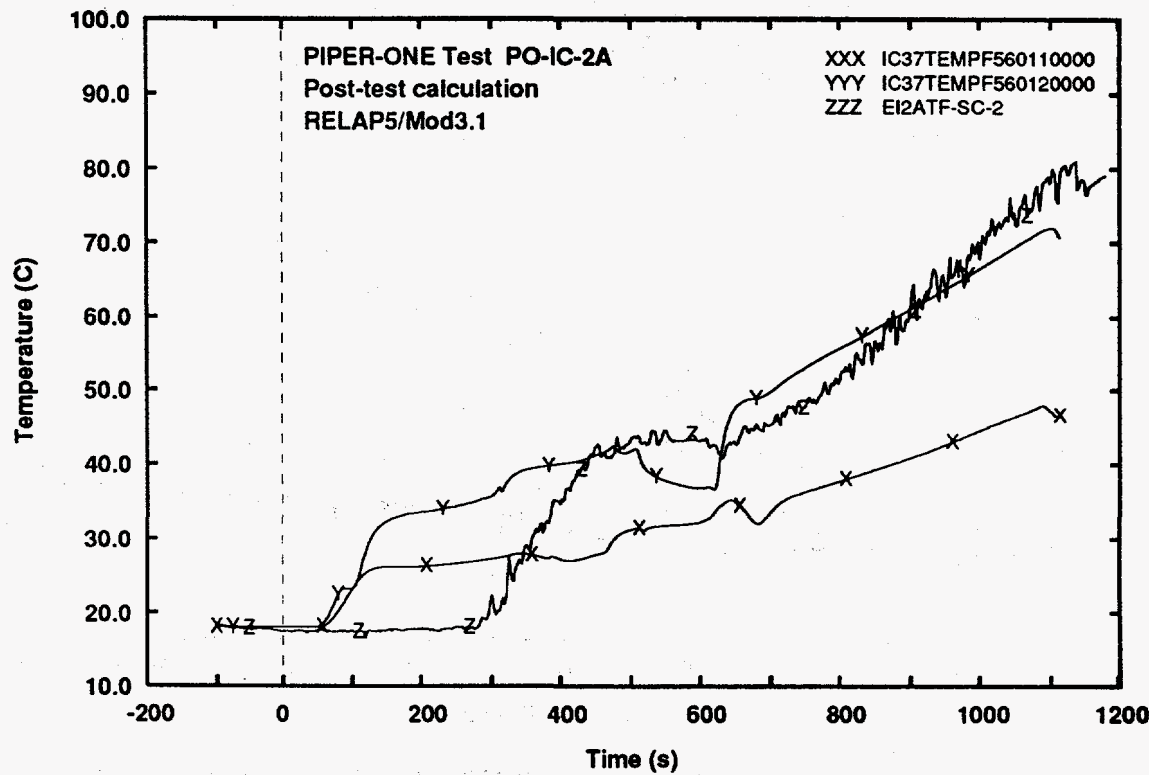


Fig. 20 - Measured and calculated trends of IC internal pool fluid temperature (level 2)

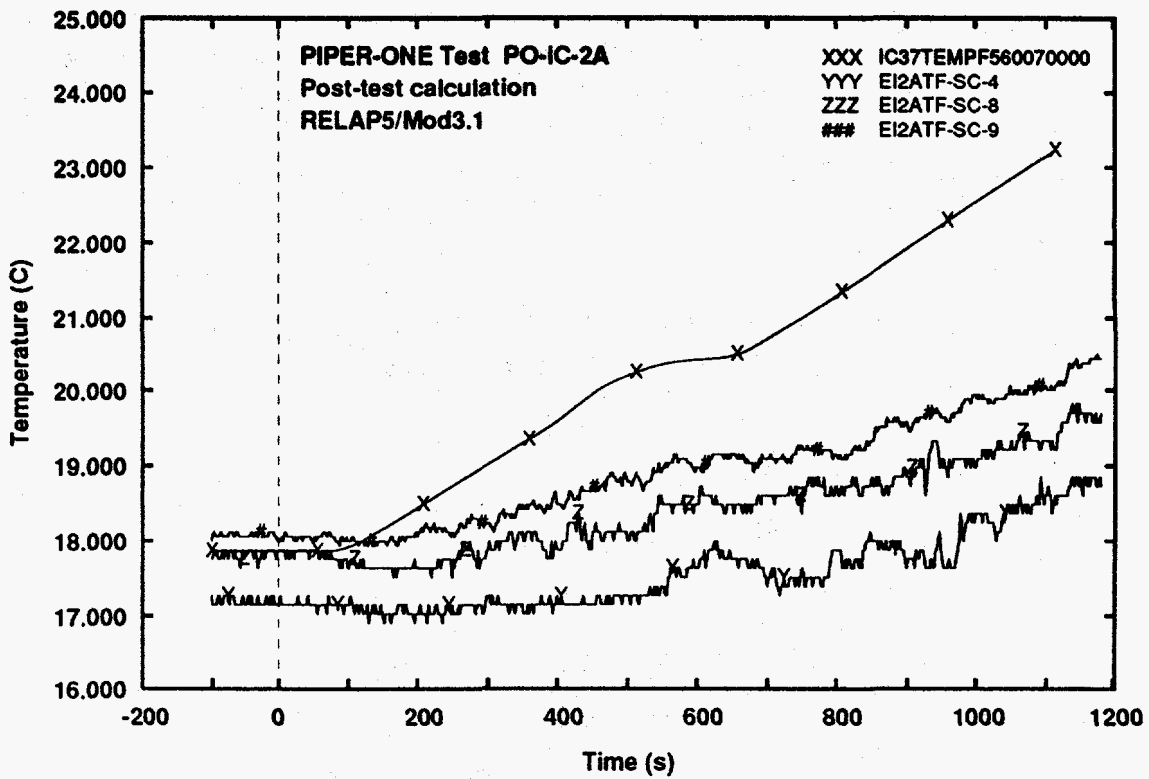


Fig. 21 - Measured and calculated trends of IC internal pool fluid temperature (middle level)

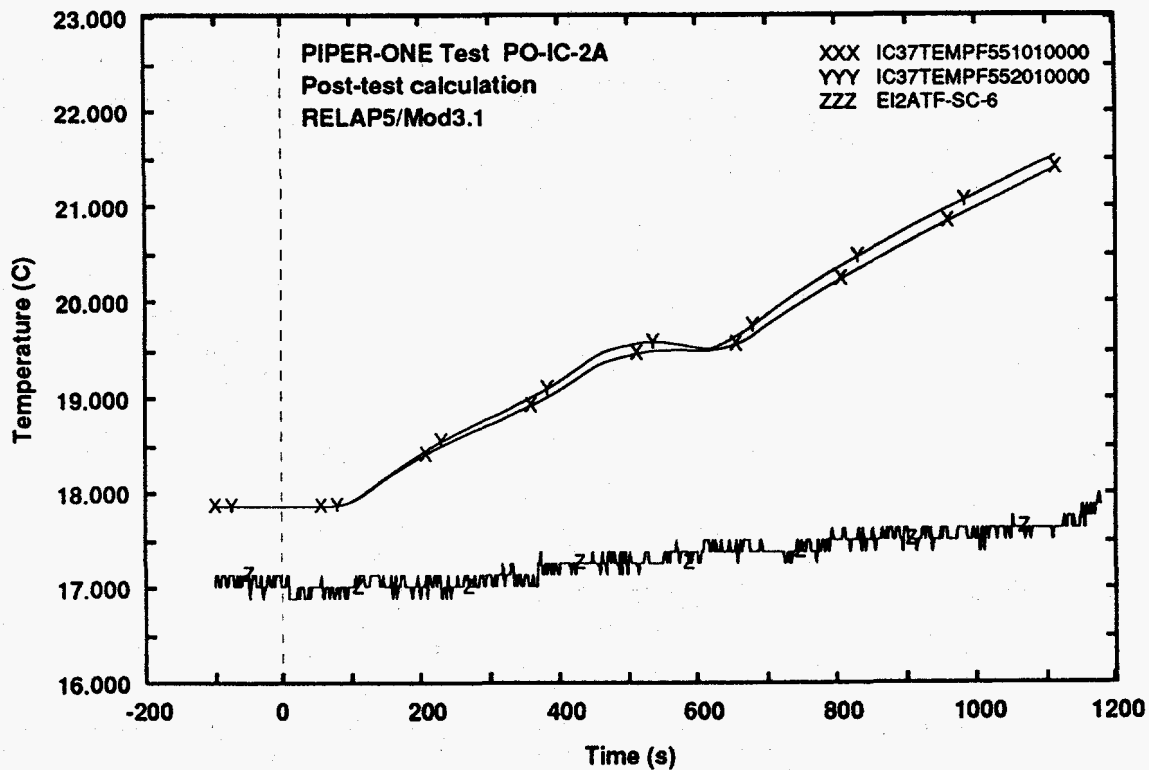


Fig. 22 - Measured and calculated trends of IC internal pool fluid temperature (bottom level)

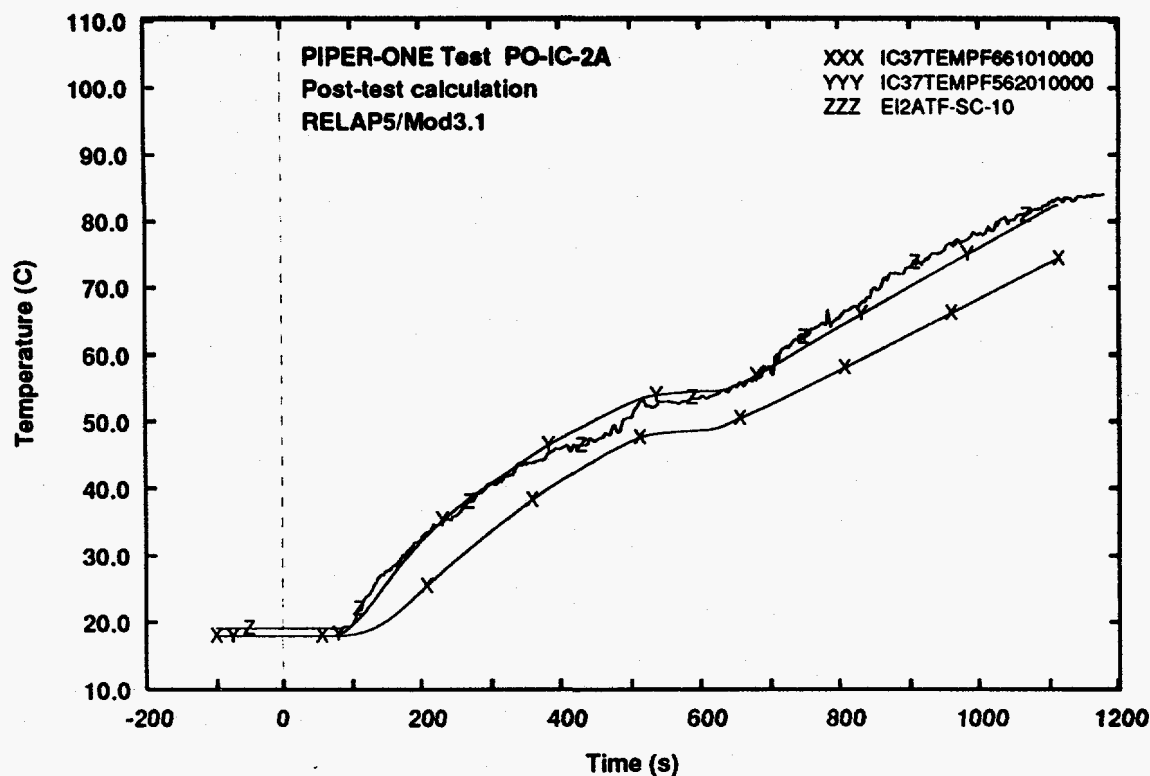


Fig. 23 - Measured and calculated trends of IC external pool fluid temperature (top level)

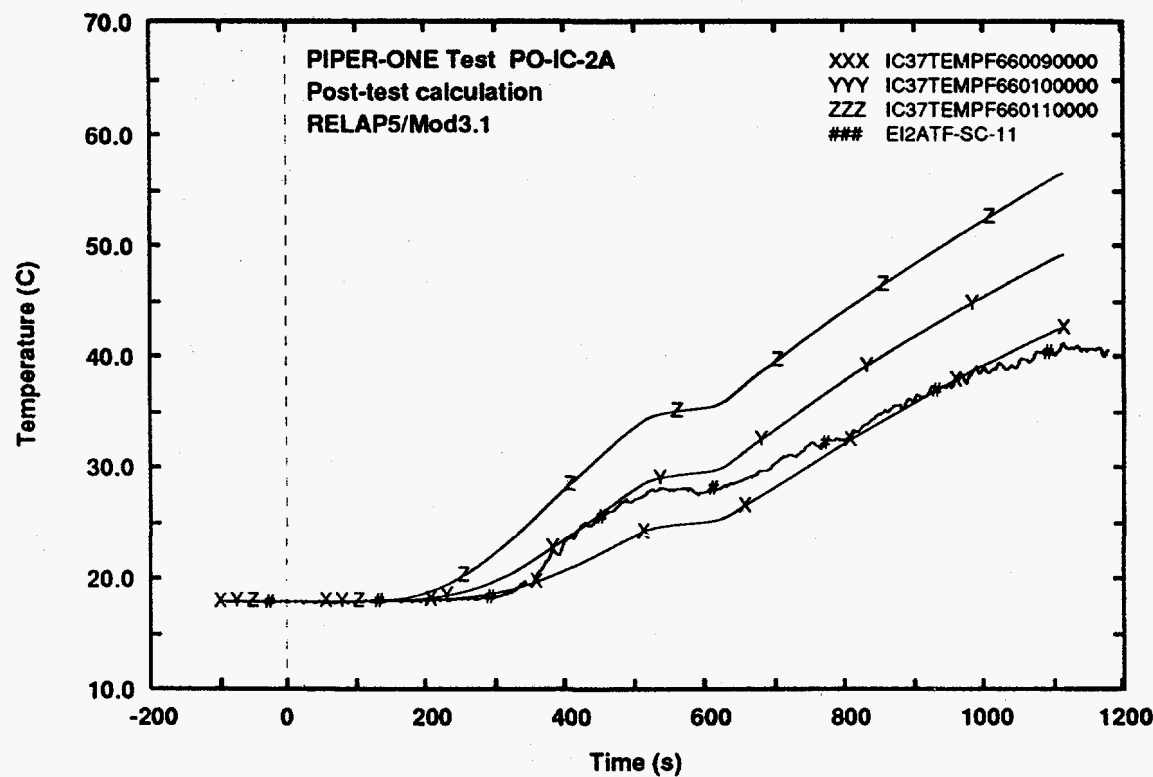


Fig. 24 - Measured and calculated trends of IC external pool fluid temperature (level 11)

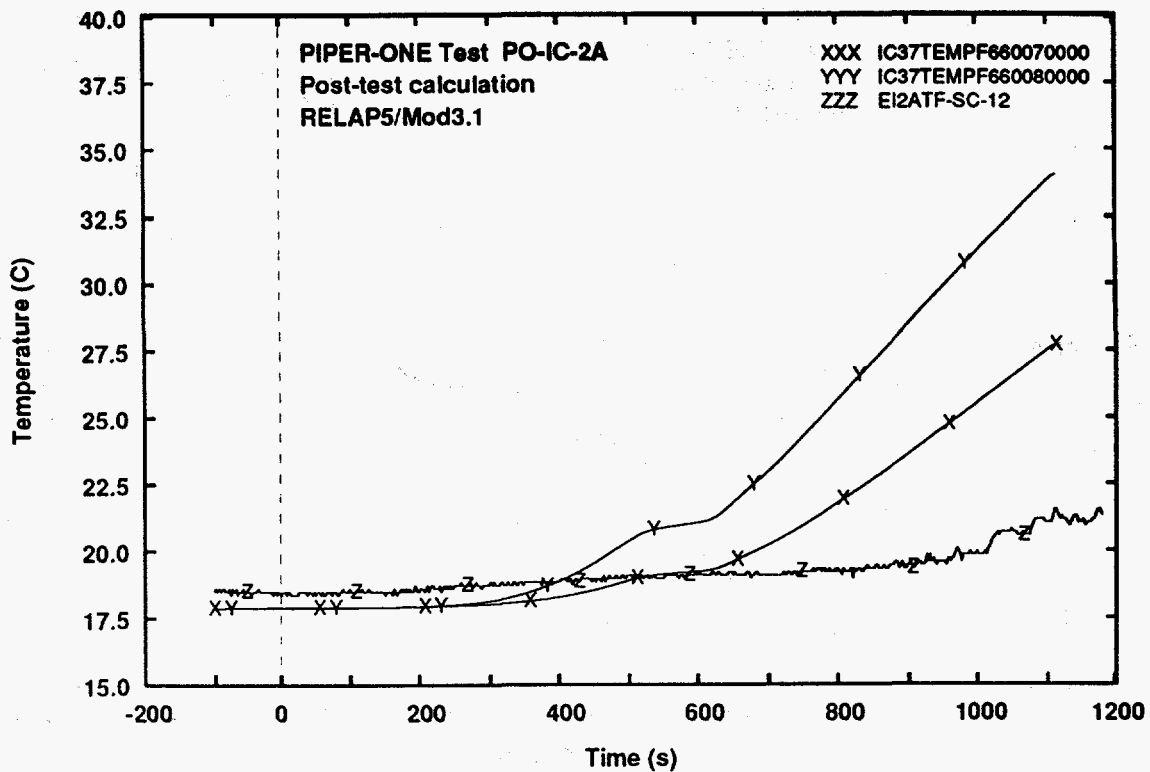


Fig. 25 - Measured and calculated trends of IC external pool fluid temperature (middle level)

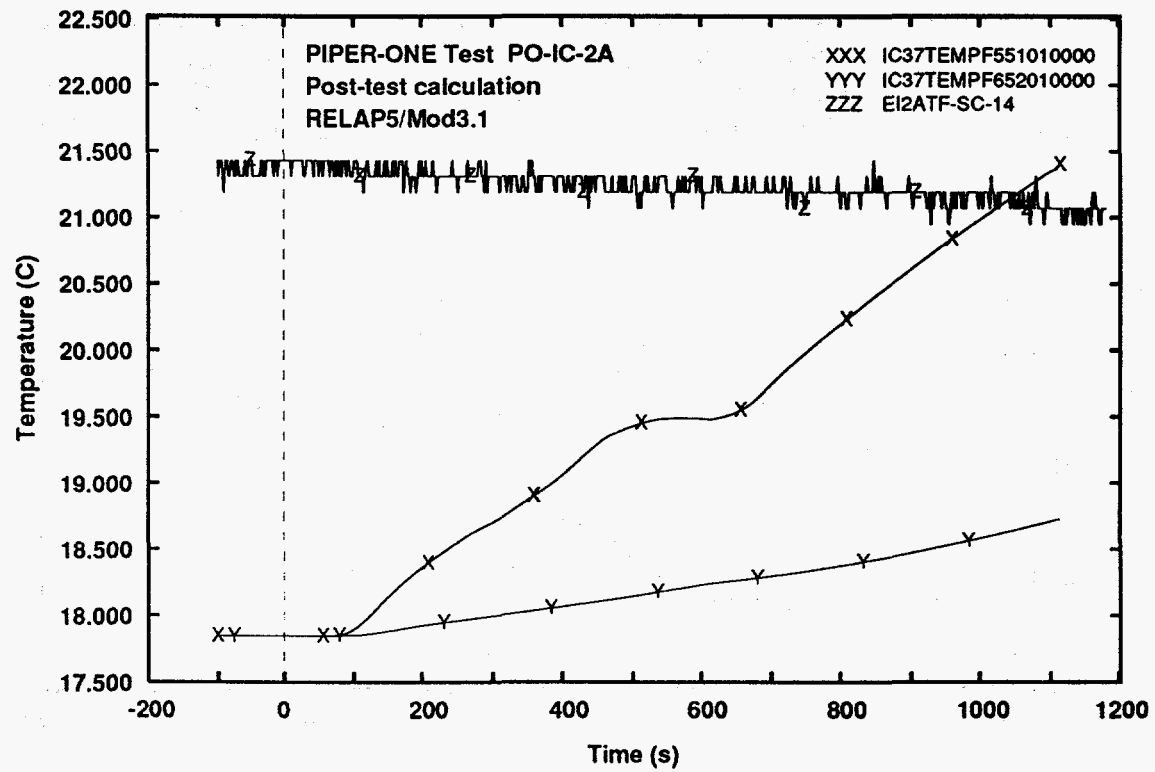


Fig. 26 - Measured and calculated trends of IC external pool fluid temperature (bottom level)

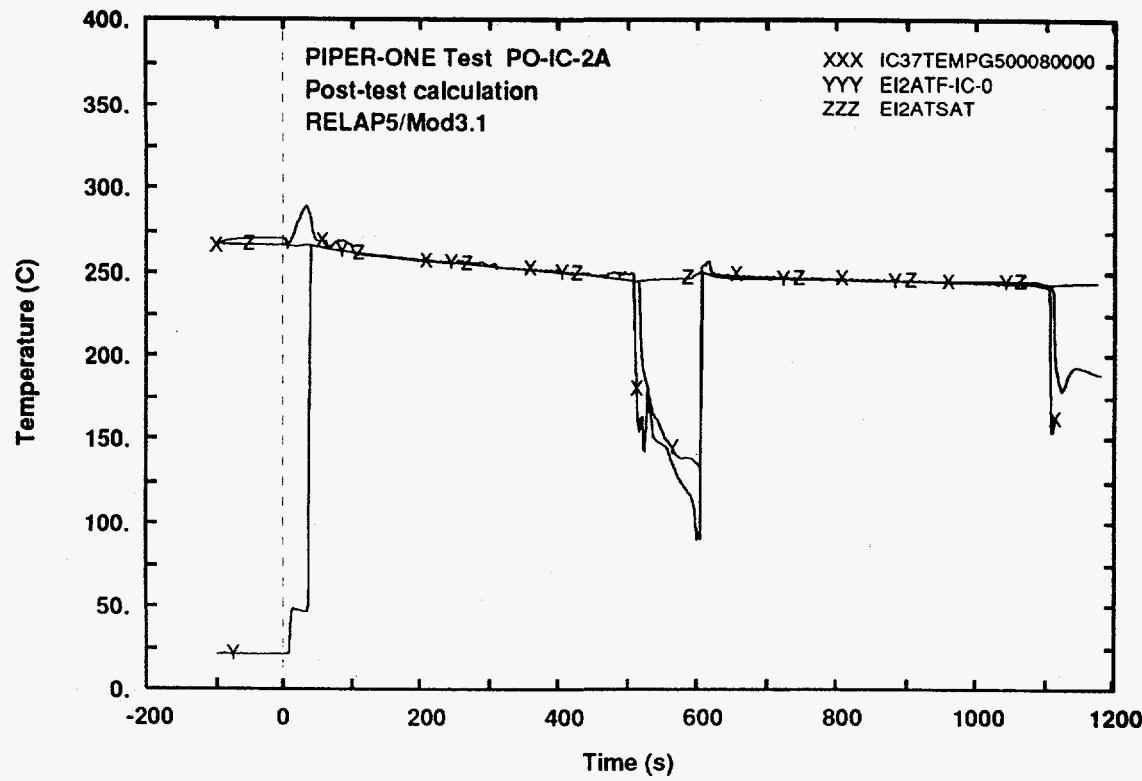


Fig. 27 - Measured and calculated trends of steam temperature at IC inlet compared with experimental saturated temperature

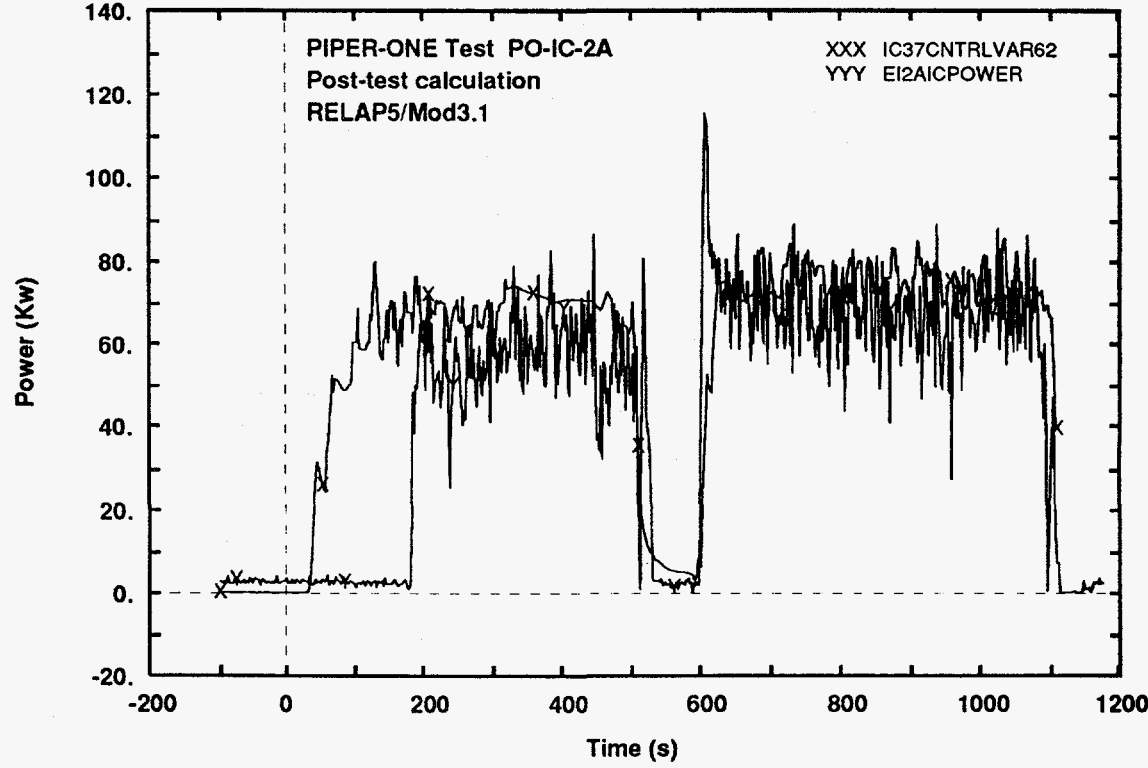


Fig. 28 - Measured and calculated trends of IC exchanged power

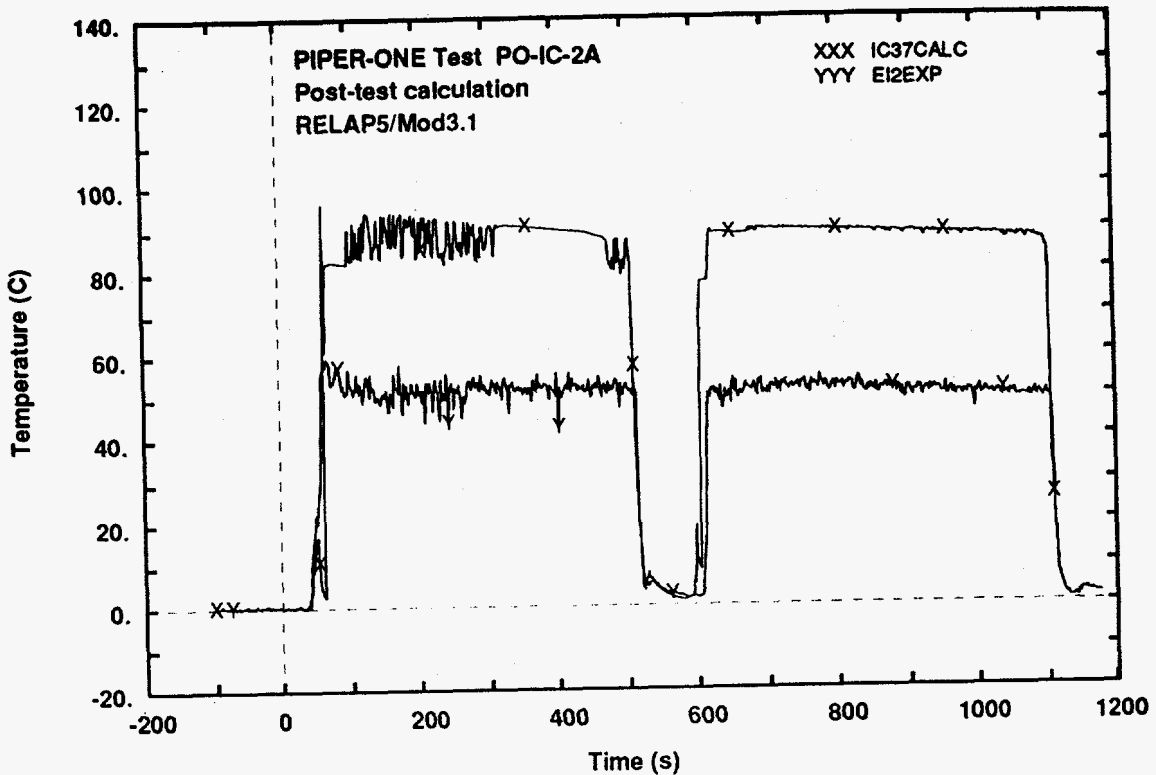


Fig. 29 - Measured and calculated trends of temperature difference between internal and external side of IC tubes wall (top elevation)

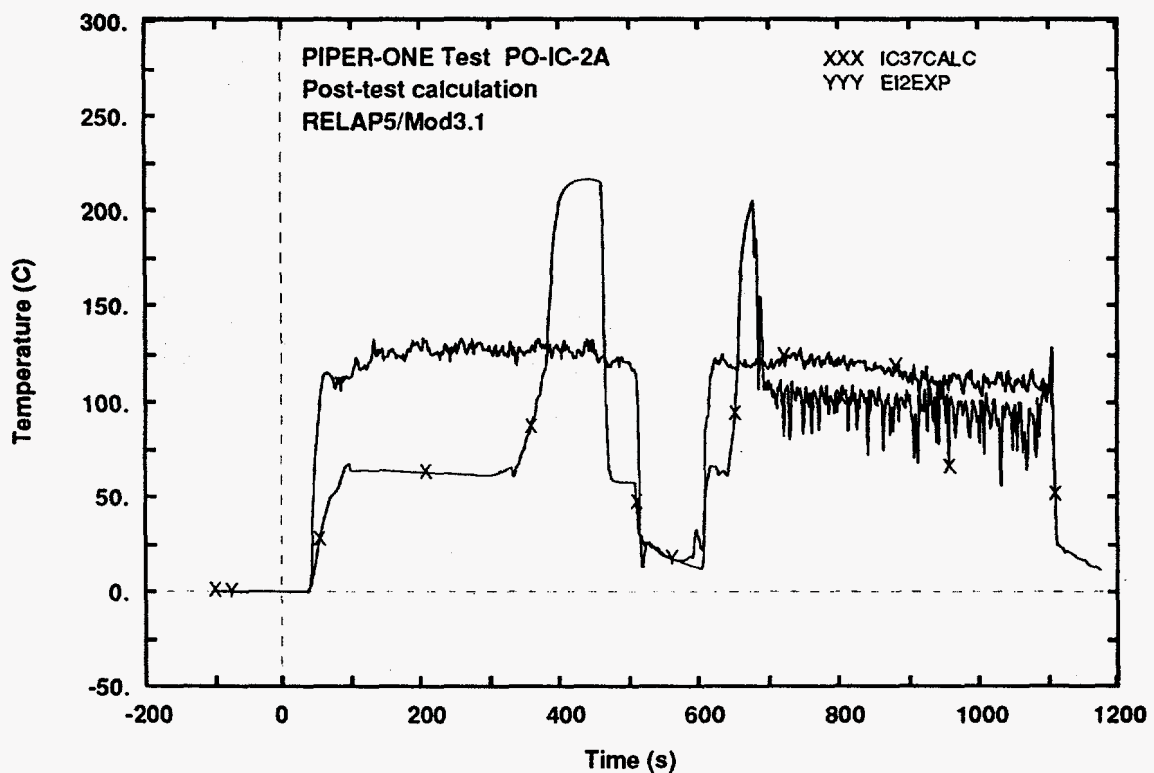


Fig. 30 - Measured and calculated trends of temperature difference between IC fluid and external side of IC tubes wall (middle elevation)

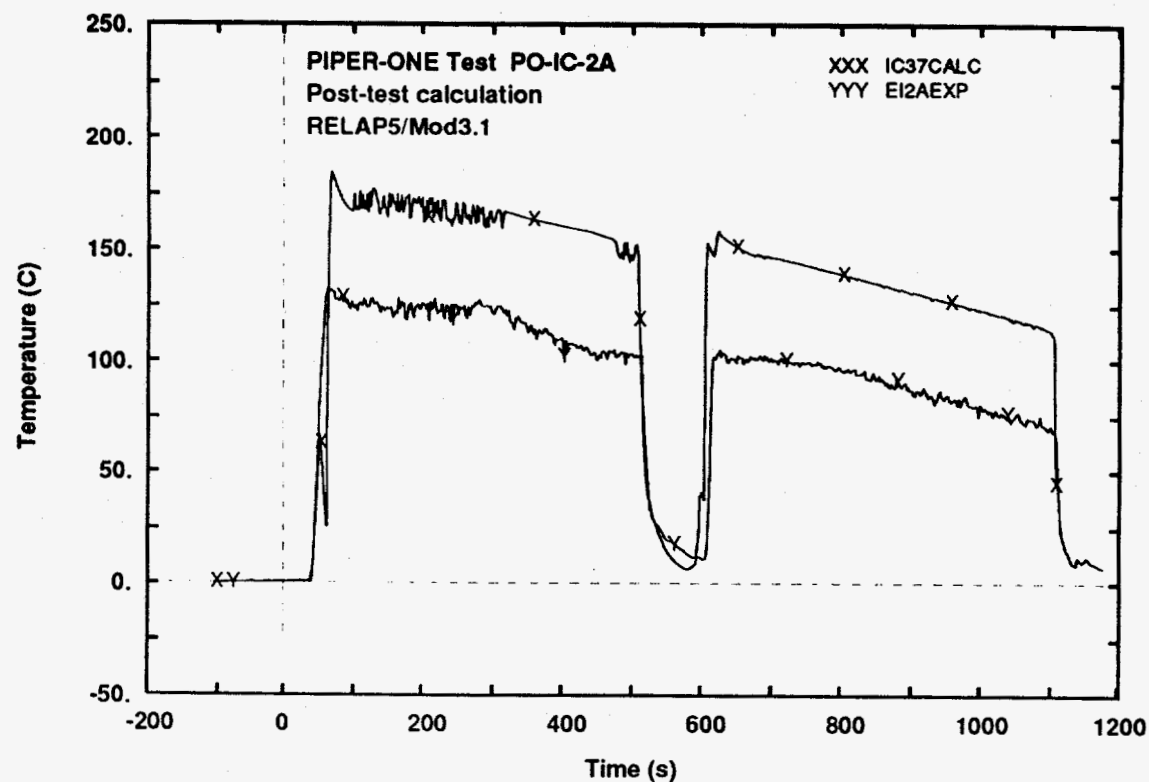


Fig. 31 - Measured and calculated trends of temperature difference between internal side of IC tubes wall and IC pool fluid temperature (top elevation)

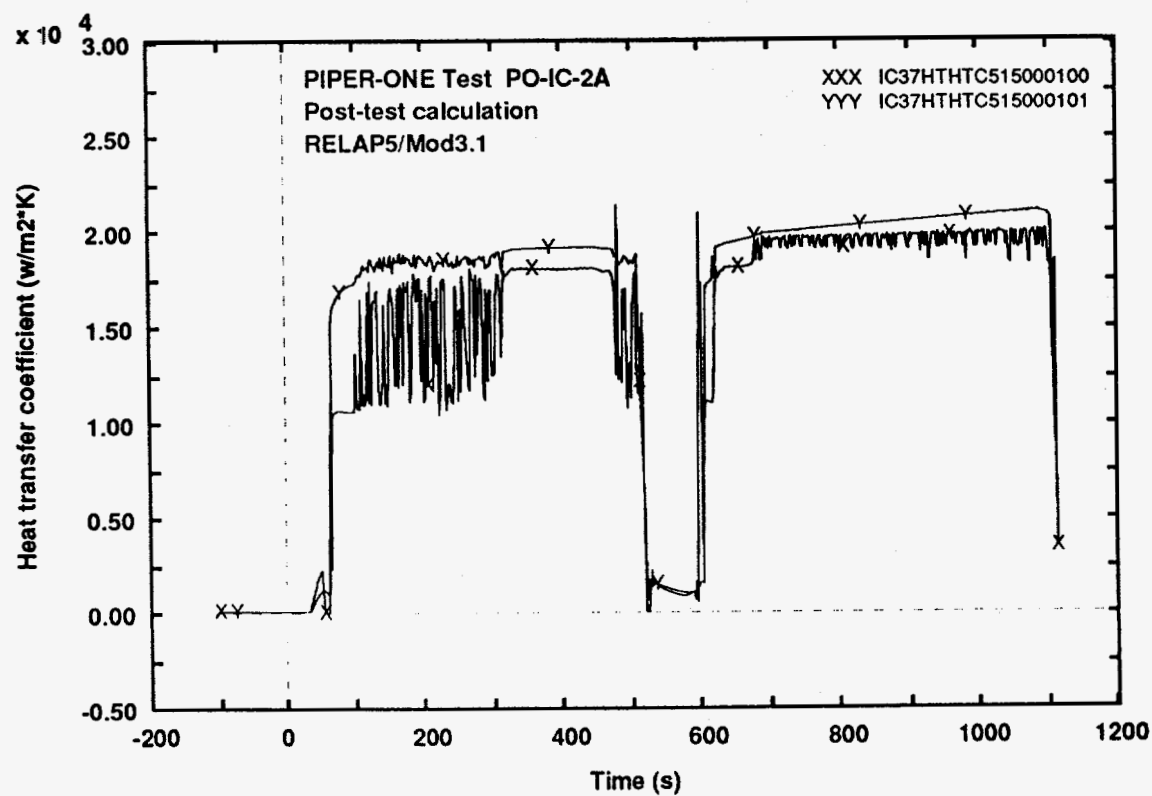


Fig. 32 - Calculated trends of the heat transfer coefficient at the inside and the outside of IC tubes wall (top elevation)

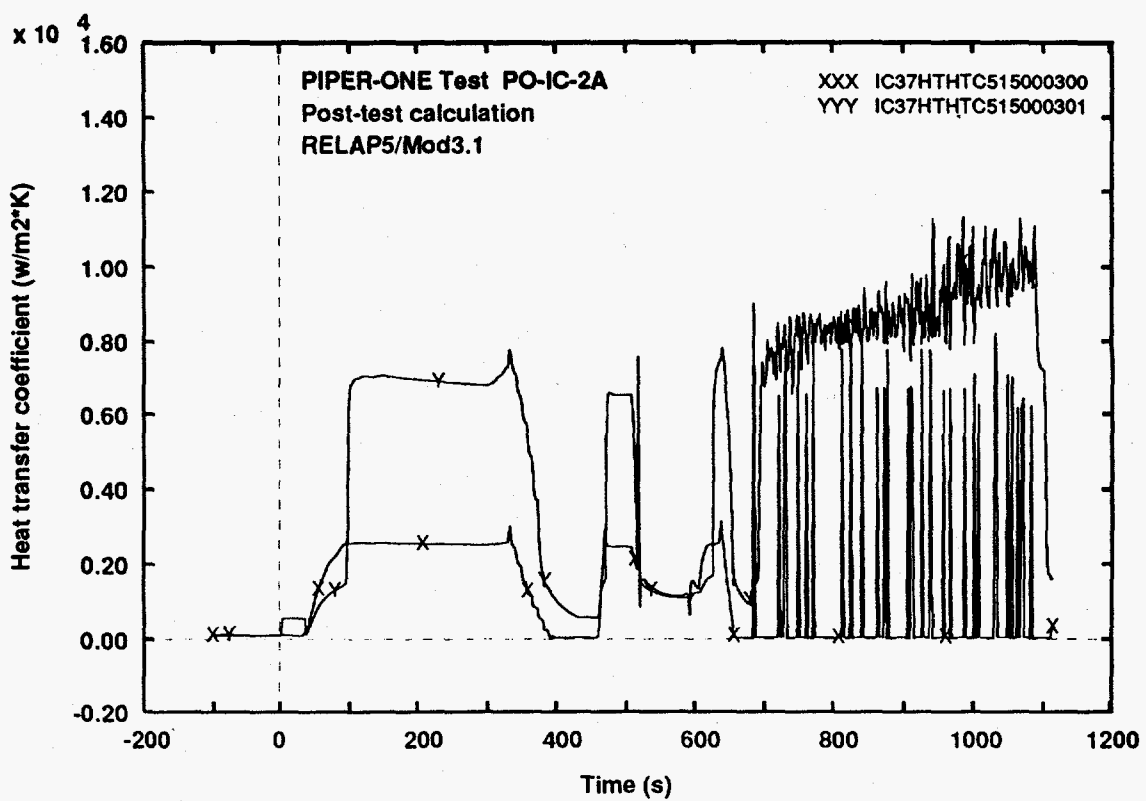


Fig. 33 - Calculated trends of the heat transfer coefficient at the inside and the outside of IC tubes wall (middle elevation)

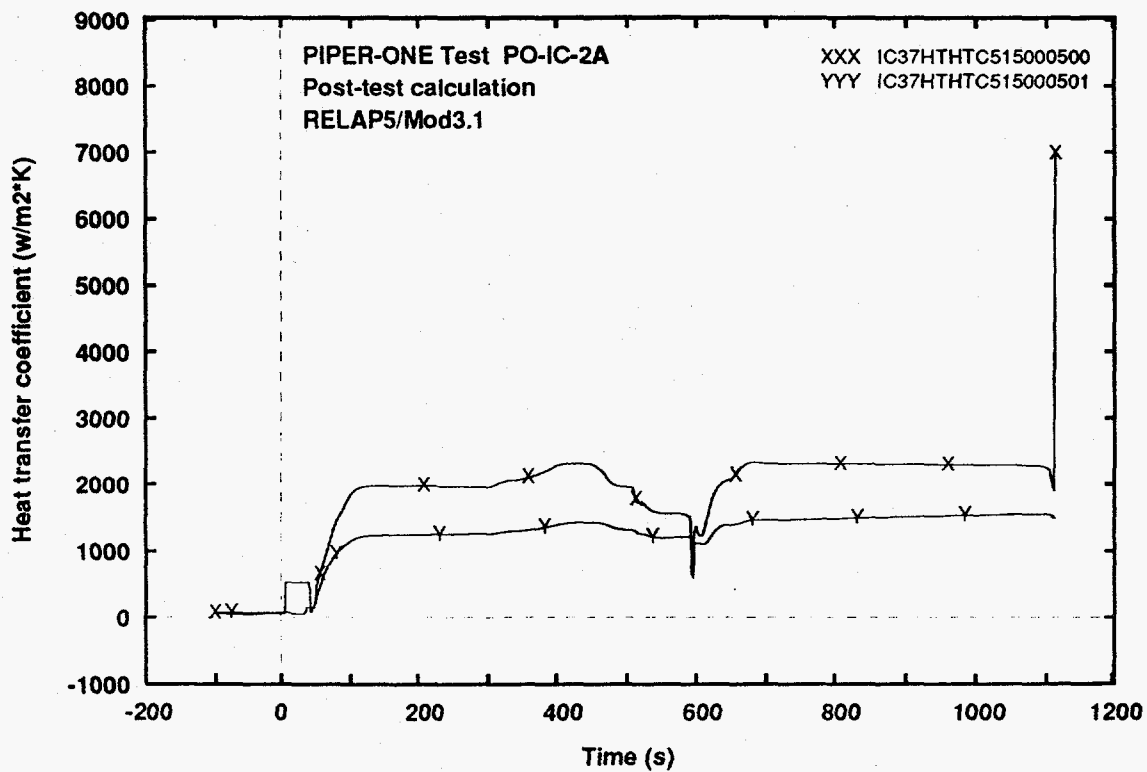


Fig. 34 - Calculated trends of the heat transfer coefficient at the inside and the outside of IC tubes wall (bottom elevation)

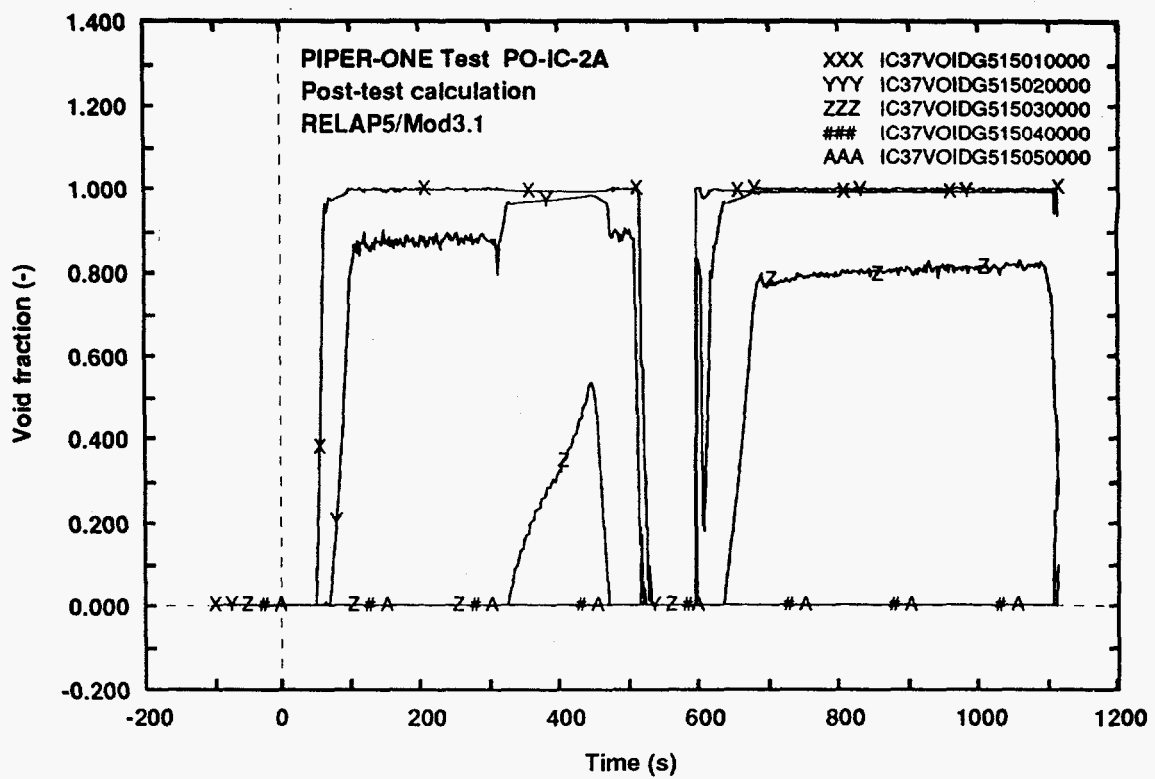


Fig. 35 - Calculated trends of IC tubes void fraction along the axis

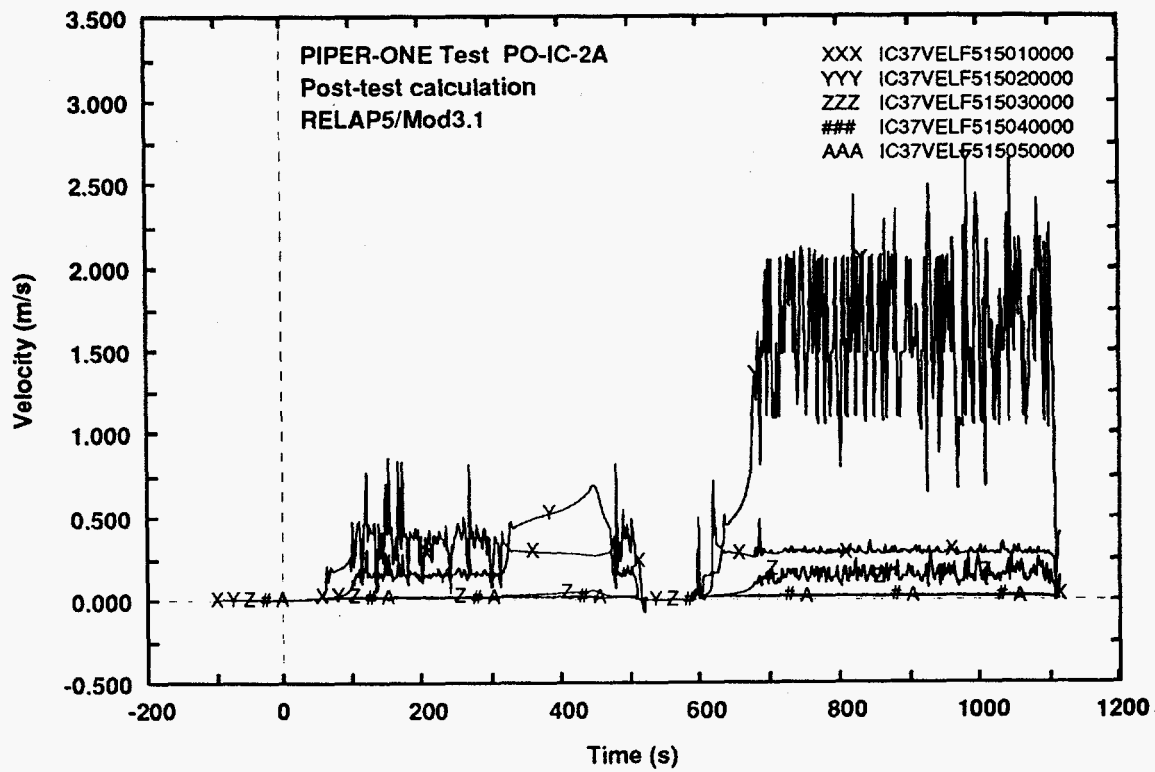


Fig. 36 - Calculated trends of IC tubes liquid velocity along the axis

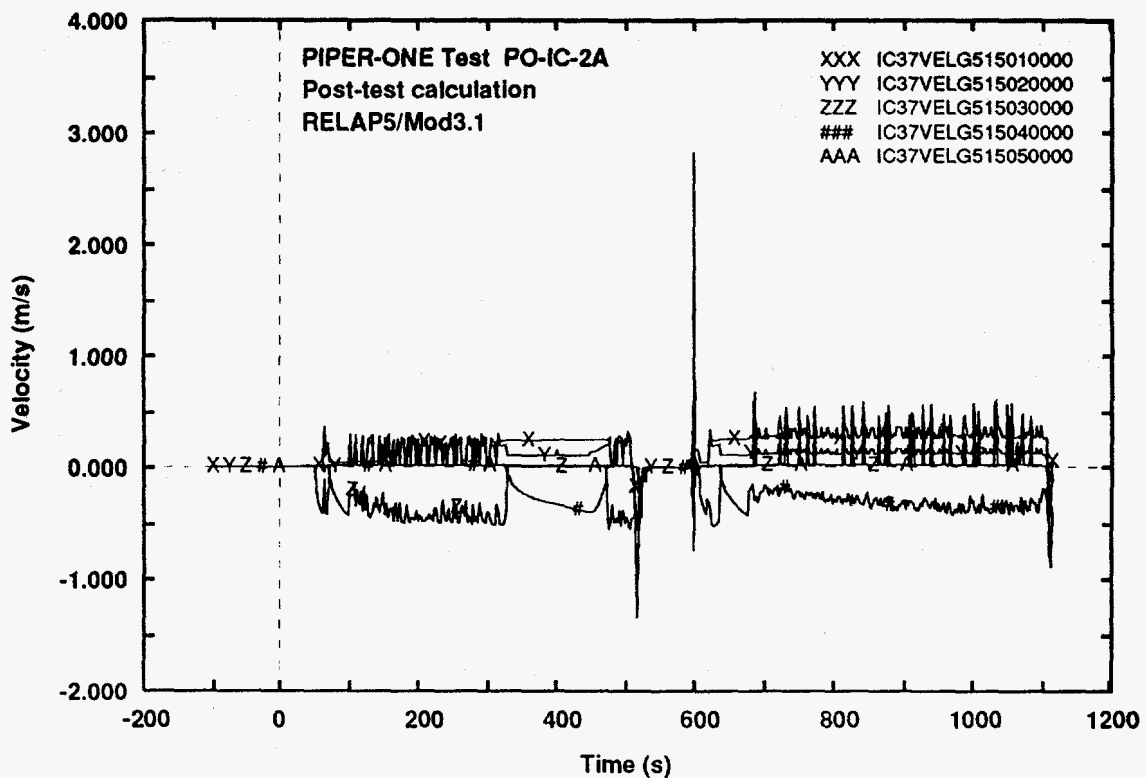


Fig. 37 - Calculated trends of IC tubes steam velocity along the axis

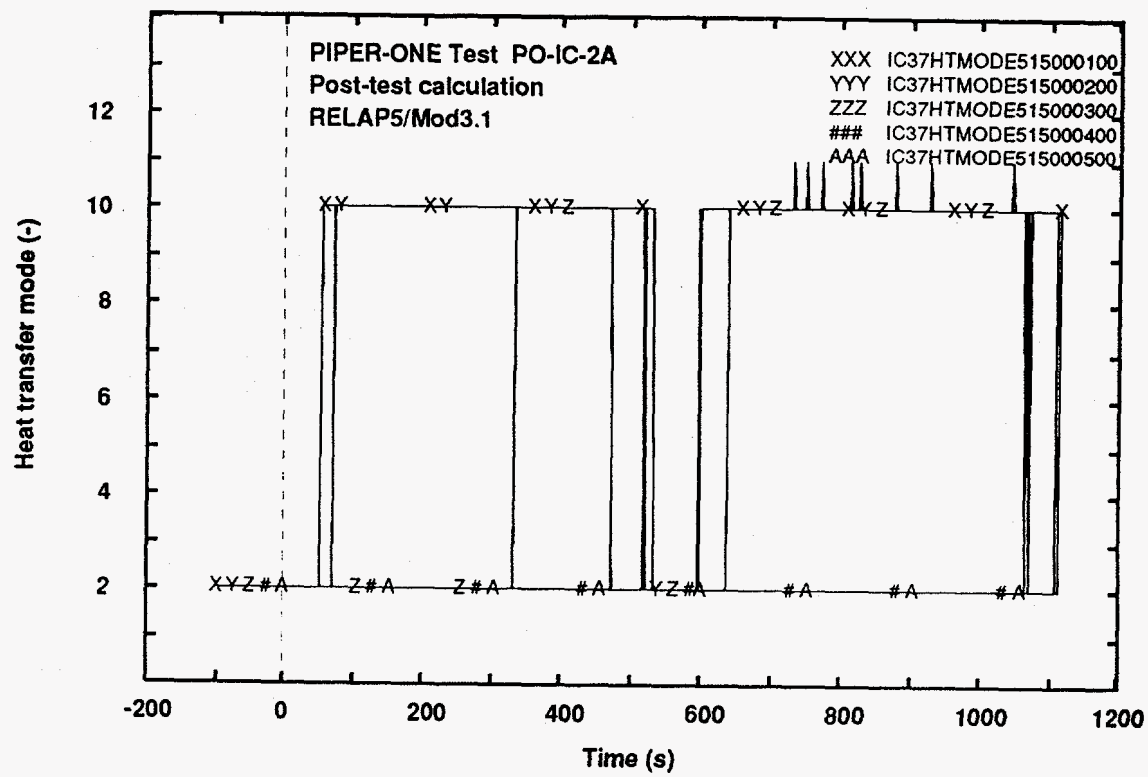


Fig. 38 - Calculated trends of IC tubes heat transfer mode (internal side)

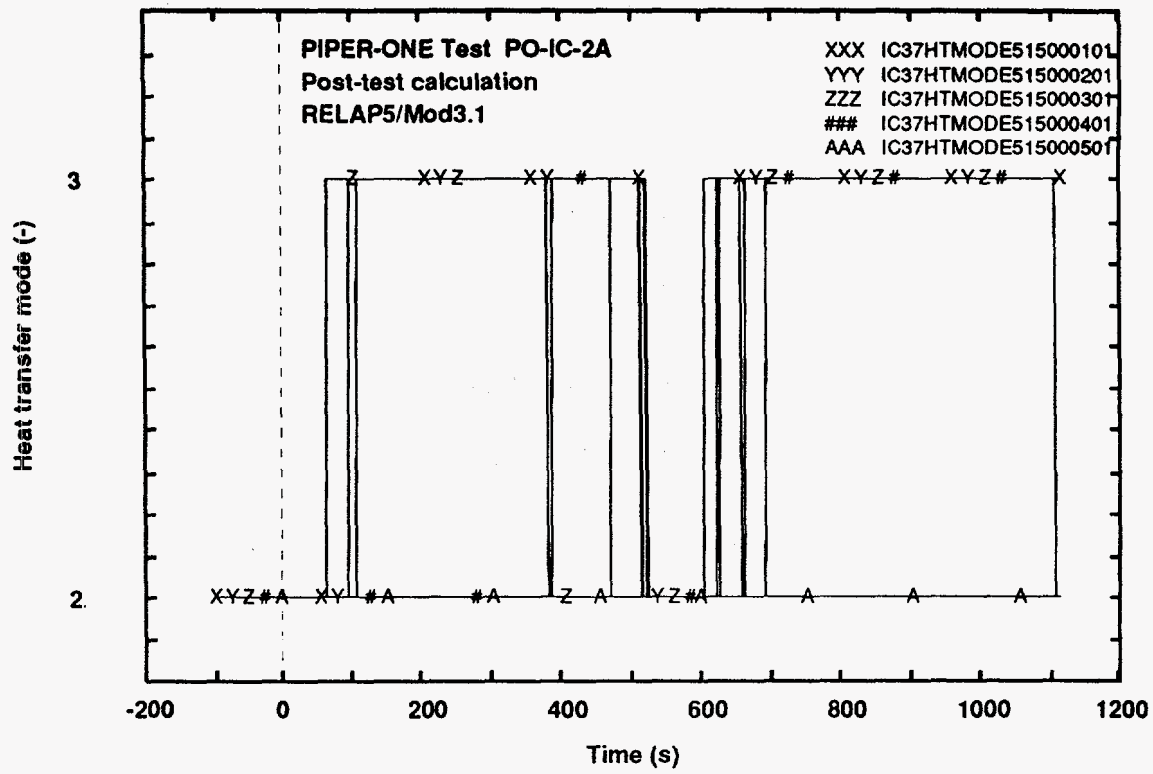
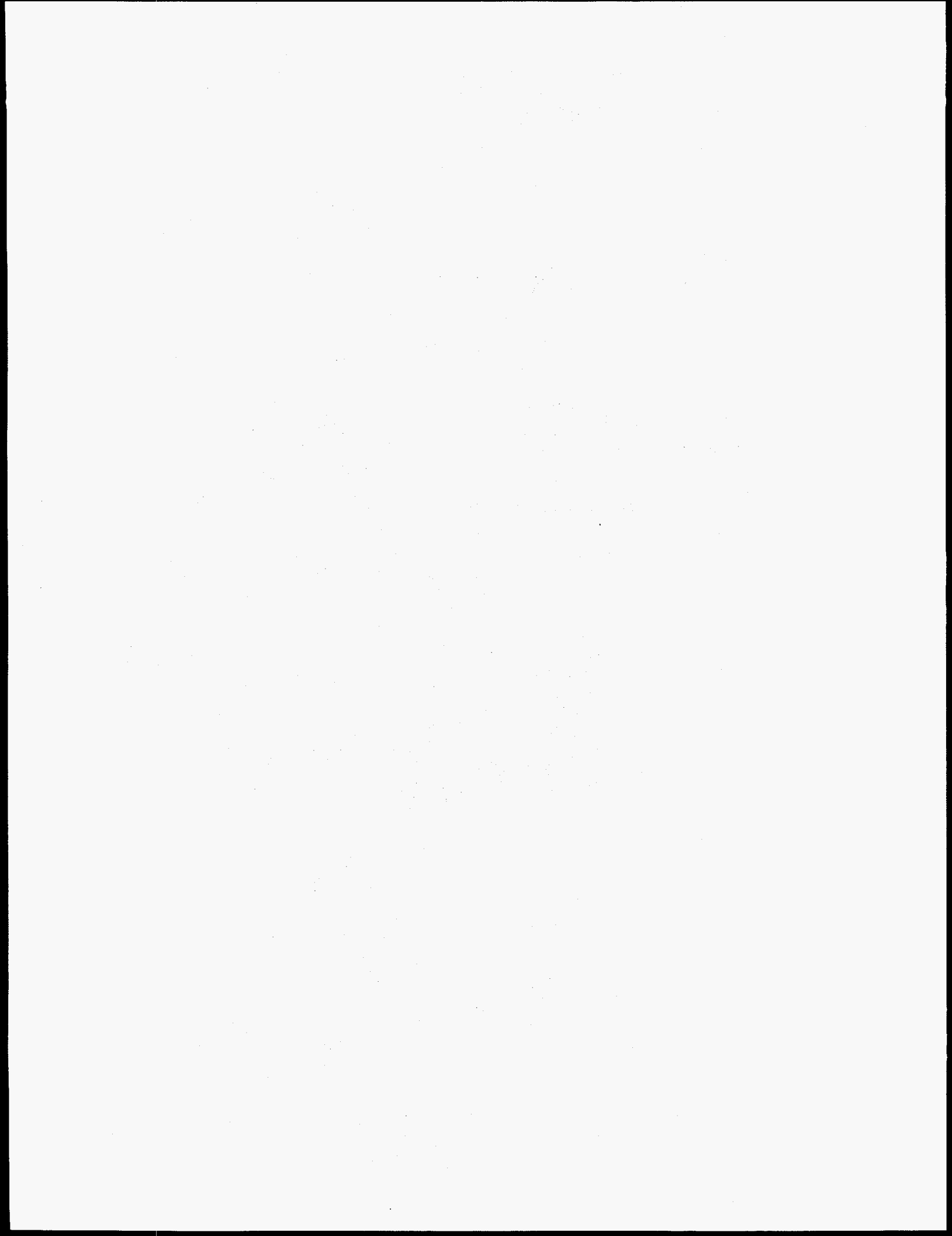


Fig. 39 - Calculated trends of IC tubes heat transfer mode (external side)

APPENDIX 4:
ICA6 Results



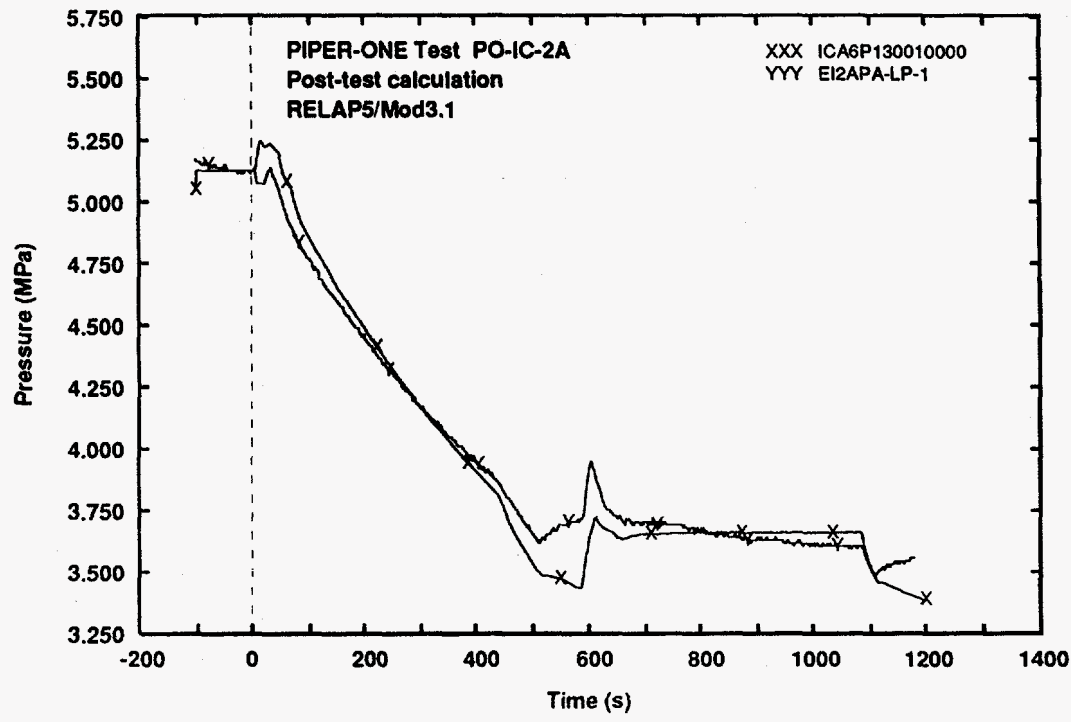


Fig. 1 - Measured and predicted trends of lower plenum pressure

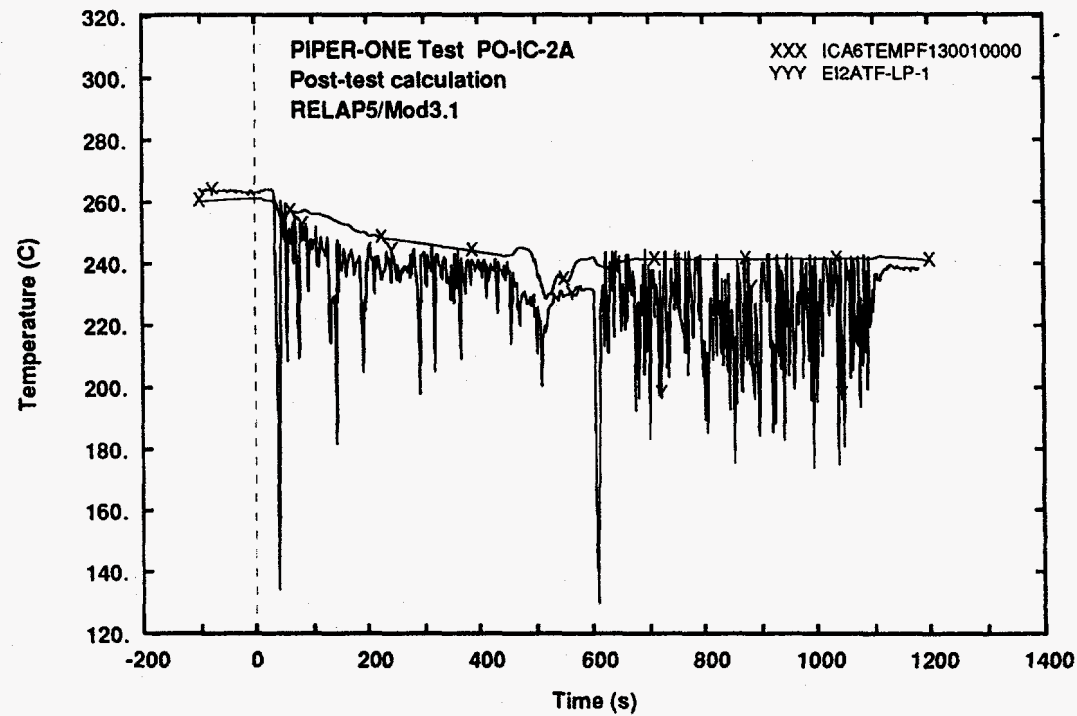


Fig. 2 - Measured and calculated trends of lower plenum temperature

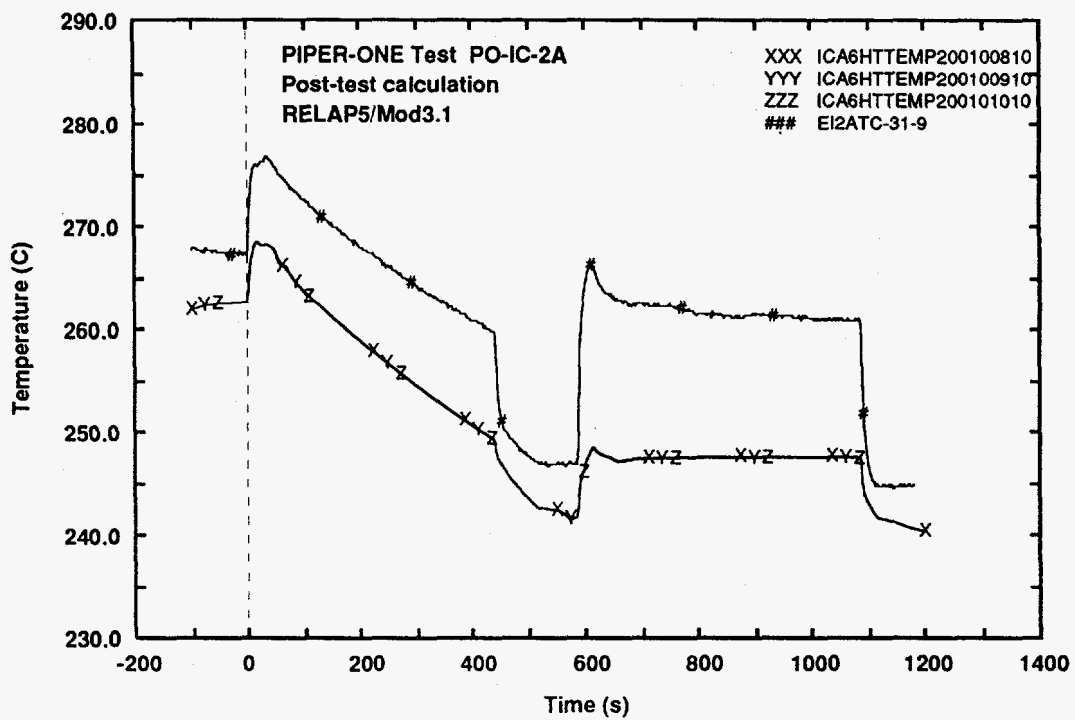


Fig. 3 - Measured and calculated trends of rod surface temperature (level 9)

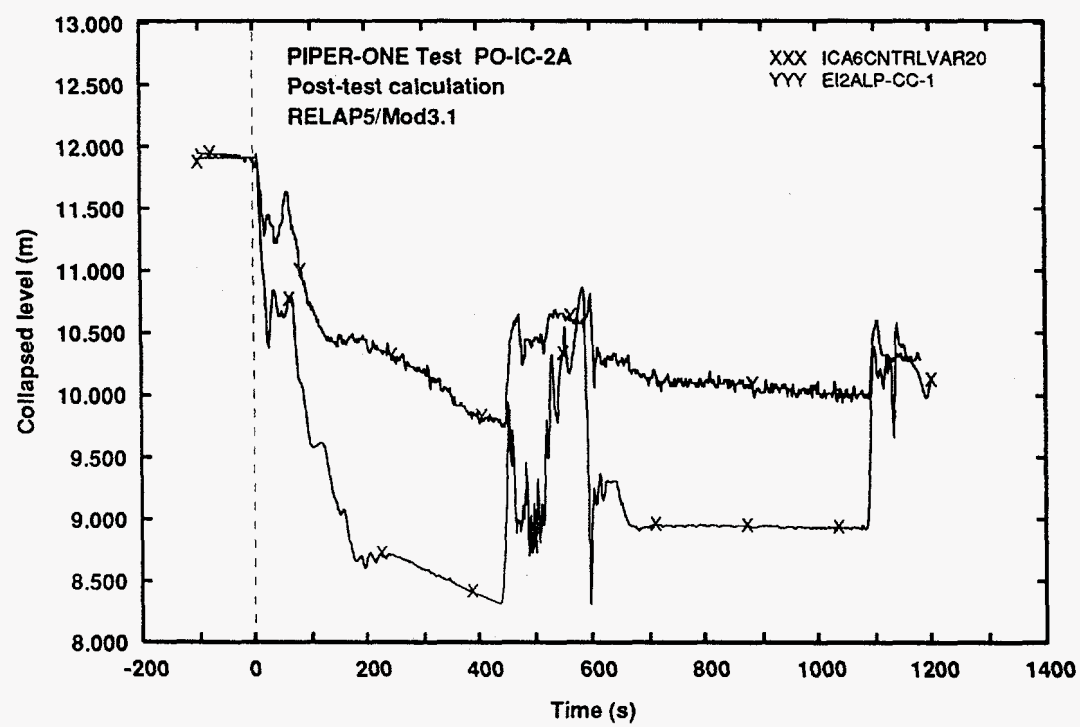


Fig. 4 - Measured and calculated trends of core level

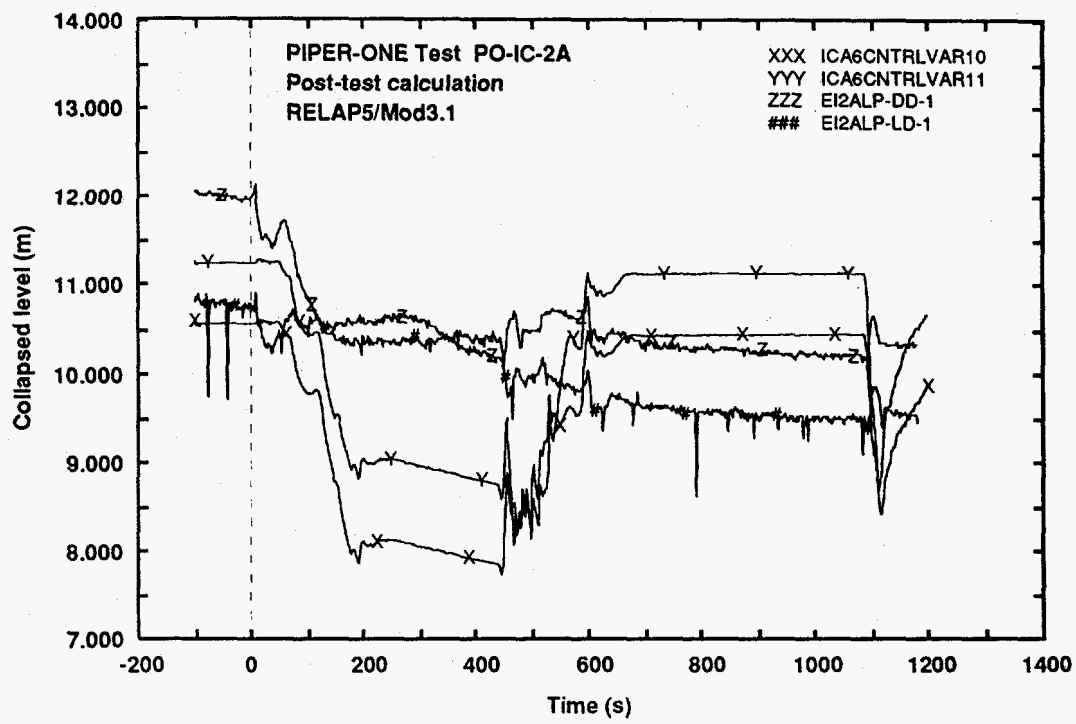


Fig. 5 - Measured and calculated trends of downcomer level

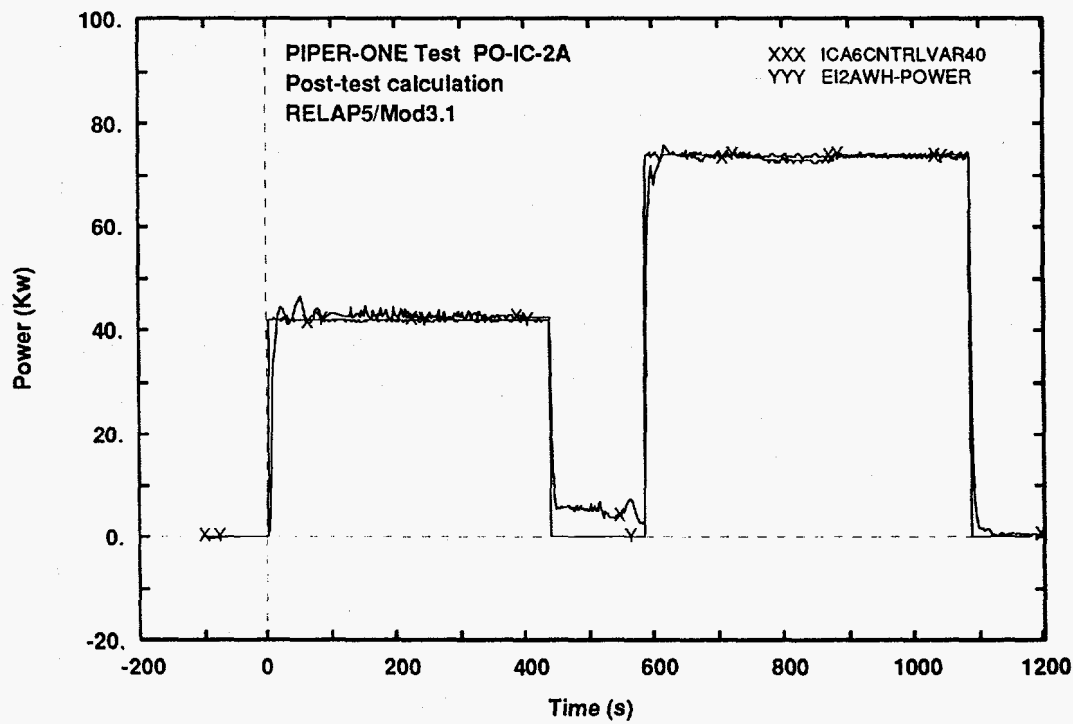


Fig. 6 - Measured and calculated trends of core power

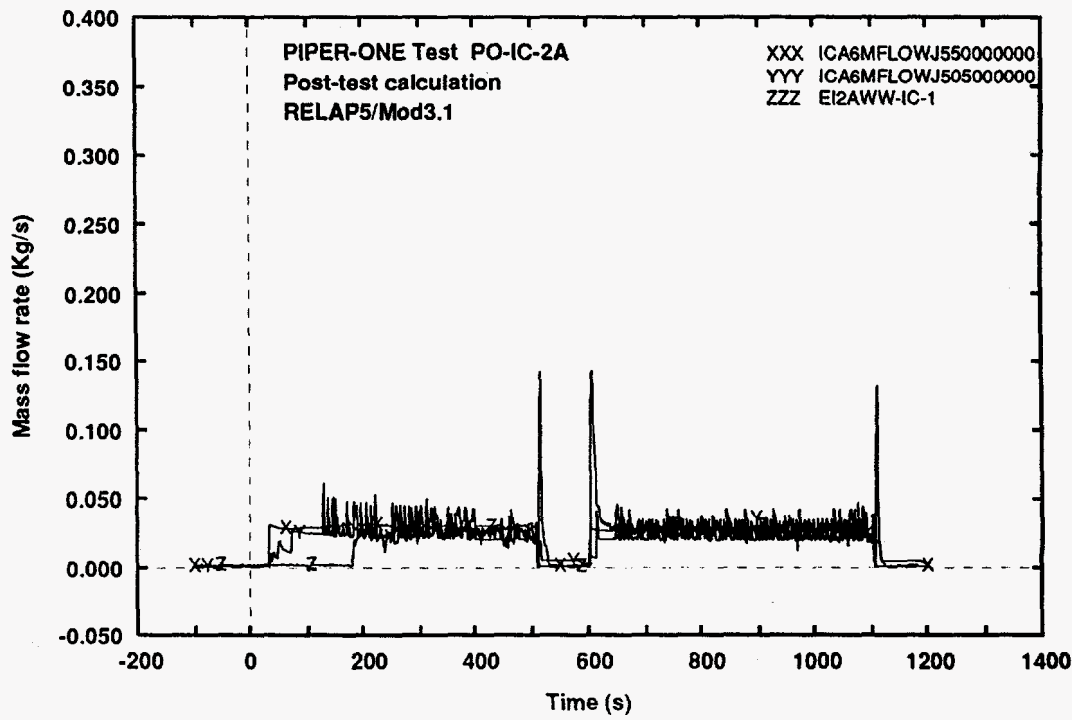


Fig. 7 - Measured and calculated trends of IC mass flow rate

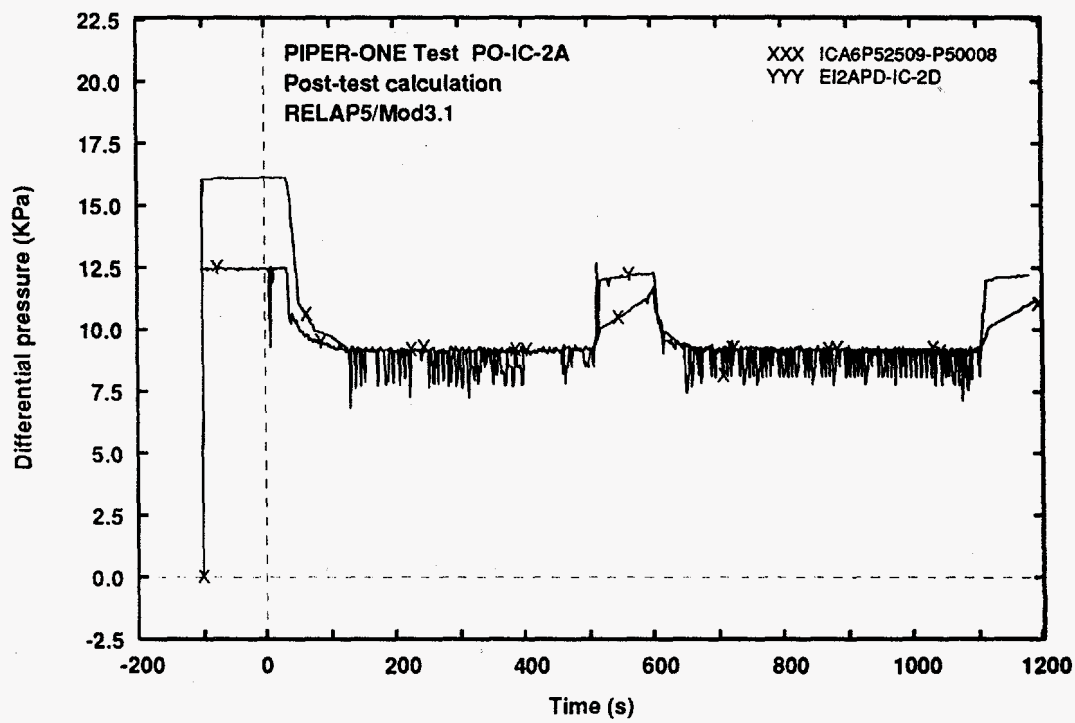


Fig. 8 - Measured and calculated trends of IC differential pressure

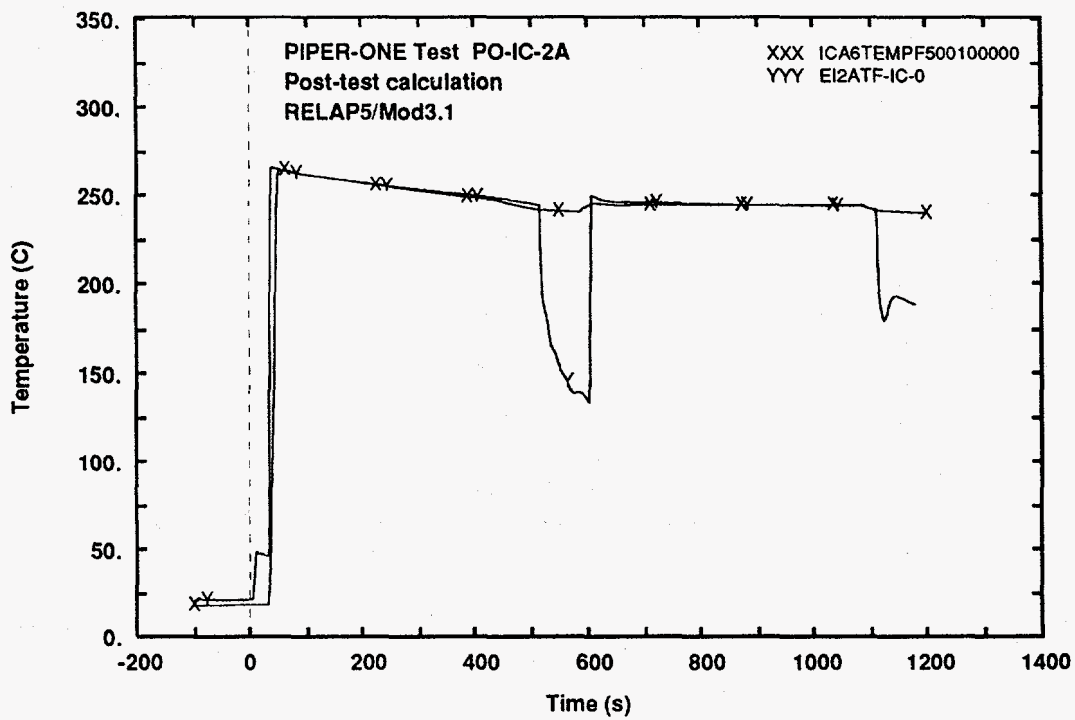


Fig. 9 - Measured and calculated trends of IC inlet fluid temperature

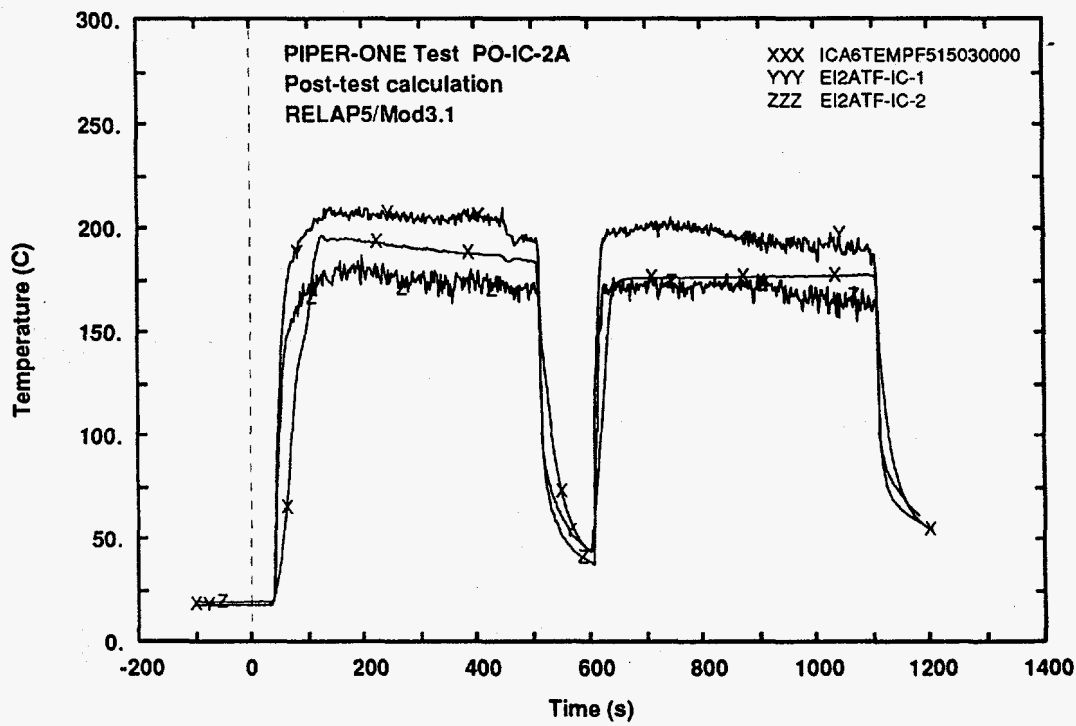


Fig. 10 - Measured and calculated trends of IC tubes fluid temperature
(middle elevation)

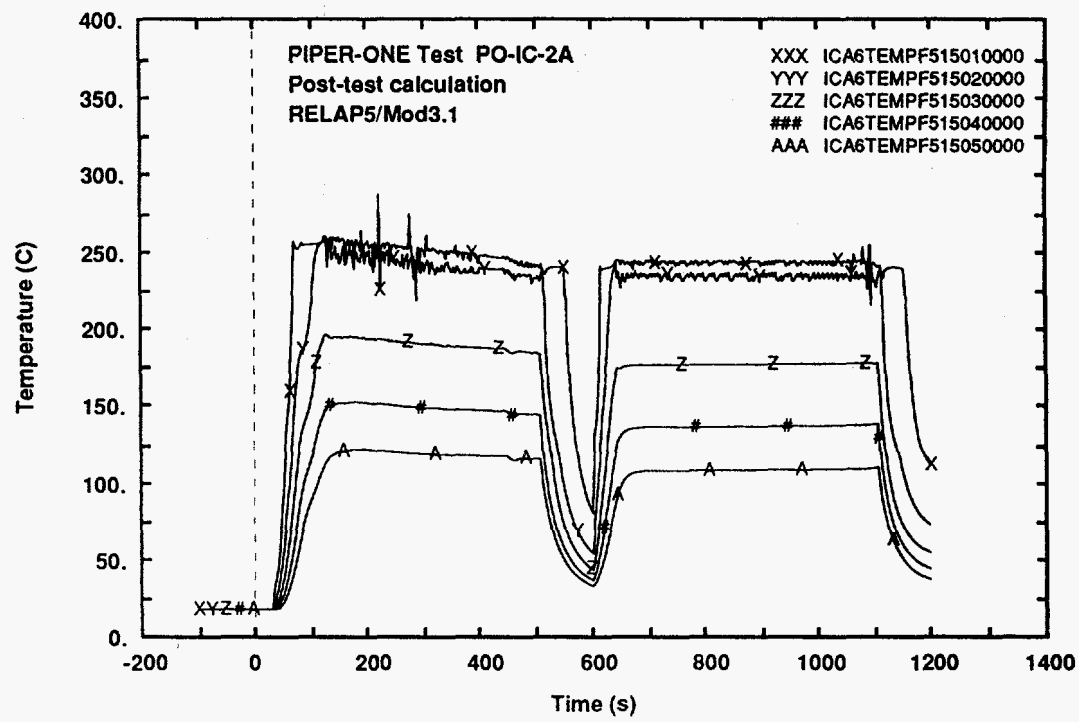


Fig. 11 - Calculated trends of IC tubes fluid temperature along the axis

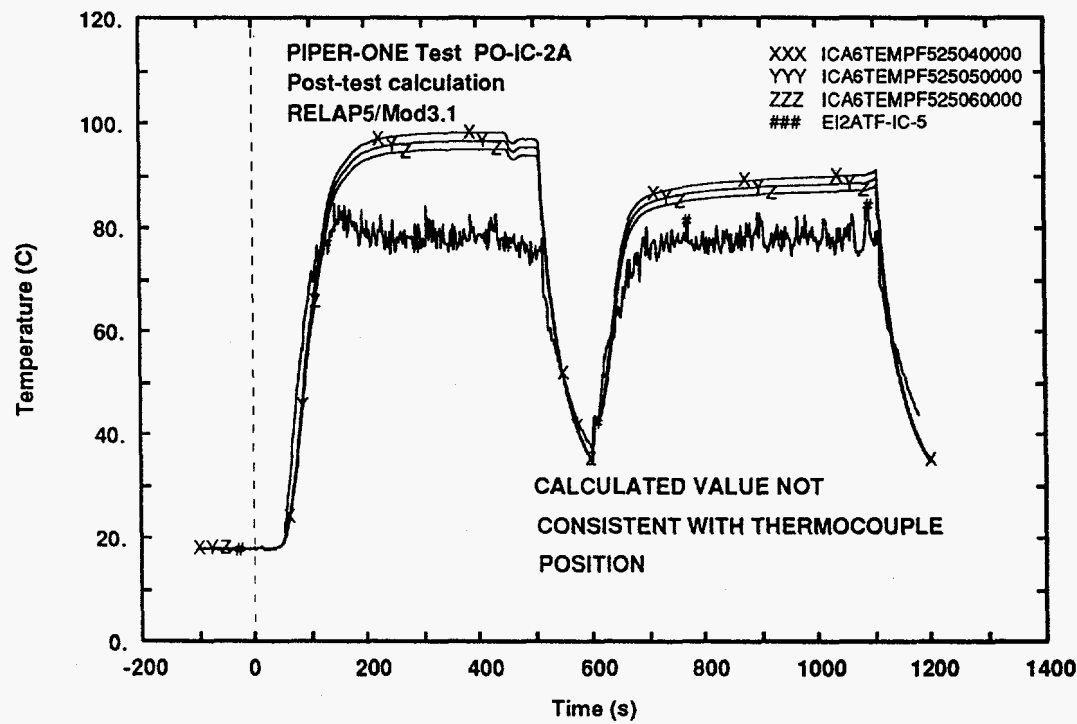


Fig. 12 - Measured and calculated trends of IC outlet fluid temperature

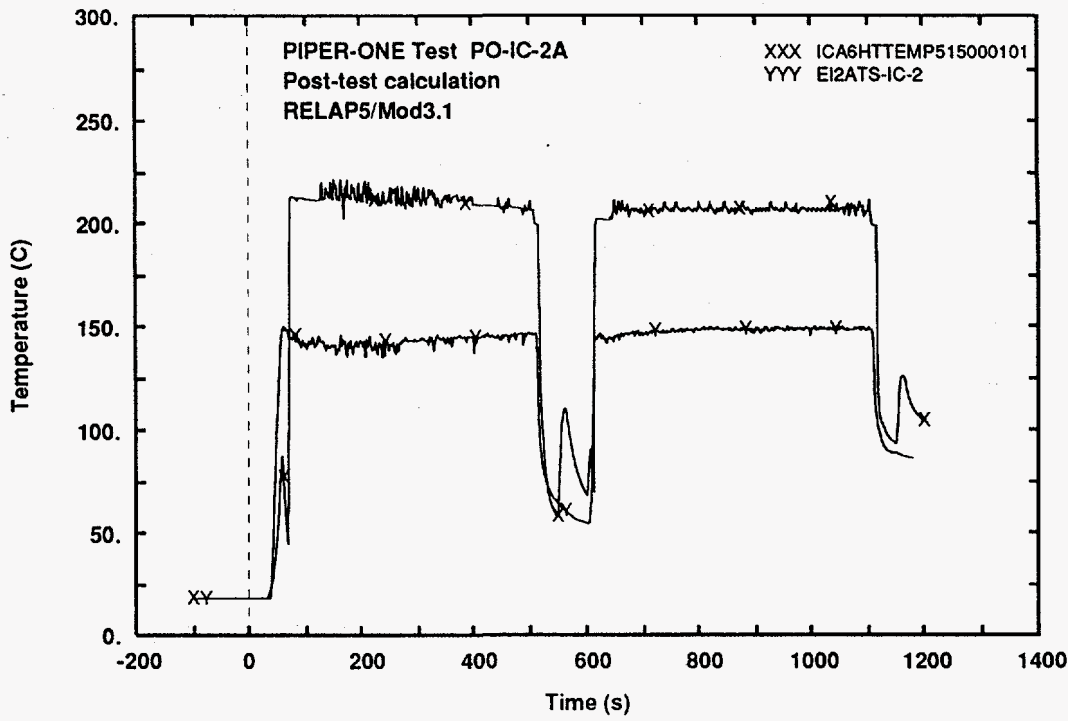


Fig. 13 - Measured and calculated trends of IC tubes wall surface temperature
(internal side top elevation)

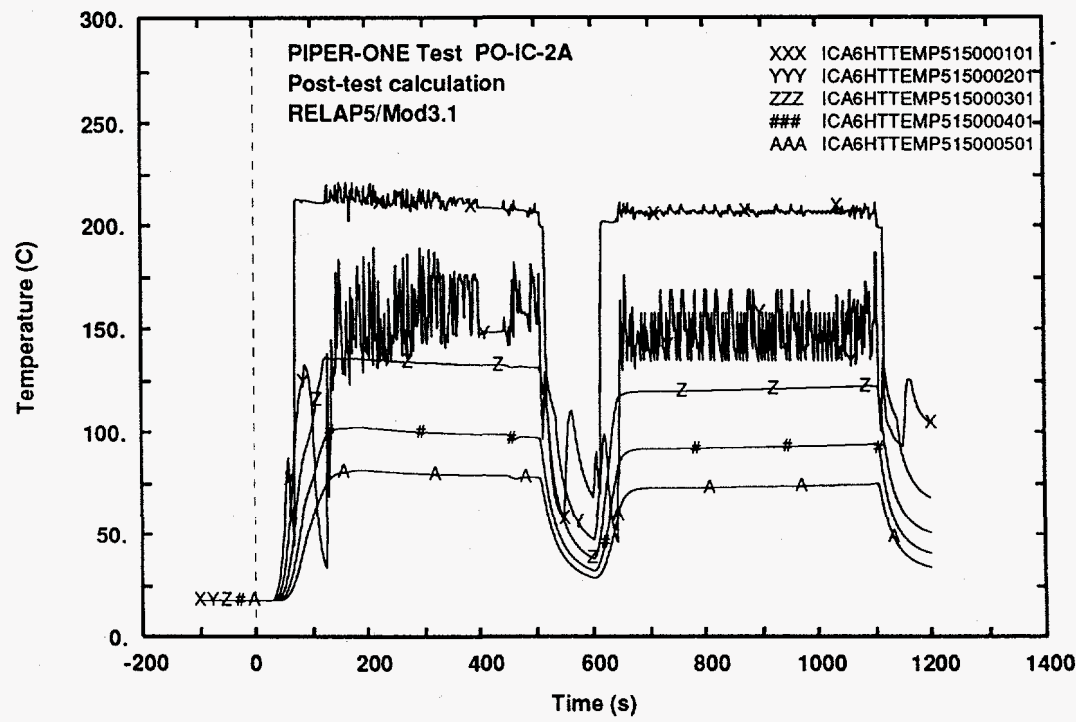


Fig. 14 - Calculated trends of IC tubes wall surface temperature along the axis
(internal side)

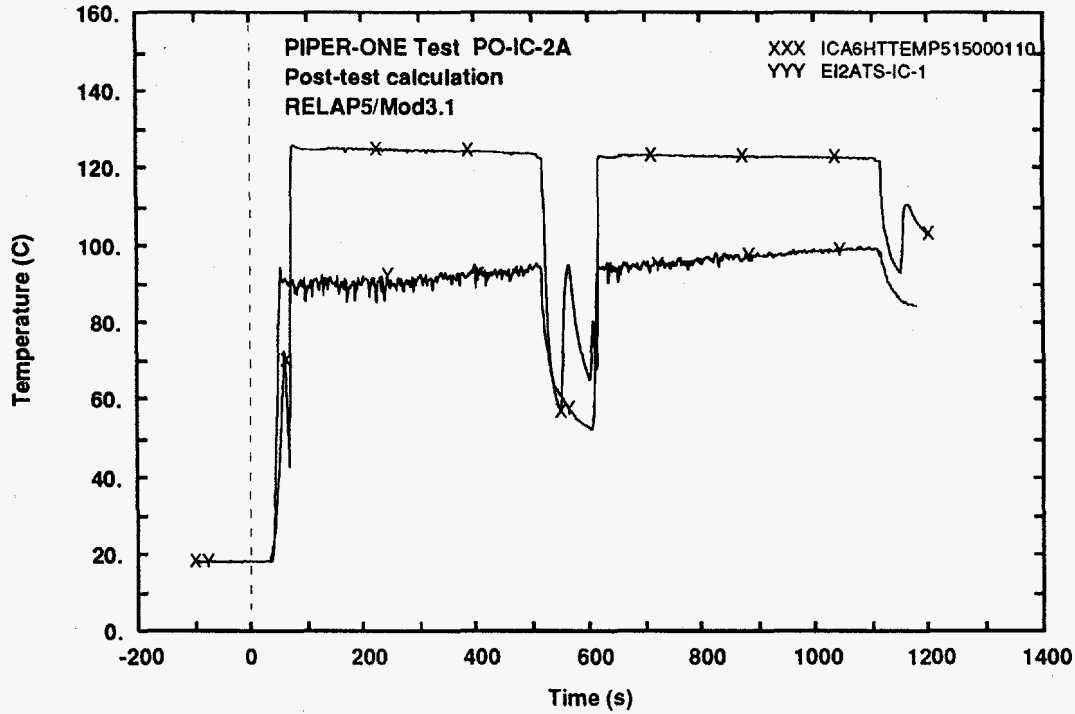


Fig. 15 - Measured and calculated trends of IC tubes wall surface temperature (external side top elevation)

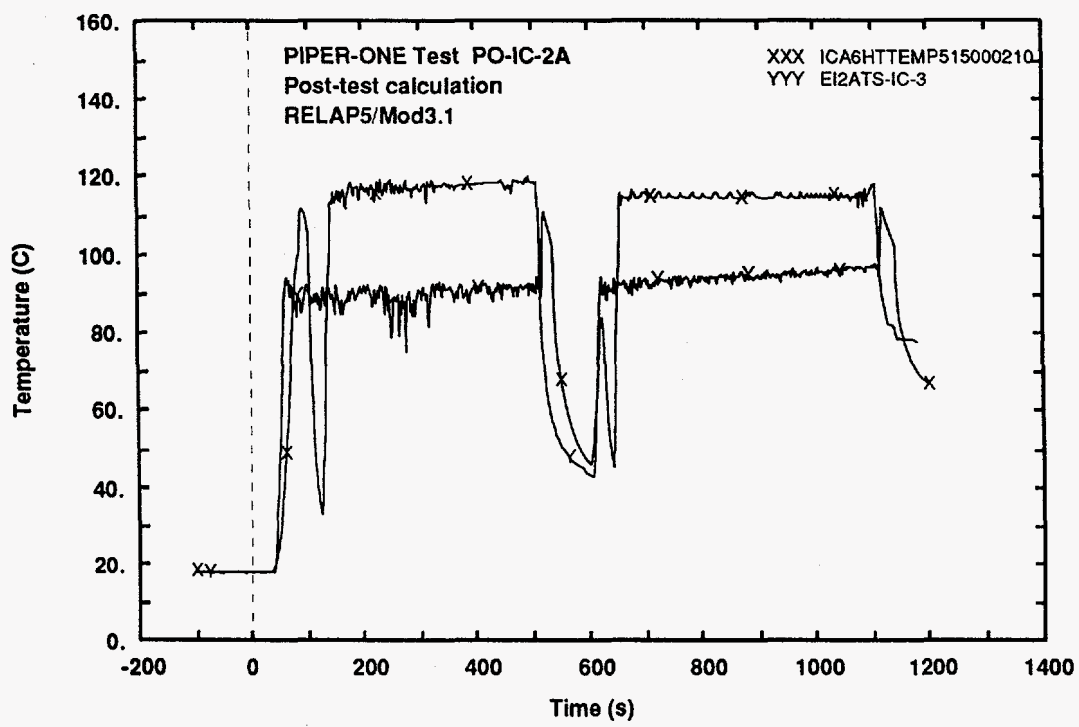


Fig. 16 - Measured and calculated trends of IC tubes wall surface temperature (external side level 3)

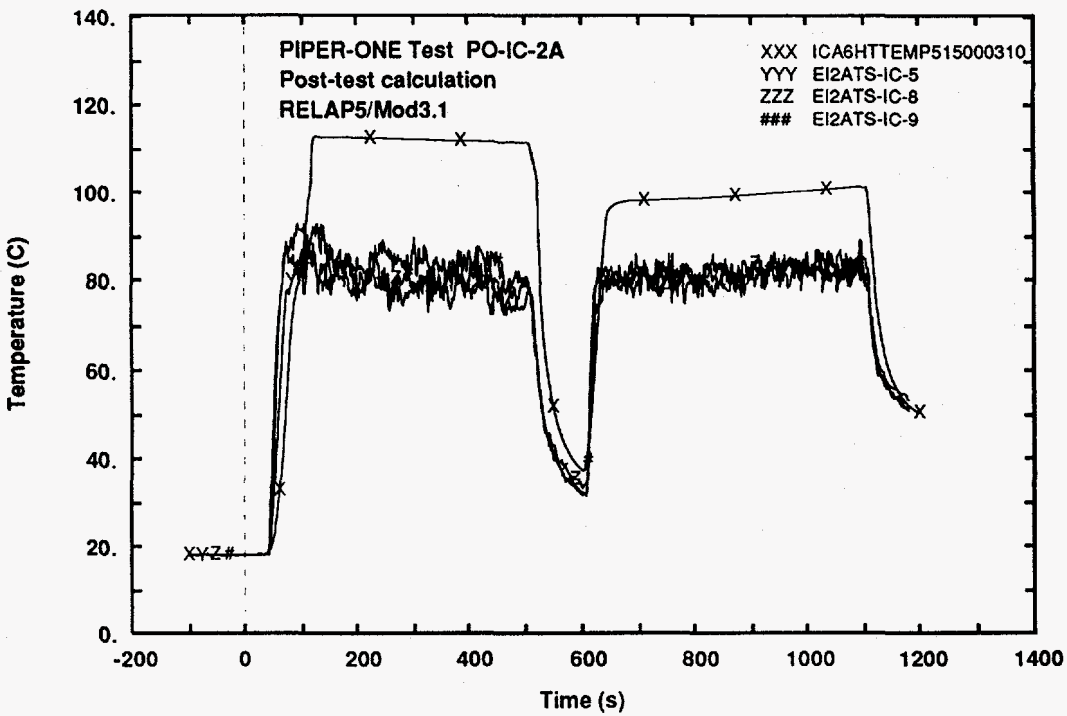


Fig. 17 - Measured and calculated trends of IC tubes wall surface temperature (external side middle elevation)

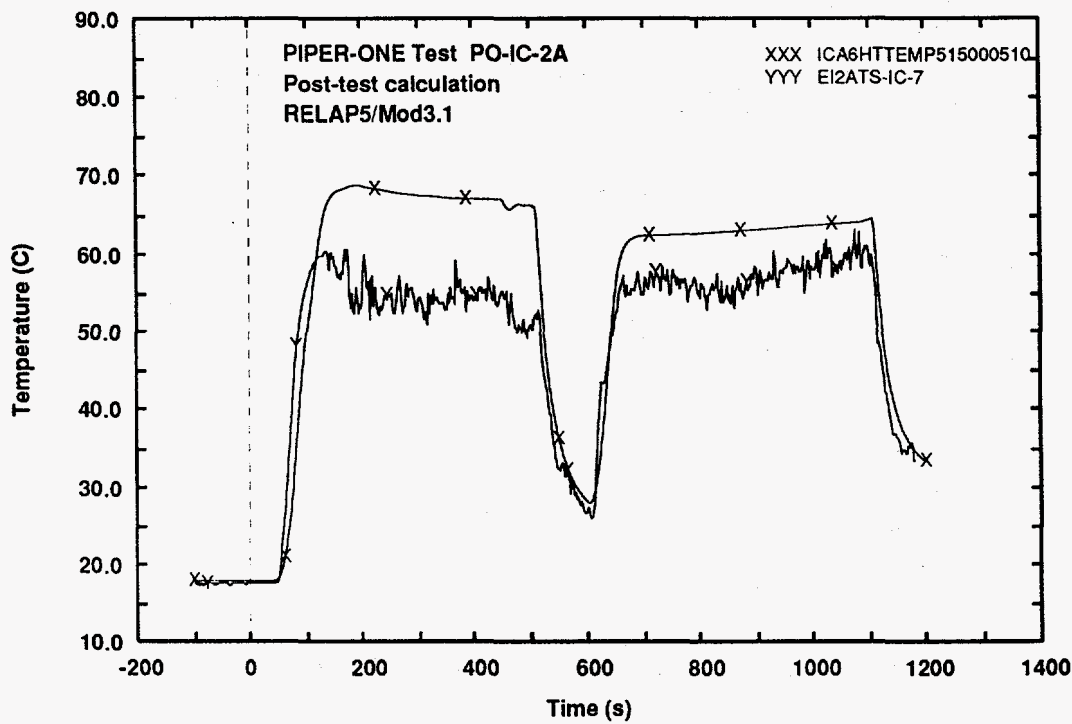


Fig. 18 - Measured and calculated trends of IC tubes wall surface temperature (external side bottom elevation)

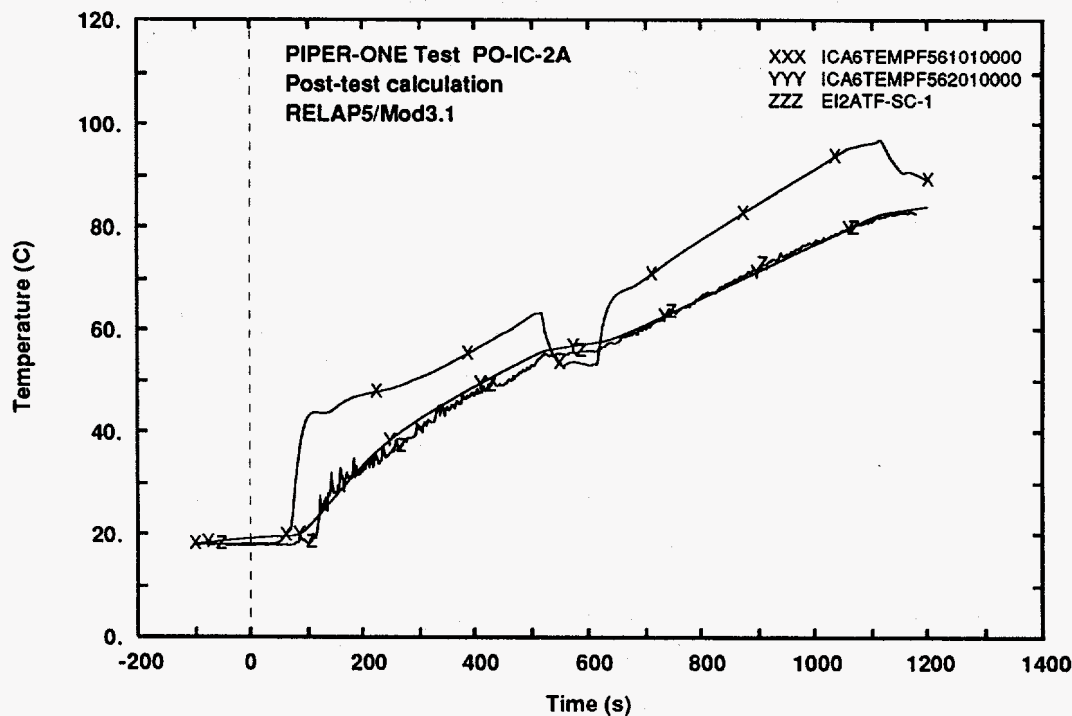


Fig. 19 - Measured and calculated trends of IC internal pool fluid temperature (top level)

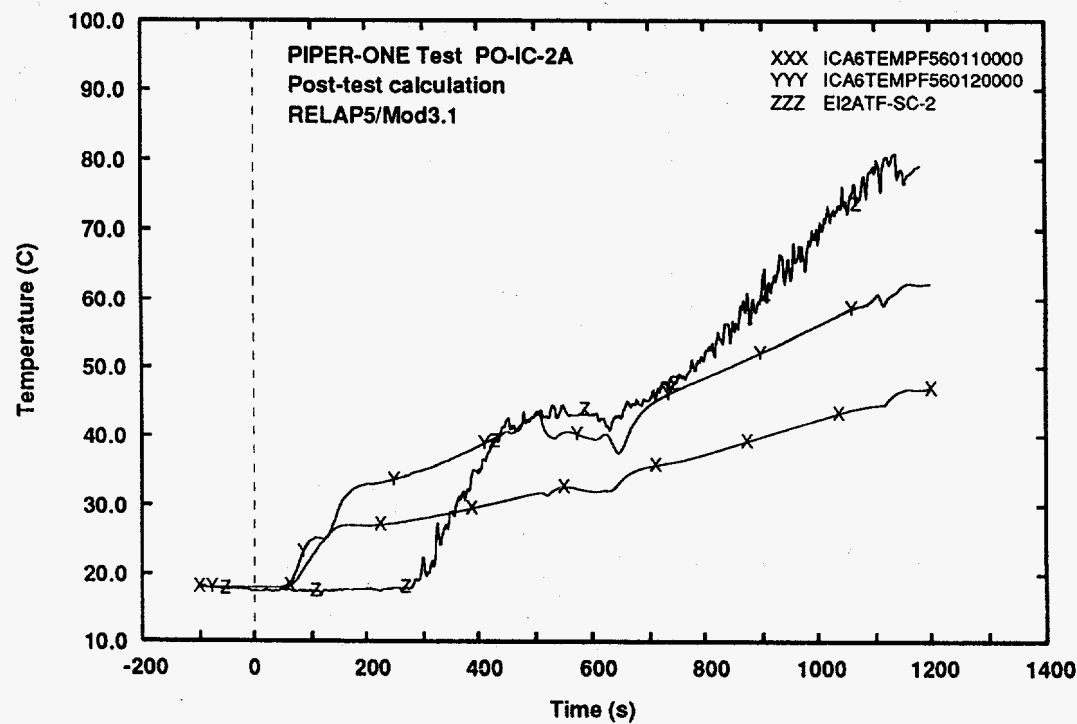


Fig. 20 - Measured and calculated trends of IC internal pool fluid temperature (level 2)

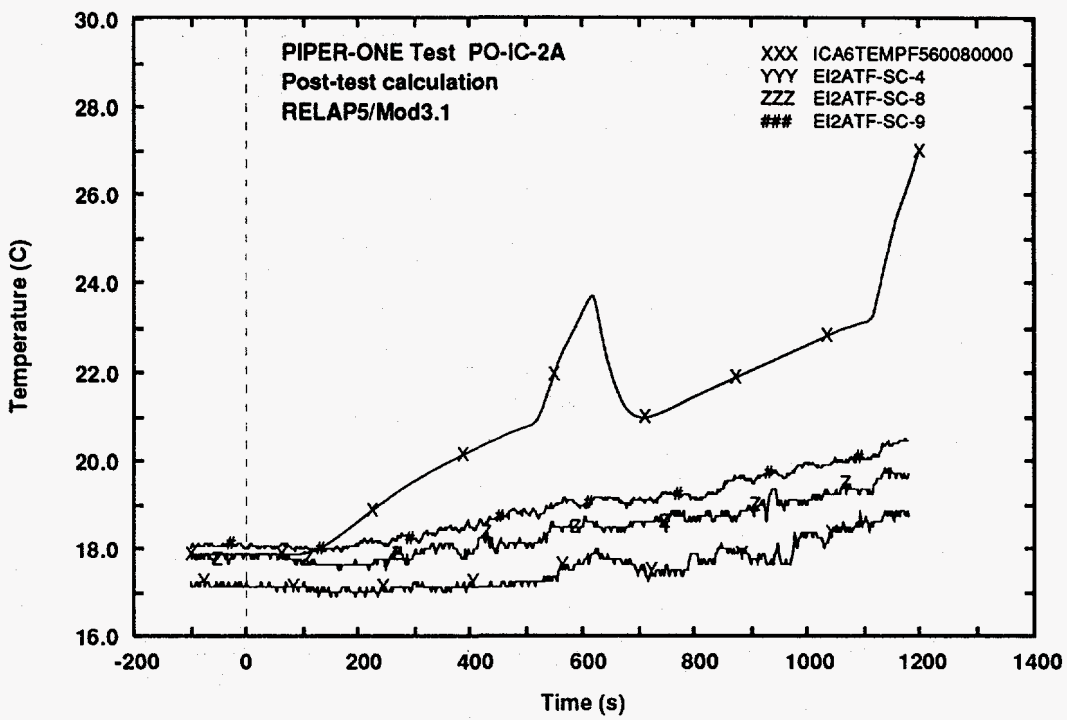


Fig. 21 - Measured and calculated trends of IC internal pool fluid temperature (middle level)

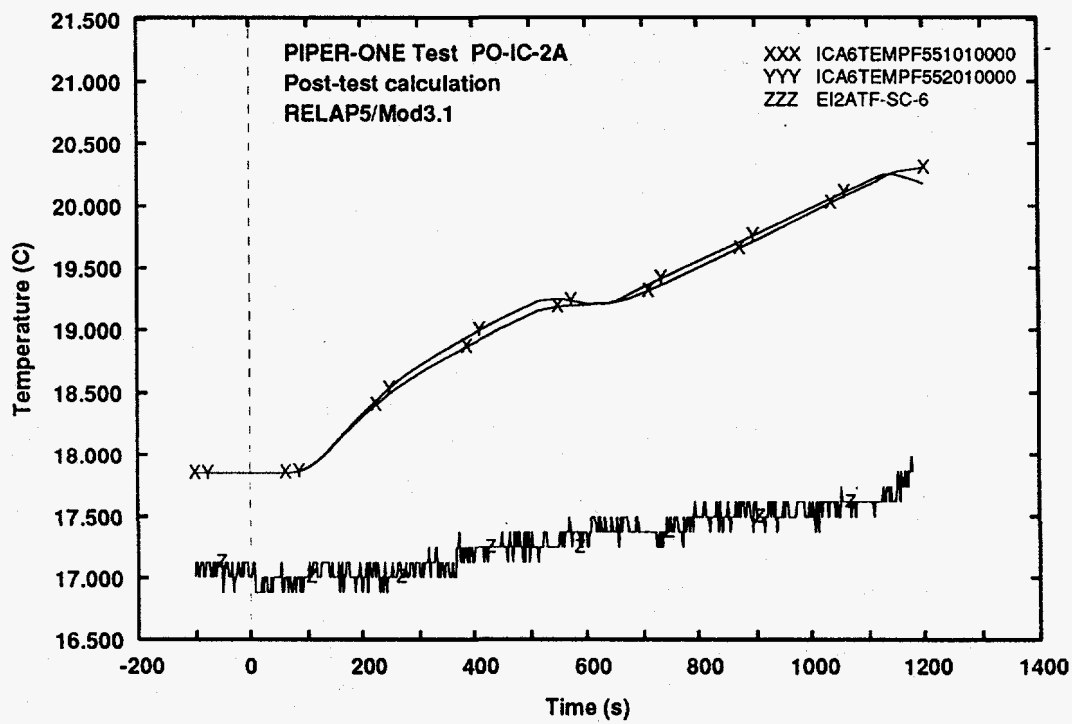


Fig. 22 - Measured and calculated trends of IC internal pool fluid temperature (bottom level)

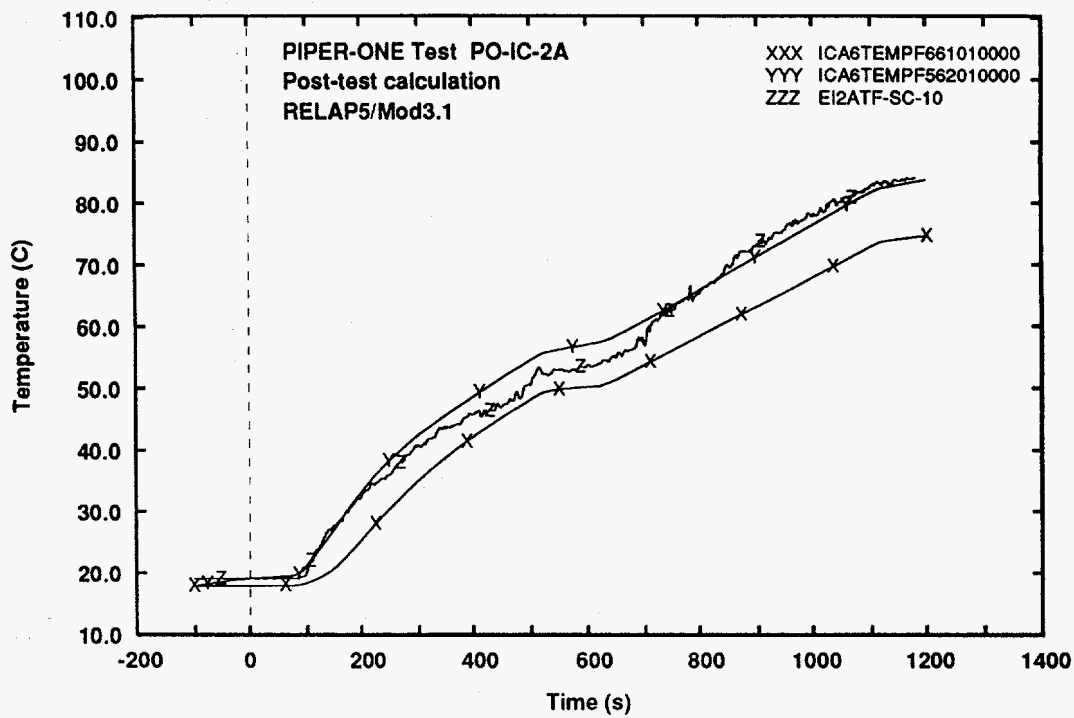


Fig. 23 - Measured and calculated trends of IC external pool fluid temperature (top level)

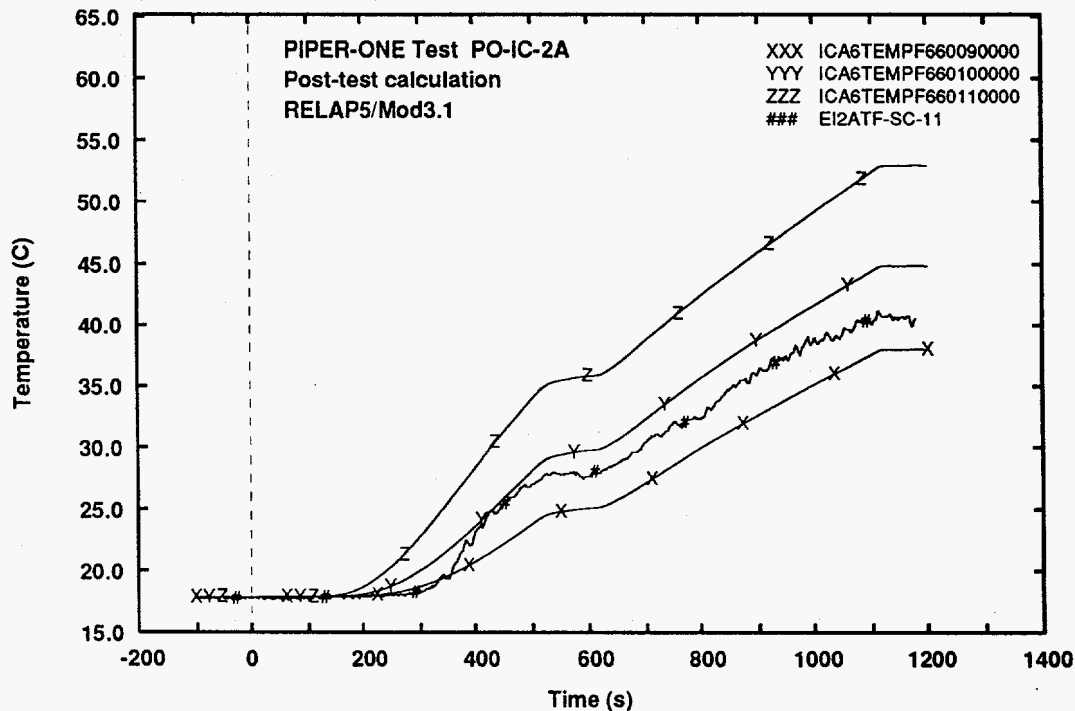


Fig. 24 - Measured and calculated trends of IC external pool fluid temperature (level 11)

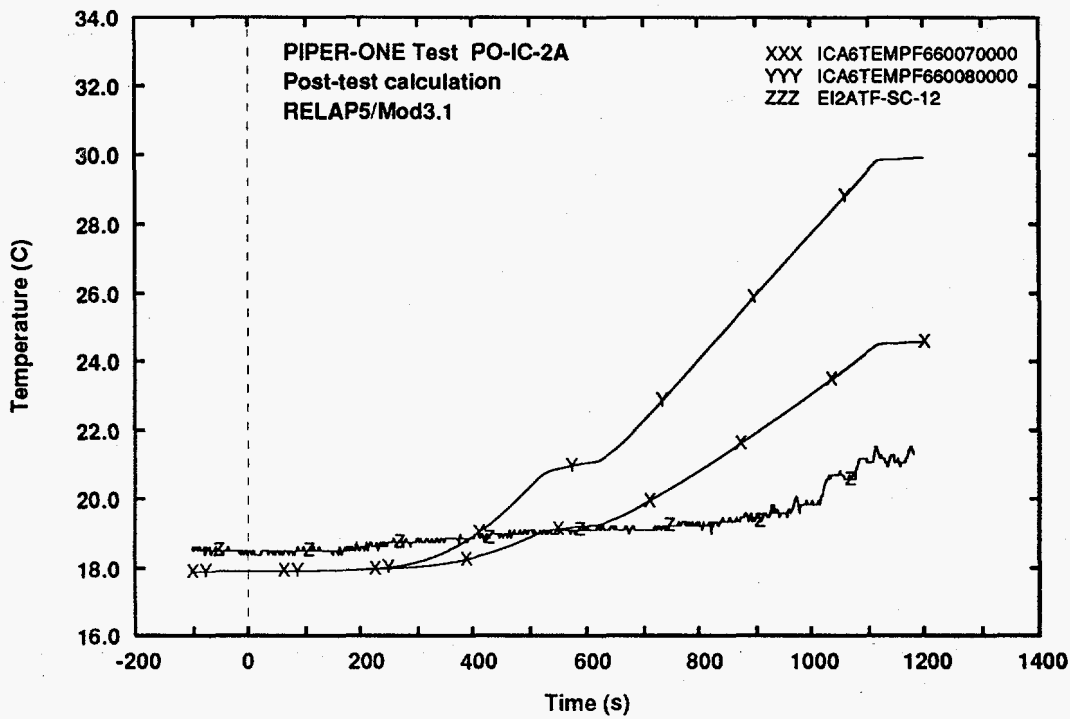


Fig. 25 - Measured and calculated trends of IC external pool fluid temperature (middle level)

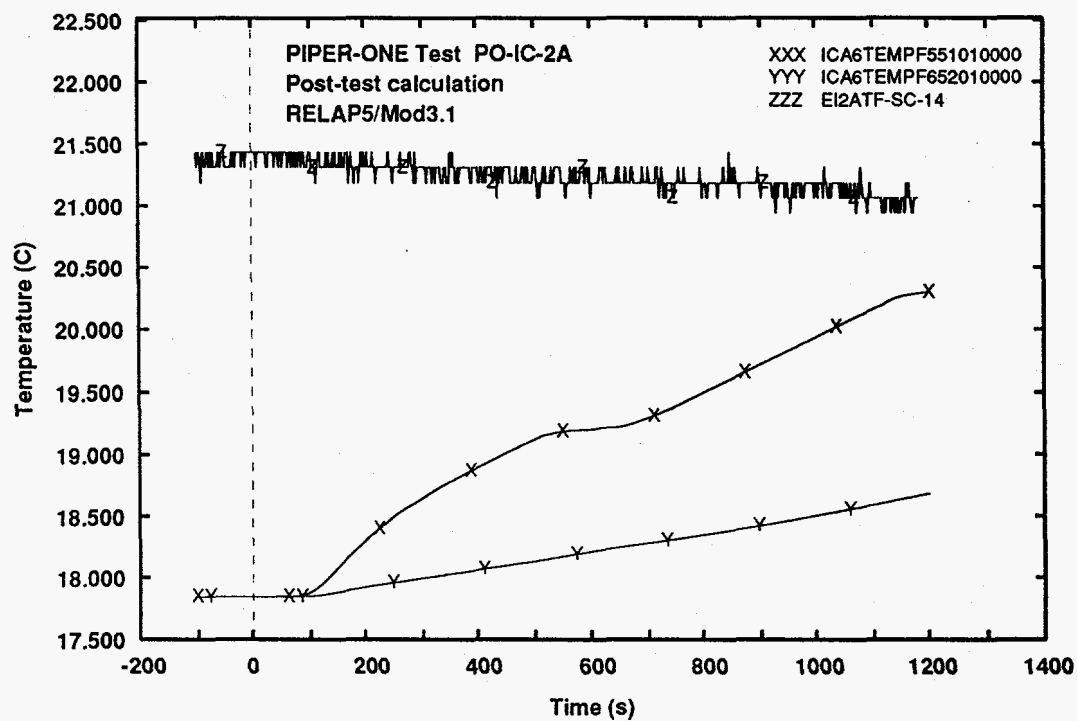


Fig. 26 - Measured and calculated trends of IC external pool fluid temperature (bottom level)

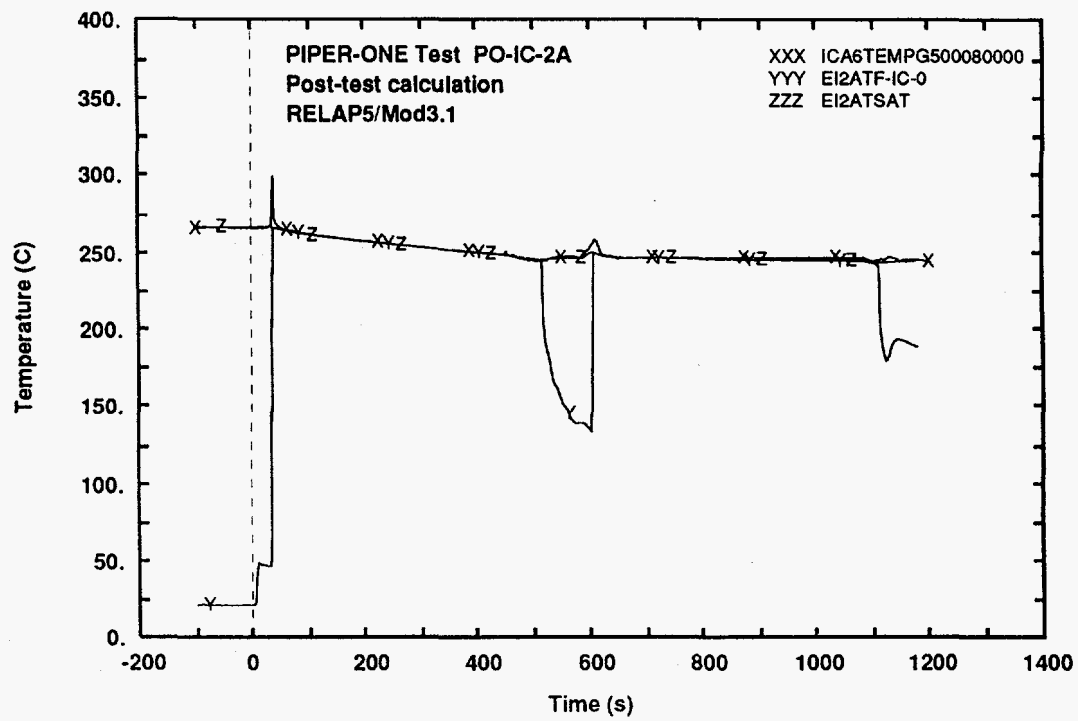


Fig. 27 - Measured and calculated trends of steam temperature at IC inlet compared with experimental saturated temperature

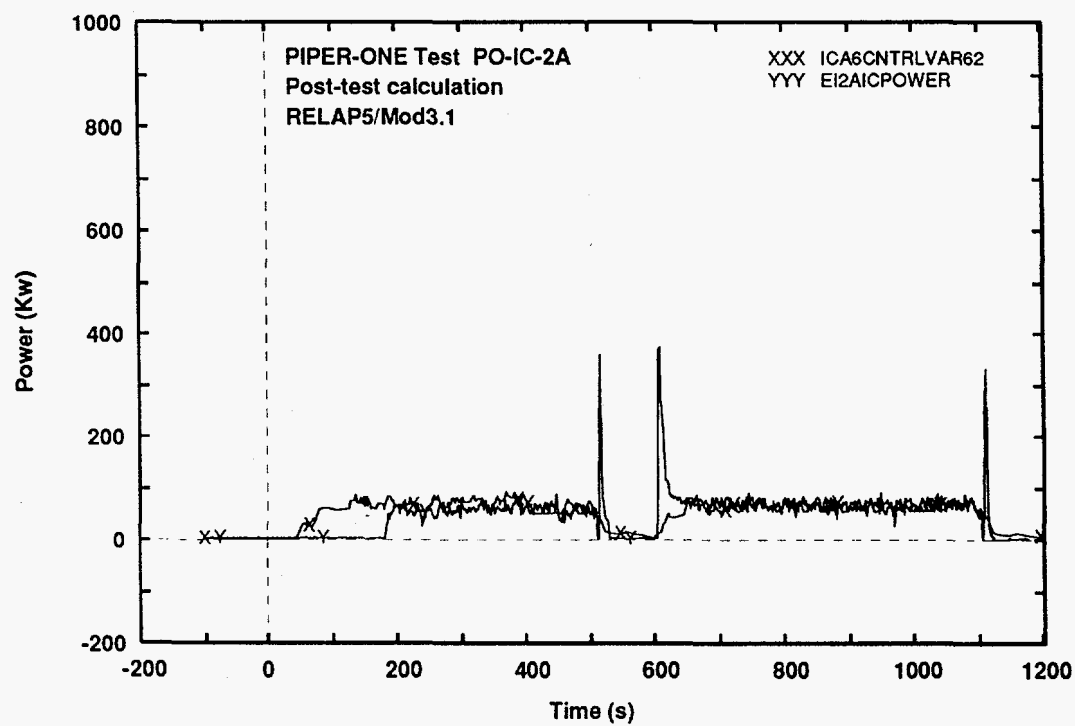


Fig. 28 - Measured and calculated trends of IC exchanged power

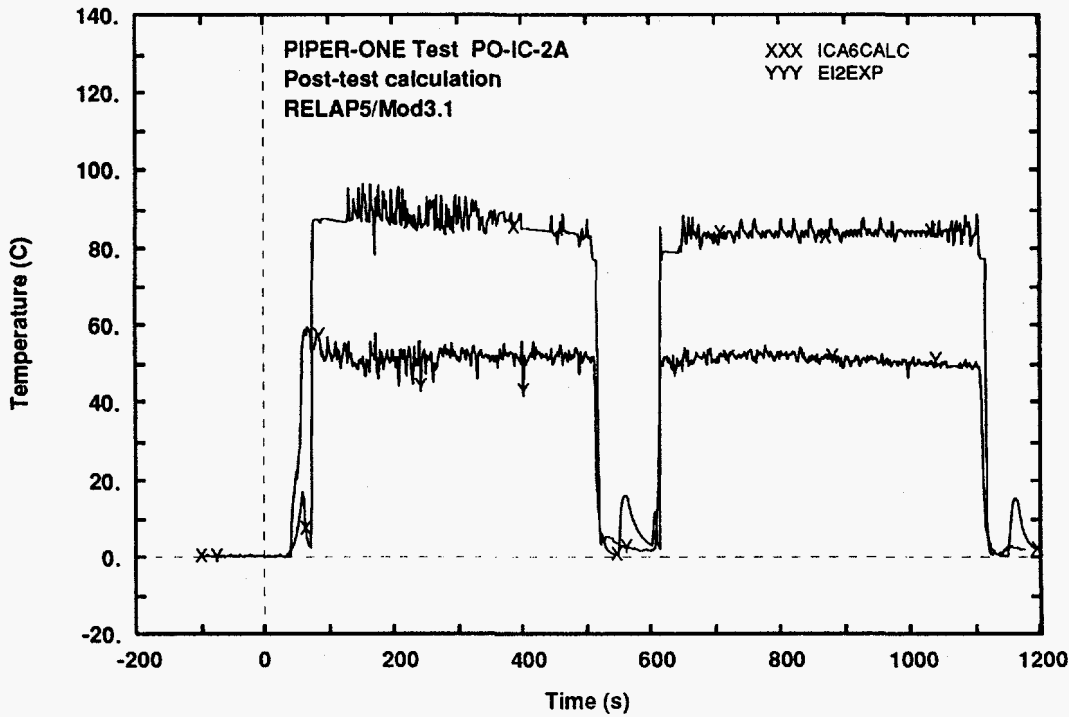


Fig. 29 - Measured and calculated trends of temperature difference between internal and external side of IC tubes wall (top elevation)

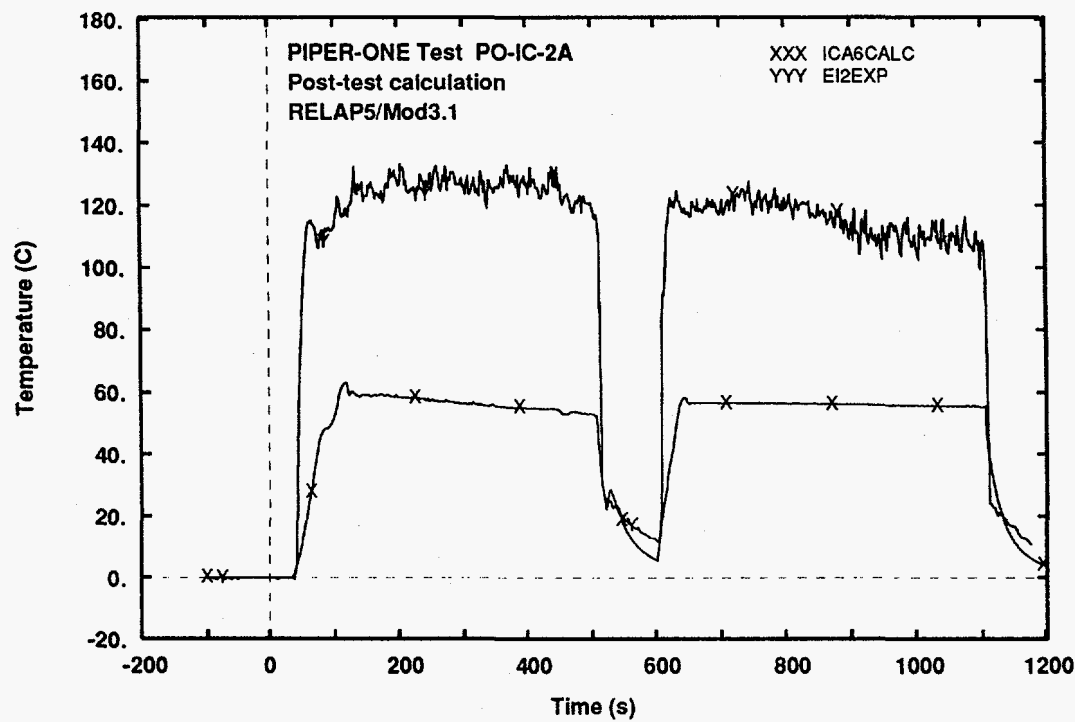


Fig. 30 - Measured and calculated trends of temperature difference between IC fluid and external side of IC tubes wall (middle elevation)

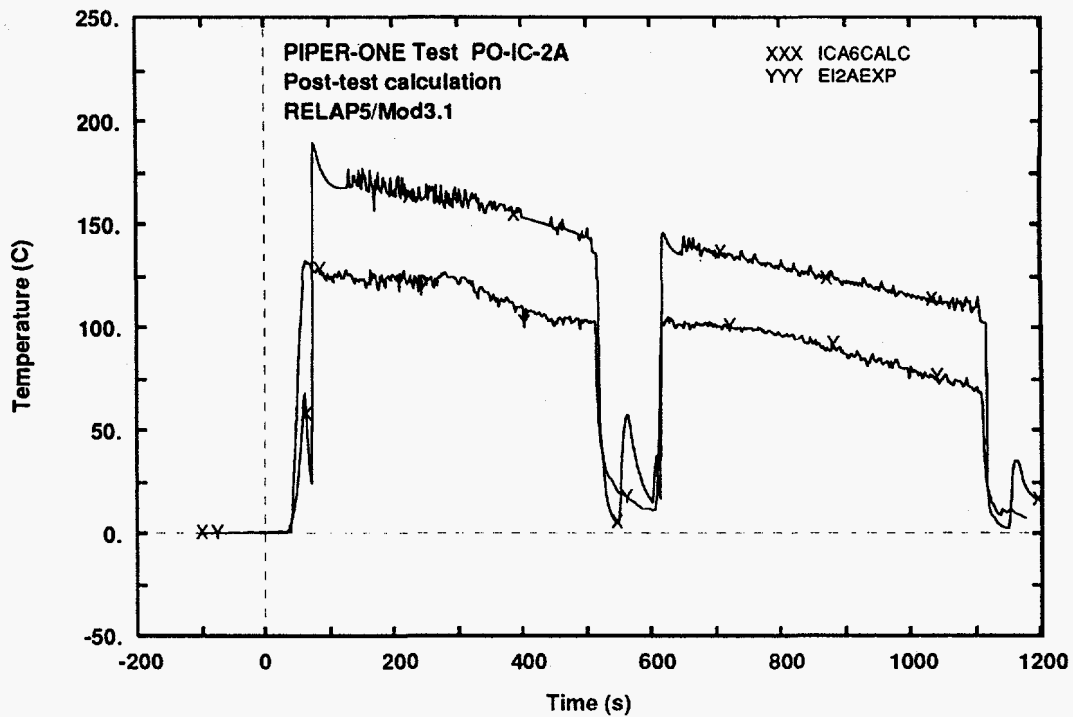


Fig. 31 - Measured and calculated trends of temperature difference between internal side of IC tubes wall and IC pool fluid temperature (top elevation)

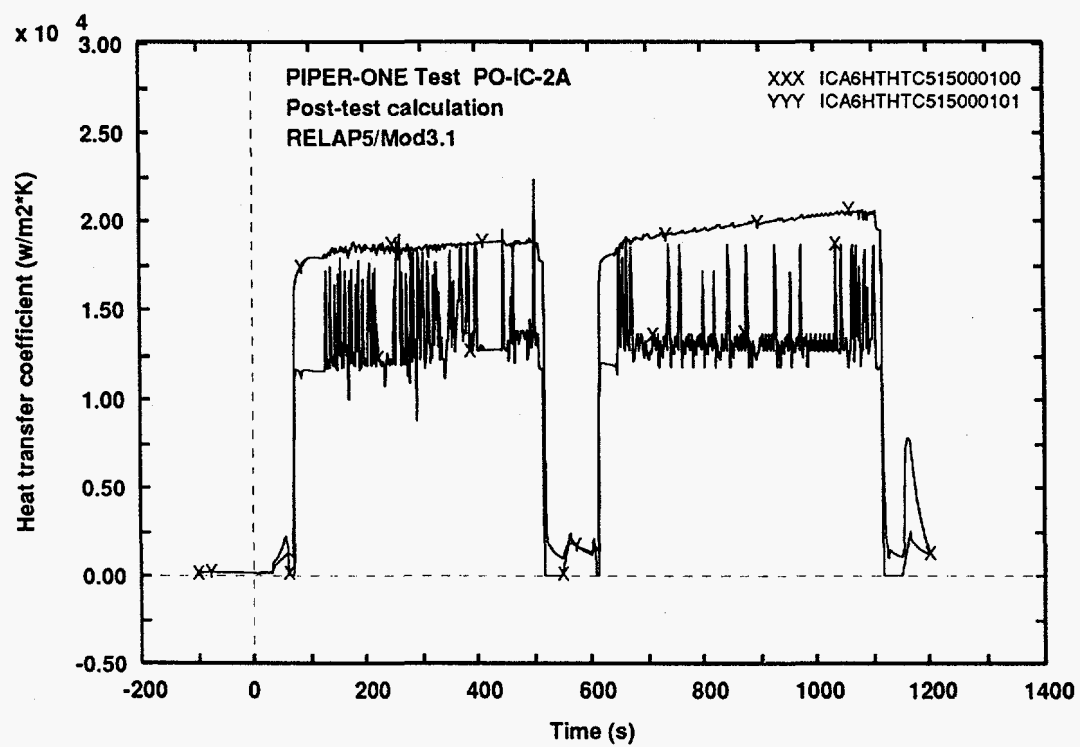


Fig. 32 - Calculated trends of the heat transfer coefficient at the inside and the outside of IC tubes wall (top elevation)

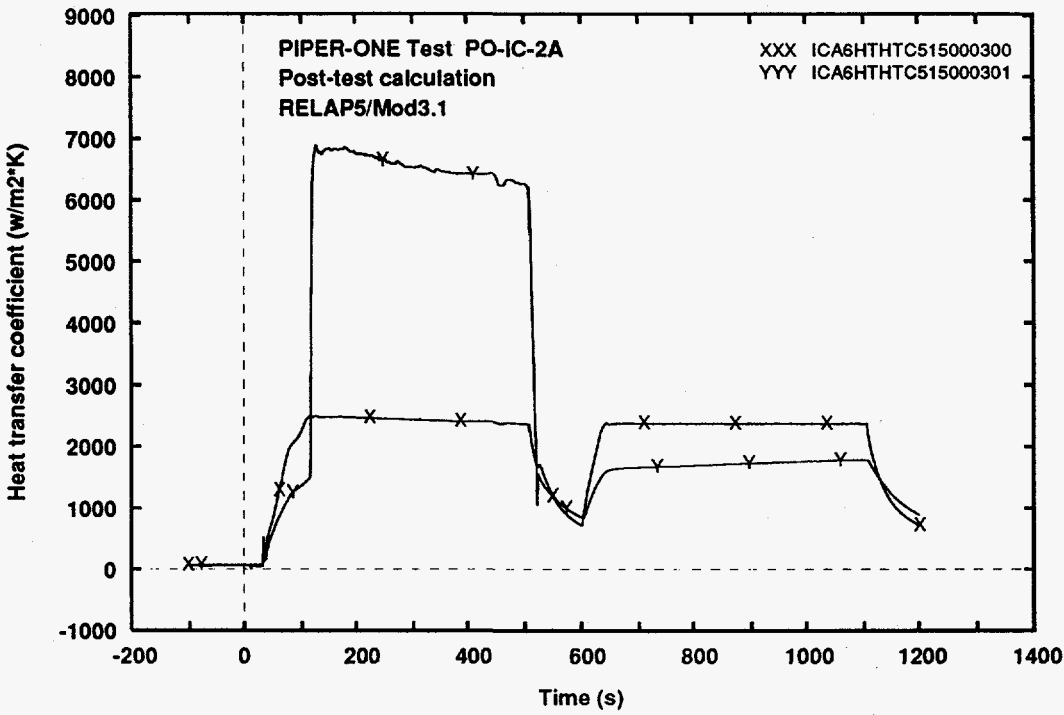


Fig. 33 - Calculated trends of the heat transfer coefficient at the inside and the outside of IC tubes wall (middle elevation)

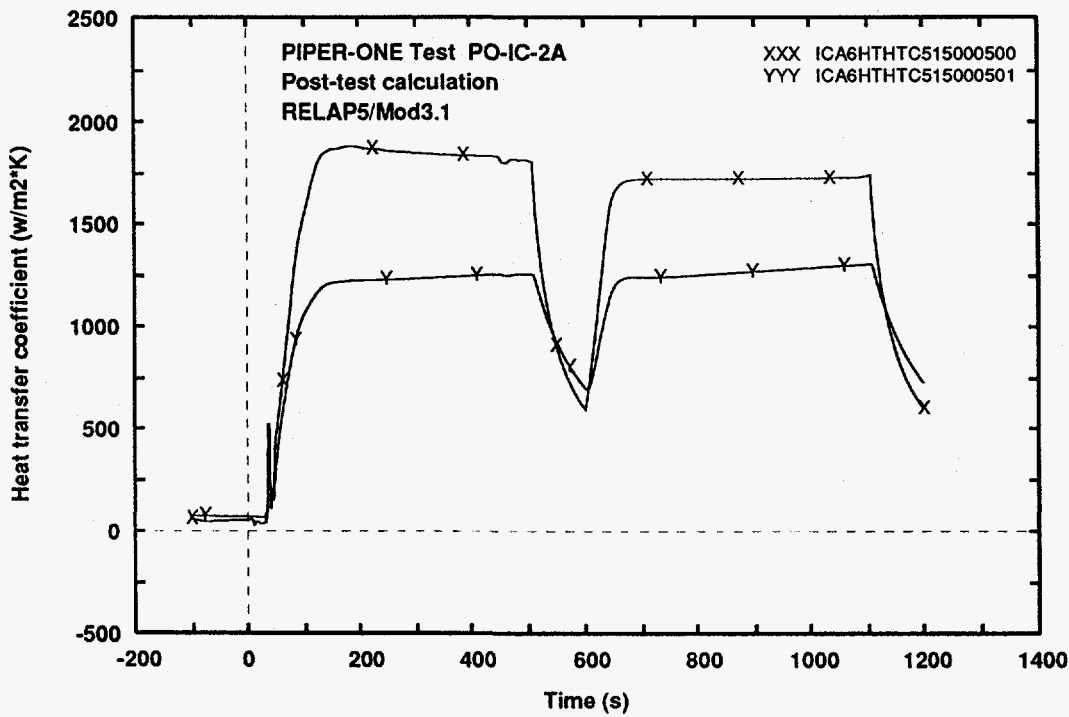


Fig. 34 - Calculated trends of the heat transfer coefficient at the inside and the outside of IC tubes wall (bottom elevation)

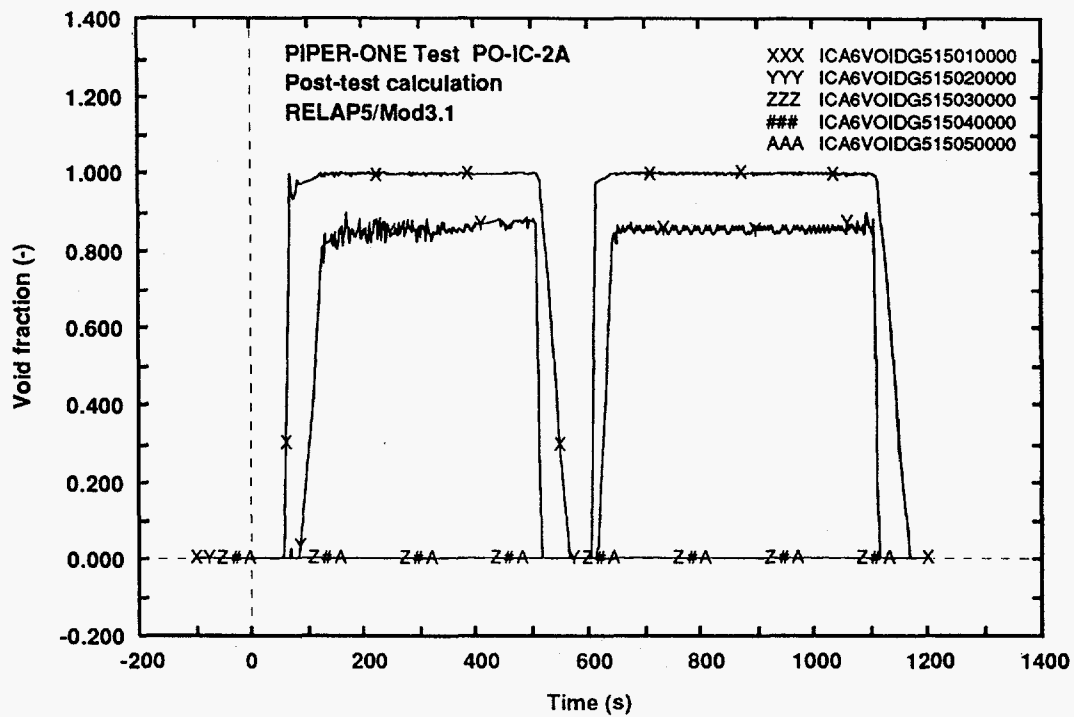


Fig. 35 - Calculated trends of IC tubes void fraction along the axis

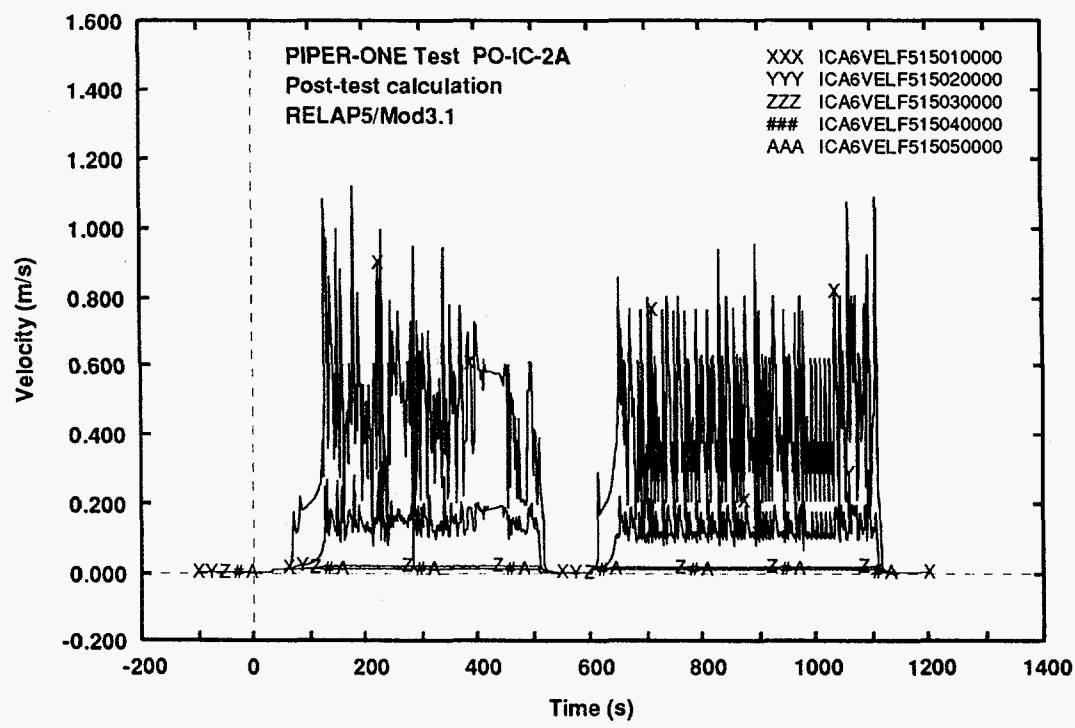


Fig. 36 - Calculated trends of IC tubes liquid velocity along the axis

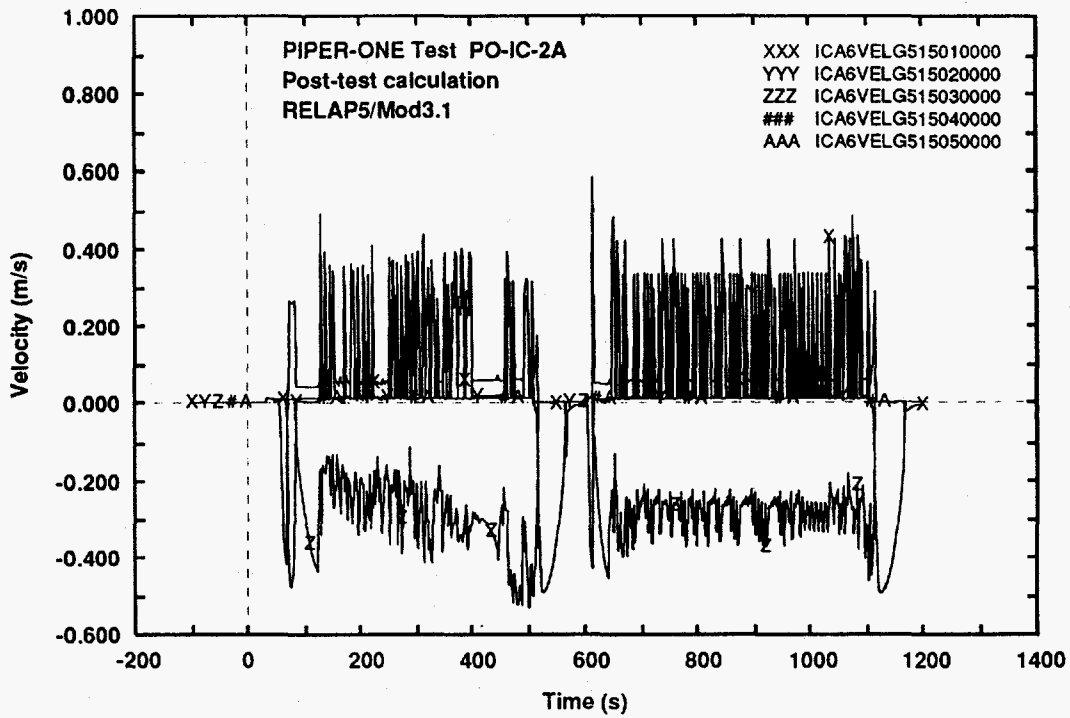


Fig. 37 - Calculated trends of IC tubes steam velocity along the axis

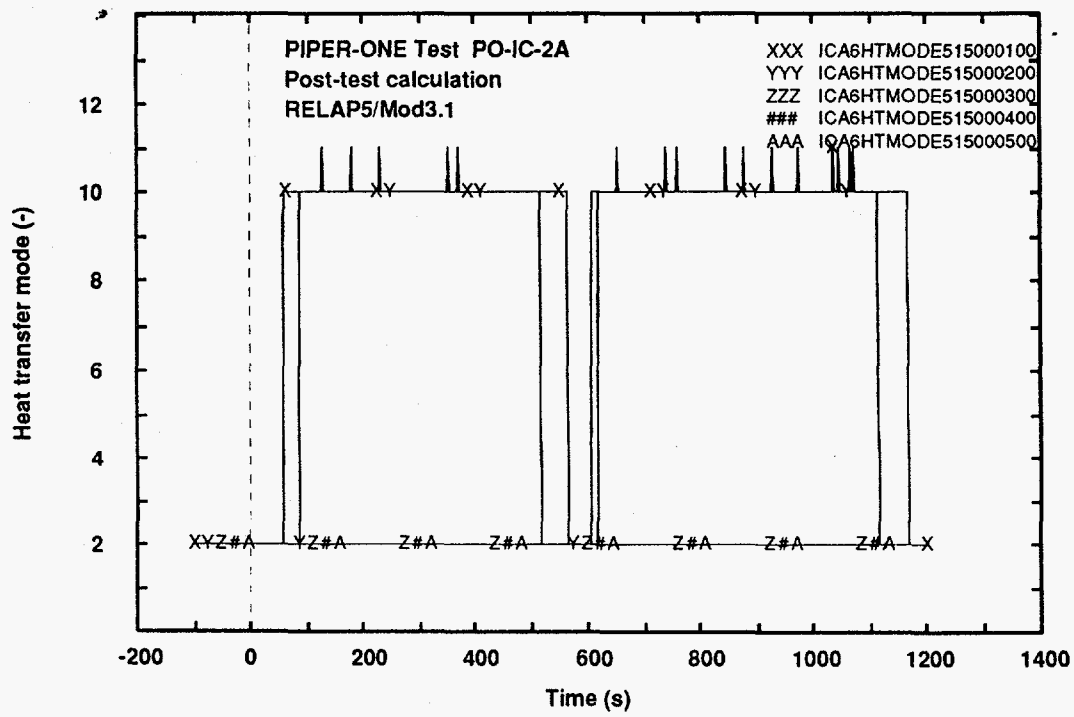


Fig. 38 - Calculated trends of IC tubes heat transfer mode (internal side)

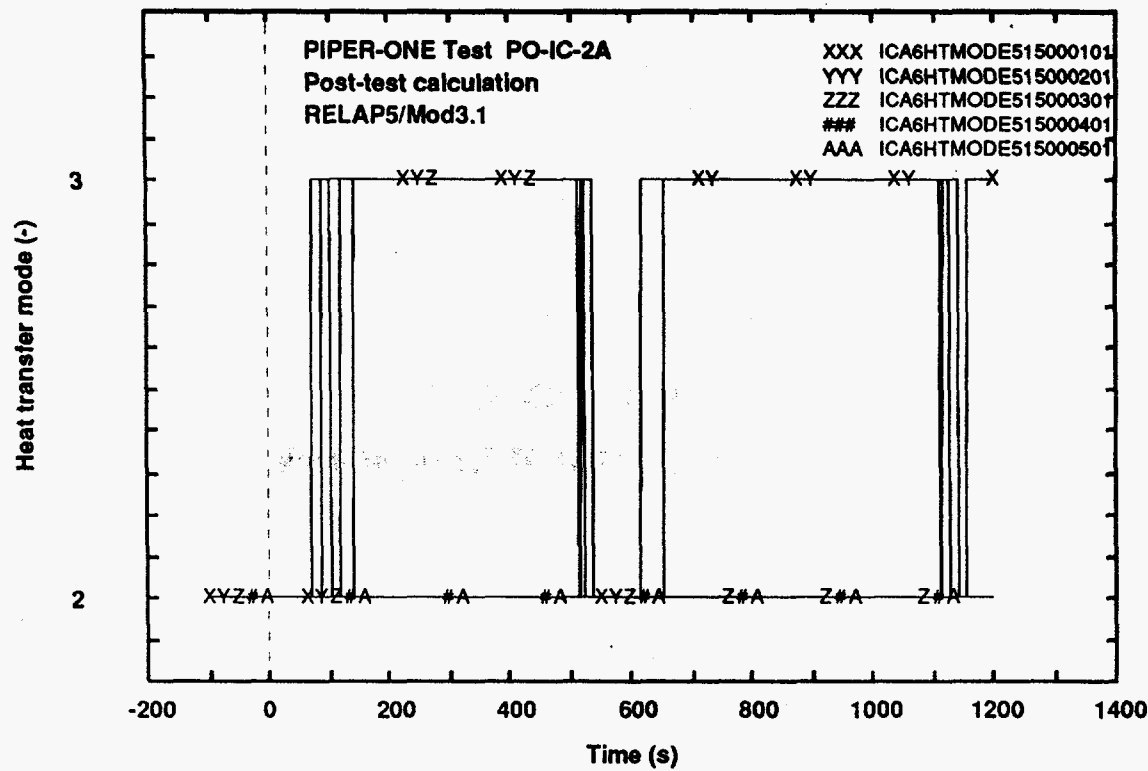
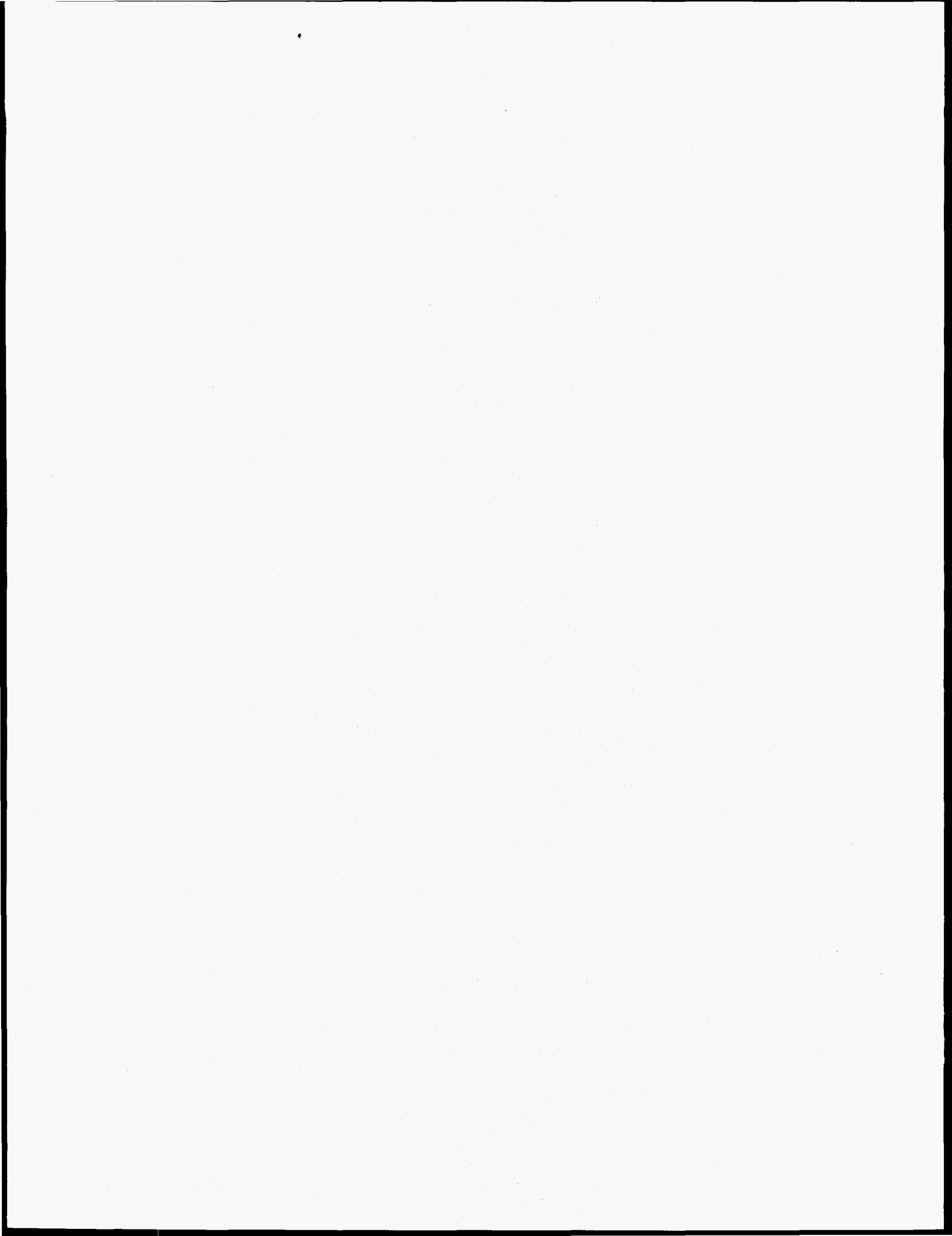


Fig. 39 - Calculated trends of IC tubes heat transfer mode (external side)

APPENDIX 5:
Listing of RELAP5/MOD3.1 input deck



```

=po-ic-02
*
*
100      new transient
*01      inp-chk
*
=====
* time steps
*      mint maxt    mie mae
201 100.  1.e-7  1.e-1  07003 20   500  500
202 600.  1.e-7  1.e-1  07003 20   1000 1000
203 636.  1.e-7  1.e-3  07003 1000  2000 2000
204 642.  1.e-7  5.e-4  07003 2000  2000 2000
205 730.  1.e-7  1.e-3  07003 1000  2000 2000
206 1200. 1.e-7  1.e-1  07003 20   1000 1000
207 1.e6  1.e-7  1.e-1  07003 20   1000 1000
*
* added minor edit request
*
20800001 htmode 515000100
20800002 htmode 515000200
20800003 htmode 515000300
20800004 htmode 515000400
20800005 htmode 515000500
20800006 htmode 515000101
20800007 htmode 515000201
20800008 htmode 515000301
20800009 htmode 515000401
20800010 htmode 515000501
*
* minor edit request
*
* pressures and fluid temperatures
301 p     130010000 * pa-lp-1
302 p     245010000 * sd
303 tempf 100010000 * lp
304 tempf 110040000 * lp middle
305 tempf 140010000 * core inlet
306 tempf 200010000 * core bot
307 tempf 200070000 * core middle
308 tempf 200140000 * core top
309 tempg 200140000 * core top
*
* fluid temperatures
310 tempf 150010000 * by guide tube
311 tempf 155010000 * bypass bot
312 tempf 165010000 * bypass middle
313 tempf 175010000 * bypass top
314 tempg 175010000 * bypass top
315 tempf 220010000 * up
316 tempg 220010000 * up
317 tempf 245010000 * sd
318 tempg 245010000 * sd
*
* fluid temperatures
319 tempf 270010000 *
320 tempg 270010000 *
321 tempf 300010000 *
322 tempf 310010000 *
323 tempf 320150000 *
324 tempf 315150000 *
325 tempf 330010000 *
326 tempf 345010000 *
327 tempf 345050000 *
*
* levels
328 cntrlvar 010    * dc-ann
329 cntrlvar 011    * dc-jp
330 cntrlvar 015    * lp
331 cntrlvar 016    * core
332 cntrlvar 017    * up
333 cntrlvar 020    * core total
334 cntrlvar 030    * bypass
335 cntrlvar 035    * ssa
336 cntrlvar 050    * fuel box exterior
*
* quality & void fraction
337 voidg 200010000 *
338 voidg 200080000 *
339 voidg 200130000 *
340 voidg 200140000 *
341 voidg 200150000 *
342 voidg 245010000 *
343 quale 200100000 *
344 quale 200110000 *
345 quale 200120000 *
*
* mass flowrates
346 mflowj 3400000000 *
347 mflowj 130010000 *
348 mflowj 130020000 *
349 mflowj 140020000 *
350 mflowj 205010000 *
351 mflowj 205020000 *
352 mflowj 360010000 *
353 mflowj 235010000 *
354 mflowj 235020000 *
*
* mass flowrates
355 mflowj 505000000 * io top
356 mflowj 245010000 *
357 mflowj 225020000 *
358 mflowj 245020000 *
359 mflowj 270020000 *
360 mflowj 563010000 *
361 mflowj 564010000 *
*
* rod surface temp
362 mflowj 4630000000 *
363 mflowj 300010000 *
*
* quality & void fraction (2nd group)
364 httemp 200100110 *
365 httemp 200100410 *
366 httemp 200100510 *
367 httemp 200100710 *
368 httemp 200100810 *
369 httemp 200100910 *
370 httemp 200101010 *
371 httemp 200101210 *
372 httemp 200101410 *
*
* trip
373 voidg 265010000 *
374 voidg 260010000 *
375 voidg 260030000 *
376 voidg 250010000 *
377 voidg 250030000 *
378 voidg 250050000 *
379 voidg 255010000 *
380 voidg 255030000 *
381 voidg 210010000 *
*
* core power
382 cntravar 040    * core power
383 cntravar 060    * ic power
384 cntravar 061    * ic power
385 cntravar 062    * ic power
386 cntravar 063    * ic power
*
* op. vlv lp-jp
501 time 0 ge null 0 98.  l *
502 time 0 ge null 0 1.e6  l *
*
* start heat losses sep. annulus
507 time 0 ge null 0 100.  l *
*
* start heat losses upp. dc
508 time 0 ge null 0 100.  l *
*
* heat losses
509 time 0 ge null 0 100.  l *
510 time 0 ge null 0 1.e6  l *
511 time 0 ge null 0 0.    l * table 801
*
* core & bypass power
513 time 0 ge null 0 100.  l * start rod heat.
515 time 0 ge null 0 500.  l * start bypass
heat.
*
* fb1 & fb2 heat losses (only fb1 utilized)
516 time 0 ge null 0 200.  l * fb1 start
517 time 0 ge null 0 1.e6  l * fb2 start
*
* op vlv ic top
520 time 0 ge null 0 104.  l * op vlv ic top
523 time 0 ge null 0 608.  l * cl vlv ic top
553 time 0 ge null 0 705.  l * op vlv ic top
554 time 0 ge null 0 1206. l * cl vlv ic top
616 520 xor 523          n * op/cl ic top
632 553 xor 554          n * op/cl ic top
633 616 or 632          n * op/cl ic top
*
* op vlv ic bot
521 time 0 ge null 0 132.  l * op vlv ic bot
522 time 0 ge null 0 608.  l * cl vlv ic bot
551 time 0 ge null 0 706.  l * op vlv ic bot
552 time 0 ge null 0 1206. l * cl vlv ic bot
615 521 xor 522          n * op/cl ic bot
630 551 xor 552          n * op/cl ic bot
631 615 or 630          n * op/cl ic bot
631 521 and 521         n * op/cl ic bot
*
* added break control for po-ic-2
549 time 0 ge null 0 710.  l *
*
* ic control water in.
550 time 0 ge null 0 608.e6  l *
551 time 0 ge null 0 690.e6  l *
635 560 xor 561          n *
*
* ic control water out.
562 time 0 ge null 0 691.e6  l *
563 time 0 ge null 0 699.e6  l *
636 562 xor 563          n *
*
* steam line (tj 433)
525 time 0 ge null 0 1.e6  n *
*
* pressure control
526 time 0 ge null 0 -1.   l *
527 time 0 ge null 0 10.   l *
528 time 0 ge null 0 99.   l * actual clo.
617 527 xor 526          n * actual op.
*
* fw control
529 time 0 ge null 0 1.e6  l *
*
* auxiliary systems
530 p   100010000 ge null 0 1.e6  l * start lpc1
532 p   100010000 ge null 0 1.e6  l * start lpc2
534 p   100010000 ge null 0 1.e6  l * start hpc1
536 p   100010000 ge null 0 1.e6  l * start lpcsb

```

```

* serv control
537 p 245010000 ge null 0 96.50e5 n *
539 p 245010000 gt null 0 200.0e5 1 *
599 p 245010000 lt null 0 92.50e5 n * clo. serv
602 537 xor 539 n * op. serv
*
* ads control
540 time 0 ge null 0 100. 1 * ads
541 p 245010000 ge null 0 70.50e5 n *
601 540 and 541 1 * op. ads
*
* draining sea
570 time 0 ge null 0 1.e6 1 * op. drain. ann
571 cntrlvar 035 ge null 0 1.e6 n * clo. dra. an.
*
* heat losses ic tank (including external pipes) & ic line liq.
580 time 0 ge null 0 200. 1 *
*
* heat losses ic line
581 time 0 ge null 0 100. 1 *
*
* heat losses sd
582 time 0 ge null 0 100. 1 *
*
* heat losses core region (external vessel)
583 time 0 ge null 0 80. 1 *
*
* end trip signal
512 time 0 ge null 0 1300. 1 * end of problem
600 512 * end of problem
*
*
*-----*
* hydraulic components
*-----*
*
* lower plenum bot
1000000 lw.plb branch
1000001 2 1
1000101 0.010709 0.3 0. 0. 90. 0.3 4.e-5 0.065
00000
1000200 000 5.045e6 1.100e6 2597.e3 0.
1001101 100010000 110000000 0.00 0. 0. 0.00000
1002101 345010000 100010000 0.00 0. 0. 0.00000
1001201 0. 0. 0.
1002201 0. 0. 0.
*
* lower plenum central
1100000 lp.mid pipe
1100001 5
1100101 0.010709 5
1100301 0.250 2
1100302 0.1443 4
1100303 0.1114 5
1100401 0.000 5
1100601 90.0 5
1100801 4.0e-5 0.065 5
1101001 00000 5
1101101 00000 4
1101201 000 5.045e6 1.100e6 2597.e3 0.0 0. 5
1101300 1
1101301 0.0 0.0 0.0 4
*
* lower plenum added br. for ic conn.
1110000 lw.ic1 branch
1110001 1 1
1110101 0.010709 0.1615 0. 0. 90. 0.1615 4.e-5 0.065
00000
1110200 000 5.045e6 1.100e6 2597.e3 0.
1111101 110010000 111000000 0.00 0. 0. 0.00000
1111201 0.0 0. 0.
*
* lower plenum added br. for ic conn.
1120000 lw.ic2 branch
1120001 1
1120101 0.010709 0.16 0. 0. 90. 0.16 4.e-5 0.065
00000
1120200 000 5.045e6 1.100e6 2597.e3 0.
1121101 111010000 112000000 0.00 0. 0. 0.00000
1121201 0.0 0. 0.
*
* lower plenum top1
1150000 lp.top1 branch
1150001 2 1
1150101 0.010709 0.1745 0. 0. 90. 0.1745 4.e-5 0.065
00000
1150200 000 5.045e6 1.120e6 2597.e3 0.
1151101 112010000 115000000 0.00 0. 0. 0.00000
1152101 115010000 120000000 0.00 0. 0. 0.00000
1151201 0.0 0. 0.
1152201 0.0 0. 0.
*
* lower plenum top2
1200000 lp.top2 pipe
1200001 2
1200101 0.00972 2
1200301 0.2 2
1200401 0.000 2
1200601 90.0 2
1200801 4.0e-5 0.065 2
1201001 00000 2
1201101 000000 1
1201201 000 5.045e6 1.120e6 2597.e3 0.0 0. 2
1201300 1
1201301 0.0 0.0 0.0 1
*
* lower plenum top3
1300000 lp.top3 branch
1300001 2 1
1300101 0.008457 0.176 0. 0. 90. 0.176 4.e-5 0.065
00000
1300200 000 5.045e6 1.120e6 2597.e3 0.
1301101 120010000 130000000 0.00 0. 0. 0.00000
1302101 130000000 145000000 0.00 0. 0. 0.00000
1301201 0.0 0. 0.
1302201 0.0 0. 0.
*
* lower plenum top4
1350000 lp.top4 branch
1350001 1
1350101 0.008457 0.2 0. 0. 90. 0.2 4.e-5 0.065
00000
1350200 000 5.045e6 1.120e6 2597.e3 0.
1351101 130010000 135000000 0.00 0. 0. 0.00000
1351201 0.0 0. 0.
*
* lower plenum top5
1400000 lp.top5 branch
1400001 2 1
1400101 0.008457 0.2 0. 0. 90. 0.2 4.e-5 0.065
00000
1400200 000 5.045e6 1.120e6 2597.e3 0.
1401101 135010000 140000000 0.00 0. 0. 0.00000
1402101 140010000 200000000 5.938e-4 0.9 0.9 0.00000
1401201 0.0 0. 0.
1402201 0.0 0. 0.
*
* core by bottom hor
1450000 by.bhor pipe
1450001 7
1450101 0.000286 7
1450301 0.2 2
1450302 0.1892 7
1450401 0.000 7
1450601 -90.0 2
1450602 0.0 7
1450801 4.0e-5 0.0 7
1451001 00000 7
1451101 00000 6
1451201 000 5.045e6 1.120e6 2597.e3 0.0 0. 7
1451300 1
1451301 0. 0.0 0.0 6
*
* guide tube - bot.by
1500000 gui.tub pipe
1500001 5
1500101 0.003953 5
1500301 0.2468 5
1500401 0.000 5
1500601 90.0 5
1500801 4.0e-5 0.0 5
1501001 00000 5
1501101 00000 4
1501201 000 5.045e6 1.120e6 2597.e3 0.0 0. 5
1501300 1
1501301 0. 0.0 0.0 4
*
* bypass vertical bot
1550000 by.vert1 branch
1550001 3 1
1550101 0.000835 0.223 0. 0. 90. 0.223 4.e-5 0.0
00000
1550200 000 5.045e6 1.120e6 2597.e3 0.
1551101 145010000 155000000 0.50e-4 1. 1. 0.00000
1552101 150010000 155000000 .827e-3 0.1 0.1 0.00000
1553101 155010000 160000000 0. 0. 0. 0.00000
1551201 0. 0. 0.
1552201 0. 0. 0.
1553201 0. 0. 0.
*
* bypass vertical n2
1600000 by.vert2 pipe
1600001 10
1600101 0.000835 10
1600301 0.2133 10
1600401 0.000 10
1600601 90.0 10
1600801 4.0e-5 0.0 10
1601001 00000 10
1601101 00000 9
1601201 000 5.045e6 1.120e6 2597.e3 0.0 0. 10
1601300 1
1601301 0. 0.0 0.0 9
*
* bypass vertical n3
1650000 by.vert3 branch
1650001 2 1
1650101 0.000835 0.2015 0. 0. 90. 0.2015 4.e-5 0.0
00000
1650200 000 5.045e6 1.120e6 2597.e3 0.
1651101 160010000 165000000 0. 0. 0. 0.00000
1652101 165010000 170000000 0. 0. 0. 0.00000
1651201 0. 0. 0.
1652201 0. 0. 0.
*
* bypass vertical n4
1700000 by.vert4 pipe
1700001 10
1700101 0.000835 10
1700301 0.235 10
1700401 0.000 10
1700601 90.0 10
1700801 4.0e-5 0.0 10
1701001 00000 10
1701101 00000 9
1701201 000 5.045e6 1.120e6 2597.e3 0.0 0. 10
1701300 1
1701301 0. 0.0 0.0 9

```

1700001 10
 1700101 0.000835 10
 1700301 0.235 10
 1700401 0.000 10
 1700601 90.0 10
 1700801 4.0e-5 0.0 10
 1701001 00000 10
 1701101 000000 9
 1701201 000 5.045e6 1.120e6 2597.e3 0.0 0. 10
 1701300 1 0.0 0.0 0.0 9
 1701301 0.0 0.0 0.0 9
 * bypass vertical n5
 1750000 by.vert5 branch
 1750001 2 1
 1750101 0.000835 0.2075 0. 0. 90. 0.2075 4.e-5 0.0
 00000
 1750200 000 5.045e6 1.120e6 2597.e3 0.
 1751101 170010000 175000000 0. 0. 0. 000000
 1752101 175010000 180000000 0. 0.1 0.1 000000
 1751201 0.0 0. 0.
 1752201 0.0 0. 0.
 * bypass horizontal top
 1800000 by.hort pipe
 1800001 5
 1800101 0.00119 5
 1800301 0.1776 5
 1800401 0.000 5
 1800601 0.0 5
 1800801 4.0e-5 0.0 5
 1801001 00000 5
 1801101 000000 4
 1801201 000 5.045e6 1.120e6 2597.e3 0.0 0. 5
 1801300 1
 1801301 0.0 0.0 0.0 4
 * core channel
 2000000 core pipe
 2000001 16
 2000101 0.002943 14
 2000102 0.003556 16
 2000301 0.265 14
 2000302 0.229 15
 2000303 0.2 16
 2000401 0.000 16
 2000601 90.0 16
 2000801 4.0e-5 0.013 16
 2001001 00000 16
 2001101 000000 15
 2001201 000 5.045e6 1.128e6 2597.e3 0.0 0. 2
 2001202 000 5.045e6 1.128e6 2597.e3 0. 0. 4
 2001203 000 5.045e6 1.128e6 2597.e3 0. 0. 6
 2001204 000 5.045e6 1.128e6 2597.e3 0. 0. 8
 2001205 000 5.045e6 1.128e6 2597.e3 0. 0. 10
 2001206 000 5.045e6 1.128e6 2597.e3 0. 0. 12
 2001207 000 5.045e6 1.128e6 2597.e3 0. 0. 14
 2001208 000 5.045e6 1.128e6 2597.e3 0. 0. 16
 2001300 1
 2001301 0. 0. 0. 0. 5
 2001302 0. 0. 0. 0. 10
 2001303 0. 0. 0. 0. 15
 * core top
 2050000 core.top branch
 2050001 2 1
 2050101 0.01028 0.22 0. 0. 90. 0.22 4.e-5 0.0
 00000
 2050200 000 5.045e6 1.151e6 2597.e3 0.
 2051101 200010000 205000000 1.649e-3 14.5 10.6 000000
 2052101 180010000 205000000 0.83e-3 0.1 0.1 000000
 2052102 0. 0. 0.
 2052201 0. 0. 0.
 * upper plenum 1
 2100000 up.col branch
 2100001 2 1
 2100101 0.01028 0.22 0. 0. 90. 0.22 4.e-5 0.0
 00000
 2100200 000 5.045e6 1.151e6 2597.e3 0.
 2101101 205010000 210000000 0. 0. 0. 000000
 2102101 210010000 220000000 0. 0. 0. 000000
 2101201 0. 0. 0.
 2102201 0. 0. 0.
 * steam separator pipe
 2200000 st.sep pipe
 2200001 20
 2200101 0.01028 2
 2200102 0.00241 20
 2200301 0.214 2
 2200302 0.2345 20
 2200401 0.000 20
 2200601 90.0 20
 2200801 4.0e-5 0.0 20
 2201001 00000 20
 2201101 000000 19
 2201201 000 5.045e6 1.151e6 2597.e3 0. 0. 10 *
 1.15e6
 2201202 000 5.045e6 1.151e6 2597.e3 0. 0. 16 *
 2201203 000 5.045e6 1.151e6 2597.e3 0.9 0. 20
 2201300 1
 2201301 0. 0. 0. 0. 19
 * bot ssa
 2250000 ssa.bot branch
 2250001 2 1
 2250101 0.007196 0.34 0. 0. 90. 0.34 4.e-5 0.052
 00000
 2250200 000 5.045e6 1.120e6 2597.e3 0.
 2251101 225010000 230000000 0. 0. 0. 000000
 2252101 225010000 290000000 0. 0. 0. 000000
 2251201 0. 0. 0.
 2252201 0. 0. 0.
 * steam separator annulus
 2300000 ssa pipe
 2300001 8
 2300101 0.007196 8
 2300301 0.512 1
 2300302 0.459 8
 2300401 0.000 8
 2300601 90.0 8
 2300801 4.0e-5 0.052 8
 2301001 00000 8
 2301101 000000 7
 2301201 000 5.045e6 1.151e6 2597.e3 0.0 0. 5
 2301202 000 5.045e6 1.151e6 2597.e3 0.0 0. 6
 2301203 000 5.045e6 1.151e6 2597.e3 0.5 0. 8
 2301300 1
 2301301 0. 0. 0. 0. 7
 * steam dome bot (k in j. 2 changed for po-ic-01)
 2350000 sdo.bot branch
 2350001 4 1
 2350101 0.01038 0.246 0. 0. 90. 0.246 4.e-5 0.0
 00000
 2350200 000 5.045e6 1.151e6 2597.e3 0.9
 2351101 220010000 235000000 0. 0. 0. 000000
 2352101 235000000 230010000 3.94e-4 100. 100. 000000
 2353101 235000000 255000000 0.00426 0.1 0.1 000000
 2354101 235010000 240000000 0. 0. 0. 000000
 2351201 0. 0. 0.
 2352201 0. 0. 0.
 2353201 0. 0. 0.
 2354201 0. 0. 0.
 * steam dome vert.left
 2400000 sd.ver.1 pipe
 2400001 4
 2400101 0.01038 4
 2400301 0.25 4
 2400401 0.000 4
 2400601 90.0 4
 2400801 4.0e-5 0.0 4
 2401001 00000 4
 2401101 000000 3
 2401201 000 5.045e6 1.151e6 2597.e3 0.9 0. 4
 2401300 1
 2401301 0. 0. 0. 0. 3
 * steam dome top left
 2450000 sdc.top branch
 2450001 2 1
 2450101 0.01038 0.365 0. 0. 90. 0.365 4.e-5 0.0
 00000
 2450200 000 5.045e6 1.151e6 2597.e3 1.
 2451101 240010000 245000000 0. 0. 0. 000000
 2452101 245000000 250000000 0. 0.1 0.1 000000
 2451201 0. 0. 0.
 2452201 0. 0. 0.
 * steam dome top hor pipe
 2500000 sd.toh pipe
 2500001 5
 2500101 0.005382 5
 2500301 0.289 5
 2500401 0.000 5
 2500601 0. 0. 5
 2500801 4.0e-5 0.0 5
 2501001 00000 5
 2501101 000000 4
 2501201 000 5.045e6 1.151e6 2597.e3 0.95 0. 5
 2501300 1
 2501301 0. 0. 0. 0. 4
 * steam dome bot hor pipe
 2550000 sd.boh pipe
 2550001 5
 2550101 0.00570 5
 2550301 0.289 5
 2550401 0.000 5
 2550601 0. 0. 5
 2550801 4.0e-5 0.074 5
 2551001 00000 5
 2551101 000000 4
 2551201 000 5.045e6 1.151e6 2597.e3 1.0 0. 5
 2551300 1
 2551301 0. 0. 0. 0. 4
 * aj connecting upper parts of sd
 2590000 aj.tsd snglun
 2590101 250010000 260000000 0.005382 0.1 0.1 000000
 2590201 1 0. 0.000 0.000
 * steam dome vert.right
 2600000 ad.ver.r pipe
 2600001 4
 2600101 0.006647 4
 2600301 0.25 4
 2600401 0.000 4
 2600601 -90.0 4
 2600801 4.0e-5 0.0 4
 2601001 00000 4
 2601101 000000 3
 2601201 000 5.045e6 1.151e6 2597.e3 1.0 0. 4
 2601300 1
 2601301 0. 0. 0. 0. 3
 * steam dome right part bottom

2650000 sdo.rib branch
 2650001 2 1
 2650101 0.006647 0.246 0. 0. -90. -0.246 4.e-5 0.0
 00000
 2650200 000 5.045e6 1.151e6 2597.e3 1.
 2651101 265010000 265000000 0. 0. 0. 0.00000
 2652101 265010000 270000000 0. 0. 0. 0.00000
 2651201 0. 0. 0.
 2652201 0. 0. 0.
 * dc top
 2700000 dc.top branch
 2700001 2 1
 2700101 0.005534 0.247 0. 0. -90. -0.247 4.e-5 0.0
 00000
 2700200 000 5.045e6 1.151e6 2597.e3 0.1
 2701101 255010000 270000000 0. 0.1 0.1 0.00000
 2702101 270010000 275000000 0. 0. 0. 0.00000
 2701201 0. 0. 0.
 2702201 0. 0. 0.
 * dc top upstream fw
 2750000 sd.tufw pipe
 2750001 4
 2750101 0.005534 4
 2750301 0.362 4
 2750401 0.000 4
 2750601 -90.0 4
 2750801 4.0e-5 0.0 4
 2751001 00000 4
 2751101 000000 3
 2751201 000 5.045e6 1.151e6 2597.e3 0.0 0. 4
 2751300 1
 2751301 0. 0. 0. 0.0 3
 * dc fw connection zone
 2800000 dc.fwz branch
 2800001 2 1
 2800101 0.005534 0.3 0. 0. -90. -0.3 4.e-5 0.0
 00000
 2800200 000 5.045e6 1.100e6 2597.e3 0.
 2801101 275010000 280000000 0. 0.1 0.1 0.00000
 2802101 280010000 285000000 0. 0. 0. 0.00000
 2801201 0. 0. 0.
 2802201 0. 0. 0.
 * dc top downstream fw
 2850000 dc.tdfw pipe
 2850001 6
 2850101 0.005534 6
 2850301 0.3 6
 2850401 0.000 6
 2850601 -90.0 6
 2850801 4.0e-5 0.0 6
 2851001 00000 6
 2851101 000000 5
 2851201 000 5.045e6 1.100e6 2597.e3 0.0 0. 6
 2851300 1
 2851301 0. 0. 0. 0.0 5
 * bypass of steam dome
 2900000 by.sd pipe
 2900001 2
 2900101 0.001269 2
 2900301 0.3295 2
 2900401 0.000 2
 2900601 0.0 2
 2900801 4.0e-5 0.04 2
 2901001 00000 2
 2901101 000000 1
 2901201 000 5.045e6 1.100e6 2597.e3 0. 0. 2
 2901300 1
 2901301 0. 0. 0. 0. 1
 * vlv of sd bypass
 2920000 vlv.edby valve
 2920101 290010000 295000000 0.001256 0.0 0.0 0.000100 1.
 1. 1.
 2920201 0 0.000 0.000 0.000
 2920300 mtrvlv
 2920301 570 571 1. 0.
 * bypass of steam dome
 2950000 by.sd2 pipe
 2950001 2
 2950101 0.002765 2
 2950301 0.39 2
 2950401 0.000 2
 2950601 0.0 2
 2950801 4.0e-5 0.04 2
 2951001 00000 2
 2951101 000000 1
 2951201 000 5.045e6 1.100e6 2597.e3 0.0 0.0 2
 2951300 1
 2951301 0. 0. 0. 0. 1
 * dc middle zone
 3000000 dc.mid1 branch
 3000001 3 1
 3000101 0.00349 0.283 0. 0. -90. -0.283 4.e-5 0.0
 00000
 3000200 000 5.045e6 1.100e6 2597.e3 0.
 3001101 285010000 300000000 0. 0. 0. 0.00000
 3002101 300010000 305000000 0. 0. 0. 0.00000
 3003101 295010000 300000000 0.00046 0.1 0.1 0.00000
 3001201 0.0 0. 0.
 3002201 0. 0. 0.
 3003201 0. 0. 0.
 * dc middle zone n2

3050000 dc.mid2 pipe
 3050001 8
 3050101 0.00349 3
 3050102 0.004261 8
 3050301 0.29 3
 3050302 0.281 8
 3050401 0.000 8
 3050601 -90.0 8
 3050801 4.0e-5 0.0 8
 3051001 00000 8
 3051101 00000 7
 3051201 000 5.045e6 1.100e6 2597.e3 0.0 0. 8
 3051300 1
 3051301 0.0 0. 0.0 7
 * dc jet pump top
 3100000 dc.jpto branch
 3100001 3 1
 3100101 0.004261 0.325 0. 0. -90. -0.325 4.e-5 0.0
 00000
 3100200 000 5.045e6 1.100e6 2597.e3 0.
 3101101 305010000 310000000 0. 0. 0. 0.00000
 3102101 310010000 320000000 0. 0. 0. 0.00000
 3103101 310010000 315000000 0. 1. 1. 0.00000
 3101201 0.0 0. 0.
 3102201 0. 0. 0.
 3103201 0.0 0. 0.
 * jet pump
 3150000 jet.pump pipe
 3150001 15
 3150101 0.0013 15
 3150301 0.273 15
 3150401 0.000 15
 3150601 -90.0 15
 3150801 4.0e-5 0.0 15
 3151001 00000 15
 3151101 00000 14
 3151201 000 5.045e6 1.100e6 2597.e3 0.0 0. 15
 3151300 1
 3151301 0.0 0. 0.0 14
 * dc annular part
 3200000 dc.ann pipe
 3200001 15
 3200101 0.0027 15
 3200301 0.273 14
 3200302 0.1 15
 3200401 0.000 15
 3200601 -90.0 15
 3200801 4.0e-5 0.0 15
 3201001 00000 15
 3201101 00000 14
 3201201 000 5.045e6 1.100e6 2597.e3 0.0 0. 15
 3201300 1
 3201301 0. 0. 0.0 14
 * dc jet pump bot
 3250000 dc.jpbo branch
 3250001 3 1
 3250101 0.00426 0.327 0. 0. -90. -0.327 4.e-5 0.0244
 00000
 3250200 000 5.045e6 1.100e6 2597.e3 0.
 3251101 315010000 325000000 0. 1. 1. 0.00000
 3252101 325010000 330000000 0. 0. 0. 0.00000
 3253101 325010000 335000000 0. 0.1 0.1 0.00000
 3251201 0.0 0. 0.
 3252201 0. 0. 0.
 3253201 0.0 0. 0.
 * dc bot
 3300000 dc.jpbo branch
 3300001 0 1
 3300101 0.000 0.185 0.89e-3 0. -90. -0.185 4.e-5 0.0244
 00000
 3300200 000 5.045e6 1.100e6 2597.e3 0.
 * added break for po-ic-2
 3310000 br.vol tmdpvol
 3310101 0. 10. 10. 0. 0. 4.e-5 0. 0.00000
 3310200 000
 3310201 0. 1.5e6 1.286e5 2.601e6 0.
 3310202 1.e6 1.5e6 1.286e5 2.601e6 0.
 * fw injection in dc
 3320000 br.j tmdpjun
 3320101 330010000 331000000 0.0
 3320200 1 549
 3320201 -1. 0. 0. 0. 0. 0.
 3320202 0. 0. 0.05 0. 0. 0.
 3320203 100. 0. 0.05 0. 0. 0.
 3320204 101. 0. 0. 0. 0. 0. 0.
 3320205 1.e6 0. 0. 0. 0. 0. 0.
 * lower plenum horizontal part
 3350000 lp.hori pipe
 3350001 4
 3350101 0.0042 2
 3350102 0.00756 4
 3350201 0. 1
 3350202 0. 2 * 18.1e-6
 3350203 0. 3
 3350301 0.257 4
 3350401 0.000 4
 3350601 0. 4
 3350801 4.0e-5 0.0 4
 3350901 0. 0. 1
 3350902 0. 0. 2 * 0.57 0.57
 3350903 0. 0. 3
 3351001 00000 4

3351101 000000 3
 3351201 000 5.045e6 1.100e6 2597.e3 0.0 0.0 4
 3351300 1
 3351301 0.0 0.0 0.0 3
 *
 * lower plenum valve
 3400000 va.lopl valve
 3400101 335010000 345000000 8.500e-4 5.0 5.0 000100 1.
 1. 1. *.
 3400201 1 0.0 0.000 0.000
 3400300 mtrvlv
 3400301 501 502 1. 0.
 *
 * lower plenum hor-2
 3450000 lp.hor2 pipe
 3450001 5
 3450101 0.00756 1
 3450102 0.00137 5
 3450301 0.16 1
 3450302 0.18 3
 3450303 0.25 5
 3450401 0.000 5
 3450601 0.0 3
 3450602 -90.0 5
 3450801 4.0e-5 0.0 5
 3450901 0. 0.0 2
 3450902 0.5 0.5 3
 3450903 0. 0.0 4
 3451001 00000 5
 3451101 000000 4
 3451201 000 5.045e6 1.100e6 2597.e3 0.0 0. 5
 3451300 1
 3451301 0.0 0. 0.0 4
 *
 * fuel box exterior top
 3600000 fuel.box branch
 3600001 2 1
 3600101 4.4896e-3 0.429 0. 0. 90. 0.429 4.e-5 0.0
 00000
 3600200 000 5.045e6 1.151e6 2597.e3 1.
 3601101 360010000 205000000 1.e-5 10. 10. 000000 *
 3602101 360000000 370010000 0. 0. 0. 000000
 3601201 0. 0. 0.
 3602201 0. 0. 0.
 * fuel box exterior
 3700000 fuel.bo pipe
 3700001 7
 3700101 4.4896e-3 7
 3700301 0.53 7
 3700401 0.000 7
 3700601 90.0 7
 3700801 4.0e-5 0.0 7
 3701001 00000 7
 3701101 000000 6
 3701201 000 5.045e6 1.151e6 2597.e3 0.0 0. 7
 3701300 1
 3701301 0. 0. 0.0 6
 * up lpca injection tank sim
 4000000 vpics tmdpvol
 4000101 0. 10. 10. 0. 0. 4.e-5 0. 00000
 4000200 000
 4000201 0. 22.7e5 4.134e4 2.601e6 0.
 4000202 1000. 22.7e5 4.134e4 2.601e6 0.
 4000203 1.e6 22.7e5 4.134e4 2.601e6 0.
 *
 * lpca injection tf in up
 4030000 up.lpcsj tmdpjun
 4030101 400000000 210010000 0.0
 4030200 1 532 p 110010000
 4030201 -1. 0.0 0. 0.
 4030202 0. 0.232 0. 0.
 4030203 0.30e6 0.232 0. 0.
 4030204 0.60e6 0.209 0. 0.
 4030205 0.86e6 0.190 0. 0.
 4030206 1.10e6 0.173 0. 0.
 4030207 1.38e6 0.148 0. 0.
 4030208 1.64e6 0.120 0. 0.
 4030209 1.90e6 0.089 0. 0.
 4030210 2.05e6 0.060 0. 0.
 4030211 2.09e6 0.048 0. 0.
 4030212 2.15e6 0.0 0. 0.
 4030213 9.00e6 0.0 0. 0.
 * by lpca injection tank sim
 4100000 vbycs tmdpvol
 4100101 0. 10. 10. 0. 0. 4.e-5 0. 00000
 4100200 000
 4100201 0. 22.7e5 4.134e4 2.601e6 0.
 4100202 1000. 22.7e5 4.134e4 2.601e6 0.
 4100203 1.e6 22.7e5 4.134e4 2.601e6 0.
 *
 * by lpca injection tf
 4130000 jby.cs tmdpjun
 4130101 410000000 175010000 0.0
 4130200 1 536 p 110010000
 4130201 -1. 0.0 0. 0.
 4130202 0. 0.116 0. 0.
 4130203 0.30e6 0.116 0. 0.
 4130204 0.60e6 0.105 0. 0.
 4130205 0.86e6 0.095 0. 0.
 4130206 1.10e6 0.086 0. 0.
 4130207 1.38e6 0.074 0. 0.
 4130208 1.64e6 0.060 0. 0.
 4130209 1.90e6 0.044 0. 0.
 4130210 2.05e6 0.030 0. 0.
 4130211 2.09e6 0.024 0. 0.
 4130212 2.15e6 0.0 0. 0.

* lpcj tank simulator
 4200000 wlpcj tmdpvol
 4200101 0. 10. 10. 0. 0. 0. 4.e-5 0. 00000
 4200200 000
 4200201 0. 28.e5 4.134e4 2.601e6 0.
 4200202 1.e6 28.e5 4.134e4 2.601e6 0.
 * lpcj injection in core.bypass
 4230000 lpcij.by tmdpjun
 4230101 420000000 165010000 0.0
 4230200 1 530 p 110010000
 4230201 -1. 0.000 0. 0.
 4230202 0. 0.360 0. 0.
 4230203 0.30e6 0.360 0. 0.
 4230204 0.50e6 0.345 0. 0.
 4230205 0.68e6 0.330 0. 0.
 4230206 0.90e6 0.310 0. 0.
 4230207 1.25e6 0.250 0. 0.
 4230208 1.41e6 0.188 0. 0.
 4230209 1.51e6 0.115 0. 0.
 4230210 1.55e6 0.069 0. 0.
 4230211 1.65e6 0. 0. 0.
 4230212 9.51e6 0. 0. 0.
 * steam line downstream
 4300000 out.sl tmdpvol
 4300101 0. 3. 10. 0. 0. 0. 4.e-5 0. 00000
 4300200 000
 4300201 0. 1.e5 4.175e5 2.506e6 1.
 4300202 1. 1.e5 4.175e5 2.506e6 1.
 4300203 1.e6 1.e5 4.175e5 2.506e6 1.
 * steam line during steady state
 4330000 steam.li tmdpjun
 4330101 245010000 430000000 0.0
 4330200 1 525
 4330201 -1. 0.0 0. 0.
 4330202 0. 0. 0.348 0.
 4330203 1.e6 0. 0.348 0.
 * pre control volume
 4400000 out.sl tmdpvol
 4400101 0. 0.5 10. 0. 0. 0. 4.e-5 0. 00000
 4400200 000
 4400201 0. 5.045e6 1.151e6 2597.e3 1.
 4400202 1. 5.045e6 1.151e6 2597.e3 1.
 4400203 1.e6 5.045e6 1.151e6 2597.e3 1.
 * pressure control for steady state
 4430000 va.lopl valve
 4430101 245010000 440000000 5.00e-3 0.0 0.0 000100 1.
 1. 1.
 4430201 1. 0. 0.0463 0.000
 4430300 mtrvlv
 4430301 617 528 1. 1.
 * fw tank simulator
 4500000 fw.vol tmdpvol
 4500101 0. 10. 10. 0. 0. 0. 4.e-5 0. 00000
 4500200 000
 4500201 0. 5.5e6 6.286e5 2.601e6 0.
 4500202 1.e6 5.5e6 6.286e5 2.601e6 0.
 * fw injection in dc
 4530000 fw.j tmdpjun
 4530101 450000000 280000000 0.0
 4530200 1 529
 4530201 -1. 0.0 0. 0.
 4530202 0. 0.0463 0. 0.
 4530203 100. 0.0463 0. 0.
 4530204 101. 0. 0. 0.
 4530205 1.46 0. 0. 0.
 * srwv tank
 4600000 outsrw tmdpvol
 4600101 0. 3. 10. 0. 0. 0. 4.e-5 0. 00000
 4600200 000
 4600201 0. 1.e5 4.175e5 2.506e6 1.
 4600202 1.e6 1.e5 4.175e5 2.506e6 1.
 * srv vlv
 4630000 va.srv valve
 4630101 245010000 460000000 1.54e-6 1.e-6 1.e-6 000100 1.
 1. 1.
 4630201 0 0.000 0.000 0.000
 4630300 mtrvlv
 4630301 602 599 100. 0.
 * ads tvol
 4700000 outads tmdpvol
 4700101 0. 10. 100. 0. 0. 0. 4.e-5 0. 00000
 4700200 000
 4700201 0. 1.e5 83224. 2.50606e6 1.
 4700202 1.e6 1.e5 83224. 2.50606e6 1.
 * ads vlv
 4730000 val.ads valve
 4730101 245010000 470000000 38.3e-6 0.1 0.1 000100 1.
 1.
 4730201 0 0.000 0.000 0.000
 4730300 trpvlv
 4730301 601
 * ic line top
 5000000 1clint pipe
 5000001 10
 5000101 3.7e-4 5
 5000102 3.7e-4 10
 5000301 0.38 5
 5000302 0.312 9

5000303 0.312 10
 5000401 0.0 10
 5000601 0. 5
 5000602 -90. 10
 5000701 0. 5
 5000702 -0.212 9
 5000703 -0.112 10
 5000801 4.0e-6 0.0 10
 5000901 0.0 0.0 4
 5000902 0.3 0.3 5
 5000903 0.0 0.0 9
 5001001 01000 5
 5001002 00000 10
 5001101 000000 9
 5001201 000 5.045e6 0.7461e5 2597.03 1. 0. 6
 5001202 000 5.045e6 0.7461e5 2597.03 1. 0. 7
 5001203 000 5.045e6 0.7461e5 2597.03 1. 0. 8
 5001204 000 5.045e6 1.1510e6 2597.03 0.5 0. 9
 5001205 000 5.045e6 0.7461e5 2597.03 0. 0. 10
 5001301 0.0 0.0 0.0 9
 *
 * vlv ic top
 5050000 vlv.icb valve
 5050101 245000000 500000000 3.e-4 10. 10. 000100 1. 1.
 1.
 5050201 0 0.000 0.000 0.000
 5050300 trpvlv
 5050301 633
 *
 * ic top
 5100000 top.icb branch
 5100001 2 0
 5100101 6.0e-4 0.2 0. 0. -90. -0.1 4.e-5 1.6e-3
 00000
 5100200 000 5.045e6 0.7461e5 2597.03 0.0
 5101101 510010000 510000000 0. 0.1 0.1 000000
 5102001 500010000 510000000 0. 0.1 0.1 000000
 5102101 0. 0. 0.
 5102201 0. 0. 0.
 *
 * ic control
 5110000 iconn tmdpvvol
 5110101 0. 10. 100. 0. 0. 0. 4.e-5 0. 00000
 5110200 000
 5110201 0. 3.5e6 6.53e5 2.603e6 0. *
 5110202 1.e6 3.5e6 6.53e5 2.603e6 0.
 *
 * vlv ic control
 5120000 vlv.icc valve
 5120101 520000000 511000000 3.e-7 100. 100. 000100 1. 1.
 1.
 5120201 0 0.000 0.000 0.000
 5120300 trpvlv
 5120301 635
 *
 * ic control
 5130000 iconn tmdpvvol
 5130101 0. 10. 100. 0. 0. 0. 4.e-5 0. 00000
 5130200 000
 5130201 0. 2.5e6 6.53e5 2.603e6 0. *
 5130202 1.e6 2.5e6 6.53e5 2.603e6 0.
 *
 * vlv ic control
 5140000 vlv.icg valve
 5140101 520000000 513000000 8.e-6 100. 100. 000100 1. 1.
 1.
 5140201 0 0.000 0.000 0.000
 5140300 trpvlv
 5140301 636
 *
 * ic tubes
 5150000 ic.tubes pipe
 5150001 5
 5150101 3.05e-3 5
 5150301 0.0632 5
 5150401 0.0 5
 5150601 -90. 5
 5150801 4.0e-6 0.018 5
 5150901 0.0 0.0 4
 5151001 00000 5
 5151101 000000 4
 5151201 000 5.045e6 0.7461e5 2597.43e3 0.0 0. 5
 5151301 0.0 0.0 0.0 4
 *
 * ic bot
 5200000 bot.icb branch
 5200001 2 0
 5200101 3.0e-4 0.1 0. 0. -90. -0.1 4.e-5 1.6e-3
 00000
 5200200 000 5.045e6 0.7461e5 2598.e3 0.0
 5201101 515010000 520000000 0. 0.1 0.1 000000
 5202101 520010000 525000000 1.7e-4 0.1 0.1 000000
 5201201 0. 0. 0.
 5202201 0. 0. 0.
 *
 * ic tube internal to the tank
 5250000 ic.tube1 pipe
 5250001 14
 5250101 2.4e-4 14
 5250301 0.1 1
 5250302 0.07875 9
 5250303 0.104 14
 5250401 0.0 14
 5250601 -90. 9
 5250602 0. 14
 5250801 4.0e-6 0.018 14
 5250901 0.0 0.0 9
 5250902 0.2 0.2 10
 5250903 0.0 0.0 13
 5251001 00000 9

5251002 01000 14
 5251101 000000 13
 5251201 000 5.045e6 0.7461e5 2597.43e3 0.0 0. 1
 5251202 000 5.045e6 0.7461e5 2597.43e3 0.0 0. 3
 5251203 000 5.045e6 0.7461e5 2597.43e3 0.0 0. 5
 5251204 000 5.045e6 0.7461e5 2597.43e3 0.0 0. 7
 5251205 000 5.045e6 0.7461e5 2597.43e3 0.0 0. 14
 5251301 0.0 0.0 0.0 13
 *
 * exit tank junct.
 5300000 ic.ej sngljun
 5300101 525010000 540000000 2.5e-4 0.1 0.1 000000
 5300201 0 0.000 0.000 0.000
 *
 * ic tube external to the tank
 5400000 ic.tube1 pipe
 5400001 27
 5400101 2.544e-4 27
 5400301 0.35 2
 5400302 0.472 22
 5400303 0.4 23
 5400304 0.3 24
 5400305 0.35 27
 5400401 0.0 27
 5400601 0. 2
 5400602 -90. 22
 5400603 0. 23
 5400604 -90. 24
 5400605 0. 27
 5400801 4.0e-6 0.018 27
 5400901 0.0 0.0 2
 5400902 0.2 0.2 3
 5400903 0.0 0.0 21
 5400904 0.3 0.3 22
 5400905 0.0 0.0 26
 5401001 01000 2
 5401002 00000 22
 5401003 01000 23
 5401004 00000 24
 5401005 01000 27
 5401101 000000 26
 5401201 000 5.045e6 0.7461e5 2597.43e3 0.0 0. 27
 5401301 0.0 0.0 0.0 26
 *
 * vlv ic bot
 5500000 vlv.icb valve
 5500101 540010000 111000000 0.06e-4 300. 1.e9 000100 1.
 1.
 5500201 0 0.000 0.000 0.000
 5500300 trpvlv
 5500301 631
 *
 * ic tank bot1
 5510000 icta.b1 branch
 5510001 3 0
 5510101 0.708 0.07875 0. 0. 90. 0.07875 4.e-5 1.6e-3
 00000
 5510200 000 1.07e5 0.7488e5 3342.43e3 0.0
 5511101 551010000 552000000 0. 0. 0. 0. 000000
 5512101 551010000 563000000 0.1 0.1 0. 0. 000000
 5513101 551010000 564000000 0.1 0.1 0. 0. 000000
 5511201 0. 0. 0.
 5512201 0. 0. 0.
 5513201 0. 0. 0.
 *
 * ic tank bot2 internal part
 5520000 icta.b2 branch
 5520001 1 0
 5520101 0.1 0.07875 0. 0. 90. 0.07875 4.e-5 1.6e-3
 00000
 5520200 000 1.07e5 0.7488e5 3342.43e3 0.0
 5521101 552010000 560000000 0. 0. 0. 0. 000000
 5521201 0. 0. 0.
 *
 * ic-tank internal part (with baffle)
 5600000 ic.tank pipe
 5600001 12
 5600002 0.0632 12
 5600003 0.07875 12
 5600004 0.07875 6
 5600005 0.0632 12
 5600006 0.0 12
 5600007 0.0 12
 5600008 0.0 12
 5600009 0.0 12
 5600010 0.0 11
 5600101 0.0000 11
 5600102 0.0 12
 5600103 0.0 12
 5600104 0.0 8
 5600105 0.0 12
 5600106 0.0 12
 5600107 0.0 12
 5600108 0.0 12
 5600109 0.0 12
 5600110 0.0 12
 5600111 0.0 12
 5600112 0.0 12
 5600113 0.0 12
 5600114 0.0 12
 5600115 0.0 12
 5600116 0.0 12
 5600117 0.0 12
 5600118 0.0 12
 5600119 0.0 12
 5600120 0.0 12
 5600121 0.0 12
 5600122 0.0 12
 5600123 0.0 12
 5600124 0.0 12
 5600125 0.0 12
 5600126 0.0 12
 5600127 0.0 12
 5600128 0.0 12
 5600129 0.0 12
 5600130 0.0 12
 5600131 0.0 12
 *
 * ic tank top1
 5610000 icta.t1 branch
 5610001 1 0
 5610101 0.087 0.0632 0. 0. 90. 0.0632 4.e-5 1.6e-3
 00000
 5610200 000 1.07e5 0.7488e5 3342.43e3 0.0
 5611101 561001000 561000000 0. 0. 0. 0. 000000
 5611201 0. 0. 0.
 *
 * ic tank top2
 5620000 icta.t2 branch
 5620001 3 0

5620101 0.659 0.1 0. 0. 90. 0.1 4.e-5 1.6e-3
 00000
 5620200 000 1.07e5 0.7488e5 3342.43e3 0.0
 5621101 561010000 562000000 0. 0. 0. 0.00000
 5622101 562000000 563010000 0.1 0.1 0. 0.00000
 5623101 562000000 564010000 0.1 0.1 0. 0.00000
 *
 * ic-tank longer ext. piping
 5630000 ic.te.pi pipe
 5630001 22
 5630101 2.248e-3 22
 5630301 0.11 4
 5630302 0.07875 11
 5630303 0.1 13
 5630304 0.0632 18
 5630305 0.11 22
 5630401 0.0 22
 5630601 0. 4
 5630602 90. 18
 5630603 0. 22
 5630801 4.0e-6 0.000 22
 5630901 0.0 0.0 3
 5630902 0.1 0.1 4
 5630903 0.0 0.0 17
 5630904 0.1 0.1 18
 5630905 0.0 0.0 21
 5631001 00000 22
 5631101 000000 21
 5631201 000 1.07e5 0.7488e5 3382.43e3 0.0 0. 2
 5631202 000 1.07e5 0.7488e5 3382.43e3 0.0 0. 4
 5631203 000 1.07e5 0.7488e5 3382.43e3 0.0 0. 6
 5631204 000 1.07e5 0.7488e5 3382.43e3 0.0 0. 8
 5631205 000 1.07e5 0.7488e5 3382.43e3 0.0 0. 10
 5631206 000 1.07e5 0.7488e5 3382.43e3 0.0 0. 22
 5631301 0.0 0.0 0.0 21
 *
 * ic-tank short ext. piping
 5640000 ic.te.p2 pipe
 5640001 22
 5640101 2.248e-3 22
 5640301 0.03 4
 5640302 0.07875 11
 5640303 0.1 13
 5640304 0.0632 18
 5640305 0.03 22
 5640401 0.0 22
 5640601 0. 4
 5640602 90. 18
 5640603 0. 22
 5640801 4.0e-6 0.000 22
 5640901 0.0 0.0 3
 5640902 0.1 0.1 4
 5640903 0.0 0.0 17
 5640904 0.1 0.1 18
 5640905 0.0 0.0 21
 5641001 00000 22
 5641101 000000 21
 5641201 000 1.07e5 0.7488e5 3382.43e3 0.0 0. 2
 5641202 000 1.07e5 0.7488e5 3382.43e3 0.0 0. 4
 5641203 000 1.07e5 0.7488e5 3382.43e3 0.0 0. 6
 5641204 000 1.07e5 0.7488e5 3382.43e3 0.0 0. 8
 5641205 000 1.07e5 0.7488e5 3382.43e3 0.0 0. 10
 5641206 000 1.07e5 0.7488e5 3382.43e3 0.0 0. 22
 5641301 0.0 0.0 0.0 21
 *
 * top of ic tank
 5650000 outic tmdpvvol
 5650101 0. 10. 100. 0. 0. 0. 4.e-5 0. 00000
 5650200 000
 5650201 0. 1.e5 83224. 2.50606e6 1.
 5650202 1.e6 1.e5 83224. 2.50606e6 1.
 *
 * top ic - tmdpvvol atmosfera
 5660000 icctop sngljun
 5660101 570010000 565000000 0.1 0.1 0.1 0.1 000000
 5660201 0 0.000 0.000 0.000
 *
 * top of ic tank
 5700000 icctop pipe
 5700001 3
 5700101 1.00 3
 5700301 0.2 3
 5700401 0.0 3
 5700601 90. 3
 5700801 4.0e-6 0.0 3
 5700901 0.0 0.0 2
 5701001 00000 3
 5701101 000000 2
 5701201 000 1.07e5 425.05e3 2504.22e3 1.0 0. 3
 5701301 0.0 0.0 0.0 2
 *
 * top ic - surge line
 5750000 icccsl sngljun
 5750101 570000000 580010000 0.1 0.1 0.1 0.1 000000
 5750201 0 0.000 0.000 0.000
 *
 * surge line del ic
 5800000 icctop pipe
 5800001 5
 5800101 0.1 5
 5800301 0.2 5
 5800401 0.0 5
 5800601 90. 5
 5800801 4.0e-6 0.0 5
 5800901 0.0 0.0 4
 5801001 00000 5
 5801101 000000 4

5801201 000 1.07e5 0.7488e5 2504.e3 0.0 0. 1
 5801202 000 1.07e5 0.7488e5 2504.e3 0.0 0. 2
 5801203 000 1.07e5 425.5e3 2504.e3 0.5 0. 3
 5801204 000 1.07e5 425.5e3 2504.e3 1.0 0. 5
 5801301 0.0 0.0 0.0 4
 * top surge line- tank ic
 5850000 icccsl sngljun
 5850101 580000000 562010000 0.1 0.1 0.1 0.1 000000
 5850201 0 0.000 0.000 0.000
 *
 * ic tank bot2 external part
 6520000 icata.b2 branch
 6520001 2 0
 6520101 0.608 0.07875 0. 0. 90. 0.07875 4.e-5 1.6e-3
 00000
 6520200 000 1.07e5 0.7488e5 3342.43e3 0.0
 6521101 652010000 660000000 0. 0. 0. 0.00000
 6522101 551010000 652000000 0. 0. 0. 0.00000
 6522101 0. 0. 0. 0.
 6522201 0. 0. 0.
 *
 * ic-tank external part (with baffle)
 6600000 ic.tanc pipe
 6600001 12
 6600101 0.608 12
 6600301 0.07875 6
 6600302 0.1 8
 6600303 0.0632 12
 6600401 0.0 12
 6600601 90. 12
 6600801 4.0e-6 1.000 12
 6600901 0.0 0.0 11
 6601001 00000 12
 6601101 000000 11
 6601201 000 1.07e5 0.7488e5 3382.43e3 0.0 0. 2
 6601202 000 1.07e5 0.7488e5 3382.43e3 0.0 0. 4
 6601203 000 1.07e5 0.7488e5 3382.43e3 0.0 0. 6
 6601204 000 1.07e5 0.7488e5 3382.43e3 0.0 0. 8
 6601205 000 1.07e5 0.7488e5 3382.43e3 0.0 0. 10
 6601206 000 1.07e5 0.7488e5 3382.43e3 0.0 0. 12
 6601301 0.0 0.0 0.0 11
 *
 * ic tank top1 external
 6610000 icata.tle branch
 6610001 2 0
 6610101 0.608 0.0632 0. 0. 90. 0.0632 4.e-5 1.6e-3
 00000
 6610200 000 1.07e5 0.7488e5 3342.43e3 0.0
 6611101 661010000 562000000 0. 0. 0. 0.00000
 6612101 660010000 661000000 0. 0. 0. 0.00000
 6611201 0. 0. 0.
 6612201 0. 0. 0.
 *
 * structures
 *
 * lower plenum bottom flange
 11001006 1 5 1 1 0.0
 11001100 0 1
 11001101 4 0.073
 11001201 1 4
 11001301 0.0 4
 11001400 0
 11001401 551.0 5
 11001501 100010000 0 1 1 0.011 1
 11001601 00000000 0 0 1 0.011 1
 11001701 0 0.0 0.0 0.0 1
 11001801 0. 100. 100. 0. 0. 0. 1. 1
 *
 * thick flange in various zones
 11002000 8 10 2 1 0.058
 11002100 0 1
 11002101 9 0.1875
 11002201 1 9
 11002301 0.0 9
 11002401 551.0 10
 11002501 1000010000 0 1 1 0.080 1
 11002502 130010000 0 1 1 0.080 2
 11002503 110040000 0 1 1 0.080 3
 11002504 210010000 0 1 1 0.080 4
 11002505 235010000 0 1 1 0.080 5
 11002506 245010000 0 1 1 0.080 6
 11002507 225010000 0 1 1 0.080 7
 11002508 220020000 0 1 1 0.080 8
 11002601 000000000 0 0 1 0.080 8
 11002701 0 0.0 0.0 0.0 0.0 8
 11002801 0. 100. 100. 0. 0. 0. 1. 8
 * added structure for n2 heat losses
 11003000 1 10 1 1 0.058
 11003100 0 1
 11003101 9 0.068
 11003201 1 9
 11003301 0.0 9
 11003401 551.0 10
 11003501 130010000 0 1 1 0.100 1
 11003601 000000000 0 2902 1 0.100 1
 11003701 0 0.0 0.0 0.0 0.0 1
 11003801 0. 100. 100. 0. 0. 0. 1. 1
 * core region cylindrical vessel
 11103000 39 5 2 1 0.0565
 11103100 0 1
 11103101 4 0.07065
 11103201 1 4
 11103301 0.0 4

11651206 5 9
11651301 0.0 9
11651401 561.0 10
11651501 000000000 0 0 1 3.2 1
11651502 000000000 0 0 1 1.9 2
11651601 140010000 0 1 1 3.2 1
11651602 135010000 0 1 1 1.9 2
11651701 0 0.0 0.0 0.0 0.0 2
11651901 0. 100. 100. 0. 0. 0. 1. 2

* core active length
12001000 14 10 2 1 0.0
12001100 0 1
12001101 3 0.0020
12001102 1 0.0025
12001103 1 0.0035
12001104 1 0.0043
12001105 1 0.0050
12001106 2 0.006115
12001201 2 3
12001202 3 4
12001203 4 5
12001204 5 6
12001205 4 7
12001206 5 9
12001301 0.04 3
12001302 0.0 5
12001303 0.96 6
12001304 0.0 9
12001401 561.0 10
12001501 000000000 0 0 1 4.24 14
12001601 200010000 10000 1 1 4.24 14
12001701 900 0.051724 0.0 0.0 1
12001702 900 0.051724 0.0 0.0 2
12001703 900 0.0689655 0.0 0.0 3
12001704 900 0.0689655 0.0 0.0 4
12001705 900 0.0689655 0.0 0.0 5
12001706 900 0.0689655 0.0 0.0 6
12001707 900 0.0689655 0.0 0.0 7
12001708 900 0.0689655 0.0 0.0 8
12001709 900 0.0689655 0.0 0.0 9
12001710 900 0.0689655 0.0 0.0 10
12001711 900 0.0689655 0.0 0.0 11
12001712 900 0.0689655 0.0 0.0 12
12001713 900 0.051724 0.0 0.0 13
12001714 900 0.051724 0.0 0.0 14

12001901 0. 100. 100. 0. 0. 0. 0. 1. 1
12001902 0. 100. 100. 0.13 0. 0. 0. 1. 2
12001903 0. 100. 100. 0. 0.13 0. 0. 0. 1. 3
12001904 0. 100. 100. 0. 0.13 0. 0. 0. 1. 4
12001905 0. 100. 100. 0. 0.13 0. 0. 0. 1. 5
12001906 0. 100. 100. 0. 0.13 0. 0. 0. 1. 6
12001907 0. 100. 100. 0. 0.13 0. 0. 0. 1. 7
12001908 0. 100. 100. 0. 0.13 0. 0. 0. 1. 8
12001909 0. 100. 100. 0. 0.13 0. 0. 0. 1. 9
12001910 0. 100. 100. 0. 0.13 0. 0. 0. 1. 10
12001911 0. 100. 100. 0. 0.13 0. 0. 0. 1. 11
12001912 0. 100. 100. 0. 0.13 0. 0. 0. 1. 12
12001913 0. 100. 100. 0. 0.13 0. 0. 0. 1. 13
12001914 0. 100. 100. 0. 0. 0. 0. 0. 1. 14

* top unheated length
12002000 2 10 2 1 0.0
12002100 2001
12002401 561. 10
12002501 000000000 0 0 1 3.664 1
12002502 000000000 0 0 1 3.2 2
12002601 200150000 0 1 1 3.664 1
12002602 200160000 0 1 1 3.2 2
12002701 0 0.0 0.0 0.0 0.0 2
12002901 0. 100. 100. 0. 0. 0. 0. 1. 2

* upper tie plate
12051001 1 5 1 1 0.0
12051100 0 1
12051101 4 0.015
12051201 1 4
12051301 0. 0 4
12051400 0
12051401 561. 0 5
12051501 200160000 0 1 1 9.896e-3 1
12051601 205010000 0 1 1 9.896e-3 1
12051701 0 0.0 0.0 0.0 1
12051801 0. 100. 100. 0. 0. 0. 0. 1. 1
12051901 0. 100. 100. 0. 0. 0. 0. 1. 1

* separator walls - flange
12201000 1 5 2 1 0.02745
12201100 0 1
12201101 4 0.1875
12201201 1 4
12201301 0. 0 4
12201401 561. 0 5
12201501 220030000 0 1 1 0.086 1
12201601 000000000 0 0 1 0.086 1
12201701 0 0.0 0.0 0.0 0.0 1
12201801 0. 100. 100. 0. 0. 0. 0. 1. 1

* separator wall
12202000 19 5 2 1 0.02745
12202100 0 1
12202101 4 0.03015
12202201 1 4
12202301 0. 0 4
12202401 561. 0 5
12202501 220030000 00000 1 1 0.2345 1
12202502 220040000 00000 1 1 0.1915 2
12202503 220040000 00000 1 1 0.043 3
12202504 220050000 10000 1 1 0.2345 19
12202601 225010000 0 0 1 0.2345 1

12202602 225010000 0 0 1 1 0.1915 2
12202603 230010000 0 0 1 1 0.043 3
12202604 230010000 0 0 1 1 0.2345 1
12202605 230010000 0 0 1 1 0.2345 5
12202606 230020000 0 0 1 1 0.2345 6
12202607 230020000 0 0 1 1 0.2345 7
12202608 230030000 0 0 1 1 0.2345 8
12202609 230030000 0 0 1 1 0.2345 9
12202610 230040000 0 0 1 1 0.2345 10
12202611 230040000 0 0 1 1 0.2345 11
12202612 230050000 0 0 1 1 0.2345 12
12202613 230050000 0 0 1 1 0.2345 13
12202614 230060000 0 0 1 1 0.2345 14
12202615 230060000 0 0 1 1 0.2345 15
12202616 230070000 0 0 1 1 0.2345 16
12202617 230070000 0 0 1 1 0.2345 17
12202618 230080000 0 0 1 1 0.2345 18
12202619 230080000 0 0 1 1 0.2345 19
12202701 0 0.0 0.0 0.0 0.0 1
12202801 0. 100. 100. 0. 0. 0. 0. 1. 19
12202901 0. 100. 100. 0. 0. 0. 0. 1. 19

* sd horizontal pipes
12501000 10 5 2 1 0.0368
12501100 0 1
12501101 4 0.047
12501201 1 4
12501301 0.0 4
12501401 561. 0 5
12501501 250010000 10000 1 1 0.279 5
12501502 255010000 10000 1 1 0.279 10
12501601 000000000 0 0 1 1 0.279 10
12501701 0 0.0 0.0 0.0 0.0 10
12501801 0. 100. 100. 0. 0. 0. 0. 1. 10

* sd horizontal pipes flanges
12502000 5 5 2 1 0.0368
12502100 0 1
12502101 4 0.1335
12502201 1 4
12502301 0.0 4
12502401 561. 0 5
12502501 250010000 5 0 1 1 0.109 1
12502502 250050000 0 0 1 1 0.109 5
12502503 255010000 0 0 1 1 0.109 3
12502504 255030000 0 0 1 1 0.109 4
12502505 255050000 0 0 1 1 0.109 5
12502601 000000000 0 0 1 1 0.109 5
12502701 0 0.0 0.0 0.0 0.0 5
12502801 0. 100. 100. 0. 0. 0. 0. 1. 5

* sd and udc pipe
12601000 17 5 2 1 0.0427
12601100 0 1
12601101 4 0.0508
12601201 1 4
12601301 0.0 4
12601401 561. 0 5
12601501 260010000 10000 1 1 0.25 4
12601502 265010000 00000 1 1 0.246 5
12601503 270010000 00000 1 1 0.247 6
12601504 275010000 10000 1 1 0.362 10
12601505 280010000 00000 1 1 0.3 11
12601506 285010000 10000 1 1 0.3 17
12601601 000000000 0 0 1 1 0.25 4
12601602 000000000 0 0 1 1 0.246 5
12601603 000000000 0 0 1 1 0.247 6
12601604 000000000 0 0 1 1 0.362 10
12601605 000000000 0 0 1 1 0.3 11
12601606 -801 00000 3502 1 0.3 17
12601701 0 0.0 0.0 0.0 0.0 17
12601801 0. 100. 100. 0. 0. 0. 0. 1. 17

* dc flanges
12602000 10 5 2 1 0.0427
12602100 0 1
12602101 4 0.146
12602201 1 4
12602301 0.0 4
12602401 561. 0 5
12602501 260010000 0 0 1 1 0.08 1
12602502 260010000 0 0 1 1 0.08 2
12602503 265010000 0 0 1 1 0.08 3
12602504 270010000 0 0 1 1 0.08 4
12602505 280010000 0 0 1 1 0.08 5
12602506 300010000 0 0 1 1 0.08 6
12602507 310010000 0 0 1 1 0.08 7
12602508 320150000 0 0 1 1 0.08 8
12602509 325010000 0 0 1 1 0.08 9
12602510 330010000 0 0 1 1 0.08 10
12602601 000000000 0 0 1 1 0.08 10
12602701 0 0.0 0.0 0.0 0.0 10
12602801 0. 100. 100. 0. 0. 0. 0. 1. 10

* sse-dc connection
12901000 4 5 2 1 0.02
12901100 0 1
12901101 4 0.0211
12901201 1 4
12901301 0.0 4
12901401 561. 0 5
12901501 290010000 10000 1 1 0.3 2
12901502 295010000 10000 1 1 0.35 4
12901601 000000000 0 0 1 1 0.3 1
12901602 000000000 0 0 1 1 0.3 2
12901603 000000000 0 0 1 1 0.35 3
12901604 000000000 0 0 1 1 0.35 4
12901701 0 0.0 0.0 0.0 0.0 4
12901801 0. 100. 100. 0. 0. 0. 0. 1. 4

* sea-dc connection flanges

12902000	4	5	2	1	0.02
12902100	0	1			
12902101	4	0.0595			
12902201	1	4			
12902301	0.0	4			
12902401	561.	5			
12902501	290010000	10000	1	1	0.070 2
12902502	295010000	10000	1	1	0.070 4
12902601	000000000	0	0	1	0.070 1
12902602	000000000	0	0	1	0.070 2
12902603	000000000	0	0	1	0.070 3
12902604	000000000	0	0	1	0.070 4
12902701	0	0.0	0.0	0.0	0.0 4
12902801	0.	100.	100.	0.	0. 0. 0. 0. 1. 4

* lower downcomer

13001000	26	5	2	1	0.0368
13001100	0	1			
13001101	4	0.0445			
13001201	1	4			
13001301	0.0	4			
13001401	551.0	5			
13001501	300010000	0	1	1	0.275 1
13001502	305010000	10000	1	1	0.28 9
13001503	310010000	0	1	1	0.26 10
13001504	320010000	10000	1	1	0.275 24
13001505	325010000	0	1	1	0.27 25
13001506	330010000	0	1	1	0.27 26
13001601	000000000	0	0	1	0.275 1
13001602	-801	00000	3503	1	0.28 9
13001603	000000000	0	0	1	0.26 10
13001604	000000000	00000	0	1	0.275 24
13001605	000000000	0	0	1	0.27 25
13001606	000000000	0	0	1	0.27 26
13001701	0	0.0	0.0	0.0	0.0 26
13001801	0.	100.	100.	0.	0. 0. 0. 0. 1. 26

* jet pump

13151000	15	5	2	1	0.0133
13151100	0	1			
13151101	4	0.0167			
13151201	1	4			
13151301	0.0	4			
13151401	551.0	5			
13151501	315010000	10000	1	1	0.273 14
13151502	315150000	0	1	1	0.1 15
13151601	320010000	10000	1	1	0.273 14
13151602	320150000	0	1	1	0.1 15
13151701	0	0.0	0.0	0.0	0.0 15
13151801	0.	100.	100.	0.	0. 0. 0. 0. 1. 15
13151901	0.	100.	100.	0.	0. 0. 0. 0. 1. 15

* lower plenum hor

13351000	7	5	2	1	0.0244
13351100	0	1			
13351101	4	0.028			
13351201	1	4			
13351301	0.0	4			
13351401	551.0	5			
13351501	335010000	10000	1	1	0.25 4
13351502	345010000	10000	1	1	0.12 7
13351601	000000000	0	0	1	0.25 4
13351602	000000000	0	0	1	0.12 7
13351701	0	0.0	0.0	0.0	0.0 7
13351801	0.	100.	100.	0.	0. 0. 0. 0. 1. 7

* lp hor flanges

13352000	3	5	2	1	0.0244
13352100	0	1			
13352101	4	0.1335			
13352201	1	4			
13352301	0.0	4			
13352401	551.0	5			
13352501	335010000	0	1	1	0.1 1
13352502	335040000	0	1	1	0.1 2
13352503	345010000	0	1	1	0.1 3
13352601	000000000	0	0	1	0.1 3
13352701	0	0.0	0.0	0.0	0.0 3
13352801	0.	100.	100.	0.	0. 0. 0. 0. 1. 3

* lp pipe

13353000	2	5	2	1	0.01905
13353100	0	1			
13353101	4	0.02413			
13353201	1	4			
13353301	0.0	4			
13353401	551.0	5			
13353501	345040000	10000	1	1	0.25 2
13353601	110020000	-10000	1	1	0.25 2
13353701	0	0.0	0.0	0.0	0.0 2
13353801	0.	100.	100.	0.	0. 0. 0. 0. 1. 2
13353901	0.	100.	100.	0.	0. 0. 0. 0. 1. 2

* ic pipe external

15000000	10	5	2	1	0.009
15000100	0	1			
15000101	4	0.010			
15000201	1	4			
15000301	0.0	4			
15000401	551.0	5			
15000501	500010000	10000	1	1	0.38 5
15000502	500060000	10000	1	1	0.212 9
15000503	500100000	00000	1	1	0.112 10
15000601	-801	00000	3507	1	0.38 1
15000602	-801	00000	3507	1	0.38 2
15000603	-801	00000	3507	1	0.38 3
15000604	-801	00000	3507	1	0.38 4
15000605	-801	00000	3507	1	0.38 5
15000606	-801	00000	3507	1	0.212 6

* ic exit piping

15000607	-801				
15000608	-801				
15000609	-801				
15000610	-801				
15000611	0				
15000612	0				
15000613	0				
15000614	0				
15000615	0				
15000616	0				
15000617	0				
15000618	0				
15000619	0				
15000620	0				
15000621	0				
15000622	0				
15000623	0				
15000624	0				
15000625	0				
15000626	0				
15000627	0				
15000628	0				
15000629	0				
15000630	0				
15000631	0				
15000632	0				
15000633	0				
15000634	0				
15000635	0				
15000636	0				
15000637	0				
15000638	0				
15000639	0				
15000640	0				
15000641	0				
15000642	0				
15000643	0				
15000644	0				
15000645	0				
15000646	0				
15000647	0				
15000648	0				
15000649	0				
15000650	0				
15000651	0				
15000652	0				
15000653	0				
15000654	0				
15000655	0				
15000656	0				
15000657	0				
15000658	0				
15000659	0				
15000660	0				
15000661	0				
15000662	0				
15000663	0				
15000664	0				
15000665	0				
15000666	0				
15000667	0				
15000668	0				
15000669	0				
15000670	0				
15000671	0				
15000672	0				
15000673	0				
15000674	0				
15000675	0				
15000676	0				
15000677	0				
15000678	0				
15000679	0				
15000680	0				
15000681	0				
15000682	0				
15000683	0				
15000684	0				
15000685	0				
15000686	0				
15000687	0				
15000688	0				
15000689	0				
15000690	0				
15000691	0				
15000692	0				
15000693	0				
15000694	0				
15000695	0				
15000696	0				
15000697	0				
15000698	0				
15000699	0				
15000700	0				
15000701	0				
15000702	0				
15000703	0				
15000704	0				
15000705	0				
15000706	0				
15000707	0				
15000708	0				
15000709	0				
15000710	0				
15000711	0				
15000712	0				
15000713	0				
15000714	0				
15000715	0				
15000716	0				
15000717	0				
15000718	0				
15000719	0				
15000720	0				
15000721	0				
15000722	0				
15000723	0				
15000724	0				
15000725	0				
15000726	0				
15000727	0				
15000728	0				
15000729	0				
15000730	0				
15000731	0				
15000732	0				
15000733	0				
15000734	0				
15000735	0				
15000736	0				
15000737	0				
15000738	0				
15000739	0				
15000740	0				
15000741	0				
15000742	0				
15000743	0				
15000744	0				
15000745	0				
15000746	0				
15000747	0				
15000748	0				
15000749	0				
15000750	0				
15000751	0				
15000752	0				
15000753	0				
15000754	0				

15600611 -801 0 3505 1 0.0632 11
 15600612 -801 0 3505 1 0.0632 12
 15600613 -801 0 3505 1 0.0632 13
 15600614 -801 0 3505 1 0.0632 14
 15600615 -801 0 3505 1 0.0632 15
 15600616 -801 0 3505 1 0.1 16
 15600701 0 0.0 0.0 0.0 1.16
 15600801 0. 100. 100. 0. 0. 0. 1. 16
 *
 * ic tank external pipes - for heat losses
 15630000 22 5 2 1 0.02625
 15630100 0 1
 15630101 4 0.0295
 15630201 1 4
 15630301 0.0 4
 15630401 551.0 5
 15630501 563010000 10000 1 1 0.11 4
 15630502 563050000 10000 1 1 0.07875 11
 15630503 563120000 10000 1 1 0.1 13
 15630504 563140000 10000 1 1 0.0632 18
 15630505 563190000 10000 1 1 0.11 22
 15630601 -801 0 3508 1 0.11 4
 15630602 -801 0 3508 1 0.07875 11
 15630603 -801 0 3508 1 0.1 13
 15630604 -801 0 3508 1 0.0632 18
 15630605 -801 0 3508 1 0.11 22
 15630701 0 0.0 0.0 0.0 22
 15630801 0. 100. 100. 0. 0. 0. 1. 22
 *
 * ic tank external pipes - for heat losses
 15640000 22 5 2 1 0.02625
 15640100 0 1
 15640101 4 0.0295
 15640201 1 4
 15640301 0.0 4
 15640401 551.0 5
 15640501 564010000 10000 1 1 0.03 4
 15640502 564050000 10000 1 1 0.07875 11
 15640503 564120000 10000 1 1 0.1 13
 15640504 564140000 10000 1 1 0.0632 18
 15640505 564190000 10000 1 1 0.03 22
 15640601 -801 0 3508 1 0.03 4
 15640602 -801 0 3508 1 0.07875 11
 15640603 -801 0 3508 1 0.1 13
 15640604 -801 0 3508 1 0.0632 18
 15640605 -801 0 3508 1 0.03 22
 15640701 0 0.0 0.0 0.0 22
 15640801 0. 100. 100. 0. 0. 0. 1. 22
 *
 * ic tank internal baffle
 16600000 14 5 2 1 0.35
 16600100 0 1
 16600101 4 0.353
 16600201 1 4
 16600301 0.0 4
 16600401 551.0 5
 16600501 552010000 00000 1 1 0.07875 1
 16600502 560010000 10000 1 1 0.07875 7
 16600503 560070000 10000 1 1 0.1 9
 16600504 560090000 10000 1 1 0.0632 13
 16600505 561010000 00000 1 1 0.0632 14
 16600601 652010000 00000 1 1 0.07875 1
 16600602 660010000 10000 1 1 0.07875 7
 16600603 660070000 10000 1 1 0.1 9
 16600604 660090000 10000 1 1 0.0632 13
 16600605 661010000 00000 1 1 0.0632 14
 16600701 0 0.0 0.0 0.0 14
 16600801 0. 100. 100. 0. 0. 0. 1. 14
 16600901 0. 100. 100. 0. 0. 0. 1. 14
 *
 * material tables
 *
 *
 20100100 tbl/fctn 1 1 * stainless steel
 20100200 tbl/fctn 1 1 * copper
 20100300 tbl/fctn 1 1 * nickel
 20100400 tbl/fctn 1 1 * boron nitride
 20100500 tbl/fctn 1 1 * inc. 600
 20100600 tbl/fctn 1 1 * filler (ceramics)
 *
 * conductivita' acciaio
 *
 20100101 1.0 15.16
 20100102 123.0 15.16
 20100103 173.0 15.16
 20100104 223.0 15.16
 20100105 273.0 15.16
 20100106 293.0 15.16
 20100107 323.0 15.62
 20100108 373.0 16.37
 20100109 423.0 17.09
 20100110 473.0 17.81
 20100111 523.0 18.50
 20100112 573.0 19.20
 20100113 623.0 19.85
 20100114 673.0 20.50
 20100115 723.0 21.13
 20100116 773.0 21.77
 20100117 823.0 22.36
 20100118 873.0 22.95
 20100119 923.0 23.53
 20100120 973.0 24.12
 20100121 1023.0 24.68
 20100122 1073.0 25.25
 20100123 1123.0 25.81
 20100124 1173.0 26.38
 20100125 1223.0 26.94
 *
 * calore specifico dell' acciaio
 *
 20100126 1273.0 27.50
 20100127 1323.0 28.05
 20100128 1373.0 28.60
 20100129 1423.0 29.15
 20100130 1473.0 29.70
 20100131 1523.0 30.25
 20100132 1573.0 30.80
 *
 * calore specifico dell' acciaio
 *
 20100151 1.0 3.58249e6
 20100152 123.0 3.58249e6
 20100153 173.0 3.58249e6
 20100154 223.0 3.58249e6
 20100155 273.0 3.58249e6
 20100156 323.0 3.58249e6
 20100157 323.0 3.69720e6
 20100158 373.0 3.85678e6
 20100159 423.0 3.99345e6
 20100160 473.0 4.10800e6
 20100161 523.0 4.21070e6
 20100162 573.0 4.29602e6
 20100163 623.0 4.37028e6
 20100164 673.0 4.43980e6
 20100165 723.0 4.50300e6
 20100166 773.0 4.56225e6
 20100167 823.0 4.62308e6
 20100168 873.0 4.68470e6
 20100169 923.0 4.75185e6
 20100170 973.0 4.82295e6
 20100171 1023.0 4.91380e6
 20100172 1073.0 5.03230e6
 20100173 1123.0 5.18398e6
 20100174 1173.0 5.37200e6
 20100175 1223.0 5.60110e6
 20100176 1273.0 5.88155e6
 20100177 1323.0 6.16200e6
 20100178 1373.0 6.44245e6
 20100179 1423.0 6.72290e6
 20100180 1473.0 7.00335e6
 20100181 1523.0 7.28380e6
 20100182 1573.0 7.56425e6
 *
 * conduttivita' mat.-2 - rame *
 *
 20100201 293.2 386.1
 20100202 373.2 376.8
 20100203 573.2 366.3
 20100204 1000.0 366.3
 20100205 2000.0 366.3
 *
 * calore spec. mat. -2- *
 *
 20100251 293.2 3.44956e6
 20100252 373.2 3.56608e6
 20100253 573.2 3.71846e6
 20100254 1000.0 3.71846e6
 20100255 2000.0 3.71846e6
 *
 * conduttivita' mat. -3- ni *
 *
 20100301 293.2 71.18
 20100302 573.2 58.62
 20100303 773.2 58.62
 20100304 1073.2 48.15
 20100305 2000.0 48.15
 *
 * calore spec. mat. -3- *
 *
 20100351 293.2 4.05384e6
 20100352 573.2 4.05384e6
 20100353 773.2 4.05384e6
 20100354 1073.2 4.05384e6
 20100355 2000.0 4.05384e6
 *
 * conduttivita' mat. -4- bn-s*
 *
 20100401 293.0 23.0
 20100402 400.0 23.0
 20100403 500.0 22.5
 20100404 600.0 22.0
 20100405 700.0 21.5
 20100406 800.0 20.9
 20100407 900.0 20.5
 20100408 1000.0 20.1
 20100409 1100.0 19.8
 20100410 1200.0 19.4
 20100411 1300.0 19.1
 20100412 2000.0 19.1
 *
 * calore spec.mat. -4- *
 *
 20100451 293.0 1.5029e6
 20100452 400.0 2.0121e6
 20100453 500.0 2.4035e6
 20100454 600.0 2.698e6
 20100455 700.0 2.9127e6
 20100456 800.0 3.0976e6
 20100457 900.0 3.2686e6
 20100458 1000.0 3.3372e6
 20100459 1100.0 3.4941e6
 20100460 1200.0 3.5891e6
 20100461 1300.0 3.6537e6
 20100462 1400.0 3.7183e6
 20100463 1500.0 3.7506e6
 20100464 2000.0 3.7506e6
 *
 * conduttivita' mat.-5- 1/600 *
 *
 20100501 294.3 14.86

20100502 366.5 15.72
 20100503 477.6 17.45
 20100504 588.8 19.19
 20100505 699.9 20.92
 20100506 811.0 22.79
 20100507 922.0 24.81
 20100508 1033.2 26.83
 20100509 1144.3 28.85
 20100510 2000.0 28.85
 *
 * calore spec. mat. -5- *
 *
 20100551 294.3 3.74292e6
 20100552 366.5 3.91995e6
 20100553 477.6 4.03698e6
 20100554 588.8 4.274e6
 20100555 699.9 4.451e6
 20100556 811.0 4.66179e6
 20100557 922.0 4.93998e6
 20100558 1033.2 5.11701e6
 20100559 1144.3 5.26032e6
 20100560 2000.0 5.26032e6
 *
 * conduttivita' mat.-6- fil. *
 *
 20100601 294.2 0.9304
 20100602 2000.0 0.9304
 *
 * calore spec. mat. -6- *
 *
 20100651 294.2 1.92975e6
 20100652 2000.0 1.92975e6
 *
 *
 * general tables
 *
 *
 * heat removal by cooling coil from sd (max 200 kw)/ heat losses
 po-ic-2
 20250100 htc-t 507
 20250101 -1.0 0.0
 20250102 0.0 0.0
 20250103 1.0 -1. *15.
 20250104 450. -1. *15.
 20250105 451. -4. *15.
 20250106 600. -4. *15.
 20250107 601. -1. *15.
 20250108 1.e6 -1. *15.
 *
 * heat removal by cooling coil from udc (max 40 kw)/ heat losses
 po-ic-2
 20250200 htc-t 508
 20250201 -1.0 0.0
 20250202 0.0 0.0
 20250203 1.0 -1. *20.
 20250204 450. -1. *20.
 20250205 451. -15. *20.
 20250206 600. -15. *20.
 20250207 601. -1. *20.
 20250208 1.e6 -1. *20.
 *
 * heat removal by cooling coil from mdc (max 10 kw) (heat losses
 po-ic-2)
 20250300 htc-t 509
 20250301 -1.0 0.0
 20250302 0.0 0.0
 20250303 1.0 20.
 20250304 1.e6 20.
 *
 * heat removal by cooling coil from lp (max 50 kw)
 20250400 htc-t 510
 20250401 -1.0 0.0
 20250402 0.0 0.0
 20250403 1.0 323.
 20250404 1.e6 323.
 *
 * heat losses from ic tank
 20250500 htc-t 580
 20250501 -1.0 0.0
 20250502 0.0 0.0
 20250503 1.0 50.
 20250504 1.e6 50.
 *
 * heat losses from steam dome top (utilized for po-sd-8)
 20250600 htc-t 582
 20250601 -1.0 0.0
 20250602 0.0 0.0
 20250603 1.0 80.
 20250604 1.e6 80.
 *
 * heat losses from ic line
 20250700 htc-t 581
 20250701 -1.0 0.0
 20250702 0.0 0.0
 20250703 1.0 50. *
 20250704 982. 50.
 20250705 1.e6 50.
 *
 * heat losses from ic tank external pipes & ic line liquid
 20250800 htc-t 580
 20250801 -1.0 0.0
 20250802 0.0 0.0
 20250803 1.0 50. *
 20250804 1.e6 50.
 *
 * heat losses from core region (external vessel)
 20250900 htc-t 583
 20250901 -1.0 0.0

20250902 0.0 0.0
 20250903 1.0 5. *
 20250904 1.e6 5.
 * heat exchange between sd, udc, mdc and lp slabs with cooling coil
 * assigned environment temperature value -
 20280100 temp 511
 20280101 -1.0 0.0
 20280102 0.0 0.0
 20280103 1.0 303.
 20280104 1.e6 303.
 * core power
 20290000 power 513
 20290001 -1.0 0.0
 20290002 0.0 0.0
 20290003 5.0 0.0416e6
 20290004 438.0 0.0416e6
 20290005 440.7 0.004e6
 20290006 586.1 0.004e6
 20290007 588. 0.07047e6
 20290008 590. 0.07330e6
 20290009 1086. 0.07330e6
 20290010 1088. 0.0
 20290011 1.e6 0.
 * bypass heaters
 20290100 htrnrate 515
 20290101 -1. 0.00
 20290102 0. 0.00
 20290103 1.99 0.00
 20290104 2.0 -2.65e3
 20290105 200. -2.65e3
 20290106 201. 0.
 20290107 1.e6 0.
 * power loss from fuel box -lower part- fbl
 20290200 htrnrate 516
 20290201 -1. 0.00
 20290202 0. 0.00
 20290203 0.01 5.90e4
 20290204 30. 5.90e4
 20290205 50. 5.90e4
 20290206 70. 5.90e4
 20290207 100. 5.90e4
 20290208 201. 7.90e4
 20290209 202. 7.90e4
 20290210 400. 10.90e4
 20290211 1003. 10.90e3
 20290212 1.e6 10.90e3
 * power loss from fuel box -upper part- fb2
 20290300 htrnrate 517
 20290301 -1. 0.00
 20290302 0. 0.00
 20290303 0.01 0.450e3
 20290304 100. 0.650e3
 20290305 360. 0.650e3
 20290306 650. 0.450e3
 20290307 1002. 5.650e4
 20290308 1003. 0.450e3
 20290309 1.e6 0.450e3
 * control variables
 *
 * dc lvl annular part1
 20500100 dc.lvl1 sum 1. 0. 1
 20500101 0. 0.1 voidf 320150000
 20500102 0. 0.273 voidf 320140000
 20500103 0. 0.273 voidf 320130000
 20500104 0. 0.273 voidf 320120000
 20500105 0. 0.273 voidf 320110000
 20500106 0. 0.273 voidf 320100000
 20500107 0. 0.273 voidf 320090000
 20500108 0. 0.273 voidf 320080000
 20500109 0. 0.273 voidf 320070000
 20500110 0. 0.273 voidf 320060000
 20500111 0. 0.273 voidf 320050000
 20500112 0. 0.273 voidf 320040000
 20500113 0. 0.273 voidf 320030000
 20500114 0. 0.273 voidf 320020000
 20500115 0. 0.273 voidf 320010000
 * dc lvl part 2
 20500200 dc.lvl2 sum 1. 0. 1
 20500201 0. 0.325 voidf 310010000
 20500202 0. 0.281 voidf 305080000
 20500203 0. 0.281 voidf 305070000
 20500204 0. 0.281 voidf 305060000
 20500205 0. 0.281 voidf 305050000
 20500206 0. 0.281 voidf 305040000
 20500207 0. 0.29 voidf 305030000
 20500208 0. 0.29 voidf 305020000
 20500209 0. 0.29 voidf 305010000
 20500210 0. 0.283 voidf 300010000
 * dc lvl part 3
 20500300 dc.lvl3 sum 1. 0. 1
 20500301 0. 0.300 voidf 285060000
 20500302 0. 0.300 voidf 285050000
 20500303 0. 0.300 voidf 285040000
 20500304 0. 0.300 voidf 285030000
 20500305 0. 0.300 voidf 285020000
 20500306 0. 0.300 voidf 285010000
 20500307 0. 0.300 voidf 280010000
 20500308 0. 0.362 voidf 275040000
 20500309 0. 0.362 voidf 275030000

20500310	0.362	voidf	275020000	* co lvl total in the core region
20500311	0.362	voidf	275010000	20502000 dc.lv.jp sum 1. 0. 1
20500312	0.247	voidf	270010000	20502001 0. 1. cntrlvar 015
*				20502002 1. cntrlvar 016
* dc lvl jet pump region				20502003 1. cntrlvar 017
20500400 dc.lvl4	sum	1. 0. 1		20502004 1. cntrlvar 018
20500401 0. 0.273	voidf	315150000	*	
20500402 0. 0.273	voidf	315140000	* core bypass level part 1	
20500403 0. 0.273	voidf	315130000	20502500 0. 0.2468 voidf 150010000	
20500404 0. 0.273	voidf	315120000	20502501 0. 0.2468 voidf 150020000	
20500405 0. 0.273	voidf	315110000	20502502 0. 0.2468 voidf 150030000	
20500406 0. 0.273	voidf	315100000	20502503 0. 0.2468 voidf 150040000	
20500407 0. 0.273	voidf	315090000	20502504 0. 0.2468 voidf 150050000	
20500408 0. 0.273	voidf	315080000	20502505 0. 0.223 voidf 155010000	
20500409 0. 0.273	voidf	315070000	20502506 0. 0.223 voidf 160010000	
20500410 0. 0.273	voidf	315060000	20502507 0. 0.2133 voidf 160010000	
20500411 0. 0.273	voidf	315050000	20502508 0. 0.2133 voidf 160020000	
20500412 0. 0.273	voidf	315040000	20502509 0. 0.2133 voidf 160030000	
20500413 0. 0.273	voidf	315030000	20502510 0. 0.2133 voidf 160040000	
20500414 0. 0.273	voidf	315020000	20502511 0. 0.2133 voidf 160050000	
20500415 0. 0.273	voidf	315010000	20502512 0. 0.2133 voidf 160060000	
*				20502513 0. 0.2133 voidf 160070000
* dc lvl total annular region				20502514 0. 0.2133 voidf 160080000
20501000 dc.lvl.a	sum	1. 0. 1		20502515 0. 0.2133 voidf 160090000
20501001 0. 1. cntrlvar	001			20502516 0. 0.2133 voidf 160100000
20501002 1. cntrlvar	002			20502517 0. 0.2015 voidf 165010000
20501003 1. cntrlvar	003		*	
20501004 0. 0.246 voidf	265010000	* core bypass level part 2		
20501005 0. 0.25 voidf	260010000	20502600 by.lvl2 sum 1. 0. 1		
20501006 0. 0.25 voidf	260020000	20502601 0. 0.235 voidf 170010000		
20501007 0. 0.25 voidf	260030000	20502602 0. 0.235 voidf 170020000		
20501008 0. 0.25 voidf	260040000	20502603 0. 0.235 voidf 170030000		
*		20502604 0. 0.235 voidf 170040000		
* dc lvl total jet pump region				20502605 0. 0.235 voidf 170050000
20501100 dc.lv.jp	sum	1. 0. 1		20502606 0. 0.235 voidf 170060000
20501101 0. 1. cntrlvar	002			20502607 0. 0.235 voidf 170070000
20501102 1. cntrlvar	003			20502608 0. 0.235 voidf 170080000
20501103 1. cntrlvar	004			20502609 0. 0.235 voidf 170090000
20501104 0. 0.327 voidf	325010000	20502610 0. 0.235 voidf 170100000		
20501105 0. 0.185 voidf	330010000	20502611 0. 0.2075 voidf 175010000	*	
*		* by lvl total from bot		
20501107 0. 0.25 voidf	260010000	20503000 dc.lv.jp sum 1. 0. 1		
20501108 0. 0.25 voidf	260020000	20503001 0. 1. cntrlvar 025		
20501109 0. 0.25 voidf	260030000	20503002 1. cntrlvar 026	*	
20501110 0. 0.25 voidf	260040000	*		
* lp lvl vertical		* sep annulus level		
20501500 lp.lvl	sum	1. 0. 1	20503500 sep.annl sum 1. 0. 1	
20501501 0. 0.30 voidf	100010000	20503501 0. 0.34 voidf 225010000		
20501502 0. 0.25 voidf	110010000	20503502 0. 0.512 voidf 230010000		
20501503 0. 0.25 voidf	110020000	20503503 0. 0.469 voidf 230020000		
20501504 0. 0.1443 voidf	110030000	20503504 0. 0.469 voidf 230030000		
20501505 0. 0.1443 voidf	110040000	20503505 0. 0.469 voidf 230040000		
20501506 0. 0.1114 voidf	110050000	20503506 0. 0.469 voidf 230050000		
20501507 0. 0.1615 voidf	111010000	20503507 0. 0.469 voidf 230060000		
20501508 0. 0.1600 voidf	112010000	20503508 0. 0.469 voidf 230070000		
20501509 0. 0.1745 voidf	115010000	20503509 0. 0.469 voidf 230080000	*	
20501510 0. 0.2 voidf	120010000	*		
20501511 0. 0.2 voidf	120020000	* core power		
20501512 0. 0.176 voidf	130010000	20504000 core.po sum 1. 0. 1		
20501513 0. 0.2 voidf	135010000	20504001 0. 0.162907 htrnr 200100101		
20501514 0. 0.2 voidf	140010000	20504002 0. 0.162907 htrnr 200100201		
*		20504003 0. 0.162907 htrnr 200100301		
* core level		20504004 0. 0.162907 htrnr 200100401		
20501600 core.lvl	sum	1. 0. 1	20504005 0. 0.162907 htrnr 200100501	
20501601 0. 0.265 voidf	200010000	20504006 0. 0.162907 htrnr 200100601		
20501602 0. 0.265 voidf	200020000	20504007 0. 0.162907 htrnr 200100701		
20501603 0. 0.265 voidf	200030000	20504008 0. 0.162907 htrnr 200100801		
20501604 0. 0.265 voidf	200040000	20504009 0. 0.162907 htrnr 200100901		
20501605 0. 0.265 voidf	200050000	20504010 0. 0.162907 htrnr 200101001		
20501606 0. 0.265 voidf	200060000	20504011 0. 0.162907 htrnr 200101101		
20501607 0. 0.265 voidf	200070000	20504012 0. 0.162907 htrnr 200101201		
20501608 0. 0.265 voidf	200080000	20504013 0. 0.162907 htrnr 200101301		
20501609 0. 0.265 voidf	200090000	20504014 0. 0.162907 htrnr 200101401	*	
20501610 0. 0.265 voidf	200100000	*		
20501611 0. 0.265 voidf	200110000	* ext fuel box level		
20501612 0. 0.265 voidf	200120000	20505000 ext.fblv sum 1. 0. 1		
20501613 0. 0.265 voidf	200130000	20505001 0. 0.53 voidf 370010000		
20501614 0. 0.265 voidf	200140000	20505002 0. 0.53 voidf 370020000		
20501615 0. 0.229 voidf	200150000	20505003 0. 0.53 voidf 370030000		
20501616 0. 0.2 voidf	200160000	20505004 0. 0.53 voidf 370040000		
*		20505005 0. 0.53 voidf 370050000		
* upper plenum level		20505006 0. 0.53 voidf 370060000		
20501700 up.lvl	sum	1. 0. 1	20505007 0. 0.53 voidf 370070000	
20501701 0. 0.22 voidf	205010000	20505008 0. 0.429 voidf 360010000	*	
*		*		
* up-sep level		* heat exchange ic		
20501800 upse.lvl	sum	1. 0. 1	20506000 ic.ht sum 1. 0. 1	
20501801 0. 0.214 voidf	220010000	20506001 0. 1. q 510010000		
20501802 0. 0.214 voidf	220020000	20506002 1. q 515010000		
20501803 0. 0.2345 voidf	220030000	20506003 1. q 515020000		
20501804 0. 0.2345 voidf	220040000	20506004 1. q 515030000		
20501805 0. 0.2345 voidf	220050000	20506005 1. q 515040000		
20501806 0. 0.2345 voidf	220060000	20506006 1. q 515050000		
20501807 0. 0.2345 voidf	220070000	20506007 1. q 520010000	*	
20501808 0. 0.2345 voidf	220080000	*		
20501809 0. 0.2345 voidf	220090000	* heat exchange ic exit pipe (in the tank)		
20501810 0. 0.2345 voidf	220100000	20506100 ic.tube sum 1. 0. 1		
20501811 0. 0.2345 voidf	220110000	20506101 0. 1. q 525010000		
20501812 0. 0.2345 voidf	220120000	20506102 1. q 525020000		
20501813 0. 0.2345 voidf	220130000	20506103 1. q 525030000		
20501814 0. 0.2345 voidf	220140000	20506104 1. q 525040000		
20501815 0. 0.2345 voidf	220150000	20506105 1. q 525050000		
20501816 0. 0.2345 voidf	220160000	20506106 1. q 525060000		
20501817 0. 0.2345 voidf	220170000	20506107 1. q 525070000		
20501818 0. 0.2345 voidf	220180000	20506108 1. q 525080000		
20501819 0. 0.2345 voidf	220190000	20506109 1. q 525090000		
20501820 0. 0.2345 voidf	220200000	20506110 1. q 525100000		
*		20506111 1. q 525110000		
		20506112 1. q 525120000		

```

20506113      1.      q      525130000
20506114      1.      q      525140000
*
* ht ic total
20506200  ic.ht.to      sum    1.  0.  1
20506201  0.  -1.  cntrlvar  060
20506202  -1.  cntrlvar  061
*
* environment heat loss from ic tank
20506300  ic.t.h1      sum    1.  0.  1
20506301  0.  0.235  htrnr  560000101
20506302  0.  0.235  htrnr  560000201
20506303  0.  0.235  htrnr  560000301
20506304  0.  0.235  htrnr  560000401
20506305  0.  0.235  htrnr  560000501
20506306  0.  0.235  htrnr  560000601
20506307  0.  0.235  htrnr  560000701
20506308  0.  0.235  htrnr  560000801
20506309  0.  0.298  htrnr  560000901
20506310  0.  0.298  htrnr  560001001
20506311  0.  0.188  htrnr  560001101
20506312  0.  0.188  htrnr  560001201
20506313  0.  0.188  htrnr  560001301
20506314  0.  0.188  htrnr  560001401
20506315  0.  0.188  htrnr  560001501
20506316  0.  0.298  htrnr  560001601
*
* heat exchange from ic tank ext pipe vertical (longer)
20507100  ic.tav1      sum    1.  0.  1
20507101  0.  1.      q      563050000
20507102  1.      q      563060000
20507103  1.      q      563070000
20507104  1.      q      563080000
20507105  1.      q      563090000
20507106  1.      q      563100000
20507107  1.      q      563110000
20507108  1.      q      563120000
20507109  1.      q      563130000
20507110  1.      q      563140000
20507111  1.      q      563150000
20507112  1.      q      563160000
20507113  1.      q      563170000
20507114  1.      q      563180000
*
* heat exchange from ic tank ext pipe vertical (short)
20507200  ic.tav2      sum    1.  0.  1
20507201  0.  1.      q      564050000
20507202  1.      q      564060000
20507203  1.      q      564070000
20507204  1.      q      564080000
20507205  1.      q      564090000
20507206  1.      q      564100000
20507207  1.      q      564110000
20507208  1.      q      564120000
20507209  1.      q      564130000
20507210  1.      q      564140000
20507211  1.      q      564150000
20507212  1.      q      564160000
20507213  1.      q      564170000
20507214  1.      q      564180000
*
* heat exchange from ic tank ext pipe all four horizontal
20507300  ic.tav3      sum    1.  0.  1
20507301  0.  1.      q      563010000
20507302  1.      q      563020000
20507303  1.      q      563030000
20507304  1.      q      563040000
20507305  1.      q      563190000
20507306  1.      q      563200000
20507307  1.      q      563210000
20507308  1.      q      563220000
20507309  1.      q      564010000
20507310  1.      q      564020000
20507311  1.      q      564030000
20507312  1.      q      564040000
20507313  1.      q      564190000
20507314  1.      q      564200000
20507315  1.      q      564210000
20507316  1.      q      564220000
*
* ht tank external total
20507500  tank.htt      sum    1.  0.  1
20507501  0.  1.  cntrlvar  063
20507502  1.  cntrlvar  071
20507503  1.  cntrlvar  072
20507504  1.  cntrlvar  073
*
*
/*

```

APPENDIX 6:
Overview of the scaling analysis



The American Society of
Mechanical Engineers

Reprinted From
Proceedings of the ASME-JSME 4th International
Conference on Nuclear Engineering
Editors: A. S. Rao, R. B. Duffey, and D. Elias
Book No. 10389C - 1996

QUALITATIVE ANALYSIS OF SCALING EFFECTS IN ISOLATION CONDENSER BEHAVIOUR WITH RELAP5/MOD3.1 THERMALHYDRAULIC CODE

Francesco D'Auria

Department of Mechanical and Nuclear Constructions
University of Pisa Via Diotisalvi, 2 - 56126 Pisa-(Italy)
Tel. +39-50-585253

Vittorio Faluomi

Department of Mechanical and Nuclear Constructions
University of Pisa Via Diotisalvi, 2 - 56126 Pisa (Italy)
Tel. +39-50-585253

ABSTRACT

This paper deals with the attempt to analyse, with the Relap5/Mod3.1 code, the scaling effects in the behaviour of Isolation Condenser taking as reference the PO-IC-02 experiment performed in the PIPER-ONE facility available at Pisa University.

The PIPER-ONE is an experimental facility simulating a General Electric BWR-6 with volume and height scaling ratio of 1/2200 and 1/1, respectively. The facility was properly modified to test the thermalhydraulic characteristics of an isolation condenser-type system.

The isolation condenser-type system consists of a once-through heat exchanger immersed in a pool with water at ambient temperature and installed at about 10 m above the core.

Several calculations have been performed with Relap5/Mod3.1 and Relap5/Mod3.1 codes, and the capabilities of code to simulate the behaviour of the isolation condenser component have been assessed. The results obtained cannot be extrapolated to the plant because of the different scaling of isolation condenser system with respect to the other components of the facility.

In this paper the effects of "scaling" changes in the facility nodalization are analysed with the use of Relap5/Mod3.1 code.

The following parameters are considered in the analysis of scaling effects:

- 1) Elevation of isolation condenser relative to the top of active fuel (TAF);
- 2) Length of Isolation Condenser tubes;
- 3) Diameter of Isolation condenser tubes;
- 4) Heat exchange area of Isolation condenser;
- 5) Inlet flow area of Isolation condenser;

A final calculation including all the modifications has also been performed.

1. INTRODUCTION

Innovative reactors, (essentially AP-600 and SBWR) are characterized by simplification in the design and by the presence of passive systems. Experimental and theoretical research are needed to qualify the new components and to characterize the new thermal-hydraulic scenarios expected during accidents. Available system codes have to be validated in order to be used for evaluating the thermal-hydraulic performances of the new systems, especially in case of long lasting transients evolving at low pressure (D'Auria et. al., 1992a).

In the frame of the activities carried out at University of Pisa related to the analysis of thermal-hydraulic situations of interest to the mentioned reactors (e.g. D'Auria et. al., 1992b and Andeucetti et al., 1991), three series of experiments have been carried out utilizing the PIPER-ONE facility. These were aimed at the experimental investigation of the behaviour of systems simulating the main features of the Gravity Driven Cooling System (GDCS, first series of experiments, Bovalini et al., 1991a) and of the reactor pressure vessel Isolation Condenser (IC, second and third series of experiments, Bovalini et al., 1992a, D'Auria et. al., 1993, Bovalini et al., 1992b, and D'Auria et. al., 1994a, respectively). At the same time Relap5/Mod2 and Mod3 codes (Carlson et al., 1990) have been extensively applied as best estimate tools to predict the transient scenarios of both SBWR and AP-600 reactors (see also D'Auria et. al., 1994b, and Barbucci et al., 1993).

The object of this paper is to evaluate the possibilities to use Relap5/Mod 3.1 code (Carlson et al., 1990) for extrapolating the behaviour of PIPER-ONE facility. In order to achieve this, a qualified Relap5/Mod3.1 nodalization (Bovalini et al., 1995) of the PIPER-ONE has been used and the considered modifications have been implemented step-by-step to investigate the single effects of each parameter in the scaling process (D'Auria et al., et al., 1992c).

2. EXPERIMENTAL FACILITY

The simplified sketch of the apparatus is shown in Fig. 1; it includes the main loop, the ECCS simulators (LPCI/CS,

	QUANTITY	UNIT	PIPER-ONE	SBWR (°)	RATIO ⁽⁺⁾ PIPER-ONE/ SBWR	IDEAL ⁽⁺⁾ VALUE OF THE RATIO PIPER-ONE/SBWR
1	Primary system volume	m ³	0.199	595.	1/2990	1/2990
2	Core height	m	3.710	2.743	1.35/1	1/1
3	Maximum nominal core power	MW	0.320	2000.	1/6200	1/2990
4	Value of 3% core power	MW	0.041 (-)	60.	1/1463	1/2990
5	Ratio (3% core power) /primary system volume	MW/m ³	0.206	0.1	2.06/1	1/1
6	Isolation condenser heat transfer area (++)	m ²	0.301	184	1/610	1/2990
7	Isolation condenser heat transfer area over primary system volume	m ⁻¹	1.512	0.31	4.9/1	1/1
8	Isolation condenser volume	m ³	0.0015	2.334	1/1556	1/2990
9	Isolation condenser volume over primary system volume	-	0.0075	0.0038	1.97/1	1/1
10	Isolation condenser heat transfer area over 3% core power	m ² /kW	7.341	3.066	2.39/1	1/1
11	Height of isolation condenser top related to bottom of active fuel	m	8.64	24.75	1/2.86	1/1
12	Diameter of a single tube	m	0.020	0.0508	1/2.54	1/1
13	Thickness of a single tube	m	0.0023	0.0023	1/1	1/1

(+) non-dimensional

(°)IC data have been taken from reference /15/

(++)only tube bundles (-)related to BWR6

Tab. 1 - Comparison between isolation condenser related data in PIPER-ONE and in SBWR.

HPCI/CS) and the systems simulating ADS, SRV and steam line, as well as the blow-down line. Ten zones can be identified in the main loop: lower plenum, core, core bypass (outside the core), guide tube region, upper plenum, region of separators and dryers, steam dome, upper down comer, lower down comer and jet pump region.

The volume scaling factor is about 1/2200, while the core cell geometry and the piezometric heads acting on the lower core support plate are the same in the model and in the reference plant.

The heated bundle consists of 16 (4x4) indirectly heated electrical rods, whose height, pitch and diameter are the same as in the reference plant (Fig. 2). The maximum available power is 320 kW, corresponding to about 25% of scaled full power of the reference BWR.

As already mentioned, the facility hardware was modified by inserting the ICS loop, which can operate at the same pressure as the main circuit.

The main component of Isolation Condenser loop is a heat exchanger consisting of a couple of flanges that support 12 pipes, 22 mm outer diameter and 0.4 m long: it is immersed in a tank of 1 m³ volume, containing stagnant water, located at 4th floor of the PIPER-ONE service structure. The heat exchanger is connected at the top and at the bottom respectively with the steam dome and the lower plenum of the main loop. In order to enhance natural convection inside the

pool, a sort of shroud has been installed that divides the pool into two parts; a hot one and a cold one, the former encompassing the IC as can be seen in Fig. 4.

The Isolation Condenser loop is instrumented with a turbine flow-meter and a differential pressure transducer on the hot side and a series of almost 30 thermocouples in various position of the IC and of the pool as can be derived from Fig. 2.

Hardware restrictions preclude the possibility to have a system correctly scaled with respect to those provided for the new generation nuclear reactors, particularly the GE SBWR. In particular, the heat transfer area of Isolation Condenser in PIPER-ONE is roughly five times larger than the ideal value (Tab.1). The distance between bottom of the active fuel and the Isolation Condenser and the height of the core itself, are two of the most important parameters differentiating PIPER-ONE from SBWR. These essentially prevent any possibility of extrapolating PIPER-ONE experimental data to SBWR.

3. EXPERIMENT

The experiment comprises two phases characterized by different values of heating power (about 40 and 75 kW, respectively), later indicated as phases A and the B of the test. They correspond to the scaled value of the core decay power and to the capability of heat removal by the IC device,

PARAMETER	SIGN	UNIT	VALUE
LP pressure	PA-LP-1	MPa	5.1
LP fluid temperature	TF-LP-1	K	262.5
Core level	LP-CC-1	m	11.9
Down comer level	LP-LD-1	m	10.7
IC line fluid temperature	TF-IC-1	K	17.5
IC pool fluid temperature	TF-SC-1	K	17.5

Tab. 2- PIPER-ONE test PO-IC-2: initial conditions

PARAMETER OR EVENT	TIME (s)
Test initiation	0.0
IC top valve opens	4.0
IC bottom valve opens	32.0
IC top valve closes	508.0
IC top valve opens again	602.0
IC top and bottom valve close	1106.0
End of test	1184.0

Tab. 3- PIPER-ONE test PO-IC-2: boundary conditions

determined from the previous test PO-SD-8 (Bovalini et al., 1992b).

As usual for the experiments carried out in the PIPER-ONE facility, the test was designed on the basis of pre-test calculations performed by Relap5/Mod3 code.

The test specifications foresaw constant heating power for 5/10 minutes for both experimental phases, in such a way that quasi-steady state conditions could be reached by the main thermal-hydraulic quantities (pressure, flow rates, collapsed levels, etc.).

In the test, the primary circuit was pressurized at the specified value by single-phase natural circulation; the heat source was provided by the core simulator and the structure heating system. Then, liquid was drained from the primary circuit for establishing the test specified liquid levels, roughly at the steam separator top elevation. After some hundreds seconds of steady conditions, with heat losses compensated by the heating cables, the test started by supplying power to the core simulator and opening the valves of the IC loop.

The initial and boundary conditions measured during the test PO-IC-02 are given in Tabs. 2 and 3.

The most significant results measured during the phases A and B are reported in the Figures 3 to 6.

Figure 5 shows the different phases of the transient; when the core power is around 40 kW, the primary pressure decreases (0.3 MPa/min), demonstrating that the power exchanged through the Isolation Condenser is greater than the supplied power. Roughly a steady condition is reached at around 75 kW (phase B), with a decrease of primary pressure of only 0.02 MPa/min. According also to the results of the test PO-SD-8, the overall power removed by the Isolation Condenser is of the order of 80 kW, corresponding to an average heat flux of about 200 kW/m² in the considered conditions. The condensate mass flow rate, registered at the drain line (Fig. 4), appears quite constant along the two phases of the test (the turbine transducer was initially blocked, but

started to operate with about 3 minutes of delay from the opening of the IC valve).

In Fig. 5, the fluid temperatures measured in three positions along the Isolation Condenser heat exchanger are compared with the steam temperature at the IC inlet (equal to the saturation temperature corresponding to the primary system pressure); in particular, the bottom curve gives an idea of the sub cooled conditions attained by the liquid exiting from the heat exchanger.

Finally, the curves in Fig. 6 essentially show the strong fluid temperature stratification in the pool: in the upper zone, the temperature increases up to about boiling conditions at the test end, while the bottom part of the pool remains at ambient temperature during all the test (fluid temperature less than 20 °C).

4. SCALING METHOD AND INPUT DECK MODIFICATIONS

4.1 The scaling method

The adopted scaling methodology is organised in the following steps (Fig. 7):

1) set-up of nodalization of considered facility and calculation of a transient to qualifying the nodalization itself. This input deck is used for the "base calculation" (D'Auria et al., 1995).

2) identification of relevant parameters for the considered transient: this step defines which parameters in the facilities have to be properly scaled to represent the reference plant behaviour.

3) consideration of the value of above parameters in the facility and scaling to the reference plant.

Parameter	Identifier	Scaling factor	Facility actual value	Facility scaled value	Reference value (Plant)
Elevation of Isolation Condenser from the core	TOIC-TAF	1/1	4.7 m	22.7 m	22.7 m
Isolation Condenser Heat exchange area	IC HTA	1/2990	0.23 m ²	0.061 m ²	184 m ²
Isolation Condenser Tubes Equivalent Diameter	IC TDH	1/1	0.02 m	0.05 m	0.05 m
Isolation Condenser Tube length	IC TL	1/1	0.314 m	2.4 m	2.4 m
Isolation Condenser flow area	IC TFA	1/2990	0.0037 m ²	0.00102 m ²	3.05 m ²

Tab. 4: Modified parameter for scaling analysis

Input deck	Parameter changed	Nodalization modifications	Remark:
POONLY1	elevation of IC (same as SBWR)	-add of a MSV to connect the old MSV to the new position of IC (30 volumes) -add a 35 volumes to the IC outlet line connecting the IC to the DC.	The dimension of added tubes and heat structures are the same as the preesistent compoenets. No heat losses are applied to these new volumes.
POONLY2	heat transfer area scaled to SBWR	change of heat slab dimensions and inner and outer cilindrical shell representing the IC tube wall to have a scaled heat transfer area nad the same values of heat slab radius as reference plant.	
POONLY3	tube diameter of IC (same as SBWR)	change of hydraulic diameter of IC tubes in the volume representing the bundle in the nodalization	
POONLY4	Length of IC tubes same as SBWR	change of length of IC tube and pool dimension. Te position of IC relatively to the pool is kept constant as in the base case nodalization.	
POONLY5	IC flow area (scaled to the SBWR)	the flow area of pipe stack representing the IC bundle has been scaled to the SBWR plant.	

Table 5: List of modifications made to the nase nodalization for parameter influence evaluation in the scaling activity.

4) set-up of individual facility nodalizations adopting the scaled values from the previous step.

5) set-up of the final nodalization with all the modifications; comparison of the results with the experimental data.

6) test calculation of a different transient adopting the scaled input deck, and comparison with plant calculation results (base case can be considered). This step has not been dealt with in the present paper.

4.2 Relevant modification to the base input deck

The standard IBM RJSC version of Relap5/Mod3.1 has been adopted.

The base nodalization of the PIPER-ONE facility has been previously developed for PO-IC-2 experiment analysis (Bovalini et al., 1995)

The list of modified parameters is given in Tab. 4. For each parameter different calculations have been performed, including sensitivities and use of different codes.

In Tab. 5 the different nodalizations and the modifications introduced are summarized.

The following constraints have been considered:

a) the overall facility volume has been kept nearly constant (overall modifications increase the total volume of 2 %), because it was already scaled to the plant;

b) the additional volumes are thermally insulated.

5. RESULTS OF CODE APPLICATION

5.1 Output relevant parameters

For evaluating the calculation results the following parameters have been used:

- System pressure;
- IC mass flowrate;
- IC fluid temperature jump from inlet to outlet ;

- Core level;
- Downcomer level;
- Temperature jump from IC fluid to inner pool fluid;
- IC exchanged power;
- Temperature jump from inner to outlet pool fluid.

Some results are given in Figs. 8 to 15. The complete evaluation of results can be found in D'Auria et al., 1995.

5.2 One-step analysis

The results of single parameter variations are given in Figs. 8 from 11. Detected differences are related to the experimental data:

PON1 (Elevation of IC same as in the SBWR plant): Large difference in the pressure trend of primary system are due to the high flow rate in the IC (higher driving force) and consequent high heat transfer between IC tubes and pool. Higher values of fluid temperature in the IC tubes (>50 K) give a lower fluid temperature jump along the IC tubes (150 K lower than in the exp. case). No relevant modifications in the phenomenological description of the transient.

PON2 (Heat transfer area scaled to SBWR): No significant differences in the overall scenario were calculated. In the IC tubes the calculated fluid temperature was 100 K lower than in the experiment. To be noted that the calculation was stopped after 800 s. due to code failure in the calculation of water properties.

PON3 (Tube diameter of IC same as in the SBWR): The calculation showed similar results as in previous case, with some differences in the primary system pressure, owing to the higher value of fluid temperature in the IC tubes (around 250 K) and at the IC outlet.

PON4 (Length of IC tubes same as SBWR): Lower values of IC tubes fluid temperature than in previous calculations have been calculated. The length of tubes allows more cooling of IC fluid from IC pool, so that the values of subcooling at the IC outlet is higher than in previous cases and also higher than experimental and base calculation values.

PON5 (IC flow area scaled to the SBWR): Similar results as PON3 calculation.

5.3 Global Effect analysis

The different modifications to the base input deck previous analysed have been considered together to evaluate the global effects in the transient. The Figs. 12 to 15 show the results.

System pressure: the elevation of IC with respect to the core mostly contributes to the different trend of pressure, lower than experimental value of 0.5-0.8 MPa (Fig. 12). This effect is due mainly to the increase of mass flow rate (Fig. 13) through the IC and the higher power exchanged (Fig. 14) in the IC itself.

Mass flow rate: the average value of mass flow rate through the IC is nearly twice (0.05 Kg/s instead of 0.025 Kg/s) than in the experimental and base case. This also affects the exchanged power, higher than in the experimental case.

Fluid temperature in IC tubes: the value of IC tubes fluid temperature is 50 K higher than in the experimental case (Fig. 15). Moreover, the temperature jump between IC inlet and outlet is 150 K lower than the experimental results. This effect is connected with the pressure trend.

6. CONCLUSIONS

With the above described scaling method the following main results have been achieved:

- the relevant phenomenological aspect of PO-IC-2 experiment (i.e. the constant value of power exchanged in IC bundle depending on downcomer level) have been also calculating by the modified (scaled-up) nodalization; so, the measured scenario can be considered applicable to the SBWR, though the experimental apparatus was not properly scaled.

The adopted method seem to be capable to handle the main phenomenological aspect of transient, and might also predict some aspects that are expected but not obtained due to limitation of facility design.

In addition, it can be noted that there is no substantial disagreement in the overall evaluation of parameters considered as reference to evaluate the scaled nodalization: the system pressure decreases, following an increment of mass flow rate of IC and the related increment of power exchanged. The subcooling is also is than in experimental case, according with the low level of energy stored in the system (low value of system pressure). Some additional interesting effects can be noted in the calculation performed with this modified nodalization : along the inner pool there is no strong thermal stratification as in the experimental case (Fig. 16) and the calculated mass flow rate through the internal pool (Fig. 17) is higher than the base value. These effects can be directly connected with the modifications of input deck, especially with the new position of Isolation Condenser with respect to the core.

REFERENCES

Andreuccetti P., Barbucci P., Donatini F., D'Auria F., Galassi G. M., Oriolo F., 1991: "Capabilities of the RELAPS in Simulating SBWR and AP-600 Thermalhydraulic Behaviour", IAEA Technical Committee Meet. (TCM) on Progress in Development and Design Aspects of Advanced Water Cooled Reactors, Rome (I).

Barbucci P., Bella L., D'Auria F., Oriolo F., 1993: "SBWR Thermalhydraulic Performance: a RELAPS/MOD2 Model Simulation", 6th Int. Top. Meet. on Nuclear Reactor Thermalhydraulics, Grenoble (F).

Bovalini R., D'Auria F., Mazzini M., 1991: "Experiments of Core Coolability by a Gravity Driven System performed in

"PIPER-ONE Apparatus", *ANS Winter Meeting*, San Francisco (CA).

Bovalini R., D'Auria F., Mazzini M., Vigni P., 1992a: "Isolation Condenser Performances in PIPER-ONE Apparatus", European Two-Phase Flow Group Meet., Stockholm (S).

Bovalini R., D'Auria F., Galassi G.M., Mazzini M., 1992b: "Piper-One Research: the Experiment PO-SD-8 Related to the Evaluation of Isolation Condenser Performance. Post-Test Analysis Carried out by Relap5/Mod3-7J code", *University of Pisa Report*, DCMN - NT 200 (92), Pisa (I).

Bovalini R., D'Auria F., Galassi G. M., Mazzini M. 1995: "Post-test Analysis of PIPER-ONE PO-IC-02 Experiment by Relap5/Mod3 Codes", *University of Pisa Report*, DCMN NT 254 (95), Pisa (I).

Carlson K.E., Riemke R.A., Rouhani S.Z., Shumway R.W., Weaver W.L..1990: "Relap5/Mod3 Code Manual - Volume II. User Guide and Input Requirements", NUREG/CR-5535.

D'Auria F., Modro M., Oriolo F., Tasaka K., 1992a: "Relevant Thermalhydraulic Aspects of New Generation LWR's" CSNI Spec. Meet. On Transient Two-Phase Flow - System Thermalhydraulics, Aix-En-Provence (F).

D'Auria F., Galassi G.M., Oriolo F., 1992b: "Thermalhydraulic Phenomena and Code Requirements for

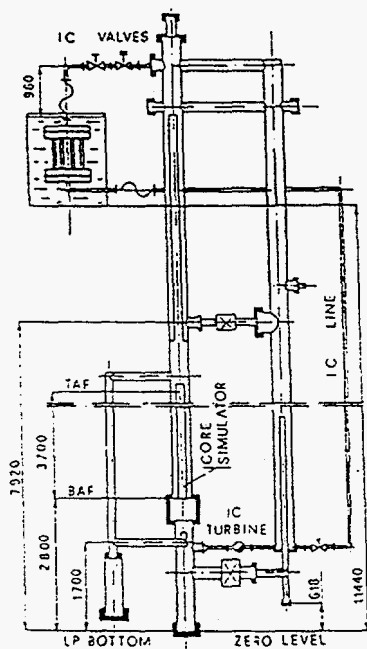


Fig. 1 - Sketch of PIPER-ONE

Future Reactors Safety Analysis", *Int. Conf. on Design and Safety of Nuclear Power Plants (ANP)* - Tokyo (J).

D'Auria F., 1992c: "Scaling and Counterpart Tests", CSNI Spec. Meeting on Transient Two-Phase Flow: System Thermalhydraulics - Aix en Provence (F).

D'Auria F., Vigni P., Marsili P., 1993: "Application of Relap5/Mod3 to the Evaluation of Isolation Condenser Performance", *Int. Conf. on Nuclear Engineering (ICONE-2)* - San Francisco (US).

D'Auria F., Galassi G.M.; Mazzini M., Pintore S., 1994a: "Ricerca Piper-One: specifiche Dettagliate della Prova PO-IC-2" *University of Pisa Report*, DCMN - NT 234(94), Pisa (I).

D'Auria F., Oriolo F., Bella L., Cavicchia V., 1994b: "AP-600 Thermalhydraulic Phenomenology: A Relap5/Mod2 Model Simulation", *Int. Conf. on New Trends in Nuclear System Thermalhydraulics* - Pisa (I). *Int. Top. Meeting on Advanced Reactor Safety* - Pittsburgh (PA).

D'Auria F., Faluomi V., 1995: "Qualitative Analysis of a scaling method for Piper-One facility", *University of Pisa Report*. to be published.

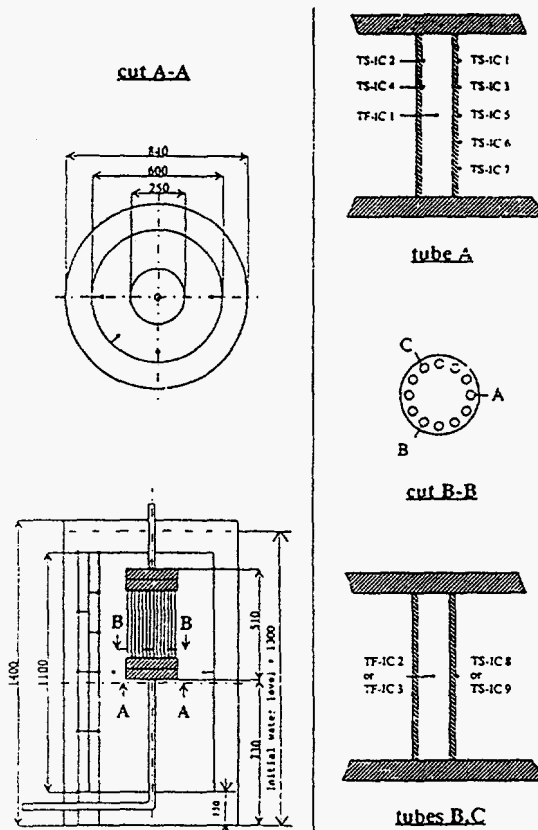


Fig. 2 - Sketch of isolation condenser pool with temperature measurement locations

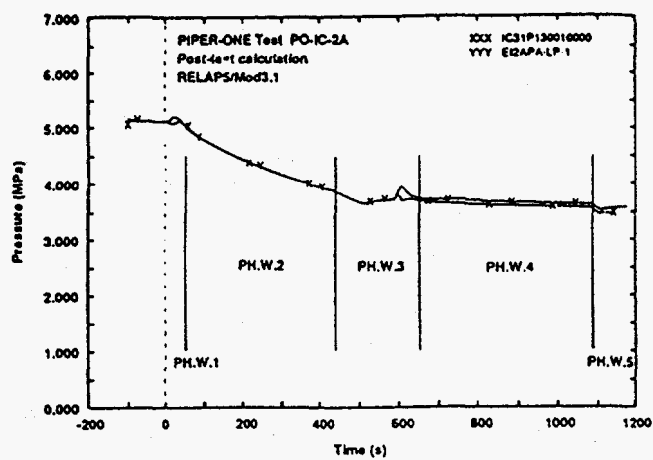


Fig. 3 - Phases of experimental transient

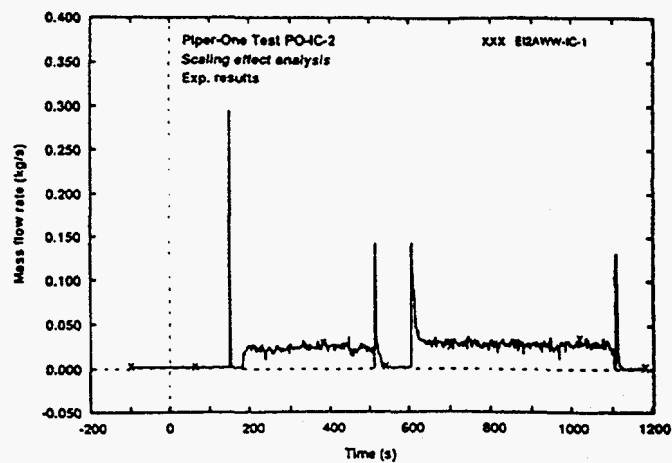


Fig. 4 - Condensate mass flow rate

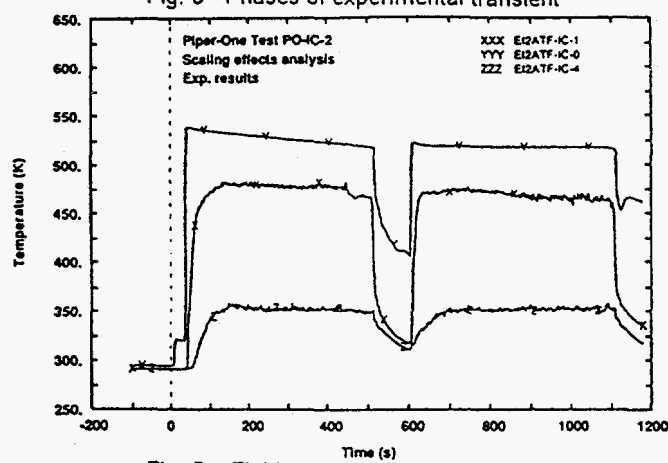


Fig. 5 - Fluid temperature along Isolation Condenser tubes

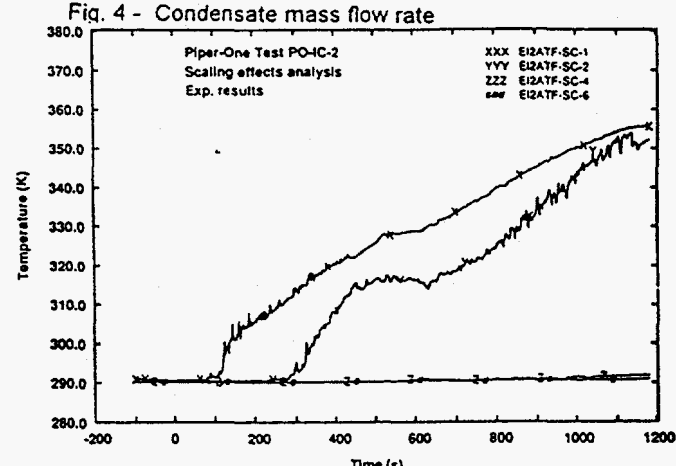


Fig 6 - Fluid temperature along the pool

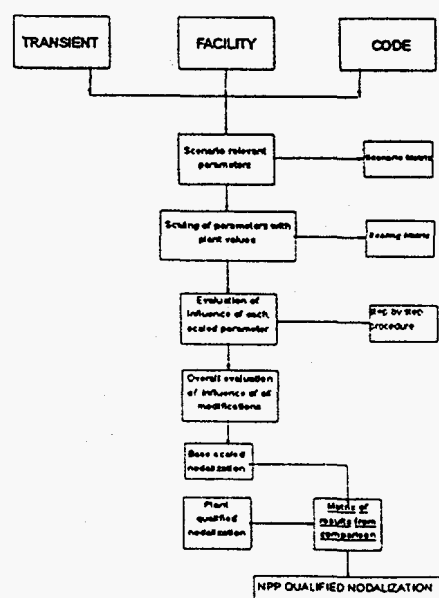


Fig. 7 - Flow chart of scaling method adopted

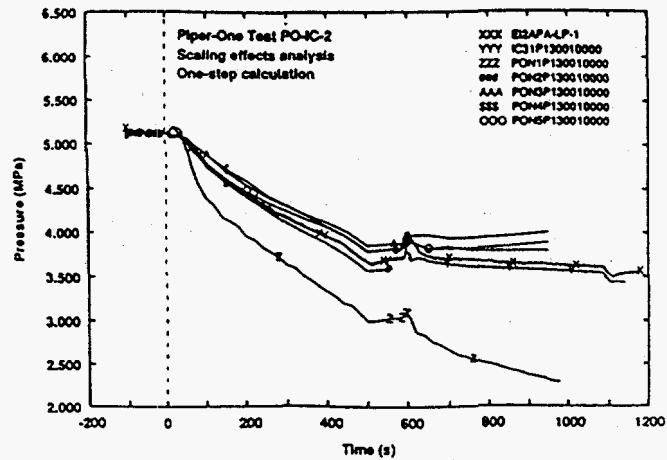


Fig. 8 - Scaling results: system pressure,
one step analysis

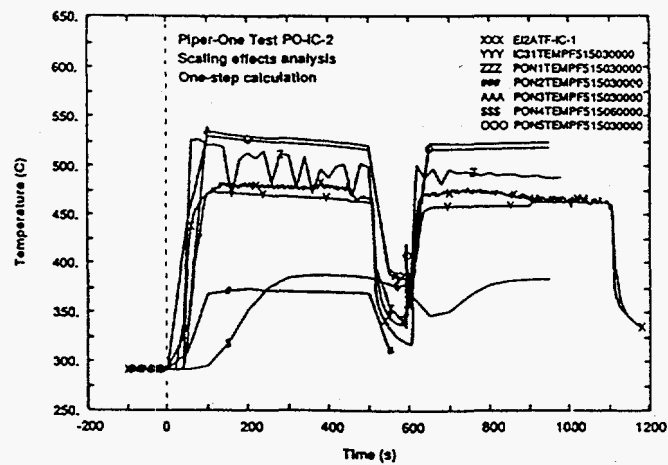


Fig. 10 - Scaling results: IC middle level tube fluid
one step analysis

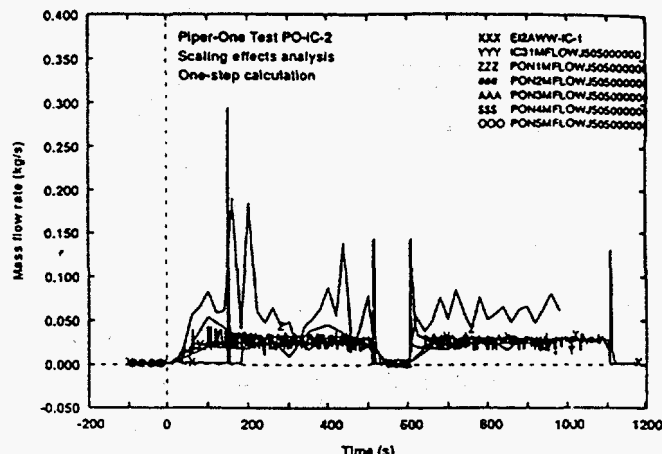


Fig. 9- Scaling results: IC mass flow rate, one step
analysis

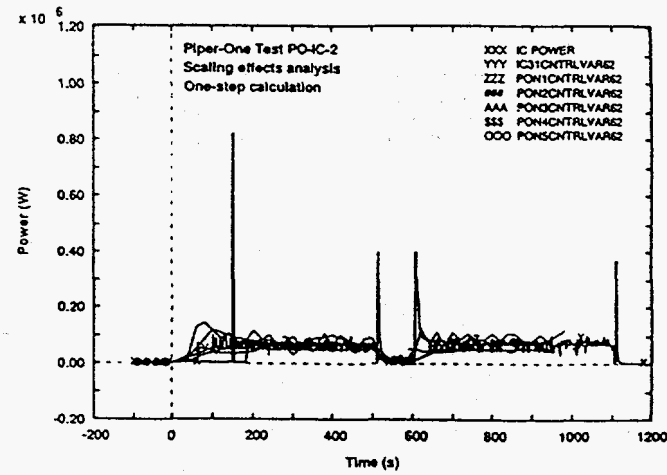


Fig. 11 - Scaling results: IC power exchanged
one step analysis

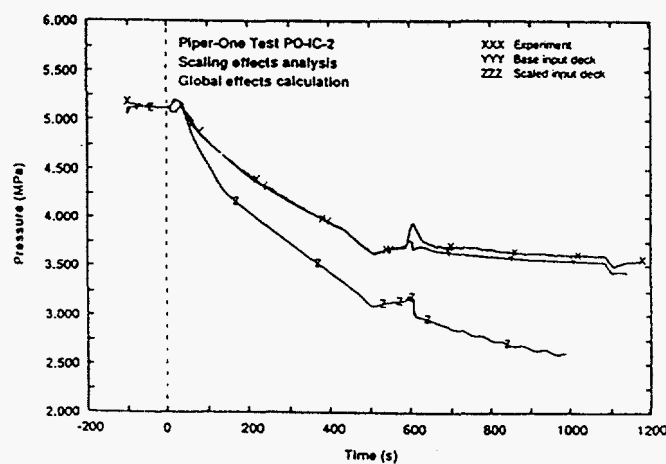


Fig. 12 - Scaling results: system pressure, global
effects analysis

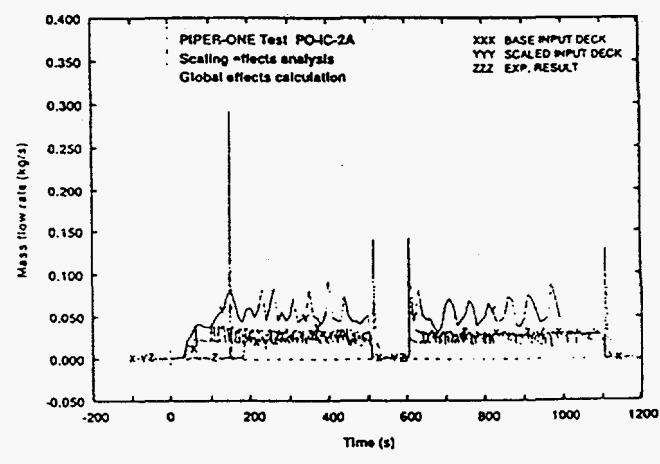


Fig. 13 - Scaling results: IC mass flowrate
effects analysis

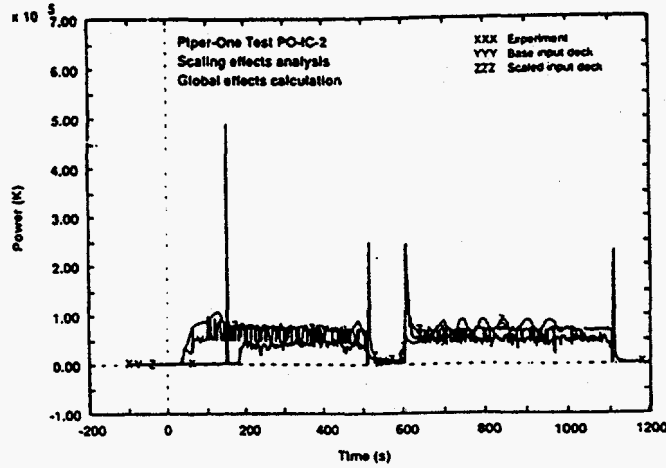


Fig. 14 - Scaling results: IC exchanged power global effects analysis

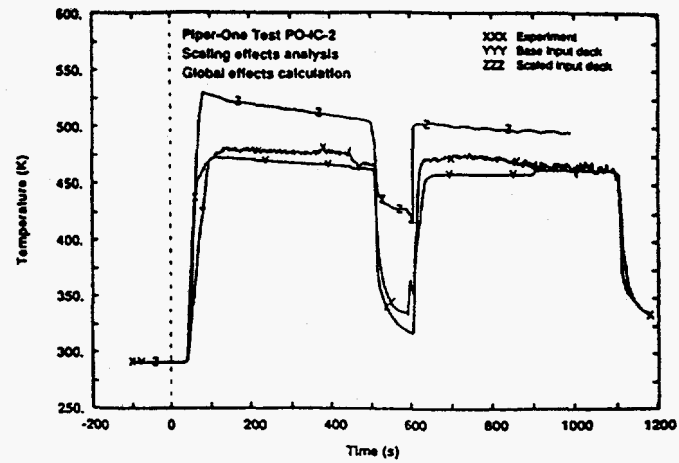


Fig. 15 - Scaling results:middle level tube fluid temperature,global effects analysis

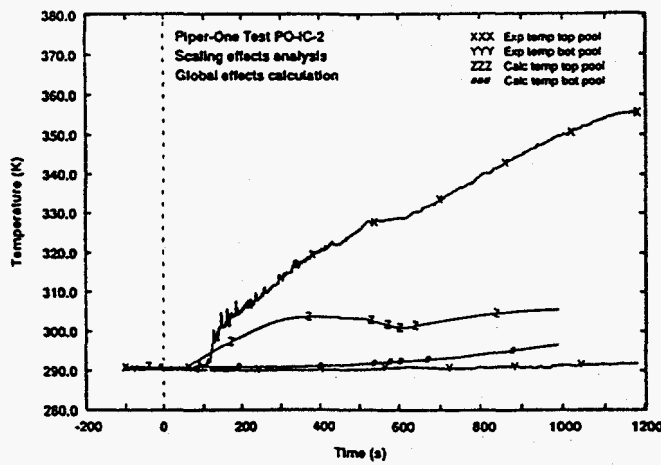


Fig. 16 - Scaling results: thermal stratification along the pool,global effects analysis

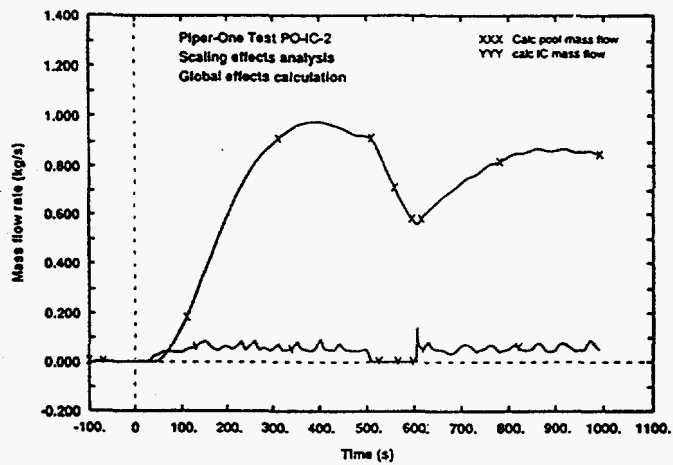


Fig. 17 - Scaling results:calculated circulation flow along the pool,global effects analysis

